Springer Earth System Sciences

Andrés Folguera
Maximiliano Naipauer
Lucía Sagripanti
Matías C. Ghiglione
Darío L. Orts
Laura Giambiagi *Editors*

Growth of the Southern Andes

Springer

Springer Earth System Sciences

Series editors

Philippe Blondel, Bath, UK
Eric Guilyardi, Paris, France
Jorge Rabassa, Ushuaia, Argentina
Clive Horwood, Chichester, UK

orlando_a_p@yahoo.com.ar

More information about this series at http://www.springer.com/series/10178

orlando_a_p@yahoo.com.ar

Andrés Folguera · Maximiliano Naipauer
Lucía Sagripanti · Matías C. Ghiglione
Darío L. Orts · Laura Giambiagi
Editors

Growth of the Southern Andes

Springer

orlando_a_p@yahoo.com.ar

Editors
Andrés Folguera
Departamento de Ciencias Geológicas,
Facultad de Ciencias Exactas y Naturales
Instituto de Estudios Andinos "Don Pablo
Groeber" UBA-CONICET
Buenos Aires
Argentina

Maximiliano Naipauer
Departamento de Ciencias Geológicas,
Facultad de Ciencias Exactas y Naturales
Instituto de Estudios Andinos "Don Pablo
Groeber" UBA-CONICET
Buenos Aires
Argentina

Lucía Sagripanti
Departamento de Ciencias Geológicas,
Facultad de Ciencias Exactas y Naturales
Instituto de Estudios Andinos "Don Pablo
Groeber" UBA-CONICET
Buenos Aires
Argentina

Matías C. Ghiglione
Departamento de Ciencias Geológicas,
Facultad de Ciencias Exactas y Naturales
Instituto de Estudios Andinos "Don Pablo
Groeber" UBA-CONICET
Buenos Aires
Argentina

Darío L. Orts
Instituto de Investigación en Paleobiología
y Geología, Universidad Nacional
de Río Negro—CONICET
General Roca (Río Negro)
Argentina

Laura Giambiagi
Centro Regional de Investigaciones
Científicas y Tecnológicas
IANIGLA, CCT Mendoza
Mendoza
Argentina

ISSN 2197-9596 ISSN 2197-960X (electronic)
Springer Earth System Sciences
ISBN 978-3-319-23059-7 ISBN 978-3-319-23060-3 (eBook)
DOI 10.1007/978-3-319-23060-3

Library of Congress Control Number: 2015954348

Springer Cham Heidelberg New York Dordrecht London
© Springer International Publishing Switzerland 2016
This work is subject to copyright. All rights are reserved by the Publisher, whether the whole or part of the material is concerned, specifically the rights of translation, reprinting, reuse of illustrations, recitation, broadcasting, reproduction on microfilms or in any other physical way, and transmission or information storage and retrieval, electronic adaptation, computer software, or by similar or dissimilar methodology now known or hereafter developed.
The use of general descriptive names, registered names, trademarks, service marks, etc. in this publication does not imply, even in the absence of a specific statement, that such names are exempt from the relevant protective laws and regulations and therefore free for general use.
The publisher, the authors and the editors are safe to assume that the advice and information in this book are believed to be true and accurate at the date of publication. Neither the publisher nor the authors or the editors give a warranty, express or implied, with respect to the material contained herein or for any errors or omissions that may have been made.

Printed on acid-free paper

Springer International Publishing AG Switzerland is part of Springer Science+Business Media (www.springer.com)

orlando_a_p@yahoo.com.ar

Contents

An Introduction to the Southern Andes (33–50°S): Book Structure 1
Andrés Folguera, Maximiliano Naipauer, Lucía Sagripanti, Matías C. Ghiglione, Darío L. Orts and Laura Giambiagi

Density and Thermal Structure of the Southern Andes and Adjacent Foreland from 32° to 55°S Using Earth Gravity Field Models 9
Orlando Álvarez, Federico Lince Klinger, Mario Gimenez, Francisco Ruiz and Patricia Martinez

Changes in Source Areas at Neuquén Basin: Mesozoic Evolution and Tectonic Setting Based on U–Pb Ages on Zircons 33
Maximiliano Naipauer and Victor A. Ramos

Cenozoic Orogenic Evolution of the Southern Central Andes (32–36°S) 63
Laura Giambiagi, José Mescua, Florencia Bechis, Gregory Hoke, Julieta Suriano, Silvana Spagnotto, Stella Maris Moreiras, Ana Lossada, Manuela Mazzitelli, Rafael Toural Dapoza, Alicia Folguera, Diego Mardonez and Diego Sebastián Pagano

The Transitional Zone Between the Southern Central and Northern Patagonian Andes (36–39°S) 99
Emilio Agustín Rojas Vera, Darío L. Orts, Andrés Folguera, Gonzalo Zamora Valcarce, Germán Bottesi, Lucas Fennell, Francisco Chiachiarelli and Víctor A. Ramos

Progression of the Deformation in the Southern Central Andes (37°S) 115
Lucía Sagripanti, Andrés Folguera, Lucas Fennell, Emilio Agustín Rojas Vera and Victor A. Ramos

orlando_a_p@yahoo.com.ar

Tectonic Evolution of the Northern Patagonian Andes (40°S) 133
Miguel E. Ramos, Andrés Folguera, Lucas Fennell, Mario Giménez and Victor A. Ramos

Cenozoic Deformational Processes in the North Patagonian Andes Between 40° and 43°S 147
Darío L. Orts, Andrés Folguera, Mario Gimenez, Francisco Ruiz, Alfonso Encinas, Emilio Agustín Rojas Vera and Federico Lince Klinger

The North Patagonian Orogen: Meso-Cenozoic Evolution from the Andes to the Foreland Area 173
Guido Gianni, Andrés Folguera, César Navarrete, Alfonso Encinas and Andrés Echaurren

Growth of the Southern Patagonian Andes (46–53°S) and Their Relation to Subduction Processes 201
Matías C. Ghiglione, Victor A. Ramos, José Cuitiño and Vanesa Barberón

Orogenic Growth of the Fuegian Andes (52–56°) and Their Relation to Tectonics of the Scotia Arc 241
Matías C. Ghiglione

Index 269

orlando_a_p@yahoo.com.ar

Contributors

Orlando Álvarez Instituto Geofísico y Sismológico Ing. Volponi, Universidad Nacional de San Juan, San Juan, Argentina; Consejo Nacional de Investigaciones Cientifícas y Técnicas (CONICET), Buenos Aires, Argentina

Vanesa Barberón Departamento de Ciencias Geológicas, Facultad de Ciencias Exactas y Naturales, Instituto de Estudios Andinos "Don Pablo Groeber" UBA-CONICET, Buenos Aires, Argentina

Florencia Bechis IIDyPCa, CONICET, Universidad Nacional de Río Negro, San Carlos de Bariloche, Argentina

Germán Bottesi Gerencia de desarrollo de no convencionales, YPF S.A., Capital Federal, Argentina

Francisco Chiachiarelli Desarrollo, YPF S.A., Neuquén, Argentina

José Cuitiño Departamento de Ciencias Geológicas, Facultad de Ciencias Exactas y Naturales, Instituto de Geociencias Básicas, Aplicadas y Ambientales (IGEBA) UBA-CONICET, Buenos Aires, Argentina

Rafael Toural Dapoza Centro Regional de Investigaciones Científicas y Tecnológicas, IANIGLA, CCT Mendoza, Mendoza, Argentina

Andrés Echaurren Departamento de Ciencias Geológicas, Facultad de Ciencias Exactas y Naturales, Instituto de Estudios Andinos "Don Pablo Groeber" UBA-CONICET, Buenos Aires, Argentina

Alfonso Encinas Departamento de Ciencias de la Tierra, Universidad de Concepción, Concepción, Chile

Lucas Fennell Departamento de Ciencias Geológicas, Facultad de Ciencias Exactas y Naturales, Instituto de Estudios Andinos "Don Pablo Groeber" UBA-CONICET, Buenos Aires, Argentina

Alicia Folguera SEGEMAR, Buenos Aires, Argentina

orlando_a_p@yahoo.com.ar

Andrés Folguera Departamento de Ciencias Geológicas, Facultad de Ciencias Exactas y Naturales, Instituto de Estudios Andinos “Don Pablo Groeber” UBA-CONICET, Buenos Aires, Argentina

Matías C. Ghiglione Departamento de Ciencias Geológicas, Facultad de Ciencias Exactas y Naturales, Instituto de Estudios Andinos “Don Pablo Groeber” UBA-CONICET, Buenos Aires, Argentina

Laura Giambiagi Centro Regional de Investigaciones Científicas y Tecnológicas, IANIGLA, CCT Mendoza, Mendoza, Argentina

Guido Gianni Departamento de Ciencias Geológicas, Facultad de Ciencias Exactas y Naturales, Instituto de Estudios Andinos “Don Pablo Groeber” UBA-CONICET, Buenos Aires, Argentina

Mario Gimenez Instituto Geofísico y Sismológico Ing. Volponi, Universidad Nacional de San Juan, San Juan, Argentina; Consejo Nacional de Investigaciones Cientifícas y Técnicas (CONICET), Buenos Aires, Argentina

Gregory Hoke Department of Earth Sciences, Syracuse University, Syracuse, NY, USA

Federico Lince Klinger Instituto Geofísico y Sismológico Ing. Volponi, Universidad Nacional de San Juan, San Juan, Argentina; Consejo Nacional de Investigaciones Cientifícas y Técnicas (CONICET), Buenos Aires, Argentina

Ana Lossada Centro Regional de Investigaciones Científicas y Tecnológicas, IANIGLA, CCT Mendoza, Mendoza, Argentina

Diego Mardonez CONICET, Universidad Nacional de San Luis, San Luis, Argentina

Patricia Martinez Instituto Geofísico y Sismológico Ing. Volponi, Universidad Nacional de San Juan, San Juan, Argentina; Consejo Nacional de Investigaciones Cientifícas y Técnicas (CONICET), Buenos Aires, Argentina

Manuela Mazzitelli CONICET, Universidad Nacional de San Luis, San Luis, Argentina

José Mescua Centro Regional de Investigaciones Científicas y Tecnológicas, IANIGLA, CCT Mendoza, Mendoza, Argentina

Stella Maris Moreiras Centro Regional de Investigaciones Científicas y Tecnológicas, IANIGLA, CCT Mendoza, Mendoza, Argentina

Maximiliano Naipauer Departamento de Ciencias Geológicas, Facultad de Ciencias Exactas y Naturales, Instituto de Estudios Andinos “Don Pablo Groeber” UBA-CONICET, Buenos Aires, Argentina

César Navarrete Departamento de Geología, F.C.N., Universidad Nacional de la Patagonia “San Juan Bosco”, YPF, Santo Domingo, Argentina

orlando_a_p@yahoo.com.ar

Darío L. Orts Instituto de Investigación en Paleobiología y Geología, Universidad Nacional de Río Negro—CONICET, General Roca (Río Negro), Argentina

Diego Sebastián Pagano CONICET, Universidad Nacional de San Luis, San Luis, Argentina

Miguel E. Ramos Departamento de Ciencias Geológicas, Facultad de Ciencias Exactas y Naturales, Instituto de Estudios Andinos "Don Pablo Groeber" UBA-CONICET, Buenos Aires, Argentina

Victor A. Ramos Departamento de Ciencias Geológicas, Facultad de Ciencias Exactas y Naturales, Instituto de Estudios Andinos "Don Pablo Groeber" UBA-CONICET, Buenos Aires, Argentina

Emilio Agustín Rojas Vera Departamento de Ciencias Geológicas, Facultad de Ciencias Exactas y Naturales, Instituto de Estudios Andinos "Don Pablo Groeber" UBA-CONICET, Buenos Aires, Argentina

Francisco Ruiz Instituto Geofísico y Sismológico Ing. Volponi, Universidad Nacional de San Juan, San Juan, Argentina

Lucía Sagripanti Departamento de Ciencias Geológicas, Facultad de Ciencias Exactas y Naturales, Instituto de Estudios Andinos "Don Pablo Groeber" UBA-CONICET, Buenos Aires, Argentina

Silvana Spagnotto Departamento de Física, Universidad Nacional de San Luis, San Luis, Argentina

Julieta Suriano Departamento de Ciencias Geológicas, Facultad de Ciencias Exactas y Naturales, Instituto de Geociencias Básicas, Aplicadas y Ambientales (IGEBA) UBA-CONICET, Buenos Aires, Argentina

Gonzalo Zamora Valcarce Complex Tectonics, Repsol S.A, Houston, TX, USA

orlando_a_p@yahoo.com.ar

An Introduction to the Southern Andes (33–50°S): Book Structure

Andrés Folguera, Maximiliano Naipauer, Lucía Sagripanti, Matías C. Ghiglione, Darío L. Orts and Laura Giambiagi

1 Introduction

This book intends to constitute a useful tool to access to data and a general discussion about the mechanisms that have been associated with the development of the Southern Andes. It is mainly conceived for Earth Science professionals working in academia and industry, as well as Ph.D and Ms students and interested readers in general.

This book is structured through a total number of 11 chapters, where the initial three are focused on general aspects such as crustal density structure and main source areas of the sedimentary basins that characterize the Southern Andes through time, while the other eight analyze the structure and evolution of particular

A. Folguera (✉) · M. Naipauer · L. Sagripanti · M.C. Ghiglione
Departamento de Ciencias Geológicas, Facultad de Ciencias Exactas y Naturales, Instituto de Estudios Andinos "Don Pablo Groeber" UBA-CONICET, Buenos Aires, Argentina
e-mail: andresfolguera2@yahoo.com.ar

M. Naipauer
e-mail: maxinaipauer@gl.fcen.uba.ar

L. Sagripanti
e-mail: lusagripanti@gmail.com

M.C. Ghiglione
e-mail: mcghiglione@gmail.com

D.L. Orts
Instituto de Investigación en Paleobiología y Geología, Universidad Nacional de Río Negro—CONICET, General Roca (Río Negro), Argentina
e-mail: dlorts@yahoo.com

L. Giambiagi
Centro Regional de Investigaciones Científicas y Tecnológicas, IANIGLA, CCT Mendoza, Mendoza, Argentina
e-mail: lgiambia@mendoza-conicet.gob.ar

© Springer International Publishing Switzerland 2016

A. Folguera et al. (eds.), *Growth of the Southern Andes*,
Springer Earth System Sciences, DOI 10.1007/978-3-319-23060-3_1

orlando_a_p@yahoo.com.ar

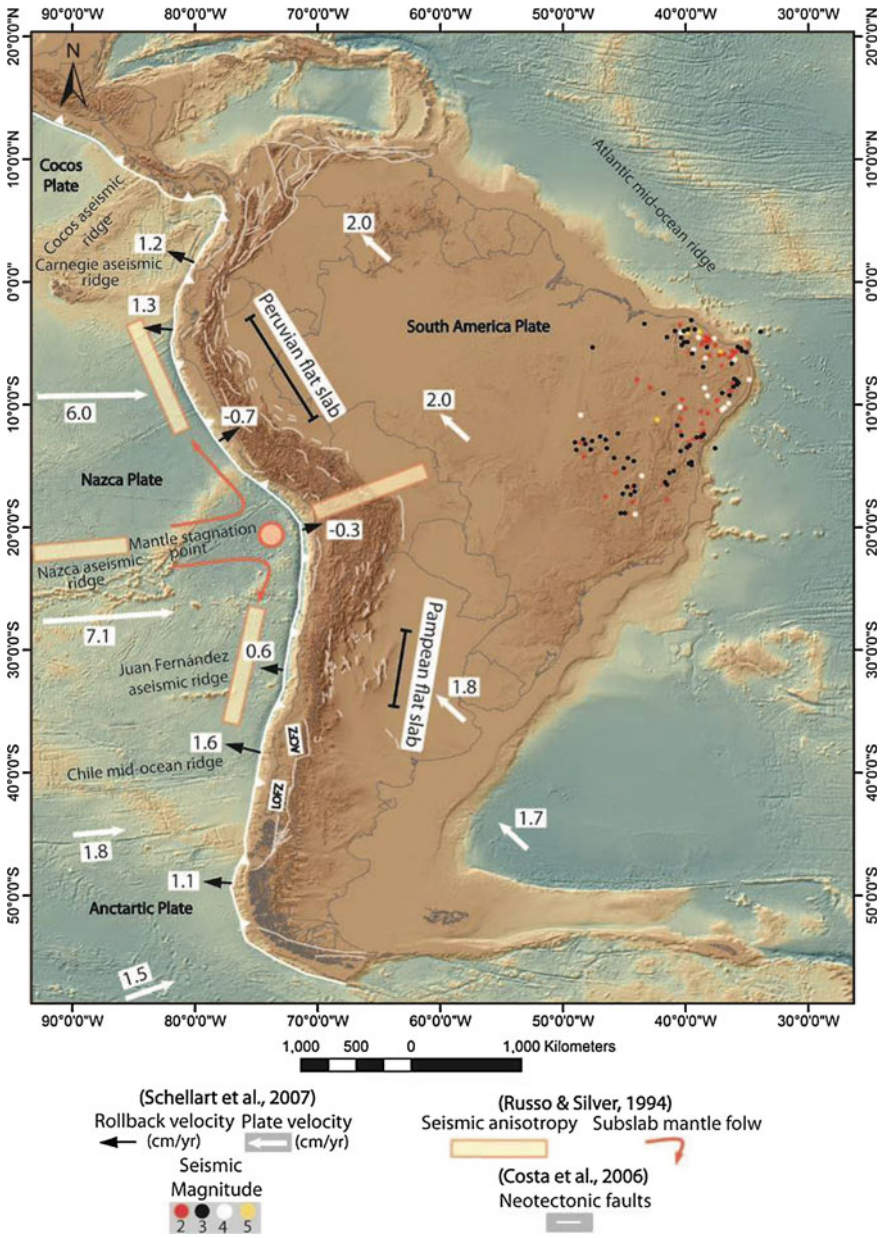


Fig. 1 The Andes, considered the product of subduction of a series of Pacific plates, have a peculiar symmetrical geometry that has been noted and analyzed in different studies. This is characterized by (i) a central plateau bordered by sub-Andean systems, (ii) north and south of it two flat slabs where deformation progressed into the foreland area as thick-skinned broad domains, (iii) two sectors north and south respectively characterized by lower elevations and narrower amplitudes and finally (iv) two transform plate boundaries that separate the South American Plate from two smaller plates. This work is focused in the area located south of the southern flat slab non formally denominated Southern Andes

orlando_a_p@yahoo.com.ar

mountain sectors ordered from north to south. The book contains maps, schemes and cross sections that constitute up-to-date proposals that use previous and new datasets. Different sources are cited at the end of each chapter that can be used to expand particular points discussed in the book.

The segment that is being analyzed in this book develops south of the Pampean flat subduction zone, one of the three flat subduction zones that affect western South America and one of the largest in the world (Fig. 1). We are referring to this segment with a non-formal denomination that is "Southern Andes" that comprises the sectors comprehended south of the Pampean flat subduction zone up to the southernmost tip of the continent (Fig. 1). This segment shows a marked fall in topography from the southern flat slab zone to the south as well as a reduction in amplitude and orogenic shortenings (Fig. 1). Schellart et al. (2007) have proposed a coherent frame to explain these morphostructural differences of the Andes along strike. The central part of the Andes coincides with the Arica bending and the broadest part of the mountain system (Fig. 1). This is explained by a stagnant asthenospheric zone produced between two divergent mantle flows west of the subduction zone of the Cocos, Nazca and Antarctic plates, revealed by mantle anisotropic studies (Russo and Silver 1994). This stagnant point would have determined a nearly stationary trench through time that is not able to retreat such as the two slab edges of the Andean subduction system, where parallel to the trench asthenospheric flows do not impede slab retreat (Fig. 1) (Schellart et al. 2007). According to Schellart et al. (2007), long subduction zones do not facilitate, and at a certain point difficult, interchange between asthenospheric compartments that are comprehended below and above the subducted slab, a process that usually occurs at subducted slab edges during slab retreat. This explains why westward displacement of the South American Plate that is imposed by the ridge push forces associated with the Atlantic Ridge is absorbed at the Arica bending latitudes as permanent deformation in the Subandean region flanking the Altiplano, and at a certain extent in the Bazilian coast as passive margin mountains (Fig. 1).

This book concentrates in the southern half of this system along a segment characterized by an important topographic gradient (Fig. 1). This constitutes a long term analysis trying to conceal and compare present morphology and acting processes with the initial stages of Andean development.

2 The Andean Segmentation

Several proposals for the Andean segmentation that attend different geological evolutions, magmatism, structure, subduction geometry and topography have been proposed, which differ substantially from each other (Fig. 2). The first classification of the Andes using plate tectonics criteria was proposed by Gansser (1973) who differentiated Northern, Central, and Southern Andes (Fig. 2a). According to this classification, the Northern Andes are developed between 10°N and 4°S, from their confluence with the Caribbean Andes to the point of inception of the Carnegie ridge

orlando_a_p@yahoo.com.ar

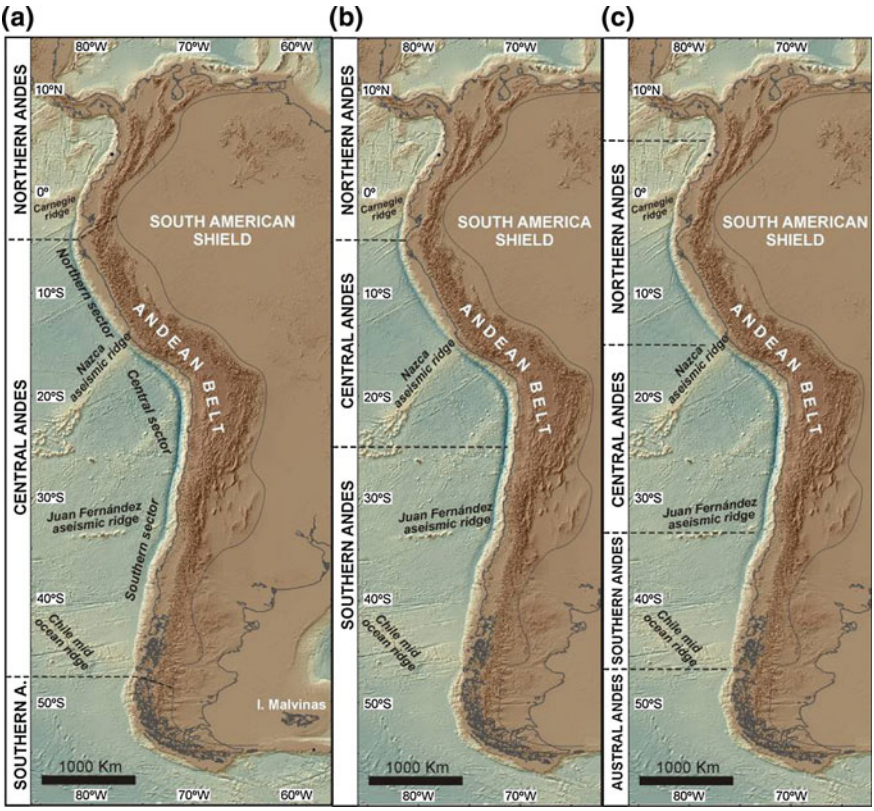


Fig. 2 Different Andean segmentation proposals according to: **a** Gansser (1973) and Ramos (1999) (*to the left*); **b** Auboin (1973) and Auboin et al. (1973) (*middle part*); **c** Tassara and Yáñez (2003) (*to the right*)

into the trench. These Andes are formed by a complex collage of different kinds of oceanic terranes mainly formed at the Galápagos hot spot that were incorporated into the accretionary wedge producing rapid expansion of the continental margin, deformation and metamorphism (see Ramos 2009 for a synthesis). The Central Andes to the south lie between 4°S and 46°30′S, between the Guayaquil Gulf and the Chile mid ocean ridge. The most striking characteristic of this long segment is that it has not experienced ocean crust accretions in Mesozoic and Cenozoic times, with a basement consolidated early since the Late Proterozoic and Early Paleozoic. Then no Mesozoic to Cenozoic metamorphic processes have affected the margin associated with collision of continental and oceanic fragments, with an evolution mainly linked to a subduction system (see Ramos 2009). The Southern Andes between 46°30′S and 52°S is again considered an accretionary orogen with the presence of metamorphic and oceanic rocks of Mesozoic age (Fig. 2a) (Gansser 1973). Ramos (1999, 2009, 2010; among others), following the classical segmentation of Gansser (1973),

orlando_a_p@yahoo.com.ar

introduced a subdivision of the Central Andes, mainly attending to changes in the Wadati-Benioff geometry, that comprehended northern (4°S–14°S), central (14°S–27°S), and southern sectors (27°S–46°30′S) (Fig. 2a).

Auboin (1973) divided the Andes in Northern, Central, and Southern (Fig. 2b). Even though this subdivision is based on geological features and paleogeography, topography, and involved orogenic cycles, it is contextualized in the geosynclinal model, reason by which this classification is presently discarded (Auboin et al. 1973).

Recently Tassara and Yáñez (2003) proposed a new subdivision, based on topography and factors inherent to the continental crust. Unlike the other two proposals, these authors divided the Andes in four segments: northern (5°N–15°S), central (15°S–33°30′S), southern (33°30′S–47°S), and austral (47°S–57°S) (Fig. 2c).

We use the informal name of "Southern Andes" for the segment south of 33°S that is the case study of this book, roughly equivalent to the Southern and Austral segments of Tassara and Yáñez (2003). This segment overlaps the southern sector of the Central and Southern Andes in terms of Gansser (1973) and Ramos (1999).

3 Morphostructural Provinces

The morphostructural Provinces in which the Andes of Chile and Argentina are usually divided are shown in Fig. 3 (Mpodozis and Ramos 1989; Tassara and Yáñez 2003). South of 33–34°S, the Andes experiment a major change in morphology derived from the transition from a flat slab to a normal subduction segment. Consequently a broad mountain system converges in a narrower and lower system to the south formed from west to east by a Costal Cordillera corresponding to a Paleozoic block composed of metamorphic and magmatic rocks, a Central Valley mainly formed by Cenozoic to Quaternary depocenters, a Main Cordillera at the Chilean-Argentinian boundary where Mesozoic to Cenozoic strata are deformed, a Frontal Cordillera corresponding to a thick-skinned basement block and at the extran-Andean zone the San Rafael block with a surficial geology equivalent to the Frontal Cordillera. South of 39°S, the Patagonian Cordillera is cored by a Mesozoic batholith and at its northern section is associated with the Precordillera Patagónica where Paleozoic to Mesozoic rocks are exposed in the foreland area.

4 Structure of the Book

The second chapter analyzes from 30 to 55°S gravity and magnetic fields with the aim of understanding density and thermal structure of the Southern Andes and adjacent foreland region, working as an introductory chapter.

The third chapter analyzes the general U–Pb ages of the detrital components of the main sedimentary sections exposed through the different Andean segments. Thus, varying provenance sources through time are discussed, as well as Andean

orlando_a_p@yahoo.com.ar

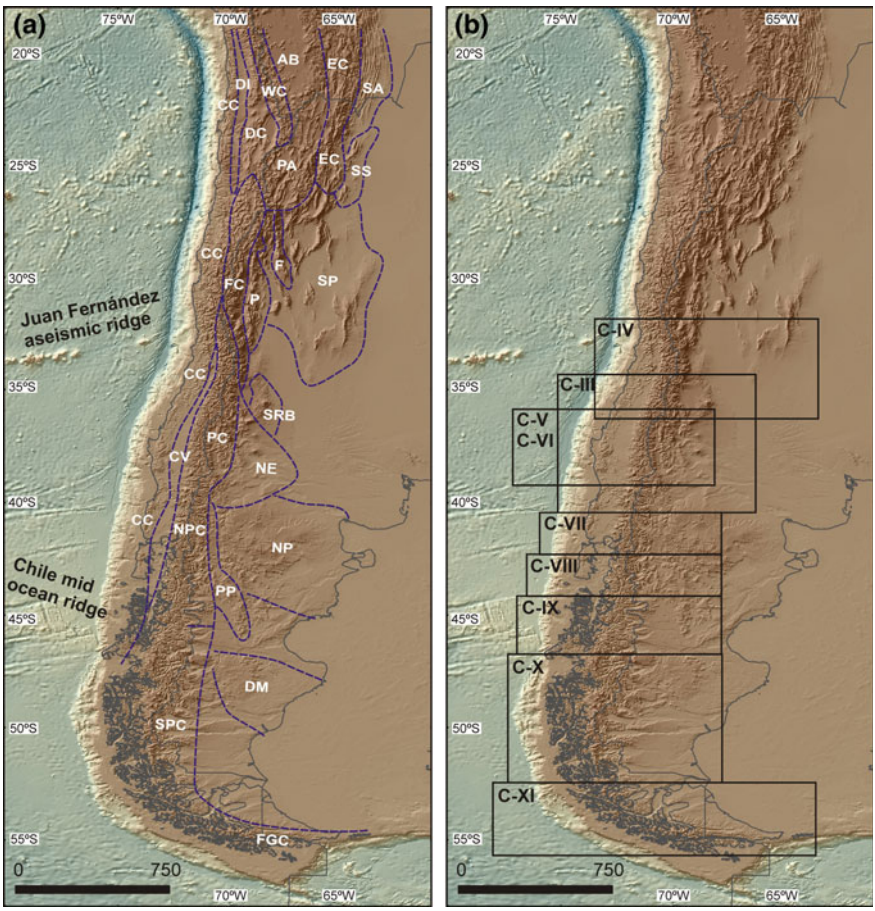


Fig. 3 *To the left* Main morphostructural provinces in which the Southern Andes are divided. *CC* Cordillera de la Costa, *DI* Depresión Intermedia, *DC* Cordillera de Domeyko, *WC* Cordillera Occidental; *PA* Puna; *AB* Altiplano Boliviano; *EC* Cordillera Oriental; *SA* Sierras Subandinas; *SS* Sistema de Santa Bárbara; *FC* Cordillera Frontal; *P* Precordillera; *F* Sistema de Famatina; *SP* Sierras Pampeanas; *CV* Valle Central; *PC* Cordillera Principal; *NE* Engolfamiento Neuquino; *SRB* Bloque de San Rafael; *NPC* Cordillera Norpatagónica; *PP* Precordillera Patagónica; *NP* Macizo Norpatagónico; *SPC* Cordillera Surpatagónica; *DM* Macizo del Deseado; *FGC* Cordillera Fueguina (based on Mpodozis and Ramos 1989; Tassara and Yáñez 2003). *To the right* Book structure (*empty rectangles* indicate areas analyzed in each chapter. The two initial chapters are focused in a regional perspective while the following eight analyze particular sectors of the Andes)

initiation uplift and exhumation based on changes on detrital compositions on the main sedimentary sections.

The fourth chapter is focused south of the present Pampean flat subduction segment, where a dramatic fall in altitude and amplitude in the Andean orogen is produced. Here, main growth stages as well as extensional periods interrupting Andean orogenesis are summarized.

orlando_a_p@yahoo.com.ar

The fifth chapter analyzes the structure and evolution of the area where the deepest and broadest part of the Neuquén embayment is incorporated into the orogenic wedge. The sixth chapter complements this through a detailed description of the development of the fold and thrust belt at 37°S, showing a complex evolutionary pattern that attends cycles of arc expansion and retraction.

The seventh chapter analyzes the segment at 39°S where the sag facies of the Neuquén embayment thin and consequently the structure changes to a narrow thick skinned system with a limited development to the foreland zone.

The eighth chapter focuses on the Cenozoic development of the Andes of North Patagonia and its relation to magmatic evolution, while the ninth chapter explores previous orogenic stages during the Late Cretaceous that show the cyclical character of the deformation.

The tenth chapter constitutes a review about the evolution and structure of the Southern Patagonian Andes and finally the eleventh chapter focuses on the Fueguian Andes at southernmost South America.

Acknowledgements The authors acknowledge Jorge Rabassa for the opportunity to show their research through this book.

References

Auboin JA (1973) Présentation de la Cordillère des Andes. Rev Géogr Phys Géol Dynam 15:5–10

Auboin JA, Borrello AV, Cecione G, Charrier R, Chotin P, Frutos J, Thiele R, Vicente JC (1973) Esquisse paleogeographique et structurale des Andes meridionales. Rev Géogr Phys Géol Dynam 15:11–71

Costa CH, Audemard MFA, Bezerra FHR, Lavenu A, Machette MN, París G (2006) An overview of the main Quaternary deformation of South America. Rev Asoc Geol Argentina 61:461–479

Gansser A (1973) Facts and theories on the Andes. J Geol Soc London 129:93–131

Mpodozis C, Ramos VA (1989) The Andes of Chile and Argentina. In: Ericksen GE, Cañas MT, Reinemud JA (eds) Geology of the Andes and Its Relation to Hydrocarbon and Mineral Resources Circumpacific Council for Energy and Mineral Resources, 11. Earth Science Series 59–90

Ramos VA (1999) Plate tectonic setting of the Andean Cordillera. Episodes 22(3):183–190

Ramos VA (2009) Anatomy and global context of the Andes: main geologic features and the Andean orogenic cycle. In: Kay SM, Ramos VA, Dickinson W (eds) Backbone of the Americas: Shallow Subduction, Plateau Uplift, and Ridge and Terrane Collision. Geological Society of America, Boulder, Memoir 204:31–65

Ramos VA (2010) The tectonic regime along the Andes: Present-day and Mesozoic regimes. Geol J 45:2–25

Russo RM, Silver PG (1994) Trench-parallel flow beneath the Nazca plate from seismic anisotropy. Science 263:1105–1111

Schellart WP, Freeman J, Stegman DR, Moresi L, May D (2007) Evolution and diversity of subduction zones controlled by slab width. Nature 446:308–311

Tassara A, Yáñez G (2003) Relación entre el espesor elástico de la litósfera y la segmentación tectónica del margen andino (15–47°S). Rev Geol de Chile 30(2):159–186

orlando_a_p@yahoo.com.ar

Density and Thermal Structure of the Southern Andes and Adjacent Foreland from 32° to 55°S Using Earth Gravity Field Models

Orlando Álvarez, Federico Lince Klinger, Mario Gimenez, Francisco Ruiz and Patricia Martinez

Abstract GOCE satellite data and EGM2008 model are used to calculate the gravity anomaly and the vertical gravity gradient, both corrected by the topographic effect, in order to delineate main tectonic features related to density variations. In particular, using the Bouguer anomaly from GOCE, we calculated the crust–mantle discontinuity obtaining elastic thicknesses in the frame of the isostatic lithospheric flexure model applying the convolution method approach. Results show substantial variations in the density, compositional and thermal structure, and isostatic and flexural behavior of the continental lithosphere along the Southern Andes and adjacent foreland region.

Keywords GOCE · EGM2008 · Isostasy · Density · Andes

1 Introduction

The study of the lithospheric structure related to density variations using gravimetric data has been improved in the past two decades. Since the early Earth gravity field models recovered from satellite orbit perturbation analysis to the last missions, specially designed for gravity information recovery such as GRACE (Gravity Recovery and Climatic Experiment) and GOCE (Gravity Field and Steady State Ocean Circulation Explorer), considerable improvements have been obtained. These satellite missions provide Earth gravity field models with increasing precision, resolution, and homogeneous coverage. The combination of data from

O. Álvarez (✉) · F. Lince Klinger · M. Gimenez · F. Ruiz · P. Martinez
Instituto Geofísico y Sismológico Ing. Volponi, Universidad Nacional de San Juan, Ruta 12-Km17, San Juan, Argentina
e-mail: orlando_a_p@yahoo.com.ar

O. Álvarez · F. Lince Klinger · M. Gimenez · P. Martinez
CONICET, Consejo Nacional de Investigaciones Cientifícas y Técnicas, Buenos Aires, Argentina

© Springer International Publishing Switzerland 2016

A. Folguera et al. (eds.), *Growth of the Southern Andes*,
Springer Earth System Sciences, DOI 10.1007/978-3-319-23060-3_2

orlando_a_p@yahoo.com.ar

different satellite missions leads to an excellent performance of both the long and short wavelengths of the gravimetric signal.

In particular, the model GO_CONS_GCF_2_DIR_R5 (Bruinsma et al. 2013) is a satellite-only model, based on a full combination of GOCE-SGG with GRACE and LAGEOS (LAser GEOdynamics Satellite). This model was obtained by the method of the direct approach , and is one of the maximum degree/order from satellite-only data (processing details are presented in Bruinsma et al. 2010; Pail et al. 2011). This allows obtaining a resolution of approximately $\lambda/2 \approx 2\pi R/N_{\max} \approx 66$ km with R being the mean Earth radius and $N_{\max} = 300$ the maximum degree and order of the harmonic expansion (Li 2001; Hofmann-Wellenhof and Moritz 2006; Barthelmes 2009).

Since the gravity field attenuates at high altitudes of satellite orbits, these satellites provide information only on the long wavelength part of the spectrum (Reguzzoni and Sampietro 2010). Thus, a way to improve the Earth gravity field model resolution is to incorporate terrestrial gravity data, as done in different models such as the EGM2008 (Pavlis et al. 2008, 2012) developed up to $N = 2190$ with $\lambda/2 = 9$ km, and EIGEN models from Förste et al. (2012) as EIGEN-6C4, also developed up to $N = 2190$ but including the last GOCE mission data. Despite its higher spatial resolution and global coverage, the disadvantage of these models is their inhomogeneous precision. For well-surveyed regions, where high quality terrestrial mean gravity anomalies are available, such as in North America, Europe, and Australia these models present geoid RMS-differences in the order of 4–6 cm (Yi and Rummel 2014). However, where surface gravity data are poor such as in South America, Africa, South-East Asia, and China regions, the RMS differences span between 20 and 38 cm (Yi and Rummel 2014).

The combined use of both kinds of models allow interpretation of medium-to-high (satellite-only models) and low (integrated models as EGM2008, EIGEN) wavelength anomalies related to crustal inhomogeneities. Nevertheless, a statistical comparison is needed between satellite-only and integrated models in order to estimate the error assessment prior to interpretation and analysis. Satellite only models ensure data quality, since these present homogeneous precision and no errors or sampling biases are present. Köther et al. (2012) explained that combined gravity models (such as EGM2008) can be used for density modeling of relatively smaller features such as shallower crustal structures, while satellite-only models are not appropriate for this purpose due to a lower spatial resolution.

Despite this, the homogeneous precision and regional coverage make them useful for regional studies, allowing interpretation of the gravity potential-derived signals at medium-to-high wavelengths (Braitenberg et al. 2011; Alvarez et al. 2012, 2014, 2015; Mariani et al. 2013; Li et al. 2013; Braitenberg 2014). In the present work, we use the satellite-only model from *GO_CONS_GCF_2_DIR_R5* (Bruinsma et al. 2013) to delineate the density and thermal structure of the Andes and adjacent foreland region from 32° to 55°S. In those regions, where the EGM2008 model (Pavlis et al. 2008, 2012) has an acceptable performance, density anomalies are interpreted as related to medium-to-low wavelengths.

orlando_a_p@yahoo.com.ar

2 Main Morphostructural Units of the Southern Andes

The northern analyzed region is located in the southern part of the Pampean flat slab zone. At these latitudes (32°S–33°S), the Andean structure is composed of a series of mountain ranges that comprises the Main Cordillera , the Frontal Cordillera, the southernmost region of the Precordillera, and the Sierras Pampeanas (Fig. 1; and see Chap. 1). The Frontal Cordillera is formed by a series of basement blocks that exposes Neo-Proterozoic to Paleozoic rocks, constituting the highest part of the fold and thrust belt at these latitudes (Ramos 1999). The Precordillera to the east is formed by thin- and thick-skinned imbricate fans, forming east-verging systems that expose Paleozoic to Triassic sequences, whose basal Laurentia-derived terms (Early Cambrian to Early Ordovician; Cuyania terrane; Fig. 1) were accreted to the Gondwana margin in Late Ordovician times (see Ramos 2004a, for a synthesis).

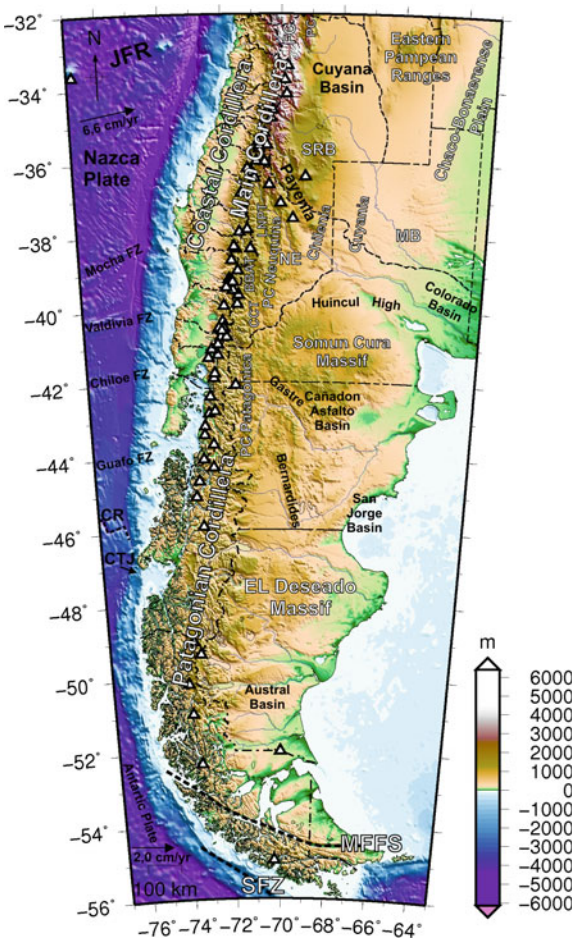


Fig. 1 Main morphostructural units mentioned in this chapter (*FC* Frontal Cordillera, *PC* Precordillera, *SRB* San Rafael Block, *NE* Neuquén Embayment, *MB* Mauidas Block, *LNPT* Loncopué Through, *BBAT* BíoBío Aluminé Through, *CCT* Collón Cura Through, *CR* Chile Rise, *CTJ* Chile Triple Junction). *MFFS* Magallanes Fagnano fault zone, *SFZ* Scotia fault zone. The Chilean–Argentinian border is indicated by a *dot* and *dashed line* and the coastal zone by a *solid black line*

orlando_a_p@yahoo.com.ar

Deformation in the Precordillera responsible for its present morphology occurred in the last 10 Ma, partly synchronous with the rise of the Pampean Ranges to the east in the foreland area (Jordan and Allmendinger 1986; Ramos et al. 2002). The thick-skinned Sierras Pampeanas constitute a set of Laramide-style basement blocks uplifted during the shallowing of the subducted Nazca Plate since late Miocene times (Ramos et al. 2002; Kay and Coira 2009). The NE region of the area under study comprises the Eastern Sierras Pampeanas that expose latest Proterozoic to Cambrian metamorphic rocks intruded by subduction-related to anorogenic magmatic rocks (Ramos 1988; Rapela et al. 1998; Lira et al. 1997). Late Miocene to Quaternary volcanic rocks unconformably overlying the Proterozoic to Paleozoic basement at the foreland area indicate the eastern migration of the volcanic arc during the flattening of the Nazca Plate in the last 17 Ma (Brogioni 1990; Kay and Gordillo 1994).

South of this region (−35°S), the Payenia volcanic zone is characterized by mainly Quaternary extensive volcanic fields, located in the back-arc zone. These young volcanic rocks overly Paleozoic to Cenozoic rocks and more locally, Mesozoic sedimentary sections of the Neuquén embayment. The Neuquén embayment is segmented by basement structures with N-to-NW structures and more locally by the Huincul Ridge, a transverse-to-the Andes regional lineament (see Ramos 1999 and references therein), corresponding to a first order structural feature (Turner and Baldis 1978), interpreted in some works as the extensional reactivation of the northern limit of the Patagonia Paleozoic terrane (Ramos et al. 2004b). North of this, the Mahuidas basement block is constituted by Precambrian metamorphic rocks intruded by Paleozoic plutonic rocks (Linares et al. 1980).

The Patagonian Cordillera to the south, a relatively narrow mountain system compared with the Central Andes to the north, is characterized by a continuous Mesozoic to Cenozoic batholith emplaced along the western slope and axial zone of the Andes, from nearly 39°S to about 52°S (Hervé et al. 2004). A strike-slip crustal structure, the Liquiñe–Ofqui fault zone (LOFZ) (Fig. 1) (Hervé et al. 1996; Cembrano et al. 1996, among others) crosses the axial part of the Northern Patagonian Andes, controlling the emplacement of the volcanic arc corresponding to the Southern Volcanic Zone (see Ramos 2009 and references therein).

Two basement-foreland cores characterize the extra-Andean region, the Somuncura Massif (Windhausen 1931) and the Deseado Massif. The central zone of these foreland Paleozoic cores is partly covered by siliceous Jurassic rocks associated with widespread synextensional volcanic activity during Pangea breakup (Uliana et al. 1985; Alric et al. 1996; Feraud et al. 1999; Ghidella et al. 2002; Ramos 2004b). These foreland cores are flanked by Mesozoic extensional basins such as Cañadón Asfalto, Río Mayo, Austral, and San Jorge Gulf basins (Fig. 1). The Precordillera Patagonica across the Patagonian foreland zone constitutes a feature separated from the Andes to the west that results from the partial inversion of these extensional basins (Ramos 1999).

orlando_a_p@yahoo.com.ar

3 The Topography-Reduced Gravity Anomaly (Ga)

The observed potential is obtained from the Earth gravity field model. The disturbing potential (T) is calculated subtracting the potential field from the reference ellipsoid (WGS84) (Janak and Sprlak 2006). This disturbing potential allows calculation of different derived quantities, related to crustal density heterogeneities. The topography reduced gravity anomaly $(\Delta_{g_{tr}})$ is the difference between the real gravity (g) at a given point (h, λ, ϕ), and the gravity of the reference ellipsoid (γ) at the same coordinates, but at the ellipsoidal height h-ζ_g (where ζ_g is the generalized height anomaly) and without considering the effect of the topographic masses above the geoid (g_t) (Molodensky et al. 1962; Hofmann-Wellenhof and Moritz 2006; Barthelmes 2009). The height h is assumed on or above the Earth surface ($h \geq h_t$). Thus, the measured gravity at the Earth surface can be used for calculation of the gravity anomaly, in the modern definition, without downward continuation or any reduction as it is a function in the space outside the masses (Barthelmes 2009).

$$\Delta_{g_{tr}}(h, \lambda, \phi) = g(h, \lambda, \phi) - g_t(h, \lambda, \phi) - \gamma\left(h - \zeta_g, \lambda, \phi\right) \quad (1)$$

For calculation of the gravity anomalies (Janak and Sprlak 2006), we used the model of GOCE *GO_CONS_GCF_2_DIR_R5* (Bruinsma et al. 2013) up to its maximum degree/order = 300 (Fig. 2), and the EGM2008 (Pavlis et al. 2008, 2012) up to degree/order = 2159 (Fig. 3). For an approximate calculation of the effect of the topographic masses, we used a global relief model which includes ocean bathymetry (ETOPO1, Amante and Eakins 2009) and a mass density distribution hypothesis. We utilized standard densities of 2670 kg/cm^3 for continental crust and a density of 1030 kg/cm^3 for the sea. The topographic effect was calculated at a height of 7000 m to ensure that all values are above the topography and in a spherical coordinate system. The topographic elements were approximated using spherical prisms or Tesseroids (Uieda et al. 2010; Alvarez et al. 2013) taking into account the Earth curvature in order to avoid the error introduced when using a planar approximation (Grombein et al. 2013; Bouman et al. 2013). All calculations were carried out with respect to the system WGS84 on a regular grid of 0.05° grid cell size. These topography corrected gravity anomalies are useful for highlighting the effects of different rock densities into the crust, geological structures and basins.

4 The Topography Corrected Vertical Gravity Gradient (Tzz)

The gravity gradient tensor (Marussi tensor) is obtained as the second derivative of the disturbing potential T (e.g., Hoffman-Wellenhof and Moritz 2006) and is composed of five independent elements. The Marussi tensor components M = T_{ij} can be expressed and solved numerically in a spherical coordinate system

orlando_a_p@yahoo.com.ar

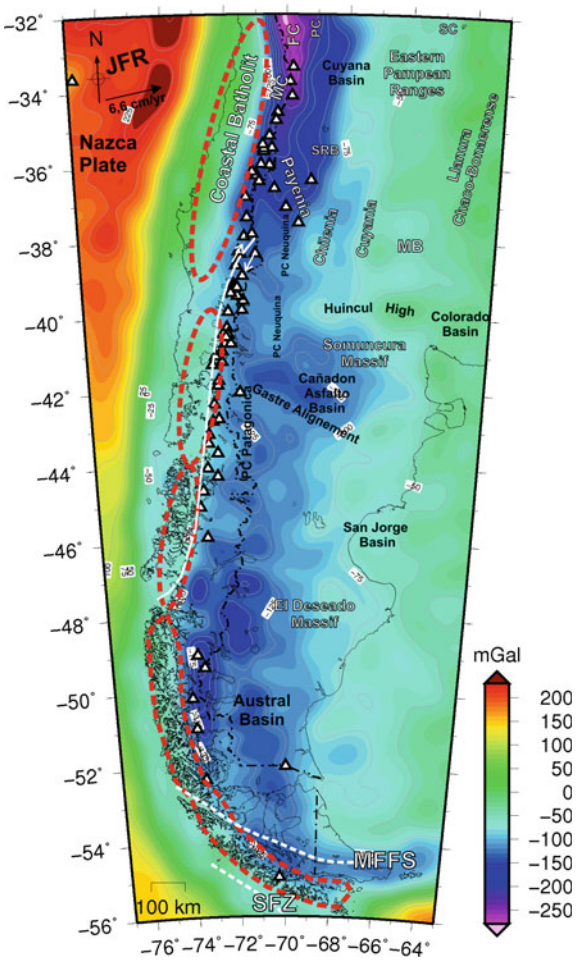


Fig. 2 Gravity anomaly from GOCE model GO_CONS_GCF_2_DIR_R5 (Bruinsma et al. 2013) corrected by the topographic effect (*FC* Frontal Cordillera, *PC* Precordillera, *SC* Sierras de Cordoba, *MC* Main Cordillera, *SRB* San Rafael Block, *MB* Mahuidas Block, and *JFR* Juan Fernandez Ridge). *Thin White dashed line* represents the Liquiñe Ofqui fault zone, *MFFS* Magallanes Fagnano fault zone, *SFZ* Scotia fault zone. The Chilean–Argentinian border is indicated by a *dot* and *dashed line* and the coastal zone by a *solid black line*

(Tscherning 1976; Rummel et al. 2011). The vertical gravity (Tzz) gradient is the second radial derivative of the disturbance potential T.

$$T_{zz} = \frac{\partial^2 T}{\partial r^2} \left[1\text{Eötvös} = 10^{-4} \frac{\text{mGal}}{\text{m}} \right] \tag{2}$$

The vertical gravity gradient highlights superficial density anomalies and allows delineating the location of an anomalous mass with better detail and accuracy than the gravity anomaly itself (Braitenberg et al. 2011). Since the Tzz is a derivative of gravity, the spectral power of gravity gradient signals is pushed to higher frequencies, resulting in a signal more focalized to the source than the gravity anomaly (Li 2001). Therefore Tzz is better for detection of the edge of geological structures and to distinguish the signal due to a smaller superficial density variation from an

orlando_a_p@yahoo.com.ar

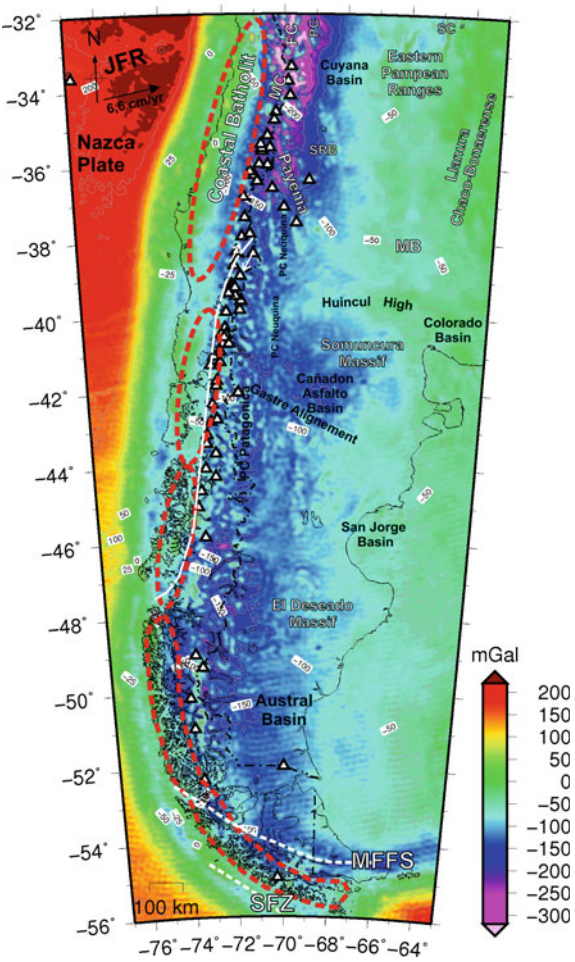


Fig. 3 Gravity anomaly from EGM2008 model (Pavlis et al. 2008, 2012) corrected by the topographic effect

extensive deeper mass, being the *Ga* more sensitive to regional signals and deeper sources (Alvarez et al. 2012). Relative denser bodies are related to a positive gradient value while a negative gradient is related to less dense bodies. Abrupt changes may indicate a high-density contrast between two different lithologies.

We calculated the vertical gravity gradient from GOCE *GO_CONS_GCF_2_DIR_R5* (Bruinsma et al. 2013) in a geocentric spherical coordinate system at the calculation height of 7000 m to ensure that all values were above the topography (Fig. 4) and also for the EGM2008 model (Fig. 5). The values were calculated on a regular grid with a cell size of 0.05°, with the maximum degree and order of the harmonic expansion ($N = 300$, $N = 2159$) for each model. The topographic effect was removed from the fields in order to eliminate the correlation with the topography (Alvarez et al. 2013) as made for the gravity anomaly. The topographic correction amounts up to tens of Eötvös for the *Tzz*, becoming higher over the

orlando_a_p@yahoo.com.ar

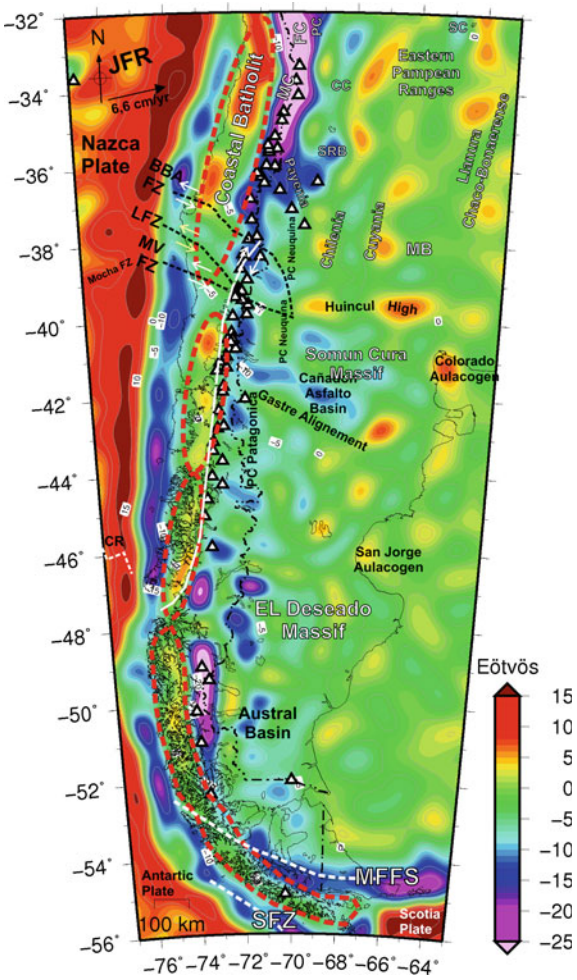


Fig. 4 Vertical gravity gradient from GOCE model GO_CONS_GCF_2_DIR_R5 (Bruinsma et al. 2013) corrected by the topographic effect (*BBAFZ* BioBio Alumine fault zone, *LFZ* Lanalhue fault zone, *MVFZ* Mocha Villarica fault zone, *MFFS* Magallanes Fagnano fault zone, *SFZ* Scotia fault zone)

maximum topographic elevations (e.g., the Main Andes) and lower over the topographic depressions such as the Chilean Trench.

After a statistical analysis and considering the sparseness of terrestrial data in the region under study (Pavlis et al. 2008, 2012), the most reliable areas to apply the EGM2008 model are mainly offshore and forearc regions comprised between 36° and 48°S. Thus, the GOCE model (TIM_R5) becomes more appropriate than the EGM2008 model in the region under study despite its lower resolution (but homogeneous precision). Results obtained by means of the EGM2008 model will only be analyzed and compared to GOCE in the regions of higher performance, in order to solve the different anomalies in greater detail. The combined use of both models, considering their best individual qualities, has been already tested in different studies (Braitenberg et al. 2011; Alvarez et al. 2012, 2014, 2015).

orlando_a_p@yahoo.com.ar

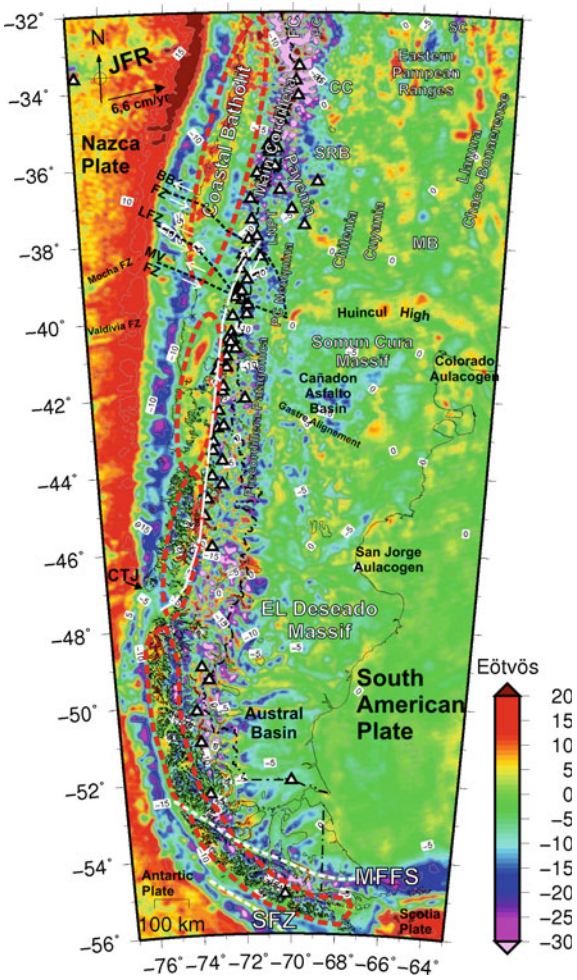


Fig. 5 Vertical gravity gradient from EGM2008 model (Pavlis et al. 2008, 2012) corrected by topographic effect. *CTJ* Chile triple junction

5 Isostatic Modeling

Isostatic theory explains the elastic behavior of the lithosphere, describing the effect of the inhomogeneous distribution of the crustal loads. The Airy model considers that different cortical sections behave in hydrostatic equilibrium, constituting a "topographic load" compensated by a "crustal root"

$$\Delta R = \frac{\sigma}{\sigma_1 - \sigma} h \tag{3}$$

where σ is the crustal density, σ_1 is the mantle density, ΔR: the crustal root or compensation and h is the topography. As this expression indicates, crustal and

orlando_a_p@yahoo.com.ar

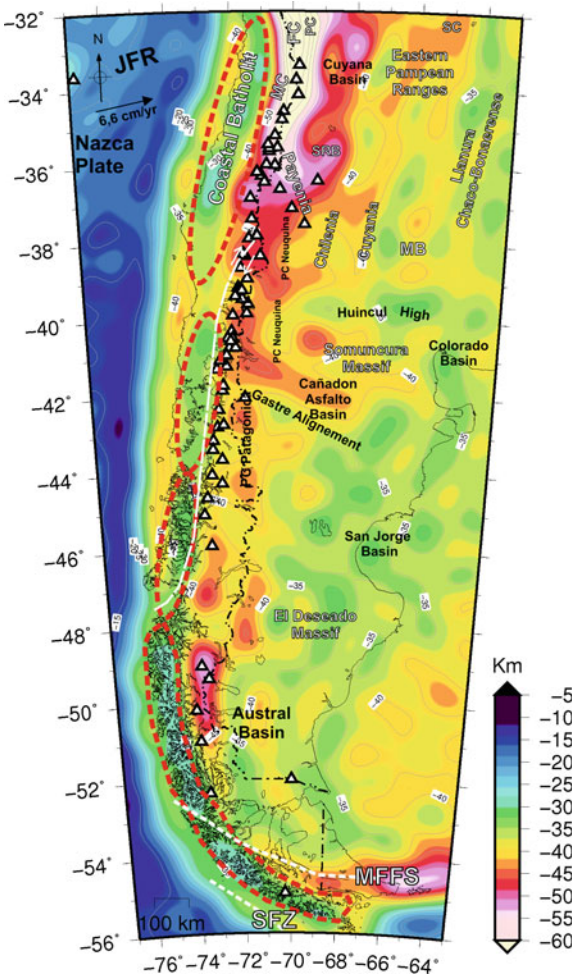


Fig. 6 Moho from GOCE model GO_CONS_GCF_2_DIR_R5 (Bruinsma et al. 2013) obtained from inversion of the Bouguer anomaly

mantle densities remain constant and consequently the depth of compensation varies in function of the topography. For calculation of the Airy response we considered a crust–mantle density contrast of 400 kg/cm^3 and the relief model ETOPO1.

Then, we obtained the depth to the crust–mantle interface (Hydrostatic Moho) by using Eq. (3), taking into account as normal crustal thickness Tn = 35 km. This Moho was then compared (by subtracting) to the crust–mantle interface (Fig. 6) obtained by inversion of the Bouguer anomaly (Fig. 2) calculated from the GOCE model *GO_CONS_GCF_2_DIR_R5* (Bruinsma et al. 2013). Near to zero values of this "residual" Moho (Fig. 7) indicates different regions that are near the isostatic equilibrium or that behave as compensated by a crustal root, while negative values indicate an overcompensation (the crustal root obtained by means of the Bouguer

orlando_a_p@yahoo.com.ar

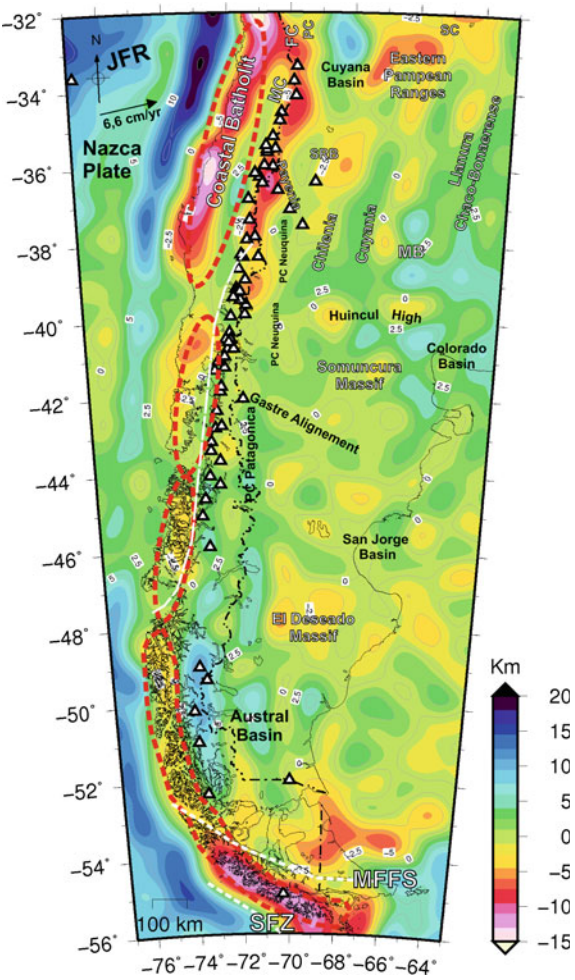


Fig. 7 Residual between the isostatic Moho (Airy) and Moho obtained by inversion of the Bouguer anomaly from GOCE model GO_CONS_GCF_2_DIR_R5 (Bruinsma et al. 2013). Near zero values indicates a hidrostatic balance, while negative values indicate an overcompensation of the crustal root and positive ones the expression of a deficiency in isostatic compensation

anomaly is deeper than the one obtained following the Airy hypothesis), and positive values indicate an undercompensation, i.e., the crustal root is not deep enough to compensate the topographic loads.

6 Effective Elastic Thickness

The compensation of the topographic masses is approximated through the Airy theoretical model that considers a local compensation and the Vening Meinesz model that indicates that the compensation is performed by a regional bending of

orlando_a_p@yahoo.com.ar

the plate, which best describes the mechanical behavior and stress state of a loaded lithosphere (Introcaso 2006).

The thickness and viscosity of the lithosphere, or lithospheric strength, is related to the thermal state, rheological and compositional properties of the crust and is well characterized by the flexural rigidity (Lowry et al. 2000). The last can be interpreted in terms of the elastic thickness (*Te*) by making some assumptions regarding the Young modulus and the Poisson ratio. *Te* defines the maximum size and wavelength of the surface loading that can be supported without an elastic break of the lithosphere. The flexural rigidity *D* can be expressed by:

$$D = T_e^3 \cdot \frac{E}{12(1 - v^2)} \tag{4}$$

where E = 100 GPA = 10^{11} N/m^2 is the Young's modulus, and v = 0.25 is the Poisson's ratio. The isostatic state and deformation of the upper crust are reflected in the spatial distribution of the *Te*, whose variation can be explained by heat flow distribution and a change in the Young modulus. A relation between *Te* and the geometry and composition of the flexured plate, external forces and the thermal structure has been reported by different authors (e.g., Göetze and Evans 1979; Lyon-Caen and Molnar 1983; Burov and Diament 1995; Hackney et al. 2006).

Different methods have been developed for estimation of the elastic thickness, as the flexural coherence analysis, the spectral methods, and the convolution approach (Braitenberg et al. 2002; Wienecke 2006). The last has the advantage of being a method of double entry that calculates the flexure parameters by the best fit of the observed crust–mantle interface obtained by gravity inversion and a crust–mantle interface computed due to a flexure model see Fig. 8 (www.lithoflex.org) (Wienecke 2006; Wienecke et al. 2007; Braitenberg et al. 2007). Isostatic modeling adopts the isostatic thin plate flexure model (e.g., Watts 2001). To estimate the elastic properties of the plate for a known load are needed a crustal load (combination of the overlying topography plus a density model) and the crust–mantle interface to be used as a reference surface (Wienecke 2006).

The topographic load was calculated using topographic/bathymetric data from ETOPO1 (Amante and Eakins 2009). The densities used for calculation were 1030 kg/m^3 for water and 2800 kg/m^3 for the crust. The undulating boundary corresponding to the Moho was calculated by gravity inversion of the Bouguer anomaly field (from GOCE *GO_CONS_GCF_2_DIR_R5*, http://icgem.gfz-potsdam.de/ICGEM/, Bruinsma et al. 2013). This method requires two input parameters, the density contrast (400 kg/m^3) and reference depth or normal crustal thickness (Tn = 35 km) (values between 30 and 40 km have been adopted in numerous works as normal crustal thickness).

The flexural rigidity was inverted in order to match the known loads with the known crustal thickness model (i.e., to model the gravity Moho in terms of an isostatic model). The elastic thickness was allowed varying in the range of 1< *Te* <

orlando_a_p@yahoo.com.ar

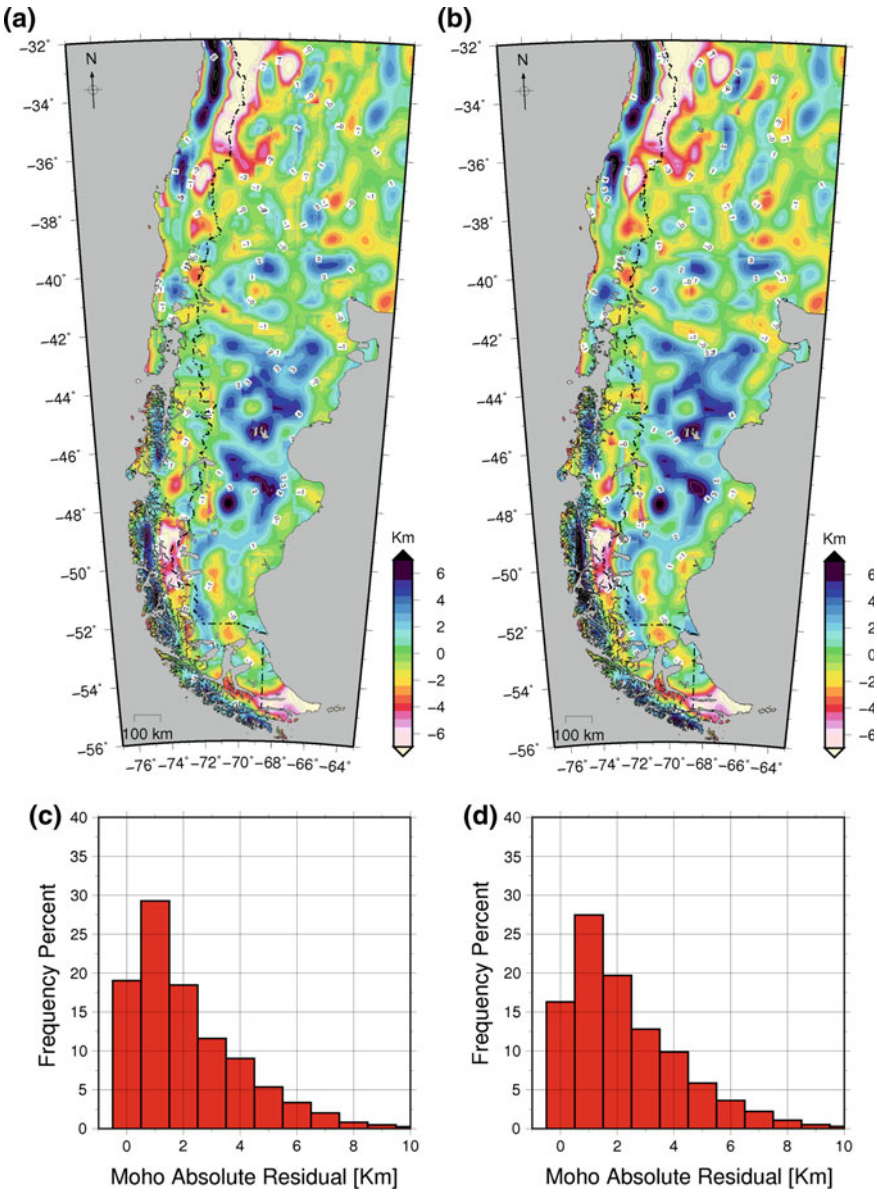


Fig. 8 *Up* Residual obtained by subtracting the crust–mantle interface obtained by gravity inversion of the Bouguer anomaly minus the crust–mantle interface obtained from the flexural model. **a** Window size 80 × 80 km. **b** Window size 120 × 120 km. *Down* Histograms of the residual Moho between the crust–mantle interface obtained by gravity inversion and the crust–mantle interface from the flexural model. More than 80 % of the error is less than 4 km. **c** Window size 80 × 80 km. **d** Window size 120 × 120 km. The residual obtained for the window size of 80 × 80 km shows a slight better fitting

orlando_a_p@yahoo.com.ar

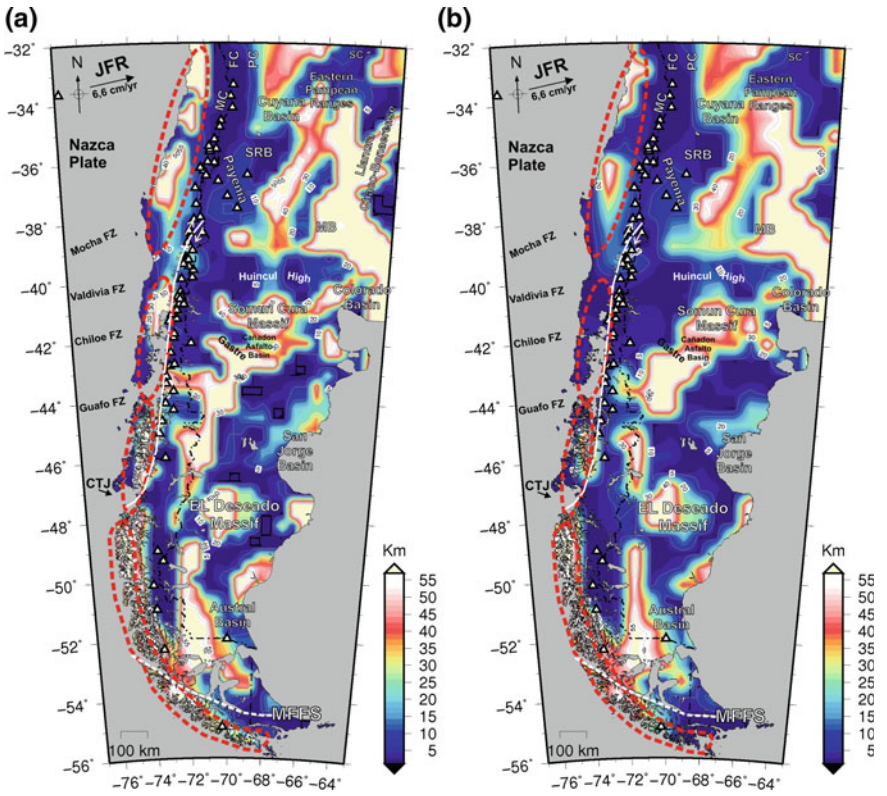


Fig. 9 Effective elastick thickness for the Southern Andes and adjacent foreland region from GOCE model. **a** Window size of 80 × 80 km. **b** Window size of 120 × 120 km

Table 1 Parameters used in the flexural modeling

Masses above sea level	ρ_s	2670 kg/m^3
Upper crustal density	ρ_{uc}	2700 kg/m^3
Lower crustal density	ρ_{lc}	2900 kg/m^3
Mean crustal density	ρ_{mc}	2800 kg/m^3
Upper mantle density	ρ_m	3300 kg/m^3
Young modulus	E	10^{11} N/m^2
Poisson ratio	Σ	0.25

60 km and was iteratively estimated over moving windows of 40 × 40 km size (Fig. 9a) and with 60 × 60 km window size (Fig. 9b). Model parameters (Table 1) and adopted densities are standard values already used by Introcaso et al. (2000); Gimenez et al. (2000, 2009); Alvarez et al. (2015) in the region under study.

orlando_a_p@yahoo.com.ar

7 Results

Low gravity values (less than −250 mGal) north of 38°S along the Andes detected in the *Ga* from GOCE (Fig. 2) and from EGM2008 (Fig. 3) are related to the negative gravimetric response of the Andean roots. Computed Moho depths (Fig. 6) are consistent in the southern section of the Pampean flat subduction zone (32–34°S) with those obtained by Gans et al. (2011), based on receiver functions. Low-gravity anomalies (Figs. 2, 3), a deep Moho (Fig. 6) and low *Te* values (Fig. 9) are a consequence of a flexural model in which the plate has little to no strength. The isostatic residual Moho (Fig. 7) indicates that this region of the Andes is over-compensated along the active arc front, while previous results had indicated that this region was near isostatic balance (Introcaso et al. 1992; Stewart and Watts 1997; Tassara and Yañez 2003; Tassara et al. 2007; Pérez-Gussinyé et al. 2008; Sacek and Ussami 2009).

Seaward of the trench at the latitudes of the Pampean flat subduction zone, the flexural outer rise of the Nazca Plate, is marked by a positive gravity anomaly higher than +200 mGal (Figs. 2, 3) and more than +20 Eötvös (Figs. 4, 5). Particularly, the Juan Fernández Ridge over the Nazca Plate is delineated by a well-defined signal in both *Tzz* and gravity anomaly differentiated from the surrounding sea-floor (Alvarez et al. 2015). The Moho is deeper along the Juan Fernández Ridge indicating an over-thickened oceanic crust beneath the ridge as described by von Huene et al. (1997) based on wide-angle seismic data and by Sandwell and Smith (1997) who related negative satellite-derived gravity anomalies to a crustal root indicative of crustal flexure from loading.

Relative low *Ga* values to the south of 38°S (Fig. 2) reflect the reduction of the Andean roots (Fig. 6) in coincidence with a segment of lower Andean elevations. In particular, between 39° and 48°S the residual Moho indicates a state near isostatic balance (Fig. 7). Contrastingly, south of the inception zone of the Chilean Ridge into the trench along the Southern Patagonian Cordillera, the residual Moho indicates an undercompensation of the Andean root.

Paleozoic sedimentary rocks exposed in the Precordillera region above the Pampean flat subduction zone are identified by a more positive gravimetric signal than the general negative gravimetric response of the Main Andes (Fig. 2). Other works (Introcaso et al. 1992; Gimenez et al. 2000, among others) had also reported, based on terrestrial gravimetric data, a high gravimetric signal for the Precordillera area (see Alvarez et al. 2012, 2014 for a detailed analysis). The Late Triassic Cuyo sedimentary basin located SE of the Precordillera is detected by low gradient values of less than −20 Eötvös and less than −150 mGal. The crust–mantle interface is shallower through the Precordillera region (Fig. 6) and behaves near the isostatic balance (Fig. 7). Higher values of *Te* are detected in this area in relation to the Main Cordillera. The *Tzz* shows a high gradient signal for the Precordillera in both GOCE (Fig. 4) and EGM2008 (Fig. 5). The flat slab region (north of 33°S) presents high-rigidity values most likely delineating the Cuyania Terrane boundaries as described by Alvarez et al. (2015). High *Te* values over flat-slab regions have been

orlando_a_p@yahoo.com.ar

related to low thermal regimes (Stewart and Watts 1997; Tassara 2005; Alvarez et al. 2015). In this sense, Pérez-Gussinyé et al. (2008) considered that flat slabs are characterized by several parameters among which high *Te* values, high shear wave velocities, thick thermal lithospheres, and low heat flows are characteristic, indicating that the continental lithosphere above these settings become cooler and consequently thicker.

East of the Precordilleran region, a broad broken foreland zone is developed associated with the Pampean flat slab, where the Eastern Sierras Pampeanas are uplifted in the eastern border of the Rio de la Plata Craton. These uplifts are represented by Neoproterozoic basement blocks which present low gradient gravity values characteristic of their composition. Gravity data indicate that these mountain ranges are developed over intermediate Moho depths (approx. 40 km), consistent with previous works (Gans et al. 2011). Even shallower Moho depths are calculated beneath the Rio de la Plata Craton to the east. We found intermediate to low *Te* values in the Eastern Sierras Pampeanas with increasing values eastwards to the foreland region; this is consistent with the residual Moho that indicates a regional overcompensation under this zone. Different authors have found that the Eastern Sierras Pampeanas are undercompensated (Introcaso et al. 1992, 2000) for wavelengths in the order of range topography (less than 50 km), based on terrestrial gravity data. This is consistent with the tectonic evolution of these ranges that were uplifted by listric faults as is the case of the Western Sierras Pampeanas (Weidmann et al. 2013).

The Payenia region and the San Rafael block south of the Pampean flat subduction zone present low *Tzz* values, a relatively deep Moho and low rigidity values. In particular, in the Payenia region the isostatic residual Moho is near-to-zero and the *Te* is near 10 km (Fig. 9), contrastingly to the San Rafael Block that is overcompensated, with a lower *Te* (less than 5 km), similarly to the Sierras Pampeanas to the north (at higher wavelength), showing the continuity of the broken foreland zone south of the Pampean flat subduction zone.

South of the Juan Fernández Ridge up to the latitudes of the triple point determined by the Chile Ridge with the trench, the region comprehended between this and the coastline is defined by a negative *Tzz* anomaly, less than −10 Eötvös. This indicates the existence of low-density materials filling the trench and a thinner crust beneath the forearc (Alvarez et al. 2014). Sediment filled slope basins, resting upon thinned continental crust that extends to about 50 km off the trench, had been recognized in free-air gravity maps and in seismic profiles of the southern Chile margin (ANCORP Working Group 2003; Flueh et al. 1998; von Huene et al. 1997). Wells et al. (2003) had found prominent free-air gravity lows following the physiographic slope and basins in areas of high sedimentation rates as in the Southern Chile continental margin. This low-gravity signal is segmented by transform zones over the Nazca plate that segment the Chile Ridge that enter obliquely to the trench. These transform faults are described as highly serpentinized crustal settings by Contreras-Reyes (2008), where oceanic lithosphere is segmented by its different ages and consequently by variable lithospheric thicknesses (Tebbens and Cande 1997).

orlando_a_p@yahoo.com.ar

West of the Main Andes, positive gravimetric values and higher *Tzz* parallel to the coastline are the expression of the Coastal Batholith exhumed along the Coastal Cordillera (Hackney et al. 2006). The residual Moho over this region indicates an overcompensation of the Coastal Batholith adjacent to an undercompensated region along the Central Valley of Chile west of the Main Andes.

At 39°S, a displacement of 100 km between the axis of the Coastal Cordillera Batholith and the Paleozoic Patagonian Batholith is observed. An interruption of the gradient signal in coincidence with this jump coincides with the Bio-Bio Aluminé lineament along the arc and retroarc zones (Garcia Morabito et al. 2003; Rosenau et al. 2006). In this region, the upper plate is segmented in the forearc zone by major fault zones with geneal NW-trends (Sick et al. 2006; Hackney et al. 2006; Krawczyk et al. 2006; Ramos et al. 2011; among others).

Between 39° and 52°S, high *Tzz* values detected along the back-arc zone are related to plutonic rocks of the Patagonian Batholith. Along this Northern region of the Patagonian retroarc, Moho depths are rather constant (Fig. 6) indicating in the residual Moho a certain degree of overcompensation (Fig. 7).

Near the Taitao peninsula, where the Chile Ridge is presently colliding, low *Ga* values (<0 mGal) and less than −10 Eötvös interrupt the high-gravity values characteristic of the Coastal Batholith. South of this low, the alternation of high and lows in the *Tzz* values probably indicates a truncated subduction channel most likely as a consequence of the collision of Chile Ridge against the continental margin in the last 3–6 My (Ranero et al. 2006; Bourgois et al. 1996; Cande and Leslie 1986).

Between 48° and 55°S, the Patagoninan Batholith is expressed by high *Tzz* values that are interrupted at 53°S by the Magallanes–Fagnano fault system (MFFS) which marks the limit between the South American and Scotia plates (Dalziel et al. 1974; Klepeis 1994; Olivero 1998; Lodolo et al. 2003; Ghiglione and Ramos 2005; Ramos 2009). Computed Moho depths (Fig. 6) are shallower in the southernmost region of the Patagonian Andes (−25 km) next to this plate limit than to the north (−35 km). The isostatic Residual Moho (Fig. 7) shows a certain degree of overcompensation which increases south of the Magallanes–Fagnano fault system.

In the north central Patagonia, the North Patagonian Massif is characterized by high *Tzz* values, with low *Ga* values indicating the existence of a crustal root. Low *Tzz* values in the south central region of the massif are the expression of the Cañadon Asfalto basin, while north of it, the Huincul High (Bettini 1984; Ramos et al. 2004a; Mosquera and Ramos 2006) is expressed by an arched and elongated anomaly of high *Tzz* values, also detected in the *Ga* maps. Positive magnetic anomalies along this feature were related to mafic and ultramafic rocks potentially emplaced in a suture between Northern Patagonia and the southern Gondwana margin (Chernicoff et al. 2008). Moho depths are shallower along the Huincul High than to the south over the Somuncura Massif. The central region of the Somuncura and Deseado Massifs to the south presents high rigidity values (Fig. 9).

orlando_a_p@yahoo.com.ar

The Deseado Massif is expressed by high *Tzz* values and shows to be slightly overcompensated isostatically. The Cretaceous sedimentary deposits filling the Austral basin, and further north in the Río Mayo embayment (Ramos and Aguirre-Urreta 1994) are denoted by low *Tzz* values at the western and southern sides of the Deseado Massif.

Acknowledgements Authors acknowledge the use of the GMT mapping software of Wessel and Smith (1998) and to Dr. L. Uieda, Dr. J. Janak, Dr. M. Sprlak, and Dr. Prof. C. Braitenberg for their usefull softwares. The authors would like to thank to CONICET and the Ministerio de Ciencia y Técnica–Agencia de Promoción Científica y Tecnológica, PICT07-1903 for financial support.

References

Alric VI, Haller MJ, Féraud G (1996) Geocronología 40Ar/39Ar del volcanismo jurasico de la Patagonia Extrandina. XIII Congreso Geologico Argentino y III Congreso Exploración de Hidrocarburos (Buenos Aires). Actas 5:243–250

Alvarez O, Gimenez ME, Braitenberg C, Folguera A (2012) GOCE satellite derived gravity and gravity gradient corrected for topographic effect in the South Central Andes region. Geophys J Int 190(2):941–959. doi:10.1111/j.1365-246X.2012.05556.x

Alvarez O, Gimenez ME, Braitenberg C (2013) Nueva metodología para el cálculo del efecto topográfico para la corrección de datos satelitales. Rev Asoc Geol Argent 70(4):422–429

Alvarez O, Nacif S, Gimenez M, Folguera A, Braitenberg A (2014) Goce derived vertical gravity gradient delineates great earthquake rupture zones along the Chilean margin. Tectonophysics 622:198–215. http://dx.doi.org/10.1016/j.tecto.2014.03.011

Alvarez O, Gimenez ME, Martinez MP, LinceKlinger F, Braitenberg C (2015) New insights into the Andean crustal structure between 32° and 34°S from GOCE satellite gravity data and EGM2008 model. In: Sepúlveda SA, Giambiagi LB, Moreiras SM, Pinto L, Tunik M, Hoke GD, Farías M (eds) Geodynamic processes in the Andes of Central Chile and Argentina, Geol Soc Lond, Special Publication, vol 399, pp 183–202. http://dx.doi.org/10.1144/SP399.3

Amante C, Eakins BW (2009). ETOPO1 1 Arc-Minute global relief model: procedures, data sources and analysis. NOAA technical memorandum NESDIS NGDC-24. National Geophysical Data Center, NOAA. doi:10.7289/V5C8276M

ANCORP Working Group (2003) Seismic imaging of a convergent continental margin and plateau in the central Andes (Andean Continental Research Project 1996 (ANCORP'96)). J Geophys Res 108(B7). http://dx.doi.org/10.1029/2002JB001771

Barthelmes F (2009) Definition of functionals of the geopotential and their calculation from spherical harmonic models. Theory and formulas used by the calculation service of the ICGEM. Scientific Technical Report. GFZ German Research Centre for Geosciences, Postdam, Germany

Bettini FH (1984) Pautas sobre cronología estructural en el área del cerro Lotena, cerro Granito y su implicancia en el significado de la dorsal del Neuquén, provincia del Neuquén. IX Congrego Geológico Argentino (San Carlos de Bariloche). Actas 2:163–169

Bouman J, Ebbing J, Fuchs M (2013) Reference frame transformation of satellite gravity gradients and topographic mass reduction. J Geophys Res 118(2):759–774

Bourgois J, Martin H, Lagabrielle Y, Le Moigne J, Frutos Jara J (1996) Subduction-erosion related to spreading-ridge subduction: Taitao Peninsula (Chile margin triple junction area). Geology 24:723–726

orlando_a_p@yahoo.com.ar

Braitenberg C (2014) Exploration of tectonic structures with GOCE in Africa and across-continents. EGU Gen Assembly Conf Abstr 16:7277

Braitenberg C, Ebbing J, Götze HJ (2002) Inverse modeling of elastic thickness by convolution method-the Eastern Alps as a case example. Earth Planet Sci Lett 202:387–404

Braitenberg C, Wienecke S, Ebbing J, Bom W, Redfield T (2007) Joint gravity and isostatic analysis for basement studies-a novel tool. EGM International Wokshop, Innovation on in EM, Grav. and Mag. Methods: a new perspective for exploration (Capri), Extended Abstracts

Braitenberg C, Mariani P, Ebbing J, Sprlak, M (2011) The enigmatic Chad lineament revisited with global gravity and gravity-gradient fields. In: Van Hinsbergen DJJ, Buiter SJH, Torsvik TH, Gaina C, Webb SJ (eds) The formation and evolution of Africa: a synopsis of 3.8 Ga of Earth history. Geol Soc London, Special Publication, vol 357, pp 329–341

Brogioni N (1990) Geología y petrografía del vulcanismo mio-plioceno de la provincia de San Luis. Rev Museo de La Plata Geología 90:197–214

Bruinsma SL, Marty JC, Balmino G, Biancale R, Förste C, Abrikosov O, Neumayer H (2010) GOCE gravity field recovery by means of the direct numerical method. In: Lacoste-Francis H (ed) Proceedings of the ESA living planet symposium, Bergen, Norway, ESA Publication (27) SP-686

Bruinsma SL, Förste C, Abrikosov O, Marty JC, Rio MH, Mulet S, Bonvalot S (2013) The new ESA satellite-only gravity field model via the direct approach. Geophys Res Lett 40:3607–3612

Burov EB, Diament M (1995) The effective elastic thickness (Te) of continental lithosphere: What does it really mean? J Geophys Res 100:3905–3927

Cande SC, Leslie RB (1986) Late Cenozoic tectonics of the southern Chile trench. J Geophys Res 91:471–496

Cembrano J, Hervé F, Lavenu A (1996) The Liquifie Ofqui fault zone: a long-lived intra-arc fault system in southern Chile. Tectonophysics 259:55–66

Chernicoff CJ, Zappettini EO, Santos JOS, Beyer E, McNaughton NJ (2008) Foreland basin deposits associated with Cuyania accretion in La Pampa Province, Argentina. Gondwana Res 13:189–203

Contreras-Reyes E (2008) Evolution of the seismic structure of the incoming/subducting oceanic Nazca plate off south-central Chile. Unpublished Ph.D. Thesis. Christian-Albrechts-Universität zu Kiel, Germany, p 143

Dalziel IWD, De Wit MF, Palmer KF (1974) Fossil marginal basin in the Southern Andes. Nature 250:291–294

Feraud G, Alric V, Fornari M (1999) 40Ar/39Ar dating of the Jurassic volcanic province of Patagonia: migrating magmatism related to Gondwana break-up and subduction. Earth Planet Sci Lett 172:83–96

Flueh ER, Vidal N, Ranero CR, Hokja A, von Huene R, Bialas J, Hinz K, Cordoba D, Danobeitia JJ, Zelt C (1998) Seismic investigation of the continental margin off- and onshore Valparaiso, Chile. Tectonophysics 288:251–263

Förste C, Bruinsma SL, Shako R, Abrikosov O, Flechtner F, Marty JC, Lemoine JM, Dahle C, Neumeyer H, Barthelmes F, Biancale R, Balmino G, König R (2012) A new release of EIGEN-6: The latest combined global gravity field model including LAGEOS, GRACE and GOCE data from the collaboration of GFZ Potsdam and GRGS Toulouse. EGU Gen Assembly Conf Abstr 14:2821

Gans C, Beck S, Zandt G, Gilbert H, Alvarado P, Anderson M, Linkimer L (2011) Continental and oceanic crustal structure of the Pampean flat slab region, western Argentina, using receiver function analysis: new high-resolution results. Geophys J Int 186:45–58

García Morabito E, Folguera A, Melnick D, Ramos VA (2003) Variabilidad en la actividad del retroarco andino entre 37 y 39°. X Congreso Geológico Chile (Concepción), Actas: p 11

Ghidella ME, Yañez G, LaBrecque HL (2002) Revised tectonic implications for the magnetic anomalies of the Western Weddell Sea. Tectonophysics 347:65–86

Ghiglione MC, Ramos VA (2005) Progression of deformation in the southernmost Andes. Tectonophysics 405:25–46

orlando_a_p@yahoo.com.ar

Gimenez ME, Martínez MP, Introcaso A (2000) A Crustal Model based mainly on Gravity data in the area between the Bermejo Basin and the Sierras de Valle Fértil- Argentina. J South Am Earth Sci 13(3):275–286

Gimenez ME, Braitenberg C, Martinez MP, Introcaso A (2009) A comparative analysis of seismological and gravimetric crustal thicknesses below the Andean Region with Flat Subduction of the Nazca Plate. Int J Geophys. doi:10.1155/2009/607458

Göetze C, Evans B (1979) Stress and temperature in the bending lithosphere as constrained by experimental rock mechanism. Geophys J Royal Astron Soc 59:463–478

Grombein T, Heck B, Seitz K (2013) Optimized formulas for the gravitational field of a tesseroid. J Geodyn 87:645–660

Hackney R, Echtler HP, Franz G, Götze HJ, Lucassen F, Marchenko D, Melnick D, Meyer U, Schmidt S, Tašárová Z, Tassara A, Wienecke S (2006) The segmented overriding plate and coupling at the South-Central Chilean Margin (36–42°S). In: Oncken O, Chong G, Franz G, Giese P, Götze HJ, Ramos VA, Strecker MR, Wigger P (eds) The Andes. Active subduction orogeny. Frontiers in Earth science series. Springer, New York, pp 355–375

Hervé F, Demant A, Pankhurst RJ, Ramírez E (1996) Age and Al-inhornblende geobarometry in the northern Patagonian batholith, Aysén, Chile. III International Symposium on Andean Geodynamics (Saint Malo), pp 579–582

Hervé F, Godoy E, Mpodozis C, Fanning CM (2004) Monitoring magmatism of the Patagonian Batholith through the U-SHRIMP dating of detrital zircons in sedimentary units of the Magallanes basin. Bolletino di Geofisica Teorica ed Applicata. Electron Files 45:113–117

Hofmann-Wellenhof B, Moritz H (2006) Physical geodesy, 2nd edn. Springer, Berlin

Introcaso A (2006) Geodesia Física. Boletin del Instituto de Fisografia y Geologia 1:1–128

Inrocaso A, Pacino MC, Fraga H (1992) Gravity, isostasy and Andean crustal shortening between latitudes 30°S and 35°S. Tectonophysics 205:31–48

Introcaso A, Pacino MC, Guspi F (2000) The Andes of Argentina and Chile: crustal configuration, isostasy, shortening and tectonic features from gravity data. Temas de Geociencia 5:31

Janak J, Sprlak M (2006) New software for gravity field modelling using spherical Armonic. Geod Cartog Hor 52:1–8

Jordan T, Allmendinger R (1986) The Sierras Pampean of Argentina: a modern analogue of Rocky Mountain foreland deformation. Am J Sci 286:737–764

Kay SM, Coira BL (2009) Shallowing and steepening subduction zones, continental lithospheric loss, magmatism, and crustal flow under the Central Andean Altiplano–Puna Plateau. In: Kay SM, Ramos VA, Dickinson WR (eds) Backbone of the Americas: shallow subduction, plateau uplift, and ridge and terrane collision. Geol Soc Am Memoirs 204. doi:10.1130/2009.1204(11)

Kay SM, Gordillo CE (1994) Pocho volcanic rocks and the melting of depleted continental lithosphere above a shallowly dipping subduction zone in the Central Andes. Contrib Miner Petrol 117:25–44

Klepeis KA (1994) The Magallanes and Deseado fault zones: Major domains of the South American-Scotia transform plate boundary in southernmost South America, Tierra del Fuego. J Geophys Res 99:22001–22014

Köther N, Götze HJ, Gutknecht BD, Jahr T, Jentzsch G, Lücke OH, Mahatsente R, Sharm R, Zeumann S (2012) The seismically active Andean and Central American margins: can satellite gravity map lithospheric structures? J Geodyn 59(60):207–218

Krawczyk CM, Mechie J, Lüth S, Tašárová Z, Wigger P, Stiller M, Brasse H, Echtler HP, Araneda M, Bataille K (2006) Geophysical signatures and active tectonics at the South-Central chilean margin. In: Oncken O, Chong G, Franz G, Giese P, Götze H-J, Ramos VA, Strecker MR, Wigger P (eds) The Andes. Active subduction orogeny. Frontiers in Earth science series. Springer, Berlin, pp 171–192

Li X (2001) Vertical resolution: gravity versus vertical gravity gradient. Lead Edge 20:901–904

Li Y, Braitenberg C, Yang Y (2013) Interpretation of gravity data by the continuous wavelet transform: the case of the Chad lineament (North-Central Africa). J Appl Geophys 90:62–70

orlando_a_p@yahoo.com.ar

Linares E, Llambias E, Latorre (1980) Geología de la Provincia de La Pampa, República Argentina y Geocronología de sus rocas metamórficas y eruptivas. Rev Assoc Geol Argent 35(1):87–146
Lira R, Millone HA, Kirschbaum AM, Moreno RS (1997) Calcalkaline arc granitoid activity in the Sierra Norte Ambargasta ranges central Argentina. J S Am Earth Sci 10:157–177
Lodolo E, Menichetti M, Bartole R, Ben-Avraham Z, Tassone A, Lippai H (2003) Magallanes-Fagnano continental transform fault (Tierra del Fuego, southernmost South America). Tectonics 22. doi:10.1029/2003TC001500
Lowry AR, Ribe NM, Smith RB (2000) Dynamic elevation of the Cordillera, western United States. J Geophys Res 105:23–371
Lyon-Caen H, Molnar P (1983) Constraints on the structure of the Himalaya from an analysis of gravity anomalies and a flexural model of the lithosphere. J Geophys Res 88:8171–8191
Mariani P, Braitenberg C, Ussami N (2013) Explaining the thick crust in Paraná basin, Brazil, with satellite GOCE gravity observations. J S Am Earth Sci 45:209–223
Molodensky MS, Eremeev VF, Yurkina MI (1962) Methods for study of the external gravity field and figure of the Earth, Israel Program of Scientific Translations, Jerusalem (Russian original 1960)
Mosquera A, Ramos VA (2006) Intraplate deformation in the Neuquén Basin. In: Kay SM, Ramos VA (eds) Evolution of an Andean margin: A tectonic and magmatic view from the Andes to the Neuquén Basin (35°–39°S latitude). Geol Soc of America, Special Paper 407: 97–124
Olivero EB (1998) Mesozoic-Paleogene geology of the marginal-Austral basin of Tierra del Fuego. Mesozoic-Paleogene geology of the marginal-Austral basin of Tierra del Fuego. III Annual Conference, IGCP Project 381, South Atlantic Mesozoic Correlations (Ushuaia), Field Trip Guide, pp 1–42
Pail R, Bruisma S, Migliaccio F, Förste C, Goiginger H, Schuh WD, Höck E, Reguzzoni M, Brockmann JM, Abrikosov O, Veicherts M, Fecher T, Mayrhofer R, Krasbutter I, Sansò F, Tscherning CC (2011) First GOCE gravity field models derived by three different approaches. J Geodyn 85:819–843
Pavlis NK, Holmes SA, Kenyon SC, Factor JK (2008) An Earth gravitational model to degree 2160: EGM2008. General Assembly of the European Geosciences Union, Vienna, Austria
Pavlis NK, Holmes SA, Kenyon SC, Factor JK (2012) The development and evaluation of the Earth Gravitational Model (EGM2008). J Geophys Res 117:B04406. doi:10.1029/2011JB008916
Perez-Gussinye M, Lowry AR, Phipps Morgan J, Tassara A (2008) Effective elastic thickness variations along the Andean margin and their relationship to subduction geometry. Geochem Geophys Geosyst 9(2) doi:10.1029/2007GC001786
Ramos VA (1988) Tectonics of the late proterozoic–early Paleozoic: a collisional history of southern South America. Episodes 11(3):168–174
Ramos VA (1999) Las Provincias Geologicas del Territorio Argentino. In: Caminos R (ed) Geologia Argentina. Instituto de Geología y Recursos Minerales 29(3):41–96
Ramos VA (2004a) Cuyania, an exotic block to Gondwana: review of a historical success and the present problems. Gondwana Res 7:1009–1026
Ramos VA (2004b) Tectonics of the southernmost Andes: a comparison between the Patagonian and the Fuegian Cordilleras. Bolletino di Geofisica Teorica ed Applicata. Electron Files 45:1–10
Ramos VA (2009) Anatomy and global context of the Andes: main geologic features and the Andean orogenic cycle. In: Kay S, Ramos VA, Dickinson W (eds) Backbone of the Americas: shallow subduction, plateau uplift, and ridge and terrane collision (Boulder). Geol Soc Am Memoirs, vol 204, pp 31–65
Ramos VA, Aguirre-Urreta MB (1994) Cretaceous evolution of the Magallanes basin. In: Salfity JA (ed) Cretaceous tectonics of the Andes. Earth Evolution Series. Braunschweig/Wiesbaden, Vieweg+Teubner Verlag, pp 315–345
Ramos VA, Cristallini E, Pérez D (2002) The Pampean flat-slab of the Central Andes. J S Am Earth Sci 15:59–78

orlando_a_p@yahoo.com.ar

Ramos VA, Riccardi A, Rolleri EO (2004a) Límites naturales del norte de la Patagonia. Rev Assoc Geol Argent 59(4):785–786

Ramos VA, Zapata T, Cristallini E, Introcaso A (2004b) The Andean thrust system: latitudinal variations in structural styles and orogenic shortening. In: McClay K (ed) Thrust tectonics and hydrocarbon systems. Am Assoc Petroleum Geologists, Memoir, vol 82(3), pp 30–50

Ramos VA, Folguera A, Garcia-Morabito E (2011) Las provincias geológicas del Neuquén. Geología y Recursos Naturales de la Provincia de Neuquén. Relatorio del VXIII Congreso Geológico Argentino, pp 317–326

Ranero C, von Huene R, Weinrebe W, Reichert C (2006) Tectonic processes along the chile convergent margin. In: Oncken O, Chong G, Franz G, Giese P, Götze H-J, Ramos VA, Strecker MR, Wigger P (eds) The Andes. Active subduction orogeny. Frontiers in Earth science series. Springer, Berlin, pp 91–121

Rapela CW, Pankhurst RJ, Casquet C, Baldo E, Saavedra J, Galindo C, Fanning CM (1998) The Pampean Orogeny of the southern proto-Andes: evidence for Cambrian continental collision in the Sierras de Cordoba. In: Pankhurst RJ, Rapela CW (eds) The proto-Andean Margin of Gondwana. Geol Soc London, Special Publication, vol 142, pp 181–217

Reguzzoni M, Sampietro D (2010) An inverse gravimetric problem with GOCE Data, International Association of Geodesy Symposia, Springer-Verlag. Gravity Geoid Earth Obs 135(5):451–456

Rosenau M, Melnick D, Echtler H (2006) Kinematic constraints on intra-arc shear and strain partitioning in the southern Andes between 38°S and 42°S latitude. Tectonics 25. doi:10.1029/2005TC001943

Rummel R, Yi W, Stummer C (2011) GOCE gravitational gradiometry. J Geodyn 85(11):777–790

Sacek V, Ussami N (2009) Reappraisal of the effective elastic thickness for the sub-Andes using 3-d finite element fexural modelling, gravity and geological constraints. Geophys J Int 179 (2):778–786

Sandwell DT, Smith WHF (1997) Marine gravity anomaly from Geosat and ERS-1 satellite altimetry. J Geophys Res 102:10039–10050

Sick C, Yoon MK, Rauch K, Buske S, Lüth S, Araneda M, Bataille K, Chong G, Giese P, Krawczyk C, Mechie J, Meyer H, Oncken O, Reichert C, Schmitz M, Shapiro S, Stiller M, Wigger P (2006) Seismic images of accretive and erosive subduction zones from the chilean margin. In: Oncken O, Chong G, Franz G, Giese P, Götze H-J, Ramos VA, Strecker MR, Wigger P (eds) The Andes. Active subduction orogeny. Frontiers in Earth science series. Springer, Berlin, pp 147–169

Stewart J, Watts AB (1997) Gravity anomalies and spatial variations of flexural rigidity at mountain ranges. J Geophys Res 102(B3):5327–5352

Tassara A (2005) Interaction between the Nazca and South American plates and formation of the Altiplano-Puna plateau: review of a flexural analysis along the Andean margin (15°–34°S). Tectonophysics 399:39–57

Tassara A, Yañez G (2003) Relación entre el espesor elástico de la litósfera y la segmentación tectónica del margen andino (15°–47°S). Rev Geol Chile 30(2):159–186

Tassara A, Swain C, Hackney R, Kirby J (2007) Elastic thickness structure of South America estimated using wavelets and satellite-derived gravity data. Earth Planet Sci Lett 253:17–36

Tebbens SF, Cande SC (1997) Southeast Pacific tectonic evolution from early Oligocene to present. J Geophys Res 102(B6):12061–12084

Tscherning CC (1976) Computation of the second-order derivatives of the normal potential based on the representation by a Legendre series. Manuscripta Geod 1:71–92

Turner JCM, Baldis BAJ (1978) La estructura transcontinental del límite septentrional de la Patagonia. VII Congreso Geológico Argentino (Bahía Blanca). Actas 2:225–238

Uieda L, Ussami N, Braitenberg CF (2010) Computation of the gravity gradient tensor due to topographic masses using tesseroids. EOS, Trans Am geophys Un 91(26)

Uliana MA, Biddle KT, Phelps DW, Gust DA (1985) Significado del vulcanismo y extensión mesojurásicos en el extremo meridional de Sudamérica. Rev Asoc Geol Argent 40(3–4):231–253

orlando_a_p@yahoo.com.ar

von Huene R, Corvalán J, Flueh ER, Hinz K, Korstgard J, Ranero CR, Weinrebe W, CONDOR scientists (1997) Tectonic control of the subducting Juan Fernández Ridge on the Andean margin near Valparaiso, Chile. Tectonics 16(3):474–488

Watts A (2001) Isostasy and flexure of the Lithosphere: Cambridge University Press, Cambridge, p 458

Wells RE, Blakely RJ, Sugiyama Y, Scholl DW, Dinterman PA (2003) Basin centered asperities in great subduction zone earthquakes: a link between slip, subsidence and subduction erosion? J Geophys Res 108(B10):2507–2536

Weidmann C, Spagnotto S, Gimenez ME, Martinez P, Alvarez O, Sanchez M, Lince Klinger F (2013) Crustal structure and tectonic setting of the south central Andes from gravimetric analysis. Geofísica Int 52:121–133

Wessel P, Smith WHF (1998) New, improved version of the generic mapping tools released. EOS Trans AGU 79(47):579

Wienecke S (2006) A new analytical solution for the calculation of flexural rigidity: significance and applications: Unpublished. Ph.D. Thesis. Free University Berlin, p 126

Wienecke S, Braitenberg C, Göetze HJ (2007) A new analytical solution estimating the flexural rigidity in the Central Andes. Geophys J Int 169:789–794

Windhausen A (1931) Geología Argentina. Geología Histórica y Regional del Territorio Argentino. Editorial J. Peuser, Buenos Aires 2, p 645

Yi W, Rummel R (2014) A comparison of GOCE gravitational models with EGM2008. J Geodyn 73:14–22

orlando_a_p@yahoo.com.ar

Changes in Source Areas at Neuquén Basin: Mesozoic Evolution and Tectonic Setting Based on U–Pb Ages on Zircons

Maximiliano Naipauer and Victor A. Ramos

Abstract The Neuquén Basin constitutes a key site to investigate how the pattern of detrital zircon age varies through time in different tectonic regimes. Here we analyze the U–Pb zircon age database published for the Southern Central Andes. In the early Mesozoic (rift stage) the source regions were locally and strongly influenced by the active volcanism coeval with the extensional tectonic activity. The rift relief associated with the synrift stage lasted until the first marine transgression corresponding to the Los Molles Formation. The source regions in the retroarc setting (sag stage) are variable and showed reversal provenance. In the Middle and Late Jurassic the magmatic arc became the most important source, but in the Early Cretaceous eastern cratonic regions were the main source areas of sediment contribution. The reversal of the provenance pattern can be either explained by the base-level fall or by a period of exhumation of the Sierras Pampeanas basement linked to generation of rift systems. The source regions in the Late Cretaceous (foreland stage) indicate an uplift of a mountain chain and exhumation along the Andean magmatic arc; although younger and distal units showed that a peripheral bulge would be growing in the eastern cratonic sector. Cawood's tectonic discrimination diagram is tested as a useful tool in the Southern Central Andes. However, it is necessary to consider more complex settings taking into account the relative positions of the magmatic arc and the orogenic front through time.

Keywords Provenance · Neuquén Basin · Geochronology · Detrital zircons

M. Naipauer (✉) · V.A. Ramos
Departamento de Ciencias Geológicas, Facultad de Ciencias Exactas y Naturales,
Instituto de Estudios Andinos "Don Pablo Groeber" UBA-CONICET,
Buenos Aires, Argentina
e-mail: maxinaipauer@gl.fcen.uba.ar

© Springer International Publishing Switzerland 2016

A. Folguera et al. (eds.), *Growth of the Southern Andes*,
Springer Earth System Sciences, DOI 10.1007/978-3-319-23060-3_3

orlando_a_p@yahoo.com.ar

1 Introduction

Several works in the past two decades have indicated the importance of U–Pb dating of detrital and igneous zircons in studies of sedimentary provenance, crustal evolution, paleogeographic reconstructions, and stratigraphic correlations (Mueller et al. 1994; Cawood and Nemchin 2001; Fedo et al. 2003; Cawood et al. 2007; Bahlburg et al. 2009; among others). More recently, different U–Pb geochronological methods as TIMS-ID, SHRIMP, and LA-ICP-MS were developed. This has increased data sets, allowing the application of statistic methods that improved the relationship between the pattern of detrital zircon ages, magmatic events, and tectonic setting of sedimentary basins (Condie et al. 2009; Cawood et al. 2012). The Neuquén basin is developed in the retroarc of the Southern Central Andes, between 31° and 41°S, (Fig. 1), with more than 6000 m of marine and continental deposits and interlayered volcanic rocks. This succession is an excellent site to investigate how the pattern of detrital zircon age varied through time in different tectonic regimes. The tectonic evolution of the basin is remarkable, since it began with synrift depocenters, continuing with a thermal retroarc (sag) stage and finishing as a foreland basin (Vergani et al. 1995; Ramos and Folguera 2005; Howell et al. 2005; Ramos 2010).

The aim of this work is to analyze the U–Pb zircon age database published for the Neuquén Basin integrated according to the different tectonic stages recognized in this sector of the Andes. At the same time the pre-Andean basement regions were revised identifying the main sediment source areas of the basin. The analysis showed variations in the sedimentary provenance through each tectonic stage: synrift, retroarc (sag stage), and foreland. Based on that was defined the most representative pattern of detrital zircon ages at each stage. Finally, the data set produced in the Neuquén Basin was compared with the patterns of detrital zircons and tectonic setting diagram proposed by Cawood et al. (2012).

2 Geological Background

The geology of the Southern Central Andes between 31° and 41°S is described through several morphotectonic units according to their stratigraphy, structure, and geological history (Fig. 1). The Main Cordillera (Principal and Frontal Cordilleras) form the axis of the Andean mountain chain at these latitudes, while the Neuquén Embayment occupies most of the extra-Andean region. In the northeastern foreland region, the San Rafael block is developed, while to the east Las Matras-Chadileuvú block is exposed, as part of a broken foreland system. East of the North Patagonian Cordillera (Ramos 1999), the North Patagonian Massif is developed, delimiting the southern part of the Neuquén Basin. In the west the Central Depression and the

orlando_a_p@yahoo.com.ar

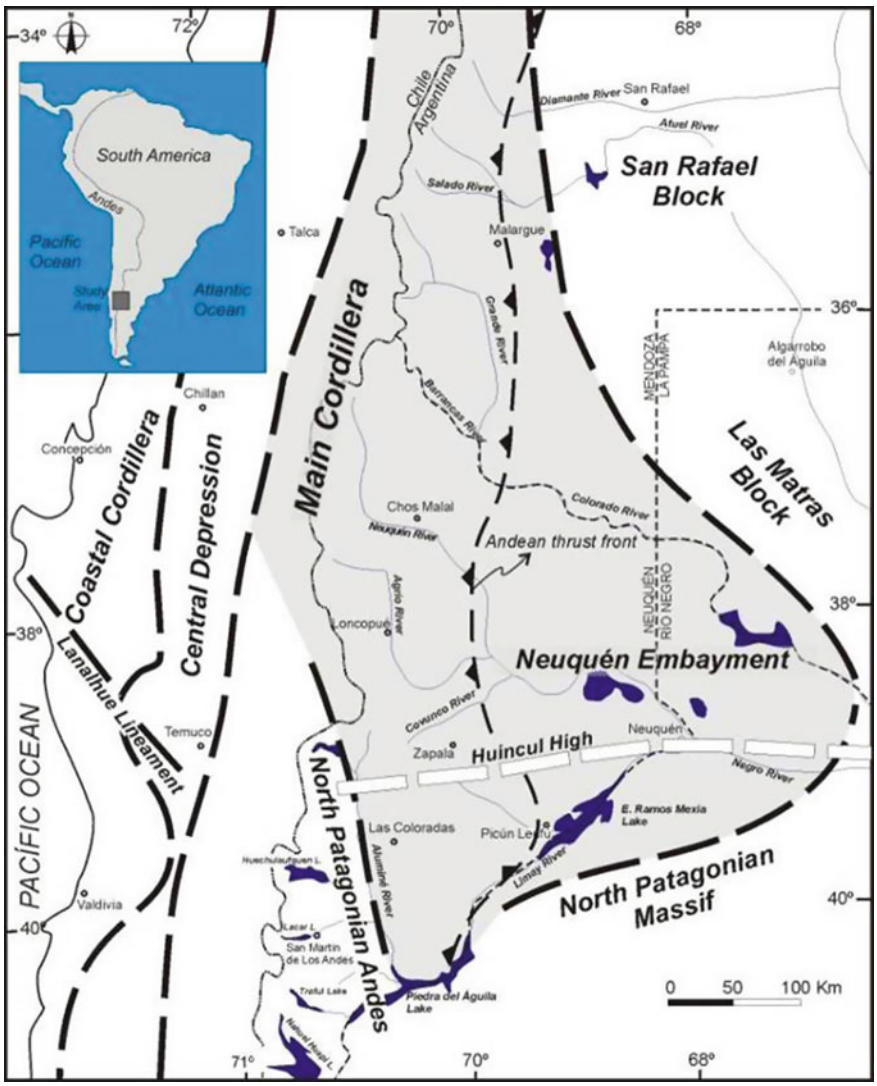


Fig. 1 Location of the main morphotectonic features in the Southern Central Andes between 34° and 41°S. The Andean thrust front, Huincul High, and Lanalhue Lineament are also shown. Argentinean geological provinces are modified from Ramos (1999) and Chilean features are taken from Pankhurst and Hervé (2007) and Hervé et al. (2013)

Coastal Cordillera are the main morphostructural features on the Chilean Andean slope (see Fig. 1).

The Main Cordillera (Darwin 1946; Stelzner 1876; Schiller 1912; Keidel 1927; Groeber 1929; Yrigoyen 1972) is characterized by thick Jurassic and Cretaceous

orlando_a_p@yahoo.com.ar

marine, continental, and volcanic sequences; the marine transgressions are from the Paleo-Pacific Ocean. Based on different structural styles, several fold and thrust belts were recognized (Ramos 1999), e.g., the Aconcagua, Malargüe, Chos Malal, Agrio, and Aluminé. The uplift and deformational stages of these fold and thrust belts are constrained between Late Cretaceous and the Cenozoic (Cobbold and Rossello 2003; Ramos and Folguera 2005; Tunik et al. 2010). East of the Andean Cordillera the orogenic front bounds the Neuquén Embayment (Bracaccini 1970; Ramos 1999), which is characterized by Late Cretaceous continental sediments and remnants of the first Atlantic ingression of Cretaceous–Paleogene age (Uliana and Dellapé 1981; Aguirre-Urreta et al. 2011). In the subsurface Jurassic–Cretaceous marine and continental sequences are also present, but deformation is milder than in the Main Andes. The structure style is a combination of thick and thin-skinned structures developed in different sectors, which at the surface are recognized as large anticline folds (Ramos 1999).

The Mesozoic and Cenozoic sedimentary and volcanic deposits of the Main Cordillera and Neuquén Embayment are included in the Neuquén Basin (Digregorio 1972; Digregorio et al. 1984; Legarreta and Uliana 1999). The stratigraphic, structural, paleontological, and tectonic knowledge of the basin was established by the pioneering works that started at the past century (Fig. 2) (Groeber 1948; Ramos 1978; Uliana and Biddle 1988; Legarreta and Uliana 1991; Vergani et al. 1995; among others).

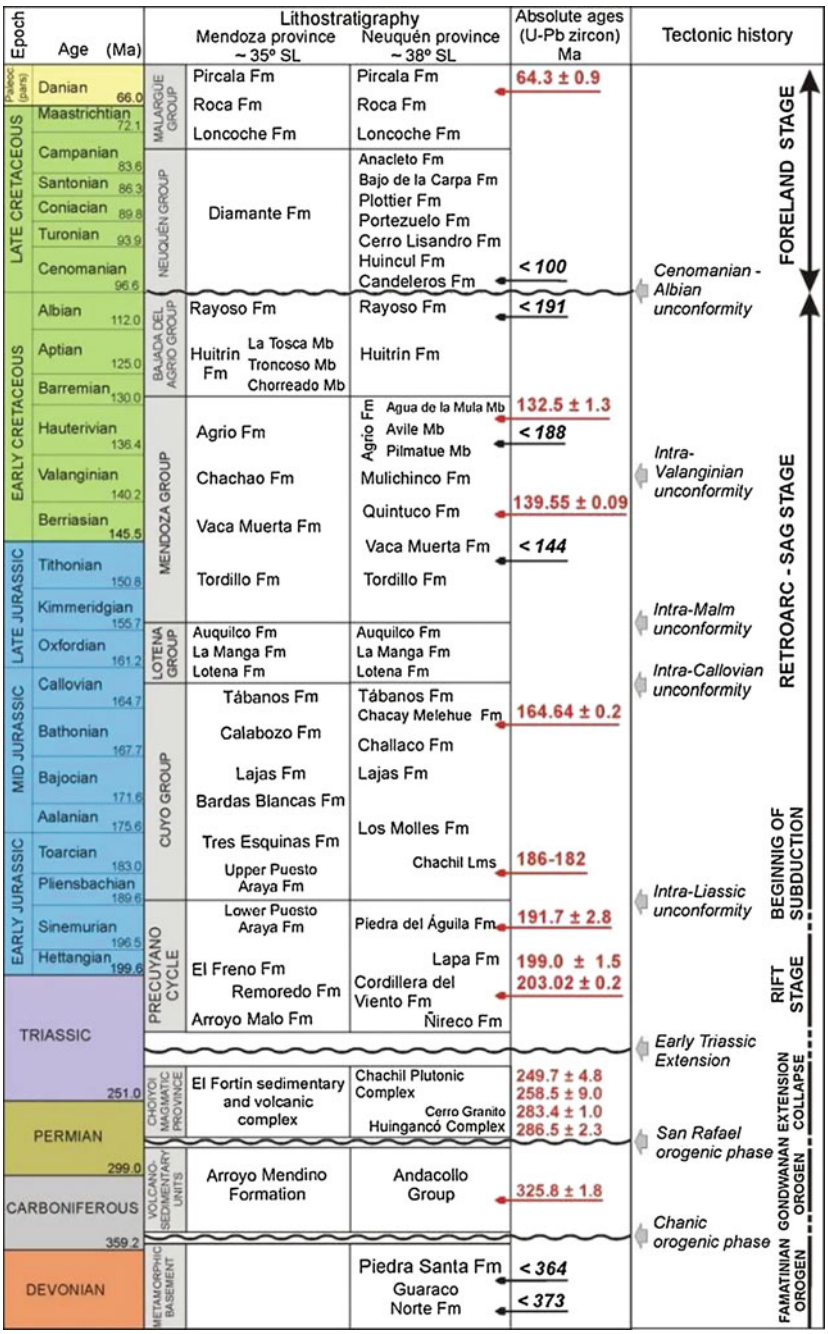
The history of the basin reflects the tectonic evolution of the Andes at these latitudes: it started in the Late Triassic with isolated rift depocenters where acidic and mafic volcanic rocks predominated over continental coarse sediments (Vergani et al. 1995; Franzese and Spalletti 2001); it continued with the first marine transgression from the Paleo-Pacific registered in the Early Jurassic with the installation of a thermal subsidence regime corresponding to the sag stage of the basin (Mpodozis and Ramos 2008). This tectonic condition lasted until the end of the Early Cretaceous and it was contemporaneous with the development of an Andean magmatic arc. The tectonic regime in the Southern Central Andes became compressive and recorded the first Andean uplift in the retroarc foreland basins ca. 100 Ma (Tunik et al. 2010; and references therein).

Metamorphic, igneous, and sedimentary rocks older than Late Triassic form the pre-Andean stratigraphic basement of the Neuquén Basin (Cingolani et al. 2011).

These rocks outcrop in the San Rafael-Las Matras-Chadileuvú blocks and in the North Patagonian Massif, which bound the northeastern and southeastern margins of the basin, respectively (Fig. 1).

Igneous and metamorphic basement rocks are exposed also through the basin area forming the core of large anticlines developed during the Andean deformation (García Morabito and Ramos 2012).

orlando_a_p@yahoo.com.ar



orlando_a_p@yahoo.com.ar

◀ **Fig. 2** Tectonostratigraphic chart of the Neuquén Basin. The *table* shows the chronostratigraphy, U–Pb zircon ages, and tectonic setting. The U–Pb ages are from Aguirre-Urreta et al. (2008, 2011), Hervé et al. (2013), Kamo and Riccardi (2009), Leanza et al. (2013), Llambías et al. (2005), Naipauer et al. (2012, 2014a), Ramos et al. (2010a), Riccardi and Kamo (2014), Sato et al. (2008), Schiuma and Llambías (2008), Tunik et al. (2010), Vennari et al. (2014), and Zappettini et al. (2012). The black italic number indicates the youngest detrital zircon U–Pb ages in metasedimentary and sedimentary rocks. The *red bold* number indicates U–Pb crystallization ages of plutonic and volcanic (tuff) rocks

3 Precambrian and Paleozoic Basement Regions

The basement of the study area is exposed in several regions along the margins of the Neuquén Basin, and constitutes the foreland region of the Southern Central Andes. In the northeastern margin of the basin, the igneous–metamorphic basement is exposed, which is included in the Frontal Cordillera and in the San Rafael, Las Matras, and Chadileuvú blocks (Fig. 3). The oldest Mesoproterozoic basement conforms small outcrops in the southern part of the Frontal Cordillera and in the San Rafael and Las Matras blocks. U–Pb (TIMS and SHRIMP) ages between 1069 and 1244 Ma were obtained by several authors in these rocks (see Varela et al. 2011; and references therein). The Mesoproterozoic orthogneiss of the Frontal Cordillera is interpreted as the Grenville basement of Chilenia terrane (Ramos and Basei 1997). While the Mesoproterozoic metaigneous rocks of San Rafael (Cingolani et al. 2005; Thomas et al. 2012) and the TTG pluton of Las Matras (Sato et al. 2004) are considered part of the basement of the Cuyania terrane (Ramos 2004). The Mesoproterozoic basement in the Pampia terrane has not been found yet, but it is possible to interpret that Pampia has a Grenville basement in the subsurface as suggested by the detrital zircon ages of many metasedimentary units from the Sierras Pampeanas (Escayola et al. 2007) and Chadileuvú Block (Chernicoff et al. 2012). The Pampia terrane is characterized by Neoproterozoic to Early Cambrian igneous and metamorphic rocks, which were accreted as crustal fragments in the western Gondwana margin during the Pampean orogenic cycle (Ramos 1988; Ramos et al. 2010b and references therein). Early Cambrian igneous rocks were dated by U–Pb on zircons east of the Neuquén Basin, in the Chadileuvú Block by Chernicoff et al. (2012) as part of the southern outcrops of the Pampia terrane (Fig. 3). Along the western border of Pampia, the Famatinian magmatic arc was developed in Ordovician times. Several calcalkaline plutons were dated by U–Pb (SHRIMP) in the Chadileuvú Block between 466 and 476 Ma (Pankhurst et al. 2006; Chernicoff et al. 2010).

The Famatinian arc is extended through the Gondwana margin for hundreds of kilometers to the north up to Peru latitudes (Casquet et al. 2010).

The southern border of the Neuquén Basin is formed by the basement of the North Patagonian Massif (Fig. 3), which was considered part of the Patagonia terrane according to some hypotheses (Ramos 1984, 2008). This basement can be separated into two main regions according to their ages. Older igneous rocks have an Early Cambrian age, recently dated by U–Pb (SHRIMP) on zircons from the Tardugno Granodiorite (Rapalini et al. 2013; Pankhurst et al. 2014); this body is exposed in the

orlando_a_p@yahoo.com.ar

northeastern part of the massif (Fig. 3). In this region, Ordovician plutons are intruded in a metasedimentary sequence of the Nahuel Niyeu Formation. These granites were dated by U–Pb (SHRIMP) in ca. 467 Ma (Rapalini et al. 2013) and the metasediment have a maximum depositional age at ca. 515 Ma (Pankhurst et al. 2006). The detrital patterns of these rocks present Mesoproterozoic peaks at ca. 1200–1000 Ma. In the central-western sectors of the North Patagonian basement are younger rocks, characterized by Late Silurian to Devonian igneous and metaigneous ages dated by U–Pb (TIMS and SHRIMP) between ca. 425 and 348 Ma (Varela et al. 2005; Pankhurst et al. 2006). These rocks form part of a magmatic arc that crosses Patagonia with a NNW-trending direction (Ramos and Naipauer 2014).

Devonian plutons are also present to the north, in the San Rafael Block, where small tonalite bodies are intrusive in Silurian sedimentary rocks. These rocks were dated by U–Pb (TIMS) at ca. 401 Ma (Cingolani et al. 2005) (Fig. 3).

Another important component of the pre-Andean basement is the Devonian metasedimentary sequences, which are exposed in the western Neuquén Basin in the Main Cordillera of Argentina and the Coastal Cordillera of Chile (Figs. 2 and 3). The outcrops of the Main Cordillera are small and conform the core of large Andean anticlines; some of them are related to the Huincul High (Fig. 3). The metasedimentary rocks of the Piedra Santa Formation (Franzese 1995) crop out in the western sector of the Huincul deformation zone; it was dated by U–Pb

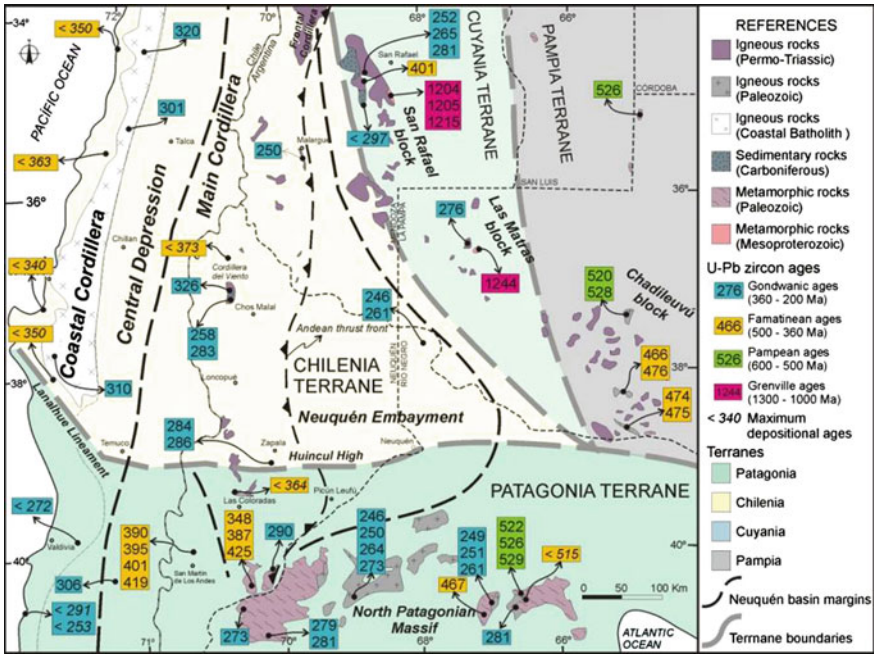


Fig. 3 Sketch map of the basement geology and U–Pb zircon ages in the Southern Central Andes. Accreted basement terranes are also shown along the western Gondwana margin (Pampia, Cuyania, Chilenia, and Patagonia). Terrane boundaries modified from Ramos (2010). Representative ages are indicated in the map and their references are cited in the text

orlando_a_p@yahoo.com.ar

(SHRIMP) on detrital zircons (Ramos et al. 2010a); these authors defined a maximum depositional age at ca. 364 Ma, but older peaks of Ordovician and Mesoproterozoic ages are also present. North of the Huincul deformation zone, a very small outcrop of metasedimentary rocks is exposed in the Cordillera del Viento (Fig. 3). These rocks are grouped in the Guaraco Norte Formation and U–Pb (SHRIMP) on detrital zircons indicated a maximum depositional age at ca. 373 Ma (Zappettini et al. 2012); the pattern of detrital zircons is completed with Ordovician and minor Mesoproterozoic peaks. Based on this fact the metasedimentary sequences of the Piedra Santa and Guaraco Norte Formations are correlated.

On the Chilean margin, metamorphic complexes occur as part of the Coastal Cordillera; these are flanked to the east by the Coastal Batholith (Fig. 3). Several works have demonstrated based on lithological differences, metamorphism, and structure that this metamorphic basement may be separated into two units: the Western and Eastern series (Hervé et al. 2007; and references therein). U–Pb (SHRIMP) ages on detrital zircons separated from these series were recently obtained; the results showed major input from Ordovician (ca. 470 Ma) sources with minor peaks at ca. 530–510 Ma and ca. 1250–950 Ma (Hervé et al. 2013). The maximum depositional ages are different: the Eastern series was defined at ca. 345 Ma and the Western series at ca. 330 Ma (Fig. 3) (Hervé et al. 2013). The Coastal Batholith yielded U–Pb zircon ages between 300 and 320 Ma. These crystallization ages are coherent with older maximum depositional ages defined for their country rocks (Hervé et al. 2013). South of the Lanalhue lineament the Coastal Batholith disappear and the Western series showed marked differences in comparison to the north in the pattern of detrital zircon ages (Hervé et al. 2013). The major peak is defined at ca. 290 Ma, which represents a younger maximum depositional age for this basement complex (Fig. 3). Another prominent peak is in the Devonian at 380 Ma, but all samples lack Ordovician and Grenville zircons (Hervé et al. 2013).

The Choiyoi magmatic province was developed in the western margin of Gondwana after the Carboniferous magmatism and the San Rafael orogenic phase of the Early Permian (Kay et al. 1989; Llambías and Sato 2011). In the southern sector of the study region the San Rafael orogenic phase and the Choiyoi magmatism are related to the Patagonia terrane collision with the southern margin of Western Gondwana (Ramos 1984, 2008). Plutonic and volcanic rocks of the Choiyoi magmatism form the most extensive basement of the Neuquén Basin. These rocks are very well represented in the Frontal Cordillera, San Rafael, Las Matras, and Chadileuvú blocks, North Patagonian Massif, Main Cordillera, and Coastal Cordillera (Fig. 3). Furthermore, volcanic rocks were found in hydrocarbon well cores drilled in subsurface of the Neuquén Embayment (Barrionuevo et al. 2014). The composition of the Choiyoi magmatism varies between mesosiliceous and siliceous and their ages between 290 and 250 Ma (Llambías and Sato 2011). In Fig. 3, the extension of this magmatism and U–Pb zircon ages for the study region are shown: ages in the San Rafael Block are from Rocha-Campos et al. (2011), in the Main Cordillera from Llambías et al. (2005, 2007), Schiuma and Llambías (2008), Sato et al. (2008) and Hervé et al. (2013), and in the North Patagonian Massif from Pankhurst et al. (2006).

orlando_a_p@yahoo.com.ar

4 Meso-Cenozoic Sedimentary and Volcanic Deposits of the Neuquén Basin

The infill of the basin started in the Late Triassic when isolated depocenters were filled with volcanic and volcaniclastic rocks and coarse sediments. These deposits were grouped in the Precuyano cycle (Gulisano 1981; Carbone et al. 2011), which was related to the tectonic subsidence of the rifting phase with typical wedge geometries. Outcrop of synrift deposits were recognized throughout the Main Cordillera from the San Juan Province (32°S) until the Neuquén Province (40°S), but in the Neuquén Embayment were these detected only in subsurface (Fig. 4). The cycle finishes in the Early Jurassic together with the first Jurassic marine ingression of the Cuyo Group (Fig. 2).

A subduction regime starts in the Early Jurassic and the Andean magmatic arc is developed along the western margin of Gondwana (Mpodozis and Ramos 2008). Tectonic subsidence ceased in the Early Jurassic when the basin underwent a thermal subsidence postrift phase. This phase continues until the Early Cretaceous and three main transgression–regression cycles were developed (Legarreta and Gulisano 1989). Marine transgressions from the Paleo-Pacific Ocean penetrated through the Andean volcanic arc flooding the retroarc region. The sedimentary and volcanic deposits can be separated into four different groups (Fig. 2): Cuyo, Lotena, Mendoza, and Bajada del Agrio (Rayoso). The distribution of these groups is shown in Fig. 4.

The retroarc-sag phase of the Neuquén Basin initiated in the Cuyo Group (Dellapé et al. 1978); it records the first marine ingression that crossed the cordilleran axis through the Curepto Pass (between 34° and 35°S) (Vicente 2005, 2006), and was initially associated with a later synrift stage. Later on the transgression flooded most of the depocenters and covered the Neuquén Embayment (Los Molles and Lajas formations) (Fig. 2). A regression culminated with fluvial and evaporate deposits in the central part of the basin (Challacó and Tábanos formations).

These deposits correspond to the Cuyo Cycle of Gulisano (1981). The Cuyo Group is developed between the Early and Middle Jurassic based on the marine invertebrate fossils (Riccardi 2008a, b).

The Loteniano–Chacayano is the second transgressive–regressive cycle (Groeber 1946; Guilisano et al. 1984) and is represented by the Lotena Group (Leanza 1992). This group includes continental sandstones and clastic platform facies on the base (Fm Lotena), typical marine carbonate facies of La Manga Formation and toward the top a thick evaporate sequence of the Auquilco Formation (Fig. 2). Ammonoid fossils from La Manga Formation have a Middle to Late Jurassic age (Callovian-Oxfordian) (Stipanicic 1951, 1966; Riccardi 2008a, b).

The last cycle is the most extended in time and comprises the Mendoza and Bajada del Agrio groups; this cycle is partially equivalent of the Andico of Groeber (1946). Typical red beds at the base of the Mendoza Group (Stipanicic et al. 1968) consist of coarse conglomerates, fluvial and aeolian sandstones, and volcaniclastic deposits of the Tordillo Formation (Kimmeridgian-Early Tithonian). Typical black

orlando_a_p@yahoo.com.ar

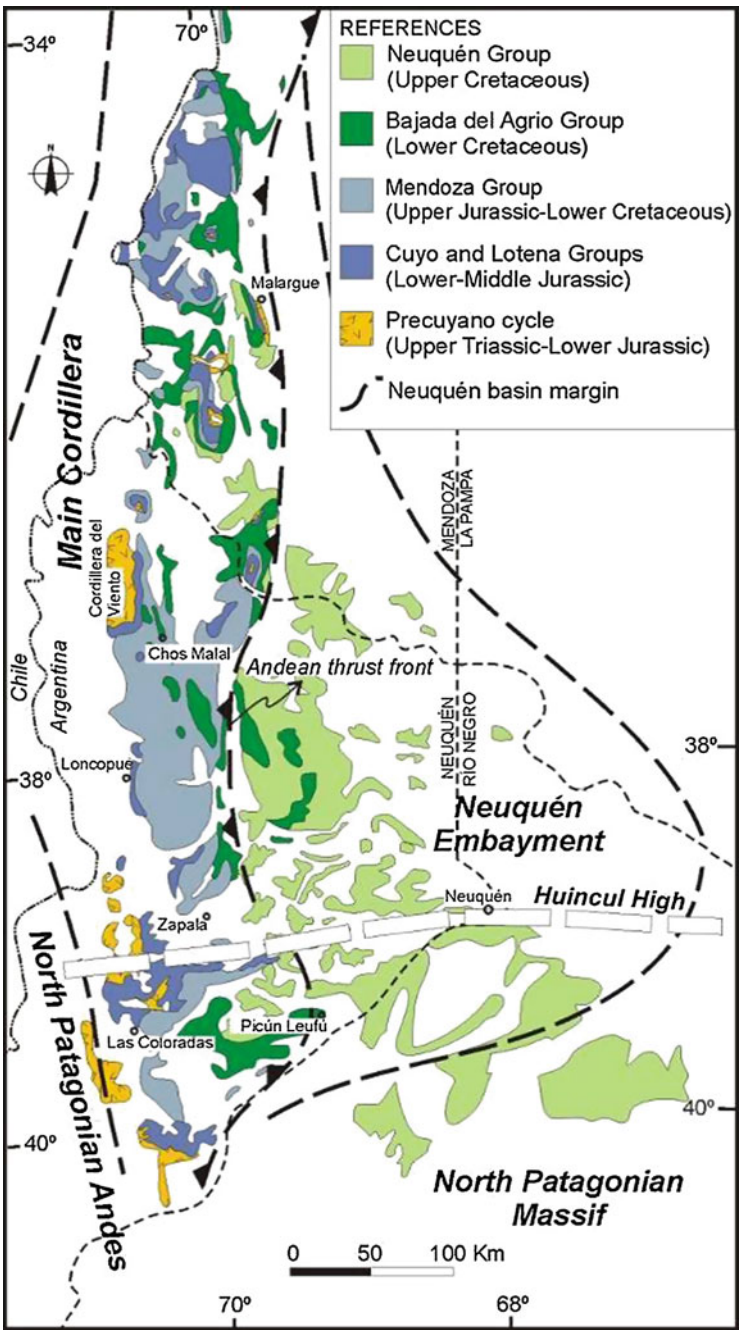


Fig. 4 Regional geological map with the sedimentary infill of the Neuquén Basin: Precuyano, Cuyo, Lotena, Mendoza, Bajada del Agrio, Neuquén, and Malargüe groups are shown

orlando_a_p@yahoo.com.ar

shale facies of the Vaca Muerta Formation (Tithonian-Early Valanginian) were deposited during a sea-level rise phase (Leanza 1973; Lenaza et al. 2011). A sharp sea-level drop occurs during the Late Valanginian and continental, mixed, and marine siliciclastic facies of the Mulichinco Formation were developed in the central part of the basin (Schwarz and Howell 2005). Finally, a thick sequence composed of black shale, carbonate, and continental sandstone facies of the Agrio Formation (Late Valanginian-early Barremian) were deposited (Fig. 2). The Bajada del Agrio Group represents the final drying stage of the basin conformably deposited on the Mendoza Group rocks. Sedimentation started again with the Huitrín Formation with shallow-marine carbonates and evaporates of a restrictive environment, followed by fluvial and aeolian sandstones and evaporates (Troncoso Member), and the sequence ended with the classical carbonate facies of the La Tosca Member (Fig. 2). These deposits are overlain by the Rayoso Formation. This is composed of a thick clastic–evaporitic sequence deposited in a predominantly continental environment. The age of this group is Aptian to Albian (Early Cretaceous) and it marks the final disconnection of the Neuquén Basin with the Paleo-Pacific Ocean. Synorogenic deposits of Neuquén Group of Late Cretaceous age (Tunik et al. 2010) are separated by an angular unconformity from the Rayoso Formation (Cobbold and Rossello 2003; Ramos and Folguera 2005).

By the Early Cretaceous the retroarc-sag phase ends and the tectonic regime changed to compressive in the southern Central Andes (Ramos 2010). Consequently, the Neuquén Basin became a foreland basin and eastward migrations of the orogenic front produced the first synorogenic deposits (Zamora Valcarce et al. 2006; Tunik et al. 2010). This occurs at approximately 100 Ma with the deposition of the red beds of the Neuquén Group and subsequently the Malargüe Group (Fig. 2). The Neuquén Group (Stipanicic et al. 1968) is composed of several formations characterized by continental red beds. In the group fine sandstones, siltstones, and pelites predominate, while conglomerates are subordinate. They are known as the *Estratos con Dinosaurios* (dinosaur beds) and their age is Cenomanian–Campanian (Late Cretaceous) (Leanza et al. 2004). The Malargüe Group, composed of several distinctive formations is separated from the Neuquén Group by an erosional unconformity, and is divided into two sectors, the Western or Andean region, and the Eastern region. One of the main stratigraphic features of the group is the record of the Roca Formation (Fig. 2), the first Atlantic marine ingression in the basin during Maastrichtian–Danian times (Aguirre-Urreta et al. 2011).

5 Provenance and U–Pb Data Background in the Neuquén Basin

The first comprehensive lithostratigraphic study and sedimentary provenance analysis in the Neuquén basin was conducted by Marchese (1971). It was based on petrographic and heavy minerals analyses from sandstones of classical profiles

orlando_a_p@yahoo.com.ar

through the entire basin. Basement source regions and Mesozoic sedimentary and volcanic units were identified. Western source areas linked with the Main Andes, composed of volcanic rocks, were defined in most of the studied units: Los Molles, Lajas, Lotena, La Manga-Auquilco, Tordillo, and Vaca Muerta formations. However, plutonic and metamorphic eastern sources increase in the Agrio (Avilé Member) and Huitrín (and Rayoso?) formations according to Marchese (1971). The provenance in the base of the Neuquén Group corresponding to the Candeleros Formation was identified as from the western volcanic sources, while to the top the Huincul Formation was derived from the east (Marchese 1971). It is important to note that these interpretations were based on geosynclinal premises, but many observations can be reinterpreted based on Plate Tectonic concepts.

Eppinger and Rosenfeld (1996) investigated the role of the source areas for the Late Jurassic–Early Cretaceous sediments of the Neuquén Basin. Based on modal analyses of sandstones and heavy-mineral studies from the Mendoza Group (except the Tordillo Formation), the authors conclude that the detritus were mainly derived from a westerly magmatic arc. A basement region, the North Patagonian Massif, acted as a permanent source for the southernmost part of the Neuquén Basin (Eppinger and Rosenfeld 1996).

More recently, petrography and geochemical analysis of sedimentary rocks were performed by Spalletti et al. (2008, 2014) in conglomerates and sandstones from the Tordillo Formation and in pelites from the Vaca Muerta Formation.

U–Pb data available for the Neuquén Basin have increased considerably, but are still insufficient. Published data include a few U–Pb ages (CA-TIMS, SHRIMP and LA-ICP-MS), and previous K-Ar, Rb-Sr, and Ar–Ar ages (Stipanicic 1967; Rapela et al. 1983; Linares et al. 1988; Pángaro et al. 2002; among others). The sedimentary provenance analysis, mainly based on new published U–Pb data in the Neuquén Basin will be analyzed for each tectonic stage.

6 Rift Stage

Analysis of sedimentary provenance in the synrift deposits have been performed in clastic sediments from the Atuel depocenter, in Mendoza Province (Fig. 4). Petrographic data in the Arroyo Malo (marine deposits), El Freno (continental deposits), and Puesto Araya (marine deposits) formations of the Precuyano cycle showed a clear provenance from volcanic sources (Lanés et al. 2008; Tunik et al. 2008). Paleocurrents analyses from these units indicated potential eastern and northeastern source regions and point out to the San Rafael Block (Lanés 2005; Tunik et al. 2008). According to these studies the main volcanic (plutonic) source rock was the Choiyoi volcanic rocks with minor participation of the Precuyano magmatism. Preliminary U–Pb detrital zircon ages from the El Freno Formation confirm these data, where the age pattern showed main peaks at ca. 204–230 Ma (Precuyano) and 250–262 Ma (Choiyoi) (Fig. 5a) (Naipauer et al. 2014b).

orlando_a_p@yahoo.com.ar

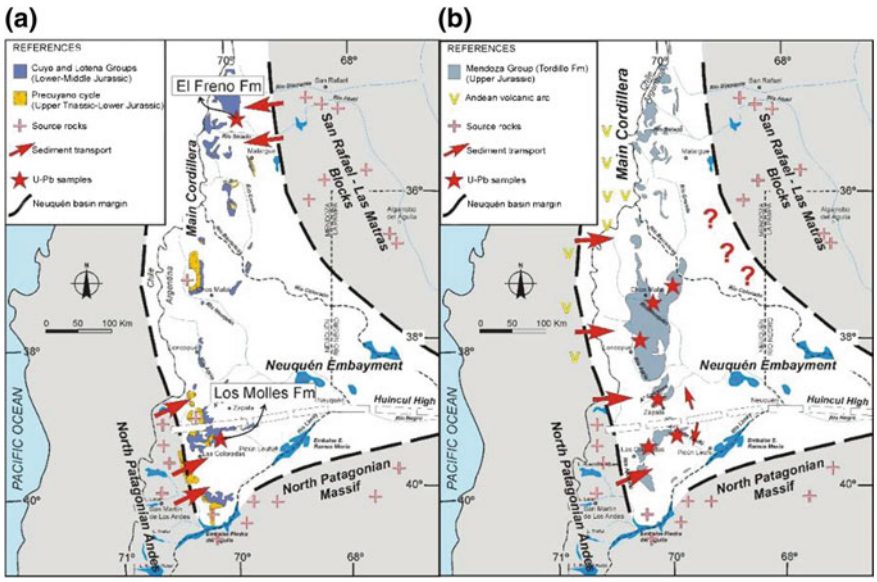


Fig. 5 Paleogeographic sketch map with potential source regions: **a** Precuyano cycle and Cuyo Group (Late Triassic to Early–Middle Jurassic); **b** Tordillo Formation, base of the Mendoza Group (Late Jurassic)

Absolute ages of the synrift volcanism, in the southern part of the basin in the Neuquén Province, range between 219 and 182 Ma (Rapela et al. 1983; Pángaro et al. 2002, 2009; Franzese et al. 2006). U–Pb zircon ages at ca. 203 and 199 Ma were recently obtained by Schiuma and Llambías (2008) for volcanic rocks from two hydrocarbon boreholes located along the Huincul High (Figs. 1 and 2). South of the Huincul High, in the Chacaico depocenter, the synrift deposits of the Lapa Formation were related to an intense volcanic and extensional tectonic environment (Muravchik et al. 2011). Further south, in the Piedra del Águila-Sañicó depocenter, a U–Pb (SHRIMP) age at 191.7 ± 2.8 Ma from a tuff intercalated in the Piedra del Águila Formation was obtained by Spalletti et al. (2010) (Fig. 2).

The source regions for the clastic sediments of the synrift Precuyano cycle were locally and strongly influenced by the active volcanism coeval with an extensional tectonic regime. The Choiyoi magmatic province represented the pre-rift and was the main source rocks of the synrift deposits. The horsts of the rift exhumed and eroded during the extensional phase of the Early Triassic exposing these volcanic rocks (Llambías et al. 2007). On this regional erosion surface the volcanic units of the Late Triassic and Early Jurassic were later deposited (Llambías et al. 2007). Different pre-Late Triassic crustal exhumation levels were developed throughout the basin since Choiyoi volcanic rocks predominate in the north (e.g., El Fortín sedimentary and volcanic complex), while plutonic rocks dominated in the south (Chachil Plutonic Complex, Cerro Granito, etc.).

orlando_a_p@yahoo.com.ar

Above the Precuyano cycle, the first marine transgression of the Cuyo Group from the Paleo-Pacific Ocean occurred and marine deposits appear for the first time on the basin. Silicified fossiliferous carbonate levels at the base outcrop in different parts of the basin, and were integrated by Leanza et al. (2013) in the Chachil Limestone (Weaver 1942). Several thin tuff layers interfingered with the carbonates were dated by U–Pb (CA-ID-TIMS) between ca. 186 and 182 Ma, and interpreted as derived from the Andean volcanic arc (Leanza et al. 2013; Riccardi and Kamo 2014). Los Molles Formation is developed over the previous carbonates; preliminary U–Pb detrital zircon ages in the Los Molles Formation demonstrated a provenance from the Choiyoi basement and Precuyano volcanic rocks present in the south (Naipauer et al. 2013) (Fig. 5a). Paleocurrents of the Los Molles Formation show NE- trends suggesting a source region to the SW (Smith and Spalletti 1995), which is coherent with the U–Pb data. A late synrift phase is interpreted at the base of the Cuyo Group based on the rift paleogeography, which shows that the horsts were not yet completely flooded at that time and remained isolated in some depocenters.

This fact confirms seismic data of the Huincul High where several authors (Silvestro and Zubiri 2008; Pángaro et al. 2002; Mosquera et al. 2011) identified normal faults affecting the sediments of Los Molles Formation.

7 Retroarc—Sag Stage

The end of the rift stage and the beginning of the retroarc stage are not clearly defined yet in the Neuquén Basin. Moreover, this change in the tectonic conditions seems to be diachronic along the basin; while in the north it began in the late Early Sinemurian (Lanés et al. 2008), in the south it began in the Early Toarcian (Pángaro et al. 2009). However, the Chachil Limestone was interpreted as an instantaneous flooding episode connected with an open sea through the Jurassic volcanic arc according to Leanza et al. (2013).

Stratigraphic and structural surface and subsurface studies in the surrounding of the Huincul High documented a period of relative tectonic quiescence since Late Toarcian, when started the thermal subsidence according to Pángaro et al. (2009). Preliminary U–Pb detrital zircon ages from Challacó Formation, in the top of the Cuyo Group, recognize a change in the provenance pattern: a Permo-Triassic source (maximum peak at ca. 270 Ma) coexists with a younger prominent peak at ca. 184 Ma derived from the Andean volcanic arc; Precuyano zircon ages are subordinate (Naipauer et al. 2014a). In the eastern sector of the Cordillera del Viento (Fig. 4) a tuff layer intercalated in the Chacay Melehue Formation, in the top of the Cuyo Group, yielded the ID–TIMS zircon age of 164.6 ± 0.2 Ma (Kamo and Riccardi 2009) (Fig. 2). This absolute age is in agreement with well-documented ammonoid fauna present in the sequence, which defined the Bathonian–Callovian boundary (late-Mid Jurassic) and confirm a near arc volcanic activity in the west (Fig. 5b).

orlando_a_p@yahoo.com.ar

The clastic sediments of the Lotena Group have a well-stratigraphic constraint but provenance studies are still poorly developed (Schiuma et al. 2002). No absolute ages in the Lotena Group were obtained; conglomerates and sandstones at the base would be key levels to analyze provenance, because in the southern sector of the basin, equivalent sediments are related to the beginning of the Huincul High uplift in the Covunco anticline (Zavala 2005).

The clastic sediments and volcanic rocks of the Mendoza Group are the most thoroughly studied in terms of sedimentary provenance. In the base of the group, red beds of the Tordillo Formation have a main source of sediment supply in basic to acidic volcanic rocks (Marchese 1971; Gulisano 1988; Spalletti et al. 2008; Mescua et al. 2008). Gulisano (1988) was the first to suggest that the source area of these clastic, pyroclastic, and volcanic materials was the Andean magmatic arc. Direct evidence of the activity of this arc is observed in the Rio Damas Formation, where andesitic volcanic rocks are interlayered in the clastic sequence (Charrier et al. 2007). The petrographic and geochemical studies agree with an Andean arc source, but provenance from acidic volcanic rocks of the Choiyoi Group was also identified (Spalletti et al. 2008; Mescua et al. 2008).

The summary of U–Pb detrital zircon ages from six analyzed samples for the Tordillo Formation indicates that the most important sediment source was the Jurassic Andean magmatic arc (peaks at ca. 144 Ma, ca. 153 Ma, and ca. 178 Ma). Two secondary source regions are defined according to the prominent peaks at ca. 218 Ma and ca. 275 Ma, which are respectively consistent with ages from the Precuyano cycle and the Choiyoi magmatic province. Less abundant age groups from the Early Palaeozoic to Precambrian could represent evidence for recycling of metamorphic basement sources in the basin (Naipauer et al. 2012, 2014a) (Fig. 5b).

Geochemical studies in black shales of the Vaca Muerta Formation were recently published (Nawratil et al. 2012; Spalletti et al. 2014), analyzing 4300 cutting samples from 58 wells of the southern part of the basin; two sections were distinguished: in the lower section siliciclastic material predominates and in the upper section mudstones and limestones with low organic content are abundant. Spalletti et al. (2014) studied the Tithonian interval of Vaca Muerta Formation; geochemical data show remarkable aspects of the sedimentary environment, provenance, and source areas. The chemical data indicated that the clastic sediments were supplied to the basin from source areas composed of igneous rocks with felsic to intermediate composition. Volcanic rocks linked with the Andean volcanic arc and older with the Choiyoi and Precuyano magmatism were interpreted as the main source rocks by Spalletti et al. (2014). Evidence of the Andean volcanic arc activity is recorded by the ash-fall tuffs interbedded in the black shales. Recently, U–Pb (CA-ID-TIMS) zircon age at 139.55 ± 0.09 Ma was obtained from equivalent tuff levels (Vennari et al. 2014). This indicates that the subaerial volcanic arc activity continued despite the marine transgression during the Early Cretaceous. These precise absolute ages showed an interesting discrepancy between biostratigraphic and absolute ages (see Vennari et al. 2014; Naipauer et al. 2014a).

An important lowstand wedge was developed in the Hauterivian during the deposition of the Agrio Formation. This is represented by the Avilé Member

orlando_a_p@yahoo.com.ar

(Legarreta and Gulisano 1989; Veiga et al. 2007, 2011) which their U–Pb (SHRIMP) detrital zircon ages showed a significant change in the age pattern in comparison with the Tordillo Formation (Naipauer et al. 2014a). The Hauterivian lowstand wedge has a decrease in the relative abundance of the Late Jurassic and Cretaceous zircon ages, as well as an increase in the abundance of the older ages (Tunik et al. 2010). The prominent age peaks show provenance from the synrift volcanism (Precuyano cycle), from the basement of the basin (Choiyoi magmatic province), and from the eastern foreland cratonic region (Grenvillian, Pampean, and Famatinian magmatic arcs) (see Fig. 6). This fact agrees with the petrographic observations made by Marchese (1971), who noted the presence of metamorphic and plutonic clastics in the Avilé Member. Besides, volcanic zircons from tuff layers intercalated in Agua de la Mula Member of the upper Agrio Formation were dated by SHRIMP at ca. 132 Ma (Aguirre-Urreta et al. 2008).

Continental sediments of the Huitrín and Rayoso formations were deposited to the end of the Early Cretaceous showing the final disconnection of the basin with the Paleo-Pacific Ocean (Veiga et al. 2005). These authors concluded that this change in the paleogeography is attributed to the Andean uplift related to the transition from a retroarc basin to a foreland-type basin. U–Pb detrital zircon ages obtained by Tunik et al. (2010) have a provenance pattern similar to those of the Agrio Formation, where no evidence of Cretaceous zircons are present, but show dominant Precambrian to Paleozoic basement sources (Fig. 6). These authors concluded that the sediments of the Agrio and Rayoso formations were derived from erosion of the foreland basement located to the east and southeast of the basin (Tunik et al. 2010). These patterns suggest a provenance reversal in the direction of paleo-drainage in the basin (Fig. 7a).

The lack of Cretaceous zircons in the basin at that time was attributed to the growth of topographic barriers such as the Huincul High in the south or the Cordillera del Viento range in the northwest (Naipauer et al. 2012, 2014a). Even though there are no Late Jurassic and Early Cretaceous detrital zircon ages in the Avilé Member and Rayoso Formation, petrographic studies have demonstrated that the magmatic arc supplied volcanic material into the basin during the Early Cretaceous (Eppinger and Rosenfeld 1996). This source is also detected in the fall tuff layers of the upper Agrio Formation (Aguirre-Urreta et al. 2008).

The reversal of the provenance pattern can be explained by the base-level fall and the creation of incised valleys in the eastern cratonic margin of the Neuquén Basin. In the eastern flank of the basin, a small outcrop of the upper Agrio Formation has been recognized as marine and conglomeratic continental facies (Sagripanti et al. 2014). The conglomerate facies were also known at the subsurface based on borehole data (Vergani et al. 2001; Barrionuevo and Pérez 2002). The occurrence of these conglomerates along the eastern flank of the basin is related to a forced regression (Vergani et al. 2001).

However, an alternative hypothesis is proposed, where uplift and exhumation of the eastern foreland region in the Early Cretaceous explains the Precambrian and Paleozoic zircon supply as well as the conglomerate facies in the Agrio Formation. This exhumation could have been related to the regional uplift occurred during the

orlando_a_p@yahoo.com.ar

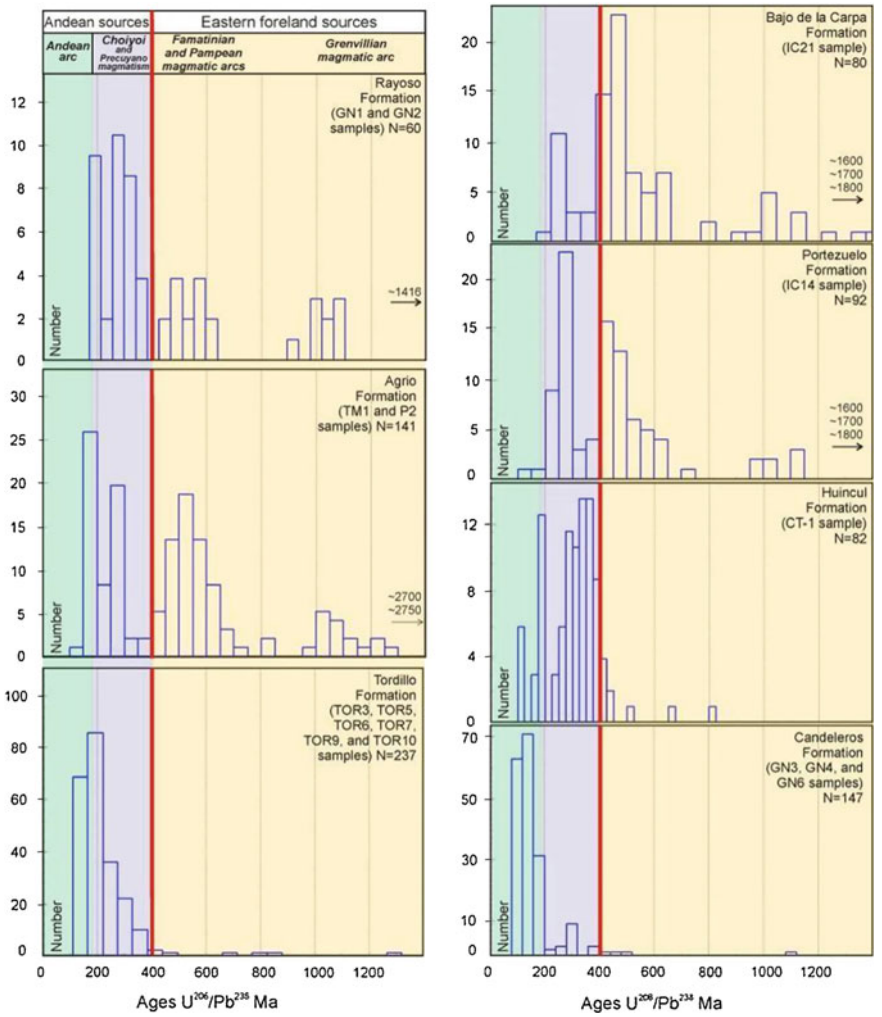


Fig. 6 Frequency histogram of the U–Pb zircon ages for all samples from the Tordillo Formation (Naipauer et al. 2012, 2014a; Agrio Formation (Tunik et al. 2010); Rayoso Formation (Tunik et al. 2010; Di Giulio et al. 2012); and Neuquén Group (Candeleros, Huincul, Portezuelos, and Bajo de la Carpa Formations) (Di Giulio et al. 2012)

Paraná plume and the opening of the South Atlantic. About 1500 km NE of the basin, between ca. 137 and 132 Ma, the mantle plume of Paraná that produced the Paraná-Etendeka LIP (*large igneous province*) was installed. This magmatism is associated with the opening of South Atlantic Ocean (Stica et al. 2013; and references therein). During this period alkaline basalts and NNW-trending narrow rift basins occurred in the Sierras Pampeanas (Kay and Ramos 1996; Lagorio 2008). Another work based on thermochronological data also suggest a period of

orlando_a_p@yahoo.com.ar

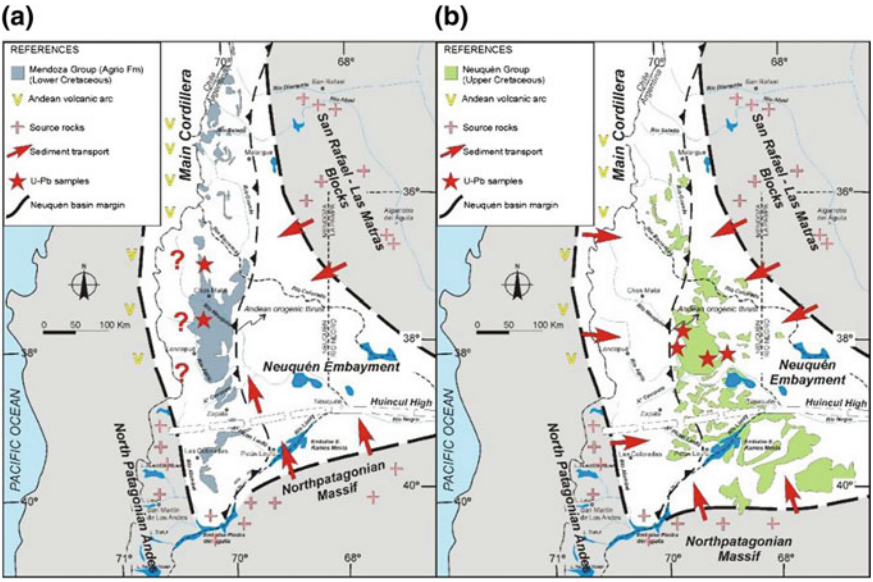


Fig. 7 Paleogeographic sketch map with the potential source region: **a** Agrio Formation, top of the Mendoza Group (Early Cretaceous); **b** Neuquén Group (Late Cretaceous)

exhumation of the Sierra Pampeanas for the Early Cretaceous linked to generation of rift systems (Bense et al. 2013). Therefore, regional uplift occurring during the Paraná plume may have exhumed part of Sierras Pampeanas supplying Precambrian and Paleozoic zircons to the Neuquén Basin in the south.

8 Foreland Stage

Several studies showed that the compressional deformation along the Andes coincides with the beginning of the westward absolute plate motion of the South America Plate (Somoza 1998; Somoza and Zaffarana 2008), associated with the final breakup of western Gondwana (Ramos 2010). Consequently, foreland basins in the backarc were recorded in the early Late Cretaceous, caused by the eastward migration of the orogenic front (Ramos 2010). In the Neuquén basin the compressive regime occurred at ca. 100 Ma with the beginning of the deposition of the red beds of the Neuquén Group (Tunik et al. 2010).

The change of tectonic regime is also reflected in the pattern of detrital zircon ages (Tunik et al. 2010; Di Giulio et al. 2012): at the base, in the Candeleros Formation, the pattern is characterized by the predominance of Jurassic and Cretaceous zircons (ca. 105–198 Ma) indicating exhumation and contribution from the Andean magmatic arc; whereas in the younger units (Huincul, Portezuelo, and

orlando_a_p@yahoo.com.ar

Bajo de la Carpa Formations) Jurassic and Cretaceous zircons are diluted and begin to dominate the oldest ages. Zircon ages comparable with Precuyano and Choiyoi magmatism are present in all units, although in the upper units (Portezuelo and Bajo de la Carpa Formations) Grenvillian, Pampean, and Famatinian zircon ages predominated (see Fig. 6). This indicates a contribution from the eastern cratonic region and a reversal pattern of provenance (Fig. 7b). The change in the provenance was related to the migration of the orogenic front to the east and the development of a peripheral bulge (Di Giulio et al. 2012); a change initially detected in the early work performed by Marchese (1971).

Recently, a sedimentary petrographic study and provenance analysis in the Anacleto Formation, in the top of the Neuquén Group, was published by Armas et al. (2014). The mineral and lithic composition of the sandstones showed the presence of igneous (plutonic and volcanic), metamorphic, and sedimentary rocks in the source areas. These results together with the paleocurrent analysis suggest that the source areas were located in the North Patagonian Massif; contemporaneous activity of the Andean magmatic arc was also interpreted (Armas et al. 2014).

9 Detrital Zircon Record and Tectonic Setting

Cawood et al. (2012) established that the pattern of detrital zircon ages reflect the tectonic setting of the basins where the sediments were generated. The relationship between the zircon pattern and the tectonic setting is principally controlled by the magma production and preservation potential in each tectonic setting; e.g., in convergent margins there is a large volume of magma generated in relation with a passive margin. Consequently, basins linked with convergent margins are characterized by younger zircons close to the time of sediment accumulation, while passive margin basins are characterized by old zircons separated by several million years of the age of sedimentation. The synsedimentary magmatic activity and their preservation in the basin is one of the main factors to distinguish the tectonic setting of the basin where zircons were deposited. Cawood et al. (2012) proposed a model diagram where the difference between the measured crystallization ages of the single grains (*CA*) and the depositional age of the sediment (*DA*) is plotted. In this diagram, three main tectonic settings were recognized, as convergent, collisional, and extensional and different basin types can be differentiated (e.g., foreland, forearc, rift, and others). We plotted the data set obtained in this work in the diagram of Cawood et al. (2012) to investigate a possible relation between the patterns of detrital zircon ages and tectonic setting in the Neuquén Basin (Fig. 8).

Figure 8 a shows detrital zircon age data plotted with respect to sediment depositional age for the Tordillo, Agrio, and Rayoso Formations following Cawood et al. (2012). The cumulative proportion curves obtained for the 237 zircon ages (6 samples) of Tordillo Formation fall clearly in the convergent setting (>30 % of population have *CA–DA* < 100 Ma), having strong similarities with trench and forearc basin settings (South California) represented in Cawood et al. (2012).

orlando_a_p@yahoo.com.ar

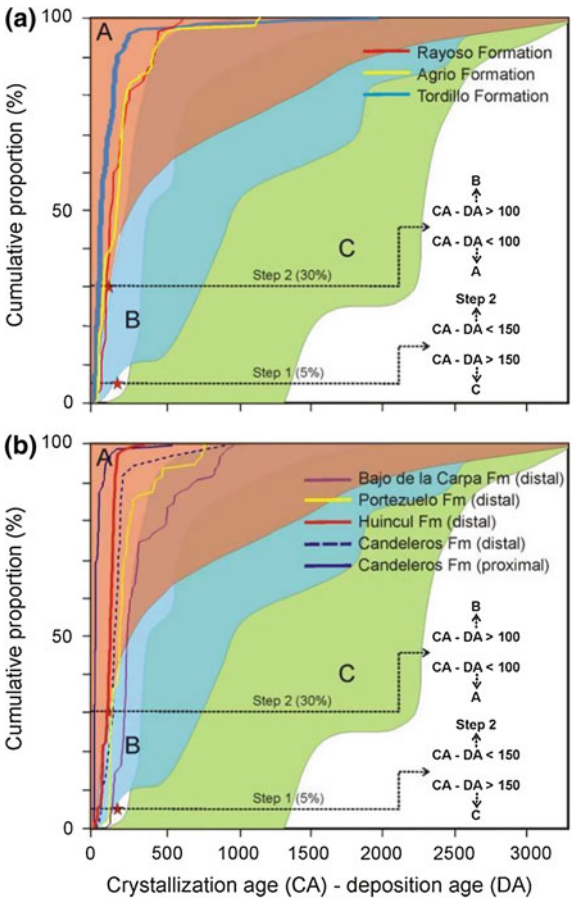


Fig. 8 Crystallization age minus deposition age versus cumulative zircon age proportion diagram (after Cawood et al. 2012); **a** Tordillo (samples TOR-03, TOR-05, TOR-06, TOR-07, TOR-09, and TOR-10), Agrio (samples TM1 and P2), and Rayoso formations (GN-02); **b** Neuquén Group: Candeleros Formation proximal facies (samples GN-03, GN-04, and GN-06) and distal facies (sample AP-07), Huincul Formation distal facies (sample CT-01), Portezuelo Formation distal facies (sample IC-14), and Bajo de la Carpa Formation distal facies (sample IC-21). U–Pb data from the Tordillo Formation after Naipauer et al. (2012, 2014a), Agrio and Rayoso Formations after Tunik et al. (2010), and Neuquén Group after Tunik et al. (2010) and Di Giulio et al. (2012). **a** Convergent setting (*brown field*), **b** Collision setting (*blue field*); and **c** Extensional setting (*green field*)

However, it is clear that the red beds of Tordillo Formation were deposited in a retroarc setting, where their input of volcanic rocks is due to its proximity to the magmatic arc. For the 141 zircon ages (two samples) of Agrio Formation and 60 zircons (one sample) of Rayoso Formation the curves have small variations, plotting in the convergent setting (Fig. 8a). Both curves and pattern of detrital zircons have more similarity with those represented as backarc basins (Terra Australis) in

orlando_a_p@yahoo.com.ar

Cawood et al. (2012). The variation observed in the Tordillo Formation is likely the result of the increased participation of older basement rocks in the source areas.

In Fig. 8b, the data set of different units from the Neuquén Group is plotted. The basal Candeleros Formation was separated in proximal and distal facies in the diagram because the only samples (147 detrital zircon ages) plotted in the convergent setting (>30 % of population have *CA–DA* < 100 Ma) were the proximal facies. The samples corresponding to distal facies for Candeleros (39 zircons), Huincul (82 zircons), Portezuelos (92 zircons), and Bajo de Carpa formations (80 zircons) fall in the collision setting (>30 % of population have *CA–DA* > 100 Ma) because older ages predominate in the patterns of detrital zircon ages. However, the deposition setting of the Neuquén Group would have been a foreland basin in an Andean convergent tectonic setting. It is also clear that these variations are due to changes in the sedimentary provenance of the zircons linked to the proximal or distal facies associated with the development of the peripheral bulge that increases the provenance of old basement sources.

Finally, the pattern of detrital zircon ages for samples from the retroarc setting in the Neuquén Basin was quite consistent with the tectonic discrimination diagram of Cawood et al. (2012). The proximal facies samples for the foreland setting were also consistent. However, the samples corresponding to distal facies in the Neuquén foreland were not consistent with a convergent setting, falling in the collisional setting of Cawood et al. (2012). We attribute this fact to the long distance to the orogenic front, and to the control that had the peripheral bulge could play in the sedimentary provenance. The uplift of the peripheral bulge, as a response to the increasing tectonic loading, exhumed the basement and produced eastern cratonic sources. Therefore, we consider the tectonic discrimination diagram of Cawood et al. (2012) as a successful tool to discriminate tectonic settings in the Southern Central Andes, which can be applied to older orogens with nonobvious tectonic settings. However, it is necessary to consider the relative position of the sedimentary sequence with respect to the magmatic arc and the potential development in foreland stages of peripheral bulges.

10 Conclusions

1. In the rift stage of the Neuquén Basin the source regions were locally and strongly influenced by the active volcanism coeval with extensional tectonic activity. The Choiyoi magmatic province represented the pre-rift stage and it was the main source rock of the synrift deposits. This extensional relief lasted until the first marine transgression at the base of the Cuyo Group in the Early Jurassic.
2. The source regions in the retroarc setting are variable and showed reversal provenance patterns in the Early Cretaceous. In the early stage of the retroarc (Middle to Late Jurassic) the magmatic arc became the most important source region of sediment supply; although older basement sources related to the Huincul High were also exhumed. In the late stage of the sag (Early Cretaceous)

orlando_a_p@yahoo.com.ar

eastern cratonic regions were the main source areas of sediment contribution. The reversal of the provenance pattern can be explained by the base-level fall and establishment of incision valleys in the eastern cratonic margin or by a period of exhumation of the Sierra Pampeanas linked to the generation of rift systems in the Early Cretaceous.

3. The source regions in the foreland stage are also variable. The basal and proximal samples of the Candeleros Formation indicate a mountain chain uplift and exhumation along the Andean magmatic arc in the west; although younger and distal units (Candeleros, Huincul, Portezuelo, and Bajo de La Carpa Formations) show that a peripheral bulge is probably growing in the eastern cratonic sector.
4. The tectonic discrimination diagram of Cawood et al. (2012) may constitute a useful tool to apply in the Southern Central Andes. However, it is necessary to consider more complex settings.

Acknowledgements Maximiliano Naipauer acknowledges the financial support of CONICET and ANPCyT PICT-2010–2099, Argentina.

References

Aguirre-Urreta MB, Pazos PJ, Lazo DG, Fanning CM, Litvak VD (2008) First U-Pb SHRIMP age of the Hauterivian stage, Neuquén Basin, Argentina. J South Am Earth Sci 26:91–99

Aguirre-Urreta MB, Tunik M, Naipauer M, Pazos PJ, Ottone EG, Fanning MC, Ramos VA (2011) Malargüe Group (Maastrichtian–Danian) deposits in the Neuquén Andes, Argentina: implications for the onset of the first Atlantic transgression related to Western Gondwana break-up. Gondwana Res 19(2):482–494

Armas P, Moreno C, Sánchez ML, González F (2014) Sedimentary palaeoenvironment, petrography, provenance and diagenetic inference of the Anacleto Formation in the Neuquén Basin, Late Cretaceous, Argentina. J South Am Earth Sci 53:59–76

Bahlburg H, Vervoort JD, Du Frane SA, Bock B, Augustsso C, Reimann C (2009) Timing of crust formation and recycling in accretionary orogens: Insights learned from the western margin of South America. Earth-Sci Rev 97:215–241

Barrionuevo M, Pérez DE (2002) Reservorios del Miembro Agrio Superior de la Formacio´n Agrio. In: Schiuma M, Hinterwimmer G, Vergani G (eds) Rocas reservorio de las cuencas productivas de la Argentina. Instituto Argentino del Petróleo, Buenos Aires, pp 447–456

Barrionuevo M, Arnosio M, Llambías EJ (2014) Nuevos datos geocronológicos en subsuelo y afloramientos del Grupo Choiyoi en el oeste de La Pampa: implicancias estratigráficas. Rev Asoc Geol Argentina 70(1):31–39

Bense FA, Löbens S, Dunkl I, Wemmer K, Siegesmund S (2013) Is the exhumation of the Sierras Pampeanas only related to Neogene flat-slab subduction? Implications from a multi-thermochronological approach. J South Am Earth Sci 48:123–144

Bracaccini O (1970) Rasgos tectónicos de las acumulaciones Mesozoicas en las provincias de Mendoza y Neuquén. Rev Asoc Geol Argentina 35(2):275–284

Carbone O, Franzese J, Limeres M, Delpino D, Martínez R (2011) El Ciclo Precuyano (Triásico Tardío - Jurásico Temprano) en la Cuenca Neuquina. In: Leanza HA, Arregui C, Carbone O, Danieli JC, Vallés JM (eds) Geología y Recursos Naturales de la Provincia de Neuquén. Relatorio del VXIII Congreso Geológico Argentino, Buenos Aires, pp 63–75

orlando_a_p@yahoo.com.ar

Casquet C, Fanning CM, Galindo C, Pankhurst RJ, Rapela CW, Torres P (2010) The Arequipa Massif of Peru: New SHRIMP and isotope constraints on a Paleoproterozoic inlier in the Grenvillian orogen. J South Am Earth Sci 29:128–142

Cawood PA, Nemchin AA (2001) Source regions for Laurentian margin sediments: constraints from U/Pb dating of detrital zircon in the Newfoundland Appalachians. Geol Soc Am Bulletin 113:1234–1246

Cawood PA, Nemchin AA, Strachan RA, Prave AR, Krabbendam M (2007) Sedimentary basin and detrital zircon record along East Laurentia and Baltica during assembly and breakup of Rodinia. J Geo Soc 164:257–275

Cawood PA, Hawkesworth CJ, Dhuime B (2012) Detrital zircon record and tectonic setting. Geology 40:875–878

Charrier R, Pinto L, Rodríguez M (2007) Tectonostratigraphic evolution of the Andean Orogen in Chile. In: Gibbonds W, Moreno T (eds) The geology of Chile. Geological Society of London, London, pp 21–116 (special Publications)

Chernicoff CJ, Zappettini EO, Santos JOS, Allchurch S, McNaughton NJ (2010) The southern segment of the Famatinian magmatic arc, La Pampa province, Argentina. Gondwana Res 17:662–675

Chernicoff CJ, Zappettini EO, Santos JOS, Godeas MC, Belousova E, McNaughton NJ (2012) Identification and isotopic studies of early Cambrian magmatism (El Carancho Igneous Complex) at the boundary between Pampia terrane and the Río de la Plata craton, La Pampa Province, Argentina. Gondwana Res 21:378–393

Cingolani CA, Llambías EJ, Basei MAS, Varela R, Chemale F Jr, Abre P (2005) Grenvillian and Famatinina-age igneous events in the San Rafael Block, Mendoza Province, Argentina: geochemical and isotopic constraints. In: Pankhurst RJ, Veiga GD (eds) Gondwana 12. Academia Nacional de Ciencias, Mendoza, p 103

Cingolani CA, Zanettini JCM, Leanza HA (2011) El basamento ígneo metamórfico. In: Leanza HA, Arregui C, Carbone O, Danieli JC, Vallés JM (eds) Geología y Recursos Naturales de la Provincia de Neuquén. Relatorio del XVIII Congreso Geológico Argentino, Buenos Aires, pp. 37–47

Cobbold PR, Rossello EA (2003) Aptian to recent compressional deformation of the Neuquén Basin, Argentina. Mar Petrol Geol 20:429–443

Condie KC, Belousova E, Griffi WL, Sircombe KN (2009) Granitoid events in space and time: constraints from igneous and detrital zircon age spectra. Gondwana Res 15:228–242

Darwin C (1946) Geological observations of South America, being the third part of the Geology of the voyage of the Beagle during 1832–1836. Smith Elder and Co., London, p 279

Dellapé DA, Pando GA, Uliana MA, Musacchio EA (1978) Foraminíferos y ostrácodos del Jurásico en las inmediaciones del arroyo Picún Leufú y la ruta 40 (Provincia del Neuquén, Argentina) con algunas consideraciones sobre la estratigrafía de la Formación Lotena. VII Congreso Geológico Argentino (Neuquén). Actas 2:489–507

Di Giulio A, Ronchi A, Sanfilippo A, Tiepolo M, Pimentel M, Ramos VA (2012) Detrital zircon provenance from the Neuquén Basin (South Central Andes): cretaceous geodynamic evolution and sedimentary response in a retroarc-foreland basin. Geology 40:559–562

Digregorio JH (1972) Neuquén. In: Leanza HF (ed) Geología regional Argentina. Academia Nacional de Ciencias, Córdoba, pp 439–505

Digregorio RE, Gulisano CA, Gutiérrez-Pleimling AR, Minitti SA (1984) Esquema de la evolución geodinámica de la Cuenca Neuquina y sus implicancias paleogeográficas. IX Congreso Geológico Argentino (San Carlos de Bariloche). Actas 2:147–162

Eppinger KJ, Rosenfeld U (1996) Western margin and provenance of sediments of the Neuquén Basin (Argentina) in the Late Jurassic and Early Cretaceous. Tectonophysics 259:229–244

Escayola MP, Pimentel M, Armstrong R (2007) Neoproterozoic backarc basin: sensitive high-resolution ion microprobe U-Pb and Sm–Nd isotopic evidence from the Eastern Pampean Ranges, Argentina. Geology 35:495–498

orlando_a_p@yahoo.com.ar

Fedo CM, Sircombe KN, Rainbird, RH (2003) Detrital zircon analysis of the sedimentary record. In: Hanchar JM, Hoskin PWO (eds) Zircon. Reviews in Mineralogy and Geochemistry, vol 53, pp 277–303

Franzese JR (1995) El Complejo Piedra Santa (Neuquén, Argentina): parte de un cinturón metamórfico neopaleozoico del Gondwana suroccidental. Rev Geol Chile 22(2):193–202

Franzese JR, Spalletti LA (2001) Late Triassic-early Jurassic continental extension in southwestern Gondwana: tectonic segmentation and pre-break-up rifting. J South Am Earth Sci 14:257–270

Franzese JR, Veiga GD, Schwarz E, Gómez-Pérez I (2006) Tectono-stratigraphic evolution of a Mesozoic graben border system: the Chachil depocentre, southern Neuquén Basin, Argentina. J Geol Soc 163:207–221

García Morabito E, Ramos VA (2012) Andean evolution of the Aluminé fold and thrust belt, Northern Patagonian Andes (38°30′–40°30′ S). J South Am Earth Sci 38:13–30

Groeber P (1929) Líneas fundamentales de la geología del Neuquén, sur de Mendoza y regiones adyacentes. Dirección Nacional de Geología y Minería, Buenos Aires, Publicación, vol 58, pp 1–110

Groeber P (1946) Observaciones geológicas a lo largo del meridiano n° 70°. 1. Hoja Chos Malal. Servicio Geológico Minero Nacional, Boletín 1(3):177–208

Groeber P (1948) Las plataformas submarinas y su edad. Rev Ciencia Investigación 6:224–231

Gulisano CA (1981) El ciclo cuyano en el norte de Neuquén y sur de Mendoza. XVIII Congreso Geológico Argentino (San Juan). Actas 3:573–592

Gulisano CA (1988) Análisis estratigráfico y sedimentológico de la Formación Tordillo en el oeste de la Provincia del Neuquén, Cuenca Neuquina, Argentina. Unpublished PhD thesis, Facultad de Ciencias Exactas y Naturales, Universidad de Buenos Aires, p 235

Guilisano CA, Gutiérrez Pleimling AR, Digregorio RE (1984) Esquema estratigrafico de la secuencia jurásica del oeste de la provincia del Neuquén. IX Congreso Geológico Argentino (San Carlos de Bariloche). Actas 1:236–259

Hervé F, Faúndez V, Calderón M, Massonne H-J, Willner AP (2007) Metamorphic and plutonic basement complexes. In: Moreno T, Gibbons W (eds) The Geology of Chile. Geological Society of London, London, pp 5–20

Hervé F, Calderón M, Fanning CM, Pankhurst RJ, Godoy E (2013) Provenance variations in the Late Paleozoic accretionary complex of central Chile as indicated by detrital zircons. Gondwana Res 23:1122–1135

Howell JA, Schwarz E, Spalletti LA, Veiga GD (2005) The Neuquén Basin: an overview. In: Veiga GD, Spalletti LA, Howell JA, Schwarz E (eds) The Neuquén Basin, Argentina: a case study in sequence stratigraphy and basin dynamics. Geological Society of London, London, Special Publications vol 352, pp 1–14

Kamo SL, Riccardi AC (2009) A new U-Pb zircon age for an ash layer at the Bathonian-Callovian boundary, Argentina. GFF 131:177–182

Kay SM, Ramos VA (1996) El magmatismo cretácico de las sierras de Córdoba y sus implicancias tectónicas. XIII Congreso Geológico Argentino and III Congreso de Exploración de Hidrocarburos, Buenos Aires. Actas 3:453–464

Kay SM, Ramos VA, Mpodozis C, Sruoga P (1989) Late Paleozoic to Jurassic silicic magmatism at the Gondwana margin: analogy to middle proterozoic in north America? Geology 17:324–328

Keidel J (1927) Sobre las relaciones geológicas entre la Puna y la Cordillera Principal o Cordillera de Los Andes. Academia Nacional de Ciencias, Córdoba, Boletín 30:295–307

Lagorio SL (2008) Early Cretaceous alkaline volcanism of the Sierra Chica de Córdoba (Argentina): Mineralogy, geochemistry and petrogenesis. J South Am Earth Sci 26:152–171

Lanés S (2005) Late Triassic to Early Jurassic sedimentation in northern Neuquén Basin, Argentina: Tectonosedimentary evolution of the first transgression. Geol Acta 3(2):81–106

Lanés S, Giambiagi L, Bechis F, Tunik M (2008) Late Triassic—Early Jurassic successions of the Atuel depocenter: sequence stratigraphy and tectonic controls. Rev Asoc Geol Argentina 63 (4):534–548

orlando_a_p@yahoo.com.ar

Leanza HA (1973) Estudio sobre los cambios faciales de los estratos limítrofes Jurásico-Cretácicos entre Loncopué y Picún Leufú, Prov. del Neuquén, Rep. Argentina. Rev Asoc Geol Argentina 28:97–132

Leanza HA (1992) Estratigrafía del Paleozoico y Mesozoico anterior a los Movimientos Intermálmicos en la comarca del cerro Chachil, provincia del Neuquén. Rev Asoc Geol Argentina 45(3–4):272–299

Leanza HA, Apesteguía S, Novas FE, de la Fuente MS (2004) Cretaceous terrestrial beds from the Neuquén Basin (Argentina) and their tetrapod assemblages. Cretac Res 25:61–87

Leanza HA, Mazzini A, Corfu F, Llambías EJ, Svensen H, Planke S, Galland O (2013) The Chachil Limestone (Pliensbachian-earliest Toarcian) Neuquén Basin, Argentina: U-Pb age calibration and its significance on the early Jurassic evolution of southwestern Gondwana. J South Am Earth Sci 42:171–185

Legarreta L, Gulisano CA (1989) Análisis estratigráfico secuencial de la Cuenca Neuquina (Triásico superior-Terciario inferior, Argentina). In: Chebli G, Spalletti L (eds) Cuencas Sedimentarias Argentinas. Serie Correlación Geológica (6) Universidad Nacional de Tucumán, pp 221–243

Legarreta L, Uliana MA (1991) Jurassic–Cretaceous marine oscillations and geometry of backarc basin fill, central Argentine Andes. In: Macdonald DIM (ed) Sedimentation, tectonics and eustasy, sea level changes at active plate margins. International Association of Sedimentologists, Oxford, Special Publication, vol 12, pp 429–450

Legarreta L, Uliana MA (1999) El Jurásico y Cretácico de la Cordillera Principal y Cuenca Neuquina. In: Caminos R (ed) Geología Argentina. Instituto de Geología y Recursos Minerales, Buenos Aires, Anales, vol 29, pp 399–432

Lenaza HA, Sattler F, Martinez RS, Carbone O (2011) La Formación Vaca Muerta y equivalentes (Jurásico Tardío– Cretácico Temprano) en la Cuenca Neuquina. In: Leanza HA, Arregui C, Carbone O, Danieli JC, Vallés JM (eds) Geología y Recursos Naturales de la Provincia de Neuquén. Relatorio del VXIII Congreso Geológico Argentino, Buenos Aires, pp 113–129

Linares E, Cagnoni MC, Do Campo M, Ostera HA (1988) Geochronology of metamorphic and eruptive rocks of southeastern Neuquén and northwestern Río Negro Provinces, Argentine Republic. J South Am Earth Sci 1(1):53–61

Llambías EJ, Sato AM (2011) Ciclo Gondwánico: la provincia magmática Choiyoi en Neuquén. In: Leanza HA, Arregui C, Carbone O, Danieli JC, Vallés JM (eds) Geología y Recursos Naturales de la Provincia de Neuquén. Relatorio del VXIII Congreso Geológico Argentino, Buenos Aires, pp 53–62

Llambías EJ, Sato AM, Basei MAS (2005) El basamento prejurásico medio en el anticlinal Chihuido, Malargüe: evolución magmática y tectónica. Rev Asoc Geol Argentina 60 (3):567–578

Llambías EJ, Leanza HA, Carbone O (2007) Evolución tectono-magmática durante el Pérmico al Jurásico Temprano en la Cordillera del Viento (37°05′ S–37°15′ S): nuevas evidencias geológicas y geoquímicas del inicio de la cuenca Neuquina. Rev Asoc Geol Argentina 62 (2):217–235

Marchese HG (1971) Litoestratigrafía y variaciones faciales de las sedimentitas mesozoicas de la Cuenca Neuquina, provincia de Neuquén, República Argentina. Rev Asoc Geol Argentina 26 (3):343–410

Mescua JF, Giambiagi LB, Bechis F (2008) Evidencias de tectónica extensional en el Jurásico Tardío (Kimmeridgiano) del suroeste de la provincia de Mendoza. Rev Asoc Geol Argentina 63(4):512–519

Mosquera A, Silvestro J, Ramos VA, Alarcón M, Zubiri M (2011) La estructura de la Dorsal de Huincul. In: Leanza HA, Arregui C, Carbone O, Danieli JC, Vallés JM (eds) Geología y recursos naturales de la provincia de Neuquén. Relatorio del XVIII Congreso Geológico Argentino, Buenos Aires, pp 385–397

Mpodozis C, Ramos VA (2008) Tectónica Jurásica en Argentina y Chile: extensión, subducción oblicua, rifting, deriva y colisiones? Rev Asoc Geol Argentina 63(4):481–497

orlando_a_p@yahoo.com.ar

Mueller PA, Heatherington AL, Wooden JL, Shuster RD, Nutman AP, Williams IS (1994) Precambrian zircons from the Florida basement: A Gondwana connection. Geology 22:119–122

Muravchik M, D'elia L, Bilmes A, Franzese JR (2011) Syn-eruptive/inter-eruptive relations in the syn-rift deposits of the Precuyano Cycle, Sierra de Chacaico, Neuquén Basin, Argentina. Sediment Geol 238:132–144

Naipauer M, García Morabito E, Marques JC, Tunik V, Rojas Vera E, Vujovich GI, Pimentel MP, Ramos VA (2012) Intraplate Late Jurassic deformation and exhumation in western central Argentina: Constraints from surface data and U-Pb detrital zircon ages. Tectonophysics 524–525:59–75

Naipauer M, García Morabito E, Manassero MJ, Ramos VA (2013) Primeras edades U-Pb en circones detríticos de la Formación Los Molles (Grupo Cuyo) del sur de la cuenca Neuquina: áreas de aporte y edad máxima de sedimentación. V Simposio Argentino del Jurásico (Trelew) Libro de Resúmenes, p 39

Naipauer M, Tunik M, Marques JC, Rojas Vera EA, Vujovich GI, Pimentel MM, Ramos VA (2014a) U-Pb detrital zircon ages of Upper Jurassic continental successions: implications for the provenance and absolute age of the Jurassic-Cretaceous boundary in the Neuquén Basin. In: Sepúlveda S, Giambiagi L, Pinto L, Moreiras S, Tunik M, Hoke G, Farías M (eds) Geodynamic processes in the Andes of Central Chile and Argentina, Geological Society of London, London, Special Publications 399 (accepted manuscript)

Naipauer M, Tapia F, Farías M, Pimentel MM, Ramos VA (2014b) Evolución mesozoica de las áreas de aporte sedimentario en el sur de los Andes Centrales: el registro de las edades U-Pb en circones. XIX Congreso Geológico Argentino (Córdoba). Actas, pp S22–44

Nawratil A, Gómez H, Larriestra C (2012) Key tools for black shales evaluation: geostatistics and inorganic geochemistry applied to Vaca Muerta Formation, Neuquén Basin, Argentina. International conference and exhibition (Singapore). Am Assoc Pet Geol, article # 41028

Pángaro F, Veiga R, Vergani G (2002) Evolución tecto-sedimentaria del área de Cerro Bandera, Cuenca Neuquina, Argentina. V Congreso de Exploración y Desarrollo de Hidrocarburos (Mar del Plata), p 16

Pángaro F, Pereira DM, Micucci E (2009) El sinrift de la Dorsal de Huincul, Cuenca Neuquina: evolución y control sobre la estratigrafía y estructura del área. Rev Asoc Geol Argentina 65 (2):265–277

Pankhurst RJ, Hervé F (2007) Introduction and overview. In: Moreno T, Gibbons W (eds) The geology of Chile. Geological Society of London, London, pp 1–4

Pankhurst R, Rapela C, Fanning C, Márquez M (2006) Gondwanide continental collision and the origin of Patagonia. Earth-Science Rev 76:235–257

Pankhurst RJ, Rapela CW, López De Luchi MG, Rapalini AE, Fanning CM, Galindo C (2014) The Gondwana connections of northern Patagonia. J Geol Soc 171(3):313–328

Ramos VA (1978) Estructura. Geología y Recursos Naturales de la Provincia de Neuquén. Relatorio del VII Congreso Geológico Argentino, pp 99–118

Ramos VA (1984) Patagonia: un continente paleozoico a la deriva? IX Congreso Geológico Argentino (San Carlos de Bariloche). Actas 2:311–325

Ramos VA (1988) Tectonics of the Late Proterozoic e Early Paleozoic: a collisional history of Southern South America. Episodes 11:168–174

Ramos VA (1999) Las provincias geológicas del territorio argentino. In: Caminos RL (ed) Geología Argentina. Segemar Anales vol 29, no 3, pp 41–96

Ramos VA (2004) Cuyania, an exotic block to Gondwana: review of a historical success and the present problems. Gondwana Res 7:1009–1026

Ramos VA (2008) Patagonia: a Paleozoic continent adrift? J South Am Earth Sci 26:235–251

Ramos VA (2010) The tectonic regime along the Andes: present-day and Mesozoic regimes. Geol J 45:2–25

Ramos VA, Basei M (1997) The basement of Chilenia: an exotic continental terrane to Gondwana during the Early Paleozoic. In: Bradshaw JD, Weaver SD (eds) Terrane Dynamics-97, International conference on terrane geology (Christchurch), conference abstracts, pp 140–143

orlando_a_p@yahoo.com.ar

Ramos VA, Folguera A (2005) Tectonic evolution of the Andes of Neuquén: Constraints derived from the magmatic arc and foreland deformation. In: Veiga GD, Spalletti LA, Howell JA, Schwarz E (eds) The Neuquén Basin: a case study in sequence stratigraphy and basin dynamics. Geological Society of London, London, Special Publications vol 252,pp 15–35

Ramos VA, Naipauer M (2014) Patagonia: where does it come from? J Iber Geol 40(2):367–379

Ramos VA, García Morabito E, Hervé F, Fanning CM (2010a) Grenville-age sources in Cuesta de Rahue, northern Patagonia: constrains from U-Pb/SHRIMP ages from detrital zircons. In: International geological congress on the southern Hemisphere. Boll Geofis vol 51, pp 42–44

Ramos VA, Vujovich G, Martino R, Otamendi J (2010b) Pampia: a large cratonic block missing in the Rodinia supercontinent. J Geodyn 50:243–255

Rapalini AE, López de Luchi M, Tohver E, Cawood PA (2013) The South American ancestry of the North Patagonian Massif: geochronological evidence for an autochthonous origin? Terra Nova 25:337–342

Rapela CW, Spalletti L, Merodio J (1983) Evolución magmática y geotectónica de la "Serie Andesitica" andina (Paleoceno-Eoceno) en la Cordillera Norpatagónica. Rev Asoc Geol Argentina 38:469–484

Riccardi AC (2008a) The marine Jurassic of Argentina: a biostratigraphic framework. Episodes 31 (3):326–335

Riccardi AC (2008b) El Jurásico de la Argentina y sus amonites. Rev Asoc Geol Argentina 63 (4):625–643

Riccardi AC, Kamo S (2014) Biostratigraphy and geochronology of the Pliensbachian-Toarcian boundary in Argentina. XIX Congreso Geológico Argentino (Córdoba). Actas T1–42

Rocha-Campos AC, Basei MAS, Nutman AP, Kleiman LE, Varela R, Llambías E, Canile FM, da Rosa ODCR (2011) 30 million years of Permian volcanism recorded in the Choiyoi igneous province (W Argentina) and their source for younger ash fall deposits in the Paraná Basin: SHRIMP U/Pb zircon geochronology evidence. Gondwana Res 19:509–523

Sagripanti L, Aguirre-Urreta B, Folguera A, Ramos VA (2014) The Neocomian of Chachahue´n (Mendoza, Argentina): evidence of a broken foreland associated with the Payenia flat-slab. In Sepúlveda S, Giambiagi L, Pinto L, Moreiras S, Tunik M, Hoke G, Farías M (eds) Geodynamic processes in the Andes of Central Chile and Argentina. Geological Society of London, London, Special Publications 399 (accepted manuscript)

Sato AM, Tickyj H, Llambías E, Basei M, González P (2004) Las Matras Block, Central Argentina (37°S–67°W): the southernmost Cuyania Terrane and its relationship with the Famatinian orogeny. Gondwana Res 7(4):1077–1087

Sato AM, Llambías EJ, Basei MAS, Leanza HA (2008) The Permian Choiyoi Cycle in Cordillera del Viento (Principal Cordillera, Argentina): over 25 Ma of magmatic activity. VI South American Symposium on Isotope Geology (San Carlos de Bariloche). In: Proceedings in CD-ROM, p 4

Schiller W (1912) La alta cordillera de San Juan y Mendoza y parte de la provincia de San Juan, Ministerio de Agricultura de La Nación, Sección Geología, Mineralogía y Minería. Buenos Aires Anales 7:1–68

Schiuma M, Llambías EJ (2008) New ages and chemical analysis on Lower Jurassic volcanism close to the Huincul High, Neuquén. Rev Asoc Geol Argentina 63(4):644–652

Schiuma M, Saavedra C, Malone P, Cevallos M, Rebori L, Vergani G (2002) Los reservorios del Grupo Lotena. In: Schiuma M, Vergani G, Hinterwimmer G (eds) Rocas reservorios de las cuencas productivas argentinas. V Congreso de Exploración y Desarrollo de Hidrocarburos (Mar del Plata), CD-ROM

Schwarz E, Howell JA (2005) Sedimentary evolution and depositional architecture of a lowstand sequence set: the Lower Cretaceous Mulichinco Formation, Neuquén Basin, Argentina. In: Veiga GD, Spalletti LA, Howell JA, Schwarz E (eds) The Neuquén Basin, Argentina: a case study in sequence stratigraphy and basin dynamics. Geological Society of London, London, Special Publications vol 252, pp 109–138

Silvestro J, Zubiri M (2008) Convergencia oblicua: modelo estructural alternativo para la Dorsal Neuquina (39°S), Neuquén. Rev Asoc Geol Argentina 63(1):49–64

orlando_a_p@yahoo.com.ar

Smith RDA, Spalletti LA (1995) Erosional, depositional and post-depositional features of a turbidite channel-fill, Jurassic, Neuquén Basin, Argentina. In: Pickering KT, Hiscott RN, Kenyon NH, Ricci Lucchi F, Smith RDA (eds) Atlas of deep water environments: architectural style n turbidite systems. Chapmen and Hall, London, pp 162–166

Somoza R (1998) Updated Nazca (Farallon)-South American relative motions during the last 40 my: Implications for mountain building in the Andes. J South Am Earth Sci 11:211–215

Somoza R, Zaffarana CB (2008) Mid-Cretaceous polar standstill of South America, motion of the Atlantic hotspots and the birth of the Andean Cordillera. Earth Planet Sci Lett 71 (1–4):267–277

Spalletti LA, Queralt I, Matheos SD, Colombo F, Maggi J (2008) Sedimentary petrology and geochemistry of siliciclastic rocks from the upper Jurassic Tordillo Formation (Neuquén Basin, western Argentina): implications for provenance and tectonic setting. J South Am Earth Sci 25:440–463

Spalletti LA, Franzese J, Morel E, D´Elia L, Zúñiga A, Fanning M (2010) Consideraciones acerca de la sedimentología, paleobotánica y geocronología de la Formación Piedra del Águila (Jurásico Inferior, Neuquén). Rev Asoc Geol Argentina 66(3):305–313

Spalletti LA, Schwarz E, Veiga GD (2014) Geoquímica inorgánica como indicador de procedencia y ambiente sedimentario en sucesiones de lutitas negras: los depósitos transgresivos titonianos (Formación Vaca Muerta) de la Cuenca Neuquina, Argentina. Andean Geol 41(2):401–435

Stelzner A (1876) Geologie der Argentinischen Republik. In: Napp R (ed) Die argentinischen Republik, Buenos Aires, p 71

Stica JM, Zalán PV, Ferrari AL (2013) The evolution of rifting on the volcanic margin of the Pelotas Basin and the contextualization of the Paraná-Etendeka LIP in the separation of Gondwana in the South Atlantic. Mar Petrol Geol 50:1–21

Stipanicic PN (1951) Sobre la presencia del Oxfordense superior en el arroyo de La Manga. Rev Asoc Geol Argentina 6(4):213–239

Stipanicic PN (1966) El Jurásico en Vega de la Veranda (Neuquén), el Oxfordense y el diastrofismo Divesiano (Agassiz-Yaila) en Argentina. Rev Asoc Geol Argentina 20(4):403–478

Stipanicic PN (1967) Consideraciones sobre las edades de algunas fases magmáticas del Neopaleozoico y Mesozoico. Rev Asoc Geol Argentina 22(2):101–133

Stipanicic PN, Rodrigo F, Baulies OL, Martínez CG (1968) Las Formaciones presenonianas en el denominado Macizo Nordpatagónico y regiones adyacentes. Rev Asoc Geol Argentina 23 (2):367–388

Thomas WA, Tucker RD, Astini RA, Denison RE (2012) Ages of pre-rift basement and synrift rocks along the conjugate rift and transform margins of the Argentine Precordillera and Laurentia. Geosphere 8(6):1366–1383

Tunik MA, Lanés S, Bechis F, Giambiagi L (2008) Análisis petrográfico de las areniscas jurásicas tempranas en el depocentro Atuel de la cuenca Neuquina. Rev Asoc Geol Argentina 63 (4):714–727

Tunik M, Folguera A, Naipauer M, Pimentel MM, Ramos VA (2010) Early uplift and orogenic deformation in the Neuquén Basin: Constraints on the Andean uplift from U-Pb and Hf isotopic data of detrital zircons. Tectonophysics 489(1–4):258–273

Uliana MA, Biddle KT (1988) Mesozoic-Cenozoic paleogeographic and geodynamic evolution of southern South America. Rev Bras Geocienc 18:172–190

Uliana MA, Dellapé DA (1981) Estratigrafía y evolución paleoambiental de la sucesión maastrichtiano-eoterciaria del Engolfamiento Neuquino (Patagonia septentrional). VIII Congreso Geológico Argentino (San Luis). Actas 3:673–711

Varela R, Basei MAS, Cingolani CA, Siga O Jr, Passarelli CR (2005) El basamento cristalino de los Andes Norpatagónicos en Argentina: geocronología e interpretación tectónica. Rev Geol Chile 32(2):167–187

Varela R, Basei MAS, González PD, Sato AM, Naipauer M, Campos Neto M, Cingolani CA, Meira TV (2011) Accretion of Grenvillian terranes to the west of the Rio de la Plata craton, west of Argentina. Int J Earth Sci 100(2):243–272

orlando_a_p@yahoo.com.ar

Veiga GD, Howell JA, Stromback A (2005) Anatomy of a mixed marine-non-marine lowstand wedge in a ramp setting. The record of a Barremian-Aptian complex relative sea-level fall in the central Neuquén Basin, Argentina. In: Veiga GD, Spalletti LA, Howell JA, Schwarz E (eds) The Neuquén Basin, Argentina: a case study in sequence stratigraphy and Basin dynamics. Geological Society of London, Special Publications, vol 252, pp 139–162

Veiga GD, Spalletti LA, Flint SS (2007) Anatomy of a fluvial lowstand wedge: the Avilé Member of the Agrio Formation (Hauterivian) in central Neuquén Basin (NW Neuquén province), Argentina. In: Nichols G, Williams E, Paola C (eds) Sedimentary environments, processes and basins, a tribute to Peter Friend. International Association of Sedimentologists, Special Publications, vol 38, pp 341–365

Veiga GD, Spalletti LA, Schwarz E (2011) El Miembro Avilé de la Formaicón Agrio (Cretácico Temprano). In: Leanza HA, Arregui C, Carbone O, Danieli JC, Vallés JM (eds) Geología y Recursos Naturales de la Provincia de Neuquén. Relatorio del VXIII Congreso Geológico Argentino, Buenos Aires, pp 161–173

Vennari VV, Lescano M, Naipauer M, Aguirre-Urreta B, Concheyro A, Schaltegger U, Armstrong R, Pimentel M, Ramos VA (2014) New constraints in the Jurassic-Cretaceous boundary in the High Andes using high-precision U-Pb data. Gondwana Res 26:374–385

Vergani GD, Tankard AJ, Belotti HJ, Welsink HJ (1995) Tectonic evolution and paleogeography of the Neuquén Basin, Argentina. In: Tankard AJ, Suárez SR, Welsink HJ (eds) Petroleum Basins of South America, Bulletin of the American Association of Petroleum Geologists, vol 62, pp 383–402

Vergani GD, Barrionuevo M, Sosa H, Pedrazzini M (2001) Análisis estratigráfico secuencial de alta resolución en las formaciones Agrio y Huitrín del Yacimiento Puesto Hernández. Boletín Inf Pet 67:76–87

Vicente JC (2005) Dynamic paleogeography of the Jurassic Andean Basin: pattern of transgression and localization of main straits through the magmatic arc. Rev Asoc Geol Argentina 60:221–250

Vicente JC (2006) Dynamic paleogeography of the Jurassic Andean Basin: pattern of regression and general considerations on main features. Rev Asoc Geol Argentina 61:408–437

Weaver C (1942) A general summary of the Mesozoic of South and Central America. In: Proceedings XVIII American Science Congress, Geology, Washington, DC, pp 149–193

Yrigoyen MR (1972) Cordillera principal. In: Leanza AF (ed) Geología regional argentina. Córdoba, Academia Nacional Ciencias, pp 345–364

Zamora Valcarce G, Zapata T, Del Pino D, Ansa A (2006) Structural evolution and magmatic characteristics of the Agrio Fold-and-thrust belt. In: Kay SM, Ramos VA (eds) Evolution of an Andean margin: a tectonic and magmatic view from the Andes to the Neuquén Basin (35°–39° lat). Geo Soc Am 407:125–145 (special paper)

Zappettini EO, Chernicoff CJ, Santos JOS, Dalponte M, Belousova E, McNaughton N (2012) Retrowedge-related Carboniferous units and coeval magmatism in the northwestern Neuquén province, Argentina. Int J Earth Sci 101(8):2083–2104

Zavala C (2005) Tracking sea bed topography in the Jurassic. The Lotena Group in the Sierra de la Vaca Muerta (Neuquén Basin, Argentina). Geol Acta 3(2):107–118

orlando_a_p@yahoo.com.ar

Cenozoic Orogenic Evolution of the Southern Central Andes (32–36°S)

Laura Giambiagi, José Mescua, Florencia Bechis, Gregory Hoke, Julieta Suriano, Silvana Spagnotto, Stella Maris Moreiras, Ana Lossada, Manuela Mazzitelli, Rafael Toural Dapoza, Alicia Folguera, Diego Mardonez and Diego Sebastián Pagano

Abstract This review explores the complex interactions of endogenic and exogenic processes in the segment of the Andes that straddle a transition from the Pampean flat slab to a normal subduction segment (32°–36°S). This segment shows remarkable along-strike variations in topographic uplift, structural elevation, amount and rate of shortening, and crustal root geometry. In the flat-slab segment, high elevations, the development of several tectonic provinces (mountain systems) and the lack of active volcanism characterize the orogen. Deformation and uplift advanced to the east, together with arc-related magmatic activity, sequentially uplifting the Principal Cordillera (20 to ~8 Ma), the Frontal Cordillera (12–5 Ma), the Precordillera (<10 Ma) and the Sierras Pampeanas (<5 Ma). In the normal subduction segment to the south, the Andes are characterized by a decrease in

L. Giambiagi (✉) · J. Mescua · S.M. Moreiras · A. Lossada · R.T. Dapoza
Centro Regional de Investigaciones Científicas y Tecnológicas, IANIGLA,
CCT Mendoza, Mendoza, Argentina
e-mail: lgiambia@mendoza-conicet.gob.ar

F. Bechis
IIDyPCa, CONICET, Universidad Nacional de Río Negro, Mitre 630,
CP 8400 San Carlos de Bariloche, Argentina

G. Hoke
Department of Earth Sciences, Syracuse University, Syracuse, NY 13244, USA

J. Suriano
Departamento de Ciencias Geológicas, Facultad de Ciencias Exactas y Naturales,
Instituto de Geociencias Básicas, Aplicadas y Ambientales (IGEBA) UBA-CONICET,
Buenos Aires, Argentina

S. Spagnotto
Departamento de Física, Universidad Nacional de San Luis, San Luis, Argentina

M. Mazzitelli · D. Mardonez · D.S. Pagano
CONICET, Universidad Nacional de San Luis, San Luis, Argentina

A. Folguera
SEGEMAR, Buenos Aires, Argentina

© Springer International Publishing Switzerland 2016

A. Folguera et al. (eds.), *Growth of the Southern Andes*,
Springer Earth System Sciences, DOI 10.1007/978-3-319-23060-3_4

orlando_a_p@yahoo.com.ar

elevation, with a big step in topography at ~35°S and the development of an active magmatic arc straddling the Argentina-Chile border. The Frontal Cordillera is only in the northern part of the normal subduction segment, disappearing at 34°S; only the Principal Cordillera remains south of this latitude. Similarly, deformation progressively advanced to the east, uplifting the Principal Cordillera (20–8 Ma), the Frontal Cordillera (<10 Ma) and the San Rafael basement block (<5 Ma). The amount of shortening systematically decreases from north to south along these two segments, but at the transitional zone between flat and normal subduction zones, there is a sharp decline from ~180 km of shortening (32°S) to ~70 km (33°40′S). South from this latitude, the amount of shortening lineally decreases until it reaches ~30 km at 35°S. Yet, interestingly, the amount of late Miocene surface uplift is opposite to the trend in crustal shortening. These along-strike variations are best explained by boundary conditions of the subduction system related to interplate dynamics controlling the overall pattern of tectonic shortening. However, local variations in mean topographic elevation, deformation styles and crustal root geometry are more likely to be due to upper-plate lithospheric strength variations. These strength variations have governed the coupling degree between brittle upper crust and ductile lower crust deformation. In the flat-slab segment, an initial thick and felsic crust favors the coupling model; while in the normal subduction segment, a thin and mafic lower crust allows the uncoupling model.

Keywords Southern Central Andes · late Miocene-Quaternary contraction · late Oligocene extension

1 Introduction

The Andes of Central Chile and Argentina (32–36°S) straddle a transition from flat slab to normal subduction (Fig. 1), making them an ideal setting to evaluate the interplay between deep, constructive mechanisms that build mountains and destructive ones that erode and sculpt the landscape in an active convergent margin. The complex interactions of endogenic and exogenic processes in the Andean orogen represent the principal aim of this review.

The topographic elevation and crustal thickness of the Andes has long been recognized to be the product of crustal shortening due the convergence of the Nazca and South American plates. While interplate dynamics control the overall pattern of tectonic shortening, this sector of the Andes shows remarkable along-strike variations in the pattern of deformation, with abrupt changes in horizontal shortening and topography. Despite these variations, orogenic width remains relatively constant. In this review, we analyze the controlling factors of these latitudinal changes, comparing different parameters, such as upper-plate lithospheric strength variations.

orlando_a_p@yahoo.com.ar

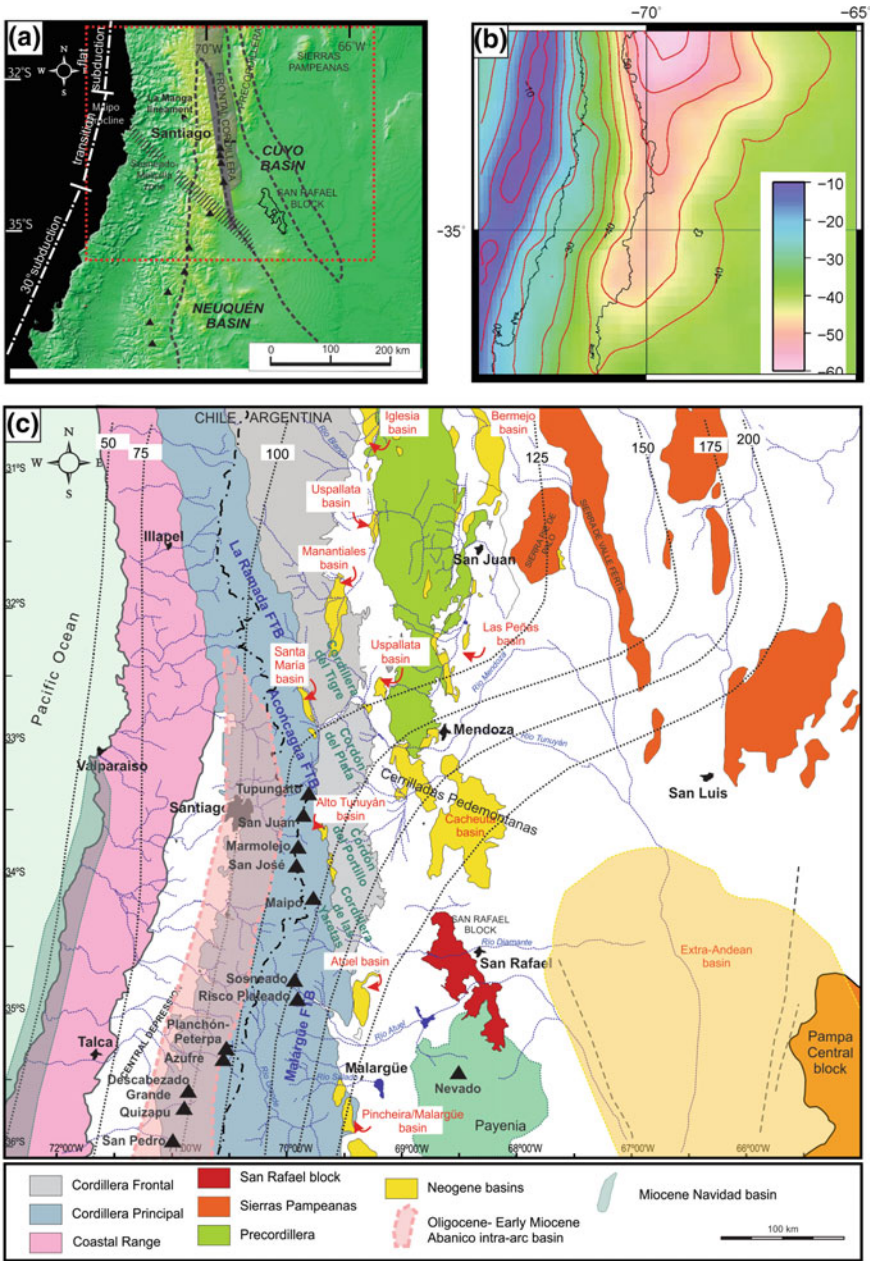


Fig. 1 **a** Shaded relief map of the Andes from 31° to 41°S, showing the study area (*rectangle*). The figure highlights the Mesozoic Cuyo and Neuquén basins, and the main structural lineaments. **b** Moho depth map taken from Tassara et al. (2006). **c** Regional map of the present-day Andean morphostructural units

orlando_a_p@yahoo.com.ar

2 Tectonic Setting

Most of the present morphology of the Andes of Central Chile and Argentina is the result of crustal shortening at the convergent plate margin since the Late Cretaceous. However, there is evidence of previous periods of deformation along the proto-Pacific margin of southwestern Gondwana (e.g., Ramos et al. 1986; von Gosen 1997; Giambiagi et al. 2011). Several Paleozoic and Mesozoic compressive, extensional and strike-slip tectonic stages created lithospheric anisotropies and weakness zones that have later defined lithospheric strength and structural styles during the Andean shortening stage.

2.1 Paleozoic Tectonics

The regional evolution during most of the Paleozoic was characterized by orogenic events related to tectonic shortening, and accretion of allochthonous terranes to the proto-Pacific margin of Gondwana (Ramos et al. 1986; Ramos 2008; Astini et al. 1995; Rapalini 2005; Varela et al. 2011; see discussion and references therein). The middle to late Ordovician Ocloyic orogen and the late Devonian to early Carboniferous Chanic orogen have been related to the collision of the Cuyania and Chilenia exotic terranes, respectively (Azcuy and Caminos 1987; Ramos 1999, 2004; Mpodozis and Ramos 1989; Davis et al. 2000; Massone and Calderón 2008; Heredia et al. 2012). Ordovician deformation has been nearly obliterated by the subsequent tectonic stages, with the exception of a few structures recognized within the study area (Giambiagi et al. 2011, 2014; Heredia et al. 2012). In contrast, the Chanic structures are well-preserved and provide evidence of a doubly vergent orogenic belt with west-vergent structures in the Frontal Cordillera, associated with high-grade metamorphic conditions, and east-vergent structures in the southern Precordillera (von Gosen 1995; Willner et al. 2011; Giambiagi et al. 2011, 2014; Heredia et al. 2012).

The Late Paleozoic was characterized by the inception of subduction along the continental margin, and a widespread contractional event referred to as the San Rafael orogeny (Azcuy and Caminos 1987; Mpodozis and Ramos 1989). The San Rafael orogenic belt follows a curved NW to NNW-trend and produced significant crustal thickening (Llambías and Sato 1990; Mpodozis and Kay 1990). Late Paleozoic rocks are affected by brittle deformation characterized by Permian thrust faults and folds striking N to NW (Japas and Kleiman 2004; Kleiman and Japas 2009; Giambiagi et al. 2011), such as the Sosneado-Melipilla deformation zone and the La Manga lineament (Fig. 1a).

orlando_a_p@yahoo.com.ar

2.2 Mesozoic Tectonics

From the Late Permian to Early Jurassic, the early break-up of Southwestern Gondwana was associated with crustal extension and thermal anomalies leading to crustal melting and locally extensive volcanism (Kontak et al. 1985; Llambías et al. 1993; Pankhurst et al. 2000). While the regional extension seems to have remained nearly stationary, showing a characteristic NNE to NE-trend (Giambiagi and Martinez 2008; Japas et al. 2008; Kleiman and Japas 2009; Giambiagi et al. 2009; Bechis et al. 2010, 2014), the locus of deformation, magmatism and rift basin opening shifted through time. The rift basins were strongly controlled by lithospheric anisotropies that were linked to the sutures and rheological contrasts generated during the Paleozoic shortening stages and terrane collisions, as well as further modifications of the thermo-mechanical state of the lithosphere during the Late Paleozoic to the Early Mesozoic evolution (Ramos and Kay 1991; Ramos 1994; Giambiagi et al. 2011; Bechis et al. 2014).

The late Permian to early Triassic evolution was characterized by the development of large volumes of bimodal volcanism under oblique extensional conditions (Giambiagi and Martinez 2008; Kleiman and Japas 2009; Giambiagi et al. 2011). This transtensional event was located over the late Paleozoic San Rafael orogenic belt and resulted in the generation of a new complex fault system, which concentrated the oblique- normal displacement related to a NNE stretching along a NNW-oriented region. Following the bimodal magmatism, several NNW-trending narrow rift basins opened and filled with continental clastic deposits during the Early to Middle Triassic, corresponding to the Cuyo Basin (Fig. 1a) and other coeval basins (Charrier 1979; Uliana et al. 1989).

During the Late Triassic to Early Jurassic, extension shifted westwards associated with the Neuquén basin opening (Uliana et al. 1989; Vergani et al. 1995) (Fig. 1a). During the Middle Jurassic to Early Cretaceous, the Neuquén Basin records an episode of thermal cooling as it filled with up to 5000 m of clastic, carbonate, and evaporite systems deposited during a sag stage (Legarreta and Uliana 1996; Vergani et al. 1995).

2.3 Cenozoic Tectonics

Between 36°S and 32°S, the Eocene to early Miocene period corresponds to a period of extensional deformation that was localized in the western slope of the Andes with the development of sedimentary-volcanic basins in an intra-arc setting (Godoy and Lara 1994; Charrier et al. 2002). The Abanico basin (Fig. 1c) concentrated the magmatic activity in this sector through the generation of extensional faults that were probably pathways for the extrusion of subduction-related magmas (Charrier et al. 2005).

orlando_a_p@yahoo.com.ar

Since ~20 Ma, deformation and uplift of the present Andes took place. The geometry of the eastern Andean ranges at the latitudes 32–36°S was strongly controlled by the orientation of basement-rooted reverse faults inherited from the compressive phase of the late Paleozoic San Rafael orogeny and, to a lesser extent, by the reactivation of the lower Paleozoic Chanic structures (Giambiagi et al. 2014). Mesozoic extensional faults also played an important role in some areas of this segment (Cristallini 1996a, b; Giambiagi et al. 2011; Mescua and Giambiagi 2012).

The study segment corresponds to the northernmost sector of the Southern Volcanic Zone (Stern and Skewes 1995). Between 33° and 35°S, magmatic activity was located in the Chilean slope of the Principal Cordillera above a relatively thin crust (<40 km) from the early Miocene until the Pliocene, and then the arc migrated over 40 km east to its current location at the border between Argentina and Chile (Fig. 1c) (Stern and Skewes 1995; Kay et al. 2005). By this time, crustal thickness was in excess of 50 km (Hildreth and Moorbath 1988). Pliocene to Quaternary magmatism is represented by a volcanic arc situated in the Principal Cordillera and by retro-arc magmatism of the Payenia volcanic province (Bermúdez et al. 1993; Stern 2004; Folguera et al. 2009). South of 35°S, Pliocene to Holocene volcanic centers are either superimposed on or immediately to the east of the Miocene magmatic arc (Kay et al. 2006).

3 Morpho-Tectonic Provinces and Deformation of the Andes Between 32° and 36°S

The Andes of Central Argentina and Chile between 32° and 36°S can be divided into two sectors with distinct tectonic characteristics: a northern sector, between 32° and 34°S and a southern sector, between 34° and 36°S (Fig. 1a). The northern sector is located in a transition zone between a subhorizontal subduction segment north of 32°S, and a zone of normal subduction south of 34°S (Stauder 1975; Barazangi and Isacks 1976; Cahill and Isacks 1992; Tassara et al. 2006; Anderson et al. 2007). Variations in the slab geometry were proposed as a cause for the abrupt southward disappearance of the Precordillera and Sierras Pampeanas systems (Jordan et al. 1983). At these latitudes, several morphostructural units composed the Andes of Argentina and Chile, which are from west to east: the Coastal Range, the Central Depression, the Principal Cordillera, the Frontal Cordillera, the Southern Precordillera, the Cerrilladas Pedemontanas range and the southern Sierras Pampeanas. The southern sector is located in the normal subduction segment, where the morphostructural units are represented by the Coastal Range, the Principal Cordillera, Frontal Cordillera and the San Rafael block (Fig. 1c).

orlando_a_p@yahoo.com.ar

3.1 Coastal Range

The Coastal Range can be divided into western and eastern sectors. The western sector with low topographic altitude (<500 m) is composed of a series of late Pliocene to Pleistocene wave-cut marine terraces (Wall et al. 1996; Rodríguez et al. 2012) carved on late Paleozoic to middle Jurassic plutons and accretionary complexes (Hervé et al. 1988; Selles and Gana 2001; Willner 2005; Richter et al. 2007). The eastern sector with altitudes up to 2000 m and relicts of high-elevated peneplains at different elevations (Brüggen 1950; Farías et al. 2008) is made up by Cretaceous plutons within an east-dipping homoclinal block of late Jurassic to early Cretaceous sedimentary and volcanic country rocks (Hervé et al. 1988; Rivano and Sepúlveda 1991; Vergara et al. 1995).

This range represents a gently east-dipping homocline of late Paleozoic to Cretaceous rocks (Wall et al. 1999). No major Andean thrust fault has been identified in this range, which is affected mainly by high-angle pre-Andean NNW to NW trending faults, like the Melipilla fault (Yáñez et al. 2002). Deformation in the Coastal Cordillera is mostly related to flexural folding and uplift of the range, without important movement along contractional structures (Giambiagi et al. 2015).

3.2 Central Depression

The Central Depression at an elevation of 700 to 500 m.a.s.l separates the Coastal Range from the Principal Cordillera. It is developed from the latitude of the city of Santiago towards the south. It consists of a Quaternary sedimentary and ignimbritic cover up to 500 m in thickness beneath the Santiago valley (Araneda et al. 2000) and basement rocks cropping out in junction ridges and isolated hills reaching 1600 m a.s.l. (Rodríguez et al. 2012).

3.3 Principal Cordillera

The Principal Cordillera can be subdivided into (a) a western sector, which comprises the Oligocene to Miocene volcanic arcs, and (b) an eastern sector corresponding to the La Ramada, Aconcagua and Malargüe fold and thrust belts (FTB). South of 33°S, the structure of the western Principal Cordillera is dominated by inversion of the late Eocene– early Miocene Abanico extensional basin with east and west-vergent reverse faults (Godoy et al. 1999; Charrier et al. 2002; Fock et al. 2006). The style of deformation of the Abanico Formation corresponds to inclined folds with wavelengths of 100s of meters to kilometers (Rivano et al. 1990). Overlying these rocks, the middle Miocene arc-related Farellones Formation is generally gently folded with dips not exceeding 15° (Vergara et al. 1988).

orlando_a_p@yahoo.com.ar

The eastern Principal Cordillera is divided latitudinally into three fold and thrust belts with distinct structural styles: la Ramada, Aconcagua and Malargüe FTBs. The La Ramada FTB, north of 32°30′S, is characterized by a hybrid thin- and thick-skin deformation, which is a consequence of the tectonic inversion of Permian-Triassic extensional structures (Cristallini et al. 1995; Jara and Charrier 2014) and of the northernmost extent of the late Triassic- early Jurassic rifting (Álvarez et al. 1996; Ramos et al. 1996a). Thin-skinned deformation of the Mesozoic Neuquén Basin sediments occurs along a *decóllement* in Jurassic gypsum (Auquilco Formation). According to Cristallini and Ramos (2000), a first stage of thin-skinned deformation lead to km-scale folding of the Neuquén Basin succession, and was followed by the inversion of the Permian-Triassic basement faults. A belt of out-of-sequence thrusts along the Argentina-Chile border was active before 9 Ma (Cristallini and Cangini 1993). This segment of the Principal Cordillera accounts for minimal shortening around ∼18 km. The majority of shortening at these latitudes occurs to the east in the Precordillera range (Cristallini et al. 1995; Cristallini and Ramos 2000).

The Aconcagua FTB (32°30′–34°S) is characterized by horizontal shortening, as high as 60 km, produced by a complex set of predominantly east-vergent thrusts and folds rooted in *decóllements* of gypsum and shale within the Neuquén Basin sedimentary successions (Kozlowski et al. 1993; Cegarra and Ramos 1996). Deformation advanced from west to east, likely involving limited inversion of Late Jurassic extensional faults in the initial steps of deformation. The main structures are imbricate thrusts developed in the central sector of the fold and thrust belt. An important episode of out-of-sequence deformation in the core of the FTB leads to the truncation of original thrust sheets and the present complex structure of the Aconcagua FTB (Cegarra and Ramos 1996). Giambiagi et al. (2015) propose that shortening in the Aconcagua FTB is accommodated by both shallow and deep detachments. The deep detachment is probably located along the mid-crustal thermally weakened brittle-ductile transition, between 15 and 20 km, while the shallow detachment is related to a ductile *decóllement* horizon at the base of the sedimentary cover.

The Malargüe FTB has been classically identified as a hybrid fold-and-thrust belt with basement thrusts and reverse faults transferring shortening to the thick Mesozoic to Cenozoic sedimentary cover (Kozlowski et al. 1993; Manceda and Figueroa 1995; Giambiagi et al. 2008; Silvestro and Atencio 2009). Here, total shortening is 26 to 30 km (Mescua et al. 2014). The northern part of the belt shares structural characteristics with the southern portion of the Aconcagua FTB, marking a transition to the thick-skinned deformation developed south of 35°S. Numerous extensional features inherited from the Triassic-Jurassic rifting episode contribute to the overall structural grain of the area (Manceda and Figueroa 1995; Giambiagi et al. 2008; Yagupsky et al. 2008; Bechis et al. 2010; Mescua et al. 2014). In many sectors, pre-existing normal faults are interpreted to have been inverted or to have controlled the location of Neogene thrusts and the vergence of the compressional

orlando_a_p@yahoo.com.ar

deformation. The main graben-bounding Mesozoic faults were inverted during the Andean deformation, like the La Manga and Río del Cobre faults at 34°30′–35°S (Mescua and Giambiagi 2012). In other sectors, low-angle basement thrusts were formed during Andean deformation, such as the Las Leñas thrust (Mescua et al. 2014), and the structures in the Bardas Blancas area at 36°S (Dimieri 1997; Dicarlo and Cristallini 2007; Giambiagi et al. 2009). Shortening in the Malargüe FTB decreases southward, from ∼30 km at 34°S to ∼10 km at 36°S (Giambiagi et al. 2012).

3.4 Frontal Cordillera

The Frontal Cordillera at this latitudes corresponds to the Cordón de la Ramada, Cordillera del Tigre, Cordón del Plata, Cordón del Portillo and Cordillera de las Yaretas ranges, where Proterozoic metamorphic rocks, early Paleozoic metasedimentary and metavolcanic rocks, late Paleozoic marine deposits, Carboniferous to Permian granitoids and Permo-Triassic volcanic rocks crop out (Polanski 1964, 1972; Heredia et al. 2012). North of 33°S, the Frontal Cordillera is uplifted by a blind ramp, deeply seated in the basement. This fault is inferred to ramp up into the Precordillera fold and thrust belt (Allmendinger et al. 1990). South of 33°S, the Frontal Cordillera is bounded by emergent faults, such as the La Carrera fault system (Caminos 1965; Folguera et al. 2004; Casa et al. 2010) consisting of four N to NNE-trending reactivated Permian structures.

3.5 Southern Precordillera

The Southern Precordillera corresponds to a bivergent mountain range developed on Paleozoic to Triassic rocks between 32° and 33°S (Cortés et al. 1997). It is a thick-skinned thrust belt, which shows a strong influence of Paleozoic and Mesozoic pre-Andean structures (Cortés et al. 1999, 2006; Folguera et al. 2004; Giambiagi et al. 2011). In particular, the Paleozoic section is restricted almost entirely to the Devonian and there is a substantial amount of Permo-Triassic volcanics, and to a lesser degree, sediments. These features distinguish it from the Precordillera north of 32°S, where traditional models have interpreted a classic thin-skinned tectonic style of a complete Paleozoic passive margin sequence with complete detachment of a deformed sedimentary cover from a basement dipping gently to the west (Allmendinger et al. 1990; Cristallini and Ramos 2000). The northern termination of the Southern Precordillera is marked by the presence of a narrow NW-trending Barreal-Las Peñas deformation zone where a high concentration of Quaternary structures are observed (Cortés et al. 2006, 2015).

orlando_a_p@yahoo.com.ar

3.6 Cerrilladas Pedemontanas

The Cerrilladas Pedemontanas region is marked by a series of elongate folds, locally broken by reverse faults displaying eastward or westward vergence (Dellapé and Hegedus 1995). The NNW-trend of these ranges is controlled by the inversion of Triassic extensional faults of the Cuyo Basin. The basin was marginally uplifted and subjected to moderate Cenozoic structural inversion of the Triassic Cuyo Basin half-grabens and associated relay/transfer faults (Legarreta et al. 1992). Triassic continental rocks are covered by Neogene to Quaternary synorogenic deposits of the Cacheuta Basin (Irigoyen et al. 2000).

3.7 San Rafael Block

The San Rafael block is located in the center-south of the Mendoza Province between 34° and 36°S, and corresponds to an uplifted basement block comprising Proterozoic basement and Permo-Triassic volcanic and sedimentary rocks (González Díaz 1964; Cortés et al. 1999; Kleiman and Japas 2009). The Santa Isabel thrust uplifts this block of Paleozoic-Mesozoic rocks over 100–200 m of late Miocene synorogenic strata of the Alvear Basin and the Pampean plain (Folguera and Zárate 2011). Motion on the Santa Isabel thrust is inferred to have occurred during the Pliocene (~3 Ma; Ramos et al. 2014). Pliocene-Quaternary retroarc volcanism of northernmost portion of the Payenia volcanic field partially covers the late Miocene Andean orogenic front (Ramos et al. 2014). This large province has been explained as related to a strong asthenospheric influx due to the steeping of the subducted Nazca plate (Folguera et al. 2009; Bertotto et al. 2009) and to a mantle plume (Burd et al. 2014).

This area presents significant neotectonic activity on its eastern edge, associated with an active fault system (Folguera et al. 2009). This fault system presents reactivations and evidence of surface rupture, such as the Malvinas fault (Bastías et al. 1993; Cisneros and Bastias 1993; Cortés et al. 2006) which was associated with the $M \sim 6.0$ earthquake on May 30th, 1929.

3.8 Sierras Pampeanas

The Sierras Pampeanas are fault-bounded basement cored uplifts that occur in the foreland, reaching heights of >3000 m and extending to ~65°W. The southernmost sector of the Sierras Pampeanas is present in the northeastern sector of the study area, between 32° and 32°30′S, and corresponds to the southernmost termination of the Sierra de Valle Fértil, the Sierra de San Luis, the southern portion of the Sierras de Cordoba, The Sierra de Chepes and a succession of small hills aligned NNE,

orlando_a_p@yahoo.com.ar

including the Cerro Barbosa and Cerro Valdivia (Costa et al. 2000; Vergés et al. 2007). This geological province is characterized by a series of crystalline basement blocks of Precambrian-early Paleozoic age, uplifted and tilted during the Late Neogene by west-vergent reverse faults (Costa et al. 1999; Perarnau et al. 2012) and separated by broad and relatively undeformed basins (Jordan et al. 1983).

East of the San Rafael block, in the Pampean plain, Folguera and Zárate (2011) described a basement block uplifted and tilted during Cenozoic compression as the Central Pampa block. This uplifted block corresponds to the southward extension of the Sierras Pampeanas, where lower Paleozoic metamorphic rocks crop out (Tickyj et al. 2002; Folguera and Zárate 2011).

4 Neogene-Quaternary Basins

Several Neogene basins, including forearc, intermontain and retro-arc foreland basins, develop between 32°S and 36°S (Figs. 1c, and 2). There are two forearc basins in Chile, the Navidad Basin and Central Depression. On the eastern flanks of the Andes there is a north-south string of intermontain basins: Manantiales, Vacas, Uspallata and Alto Tunuyán. In the foreland, local, well-exposed depocenters include the Las Peñas, Cacheuta and Pincheiras/Malargüe basins.

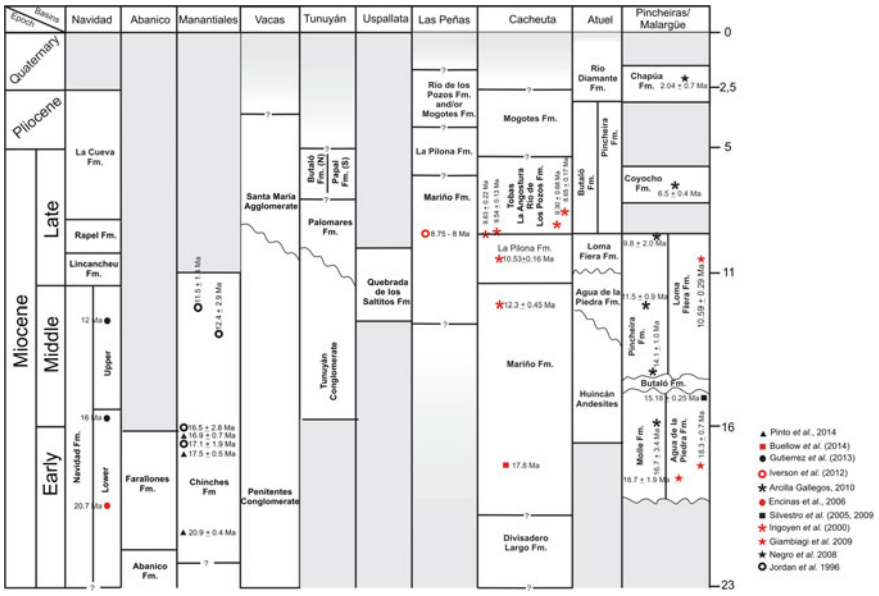


Fig. 2 Stratigraphic chart of the Neogene-Quaternary synorogenic basins

orlando_a_p@yahoo.com.ar

4.1 Forearc Basins

The Navidad Basin is a marine forearc basin exposed on the Chilean coast (Cecioni 1980) and described in offshore boreholes (Mordojovich 1981). The sediments of the basin extend from Southern Chile to Northern Chile (Ibaraki 1992; Encinas et al. 2008). Encinas et al. (2006) proposed a unified stratigraphic framework for the Navidad Formation. The exposures of the Navidad Basin sequence are shallow water fossil assemblages and shallow water sedimentary facies, followed by a subsequent major episode of subsidence in the late Miocence (Encinas et al. 2008) before re-emergence of the western basin margin at the Chilean coast.

Separating the Coastal Range and the Principal Cordillera, the Neogene Central Depression basin, developed above the Paleogene Abanico Basin (Godoy et al. 1999), hosts early to middle Miocene volcanic and volcaniclastic deposits of the Farallones Formation (Charrier et al. 2002). There is a thin veneer of Quaternary sedimentary cover, but not appreciable accumulation of Neogene terrestrial sedimentary rocks.

4.2 Intermontain Basins

Three Neogene intermontain basins occupy positions either in or straddling the Cordillera. The Manantiales basin is located between the Frontal Cordillera and the Precordillera at ~32°S (Fig. 1c), in the flat-slab zone (Pérez 1995, 2001; Jordan et al. 1996). A geochronologically constrained magnetostratigraphy was constructed by Jordan et al. (1996) in the Chinches Formation and documents continuous deposition beginning at ~19 Ma. Sedimentation ended somewhere between 10 and 8 Ma. The total thickness of sediments is ~3600 m of continental deposits. U–Pb ages on detrital zircons indicate that it developed between 22 and 16 Ma (Porras 2013), consistent with the magnetic polarity stratigraphy (Jordan et al. 1996).

In map view, the Manantiales Basin extends south into the Vacas Basin, although, Vicente (2005) recognized two coarse units limited by angular unconformities that are distinct from the Manantiales Basin (Penitentes Conglomerate—early Miocene—and the Santa María Agglomerate—late Miocene). The Penitentes Conglomerates unconformably rests upon the Cretaceous strata and the Permo-Triassic Choiyoi Group and are typical proximal synorogenic deposits with boulders and blocks of Mesozoic units. The Santa María Agglomerate is subhorizontal and rests unconformably over Permo-Triassic volcanic rocks, Jurassic strata or the Penitentes Conglomerates. This unit corresponds to distal volcaniclastic facies laterally related to the Aconcagua volcanic Complex.

The Alto Tunuyán Basin, located between Principal and Frontal cordilleras (Fig. 1c), is filled with up to 1400 m of alluvial fans facies composed of conglomerates, sandstones and mudstones (Tunuyán Conglomerates, Palomares and Butaló Formations). According to Giambiagi et al. (2001), clast composition and

orlando_a_p@yahoo.com.ar

paleocurrents are related to the migration of the deformation from the Aconcagua FTB to the Frontal Cordillera. Calculated paleoelevation for the basin is 1.4 ± 0.3 km, suggesting 2 km of topographic uplift after its filling (Hoke et al. 2014).

The Uspallata Basin is the southernmost extension of the 300 km long Uspallata-Calingasta, Iglesia Valley and lies between the Frontal Cordillera and Precordillera (Fig. 1c). The sediments of the Uspallata Basin were deposited in an arid fluvial system (Mahoney et al. 2014; Hoke et al. 2014), assigned by Cortés (1993) to the Quebrada de los Saltitos Formation. An available U–Pb age from a resedimented tuff and detrital sandstone suggests that sedimentation took place from at least 9–12 Ma, which is significantly younger (>5 Ma) than synorogenic deposits in the Cacheuta Basin to the east (Mahoney et al. 2014). Paleoelevation studies yield a paleoelevation of 1.2 km ± 0.3 km during its development, substantially lower than its modern elevation (Hoke et al. 2014).

4.3 Foreland Basins

The Las Peñas Basin (Fig. 1c) contains >2000 m of continental sedimentary strata (Vergés et al. 2007; Iverson et al. 2012). Despite its thickness and its regional importance as the easternmost exposed synorogenic basin strata along the flat slab segment, there are no detailed sedimentological studies of this basin. The sediments of the Las Peñas basin are based on lithostratigraohic correlation with the units found in the Cacheuta Basin, since there are no absolute age constrains in this area. Detrital zircon analysis of a tuffaceous sample indicating a maximum depositional age of 8.75 Ma indicates that the Precordillera was uplifted by that time (Iverson et al. 2012).

The Cacheuta Basin has its western margin on the Las Carreras fault system and the Frontal Cordillera (Fig. 1c). Containing up to 4000 m of continental sediments, the Cacheuta Basin records the uplift history of the Principal Cordillera, Frontal Cordillera and the southernmost Precordillera in the transitional zone between flat and normal subduction segments. According to Irigoyen et al. (2000) the earlier phase of Andean deformation recorded in this basin corresponds to basal alluvial conglomerates (Mariño Formation), correlated with prior to 15.7 Ma deformation in the west of Aconcagua FTB. However, a ca. 18 Ma U/Pb age from a volcanic tuff near the base of the succession constrains initial basin subsidence to >18 Ma, in accordance with mammal fossil age obtained by Cerdeño and Vucetich (2007), and suggests that previous magnetostratigraphic age constraints require revision (Buelow et al. 2014).

The Atuel basin is located between the Atuel and Barrancas rivers, east of the Principal Cordillera and over the northernmost part of the normal subduction segment (Fig. 1c). The Cenozoic synorogenic deposits correspond to Agua de la Piedra, Loma Fiera, Pincheiras, Butaló and Río Diamante Formations (Combina and Nullo 2008). The stratigraphy of this basin is partially coincident with Pincheiras/Malargüe basins but with different ages (Arcila Gallego 2010).

orlando_a_p@yahoo.com.ar

The Pincheiras/Malargüe basins record Neogene activity in the eastern slope of the Andes between 35°S and 36°S (Fig. 1c). Five synorogenic sub-basins were recognized: Horqueta, Pincheiras, Ventana, Río Grande and Palauco with volcanic, volcaniclastics and clastics records that are between 150 and 1500 m thick (Silvestro et al. 2005; Silvestro and Atencio 2009; Arcila Gallegos 2010). Radiometric dating of andesitic lavas at the base of the synorogenic deposits and of basalts at the top, constrained the age of the northern basins (Horqueta, Pincheiras and Ventana) between 15.1 and 6.7 Ma (Silvestro et al. 2005). The southern basins, Río Grande and Palauco, were fed by proximal to distal clastic and volcaniclastic deposits, constrained between 18 and 8 Ma (Silvestro and Atencio 2009).

4.4 Extra-Andean Basins

The eastern depositional zone was interpreted as a backbulge (Folguera and Zárate 2009), where thinner (200–300 m) and finer sediments deposits were deposited (Fig. 1c). Folguera and Zárate (2009, 2011) proposed two stages of continental deposition (after the Paranaense marine regression) separated by a regional unconformity, late Miocene, Río Azul Formation and the Pliocene units. The Río Negro Formation corresponds to reddish to brown silts and sandy silts interpreted as eolian and floodplain deposits (Folguera and Zárate 2011) with volcanic provenance related to the Andes (Visconti 2007). Folguera and Zárate (2009) propose that the central block of La Pampa was uplifted and tilted to the east in the late Miocene, producing a regional unconformity and the migration of the depocentre southwards of 38°S.

5 Cenozoic Tectonic Evolution

5.1 The Late Cretaceous-Paleocene Deformational Event

Andean orogeny initiated in several segments with episodes of contractional deformation during the Late Cretaceous as back-arc basins that began to be tectonically inverted (Mpodozis and Ramos 1989). This late Cretaceous-Paleocene shortening event has been recorded in the Principal Cordillera in the southern part of the study area (Orts et al. 2012; Tapia et al. 2012; Mescua et al. 2013), and further south (Tunik et al. 2010; Spagnuolo et al. 2012). These early synorogenic deposits were deposited in continental environments during the Cenomanian (Tunik et al. 2010). Foreland flexural subsidence increased during the Maastrichtian, culminating with the first Atlantic marine ingression that, according to marine deposits, reached the Cretaceous orogenic front (Tunik 2003; Aguirre-Urreta et al. 2011).

orlando_a_p@yahoo.com.ar

5.2 The Eocene—early Miocene Extensional Event

During the Eocene to the early Miocene, a protracted extensional event took place with deformation concentrated in the western sector of the Principal Cordillera (Charrier et al. 2002). Mpodozis and Cornejo (2012) suggested that the observed extension is linked to a segmented roll back subduction event of the Nazca Plate. Normal faulting was associated with crustal thinning and tholeiitic magmatism of the Abanico Formation (Fig. 3) (Nyström et al. 1993; Kay and Kurtz 1995; Zurita et al. 2000; Muñoz et al. 2006), whose $^{40}Ar/^{39}Ar$ ages at the latitude of Santiago (33°S) range from 35 to 21 Ma (Muñoz et al. 2006). The extensional basin was filled with up to 3000 m of volcaniclastic deposits, and acidic to intermediate lavas with sedimentary intercalations (Charrier et al. 2002). Even though geochemical analyses suggest it was formed upon a ca. 30–35 km thick continental crust (Nyström et al. 2003; Kay et al. 2005; Muñoz et al. 2006), there is no evidence of marine sedimentation.

During this period, the Coastal Range should have been elevated due to isostatic compensation of the late Cretaceous-Paleocene crustal thickening event, and locally by isostatic rebound close to the east-dipping Abanico master fault (Charrier et al. 2009). Further east, in the Neuquén Basin, Paleocene distal continental sediments were deposited tapering towards the east (Melchor and Casadío 2000).

The extensional structures of the Abanico Basin have been obliterated by the later contractional faults. Inferred master faults have been suggested to be located beneath the Central Depression (Godoy et al. 1999; Fock et al. 2006). Apatite and zircon fission track cooling ages from the eastern Coastal Cordillera constrain an exhumation period between 36 and 42 Ma (Farías et al. 2008), which could be related to uplift of the rift shoulder west of the master fault (Fock et al. 2006; Charrier et al. 2009) at the beginning of late Eocene extension, or uplift as a consequence of crustal shortening during the end of the Late Cretaceous to Eocene compression. Much more speculative is the existence of eastern basin-border faults (Davidson 1971; Godoy 1991; Charrier et al. 1996, 2002; Godoy et al. 1999; Fock et al. 2006; Piquer et al. 2010). More structural studies are needed.

5.3 The early Miocene (21–16 Ma)—Major Shortening Event in Principal Cordillera

The last major shortening event began during the early Miocene with the inversion of the Abanico Basin (Godoy et al. 1999; Charrier et al. 2002; Fock et al. 2006). The onset of deformation in the western slope is marked by the change from low-K Abanico Formation tholeiites to calc-alkaline dacites of the Teniente Volcanic Complex at ~34°S (Fig. 3) (Kay et al. 2005, 2006), between 21 and 19 Ma (Charrier et al. 2002, 2005). This deformation was coeval with the development of the early to middle Miocene Farellones volcanic arc (Vergara et al. 1999) in the northern study sector, and magmatic activity of the Cordón del Burrero Volcanic

orlando_a_p@yahoo.com.ar

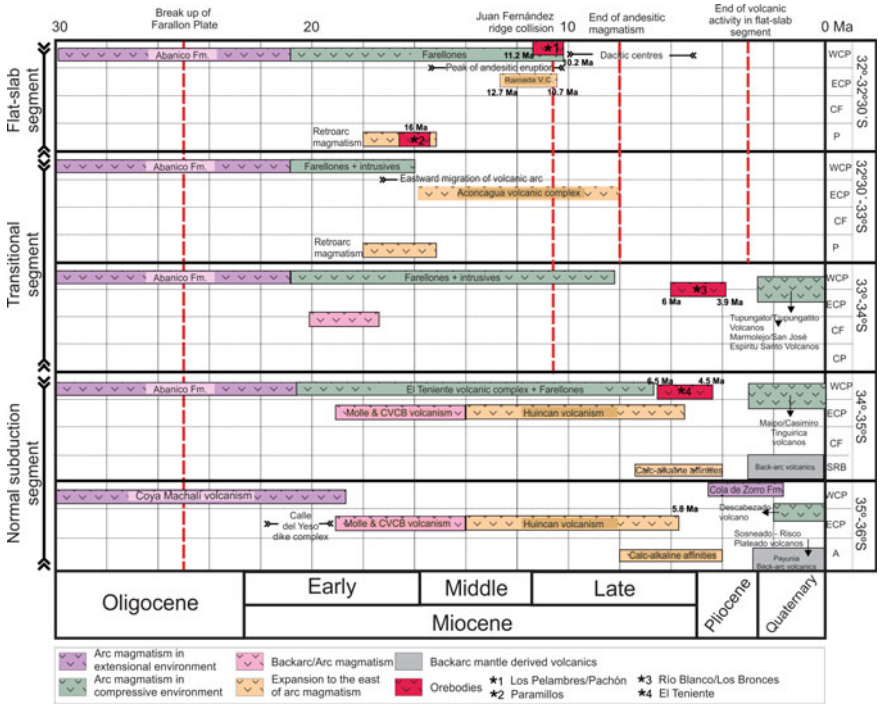


Fig. 3 Comparative chart for the magmatism present at the different study latitudes: 32°–32.5°, 32.5°–33°, 33°–34°, 34°–35° and 35°–36°S

Complex (∼18 Ma) in the southern sector at ∼35°S (Sruoga et al. 2008). During this period, back-arc magmatism is represented in the Precordillera by subvolcanic and volcanic complexes, such as the La Peña alkaline complex (Villar and Zappettini 2000; Zappettini et al. 2013). The tectonic regime for the emplacement of these complexes has been suggested by Pagano et al. (2014) to correspond to a transtensional setting developed locally in the Precordillera during the early Miocene (19 Ma).

Deformation and uplift of the western Principal Cordillera is related to the generation of a main *decóllement* deeply rooted at the contact between the Moho and mantle sub-arc lithosphere, around 40 km in depth (Giambiagi et al. 2015). Eastward movement of the upper crust relative to the stable and long-lived lower crustal MASH zone proposed by Muñoz et al. (2012) could explain the up to 40 km width of the Farellones volcanic arc. The main uplifted sectors for this period are the eastern Coastal Cordillera and the western Principal Cordillera. The passive uplift of both sectors is in agreement with provenance studies of heavy mineral assemblages for the lower Navidad Formation (Rodríguez et al. 2012) whose radiometric ages indicate deposition during 23–18 Ma (Gutiérrez et al. 2013), and apatite fission track (AFT) age (18.3 ± 2.6 Ma) for late Cretaceous deposits (Fock

orlando_a_p@yahoo.com.ar

2005). The coeval uplift of the eastern Coastal Cordillera and the Principal Cordillera leads to the formation of a depocentre filled by up to 3000 m of arc-related volcanics of the Farellones Formation (Vergara et al. 1988; Elgueta et al. 1999; Godoy et al. 1999). 20–18 Ma marks the onset of deformation in the eastern FTBs (Fig. 4) (Cegarra and Ramos 1996; Cristallini and Ramos 2000; Pérez 2001; Giambiagi and Ramos 2002; Silvestro et al. 2005; Mescua et al. 2014), linked to the eastward propagation of the main *décollement* (Giambiagi et al. 2015). During the 18–15 Ma interval, driving forces cannot supply the energy needed to elevate the western Principal Cordillera and the orogen begins to grow in width to lower the taper by propagating forward towards the foreland (e.g. Davis et al. 1983). The shift in the locus of deformation is likely related to the rapid ascent of subduction-related, mantle-derived magmas that had little interaction with the upper lithosphere in the western Precordillera (Muñoz et al. 2012).

During this period, the northern sector of the Aconcagua FTB achieves the majority of its shortening (Cegarra and Ramos 1996; Cristallini and Ramos 2000), prior to the volcanism of the Aconcagua complex (15.8–8.6 Ma—Ramos et al. 1996b). Synorogenic strata recording orogenic evolution are preserved in the sedimentary basins within the eastern Principal Cordillera (Manantiales, Vacas and Alto Tunuyán basins) and in the foreland along the orogenic front (Cacheuta, Atuel, Las Peñas and Río Grande- Palauco).

5.4 The middle Miocene (15–11 Ma) Eastward Volcanic Migration

This is a period, in the northern segment (32–34°S), of high crustal shortening concentrated along the eastern Principal Cordillera and the Cordón de la Ramada in Frontal Cordillera (Fig. 4) (Cristallini and Ramos 2000). The crust nearly achieves its present thickness, with an eastward shift in the crustal root (Giambiagi et al. 2015). Important space creation due to flexural compensation of the tectonic load, immediately to the east of the La Ramada and Aconcagua FTB, is registered in the foreland basins (Irigoyen et al. 2000; Pérez 2001). In the early late Miocene, the slab inclination begins to decrease north of 33°S, and volcanism migrates from the Principal Cordillera (Fig. 3), where it was active between 15 and 9 Ma (Aconcagua and La Ramada volcanic complex—Ramos et al. 1996b; Pérez and Ramos 1996), to the Sierras Pampeanas (Kay and Abbruzzi 1996). South of 33°S, the volcanic activity wanes (Fig. 3), and only very localized activity is recorded since the upper middle Miocene to the late Pliocene, in agreement with a highly compressive stress regime in the arc region. The present volcanic arc develops in the latest Pliocene along the drainage divide.

In the southern segment (34°–36°S), the eastern sector of the Malargüe FTB was deformed during this period (Fig. 4) (Kozlowski et al. 1993; Silvestro et al. 2005; Giambiagi et al. 2008; Turienzo et al. 2012). This deformation reflects significant

orlando_a_p@yahoo.com.ar

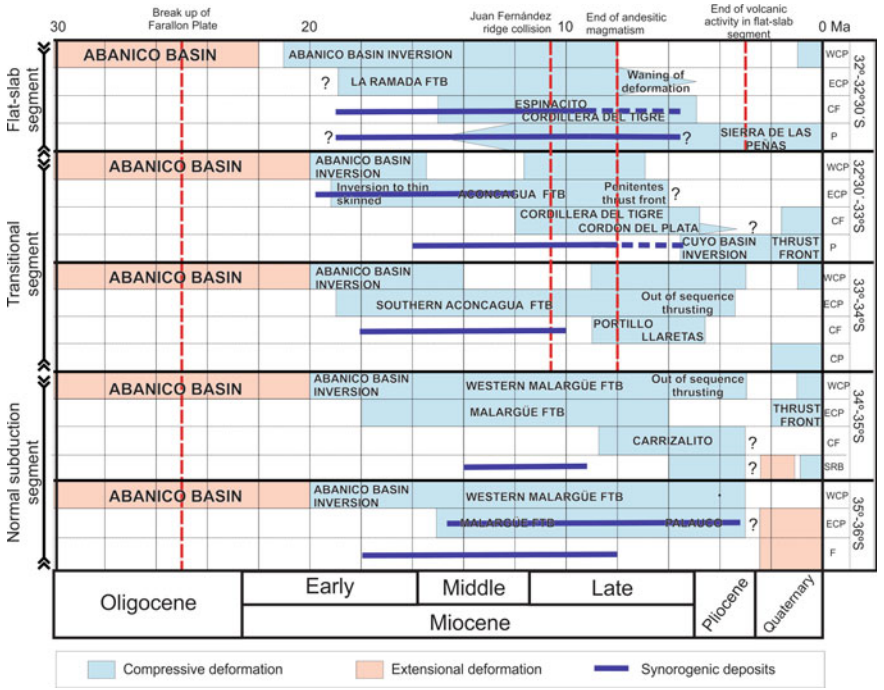


Fig. 4 Comparative chart for the main Cenozoic episodes of deformation between 32° and 26°S

shortening in a complex structural style that involves the inversion of Mesozoic normal faults and the formation of Andean thrusts (Giambiagi et al. 2012; Mescua et al. 2014). For example, the Las Leñas thrust, at 35°S, accumulated almost 20 km of shortening between 16 and 10 Ma (Mescua et al. 2014). In the southernmost part of the study area, the orogenic front expanded to the east resulting in a wide zone of deformation that includes the Sierra Azul and Sierra de Palauco Ranges (Yagupsky et al. 2008; Silvestro and Atencio 2009; Giambiagi et al. 2009). Synorogenic deposition accompanied the eastward advance of deformation within the Principal Cordillera, resulting in the formation of the Pincheira-Ventana Basin (35°30′S) between 16 and 7 Ma (Silvestro et al. 2005). Syn-orogenic magmatic activity of the Huincán cycle, with clear calk-alkaline characteristics, begins at ∼14 Ma (Baldauf 1997; Nullo et al. 2002; Sruoga et al. 2009), and records an important expansion of the magmatic arc to the east, contemporaneous with crustal deformation. The geochemistry of these rocks reflects the increase in crustal thickness that took place during this period (Nullo et al. 2002).

orlando_a_p@yahoo.com.ar

5.5 The late Miocene (10–6 Ma): Uplift of the Southern Precordillera

At the beginning of this phase, around 10–9 Ma, the crust in the Aconcagua FTB achieves its present maximum thickness of 50 km (Giambiagi et al. 2015), in accordance with isotopic analysis (Kay et al. 2005). At this point, driving forces can no longer supply the energy needed to thicken the crust and uplift the range, and the crustal root was likely to grow laterally in width instead of increasing its depth, with a reduction in shortening rates. This is in accordance with Muñoz et al.'s (2012) proposed deep crustal hot zones. The hot zone develops due to repeated basalt intrusion into the lower crust, inducing a significant thermal perturbation increasing melt component (Muñoz et al. 2012). This promotes the ductile behavior of the lowermost crust and the widening of the crustal root.

During this period in the northern sector, the flat slab is migrating eastward, and arc volcanism sweeps eastward from the Precordillera across the Sierras Pampeanas leaving a small volume of volcanism and subvolcanic bodies with subduction signatures (Kay et al. 1991) and ages between 9.5 and 2 Ma (Ramos et al. 2002) restricted to the southern Sierras Pampeanas (31°–33°S). In contrast, south of 33°S, on the western side of the Principal Cordillera, the Teniente Plutonic Complex (at 34°S) intrudes the Abanico and Farellones formations between 12 and 7 Ma (Fig. 3) (Kay and Kurtz 1995; Kurtz et al. 1997; Kay et al. 2005).

Uplift of the Southern Precordillera (32°–33°S) has been constrained to initiate by ~10 Ma based on reconstruction of a Miocene paleo-landscape remnant (Walcek and Hoke 2012). This was coeval with the migration of magmatism to the Sierras Pampeanas (Kay et al. 1991) and the uplift of the Cordillera del Tigre range (Ramos et al. 2002).

During the upper late Miocene (8–6 Ma), the sedimentary record indicates important uplift of the Frontal Cordillera between 33°30′ and 34°30′S (Irigoyen et al. 2000; Giambiagi et al. 2003). An apatite (U-Th)/He thermochronology study in the Frontal Cordillera between 32°50′ and 33°40′ found that very little exhumation would have occurred over the Cenozoic. Initially, pre-Miocene exhumation rates are ~10 m/My and increase to 100–60 m/My at 25 Ma, with an inferred onset of rapid river incision between at ~10 Ma, roughly within geologic constraints (Hoke et al. 2015).

In the Principal Cordillera, between 34° and 36°S, out of sequence thrusting occurs in the El Fierro and Las Leñas thrusts (Fig. 4) (Godoy et al. 2009; Kozlowski et al. 1993; Mescua et al. 2014). Based on thermochronology studies in Chile, a period of high exhumation since 8 Ma is proposed for the western Principal Cordillera (Spikings et al. 2008), which could be either related to the activity of these structures or the inversion of the eastern master faults of the Abanico Basin, as proposed by Piquer et al. (2010) and Tapia et al. (2012). According to Maksaev et al. (2009), this period of high exhumation took place between 6 and 3 Ma. The

orlando_a_p@yahoo.com.ar

frontal structures of the belt, like the Malargüe anticline, are also active in this period, as recorded in foreland basin deposits of the Loma Fiera Formation (dated as younger than 10 Ma by Baldauf 1997) and the Malargüe Basin (Silvestro et al. 2005).

The Huincán arc volcanics reached the orogenic front (Figs. 3 and 4), with eruptions along the Sosneado thrust with ages between 10 and 5 Ma (Baldauf 1997; Nullo et al. 2002). Coeval volcanics in the internal FTB have been dated between 10 and 6 Ma (Sruoga et al. 2009).

5.6 The Pliocene (5–2.5 Ma) Foreland Deformation

During the Pliocene, in the flat-slab region (north of 33°30′S), deformation migrates to the east to the Sierras Pampeanas (Ramos et al. 1996a, b). In the Andean region, activity is focused along the Precordillera- Frontal Cordillera orogenic front and in strike-slip structures in the eastern Principal Cordillera. Magmatic activity decreases markedly, and ceases completely by 2 Ma. In contrast, south of that latitude, the magmatic activity reassumed its current locus along the High Andean drainage divide, with the formation of the Tupungato, San José, Marmolejo, Maipo, Sosneado, Risco Plateado, Tinguiririca, Planchón-Peteroa, and other volcanic centres (Fig. 1c) (Stern 2004).

In the transitional zone between the flat-slab and normal subduction segments, contractional deformation occurs only in the eastern Frontal Cordillera with generation of thrusts affecting the Miocene to early Pliocene synorogenic deposits of the Cacheuta Basin, and in the Cerrilladas Pedemontanas, with the generation of an angular unconformity in the synorogenic units (Yrigoyen 1993; Irigoyen et al. 2000).

The widening of the crustal root during this stage favors the Coastal Cordillera uplifts by isostatic rebound, evidenced by the emergence of marine deposits between 4.4 and 2.7 Ma (Encinas et al. 2006). This process would have partially blocked the drainage, inducing sedimentation in the Central depression (Farías et al. 2008). The widening of the crustal root could in turn be responsible for the increase in topographic elevation by isostatic compensation. The enhanced erosion related to increased relief between 6 and 3 Ma suggested by Maksaev et al. (2009) could be attributed to this phenomenon.

In the Malargüe FTB, the Pliocene is a period of subdued deformation. Minor thrusting takes place along the orogenic front (Giambiagi et al. 2008), and exhumation in the southern part of the western Principal Cordillera has been attributed to fault activity from 5 to 1 Ma (Spikings et al. 2008). At these latitudes, in the foreland area, extensional tectonics was interpreted to be coeval with the flooding of the huge basaltic Payenia Volcanic Complex (Folguera et al. 2009; Ramos et al. 2014), developed in the last two million years (Ramos and Folguera 2011).

orlando_a_p@yahoo.com.ar

5.7 The Quaternary (2.5–0 Ma)

During the Quaternary, the active orogenic front is located at the foothills of the Andes (Costa et al. 2000). Major historical earthquakes have been recorded in this portion of Andes foreland between 30° and 34°S (Alvarado et al. 2005).

Between 31° and 33°S, active faults affect Pleistocene deposits in the border between Frontal Cordillera and Precordillera (Cortés and Cegarra 2004; Terrizzano et al. 2010), while Pleistocene to Holocene sediments are disrupted at the eastern border of the Precordillera and both flanks of Meseta del Guadal (Bastías et al. 1993; Ahumada and Costa 2009; Moreiras et al. 2014; García and Casa 2015). These features demonstrate Quaternary propagation of the deformation into the foreland following the scheme of eastward migration of the orogenic front. Indeed, recent activity of the eastern thrust of Barrancas anticline (68.75°W) related to Mb = 6.0 Mendoza earthquake of 1985 (INPRES 1985; Triep 1987) confirm eastward migration is ongoing.

Neotectonic studies show wide-spread Quaternary activity along the major faults of the Sierra de San Luis and Comechingones in the southernmost sector of the Sierras Pampeanas (Costa and Vita-Finzi 1996) revealing significant paleo- magnitudes (Costa and Vita-Finzi 1996; Costa et al. 2000, 2001). However, low magnitude earthquakes occur at present in this range.

Distribution of shallow earthquake epicenters in the Andes between 32° and 36°S gives important clues for the Quaternary deformation along the Southern Central Andes. The back-arc seismicity has been studied using short-period seismic networks: (1) PANDA—1988; (2) PMRES—1999; (3) CHARGE—2000–2002, (4) CHARSME—2002–2004, (5) PASSCAL—2008–2010, (6) SIEMBRA—2007–2008, (7) BSR—2009-Present, (8) ONDAS—2014-Present, and three experiments for the aftershocks of the Maule earthquake (2010). In the northern sector, crustal earthquakes occur in the longitudinal valley separating the Frontal and Principal cordilleras and in the eastern Sierras Pampeanas. The historical seismicity during the last ~250 years (INPRES 2005) also shows a concentration of larger sized earthquakes in the western Sierras Pampeanas, where the most recent occurred in 1977 in the vicinity of the Sierra Pie de Palo (Mw 7.4 Caucete Earthquake). In the southern sector, crustal seismicity is concentrated along the Malargüe FTB. Spagnotto et al. (2015) show a nine time increment of seismicity in the arc region at 35°S related to an static stress change during the Mw = 8.8 Maule 2010 earthquake.

In the Chilean slope of the Andes, shallow seismic activity is distributed mainly along the western flank of the Principal Cordillera, at depths of 12 and 15 km (Barrientos et al. 2004) and beneath the Central depression, at depths shallower than 20 km (Farías et al. 2010). This suggests that, at least the western portion of the Main *décollement* is active today. This is in agreement with minor Quaternary movement along the San Ramón fault, whose scarp has been linked to the vertical offsets (0.7–1.1 km) of the peneplains present in the western Principal Cordillera, before 2.3 Ma (Farías et al. 2008; Armijo et al. 2010).

orlando_a_p@yahoo.com.ar

In the High Andes, near the drainage divide, most shallow earthquakes >Mw 5 show focal mechanisms reflecting strike-slip kinematics (Barrientos et al. 2004), such as the Mw 6.9 Las Melosas earthquake (Alvarado et al. 2005). Beneath the eastern part of the Frontal Cordillera and the Cuyo Basin shallow focal mechanisms are related to contractional kinematics (Alvarado et al. 2007). The neotectonics of the Andean retrowedge at this latitude is characterized by movement along buried faults that fold Quaternary deposits (García and Casa 2015).

6 Discussion

6.1 Causes of Latitudinal Variations in Topographic Uplift, Shortening and Slab Geometry

The Andes of west-central Argentina and central Chile (32° and 36°S) lie within the transition from flat subduction (Pampean flat slab segment) to normal subduction segments, and host important along-strike variations in topographic uplift, structural elevation, amount and rate of shortening, and crustal root geometry. In the flat-slab segment, high elevations (an average of 4.5 km), several tectonic provinces and the lack of active volcanism characterize the orogen. Deformation and uplift advanced to the east, together with arc-related magmatic activity, sequentially uplifting the different morphostructural units (Fig. 1): the Principal Cordillera between 20 and ~8 Ma, the Frontal Cordillera between 12 and 5 Ma and the Precordillera in the last 10 Ma. Finally, the Sierras Pampeanas (up to 700 km away from the trench) were uplifted during the latest Miocene to Pleistocene (Ramos et al. 2002). Magmatic activity also migrated eastwards, with arc activity focused in the La Ramada and Aconcagua FTB before 10–8 Ma, after which magmatism was restricted to minor dacitic eruptions, shutting down in the Andean domain by ~5–3 Ma. Since ~7 Ma, arc-related magmatic activity started in the Sierras Pampeanas. The last volcanism in the flat-slab segment corresponds to the San Luis ranges (33°S), with Ar/Ar ages of 1.9 Ma (Urbina et al. 1997).

In the normal subduction segment, between 33°30′ and 36°S, the Andes are characterized by a decrease in elevation, with a big step in topography at ~35°S (the highest point, Cerro Marmolejo, of 6100 m, is an extinct volcano in the northern part of the segment) and the development of an active magmatic arc straddling the Argentina-Chile border. The Frontal Cordillera is only in the northern part of the normal subduction segment, disappearing at 34°S, leaving only the Principal Cordillera to the south.

The amount of shortening systematically decreases from north to south, but at the transitional zone between flat and normal subduction segments, there is a sharp decline from ~180 km of shortening (32°S—Cristallini and Ramos 2000) to ~70 km (33°40′S—Giambiagi et al. 2015). South from this latitude, the amount of shortening lineally decreases until it reaches ~30 km at 35°S (Mescua et al. 2014).

orlando_a_p@yahoo.com.ar

Yet, interestingly, the amount of late Miocene surface uplift is opposite that of the trend in crustal shortening (Hoke et al. 2014).

The cause of the southwards decrease in topography and tectonic shortening is debated, and numerous controls have been assigned to this phenomenon, such as variation in subduction dynamics, age and geometry of the slab (e.g. Jordan et al. 1983; Ramos et al. 2004, 2014; Folguera et al. 2009; Folguera and Ramos 2011; Ramos 2010), rheological and inherited fabric of the South American plate (e.g. Tassara and Yáñez 2003; Ramos et al. 2004; Oncken et al. 2006), and climate variations (e.g. Lamb and Davis 2003). It is clear from all these studies that one factor alone cannot account for the latitudinal variations in deformation and topographic uplift in the Southern Central Andes; although the degree of influence that these parameters have in Andean mountain building remains unclear. A crucial problem in understanding these mechanisms is distinguishing between the effects of the stresses generated from convergence from those associated with strength variations in the upper plate. Over the latitudes of this review, the Nazca Plate is subducting at a similar rate and dip. Therefore, the subduction kinematic patterns, such as convergence rate and obliquity, can be neglected.

The jump in structural shortening correlates with the arcuate shape in the Andean margin at 33°S, known as the Maipo Orocline (Farías et al. 2010). South of this latitude, up to 40°S, clockwise vertical-axis rotations have been measured in Late Jurassic to Neogene rocks, suggesting a close correlation between the southwards drop in horizontal shortening and clockwise block rotations (Arriagada et al. 2013). The precise correlation between this jump in shortening and the southernmost limit of the flat-slab segment strengthen the idea that flattening of the slab favors the upper crustal deformation. Giambiagi et al. (2012) argued that the amount of shortening has been shaped in large part by boundary conditions of the subduction system related to interplate dynamics, but second order features respond to the geological history of the upper plate, which determines its strength. They explained the variation as due to the interplay between deeply seated and shallow structures and propose two models of crustal deformation (Fig. 5). For a balanced cross section model at 33°40′S, the locus of upper-crustal shortening is aligned with respect to the maximum crustal thickness (Fig. 5a). Yet at 35°40′S, upper-crustal shortening is uncoupled from the lower-crustal deformation and thickening (Fig. 5b). The degree of coupling between brittle upper crust and ductile lower crust deformation has a strong influence on mean topographic elevation. In the northern sector of the study area, an initial thick and felsic crust favors the coupling model; while in the southern sector, a thin and mafic lower crust allows the uncoupling model. Their results indicate that interplate dynamics may control the overall pattern of tectonic shortening, however local variations in mean topographic elevation, deformation styles and crustal root geometry are not fully explained and are more likely due to upper-plate lithospheric strength variations. This could explain the jump in crustal shortening at 33°S, related to lithospheric strength variations due to flattening of the slab.

In accordance to this model, a suggested Payenia paleo-flat slab, between 34° and 37°S, has been proposed to control the eastward advance of deformation and

orlando_a_p@yahoo.com.ar

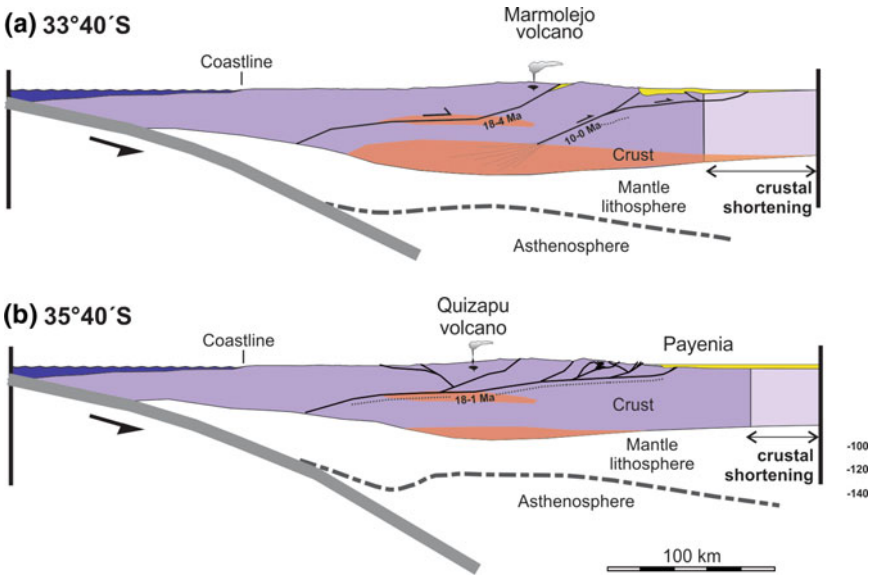


Fig. 5 Conceptual models for the 33°40′S (**a**) and 35°40′S (**b**) crustal deformation styles, taken from Giambiagi et al. (2012). **a** The northern model shows a coupling between upper crustal brittle deformation and lower crustal ductile deformation (areas in pink), and an alignment between the localization of brittle deformation and the maximum crustal thickness. **b** In the southern model, the upper crustal shortening, located in the Atlantic slope of the Andes, is uncoupled from the ductile lower crustal deformation zone, present in the Pacific slope of the Andes

uplift during the middle—late Miocene (Ramos et al. 2014, and references therein). This proposal is based partially in similarities with the Pampean flat-slab segment: including recent uplift east of the Andes in the San Rafael block, which has been assimilated to a broken foreland, and the expansion of arc activity in the same direction. The Pliocene (<2 Ma) to recent steepening of the slab is interpreted to have caused the collapse of the San Rafael block and the extrusion of the OIB-related basalts of the Payenia volcanic province, with a source in the asthenospheric mantle wedge (Burd et al. 2008; Germa et al. 2010). Although the hypothesis of the Payenia flat-slab provides an elegant explanation for some of the first-order features of the Andes at these latitudes, many questions are still unanswered and present areas for future research. The first issue is related to the cause of slab flattening: What are the causes for anomalous slab bouyancy? Another question is the reason for the expansion of arc-related magmatic activity. In contrast to the present Pampean flat-slab, arc magmatism in the Principal Cordillera seems to have not shut down in this segment. Variations in the convergence rate can explain arc widening because of invigorated dynamics in the sub-arc mantle with increased

orlando_a_p@yahoo.com.ar

velocity (Molnar et al. 1979; Shimozuru and Kubo 1983). These questions should be explored in more depth. We hope that future work, including comparisons with other regions and numerical modeling, can provide some clues to test the flat slab model.

7 Conclusions

The structural features of the Andean segment between 32° and 36°S are related to the characteristics of the Chilean subduction system. At these latitudes, different subduction angles clearly determined two segments. North of 33°S, the Pampean flat-slab is developed, with the slab dipping <5°; while south of 34°S, the slab has a "normal" dip of ~30°, with a transitional zone between 33° and 34°S. This sector of the orogen hosts important along-strike variations in topographic uplift, structural elevation, amount and rate of shortening, and crustal root geometry. In the flat-slab segment, high elevations (an average of 4.5 km), several tectonic provinces and the lack of active volcanism characterize the orogen. Deformation and uplift advanced to the east, together with arc-related magmatic activity, sequentially uplifting the Principal Cordillera (20 and ~8 Ma), the Frontal Cordillera (12 and 5 Ma), the Precordillera (<10 Ma) and the Sierras Pampeanas (<5 Ma). Magmatic activity also migrated eastwards, with arc activity focused in the La Ramada and Aconcagua FTB before 10–8 Ma, shutting down in the Andean domain by ~5–3 Ma. Since ~7 Ma, arc-related magmatic activity started in the Sierras Pampeanas.

In the normal subduction segment, the Andes are characterized by a decrease in elevation, with a big step in topography at ~35°S and the development of an active magmatic arc straddling the Argentina-Chile border. The Frontal Cordillera is only in the northern part of the normal subduction segment, disappearing at 34°S; south of this latitude, only the Principal Cordillera remains. The amount of shortening systematically decreases from north to south, but at the transitional zone between flat and normal subduction segments, there is a sharp decline from ~180 km of shortening (32°S) to ~70 km (33°40′S). South from this latitude, the amount of shortening lineally decreases until it reaches ~30 km at 35°S. Yet, interestingly, the amount of late Miocene surface uplift is opposite that of the trend in crustal shortening.

The jump in structural shortening correlates with the arcuate shape in the Andean margin at 33°S, known as the Maipo Orocline. The precise correlation between this jump in shortening and the southernmost limit of the flat-slab segment strengthen the idea that flattening of the slab favors the upper crustal deformation. The amount of shortening has been shaped in large part by boundary conditions of the subduction system related to interplate dynamics, but second order features respond to the geological history of the upper plate, which determines its strength. The degree of coupling between brittle upper crust and ductile lower crust deformation has a strong influence on mean topographic elevation. In the flat-slab and transitional

orlando_a_p@yahoo.com.ar

segments, an initial thick and felsic crust favors the coupling model; while in the normal subduction segment, a thin and mafic lower crust allows the uncoupling model.

Acknowledgements LG, GDH, SMM acknowledge IGCP program 586Y "Geodynamic Processes in the Andes" for stimulating much of the material presented here. This research was supported by grants from the CONICET (PIP 639, PIP 5843 and PIP 112,201,101-484) and the Agencia de Promoción Científica y Tecnológica (PICT 07-10,942 and PICT-2011-1079) to LG, JM, JS, FB and SMM. GDH also acknowledges the Donors of the American Chemical Society Petroleum Research Fund for supporting his participation in this contribution.

References

Aguirre-Urreta B, Tunik M, Naipauer M, Pazos P, Ottone G, Fanning M, Ramos VA (2011) Malargüe Group (Maastrichtian–Danian) deposits in the Neuquén Andes, Argentina: implications for the onset of the first Atlantic transgression related to Western Gondwana break-up. Gondwana Res 19:482–494

Ahumada EA, Costa CH (2009) Antithetic linkage between oblique Quaternary thrusts at the Andean front, Argentine Precordillera. J South Am Earth Sci 28:207–216

Allmendinger RW, Figueroa D, Snyder D, Beer J, Mpodozis C, Isacks BL (1990) Foreland shortening and crustal balancing in the Andes at 30°S latitude. Tectonics 9:789–809

Alvarado P, Beck S, Zandt G, Araujo M, Triep E (2005) Crustal deformation in the south-central Andes back-arc terranes as viewed from regional broad-band seismic wave form modelling. Geophys J Int. doi:10.111/j.1365-246X.2005.02759

Alvarado P, Beck S, Zandt G (2007) Crustal structure of the south-central Andes Cordillera and backarc region from regional wave form modeling. Geophys J Int 121:858–875

Álvarez PP, Godoy E, Aguirre-Urreta MB (1996) Jurásico marino de la Alta Cordillera de Chile Central, Región Metropolitana. In: XIII Congreso Geológico Argentino (Buenos Aires), Actas 5:181

Anderson M, Alvarado P, Zandt G, Beck S (2007) Geometry and brittle deformation of the subducting Nazca Plate, Central Chile and Argentina. Geophys J Int 171(1):419–434

Araneda M, Avendaño M, Merlo C (2000) Modelo gravimétrico de la cuenca de Santiago, etapa III final. In: IX Congreso Geológico DE Chile (Puerto Varas) 404–408

Arcila Gallego PA (2010) Los depósitos sinorogénicos del sur de Mendoza y su relación con la faja plegada y corrida de Malargüe (35°–36°S), Mendoza. Argentina. Unpubl. Ph.D. thesis. Facultad de Ciencias Exactas y Naturales, Universidad de Buenos Aires, p 379

Armijo R, Rauld R, Thiele R (2010) The West Andean Thrust, the San Ramón Fault, and the seismic hazard for Santiago, Chile. Tectonics 29: TC2007 doi:10.1029/2008TC002427

Arriagada C, Ferrando R, Córdova L, Morata D, Roperch P (2013) The Maipo Orocline: a first scale structural feature in the Miocene to Recent geodynamic evolution in the central Chilean Andes. Andean Geol 40:419–437

Astini RA, Benedetto JL, Vaccari NE (1995) The early Palaeozoic evolution of the Argentine Precordillera as a Laurentian rifted, drifted and collided terrane: a geodynamic model. Geol Soc Am Bulletin 107:253–273

Azcuy CL, Caminos R (1987) Diastrofismo. In: Archangelsky S (ed) El Sistema Carbonífero en la República Argentina. Cordoba, Academia Nacional de Ciencias, pp 239–251

Baldauf PE (1997) Timing of the uplift of the Cordillera Principal, Mendoza Province, Argentina. Unpubl. Ph.D. thesis, George Washington University: p 356

Barazangi M, Isacks BL (1976) Spatial distribution of earthquakes and subduction of the Nazca plate beneath South America. Geology 4:686–692

orlando_a_p@yahoo.com.ar

Barrientos S, Vera E, Alvarado P, Monfret T (2004) Crustal seismicity in central Chile. J S Am Earth Sci 16:759–768

Bastías H, Tello GE, Perucca LP, Paredes JD (1993) Peligro sísmico y neotectónica. In: Ramos VA (ed) Geología y recursos naturales de la provincia de Mendoza. Relatorio XII Congreso Geológico Argentino 6(1):645–658

Bechis F, Giambiagi L, García V, Lanés S, Cristallini E, Tunik M (2010) Kinematic analysis of a transtensional fault system: the Atuel depocenter of the Neuquén Basin, Southern Central Andes, Argentina. J Struct Geol 32:886–899

Bechis F, Cristallini E, Giambiagi L, Yagupsky D, Guzmán C, García V (2014) Transtensional tectonics induced by oblique reactivation of previous lithospheric anisotropies during the Late Triassic to Early Jurassic rifting in the Neuquén basin: insights from analog models. J Geodyn 79:1–17

Bermúdez A, Delpino D, Frey F, Saal A (1993) Los basaltos de retroarco extrandinos. In: Ramos VA (ed) Geología y recursos naturales de Mendoza. Relatorio XII Congreso Geológico Argentino y II Congreso de Exploració de Hidrocarburos 161–172

Bertotto GV, Cingolani CA, Bjerg EA (2009) Geochemical variations in Cenozoic back-arc basalts at the border of La Pampa and Mendoza provinces, Argentina. J S Am Earth Sci 28:360–373

Brüggen J (1950) Fundamentos de la Geología de Chile. Instituto Geográfico Militar, Santiago 374

Buelow EK, Suriano J, Mahoney B, Mescua JF, Giambiagi LB, Kimbrough DL (2014) Stratigraphic analysis of the neogene Cacheuta Basin: a record of orogenic exhumation and basin inversión in the South Central Andes. Geol Soc Am Ann Meet 1

Burd A, Booker JR, Pomposiello MC Favetto A, Larsen J, Giordanengo G, Bernal LO (2008) Electrical conductivity beneath the Payún Matrú volcanic field in the Andean back-arc of Argentina near 36.5°S: insights into the magma source. In: VII International Symposium of Andean Geodynamics (Nice), pp 90–93

Burd AI, Booker JR, Mackie R, Favetto A, Pomposiello MC (2014) Three-dimensional electrical conductivity in the mantle beneath the Payún Matrú Volcanic Field in the Andean backarc of Argentina near 36.5° S: evidence for decapitation of a mantle plume by resurgent upper mantle shear during slab steepening. Geophys J Int 198(2):812–827

Cahill T, Isacks BL (1992) Seismicity and shape of the subducted Nazca plate. J Geophys Res 97:17503–17529

Caminos R (1965) Geología de la vertiente oriental del Cordón del Plata, Cordillera Frontal de Mendoza. Rev Asoc Geol Argentina 20(3):351–392

Casa A, Cortéz JM, Borgnia M (2010) Evidencias de deformación pleistocena en el sistema de fallas de La Carrera (32°40′–33°15′S), Cordillera Frontal de Mendoza. Rev Asoc Geol Argentina 67:91–104

Cecioni G (1980) Darwin's Navidad embayment, Santiago region, Chile, as a model of the southeastern Pacific shelf. J Petrol Geol 2–3:309–321

Cegarra M, Ramos VA (1996) La faja plegada y corrida del Aconcagua. In: Ramos VA (ed) Geología de la Región del Aconcagua, Dirección Nacional del Servicio Geológico, Buenos Aires, Anales 24:386–422

Cerdeño E, Vucetich MG (2007) The first rodent from the Marino Formation (Miocene) at Divisadero Largo (Mendoza Argentina) and its biochronological implications. Rev Geol Chile 34:199–207

Charrier R (1979) El Triásico de Chile y regiones adyacentes en Argentina: una reconstrucción paleogeográfica y paleoclimática. Comunicaciones 26:1–47

Charrier R, Wyss A, Flynn J, Swisher C, Norell M, Zapatta F, McKenna M, Novacek M (1996) New evidence for Late Mesozoic-Early Cenozoic evolution of the Chilean Andes in the Upper Tinguiririca Valley (35°S), Central Chile. J South Am Earth Sci 9:393–422

Charrier R, Baeza O, Elgueta S, Flynn J, Gans P, Kay SM, Muñoz N, Wyss A, Zurita E (2002) Evidence for Cenozoic extensional basin development and tectonic in- version south of the flat-slab segment, southern Central Andes, Chile (33°–36°S.L.). J South Am Earth Sci 15:117–139

orlando_a_p@yahoo.com.ar

Charrier R, Bustamante M, Comte D, Elgueta S, Flynn JJ, Iturra N, Muñoz N, Pardo M, Thiele R, Wyss AR (2005) The Abanico Extensional Basin: regional extension, chronology of tectonic inversion and relation to shallow seismic activity and Andean uplift. Neues Jb Geol Paläontol Abh 236:43–77

Charrier R, Farías M, Maksaev V (2009) Evolución tectónica, paleogeográfica y metalogénica durante el Cenozoico en los Andes de Chile norte y central e implicaciones para las regiones adyacentes de Bolivia y Argentina. Rev Asoc Geol Argentina 65:5–35

Cisneros H, Bastias H (1993) Neotectónica del borde oriental del Bloque de San Rafael. In: XII Congreso Geológico Argentino (Mendoza), 270–276

Combina A, Nullo F (2008) El 'diacronismo' de la Formación Agua de la Piedra (Terciario, Mendoza). In: XVII Congreso Geológico Argentino (San Salvador de Jujuy), Actas 1:87–88

Cortés JM (1993) El frente de corrimiento de la Cordillera Frontal y el extremo sur del valle de Uspallata, Mendoza. In: XII Congreso Geológico Argentino y II Congreso de Exploración de Hidrocarburos (Mendoza), Actas 3:168–178

Cortés JM, Cegarra M (2004) Plegamiento cuaternario transpresivo en el piedemonte suroccidental de la Precordillera sanjuanina. Rev Asoc Geol Argentina, Special Publication 7:68–75

Cortés JM, González Bonorino G, Koukharsky M, Pereyra F, Brodtkorb A (1997) Hoja geológica 3369–09, Uspallata, Mendoza. Servicio Geologico Minero Nacional, p 142

Cortés JM, Vinciguerra P, Yamín M, Pasini MM (1999) Tectónica cuaternaria de la region andina del Nuevo Cuyo (28°–38°LS). In: Caminos R (ed) Geología Argentina, Segemar Anales 29:760–778

Cortés JM, Casa A, Pasini M, Yamin M, Terrizzano C (2006) Fajas oblicuas de deformación neotectónica en precordillera y Cordillera Frontal (31°30′–33°30′LS). Controles paleotectónicos. Rev Asoc Geol Argentina 61:639–646

Cortés JM, Terrizzano C, Pasini, M (2015) Quaternary tectonics along oblique deformation zones in the Central Andean retro-wedge between 31°30′ and 35°S. In: Sepúlveda S, Giambiagi L, Moreiras SM, Pinto L, Tunik M, Hoke G, Farías M (eds) Geodynamic Processes in the Andes of Central Chile and Argentina. Geol Soc London, Special Publication 399:267–291

Costa C, Vita-Finzi C (1996) Late Holocene faulting in the southeast Sierras Pampeanas of Argentina. Geology 24:1127–1130

Costa C, Giaccardi A, González Díaz E (1999) Palaeolandsurfaces and neotectonic anaylsis in the southern Sierras Pampeanas, Argentina. In: Smith B, Whalley W, Warke P (eds) Uplift, Erosion and Stability: Perspectives on longterm Landscape Development. Geol Soc London, Special Publication 162:229–238

Costa C, Gardini C, Diederix H, Cortés JM (2000) The Andean orogenic front at sierra de las Peñas-Las Higueras, Mendoza, Argentina. J S Am Earth Sci 13:287–292

Costa C, Murillo M, Sagripanti G, Gardini C (2001) Quaternary intraplate deformation in the southern Sierras Pampeanas, Argentina. J Seismol 5:399–409

Cristallini EO (1996a) La faja plegada y corrida de la Ramada. In: Ramos VA (ed) Geología de la región del Aconcagua. Provincias de San Juan y Mendoza. Dirección Nacional del Servicio Geológico, Anales 24(13):349–385

Cristallini EO (1996b) Plegamiento por despegue en la Alta cordillera de San Juan a los 32°S, Argentina. XIII Congreso Geológico Argentino y III Congreso de Exploración de Hidrocarburos (Mendoza), Actas 2:325–336

Cristallini E, Cangini A (1993) Estratigrafia y estructura de las nacientes del rio Volcan, Alta Cordillera de San Juan. XII Congreso Geológico Argentino, II Congreso de Exploración de Hidrocarburos (Mendoza). Actas 3:85–92

Cristallini E, Ramos VA (2000) Thick-skinned and thin-skinned thrusting in La Ramada Fold and Thrust belt: crustal evolution of the High Andes of San juan, Argentina (32°SL). Tectonophys 317:205–235

Cristallini E, Mosquera A, Ramos VA (1995) Estructura de la Alta Cordillera de San Juan. Rev Asoc Geol Argentina 49(1–2):165–183

orlando_a_p@yahoo.com.ar

Davidson J (1971) Contribución al estudio geológico de los Andes Meridionales Centrales: Geología del área de las Nacientes del Teno, Provincia de Curicó. Unpubl Memoria de Título Universidad de Chile, p 145

Davis DM, Suppe J, Dahlen FA (1983) Mechanics of fold-and-thrust belts and accretionary wedges. J Geophys Res 88:1153–1172

Davis JS, Roeske SM, McClelland WC, Kay SM (2000) Mafic and ultramafic crustal fragments of the southwestern Precordillera terrane and their bearing on tectonic models of the early Paleozoic in western Argentina. Geology 28:171–174

Dellapé D, Hegedus A (1995) Structural inversion and oil occurrence in the Cuyo basin of Argentina. Petroleum Basins of South America. In: Tankard A, Suárez R, Welsink H (eds) Am Assoc Petrol Geol Bulletin 62:369–367

Dicarlo DJ, Cristallini E (2007) Estructura de la margen norte del Río Grande, Bardas Blancas, provincia de Mendoza. Rev Asoc Geol Argentima 62(2):187–199

Dimieri L (1997) Tectonic wedge geometry at Bardas Blancas, southern Andes (36°S). Argentina. J Struct Geol 19(11):1419–1422

Elgueta S, Charrier R,Thiele R (1999) Volcanogenic sedimentation model for the Miocene Farellones Formation, Andean Cordillera, Central Chile. In: IV International Symposium of Andean Geodynamics (Göttingen), Germany, pp 228–231

Encinas A, Le Roux JP, Buatois LA, Nielsen SN, Finger KL, Fourtanier E, Lavenu A (2006) Nuevo esquema estratigráfico para los depósitos marinos mio-pliocenos del área de Navidad (33°–34°S). Chile central. Rev Geol Chile 33(2):221–246

Encinas A, Finger KL, Nielsen SN, Lavenu A, Buatois LA, Peterson D, Le Roux JP (2008) Rapid and major coastal subsidence during the lateMiocene in south central Chile. J S Am Earth Sci 25:157–175

Farías M, Charrier R, Carretier S, Martinod J, Fock A, Campbell D, Cáceres J, Comte D (2008) Late Miocene high and rapid surface uplift and its erosional response in the Andes of central Chile (33°–35°S). Tectonics. doi:10.1029/2006TC002046

Farías M, Vargas G, Tassara A, Carretier S, Baize S, Melnick D, Bataille K (2010) Land-Level changes produced by the Mw 8.8 2010 Chilean earthquake. Science. doi:10.1126/science.1192094

Fock A (2005) Cronología y tectónica de la exhumación en el Neógeno de los Andes de Chile central entre los 33° y los 34° S, Tésis para optar al grado de Magíster en Ciencias, Mención Geología, Memoria para optar al título de Geólogo, Departamento de Geología, Universidad de Chile, Santiago, pp179

Fock A, Charrier R, Farías M, Muñoz M (2006) Fallas de vergencia Oeste en la Cordillera Principal de Chile Central: Inversión de la cuenca de Abanico (33°–34°S). Rev Asoc Geol Argentina, Special Publication 10:48–55

Folguera A, Ramos VA (2011) Repeated eastward shifts of arc magmatism in the southern Andes: a revision to the long-term pattern of Andean uplift and magmatism in the southern Andes. J S Am Earth Sci 32(4):530–545

Folguera A, Zárate M (2009) La sedimentación neógena continental en el sector extrandino de Argentina central. Rev Asoc Geol Argentina 64(4):692–712

Folguera A, Zárate M (2011) Neogene sedimentation in the Argentine foreland between 34°30′S and 41°S and its relation to the Andes evolution. In: Salfity, JA, Marquillas R A (eds) Cenozoic geology of the Central Andes of Argentina: Salta, SCS Publisher, p 123–134

Folguera A, Etcheverría M, Pazos P, Giambiagi LB, Cortés JM, Fauqué L, Fusari C, Rodríguez MF (2004) Descripción de la Hoja Geológica Potrerillos (1:100.000). Subsecretaría de Minería de la Nación, Dirección Nacional del Servicio Geológico, p 262

Folguera A, Naranjo JA, Orihashi Y et al (2009) Retroarc volcanism in the northern San Rafael block (34°–35°30′S), southern Central Andes: occurrence, age, and tectonic setting. J Volcanol Geotherm Res 186:169–185

orlando_a_p@yahoo.com.ar

García VH, Casa AL (2015). Quaternary tectonics and seismic potencial of the Andean retrowedge at 33°–34°S. In: Sepúlveda SA, Giambiagi LB, Moreiras SM, Pinto L, Tunik M, Hoke GD, Farías M (eds) Geodynamic Processes in the Andes of Central Chile and Argenti na. Geol Soc London, Special Publication 399:311–327

Germa A, Quidelleur X, Gillot PY, Tchilinguirian P (2010) Volcanic evolution of the backarc Pleistocene Payun Matru Volcanic Field (Argentina). J S Am Earth Sci 29(3):717–730

Giambiagi LB, Ramos VA (2002) Structural evolution of the Andes in a transitional zone between flat and normal subduction (33°30′–33°45′S), Argentina and Chile. J South Am Earth Sci 15 (1):101–116

Giambiagi L, Martinez AN (2008) Permo-Triassic oblique extension in the Potrerillos-Uspallata area, western Argentina. J S Am Earth Sci 26:252–260

Giambiagi LB, Tunik MA, Ghiglione M (2001) Cenozoic tectonic evolution of the Alto Tunuyán foreland basin above the transition zone between the flat and normal subduction segment (33° 30′–34°S), western Argentina. J South Am Earth Sci 14:707–724

Giambiagi L, Ramos V, Godoy E, Alvarez PP, Orts S (2003) Cenozoic deformation and tectonic style of the Andes, between 33° and 34° south latitude. Tectonics 22(4):15–18

Giambiagi L, Bechis F, García V, Clark AH (2008) Temporal and spatial relationship between thick- and thin-skinned deformation in the Malargüe fold and thrust belt, southern Central Andes. Tectonophys 459:123–139

Giambiagi L, Ghiglione M, Cristallini E, Bottesi G (2009) Kinematic models of basement/cover interactions: insights from the Malargüe fold and thrust belt, Mendoza, Argentina. J Struct Geol 31:1443–1457

Giambiagi L, Mescua J, Bechis F, Martínez A, Folguera A (2011) Pre-Andean deformation of the Precordillera southern sector, Southern Central Andes. Geosphere 7(1):1–21

Giambiagi L, Mescua JF, Bechis F, Tassara A, Hoke G (2012) Thrust belts of the Southern Central Andes: along strike variations in shortening, topography, crustal geometry and denudation. Geol Soc Am Bull 124(7–8):1339–1351

Giambiagi L, Mescua J, Heredia N, Farías P, García Sansegundo J, Fernández C, Stier S, Pérez D, Bechis F, Moreiras SM, Lossada A (2014) Reactivation of Paleozoic structures during Cenozoic deformation in the Cordón del Plata and Southern Precordillera ranges (Mendoza, Argentina). J Iber Geol 40(2):309–320

Giambiagi L, Tassara A, Mescua J, Tunik M, Alvarez PP, Godoy E, Hoke G, Pinto L, Spagnotto S, Porras H, Tapia F, Jara P, Bechis F, García VH, Suriano J, Pagano SD (2015) Evolution of shallow and deep structures along the Maipo-Tunuyán transect (33°40′S): from the Pacific coast to the Andean foreland. In Sepúlveda S, Giambiagi L, Pinto L, Moreiras S, Tunik M, Hoke G, Farías M (eds) Geodynamic Processes in the Andes of Central Chile and Argentina. Geol Soc London, Special Publications 399:63–82

Godoy E (1991) El Corrimiento del Fierro reemplaza a la discordancia intrasenoniana en el rio Cachapoal, Chile Central. In: VI Congreso Geológico de Chile (Viña del Mar), pp. 635–639

Godoy E, Lara L (1994) Segmentación estructural andina a los 33°–34°: nuevos datos en la Cordillera Principal. In: Proceedings VII Congreso Geológico Chile (Concepción), pp. 1344–1348

Godoy E, Yanez G, Vera E (1999) Inversion of an Oligocene volcano-tectonic basin and uplifting of its superimposed Miocene magmatic arc in the Chilean Central Andes: first seismic and gravity evidences. Tectonophys 306(2):217–336

Godoy E, Schilling M, Solari M, Fock A (2009) Carta Rancagua. Escala 1:100.000: Santiago, Servicio Nacional de Geología y Minería. Serie Geología Básica n° 118:50

González Díaz EF (1964) Rasgos geológicos y evolución geomorfológica de la Hoja 27d (San Rafael) y zona occidental vecina (Provincia de Mendoza). Rev Asoc Geol Argentina 19:151–188

Gutiérrez N, Hinojosa L, Le Roux JP, Pedroza V (2013) Evidence for an Early-Middle Miocene age of the Navidad Formation (central Chile): Paleontological, paleoclimatic and tectonic implications. Andean Geol 40(1):1–26

orlando_a_p@yahoo.com.ar

Heredia N, Farias P, García-Sansegundo J, Giambiagi L (2012) The basement of the Andean Frontal Cordillera in the Cordón del Plata (Mendoza, Argentina): Geodynamic evolution. Andean Geol 39(2):242–257

Hervé F, Munizaga F, Parada MA, Brook M, Pankhurst R, Snelling NJ, Drake R (1988) Granitoids of the Coastal Range of central Chile: geochronology and geologic setting. J South Am Earth Sci 1:185–194

Hildreth W, Moorbath S (1988) Crustal contributions to arc magmatism in the Andes of central Chile. Contrib Mineral Petrol 98:455–489

Hoke GD, Giambiagi L, Garzione CN, Mahoney B, Strecker M (2014) Neogene paleoelevation of intermontane basins in a narrow, compressional mountain range, southern Central Andes of Argentina. Earth Planet Sci Lett 406:153–164

Hoke G, Graber NR, Mescua JF, Giambiagi L, Fitzgerald P, Metcalf J (2015) Near pure surface uplift of the Argentine Frontal Cordillera: insights from (U–Th)/He thermochronometry and geomorphic analysis. In: Sepúlveda S, Giambiagi L, Pinto L, Moreiras S, Tunik M, Hoke G, Farías M (eds) Geodynamic Processes in the Andes of Central Chile and Argentina. Geol Soc London, Special Publications 399:383–399

Ibaraki M (1992) Geologic age of biosiliceous sediments in Perú and Chile based upon planktonic foraminifera. Revista Geológica de Chile 19(1):61–66

INPRES (1985) El terremoto de Mendoza, Argentina del 26 de enero de 1985, Informe general, San Juan: p 137

INPRES (2005) Listado de sismos históricos de Argentina. On-line

Irigoyen MV, Buchan KL, Brown RL (2000) Magnetostratigraphy of Neogene Andean foreland-basin strata, lat. 33°S, Mendoza Province Argentina. Geol Soc Am Bull 112:803–816

Iverson O, Mahoney JB, Giambiagi L, Benusa KM, Kimbrough D (2012) Neogene basin evolution in the Las Peñas basin, Salagasta Region, Mendoza, Argentina. Rocky Mountain Geol Soc Am Meeting. https://gsa.confex.com/gsa/2012RM/finalprogram/abstract_203729.htm

Japas MS, Kleiman LE (2004) El ciclo Choiyoi en el bloque de San Rafael (Mendoza): de la orogénesis tardía a la relajación mecánica. Rev Asoc Geol Argentina 7:89–100

Japas MS, Cortés JM, Pasini M (2008) Tectónica extensional triásica en el sector norte de la cuenca Cuyana, Precordillera Sur: Primeros datos cinemáticos. Rev Asoc Geol Argentina 63:213–222

Jara P, Charrier R (2014) Nuevos antecedents estratigráficos y geocronológicos para el Meso-Cenozoico de la cordillera Principal de Chile entre 32° y 32°30′S: Implicancias estructurales y paleogeográficas. Andean Geol 41(1):174–209

Jordan TE, Isacks BL, Allmendinger RW, Brewer JA, Ramos VA, Ando CJ (1983) Andean tectonics related to geometry of subducted Nazca plate. Geol Soc Am Bull 94:341–361

Jordan T, Tamm V, Figueroa G, Flemmings PB, Richards D, Tabutt K, Cheatham T (1996) Development of the Miocene Manantiales foreland basin, Principal Cordillera, San Juan. Argentina. Rev Geol Chile 23(1):43–80

Kay SM, Abbruzzi JM (1996) Magmatic evidence for Neogene lithospheric evolution of the central Andean "flat-slab" between 30°S and 32°S. Tectonophys 259:15–28

Kay S M, Kurtz A (1995) Magmatic and tectonic characterization of the EI Teniente Region, internal report, Corp Nac Cobre, Santiago, Chile, p 80

Kay S, Mpodozis C, Ramos VA, Munizaga F (1991) Magma source variations for mid-late Tertiary magmatic rocks associated with a shallowing subduction zone and a thickening crust in the central Andes (28° to 33°S). In: Harmon, RS, Rapela CW (eds) Andean Magmatism and its Tectonic Setting, Geol Soc of America, Special Paper 265:113–137

Kay SM, Godoy E, Kurtz A (2005) Episodic arc migration, crustal thickening, subduction erosion, and magmatism in the south central Andes. Geol Soc Am Bull 117:67–88

Kay SM, Burns M, Copeland P (2006) Upper Cretaceous to Holocene magmatism and evidence for transient Miocene shallowing of the Andean subduction zone under the northern Neuquén Basin. In: Kay S M, Ramos VA (eds) Evolution of An Andean Margin: A Tectonic and Magmatic View From the Andes to the Neuquén Basin (35°–39°S). Geol Soc America, Special Paper 407:19–60

orlando_a_p@yahoo.com.ar

Kleiman LE, Japas MS (2009) The Choiyoi volcanic province at 34°–36°S (San Rafael, Mendoza, Argentina): Implications for the Late Paleozoic evolution of the southwestern margin of Gondwana. Tectonophys 473:283–299

Kontak DJ, Clark AH, Farrar E, Strong DF (1985) The rift-associated Permo-triassic magmatism of the Eastern Cordillera: a precursor to the Andean orogeny. In: Pitcher WS, Atherton MP, Cobbing EJ, Beckinsale RD (eds) Magmatism at a plate edge-The Peruvian Andes. Wiley, New York, pp 36–44

Kozlowski E, Manceda R, Ramos VA (1993) Estructura. In: Ramos V A (ed) Geología y Recursos Naturales de Mendoza. Relatorio del XII Congreso Geológico Argentino y II Congreso de Exploración de Hidrocarburos (Mendoza), 235–256

Kurtz A, Kay SM, Charrier R, Farrar E (1997) Geochronology of Miocene plutons and exhumation history of the El Teniente region, Central Chile (34°–35°S). Rev Geol Chile 24(1):75–90

Lamb S, Davies P (2003) Cenozoic climate change as a possible cause for the rise of the Andes. Nature 425:792–797

Legarreta L, Uliana MA (1996) The Jurassic succession in west-central Argentina: stratal patterns, sequences and paleogeographic evolution. Palaeogeo Palaeocli Paleoec 20:303–330

Legarreta L, Kokogian DA, Dellapé DA (1992) Estructuración terciaria de la Cuenca Cuyana: ¿Cuánto de inversión tectónica? Rev Asoc Geol Argentina 47(1):83–86

Llambías EJ, Sato AM (1990) EI batolito de Colanguil (29°-31°S) Cordillera Frontal Argentina: estructura y marco tectonico. Rev Geol Chile 17:89–108

Llambías EJ, Kleiman LE, Salvarredi JA (1993) Magmatismo gondwánico de Mendoza. In: Ramos VA (ed) Geología y Recursos Naturales de Mendoza. Relatorio XII Congreso Geológico Argentino, 53–64

Mahoney JB, Kimbrough DL, Hoke GD, Mescua JF, Giambiagi LB, Buelow EK, Hutter A, Leidel A (2014) Cuenca Uspallata: an intermontane basin records episodic uplift of the Cordillera Frontal and Precordillera in the Late Miocene, Geol Soc Am Annual Meeting, 143–148

Maksaev V, Munizaga F, Zentilli M, Charrier R (2009) Fission track thermochronology of Neogene plutons in the Principal Andean Cordillera of central Chile (33–35°S): Implications for tectonic evolution and porphyry Cu-Mo mineralization. Andean Geol 36(2):153–171

Manceda R, Figueroa D (1995) Inversion of the Mesozoic Neuquén rift in the Malargüe fold and thrust belt, Mendoza, Argentina. In: Tankard AJ, Suárez R, Welsink HJ (eds) Petroleum basins of South America, Memoir 62. Am Assoc Petrol Geol Bull, 369–382

Massone HJ, Calderón M (2008) P-T evolution of metapelites from the Guarguaraz Complex, Argentina: evidence for Devonian crustal thickening close to the western Gondwana margin. Rev Geol Chile 35(2):215–231

Melchor R, Casadío S (2000) Hoja Geológica 3766-I, Santa Isabel. Servicio Geológico Minero Nacional, Boletín 344:43

Mescua JF, Giambiagi LB (2012) Fault inversion vs. new thrust generation: a case study in the Malargüe fold-and-thrust belt Andes of Argentina. J Struct Geol 35:51–63

Mescua J, Giambiagi L, Ramos VA (2013) Late Cretaceous Uplift in the Malargüe fold-and-thrust belt (35°S), southern Central Andes of Argentina and Chile. Andean Geol 40(1):102–116

Mescua JF, Giambiagi LB, Tassara A, Gimenez M, Ramos VA (2014) Influence of pre-Andean history over Cenozoic foreland deformation: Structural styles in the Malargüe fold-and-thrust belt at 35°S Andes of Argentina. Geosphere 10(3):585–609

Molnar P, Freedman D, Shih JS (1979) Lengths of intermediate and deep seismic zones and temperatures in downgoing slabs of lithosphere. Geophys J Royal Astronom Soc 56:41–54

Mordojovich C (1981) Sedimentary basins of Chilean Pacific Offshore. In: Halbouty MT (ed) Energy resources of the Pacific Region. Asoc Argent Petrol Gas, Stud Geol, 63–82

Moreiras SM, Giambiagi LB, Spagnotto S, Nacif S, Mescua J, Toural R (2014) El frente orogénico activo de los Andes centrales a la latitud de la ciudad de Mendoza (32°50S–33°S). Andean Geol 41(2):261–342

Mpodozis C, Cornejo P (2012) Cenozoic Tectonics and Porphyry Copper Systems of the Chilean Andes. Geology and genesis of major copper deposits and districts of the world: a tribute to Richard H. Sillitoe. Soc Econ Geol, Boulder, 329–360

orlando_a_p@yahoo.com.ar

Mpodozis C, Kay SM (1990) Provincias magmáticas ácidas y evolución tectónica de Gondwana. Andes Chilenos, 28°–31°S. Rev Geol Chile 17(2):153–180

Mpodozis C, Ramos VA (1989) The Andes of Chile and Argentina. In: Ericksen GE, Cañas Pinochet MT, Rieinemud JA (eds) Geology of the Andes and its Relation to Hydrocarbon and Mineral Resources. Circumpacific Council for Energy and Mineral Resources, Earth Science Series, 11:59–90

Muñoz M, Fuentes F, Vergara M, Aguirre L, Nyström JO, Féraud G, Demant A (2006) Abanico East Formation: petrology and geochemistry of volcanic rocks behind the Cenozoic arc front in the Andean Cordillera, central Chile (33°50′S). Rev Geol Chile 33:109–140

Muñoz M, Charrier R, Fanning CM, Maksaev V, Deckart K (2012) Zircon trace element and O-Hf isotope analyses of mineralized intrusions from El Teniente Ore Deposit, Chilean Andes: Constraints on the source and magmatic evolution of porphyry Cu-Mo related magmas. J Petrol 53:1091–1122

Nullo F, Stephens GC, Otamendi J, Baldauf PE (2002) El volcanismo terciario del sur de Mendoza. Rev Asoc Geol Argentina 57(2):119–132

Nyström JO, Parada MA, Vergara M (1993) Sr- Nd isotope composition of Cretaceous to Miocene volcanic rocks in central Chile: A trend towards a MORB signature and a reversal with time. II Int Symp Andean Geodynamics, París, pp 411–414

Nyström JO, Vergara M, Morata D (2003) Tertiary volcanism during extension in the Andean foothills of central Chile (33°15′–33°45′S). Geol Soc Am Bull 115:1523–1537

Oncken O, Hindle D, Kley J, Elger K, Victor P, Schemmann K (2006) Deformation of the central Andean upper plate system: Facts, fiction, and constraints for plateau models. In: Oncken O, Chong G, Franz G, Giese P, Götze H-J, Ramos VA, Strecker MR, Wigger P (eds) The Andes: Active Subduction Orogeny, Frontiers Earth Sci, Springer, Berlin, 21:3–27

Orts D, Folguera A, Gimenez M, Ramos VA (2012) Variable structural controls through time in the Southern Central Andes (∼36°S). Andean Geol 39:220–241

Pagano DS, Galliski MA, Márquez-Zavalía MF (2014) Emplacement of the La Peña alkaline igneous complex, Mendoza, Argentina (33°S): Implications for the early Miocene tectonic regime in the retroarc of the Andes. J S Am Earth Sci 50:48–66

Pankhurst RJ, Rapela CW, Fanning CM (2000) Age and origin of coeval TTG, I- and S-type granites in the Famatinian belt of NW Argentina. Trans Royal Soc Edinburgh. Earth Sci 91:151–168

Perarnau M, Alvarado P, Saez M (2012) Estimación de la estructura cortical de velocidades sísmicas en el suroeste de la Sierra de Pie de Palo, provincia de San Juan (Argentina). Rev Asoc Geol Argentina 67(4):473–480

Pérez DJ (1995) Estudio geológico del Cordón del Espinacito y regiones adyacentes, provincia de San Juan. Unpubl. Ph.D. thesis. Universidad de Buenos Aires: p 262

Pérez DJ (2001) Tectonic and unroofing history of Neogene Manantiales foreland basin deposits, Cordillera Frontal (32°30′S), San Juan Province, Argentina. J South Am Earth Sci 14:693–705

Pérez DJ, Ramos VA (1996) Los depósitos sinorogénicos. In: Ramos V.A (ed) Geología de la Región del Aconcagua. Provincias de San Juan y Mendoza. Dirección Nacional del Servicio Geológico, Anales 24(11):387–422

Piquer J, Castelli JC, Charrier R, Yáñez G (2010) El Cenozoico del alto río Teno, Cordillera Principal, Chile central: estratigrafía, plutonismo y su relación con estructuras profundas. Andean Geol 37:32–53

Polanski J (1964) Descripción de la Hoja 25a, Volcán San José, provincia de Mendoza, Dirección Nacional de Geolía y Minería, Buenos Aires 98: p 1–94

Polanski J (1972) Carta Geológica Económica de la República Argentina escala 1:200,000, Descripción geológica de la hoja 24 a-b Cerro Tupungato, provincia de Mendoza. Buenos Aires, Dirección Nacional de Geología y Minería, p 110

Porras H (2013) Registro del levantamiento de la Cordillera de los Andes durante el Mioceno basado en las características geoquímicas y mineralógicas de los depósitos sintectónicos de la Cuenca del Alto Tunuyán. (33° 30′S Argentina). Unpubl. MS thesis. Universidad de Chile: p 250

orlando_a_p@yahoo.com.ar

Ramos VA (1994) Terranes of Southern Gondwanaland and Their Control in the Andean Structure (30°–33°S Latitude). In: Reutter K, Scheuber E, Wigger PJ (eds) Tectonics of the Southern Central Andes, Springer, Berlin, 249–261

Ramos VA (1999) Los depósitos sinorogénicos terciarios de la región andina. In: Caminos RL (ed) Geología Argentina. Segemar Anales 29(3):41–96

Ramos VA (2004) Cuyania, an exotic block to Gondwana: review of a historical success and the present problems. Gondwana Res 7:1009–1026

Ramos VA (2008) The basement of the central Andes: the Arequipa and related Terranes. Ann Rev Earth Planet Sci 36:289–324

Ramos VA (2010) The tectonic regime along the Andes: Present-day and Mesozoic regimes. Geol J 45(1):2–25

Ramos VA, Kay SM (1991) Triassic rifting and associated basalts in the Cuyo basin, central Argentina. In: Harmon R S, Rapela C W (eds), Andean Magmatism and Its Tectonic Setting, Geol Soc of America, Special Paper 265:79–91

Ramos VA, Folguera A (2011) Payenia volcanic province in Southern Andes: an appraisal of an exceptional Quaternary tectonic setting. J Volcanol Geotherm Res 201:53–64

Ramos VA, Jordan TE, Allmendinger RW, Mpodozis C, Kay SM, Cortés JM, Palma M (1986) Paleozoic terranes of the central Argentine-Chilean Andes. Tectonics 5:855–880

Ramos VA, Aguirre-Urreta B, Alvarez P, Cegarra M, Cristallini EO, Kay SM, Lo Forte GL, Pereyra FX, Pérez DJ (1996a) Geología de la región del Aconcagua, provincias de San Juan y Mendoza. Dirección Nacional del Servicio Geológico, Buenos Aires, Anales 24:510

Ramos VA, Cegarra M, Cristallini E (1996b) Cenozoic tectonics of the High Andes of west-central Argentina. Tectonophys 259:185–200

Ramos VA, Cristallini EO, Pérez DJ (2002) The Pampean flat-slab of the Central Andes. J South Am Earth Sci 15:59–78

Ramos VA, Zapata T, Cristallini E (2004) The Andean thrust system latitudinal variations in structural styles and orogenic shortening. In: McClay KR (ed) Thrust Tectonics and Hydrocarbons Systems: Am Assoc Petrol Geol, Memoir 82(9):30–50

Ramos VA, Litvak V, Folguera A, Spagnuolo M (2014) An Andean tectonic cycle: From crustal thickening to extension in a thin crust (34°–37°SL). Geosc Frontiers 5:351–367

Rapalini A (2005) The accretionary history of southern South America from the latest Proterozoic to the late Palaeozoic; some palaeomagnetic constraints. Geol Soc London, Special Publication 246:305–328

Richter PP, Ring U, Willner AP, Leiss B (2007) Structural contacts in subduction complexes and their tectonic significance: the Late Paleozoic coastal accretionary wedge of central Chile. J Geol Soc London 164:203–214

Rivano S, Sepulveda P (1991) Hoja Illapel, Región de Coquimbo. Servicio Nacional de Geología y Minería, Santiago, Carta Geológica de Chile 1: 250.000: p 132

Rivano S, Godoy E, Vergara M, Villarroel R (1990) Redefinición de la Formación Farellones en la Cordillera de los Andes de Chile Central (32°–34°S): Revi Geol Chile 17:205–214

Rodriguez MP, Pinto Lincoñir L, Encinas A (2012) Cenozoic erosion in the Andean forearc in Central Chile (33°–34°S): Sediment provenance inferred by heavy mineral studies. In: Rasbury ET, Hemming SR, Riggs NR (eds) Mineralogical and Geochemical Approaches to Provenance. Geol Soc of America, Special Paper 487:141–162

Selles D, Gana P (2001) Mapa geológico del área Talagante-San Francisco de Mostazal, Santiago de Chile, escala 1:100.000. Servicio Nacional de Geología y Minería, Santiago: p 99

Shimozuru D, Kubo N (1983) Volcano spacing and subduction. In: Shimozuru D, Yokoyama I (eds) Arc Volcanism: Physics and Tectonics.Terra Scientific Tokyo: 141–151

Silvestro J, Atencio M (2009) La cuenca cenozoica del río Grande y Palauco: edad, evolución y control estructural, faja plegada de Malargüe. Rev Asoc Geol Argentina 65(1):154–169

Silvestro J, Kraemer P, Achilli F, Brinkworth W (2005) Evolución de las cuencas sinorogénicas de la Cordillera Principal entre 35°–36° S, Malargüe. Rev de la Asoc Geol Argentina 60(4):627–643

orlando_a_p@yahoo.com.ar

Spagnotto S, Triep E, Giambiagi L, Lupari M (2015) Triggered seismicity in the Andean arc region via static stress variation by the Mw=8.8, February 27, 2010, Maule Earthquake. J S Am Earth Sci 63:36–47

Spagnuolo M, Folguera A, Litvak V, Rojas Vera EA, Ramos VA (2012) Late Cretaceous arc rocks in the Andean retroarc region at 36.5°S: Evidence supporting a Late Cretaceous slab shallowing. J S Am Earth Sci 38:44–56

Spikings R, Dungan M, Foeken J, Carter A, Page L, Stuart F (2008) Tectonic response of the central Chilean margin (35–38°S) to the collision and subduction of heterogeneous oceanic crust: a thermochronological study. J Geol Soc London 165:941–995

Sruoga P, Rubinstein NA, Etcheverría MP, Cegarra M, Kay SM, Singer B, Lee J (2008) Estadío inicial del arco volcánico neógeno en la Cordillera Principal de Mendoza (35°S). Rev Asoc Geol Argentina 63(3):469–545

Sruoga P, Rubinstein NA, Etcheverría MP, Cegarra M (2009) Volcanismo neógeno y mineralización asociada, Cordillera Principal, Mendoza (35°S). XII Congreso Geológico de Chile (Santiago de Chile): p 4

Stauder W (1975) Subduction of the Nazca plate under Peru as evidenced by focal mechanisms and by seismicity. J Geophys Res 80:1053–1064

Stern C (2004) Active Andean volcanism: its geologic and tectonic setting. Rev Geol Chile 31 (2):161–206

Stern CR, Skewes MA (1995) Miocene to present magmatic evolution at the northern end of the Andean Southern Volcanic Zone, central Chile. Rev Geol de Chile 22(2):261–272

Tapia F, Farías M, Astaburugada D (2012) Deformación cretácica-paleocena y sus evidencias en la cordillera de los Andes de Chile Central (33.7–36°S). XI Congreso Geológico de Chile (Antofagasta), pp 232–234

Tassara A, Yáñez C (2003) Relación entre el espesor elástico de la litosfera y la segmentación tectónica del margen andino (15–47°S). Rev Geol Chile 30:159–186

Tassara A, Goetze HJ, Hackney R (2006) Three-dimensional density modeling of the Nazca plate and the Andean continental margin. J Geophys Res. doi:10.1029/2005JB003976

Terrizzano CM, Fazzito SY, Cortés JM, Rapalini AE (2010) Studies of Quaternary deformation zones through geomorphic and geophysical evidence: a case in the Precordillera Sur, Central Andes of Argentina. Tectonophysics 490:184–196

Tickyj H, Llambías EJ, Melchor RN (2002) Ordovician rocks from La Pampa province, Argentina. In: Aceñolaza FG (ed) Aspects of the ordovician system in Argentina. Instituto Superior de Correlación Geológica, Serie Correlación Geológica (16):257–266

Triep E (1987) La falla activada durante el sismo principal de Mendoza de 1985 e implicacias tectónicas. X Congreso Geológico Argentino (San Miguel de Tucumán). Actas 1:199–202

Tunik M (2003) Interpretación paleoambiental de la Formación Saldeño (Cretácico superior), en la Alta Cordillera de Mendoza, Argentina. Rev de la Asoc Geol Argentina 58:417–433

Tunik M, Folguera A, Naipauer M, Pimentel M, Ramos VA (2010) Early uplift and orogenic deformation in the neuquén basin: constraints on the Andean uplift from U–Pb and Hf isotopic data of detrital zircons. Tectonophys 489(1–4):258–273

Turienzo M, Dimieri L, Frisicale C, Araujo V, Sánchez N (2012) Cenozoic structural evolution of the Argentinean Andes at 34°40′S: a close relationship between thick and thin-skinned deformation. Andean Geol 39(2):317–357

Uliana MA, Biddle KT, Cerdán J (1989) Mesozoic extension and the formation of Argentine sedimentary basins. In: Tankard A, Balkwill H A (eds) Extensional tectonics and stratigraphy of the North Atlantic Margins. Am Assoc Petrol Geol Bulletin 46:599–614

Urbina N, Sruoga P, Malvicini L (1997) Late Tertiary gold-bearing volcanic belt in the Sierras Pampeanas of San Luis, Argentina. Int Geol Rev 39:287–306

Varela R, Basei MAS, González PD, Sato AM, Naipauer M, Campos Neto M, Cingolani CA, Meira VT (2011) Accretion of Grenvillian terranes to the southwestern border of the Río de la Plata craton, western Argentina. Int J Earth Sci 100(2–3):243–272

orlando_a_p@yahoo.com.ar

Vergani GD, Tankard AJ, Belotti HJ, Welsink HJ (1995) Tectonic evolution and paleogeography of the Neuquén Basin, Argentina. In: Tankard AJ, Suárez R, Welsink HJ (eds) Petroleum Basins of South America. Am Assoc Petrol Geol Bulletin, Memoir 62:383–402

Vergara M, Charrier R, Munizaga F, Rivano S, Sepulveda P, Thiele R, Drake R (1988) Miocene volcanism in the central Chilean Andes (31°30′S–34°35′S). J South Am Earth Sci 1:199–209

Vergara M, Levi B, Nyström JO (1995) Jurassic and Early Cretaceous island arc volcanism, extension and subsidence in the Coast Range of central Chile. Geol Soc Am Bulletin 107:1427–1440

Vergara M, Morata D, Hickey-Vargas R (1999) Cenozoic tholeiitic volcanism in the Colbún area, Linares Precordillera, Central Chile (35°35′–36°S). Rev Geol Chile 26(1):23–41

Vergés J, Ramos V, Meigs A (2007) Crustal wedging triggering recent deformation in the Andean thrust front between 32°S and 33°S: Sierras Pampeanas-Precordillera interaction. J Geophys Res 112: B03S15 doi:10.1029/2006JB004287

Vicente JC (2005) Conglomerados Penitentes vs. Aglomerados Santa María: el frente de corrimiento polifásico del Aconcagua revisitado. xvi Congreso Geológico Argentino (La Plata). Actas 2:185–192

Villar LM, Zappettini EO (2000) El Complejo alcalino Paleógeno de Puesto La Peña. Simposio Internacional Magmatismo Andino. IX Congreso Geológico de Chile, Actas 2:697–701

Visconti G (2007) Sedimentología de la Formación Cerro Azul (Mioceno superior) de la provincia de La Pampa, Argentina. Unpubl. Ph.D. thesis. Universidad de La Pampa, Facultad de Ciencias Exactas y Naturales: p 208

Von Gosen W (1995) Polyphase structural evolution of the southwestern Argentine Precordillera. J South Am Earth Sci 8:377–404

Von Gosen W (1997) Early Paleozoic and Andean structural evolution in the Rio Jáchal section of the Argentine Precordillera. J S Am Earth Sci 10:361–388

Walcek A, Hoke G (2012) Surface uplift and erosion of the southern Argentine Precordillera. Geomorphology 153–154:156–168

Wall R, Gana P, Gutiérrez A (1996) Mapa geológico del área de San Antonio- Melipilla, regiones de Valparaíso, Metropolitana y del Libertador General Bernardo O'Higgins. Servicio Nacional de Geología y Minería, mapa 1:100.000. Santiago 2:20

Wall R, Sellés D, Gana P (1999) Mapa geológico Tiltil-Santiago, Región Metropolitana. Servicio Nacional de Geología y Minería, Mapa geológico N° 9

Willner AP (2005) Pressure-temperature evolution of a Late Paleozoic paired metamorphic belt in north-central Chile (34°–35°30′S). J Petrol 46(9):1805–1833. doi:10.1093/petrology/egi035

Willner AP, Gerdes A, Massone HJ, Schmidt A, Sudo M, Thomson SN, Vujovich G (2011) The geodynamics of collision of a microplate (Chilenia) in Devonian times deduced by the pressure temperature time evolution within part of a collisional belt (Guarguaraz Complex, W-Argentina). Contributions Mineralogy and Petrology: doi:10.1007/s00410-010-0598-8

Yagupsky D, Cristallini E, Fantín J, Zamora Valcarce G, Bottesi G, Varadé R (2008) Oblique half-graben inversion of the Mesozoic Neuquén Rift in the Malargüe Fold and Thrust Belt, Mendoza, Argentina: New insights from analogue models. J Struct Geol 30:839–853

Yañez G, Cembrano J, Pardo M, Ranero C, Sellés D (2002) The Challenger-Juan Fernandez-Maipo major tectonic transition of the Nazca-Andean subduction system at 33–34°: Geodynamic evidence and implications. J South Am Earth Sci 15:23–38

Yrigoyen M (1993) Los depósitos sinorogénicos terciarios. In: Ramos V (ed) Geología y Recursos Naturales de Mendoza. Relatorio del XII Congreso Geológico Argentino y II Congreso de Exploración de Hidrocarburos:123–148

Zappettini EO, Villar LM, Hernández LB, Santos JO (2013) Geochemical and Isotopic Constraints on the Petrogenesis of the Puesto La Peña Undersaturated Potassic Complex, Mendoza Province, Argentina. Geodynamic Implications, Lithos 162–163:301–316

Zurita E, Muñoz N, Charrier R, Harambour PS, Elgueta S (2000) Madurez termal de la materia orgánica de la Formación Abanico = Coya Machalí, Cordillera Principal, Chile Central: resultados e interpretación. IX Congreso Geológico de Chile (Puerto Varas): 726–730

orlando_a_p@yahoo.com.ar

The Transitional Zone Between the Southern Central and Northern Patagonian Andes (36–39°S)

Emilio Agustín Rojas Vera, Darío L. Orts, Andrés Folguera, Gonzalo Zamora Valcarce, Germán Bottesi, Lucas Fennell, Francisco Chiachiarelli and Víctor A. Ramos

Abstract The transition zone from the Southern Central to the North Patagonian Andes is characterized by a low topography and low shortenings. During its evolution, an extensional event in late Oligocene times affected the western section of the Late Cretaceous to Eocene fold and thrust belt. Late early Miocene contraction then constructed most of the eastern Andean slope as in sequence structures stacked in the frontal sector of the fold and thrust belt. However, out of sequence structures derived mainly from the inversion of the late Oligocene extensional depocenters uplifted the axial Andean zone at these latitudes. Contractional and extensional stages coincide with periods in which the arc expanded and retracted, respectively. Shortening gradients from 30 km in the north to only 11 km in the south and development of synorogenic depocenters are linked to arc dynamics.

Keywords Neuquén basin · Fold and thrust belt · Tectonic inversion · Late Oligocene extension

E.A. Rojas Vera (✉) · A. Folguera · L. Fennell · V.A. Ramos
Departamento de Ciencias Geológicas, Facultad de Ciencias Exactas y Naturales, Instituto de Estudios Andinos "Don Pablo Groeber" UBA-CONICET, Buenos Aires, Argentina
e-mail: erv081@yahoo.com.ar

D.L. Orts
Instituto de Investigación en Paleobiología y Geología, Universidad Nacional de Río Negro—CONICET, General Roca (Río Negro), Argentina

G. Zamora Valcarce
Complex Tectonics, Repsol S.A, Houston, TX, USA

G. Bottesi
Gerencia de desarrollo de no convencionales, YPF S.A, Capital Federal, Argentina

F. Chiachiarelli
Desarrollo, YPF S.A, Neuquén, Argentina

© Springer International Publishing Switzerland 2016

A. Folguera et al. (eds.), *Growth of the Southern Andes*,
Springer Earth System Sciences, DOI 10.1007/978-3-319-23060-3_5

orlando_a_p@yahoo.com.ar

1 Introduction and Geological Setting

This chapter analyzes the structure at the transitional zone between the Southern Central and Northern Patagonian Andes (36–39°S) and its evolution since the early opening of the South Atlantic Ocean to the last stages of Andean growth in late Miocene times.

The study area comprehends the western part of the Neuquén Basin that was incorporated into the orogenic wedge as the Agrio, Chos Malal, and Malargüe fold and thrust belts (Fig. 1). This deformation exposed Paleozoic to Cretaceous sections through different deformational stages. The basement of the Neuquén Basin is

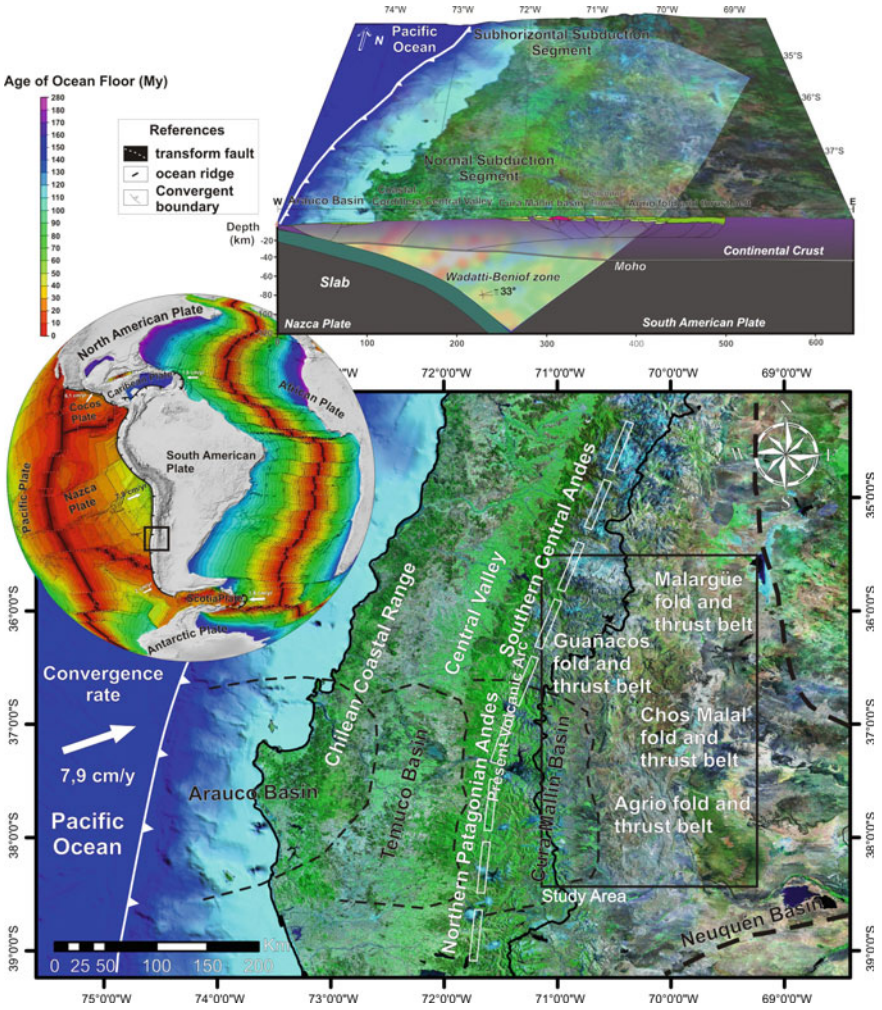


Fig. 1 Location of the study area at the transition zone between the Southern Central Andes and the Northern Patagonian Andes from the axial zone of the Andes to the retroarc zone

orlando_a_p@yahoo.com.ar

exposed in different structures of the western sector of the fold and thrust belt and is composed of the Andacollo Group (Hervé et al. 2013) with more than 2700 m of Carboniferous marine shales and ignimbrites highly deformed by the Gondwanian orogeny (Giacosa et al. 2014). These rocks are covered by the Choiyoi Group composed of more than 2000 m of Permian to Triassic volcanic and sedimentary rocks (Stipanicic et al. 1968; Ramos et al. 2011) and the Late Triassic to Early Jurassic Pre-Cuyano corresponding to sediments and volcaniclastic sections with variable thicknesses from 50 to 3000 m. These sequences have synextensional geometries identified in seismic lines (Gulisano and Gutiérrez Pleimling 1994) related to the early synrift stage of the Neuquén Basin. Outcrops of these units are associated with larger structures such as the Cordillera del Viento at the western part of the Chos Malal fold and thrust belt (Fig. 2), Domuyo, Sierra Azul, Sierra de Reyes, and Sierra de Cara Cura at the Malargüe fold and thrust belt. By the Early Jurassic, a Pacific-derived transgression flooded the western part of the basin, recorded by the Cuyo Group (Gulisano 1981) composed of offshore shales, turbidites, and platform sandstones. This unit is exposed from the western Agrio fold and thrust belt to the north in the Cordillera del Viento, Sierra de Reyes, Sierra de Cara Cura, Sierra Azul, and Domuyo anticline (Figs. 2 and 3).

Over these, Middle to Late Jurassic sequences of the Lotena Group were deposited (Legarreta and Gulisano 1989) (Figs. 1 and 2) representing a transgressive event composed of continental sandstones of the Tordillo Formation and evaporates of the Auquilco Formation. These evaporates are the main detachment level of the fold and thrust belt at these latitudes.

The lower part of the Mendoza Group corresponds to a second Pacific transgression in Late Jurassic to Early Cretaceous times, represented by the Vaca Muerta Formation, composed of 1400 m of shales and limestones (Legarreta and Gulisano 1989). Over these, the Mulichinco Formation represents a rapid fall in sea level that is followed by the Agrio Formation that is interpreted as another Pacific transgression. A Cretaceous regressive event is marked by the Huitrín and Rayoso formations, composed of evaporates, fluvial, and lacustrine deposits. A regional unconformity separates these units from the overlaying fluvial to lacustrine Neuquén Group. Tunik et al. (2010) dated the basal levels of this unit in 99 Ma, interpreting this as the first foreland basin associated with the proto-Andes at these latitudes. As part of this foreland stage, a Late Cretaceous to Paleocene Atlantic transgression corresponding to the Malargüe Group is exhumed in the eastern fold and thrust belt (Barrio 1990; the basin Aguirre-Urreta et al. 2011).

Late Cretaceous to Eocene arc-related volcanic and sub-volcanic rocks are emplaced in the western part of the Agrio and Chos Malal fold and thrust belts (Figs. 1 and 2) (Groeber 1956; Zöllner and Amos 1973; Rapela and Llambías 1985; Llambías and Rapela 1989; Zamora Valcarce et al. 2006). Previous to the emplacement of this magmatic suite, within-plate basaltic to andesitic intrusives with 91.97 ± 4.06 Ma age cut the contractional structure of the western Agrio fold and thrust belt, indicating that contractional deformation started in this sector before the Late Cretaceous (Zamora Valcarce et al. 2006). A Late Cretaceous to Paleocene

orlando_a_p@yahoo.com.ar

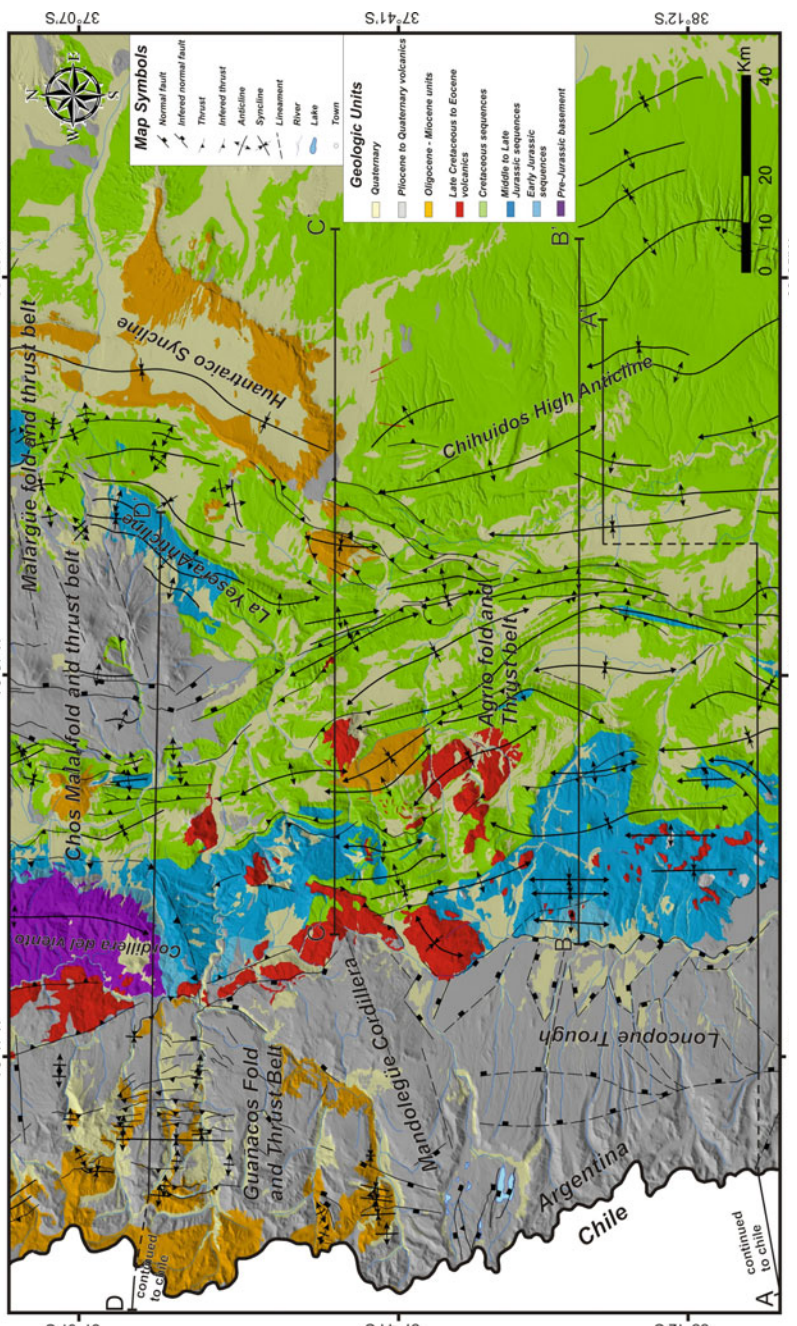


Fig. 2 Geological map of the Agrio and southern Chos Malal fold and thrust belts in the retroarc zone

orlando_a_p@yahoo.com.ar

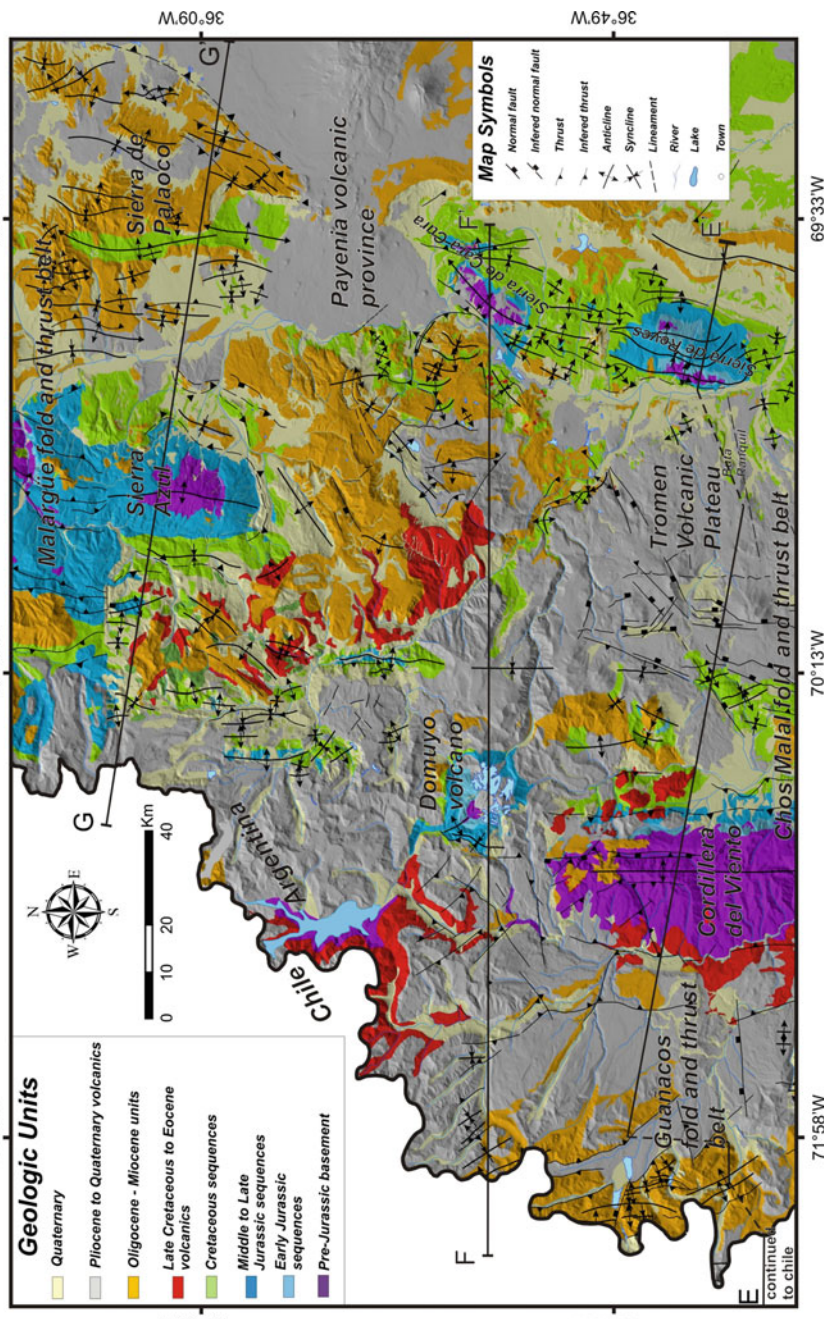


Fig. 3 Geological map of the northern Chos Malal and southern Malargüe fold and thrust belts

orlando_a_p@yahoo.com.ar

arc expansion has been interpreted coetaneous to this contractional deformation based on the age of the magmatic rocks emplaced at the retroarc zone (Ramos and Folguera 2005).

Oligocene to early Miocene volcanic rocks of the Charilehue and Palauco Formations (Uliana 1978; Ramos and Barbieri 1989) (Fig. 3) are associated with an extensional stage that affected the retroarc zone interrupting the Andean contraction. This stage is represented at the arc zone by the Cura Mallín Formation (Sarris 1964; Niemeyer and Muñoz 1983; Leanza et al. 2002; Croft et al. 2003; Vergara et al. 1997; Suárez and Emparán 1997; Jordan et al. 2001; Burns 2002). Unconformably overlying these sections late Miocene ignimbrites, lava flows and minor sedimentary sequences of the Trapa Trapa and Cajón Negro Formations were deposited (Pesce 1981; Niemeyer and Muñoz 1983; Utgé et al. 2009). Kay et al. (2006) interpreted these units as a late Miocene eastward arc expansion over the Chos Malal fold and thrust belt, similarly to the processes that occurred to the north in the Pampean flat slab zone.

Late Miocene synorogenic deposits of the Tralalhué and Puesto Burgos Formations contemporaneous to this stage are associated with the inversion of late Oligocene extensional structures and local reactivation of Cretaceous to Eocene contractional structures (Ramos 1999; Repol et al. 2002; Leanza and Hugo 2001; Zamora Valcarce et al. 2006).

After these mountain building processes, Pliocene to Quaternary arc rocks (Figs. 2 and 3) are erupted at the Main Andes area to the retroarc region. Over the Main Andes, Pliocene to early Quaternary volcanic rocks of the Cola de Zorro Formation and late Pleistocene to Holocene volcanic centers (Vergara and Muñoz 1982; Lara et al. 2001) in the Loncopué Trough, Tromen volcanic Plateau, and Payenia volcanic field (Stern 1989; Kay et al. 2006; Galland et al. 2007; Varekamp et al. 2010) locally show synextensional geometries (Folguera et al. 2006; Melnick et al. 2006; Rojas Vera et al. 2010, 2014b).

2 The Agrio and Southern Chos Malal Fold and Thrust Belts

A series of structural transects were constructed on Move™ Software of Midland Valley using surface, borehole, seismic, and gravity data. For the restorations, we used flexural slip algorithms in structures with varying thicknesses in strata and line length unfold in minor structures detached in the sedimentary column.

The southernmost transect *A*–*A′* was performed at 38°S (Fig. 4), which integrates structures of the Main Andes in Chile and the Agrio fold and thrust belt. The section through the Agrio fold and thrust belt (Fig. 2) is partially based on Zamora Valcarce (2007), while the western slope of the Andes is from Radic (2010). Structures located in the Loncopué Trough are locally measured from field data, while sedimentary thicknesses are approximated from gravity data (Rojas Vera et al. 2010).

orlando_a_p@yahoo.com.ar

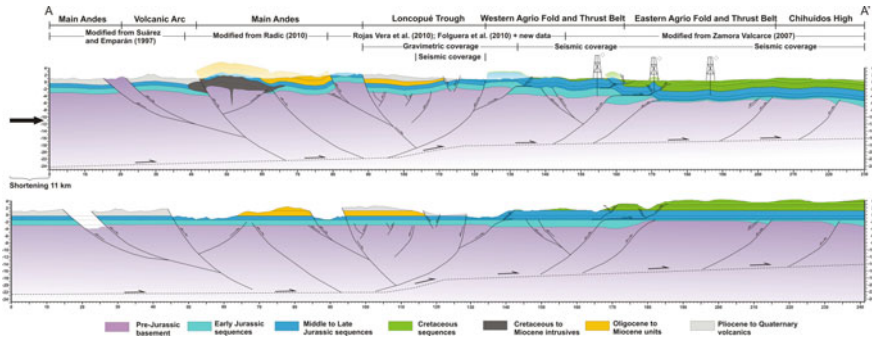


Fig. 4 *A–A′* structural cross section performed at 38°S that includes the Main Andes and the Agrio fold ant thrust belt. Note that the restoration shows only 11 km of shortening (see Fig. 2 for location) (modified from Rojas Vera et al. 2014a)

The decollement level within the basement is located at 15–24 km depth, dipping 5–3°W (Zapata et al. 1999; Zamora Valcarce et al. 2006). This section shows deformation of three partially overlapped basins: (1) the Mesozoic Neuquén Basin, mostly exhumed to the east in the Agrio fold and thrust belt; (2) the Oligocene to Miocene Cura Mallín Basin in the western part; and (3) thick sequences of Pliocene to Quaternary strata from the Loncopué Trough and the Main Andes (Fig. 2).

Over the western slope of the Andes along transect *A–A′* (Fig. 4), Early Jurassic sequences of the Nacientes del Bío Bío Formation are exposed (Suárez and Emparán 1997), which are equivalent to the Cuyo Group exposed at the western part of the Agrio fold and thrust belt on the eastern Andean side. Gravimetric models indicate that at the mid part of the section in the Loncopué Trough axis, those Early Jurassic successions would be buried beneath thick packages of Cenozoic and Quaternary strata as deep as 4–5 km (Rojas Vera et al. 2010). The Loncopué Trough is controlled by west-dipping normal faults, whose hanging wall is covered by Mesozoic to Cenozoic strata, visualized in seismic data and partially in the field (Jordan et al. 2001).

To the east, the Agrio fold and thrust belt exposes younger sequences of Early Cretaceous age in predominantly short-wavelength structures indicative of a thin-skinned mechanics of deformation. However, at the eastern deformational front, a long-wavelength anticline denominating the Chihuidos High is uplifted (Fig. 2), interpreted as a mild tectonic inversion of an array of Late Triassic extensional faults (Zamora Valcarce et al. 2006). The restoration of this transect resulted in a total shortening of 11 km which is equivalent to 4.78 % of the initial length.

The *B–B′* section (Fig. 5) is characterized by a series of basement structures at the western sector of the fold and thrust belt that transfer shortening to the upper sedimentary section producing thin-skinned structures. This complex structural geometry was described by Zapata et al. (1999) and Zamora Valcarce et al. (2006), based on well and seismic data, showing that the structures are detached at shallow

orlando_a_p@yahoo.com.ar

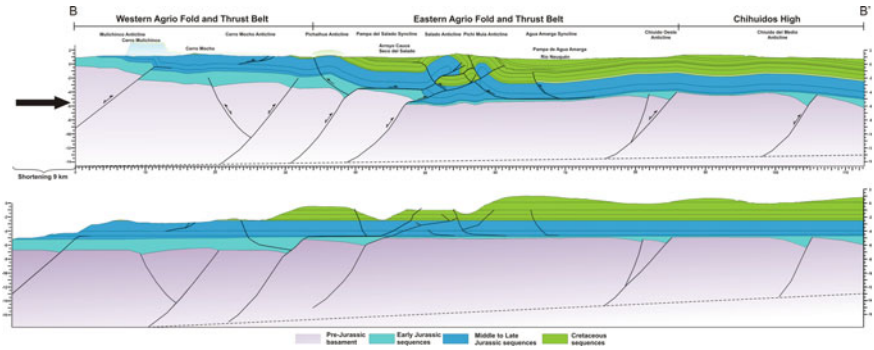


Fig. 5 *B–B′* structural cross section performed at 38°S that crosses the Main Andes region and the Agrio fold and thrust belt. Note that the restoration shows only 9 km of shortening (see Fig. 2 for location) (modified from Rojas Vera et al. 2014a)

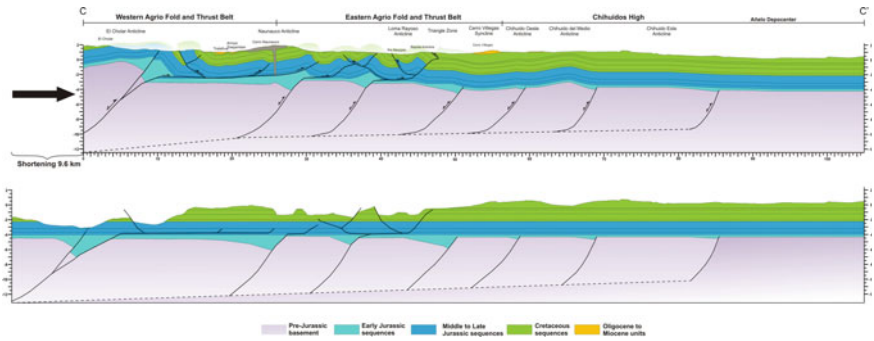


Fig. 6 *C–C′* structural cross section performed over the northern part of the Agrio fold and thrust belt (see Fig. 2 for location)

levels in the Auquilco Formation forming anticlines of 2–4 km in wavelength. A total shortening of 9 km was obtained for this section from the palinspastic restoration (Fig. 5).

The *C–C′* cross section (Fig. 2) is again the result of a combination of thin- and thick-skinned structures. Over the western part of the section, the Cholar Anticline is developed (Fig. 6), as an east vergent basement structure with a wavelength of more than 12 km, interpreted as the southern continuation of the Cordillera del Viento developed in the western part of the Chos Malal fold and thrust belt.

Immediately to the east, the presence of a backthrust defines a triangle zone. Zamora Valcarce et al. (2006) and Rojas Vera et al. (2014a) based on seismic information show how uplift of basement structures transfer displacements to shallower levels forming the Loma Rayoso Anticline, uplifted by a backthrust. The Chihuidos high to the east of this triangle zone is again the result of tectonic inversion of Early Jurassic extensional structures. Along this transect, Miocene

orlando_a_p@yahoo.com.ar

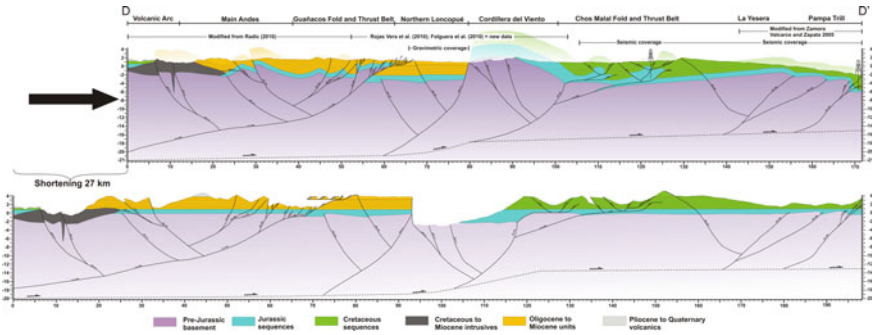


Fig. 7 *D–D′* structural cross section performed over the Agrio and Guañacos fold and thrust belts (see Fig. 2 for location) (modified from Rojas Vera et al. 2014a)

volcanic products are sealing part of the contractional structures, such as in the case of the Cerro Villegas syncline over which Miocene volcanic rocks are emplaced in the core. Restoration of the section yielded a total shortening of 9.6 km.

The *D–D′* section at 37°S (Fig. 7) has been discussed extensively during the 1990s, proposing contrasting models that explained shortening and topography (Ramos and Barbieri 1989; Kozlowski et al. 1996; Chauveau et al. 1996; Booth and Coward 1996; and Zapata et al. 1999). This is explained at the Chos Malal fold and thrust belt, by a deep decollement at 15–20 km (Zapata et al. 1999; Zamora Valcarce et al. 2006) and shallower detachments in Late Jurassic levels. Surface data show fault bend and fault propagation folds that alternate with some back-thrusts that accommodate contractional deformation. To the east, this shortening is transferred to basement structures in the deformational front such as the La Yesera and Pampa Trill anticlines (Fig. 7). The westernmost part of the Chos Malal fold and thrust belt is defined by the Cordillera del Viento basement block, where Late Paleozoic sequences crop out over a west-dipping high-angle fault.

The northern Loncopué Trough is located immediately to the west and is characterized by west-dipping high-angle faults identified in seismic lines (Jordan et al. 2001), that controls a depocenter filled by Oligocene to Miocene sequences. To the west, inversion of Oligocene to Miocene extensional depocenters at the Guañacos fold and thrust belt is associated with a narrow fan of west-dipping thrusts detached from the late Oligocene to early Miocene shales and limestones of the Cura Mallín Formation. This imbricate system was modeled using the 2D Move software and fold bend fault geometries proposed by Suppe (1983). Following Boyer and Elliott´s (1982) classification, we recognize these geometries as the basal part of an antiformal stack whose upper folded thrust has been eroded accommodating substantial amounts of shortening. Over the western slope of the Andes, a series of backthrusts stacked late Oligocene to early Miocene sequences and their basement according to Radic (2010). Therefore the Main Andes become a double vergent thick-skinned system at these latitudes.

orlando_a_p@yahoo.com.ar

In order to estimate shortenings, we have restored this section using a flexural slip algorithm (2DMove software). This yielded a higher shortening, compared to the southern transects, of 27 km, representing 13.6 % of the initial length. Comparing this section to the immediate-southern section (Fig. 4), a total shortening difference of 16 km exists. This is due basically to the development of the Guañacos fold and thrust belt frontal imbricate system, which is absent in the south. The remaining 6 km are due to a larger shortening achieved in the Chos Malal fold and thrust belt in comparison to the Agrio fold and thrust belt to the south.

3 The Northern Guañacos and Malargüe Fold and Thrust Belts

The *E–E′* section (Figs. 3 and 8) crosses the northernmost Guañacos and northernmost Chos Malal fold and thrust belts at its transition to the Malargüe fold and thrust belt. Again, this section exhibits an alternation between thick- and thin-skinned structures, although a difference in comparison to the southern transects, is that the orogenic front is formed by basement structures that insert in Late Jurassic evaporates, forming complex narrow contractional belts that accommodated more shortening.

To the west, deformation at the eastern Guañacos fold and thrust belt is explained as involving at least two contractional stages: an older stage that stacked the upper Tertiary sequence over a shallow decollement and a younger one that shortened the basement, folding previous thin-skinned deformations (Fig. 8). This section has been restored using flexural slip and line length algorithms, yielding a total shortening of 26.5 km that represents a 11.7 % of the initial length, similarly to the section immediately to the south.

To the north, the structural cross section performed in the southern part of the Malargüe fold and thrust belt is *F–F′* (Figs. 3 and 9) that crosses the northern Cordillera del Viento and the Domuyo anticline, with an anomalous height due to the presence of a Pliocene intrusive. To the east, the Puntilla de Huicán structure

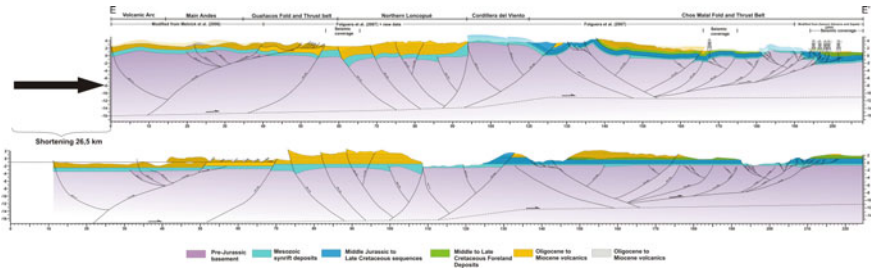


Fig. 8 *E–E′* structural cross section performed over the transitional zone from the Chos Malal to the Malargüe fold and thrust belts (see Fig. 3 for location) (modified from Rojas Vera et al. 2014a)

orlando_a_p@yahoo.com.ar

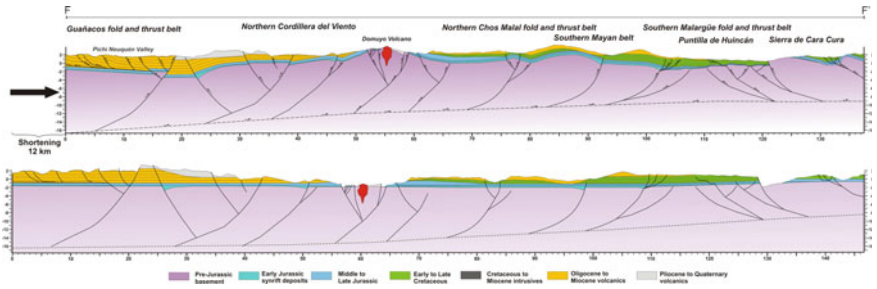


Fig. 9 *F–F′* structural cross section performed over the southern Malargüe fold and thrust belt (see Fig. 3 for location)

(Galarza et al. 2009) is a doubly vergent basement structure that folds at surface late Oligocene volcanic products. In the eastern deformational front, the Sierra de Cara Cura shows a deeper level of exhumation with Late Triassic sequences at its core (Fig. 9).

This section has been restored using flexural slip and line length algorithms, yielding a total shortening of 12 km. In comparison to the immediate-southern sections, this lower shortening can be explained by the absence of the Guañacos fold and thrust belt at these latitudes over the eastern Andean slope.

The northernmost *G–G′* section (Fig. 10) crosses entirely the Malargüe fold and thrust belt (Orts et al. 2012).

Deformational mechanisms are similar to the southern sections, although in this case temporal constraints show an inner sector initially constructed in Late Cretaceous times and an eastern sector mainly built in Cenozoic times. The Portezuelos Colorados syncline is a Late Cretaceous depocenter filled by synorogenic strata coming from the western fold and thrust belt (Orts et al. 2012). This indicates that most of the Andes in Chile had a first phase of development in Late Cretaceous times. To the east, the Sierra Azul anticline is a Neogene uplift,

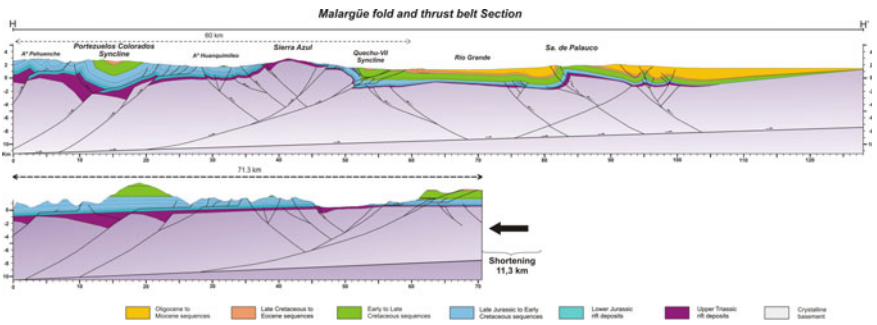


Fig. 10 *G–G′* structural cross section performed over the Malargüe fold and thrust belts (see Fig. 3 for location) (modified from Orts et al. 2012)

orlando_a_p@yahoo.com.ar

constrained by the age of the youngest deformed sequences (18 Ma; Silvestro and Atencio 2009). This cross section between the drainage divide area and the emergent orogenic front was balanced, yielding a total shortening of only 11.3 km.

4 Structural Evolution of the Retroarc Zone at the Transition Between the Southern Central and Patagonian Andes (36°–39°S)

The Agrio fold and thrust belt (*A*–*A*′, *B*–*B*′, *C*–*C*′) shows low shortenings near 11 km in a 240 km long section. To the north, at the Chos Malal fold and thrust belt latitudes, the Guañacos fold and thrust belt in the west involves a deformational front with thin-skinned structures that determines a total shortening up to 27 km along the transect. These differences can be linked to the differential migration of the magmatic arc through time (see next chapter). During the Late Cretaceous to the Eocene, the initial eastward expansion of the arc series reached the Cordillera del Viento and even expanded toward the Río Grande area. This pronounced eastern migration of the arc series in Late Cretaceous to Eocene times is associated with a higher exhumation and relatively high shortenings through many structures of the northern analyzed sector across the Malargüe fold and thrust belt. Similarly, a late Miocene arc expansion (Kay et al. 2006) coincides with the final construction of the Guañacos fold and thrust belt and eastern parts of the Malargüe and Chos Malal fold and thrust belts (see next chapter).

A Late Cretaceous exhumation (100 to 90–70 Ma) is determined for the inner sector of the fold and thrust belt based on limited amounts of fission track data (Burns 2002; Kay et al. 2006; Zamora Valcarce et al. 2009) and synorogenic strata (Tunik et al. 2010; Fenell et al. 2015) (Fig. 11). Late Eocene exhumation seems to be a more restricted phenomenon, revealed for the western Main Andes by fission track data (Gräffe et al. 2002) and regional angular unconformities locally found in the orogenic front area (Cobbold and Rossello 2003). After this mountain building event, an arc westward retraction in late Oligocene to early Miocene times coincides with an extensional reactivation of the fold and thrust belt (Muñoz et al. 2000; Jordan et al. 2001; Charrier et al. 2002; Kay et al. 2006; Rojas Vera et al. 2010; Folguera et al. 2010; Spagnuolo et al. 2012).

The late Miocene contractional stage (Fig. 11) was the responsible for the final construction of the fold and thrust belt, associated at the Malargüe fold and thrust belt with synorogenic basins developed to the east of Sierra Azul at the Río Grande and Palaoco depocenters (Silvestro and Atencio 2009) at the time of a renewed arc foreland expansion. To the south, Neogene synorogenic depocenters at the Agrio fold and thrust belt, where the arc did not migrate are more restricted (Zamora Valcarce et al. 2006, 2009).

orlando_a_p@yahoo.com.ar

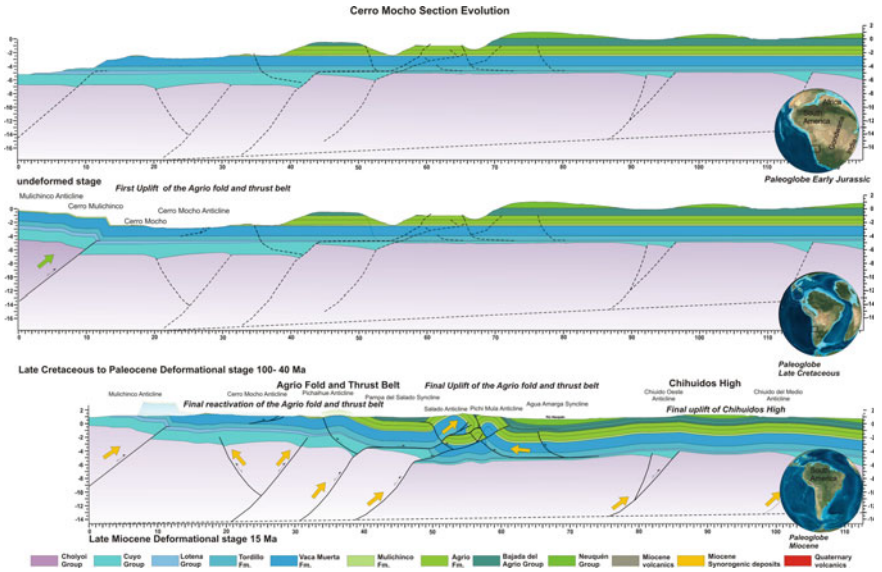


Fig. 11 Structural development of the Agrio fold and thrust belt

Acknowledgements The Authors acknowledge the financial support of CONICET and ANPCyT PICT-1490-2010, Argentina.

References

Aguirre-Urreta MB, Tunik M, Naipauer M, Pazos PJ, Ottone EG, Fanning MC, Ramos VA (2011) Malargüe group (Maastrichtian–Danian) deposits in the Neuquén Andes, Argentina: implications for the onset of the first Atlantic transgression related to Western Gondwana break-up. Gondwana Res 19(2):482–494

Barrio CA (1990) Late Cretaceous-early tertiary sedimentation in a semi-arid foreland basin (Neuquén Basin, Western Argentina). Sediment Geol 66:255–275. doi:10.1016/0037-0738(90)90063-Y

Booth JLM, Coward MP (1996) Basement faulting and inversion of the NW Neuquén basin, Argentina. In: III international symposium andean geodynamics Saint Malo, France, pp 295–298

Boyer S, Elliott D (1982) Thrust systems. Am Assoc Pet Geol Bull 66:621–628. doi:10.1306/03B5A77D-16D1-11D7-8645000102C1865D

Burns W (2002) Tectonics of the Southern Andes from stratigraphic, thermochronologic, and geochemical perspectives. PhD thesis (Unpublished), Cornell University, pp 218

Chauveau V, Nivière B, Cobbold PR, Rossello EA, Ballard J-F, Eichenseer HT (1996) Structure of the andean foothills, Chos Malal region, Neuquén Basin, Argentina. In: III international symposium andean geodynamics, Saint Malo, extented abstracts, Ed. ORSTOM, pp 315–318

Charrier R, Baeza O, Elgueta S, Flynn J, Gans P, Kay S, Muñoz N, Wyss A, Zurita E (2002) Evidence for Cenozoic extensional basin development and tectonic inversion south of the flat-slab segment, southern Central Andes, Chile (33°–36°S.L.). J South Am Earth Sci 15:117–139. doi:10.1016/S0895-9811(02)00009-3

orlando_a_p@yahoo.com.ar

Cobbold PR, Rossello EA (2003) Aptian to recent compressional deformation, foothills of the Neuquén Basin, Argentina. Mar Pet Geol 20:429–443. doi:10.1016/S0264-8172(03)00077-1

Croft DA, Radic JP, Zurita E, Charrier R, Flynn JJ, Wyss AR (2003) A miocene toxodontid (Mammalia: Notoungulata) from the sedimentary series of the cura-mallín Formation, Lonquimay, Chile. Rev Geol Chile 30:285–298. doi:10.4067/S0716-02082003000200008

Fenell L, Folguera A, Naipauer M, Gianni G, Rojas Vera EA, Bottesi G, Ramos VA (2015) Cretaceous deformation of the Southern Central Andes: synorogenic growth strata in the Neuquén Group (35°30′–37°S). Basin Res. In Press

Folguera A, Zapata T, Ramos VA (2006) Late Cenozoic extension and the evolution of the Neuquén Andes. In: Kay SM, Ramos VA (eds) Evolution of an Andean margin: a tectonic and magmatic view from the Andes to the Neuquén Basin (35°–39°S lat). Geol Soc of America, Special Paper vol 407, pp 267–285

Folguera A, Rojas Vera E, Bottesi G, Zamora Valcarce G, Ramos VA (2010) The Loncopué Trough: a Cenozoic basin produced by extension in the southern Central Andes. J Geodyn 49:287–295. doi:10.1016/j.jog.2010.01.009

Galarza BJ, Zamora Valcarce G, Folguera A, Bottesi GL (2009) Geología y evolución tectónica del frente cordillerano a los 36°30′S: bloques de Yihuin-Huaca y Puntilla de Huincán. Mendoza. Rev Asoc Geol Argentina 65:170–191

Galland O, Hallot E, Cobbold PR, Ruffet G, de Bremond d'Ars J (2007) Volcanism in a compressional Andean setting: a structural and geochronological study of Tromen volcano (Neuquén province, Argentina). Tectonics 26: 1–24. TC4010. doi:10.1029/2006TC002011

Giacosa R, Allard J, Foix N, Heredia N (2014) Stratigraphy, structure and geodynamic evolution of the Paleozoic rocks in the Cordillera del Viento (37° S latitude, Andes of Neuquén, Argentina). J Iberian Geol 40:331–348. doi:10.5209/rev_JIGE.2014.v40.n2.45301

Gräffe K, Glodny J, Seifert W, Rosenau M, Echtler H (2002) Apatite fission track thermochronology of granitoids at the south Chilean active continental margin (37 S–42 S): implications for denudation, tectonics and mass transfer since the Cretaceous. In: V International Symposium on Andean Geodynamics (Toulouse)

Groeber P (1956) La Serie Andesítica patagónica. Sus relaciones, posición y edad. Rev la Asoc Geol Argentina 9:39–42

Gulisano CA (1981) El ciclo cuyano en el norte de Neuquén y sur de Mendoza. In: XI Congreso Geológico Argentino (San Juan), Actas vol 3, pp 573–592

Gulisano CA, Gutiérrez Pleimling A (1994) The Jurassic of the Neuquen Basin. b) Mendoza Province field guide. Publicación 46. Dirección Nacional del Servicio Geológico, Buenos Aires

Hervé F, Calderón M, Fanning CM, Pankhurst RJ, Godoy E (2013) Provenance variations in the Late Paleozoic accretionary complex of central Chile as indicated by detrital zircons. Gondwana Res 23:1122–1135. doi:10.1016/j.gr.2012.06.016

Jordan T, Burns W, Veiga R (2001) Extension and basin formation in the southern Andes caused by increased convergence rate: a mid-Cenozoic trigger for the Andes. Tectonics 20:308–324. doi:10.1029/1999TC001181

Kay S, Burns W, Copeland PC, Mancilla O (2006). Upper Cretaceous to Holocene magmatism and evidence for transient Miocene shallowing of the Andean subduction zone under the northern Neuquén Basin. In: Kay SM, Ramos VA (eds) Evolution of an Andean margin: a tectonic and magmatic view from the Andes to the Neuquén Basin (35°–39°S lat). Geol Soc of America, Special Paper, vol 407, pp 19–60

Kozlowski EE, Cruz CE, Sylwan CA (1996) Geología estructural de la zona de Chos Malal, Cuenca Neuquina, Argentina. Relatorio del XIII Congreso Geológico Argentino y III Congreso de Exploración de Hidrocarburos 1:15–26

Lara L, Rodríguez C, Moreno H, Pérez de Arce C (2001) Geocronología K-Ar y geoquímica del volcanismo plioceno superior-pleistoceno de los Andes del sur (39–42°S). Rev Geol Chile. doi:10.4067/S0716-02082001000100004

Leanza HA, Hugo CA (2001) Hoja Geológica Zapala 3969-1, Provincia del Neuquén, Escala 1:250.000. Servicion Geológico y Minerio Argentino, Bulletin vol 275. Buenos Aires, 128 pp

orlando_a_p@yahoo.com.ar

Leanza HA, Volkheimer W, Hugo CA, Melendi DL, Rovere E (2002) Lutitas negras lacustres cercanas al límite Paleógeno-Neógeno en la region noroccidental de la provincia del Neuquén: Evidencias palinológicas. Rev Asoc Geol Argentina 57:280–288

Legarreta L, Gulisano CA (1989) Análisis estratigráfico secuencial de la Cuenca Neuquina (Triásico superior-Terciario inferior, Argentina). In: Chebli G, Spalletti L (eds) Cuencas Sedimentarias Argentinas. Serie Correlación Geológica (6) Universidad Nacional de Tucumán, pp 221–243

Llambías EJ, Rapela CW (1989) Las volcanitas de Collipilli, Neuquén (37°S) y su relación con otras unidades paleógenas de la cordillera. Rev Asoc Geol Argentina 44:224–236

Melnick D, Rosenau M, Folguera A, Echtler H (2006) Neogene tectonics of the Western flank of the Neuquén Andes, 37°–39°30′S. In: Kay SM, Ramos VA (eds) Evolution of an Andean margin: a tectonic and magmatic view from the Andes to the Neuquén Basin (35°–39°S lat). Geol Soc of America, Special Paper vol 407, pp 73–95

Muñoz J, Troncoso R, Duhart P, Crignola P, Farmer L, Stern CR (2000) The relation of the mid-Tertiary coastal magmatic belt in south-central Chile to the late Oligocene increase in plate convergence rate. Rev Geol Chile 27:177–503

Niemeyer H, Muñoz J (1983) Geología de la hoja 57 Laguna de la Laja, Región de Bío Bío, escala 1:250,000, Servicio Nacional Geologia Mineria Chile, Santiago, Chile

Orts DL, Folguera A, Giménez M, Ramos V (2012) Variable structural controls through time in the Southern Central Andes (∼ 36°S). Andean Geol 39:220–241

Pesce AH (1981) Estratigrafía de las nacientes del Río Neuquén y Nahueve, provincia del Neuquén. In: Relatorio del VIII Congreso Geológico Argentino, San Luis, Argentina

Radic JP (2010) Las cuencas cenozoicas y su control en el volcanismo de los Complejos Nevados de Chillán y Copahue-Callaqui (Andes del Sur, 36–39°S). Geology 37:220–246

Ramos VA (1999) Las provincias geológicas del territorio argentino. In: Caminos RL (ed) Geología Argentina. Segemar Anales 29(3): 41–96

Ramos V, Barbieri M (1989) El volcanismo Cenozoico de Huantraico: Edad y relaciones isotópicas iniciales, provincia del Neuquén. Rev Asoc Geol Argentina 43:210–223

Ramos VA, Folguera A (2005) Tectonic evolution of the Andes of Neuquén: Constraints derived from the magmatic arc and foreland deformation. In: Veiga GD, Spalletti LA, Howell JA, Schwarz E (eds) The Neuquén Basin: a case study in sequence stratigraphy and basin dynamics, vol 252. Geol Soc London, Special Publications, pp 15–35

Ramos VA, Mosquera A, Folguera A, García Morabito E (2011) Evolución tectónica de los Andes y del Engolfamiento Neuquino adyacente. In: Leanza HA, Arregui C, Carbone O, Danieli JC, Vallés JM (eds) Geología y Recursos Naturales de la Provincia de Neuquén. Relatorio del VXIII Congreso Geológico Argentino, Buenos Aires, pp 335–348

Rapela C, Llambías E (1985) La secuencia andesítica terciaria de Andacollo, Neuquén, Argentina. In: Relatorio IV Congreso Geológico Chileno, Antofagasta, Chile

Repol D, Leanza H, Sruoga P, Hugo C (2002) Evolución tectónica del Cenozoico de la comarca de Chorriaca, Provincia del Neuquén, Argentina. In: XV Congreso Geológico Argentino (El Calafate) Actas, vol 3, pp 200–205

Rojas Vera EA, Folguera A, Valcarce GZ, Giménez M, Ruiz F, Martínez P, Bottesi G, Ramos VA (2010) Neogene to quaternary extensional reactivation of a fold and thrust belt: the Agrio belt in the Southern Central Andes and its relation to the Loncopué trough (38°–39°S). Tectonophysics 492: 279–294. doi:10.1016/j.tecto.2010.06.019

Rojas Vera EA, Folguera A, Zamora Valcarce G, Bottesi G, Ramos VA (2014a) Structure and development of the Andean system between 36° and 39°S. J Geodyn 73:34–52. doi:10.1016/j.jog.2013.09.001

Rojas Vera EA, Sellés D, Folguera A, Gímenez M, Ruíz F, Orts D, Zamora Valcarce G, Martínez P, Bechis F, Ramos VA (2014b) The origin of the Loncopué Trough in the retroarc of the Southern Central Andes from field, geophysical and geochemical data. Tectonophysics 637:1–19. doi:10.1016/j.tecto.2014.09.012

Sarris M (1964) Informe geológico de la zona de Río Palao, Dto. Minas– Provincia de Neuquén: Yacimientos Carboníferos Fiscales, Open File Report 907, pp 20

orlando_a_p@yahoo.com.ar

Silvestro J, Atencio M (2009) La cuenca cenozoica del Río Grande y Palauco: edad, evolución y control estructural, faja plegada de Malargüe. Rev Asoc Geol Argentina 65(1):154–169

Spagnuolo MG, Folguera A, Litvak V, Vera EAR, Ramos VA (2012) Late Cretaceous arc rocks in the Andean retroarc region at 36.5°S: evidence supporting a Late Cretaceous slab shallowing. J South Am Earth Sci 38:44–56. doi:10.1016/j.jsames.2012.05.002

Stern C (1989) Pliocene to present migration of the volcanic front, Andean Southern Volcanic Zone. Andean Geol 16:145–162. doi:10.5027/andgeoV16n2-a02

Stipanicic PN, Rodrigo F, Baulies OL, Martínez CG (1968) Las Formaciones presenonianas en el denominado Macizo Nordpatagónico y regiones adyacentes. Rev Asoc Geol Argentina 23 (2):367–388

Suárez M, Emparán C (1997) Hoja Curacautín 71, Regiones de la Araucanía y del Bío Bío: escala 1:250,000. Servicio Nacional de Geología y Mineria de Chile, pp 105

Suppe J (1983) Geometry and kinematics of fault-bend folding. Am J Sci 283:684–721

Tunik M, Folguera A, Naipauer M, Pimentel MM, Ramos VA (2010) Early uplift and orogenic deformation in the Neuquén Basin: constraints on the Andean uplift from U–Pb and Hf isotopic data of detrital zircons. Tectonophysics 489(1–4):258–273

Uliana M (1978) Estratigrafía del Terciario. In: Relatorio VII Congreso Geológico Argentino, pp 67–84

Utgé S, Folguera A, Litvak V, Ramos VA (2009) Geología del sector norte de la cuenca de Cura Mallín: zona de las Lagunas de Epulafquen (36°40′–50′S, 71°–71°10′O). Rev Asoc Geol Argentina 64:231–248

Varekamp J, Hesse A, Mandeville C (2010) Back-arc basalts from the Loncopue graben (Province of Neuquen, Argentina). J Volcanol Geoth Res 197:313–328. doi:10.1016/j.jvolgeores.2010.04.003

Vergara M, Muñoz J (1982) La Formación Cola de Zorro en la Alta Cordillera andina chilena (36°–39° Lat. S), sus características petrográficas y petrológicas: una revisión. Rev Geol Chile 17:31–46

Vergara M, López-Escobar L, Hickey-Vargas R (1997) Geoquímica de las rocas volcánicas miocenas de la cuenca intermontana de Parral y Ñuble. In: VIII Congr. Geológico Chil

Zamora Valcarce G (2007) Estructura y Cinemática de la faja plegada y corrida del Agrio, Cuenca Neuquina. PhD thesis, Universidad de Buenos Aires, Buenos Aires, pp 303

Zamora Valcarce G, Zapata T, Del Pino D, Ansa A (2006) Structural evolution and magmatic characteristics of the Agrio fold-and-thrust belt. In: Kay SM, Ramos VA (eds) Evolution of an Andean margin: a tectonic and magmatic view from the Andes to the Neuquén Basin (35°–39° S lat). Geol Soc of America, Special Paper vol 407, pp 125–145

Zamora Valcarce G, Zapata T, Ramos VA, Rodríguez F, Bernardo ML (2009) Evolución tectónica del frente andino en neuquén. Rev Asoc Geol Argentina 65:192–203

Zapata T, Brissón I, Dzelalija F (1999) The role of basement in the Andean fold and thrust belt of the Neuquén Basin. In: Proceedings thrust tectonics, London, England, pp 122–124

Zöllner W, Amos AJ (1973) Descripción geológica de la Hoja 32b, Chos Malal(Prov. Neuquén), Bull. 143, 91 pp, Serv. Geol. Minero Argent., Buenos Aires

orlando_a_p@yahoo.com.ar

Progression of the Deformation in the Southern Central Andes (37°S)

Lucía Sagripanti, Andrés Folguera, Lucas Fennell, Emilio Agustín Rojas Vera and Victor A. Ramos

Abstract This chapter analyzes the deformational pulses and mechanisms that affected the Southern Central Andes across 37°S. Four zones were analyzed in detail that from west to east are the Cordillera del Viento, the Tromen volcanic plateau, the Sierra de Reyes, and the Chachahuén volcanic complex. Each of these zones shows evidence of one or more deformational stages that affected the Andean margin from the Late Cretaceous onwards. Due to the contrasting structure and geology, different methodologies were applied for their study, (i) balanced structural cross sections to represent structure at depth, (ii) use of potential methods (gravimetry and magnetometry) for a subsurface constraint, (iii) geochronological analyses using U/Pb dating of detrital zircons in synorogenic sequences to determine maximum ages and source areas, (iv) morphometric analyses in the drainage network in order to analyze the activity of neotectonic structures during landscape evolution. As a result, an evolutionary model is presented for the Southern Central Andes in which four pulses of deformation were recognized in agreement with previous proposals, although with a variable distribution reflecting a complex pattern. In particular, the Cordillera del Viento area in the westernmost sector registers an uplift stage that occurred during the Late Cretaceous followed by a late Miocene reactivation. The mechanisms associated with this uplift are related to the selective reactivation of half-grabens and generation of new thrusts cutting through the extensional architecture. To the east, the Tromen volcanic plateau registers a pre-Miocene stage of uplift, later affected by a neotectonic reactivation. Localization of neotectonic activity could be related to the emplacement of asthenospheric material and consequent weakening of the upper crust, as revealed by magnetotelluric studies. In the orogenic front, the Sierra de Reyes was initially uplifted during Eocene times and subsequently suffered a strong reactivation during the Neogene. This last stage produced synorogenic successions in the Sierra de

L. Sagripanti (✉) · A. Folguera · L. Fennell · E.A. Rojas Vera · V.A. Ramos
Departamento de Ciencias Geológicas, Facultad de Ciencias Exactas y Naturales, Instituto de Estudios Andinos "Don Pablo Groeber" UBA-CONICET, Buenos Aires, Argentina
e-mail: lusagripanti@gmail.com

© Springer International Publishing Switzerland 2016

A. Folguera et al. (eds.), *Growth of the Southern Andes*,
Springer Earth System Sciences, DOI 10.1007/978-3-319-23060-3_6

orlando_a_p@yahoo.com.ar

Reyes foredeep describing an unroofing sequence. Finally, the Neogene deformational stage exhumed Lower Cretaceous sequences in the foreland region before 7 Ma expanding considerably the orogenic wedge. Thus, the Chos Malal fold and thrust belt shows a foreland sequence development between the Upper Cretaceous and Eocene, that was followed by a sudden expansion of the orogenic wedge in late Miocene times and reactivation of the western sectors. Finally, Quaternary out-of-sequence thrusts define an active orogenic front at the midsection of the fold and thrust belt.

Keywords Southern Central Andes · Deformational stages · Tectonic evolution

1 Introduction

The Malargüe, Chos Malal, and Agrio fold and thrust belts had been generally considered fossilized for the last ~12–10 Ma in terms of contractional deformation. These belts had periods of construction that started in the Late Cretaceous–Eocene, with variable reactivations in late Miocene times, evidenced by synorogenic deposits, cross-cutting relationships, and limited amounts of fission track data (Ramos 1998; Rojas Vera et al. 2014; Sagripanti et al. 2011, 2012; Zamora Valcarce et al. 2006, 2009). However, discrete sectors of the Chos Malal fold and thrust belt have been distinguished due to neotectonic structures affecting Pleistocene volcanic products of the Tromen volcanic plateau (Folguera et al. 2008; Galland et al. 2007; Sagripanti et al. 2015). The particular location of these young structures, far to the west of the orogenic front, has not been satisfactorily explained yet.

The main aim of this chapter is to describe the deformational pulses and mechanisms that affected the Southern Central Andes in a transect at 37°S. An evolutionary model with four pulses of deformation are recognized responsible for the uplift of four analyzed mountain systems that, from west to east, are the Cordillera del Viento, constituting the easternmost front of the Guañacos fold and thrust belt, the Tromen volcanic plateau, comprehended in the Chos Malal fold and thrust belt, and the Sierra de Reyes and the Chachahuén volcanic complex in the foreland zone (Fig. 1).

These systems have been constructed by tectonic inversionof Late Triassic–Early Jurassicnormal faults (Charrier 1979; Charrier et al. 2007; Cobbold and Rossello 2003; Giambiagi et al. 2008; Orts and Ramos 2006) associated with variable amounts of thin-skinned deformation in sag facies of Early Jurassic to Early Cretaceous ages of the Neuquén Basin (Manceda and Figueroa 1995; Zamora Valcarce and Zapata 2005). Contractional stages were explained by shallow subduction settings, evidenced by migration and expansion of the volcanic arc and deformation in the foreland area, followed by periods of extensional relaxation

orlando_a_p@yahoo.com.ar

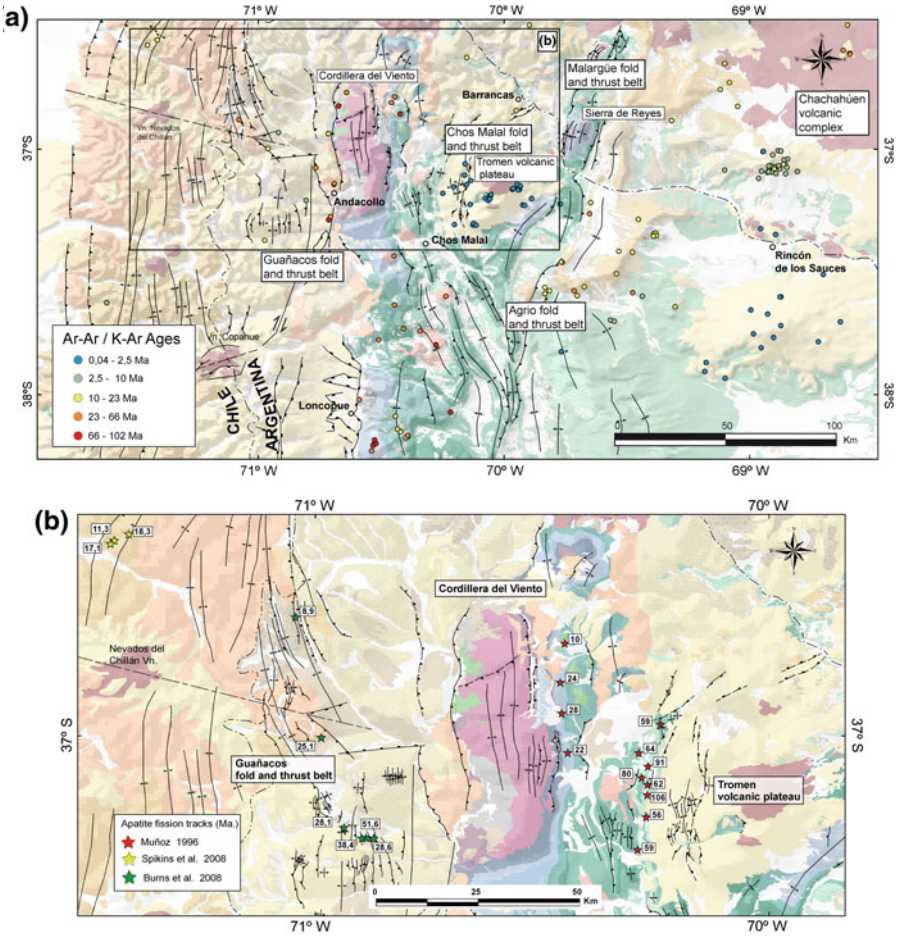


Fig. 1 **a** Compilation of available radiometric ages (Ar/Ar–K/Ar) in the study area from previous works (Cobbold and Rossello 2003; Dyhr et al. 2013; Franchini et al. 2003; Galland et al. 2007; Jordan et al. 2001; Kay and Copeland 2006; Kay et al. 2006a, b; Llambías and Rapela 1989; Perez and Condat 1996; Ramos and Barbieri 1989; Rodrigues et al. 2009; Spagnuolo et al. 2012; Zamora Valcarce et al. 2006). **b** Compilation of fission track ages performed in apatites from the inner sector of the Chos Malal and Guañacos fold and thrust belts

associated with within-plate volcanism (James and Sacks 1999; Kay et al. 2006a). Gutscher (2002) and Ramos et al. (2002) related foreland deformation during shallow subduction stages to the shallowing of brittle–ductile transitions at the area of arc expansion that favored foreland crustal deformation. Shallow subduction hypothesis at these latitudes is based on the study and dating of the Chachahuén

orlando_a_p@yahoo.com.ar

volcanic complex, a late Miocene volcanic center emplaced in the extra-Andean region with ages between 10 and 2.5 Ma (Kay et al. 2006b) (Fig. 1). This foreland magmatism is associated with a volcanic track that covers vast sectors of the Malargüe and Chos Malal fold and thrust belts (Nullo et al. 2002; Spagnuolo et al. 2012).

Thermal history of the area is known mainly from apatite fission track ages. Muñoz (1996) concluded from data of the inner part of the Chos Malal fold and thrust belt that three different periods of exhumation have occurred in 20–40, 70, and 80–100 Ma respectively. Particularly, at the Cordillera del Viento area (Fig. 1), Ar/Ar ages in Permian intrusives, interpreted as exhumation ages, have yielded 66–100 Ma indicating an exhumation stage during the Late Cretaceous (Kay et al. 2006a), in coincidence with fission track data available in the area. Furthermore, Burns et al. (2006) presented fission track data in Oligocene–Miocene rocks that indicated a late Miocene contractional pulse.

2 Cordillera Del Viento Area

The Cordillera del Viento is a contractional structure related to the tectonic inversion of Late Triassic normal faults that expose the deepest structural levels in the whole Malargüe and Chos Malal fold and thrust belts (see previous chapter) (Fig. 2) (Vergani et al. 1995; Zamora Valcarce et al. 2006; Zapata et al. 1999).

The eastern flank of the Cordillera del Viento shows the clearest evidence of synextensional sedimentation for the Late Triassic successions. Detailed mapping of the geology and the structure of this region provides accurate descriptions of the synextensional packages and their relation to the structure (Sagripanti et al. 2014a). These growth strata are recognized at different scales, being systematically associated with inverted and non-inverted normal faults. In particular, along the Butalón valley, a roughly North–South (N-S) scarp exposes a series of volcano-sedimentary depocenters 600 m thick with synrift geometries in direct relation to NW extensional faults. These extensional depocenters are selectively inverted showing the extensional architecture as a series of grabens and horsts of 500–400 m in amplitude. These are internally deformed through combined mechanisms that involve inversion of normal faults and also primary reverse faults cutting through the synextensional fillings.

To the south, next to the arroyo Tucuyo (Fig. 2b), the Cordillera del Viento Formation is preserved in small-scale depocenters associated with NE normal faults. The frontal eastern thrust of the Cordillera del Viento at these latitudes exposes a 1.400 m thick section describing a synextensional succession.

orlando_a_p@yahoo.com.ar

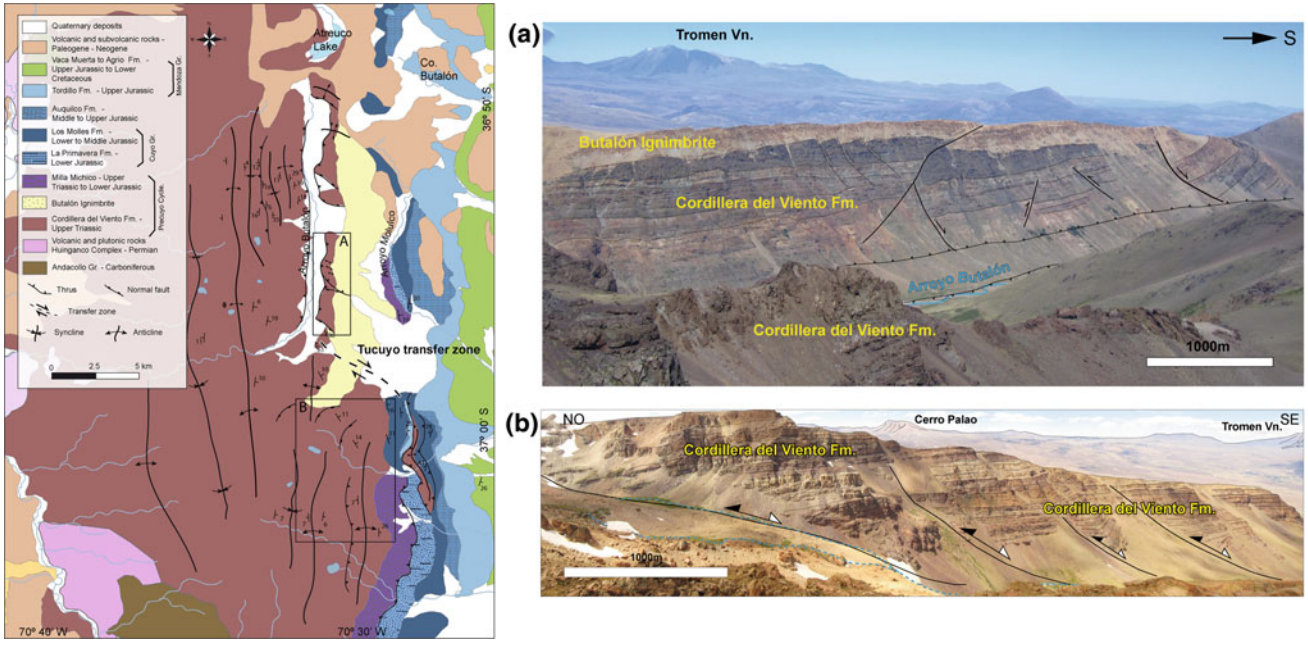


Fig. 2 Geological map of the eastern slope and axial zone of the Cordillera del Viento (Folguera et al. 2007; Leanza et al. 2005; Llambías et al. 2007). **a** East view of the main structures in the northern Cordillera del Viento high, defining a triangular zone between two reverse faults with opposite polarities exposing the Cordillera del Viento Formation. **b** Four small half-grabens associated with NE-trending normal faults are segmenting the axial part of the Cordillera del Viento uplift showing an abrupt change in polarity with respect to the northern section

orlando_a_p@yahoo.com.ar

3 Tromen Volcanic Plateau

To the east, the next area is the Tromen volcanic plateau located in the Andean retroarc zone at 36°–37°S, as part of the Southern Volcanic Zone (Jordan et al. 1983; Ramos and Aleman 2000). This sector, located to the west of the orogenic front area, has been the focus of extensive debate about its present mechanisms of deformation (Folguera et al. 2008; Galland et al. 2007; Messager et al. 2010).

Neotectonic activity has been described in the western slope of the Tromen volcanic plateau, reactivating specific structures of the Chos Malal fold and thrust belt (Galland et al. 2007). The neotectonic structures are anticlines and synclines with an echelon distribution associated with NE extensional and NW to NNW contractional structures, which are interpreted to be related to certain amounts of dextral strike-slip displacements associated with shortening (Sagripanti et al. 2015). Morphometric analyses through the fluvial network allow the recognition of a nonequilibrium state for most of the fluvial channels that drain these structures. Deflected channels and wind gaps are indicative of a reorganization of the fluvial drainage pattern, where the rivers are forced to change their original courses by growing Quaternary structures. In some cases, the channels have migrated laterally toward the tips of the uplifting areas, where they form confluences with transverse rivers.

In a regional analysis, 3D inversion of MT array data reveals a complex lower lithospheric and asthenospheric structure beneath the Tromen and Payenia volcanic plateaus (Burd et al. 2014) (Fig. 3). An asthenospheric anomaly, emerging from the 410-km-mantle discontinuity, is spatially associated with the development of the Payenia volcanic plateau. Thus, this volcanic field, and particularly the Tromen volcanic plateau, is identified as a plume-related feature. Particularly, beneath the western slope of the Tromen volcanic plateau, where neotectonic deformation has been described, this anomaly becomes rather shallow, reaching more than 40 km from the surface (Fig. 3). Therefore, neotectonic deformation affecting the mid-sections of the Chos Mala fold and thrust belt could be related to thermal weakening of the upper crust due to the development of this asthenospheric anomaly.

Based on these observations, the retroarc zone is presently absorbing shortening associated with minor amounts of right-lateral displacements, similarly to the Liquiñe-Ofqui fault system (LOFS) and Antiñir- Copahue fault system (ACFS) to the south and west, respectively, which run through the arc front (Fig. 3). Strain partitioning linked to the oblique convergence between Nazca and South American plates would differ substantially with respect to the situation in the south. While between 46° and 38°S right-lateral displacements are absorbed at the arc zone, where the crust is thermally debilitated due to magmatic addition, north of these latitudes these lateral displacements would be absorbed at the retroarc zone where the crust is intruded by magmas coming from an impacting plume, as 3D inversion of MT array data reveals. Localized out-of-sequence neotectonic deformation and related modifications to the fluvial network could therefore be in association with these sublithospheric phenomena.

orlando_a_p@yahoo.com.ar

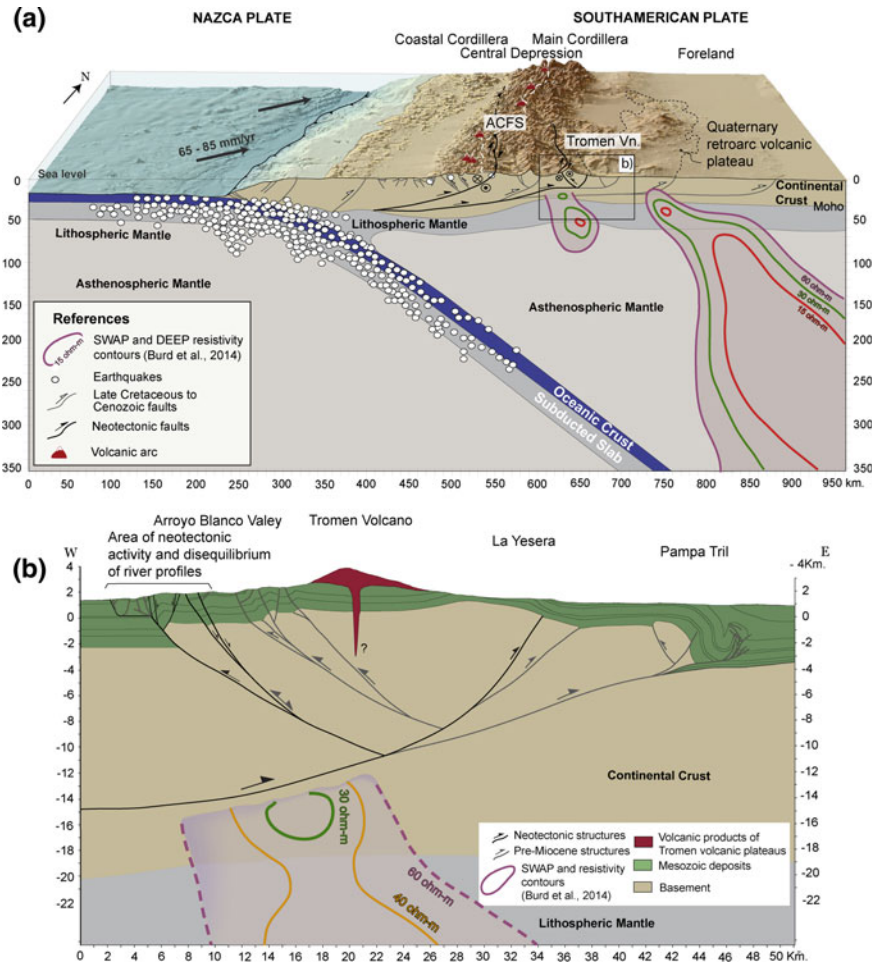


Fig. 3 **a** Digital elevation model with a cross-section that represents upper crustal structure at 37°S (after Folguera et al. 2004, 2006, 2011; Rojas Vera et al. 2014; Sagripanti et al. 2015; Zamora Valcarce et al. 2006) Seismicity and geometry of the subduction zone are taken from Pesicek et al. (2012), while the resistivity anomalies in the mantle and lower crust are a cross-section of the 3D model of Burd et al. (2014). Neotectonic structural systems are represented with thicker lines, along the arc front (ACFS) and the retroarc zone in the Tromen volcanic plateau area. **b** Detail of the inferred mantle plume from the 3D model impacting the lower crust and correlation with neotectonic deformation in the Tromen volcanic plateau (Burd et al. 2014)

4 Sierra de Reyes Area

The following structure from west to east corresponds to the Sierra de Reyes range. This structure is aligned with the orogenic front that is associated with a Neogene foredeep to the east. This deformational stage is constrained by an unconformity

orlando_a_p@yahoo.com.ar

between the Late Oligocene Palauco Formation and the Neogene sedimentary cover (Fig. 4a). Neogene synorogenic deposits are located in the Pampa de Carrizalito depocenter, east of the Sierra de Reyes range, which represents the best record of late Miocene sedimentation in the orogenic front area between 35° and 39°S. However, an angular unconformity between Eocene sections of the upper Malargüe Group and upper Oligocene to lower Miocene rocks of the Palauco Formation is exhumed, indicating an older uplift history.

The Pampa de Carrizalito depocenter can be temporally correlated with the Estratos de Molina depocenter located 80 km to the north, whose lower terms have been dated in 18.12 ± 0.24 Ma (Ar/Ar) by Silvestro and Atencio (2009) (Fig. 4a, b). Petrographic and U/Pb dating on these synorogenic deposits were carried out in order to determine provenance (Sagripanti et al. 2011, 2012) (Fig. 4c). This 370 m thick sequence is composed of polymictic fluvial conglomerates and sandstones with important variations on clast composition, associated with NE–SW fluvial systems (Sagripanti et al. 2012). Lower units consist of volcaniclastic facies that grade upwardly to clastic wedges whose composition is derived from the erosion of the Jurassic to Cretaceous sequences exhumed in the eastern slope of Sierra de Reyes. The base of the section has volcaniclastic facies containing basalt clasts due to the rework of the underlying Palauco Formation. Facies with participation of volcanic clasts, typical of the lower terms, are less developed in the middle and upper parts of the profile. At the top of the sequence there is no trace of volcanic material. Basal sedimentary wedges composed of detritus coming from late Oligocene to early Miocene sequences are followed upwardly by beds with sandstone and limestone clasts sources. Finally, Gypsum clasts replace the previous sources, and these in turn are replaced by shale clasts toward the top of the sequence. All these sources reflect a typical unroofing sequence with respect to stratigraphic order developed in the eastern Sierra de Reyes flank. (Fig. 4). The U/Pb detrital zircon data confirm the unroofing sequence, and indicate important source changes through the synorogenic sedimentation. The registered different age ranges observed through the Neogene synorogenic sequence are derived from different sectors of the eastern foreland region and the western Andean domain. Dominant sources correspond to Permian, Triassic, and typically Andean (Jurassic and Cretaceous) components. Less represented sources are the Rio de la Plata cratón components (Archean and Paleoproterozoic ages), and other components derived from the Andean foothills corresponding to the Pampia terrane basement (Mesoproterozoic, Neoproterozoic, and Early Cambrian ages), Cuyania terrane basement (Mesoproterozoic ages) and the Famatinian magmatic arc (Sagripanti et al. 2011).

As mentioned, Andean zircons are represented by Jurassic and Cretaceous populations. Among these, two main groups are recognized (i) the 190–180 Ma period, which is present all along the sequence, and (ii) the 120–60 Ma, particularly dominant toward the base and diluting upwardly. Different evidence suggests that a Late Cretaceous relief was uplifted and exhumed west of the described orogenic front. Detritus with Andean ages at the Pampa de Carrizalito depocenter are clearly related to this feature. However, Jurassic to Cretaceous prominent peaks are most probably related to the exhumation of Jurassic and Cretaceous granitoids, which are

orlando_a_p@yahoo.com.ar

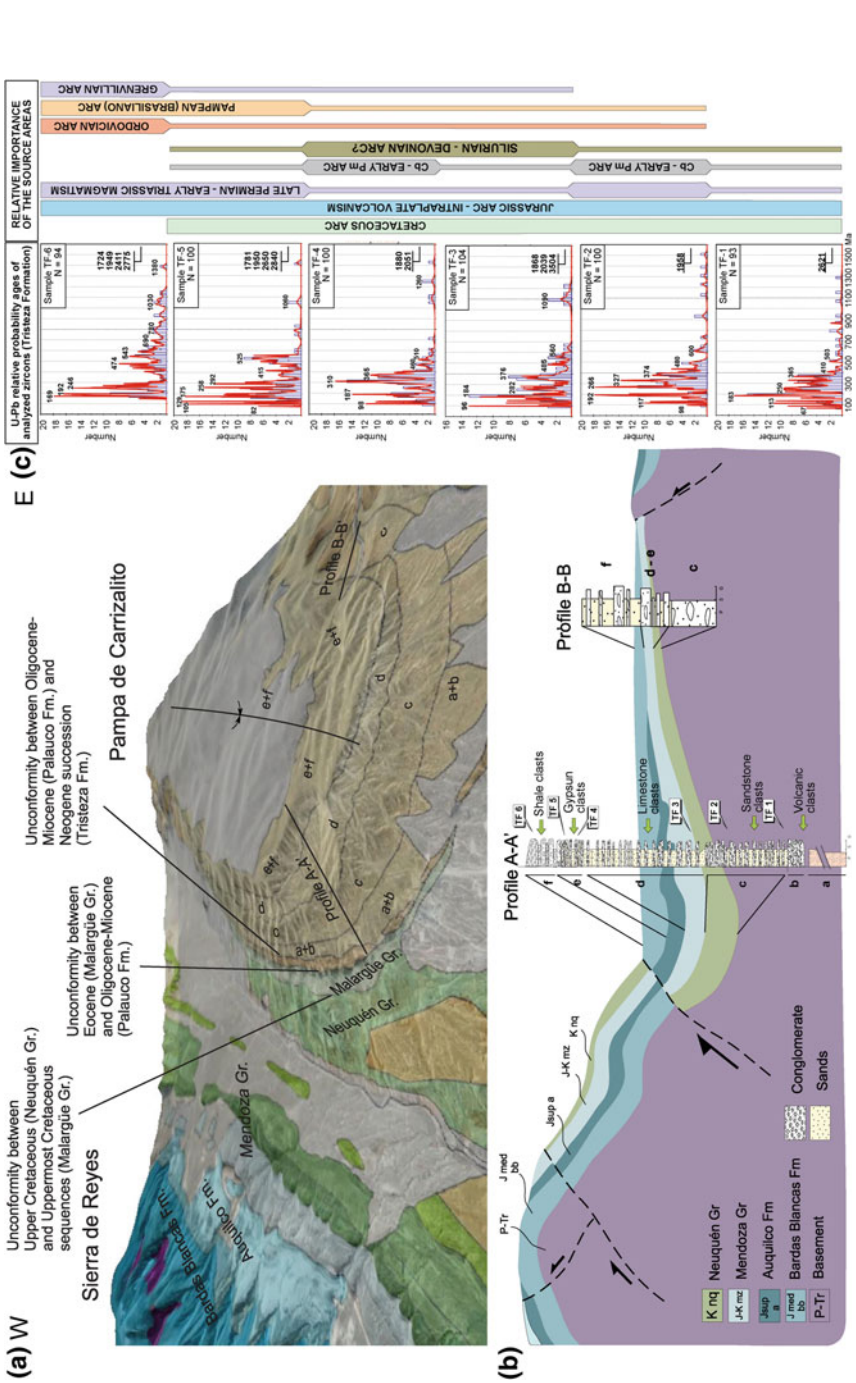


Fig. 4 **a** Landsat image and geological map draped over DEM, showing location of section surveyed at the Pampa de Carrizalito depocenter. **b** Different clast provenances are recognized and correlated through the Neogene Pampa de Carrizalito foreland depocenter (*a*, *b*, *c*, *d*, *e*, *f* are the units recognized in both profiles characterized by contrasting compositions). **c** U/Pb age histogram distribution and probability curves of analyzed zircons are indicated on the right column

orlando_a_p@yahoo.com.ar

present at the western slope of the Andes. This fact implies that the Late Cretaceous relief was at that time not such a prominent feature. On the other hand, Cretaceous U/Pb detrital zircon ages disappear upwards, while Jurassic ones are persistent all along the stratigraphy column. This is somehow puzzling if we accept that both populations come from the Main Andes. If the apparent dilution of Cretaceous components is related to the uplift of a mountain barrier that inhibited Andean provenance through time, Jurassic ages should also disappear. Therefore, while Cretaceous zircons diluted during the growth of the Andes, Jurassic populations persisted, indicating most likely a recycling from the surrounding Mesozoic sedimentary rocks. Simultaneously with the Late Cretaceous source dilution the pre-Andean component increases (Famatinian, Pampean and Grenvillian zircon ages). This is interpreted as a migration of the orogenic front toward the east and the development of a broken foreland, such as the San Rafael basement block during the last stages of the analyzed synorogenic depocenter that suministrated older basement populations (Famatinian, Pampean, and Grenvillian zircon ages). This broken foreland would have been produced during the proposed shallow subduction episode in the region (Ramos and Kay 2006; Litvak et al. 2008).

5 Chachahuén Volcanic Complex

The eastern flank of the Neuquén Basin is characterized by Titho-Neocomian sequences exhumed far away from the thrust front located at 69° 40′W. Patchy exposures of Mesozoic marine deposits near the Chachahuén volcanic complex have been known for many years, since the early oil exploration conducted by Padula (1948). At this area peculiar conglomeratic facies were described at the subsurface based on borehole data (Barrionuevo and Perez 2002; Vergani et al. 2001).

The Lower Cretaceous rocks exposed in the Chachahuén volcanic complex are gently dipping to the southwest. This homoclinal structure defines a smooth anticline nose plunging to the SW with a half-wavelength of 2 km. Sills associated with this volcanic center are emplaced in the Lower Cretaceous sequences.

As seen in many areas of the Main Andes (see Ramos et al. 1996), during compressional stages, $\sigma 1$ is horizontal while $\sigma 3$ is vertical. The positive dilatancy associated with $\sigma 3$ controls the emplacement of sills during contraction in these settings (Ramsay and Huber 1983). As the age of the sills are constrained in 7 ± 0.4 Ma in the Chachahuén volcanic complex by Kay et al. (2006b), we can bracket the age of deformation and therefore the exposition of the Early Cretaceous sections by late Miocene times (Sagripanti et al. 2014b).

The comparison between different structural cross-sections at neighbor latitudes suggests that even though an effective decollement has allowed inversion of the half-graben systems toward the foreland zone in late Miocene times (Fig. 5) (Giambiagi et al. 2012; Zamora Valcarce et al. 2011), local heating associated with volcanic activity in the Chachahuén volcanic complex, which lasted almost three million years in the area (from 7.8 ± 0.6 Ma to 4.85 ± 0.03 Ma), could be an

orlando_a_p@yahoo.com.ar

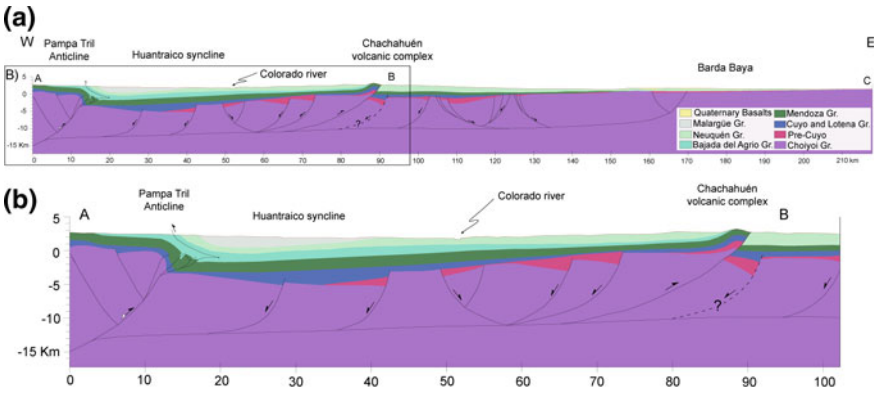


Fig. 5 **a** Regional structural cross-section from the Pampa Tril anticline to the non-deformed area. **b** Detail of the previous section from the Pampa Tril anticline to the Chachahuén volcanic complex (modified from Cristallini et al. 2006; Rojas Vera et al. 2010; Zamora Valcarce and Zapata 2005)

important factor in the development of brittle-ductile transitions far away from the orogenic front (Kusznir and Park 1986; Springer and Förster 1998). Similar structures developed anomalously far of the orogenic front have been described in the Sierras Pampeanas further north (Ramos et al. 2002).

6 Discussion: Evolution of the Andean System at 37°S

A Late Cretaceous arc migration is registered at 37°S from the description of arc-related products emplaced in the Cordillera del Viento area (Franchini et al. 2003; Llambías et al. 1978). An Upper Cretaceous exhumation pulse is registered at these latitudes from radiometric and fission track ages (Burns 2002; Burns et al. 2006; Kay 2002) (Fig. 6a) indicating that the innermost part of the orogen was deformed at the initial stages of the Andean cycle, presumably in association with a shallowing of the subducted slab. This contractional phase coexisted with the deposition of the Neuquén Group related to synorogenic sedimentation in the foreland zone (Di Giulio et al. 2012; Tunik et al. 2010). Growth evidences in proximal facies of the Neuquén Group validate this deformational stage during Late Cretaceous times (Fennell et al. 2014; Orts and Ramos 2006; Sánchez and Asurmendi 2014).

During Paleocene–Eocene times, contractional deformation migrated to the east, to the Sierra de Reyes region. This period is characterized by a high-stand sea level that produced Atlantic marine ingressions that fed the foredeep region. In the study area, an angular unconformity between the Malargüe Group (Pircala Formation—Eocene) and the late Oligocene rocks of the Palauco Formation indicates an Eocene uplift (Cobbold and Rossello 2003; Groeber 1929; Rojas Vera et al. 2014; Sagripanti et al. 2012) (Fig. 6b).

orlando_a_p@yahoo.com.ar

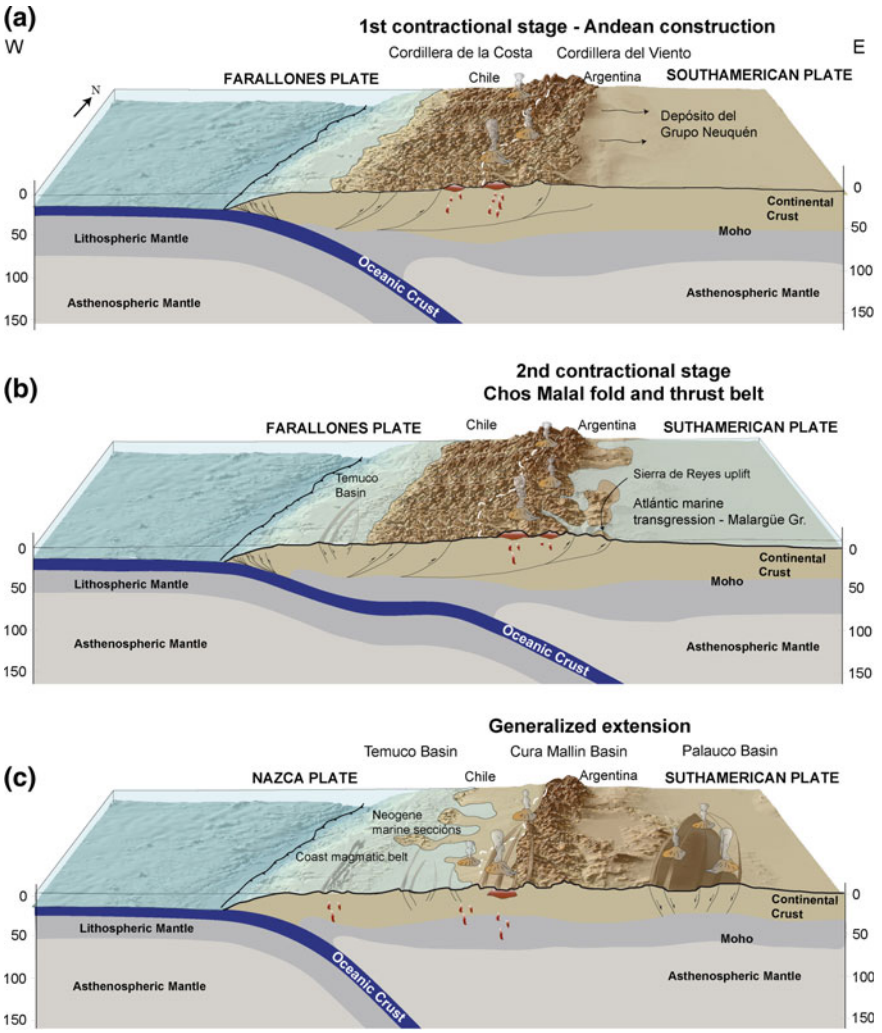


Fig. 6 Block diagram showing main deformational pulses that affected the Andes at 37°S. **a** Late Cretaceous stage, with the early development of the fold and thrust belt and the foreland basin. **b** Paleocene–Eocene contractional pulse that reached the Sierra de Reyes. **c** Late Oligocene—early Miocene extensional stage. **d** Late Miocene contractional pulse and second arc migration reaching the foreland area. **e** Pleistocene—Holocene contractional stage in the Chos Malal fold and thrust belt presumably linked to thermally weakened zones

An extensional stage has been proposed for the late Oligocene—Early Miocene period from the forearc to the foreland area (see Kay et al. 2006a, for a general revision) (see previous chapter). The Temuco Basin in the forearc, the Cura Mallin Basin in the Main Cordillera, and the Palauco Basin in the foreland region have been related to extension, interrupting Andean growth. These basins were inverted

orlando_a_p@yahoo.com.ar

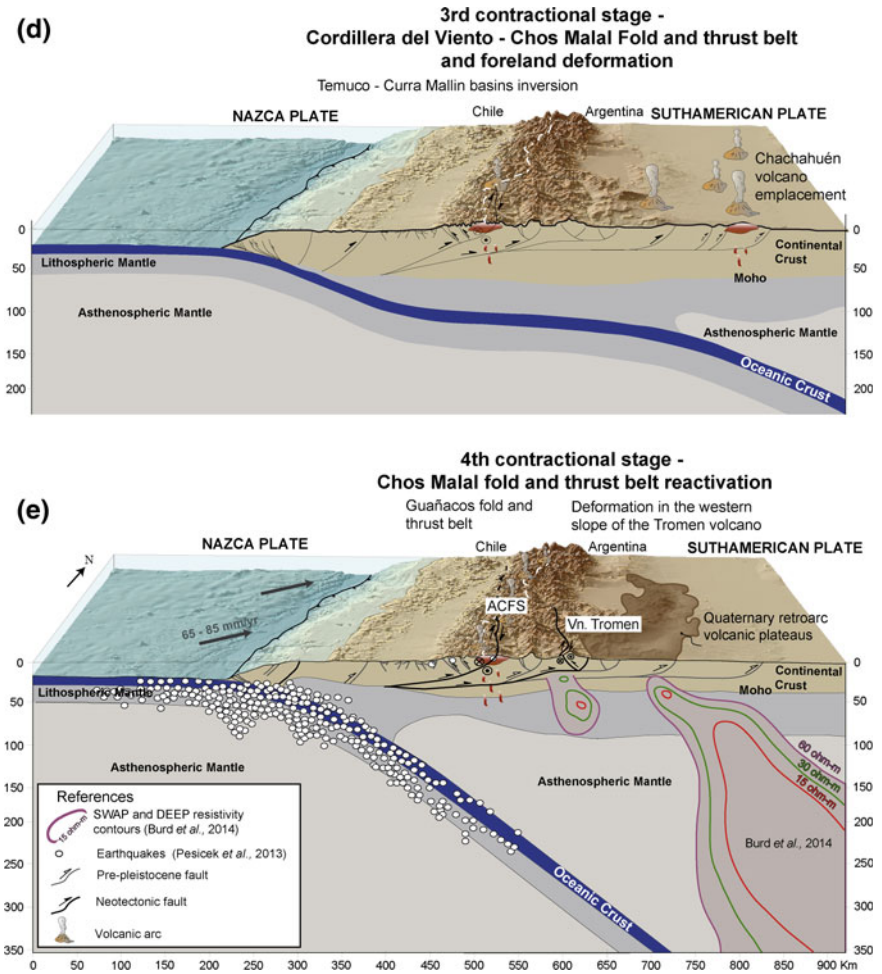


Fig. 6 (continued)

during the late Miocene and incorporated in the fold and thrust belt. This contractional stage affected simultaneously a series of structures of the fold and thrust belt, from the Cordillera del Viento, to the Chos Malal fold and thrust belt, the Tromen volcanic plateau and even some discrete sectors of the foreland area (Fig. 6c, d). Synorogenic deposits associated with the eastern front of the Sierra de Reyes register an unroofing sequence indicating an important migration of the orogenic front at this time (Sagripanti et al. 2011).

During this period, a second arc migration is evidenced by the superficial development of the Charilehue Formation representing the lower Miocene arc (Nullo et al. 2002; Spagnuolo et al. 2012). This arc migration reached the easternmost edge of the Neuquén Basin in the Chachahuén volcanic complex (Kay et al. 2006a, b;

orlando_a_p@yahoo.com.ar

Ramos and Kay 2006; Sagripanti et al. 2014b) (Fig. 6d), where Lower Cretaceous deposits (Agrio Formation) are structured during this contractional stage. Finally, neotectonic activity registered in the Tromen volcanic plateau would constitute a late reactivation of a pre-Miocene doubly vergent structure associated at depth with a contractional basement wedge. This activity would be related to a shallow asthenospheric anomaly, located at less than 40 km below surface, just beneath the western slope of the Tromen volcanic plateau (Burd et al. 2014; Sagripanti et al. 2015) (Fig. 6e). This sublithospheric anomaly could not only explain the development of the Payenia plateau, but also the contractional reactivation of selected structures in the western part of the Chos Malal fold and thrust belt as out-of-sequence structures, fossilizing the eastern sector.

References

Barrionuevo M, Perez DE (2002) Reservorios del Miembro Agrio Superior de la Formación Agrio. In: Schiuma M, Hinterwimmer G, Vergani G (eds) Rocas Reservorio de las Cuencas Productivas de la Argentina. Instituto Argentino del Petróleo, Buenos Aires, pp 447–456

Burd AI, Booker JR, Mackie R, Favetto A, Pomposiello MC (2014) Three-dimensional electrical conductivity in the mantle beneath the Payún Matrú Volcanic Field in the Andean back-arc of Argentina near 36.5°S: decapitation of a mantle plume by resurgent upper mantle shear during slab steepening. Geophys J. doi:10.1093/gji/ggu145

Burns WM (2002) Tectonics of the Southern Andes from stratigraphic, thermochronologic, and geochemical perspectives. Unpublished PhD thesis. Cornell University, p 204

Burns WM, Jordan TE, Copeland P, Kelley Shari A (2006) The case for extensional tectonics in the Oligocene-Miocene Southern Andes as recorded in the Cura Mallín basin (36°–38°S). In: Kay SM, Ramos VA (eds) Evolution of an Andean Margin: a tectonic and magmatic view from the Andes to the Neuquén Basin (35°–39°S Lat). Geological Society of America, Special Paper 407, pp 163–184

Charrier R (1979) El Triásico en Chile y regiones adyacentes de Argentina. Dep. Geol. Comun. Universidad de Chile vol 26, pp 1–37

Charrier R, Pinto L, Rodríguez M (2007) Tectonostratigraphic evolution of the Andean Orogen in Chile. In: Gibbonds W, Moreno T (eds) The geology of Chile. Geological Society London, Special Publications pp 21–116

Cobbold PR, Rossello EA (2003) Aptian to recent compressional deformation of the Neuquén Basin, Argentina. Mar Petrol Geol 20:429–443

Cristallini EO, Bottesi G, Gavarrino A, Rodriguez L, Tomezzoli R, Comeron R (2006) Synrift geometry of the Neuquén Basin in northeastern Neuquén Province, Argentina. In: Kay SM, Ramos VA (eds) Evolution of an Andean margin: a tectonic and magmatic view from the Andes to the Neuquén Basin (35°–39°S lat). Geological Society of America, Special Paper 407, pp 147–162

Di Giulio A, Ronchi A, Sanfilippo A, Tiepolo M, Pimentel M, Ramos VA (2012) Detrital zircon provenance from the Neuquén Basin (South Central Andes): Cretaceous geodynamic evolution and sedimentary response in a retroarc-foreland basin. Geology 40:559–562

Dyhr CT, Holm PM, Llambias EJ, Scherstén A (2013) Subduction controls on Miocene back-arc lavas from Sierra de Huantraico and La Matancilla and new 40Ar/39Ar dating from the Mendoza Region, Argentina. Lithos 179:67–83

orlando_a_p@yahoo.com.ar

Fennell L, Chiachiarelli F, Orts DL, Echaurren A, Kietzmann D, Rojas Vera EA, Folguera A (2014) Levantamiento cretácico superior de la Faja Plegada y Corrida de Malargüe: Evidencias de crecimiento en el Grupo Neuquén. XIX Congreso Geológico Argentino (Córdoba), Actas, pp 1586–1587

Folguera A, Ramos VA, Hermanns RL, Naranjo J (2004) Neotectonics in the foothills of the southernmost central Andes (37°–38°S): Evidence of strike-slip displacement along the Antiñir-Copahue fault zone. Tectonics 23. doi:10.1029/2003TC001533

Folguera A, Ramos VA, González Díaz EF, Hermanns RL (2006) Miocene to quaternary deformation of the Gianacos fold-and-thrust belt in the Neuquén Andes between 37° and 37° 30′S. In: Kay SM, Ramos VA (eds) Evolution of an Andean margin: a tectonic and magmatic view from the Andes to the Neuquén Basin (35°–39°S Lat). Geological Society of America, Special Paper 407, pp 247–266

Folguera A, Ramos VA, Zapata TR, Spagnuolo MG (2007) Andean evolution at the Guañacos and Chos Malal fold and thrust belts (36° 30′–37°S). J Geodyn 44:129–148

Folguera A, Bottesi G, Zapata T, Ramos VA (2008) Crustal collapse in the Andean backarc since 2 Ma: Tromen volcanic plateau, Southern Central Andes (36°40′–37°30′S). Tectonophysics 459:140–160

Folguera A, Orts D, Spagnuolo M, Rojas Vera E, Litvak V, Sagripanti L, Ramos ME, Ramos VA (2011) A review of Late Cretaceous to Quaternary palaeogeography of the southern Andes. Biol J Linn Soc 103:250–268

Franchini M, López-Escobar L, Schalamuk IB, Meinert L (2003) Magmatic characteristics of the Paleocene Cerro Nevazón region and other Late Cretaceous to Early Tertiary calc-alkaline subvolcanic to plutonic units in the Neuquén Andes, Argentina. J South Am Earth Sci 16:399–421

Galland O, Hallot E, Cobbold PR, Ruffet G, de Bremond d'Ars J (2007) Volcanism in a compressional Andean setting : A structural and geochronological study of Tromen volcano (Neuquén province, Argentina). Tectonics 26. doi:10.1029/2006TC002011

Giambiagi L, Bechis F, García V, Clark AH (2008) Temporal and spatial relationships of thick- and thin-skinned deformation: A case study from the Malargüe fold-and-thrust belt, southern Central Andes. Tectonophysics 459:123–139

Giambiagi L, Mescua J, Bechis F, Tassara A, Hoke G (2012) Thrust belts of the southern Central Andes: Along-strike variations in shortening, topography, crustal geometry, and denudation. Geol Soc Am Bulletin 124, pp 1339–1351

Groeber P (1929) Líneas fundamentales de la geología del Neuquén, sur de Mendoza y regiones adyacentes. Dirección General de Minas, Geología e Hidrología, Buenos Aires, Publicación, vol 58, p 110

Gutscher MA (2002) Andean subduction styles and their effect on thermal structure and interplate coupling. J South Am Earth Sci 15:3–10

James D, Sacks S (1999) Cenozoic formation of the Central Andes: a geophysical perspective. In: Skinner B (ed) Geology and ore deposits of the central Andes. Soc of Economic Geol, London, Special Publication, p 25

Jordan TE, Isacks BL, Allmendinger RW, Brewer JA, Ramos VA, Clifford JA (1983) Andean tectonics related to geometry of subducted Nazca plate. Geol Soc Am Bull 94:341–361

Jordan TE, Burns WM, Veiga R, Pángaro F, Copeland P, Kelley S, Mpodozis MC (2001) Extension and basin formation in the southern Andes caused by increased convergence rate. A mid-Cenozoic trigger for the Andes. Tectonics 20:308–324

Kay SM (2002) Tertiary to recent transient shallow subduction zones in the Central and Southern Andes. XV Congreso Geológico Argentino, (Calafate), Actas, pp 282–283

Kay SM, Copeland P (2006) Early to middle Miocene backarc magmas of the Neuquén Basin: Geochemical consequences of slab shallowing and the westward drift of South America. In: Kay SM, Ramos VA (eds) Evolution of an Andean margin: a tectonic and magmatic view from the Andes to the Neuquén Basin (35°–39°S Lat). Geological Society of America, Special Paper 407, pp 185–213

orlando_a_p@yahoo.com.ar

Kay SM, Burns WM, Copeland P, Oscar M (2006a) Upper Cretaceous to Holocene magmatism and evidence for transient Miocene shallowing of the Andean subduction zone under the northern Neuquén Basin. In: Kay SM, Ramos VA (eds) Evolution of an Andean margin: a tectonic and magmatic view from the Andes to the Neuquén Basin (35°–39°S Lat). Geological Society of America, Special Paper 407, pp 19–60

Kay SM, Mancilla O, Copeland P (2006b) Evolution of the late Miocene Chachahuén volcanic complex at 37°S over a transient shallow subduction zone under the Neuquén Andes. In: Kay SM, Ramos VA (eds) Evolution of an Andean margin: a tectonic and magmatic view from the Andes to the Neuquén Basin (35°–39°S Lat). Geological Society of America, Special Paper 407, pp 215–246

Kusznir NJ, Park RG (1986) The extensional strength of the continental lithosphere: its dependence on geothermal gradient, and crustal composition and thickness. In: Coward MP, Dewey JF, Hancock PL (eds) Continental extension tectonics. Geological Society of London, Special Publication 28, pp 35–52

Leanza HA, Llambías EJ, Carbone O (2005) Unidades estratigráficas limitadas por discordancias en los depocentros de la Cordillera del Viento y la Sierra de Chacaico durante los inicios de la Cuenca neuquinca. VI Congreso de Exploracion Y Desarrollo de Hidrocarburos (Mar del Plata), Tecnical works, p 13

Litvak V, Folguera A, Ramos VA (2008) Determination of an arc-related signature in Late Miocene volcanism over the San Rafael Block, Southern Central Andres (34°30′–37°) Argentina: the Payenia shallow subduction zone. VII International Symposium on Andean Geodynamics (Niza), pp 289–291

Llambias EJ, Rapela CW (1989) Las volcanitas de Collipilli, Neuquén (37°S) y su relación con otras unidades paleógenas de la cordillera. Rev Asoc Geol Argent 44(1–4):224–236

Llambías EJ, Danderfer J, Palacios M, Brogioni N (1978) Las rocas igneas cenozoicas del volcán Domuyo y áreas adyacentes. VII Congreso Geológico Argentino (Neuquén), Actas, vol 2, pp 569–584

Llambías EJ, Leanza HA, Carbone O (2007) Evolución tectono-magmática durante el Pérmico al Jurásico Temprano en la Cordillera del Viento (37°05′S–37°15′S): nuevas evidencias geológicas y geoquímicas del inicio de la cuenca Neuquina. Rev Asoc Geol Argent 62(2):217–235

Manceda R, Figueroa D (1995) Inversion of the Mesozoic Neuquén rift in the Malargüe fold and thrust belt, Mendoza, Argentina. In: Tankard AJ, Suárez R, Welsink HJ (eds) Petroleum basins of South America, Memoir 62. Am Assoc Petroleum Geologists, pp 369–382

Messager G, Nivière B, Martinod J, Lacan P, Xavier J-P (2010) Geomorphic evidence for PlioQuaternary compression in the Andean foothillsof the southern Neuquén Basin, Argentina. Tectonics 29. doi:10.1029/2009TC002609

Muñoz N (1996) The thermal evolution of Jurassic and Cretaceous source rocks in the Malargüe thrust belt, Argentina: implications for hydrocarbon exploration. Independent project report. Unpublished MSc course in Basin Evolution and dynamics. Department of Geology. Royal Holloway University of London, p 98

Nullo FE, Stephens GC, Otamendi J, Baldauf Paul E (2002) El volcanismo del Terciario superior del sur de Mendoza. Rev Asoc Geol Argent 57:119–132

Orts S, Ramos VA (2006) Evidence of middle to late Cretaceous compressive deformation in the high Andes of Mendoza, Argentina. Backbone of the Americas (Mendoza), p 65

Padula LA (1948) Sobre la presencia del Hauterivense marino en la Sierra de Chachahuén, Provincia de Mendoza. Boletín Inf Pet 287:49–53

Perez MA, Condat P (1996) Geología de la Sierra de Chachahuén, Área CNQ-23, Puelen: Buenos Aires, Argentina. Geólogos Asociados, YPF, Unpublished report, p 82

Pesicek JD, Engdahl ER, Thurber CH, DeShon HR, Lange D (2012) Mantle subducting slab structure in the region of the 2010 M8.8 Maule earthquake (30-40°S), Chile. Geophys J Int 191:317–324

orlando_a_p@yahoo.com.ar

Ramos VA (1998) Estructura del sector occidental de la faja plegada y corrida del Agrio, cuenca neuquina, Argentina. X Congreso Latinoamericano de Geología (Buenos Aires), pp 105–110
Ramos VA, Aleman A (2000) Tectonics of the Andes. In: Cordani UG, Milani EJ, Filho T, Campos DA (eds) Tectonic Evolution of South America, IGC, Río de Janeiro, pp 635–685
Ramos VA, Barbieri M (1989) El volcanismo Cenozoico de Huantraico: Edad y relaciones isotópicas iniciales, provincia del Neuquén. Rev Asoc Geol Argent 43:210–223
Ramos VA, Kay SM (2006) Overview of the evolution of the southern Central Andes of Mendoza and Neuquén (35°–39°S latitude). In: Kay SM, Ramos VA (eds) Evolution of an Andean margin: a tectonic and magmatic view from the Andes to the Neuquén Basin (35°–39°S Latitude). Geological Society of America, Special Paper, vol 407, pp 1–17
Ramos VA, Cegarra M, Cristallini EO (1996) Cenozoic tectonics of the high Andes of west-central Argentina (30°–36°S latitude). Tectonophysics 259:185–200
Ramos VA, Cristallini EO, Perez DJ (2002) The Pampean flat-slab of the Central Andes. J South Am Earth Sci 15:59–78
Ramsay J, Huber M (1983) The techniques of modern structural geology. Academic Press, London, p 307
Rodrigues N, Cobbold PR, Loseth H, Ruffet G (2009) Widespread bedding-parallel veins of fibrous calcite ('beef') in a mature source rock (Vaca Muerta Fm, Neuquén Basin, Argentina): evidence for overpressure and horizontal compression. J Geol Soc Lond 166:695–709
Rojas Vera EA, Folguera A, Valcarce GZ, Giménez M, Ruiz F, Martínez P, Bottesi G, Ramos VA (2010) Neogene to Quaternary extensional reactivation of a fold and thrust belt: the Agrio belt in the Southern Central Andes and its relation to the Loncopué trough (38°–39°S). Tectonophysics 492:279–294
Rojas Vera EA, Folguera A, Zamora Valcarce G, Bottesi G, Ramos VA (2014) Structure and development of the Andean system between 36° and 39°S. J Geodyn 73:34–52
Sagripanti L, Bottesi G, Naipauer M, Folguera A, Ramos VA (2011) U/Pb ages on detrital zircons in the southern central Andes Neogene foreland (36°–37°S): Constraints on Andean exhumation. J South Am Earth Sci 32:555–566
Sagripanti L, Bottesi G, Kietzmann D, Folguera A, Ramos VA (2012) Mountain building processes at the orogenic front. A study of the unroofing in Neogene foreland sequence (37°S). Andean Geol 39:201–219
Sagripanti L, Folguera A, Giménez M, Rojas Vera EA, Fabiano JJ, Molnar N, Fennell L, Ramos VA (2014a) Geometry of middle to late Triassic extensional deformation pattern in the Cordillera del Viento (Southern Central Andes): a combined field and geophysical study. J Iber Geol 40:349–366
Sagripanti L, Aguirre-Urreta B, Folguera A, Ramos VA (2014b) The Neocomian of Chachahuén (Mendoza, Argentina): evidence of a broken foreland associated with the Payenia flat-slab. In Sepúlveda S, Giambiagi L, Pinto L, Moreiras S, Tunik M, Hoke G, Farías M (eds) Geodynamic processes in the Andes of Central Chile and Argentina, vol 399, Geological Society of London, Special Publications, doi:10.1144/SP399.9
Sagripanti L, Rojas Vera EA, Gianni GM, Folguera A, Harvey JE, Farías M, Ramos VA (2015) Neotectonic reactivation of the western section of the Malargüe fold and thrust belt (Tromen volcanic plateau, Southern Central Andes). Geomorphology 232:164–181
Sánchez ML, Asurmendi E (2014) Modelo de depósito de la Formación Cerro Lisandro: lóbulos de desembocadura y deltas de tipo Gilbert. Cretácico superior, región central de cuenca Neuquina, Argentina. Rev Mex Ciencias Geológicas 31:141–162
Silvestro J, Atencio M (2009) La cuenca Cenozoica del Río Grande y Palauco: edad, evolución y control estrutural, Faja plegada y corrida de Malargüe (36°S). Rev Asoc Geol Argentina 65:154–169
Spagnuolo MG, Litvak VD, Folguera A, Bottesi G, Ramos VA (2012) Neogene magmatic expansion and mountain building processes in the southern Central Andes, 36–37°S, Argentina. J Geodyn 53:81–94
Springer M, Förster A (1998) Heat-flow density across the Central Andean. Tectonophysics 306:377–395

orlando_a_p@yahoo.com.ar

Tunik M, Folguera A, Naipauer M, Pimentel M, Ramos VA (2010) Early uplift and orogenic deformation in the Neuquén Basin: Constraints on the Andean uplift from U-Pb and Hf isotopic data of detrital zircons. Tectonophysics 489:258–273

Vergani G, Tankard AJ, Belotti HJ, Welsink HJ (1995) Tectonic Evolution and Paleogeography of the Neuquén Basin, Argentina. In: Tankard J, Suarez SR, Welsink J (eds) Petroleoum Basin of South America: Am Assoc Petroleum Geologists, Memori, vol 62, pp 383–402

Vergani G, Barrionuevo M, Sosa H, Pedrazzini M (2001) Análisis estratigráfico secuencial de alta resolución en las formaciones Agrio y Huitrin del Yacimiento Puesto Hernández, Cuenca Neuquina, Argentina. Boletín Inf Pet 67:76–87

Zamora Valcarce G, Zapata T (2005) Estilo estructural del frente de la faja plegada neuquina a los 37°S. VI Congreso de Exploracion Y Desarrollo de Hidrocarburos (Mar del Plata), p 16

Zamora Valcarce G, Zapata T, Del Pino D, Ansa A (2006) Structural evo-lution and magmatic characteristics of the Agrio Fold-and-thrust belt. In: Kay SM, Ramos VA (eds) Evolution of an Andean margin: a tectonic and magmatic view from the Andes to the Neuquén Basin (35°–39° lat), vol 407. Special Paper, Geo Soc of America, pp 125–145

Zamora Valcarce G, Zapata T, Ramos VA, Rodríguez F, Bernardo ML (2009) Evolución tectónica del frente andino en neuquén. Rev Asoc Geol Argent 65:192–203

Zamora Valcarce G, Zapata T, Ramos VA (2011) La Faja Plegada y corrida del Agrio. In: Leanza H, Arregui C, Carbone O, Danieli J, Vallés JM (eds) Geología y Recursos Naturales de la Provincia de Neuquén. Relatorio del VXIII Congreso Geológico Argentino (Nauquén), pp 367–374

Zapata T, Brissón I, Dzelalija F (1999) La Estructura de la faja plegada y corrida andina en relación con el control del basamento de la Cuenca Neuquina. Boletín Inf Pet 60:112–121

orlando_a_p@yahoo.com.ar

Tectonic Evolution of the Northern Patagonian Andes (40°S)

Miguel E. Ramos, Andrés Folguera, Lucas Fennell, Mario Giménez and Victor A. Ramos

Abstract This chapter is focused on the tectonic evolution of the North Patagonian Andes comprised between 38° and 40°S. Field recognition of main structures allowed establishing a structural control for the main sedimentary packages that coexisted with Andean development. These structures affect Miocene strata at the eastern deformational front, indicating a last stage of development, although cooling ages suggest a Mid to Late Cretaceous exhumation of the Paleozoic basement exposed at the westernmost sector. Synextensional deposits of late Oligocene age imply an interruption of Andean constructional mechanisms at these latitudes. Finally, seismic tomographies at these latitudes show an area of relatively low seismic velocities in the orogenic front area, separated from the arc front zone. Computed elastic thicknesses from gravity data show a good correlation with these areas with abnormal heat flow associated with retroarc stretching and magmatic emplacement in the last 5–2 Ma.

Keywords North Patagonian Andes · Late Oligocene and Pliocene to Quaternary retroarc extension

M.E. Ramos (✉) · A. Folguera · L. Fennell · V.A. Ramos
Departamento de Ciencias Geológicas, Facultad de Ciencias Exactas y Naturales, Instituto de Estudios Andinos "Don Pablo Groeber" UBA-CONICET, Buenos Aires, Argentina
e-mail: miguelestebanramos@hotmail.com

M. Giménez
Instituto Geofísico y Sismológico Ing. Volponi, Universidad Nacional de San Juan, Ruta 12-Km17, San Juan, Argentina

M. Giménez
Consejo Nacional de Investigaciones Cientifícas y Técnicas (CONICET), Buenos Aires, Argentina

© Springer International Publishing Switzerland 2016

A. Folguera et al. (eds.), *Growth of the Southern Andes*,
Springer Earth System Sciences, DOI 10.1007/978-3-319-23060-3_7

orlando_a_p@yahoo.com.ar

1 Introduction

The transitional zone from the arc to the western retroarc at the Villarrica-Lanín volcanoes latitudes is considered a key area to recognize the main constructional stages that shaped the North Patagonian Andes and their mechanisms (Fig. 1). This area has been recently related to a tearing of the Nazca Plate as suggested by a strong segmentation of the subducted slab (Fig. 2) (Pesicek et al. 2012). Based on this work, around 5 Ma ago at ~39–40°S a steeper nearly vertical subduction zone was replaced by a ~30°E subduction zone that led to the present configuration (Bohm et al. 2002; Lüth et al. 2004).

This segment has few structural and tectonic analyses due to a difficult access, a rather homogeneous stratigraphy and no hydrocarbon interest. This chapter analyzes depocenter geometry through field and gravimetric data that were incorporated into the fold and thrust belt. Additionally, it gives general constraints about timing of inversion of those depocenters into the orogenic wedge over the Argentinian slope of the Andes. The retroarc zone at these latitudes is characterized by the superposition of different sedimentary prisms, corresponding to the Late Triassic, late Oligocene–early Miocene, late Miocene, and Quaternary basins. Understanding the geometry of these basins and their relation to the Andean formation are the main objectives of this chapter.

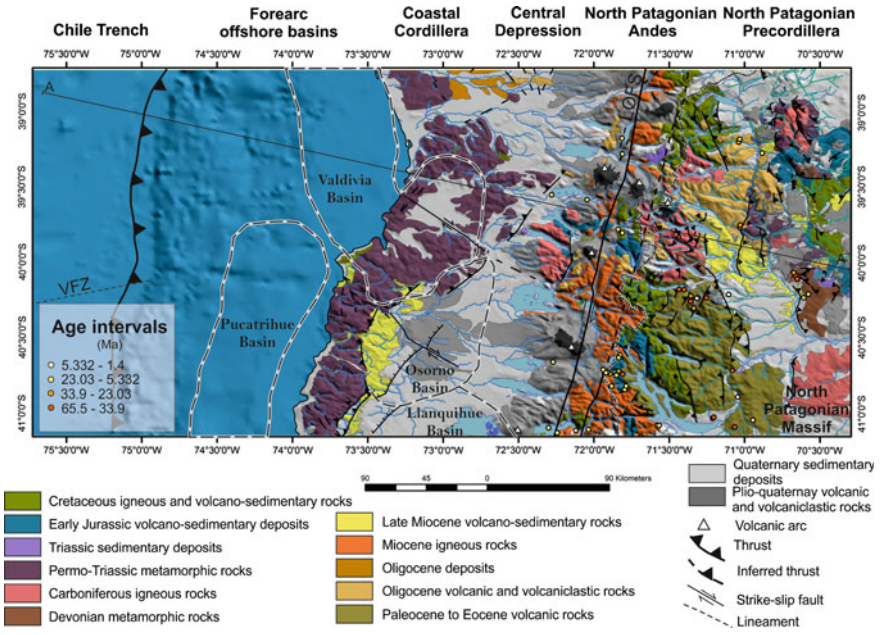


Fig. 1 Simplified geological map between the 39° and 41°S with the main structures of the western-intra and back-arc zones. The A–A′ line shows the structural profile depicted in Fig. 2a. *Color dots* indicate available Cenozoic ages for the intra- and retroarc volcanic rocks

orlando_a_p@yahoo.com.ar

2 Geological Setting

North Patagonian Andean evolution is initially linked to the subduction of the Farallón (previously to 26 Ma) and then the Nazca plates (Cande and Leslie 1986). During the Paleogene, the Farallón Plate subducted obliquely northward, up to its breakup into the Cocos and Nazca Plates (Pardo-Casas and Molnar 1987). This provoked the present relative convergence velocity of 8 cm/a in the N78ºE direction (Somoza 1998). This mild obliquity of the convergence since 26 Ma was associated with a certain degree of strain partitioning of the upper plate, with a major dextral strike-slip N-trending fault zone, known as the Liquiñe-Ofqui Fault system (Fig. 1) that runs through the axial North Patagonian Andes for over 1000 km from 39º 30′ to 47°S (Hervé 1976; Forsythe and Nelson 1985; Cembrano and Lara 2009; Thomson 2002).

The North Patagonian Andes can be divided into a series of morphostructural systems (Figs. 2, 3) (Diraison et al. 1998; García Morabito and Ramos 2012; Giacosa et al. 2005). These systems exhumed a variety of units that range from the Paleozoic, characterized by plutonic and metamorphic rocks (see Thomson and Hervé 2002, for a synthesis) to Cenozoic volcano-sedimentary rocks (Jordan et al. 2001; Radic et al. 2002). In an offshore forearc position between ~38 and 40ºS, the Valdivia basin (González 1989) has concentrated subsidence in Cretaceous, Eocene, and Miocene times (Fig. 1). To the east, the Coastal Cordillera was interpreted as a Late Carboniferous accretionary prism intruded by Neopaleozoic plutonic rocks (Munizaga et al. 1988; Thomson and Hervé 2002) that extend along the Chilean coast. The eastern sector of this Coastal Cordillera is partly covered by Miocene volcanic and sedimentary units (Vergara and Munizaga 1974) corresponding to a series of depocenters such as the Osorno and Llanquihue basins (Fig. 1). These have been gathered in the Central Depression, corresponding to a 1000-km-long low zone located in the forearc region (Lavenu and Cembrano 1999). These depocenters are exhumed along the Liquiñe-Ofqui Fault system in the eastern limit of the Central Depression, where they are incorporated in the North Patagonian Andes.

The drainage divide area corresponding to the political boundary between Argentina and Chile is constituted by the Patagonian Andes (Fig. 1). A series of stratovolcanoes rises over this structural relief up to 1500 m, among which the Villarrica, Quetrupillán, and Lanín are the most prominent. These volcanic centers are aligned together with monogenic Quaternary volcanic fields through NE and W–NW structures (Lavenu and Cembrano 1999; Lara 2004). Here, the Paleozoic basement is exposed at the eastern-frontal sector by a series of thrusts and backthrusts (Turner 1965; García Morabito and Ramos 2012). Cretaceous plutonic rocks are exposed in batholiths (Pankhurst et al. 1992, 1999) exhumed by structures mainly rooted at the Chilean slope. In this magmatic suite, the Liquiñe-Ofqui Fault system controlled the emplacement of younger Miocene plutons that are along the axial part of the Patagonian Andes (Fig. 2a) (Munizaga et al. 1988; Hervé 1976, 1984; Hervé et al. 1979).

orlando_a_p@yahoo.com.ar

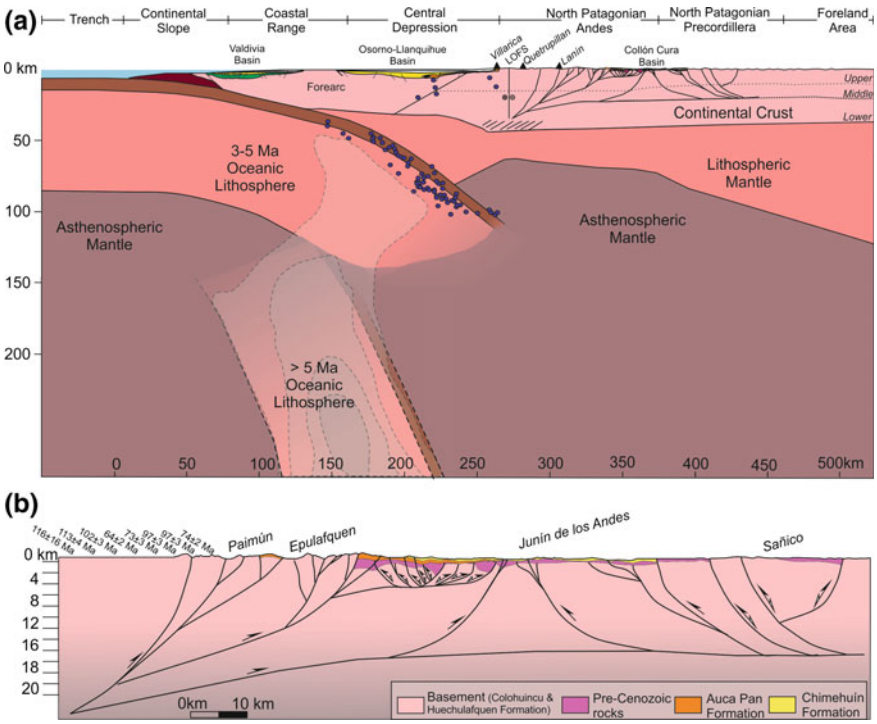


Fig. 2 **a** Lithospheric cross section across the southern Andes at 39–40°S (see Fig. 1 -A to A´- for location in map view). Lower crustal geometry is based on the density model of Tašárová (2007). Crustal and interplate seismicity are based on Dzierma et al. (2012). Superimposed tomography contours of Pesicek et al. (2012) were interpreted as a detached subducted slab at ∼5–3 Ma. Forearc structure is based on González (1989), while retroarc structure is based on data of this work. **b** Balanced cross section on the eastern slope of the Andes from the drainage divide area to the foreland zone across Junín de los Andes town. Note three distinctive areas, two where the basement is exposed, and an intermediate where it is covered by Cenozoic sections. Basement depth beneath main sedimentary depocenters was calculated from a gravity model. Note two opposite verging structural systems interfering at Junín de los Andes longitude

North of 39ºS, these rocks are covered by the late Oligocene to early Miocene Cura Mallín Basin composed of volcanic and volcaniclastic rocks locally interfingered with lacustrine and delta deposits (Suárez and Emparan 1995, 1997). This is an intra-arc basin formed during the late Oligocene–early Miocene— extensional stage that affected vast portions of the North Patagonian Andes (Suárez and Emparan 1995; Muñoz et al. 2000; Jordan et al. 2001; Burns et al. 2006; Melnick et al. 2006; Radic et al. 2002; Radic 2010). The Cura Mallín Basin is composed of a series of diachronous depocenters that span from 27 to 16 Ma along the axial zone and western Andean slope (Suárez and Emparan 1997; Radic et al. 2002; Burns et al. 2006). Locally, over the eastern Andean slope, Franzese et al. (2011) described a relatively contemporaneous Aluminé depocenter, composed of

orlando_a_p@yahoo.com.ar

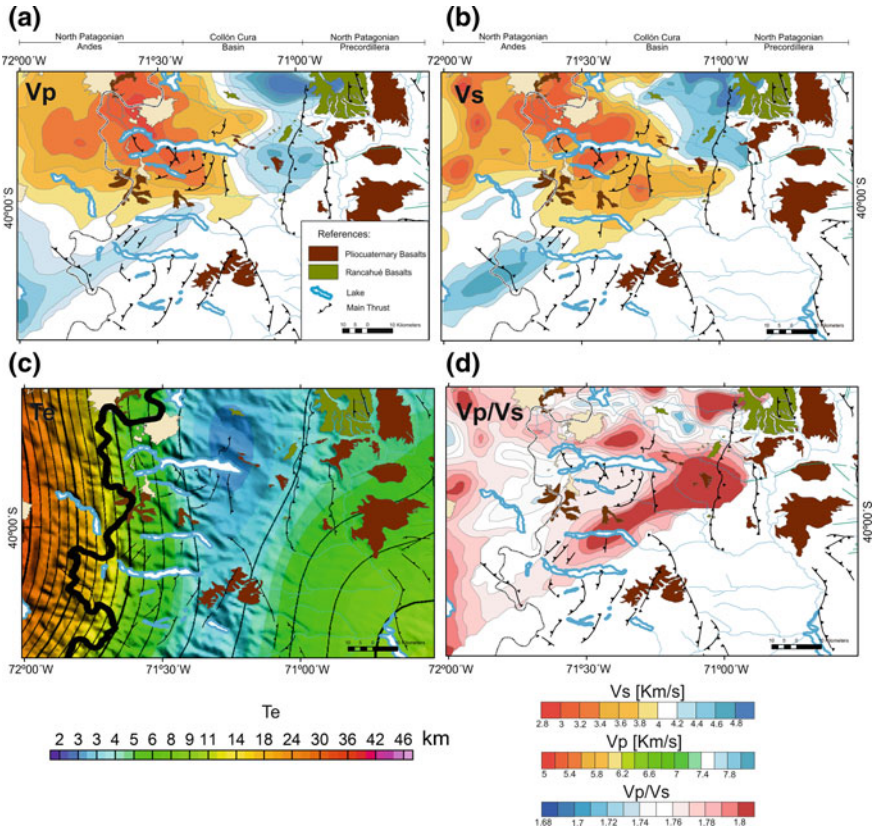


Fig. 3 Seismic velocity structure of the retroarc area at 39–40°S. **a** Vp anomalies at 10 km in depth; **b** Vs anomalies at 10 km in depth; **d** Vp/Vs anomalies at 10 km in depth (Dzierma et al. 2012). Note the spatial correlation that exists between arc and retroarc volcanic centers and related lava fields and seismic low-velocity zones. In particular, note a low-velocity anomaly associated with the volcanic arc particularly pronounced beneath the Villarrica, Quetrupillán, and Lanín Volcanoes. **c** Elastic thicknesses (Te) computed from gravity data that show lower values at the sites of low Vp and Vs

thick clastic deposits derived from the erosion of the crystalline basement, volcanic, volcaniclastic, and epiclastic rocks.

The Collón Cura Basin, to the east of the Patagonian Andes, separates an area of inverted Paleogene depocenters from the North Patagonian Precordillera. The Collón Cura Formation, the main unit filling this basin, was dated by Mazzoni and Benvenuto (1990) in the Río Collón Curá in 15–11 Ma. These are tuffs, ignimbrites, and reworked fluvial deposits, included in the Chimehuín Formation that agglutinates the Collón Cura Formation and the overlying Río Negro Formation of Pliocene age (Turner 1965; Cucchi and Leanza 2005). Spalletti and Dalla Salda (1996) had interpreted this basin as a pull-apart depocenter, based on its geometry and some sedimentary considerations. Contrastingly, Ramos and Cortés (1984)

orlando_a_p@yahoo.com.ar

showed that these sedimentary sections were formed by synorogenic deposits, related to the eastward migration of the orogenic front. Similarly, Giacosa et al. (2005) proposed a foreland basin for the origin of these sedimentary successions. More recently, Ramos et al. (2011), García Morabito et al. (2011), and García Morabito and Ramos (2012) described at these latitudes progressive unconformities in the wedge top of the fold and thrust belt, associated with Neogene contractional structures.

An isolated depocenter north of the Collón Cura Basin accommodates a succession of late Oligocene to Miocene rocks. The volcanic rocks of the Auca Pan Formation (Turner 1965, 1973) constitute the dominant exposures of this structural depression, described as the Auca Pan depocenter. These magmatic rocks of the Auca Pan Formation were dated in 29.6 ± 1.2 Ma (K/Ar age, Ramos et al. 2014).

To the east, the North Patagonian Precordillera system is divided into two particular sectors; a western part where mainly Neogene deposits are openly folded and an eastern sector where Triassic depocenters are partly inverted (Franzese and Spalletti 2001; García Morabito et al. 2011; D'Elia et al. 2012). This system has been described as a thick-skinned west-vergent structural belt (García Morabito et al. 2011) that is segmented by NE and W–NW extensional faults that are selectively inverted (D'Elia et al. 2012). The inverted Sañicó depocenter is the southernmost expression of the Precordillera. Its volcano-sedimentary filling corresponds to the Late Triassic Precuyano and Early Jurassic Cuyano cycles (Gulisano et al. 1984; Gulisano 1993) that constitute the syn-rift constituted during the Pangea breakup at these latitudes.

3 Upper Crustal Structure

A structural transect has been performed across the North Patagonian Andes and the North Patagonian Precordillera region identifying and analyzing in detail the following domains (Fig. 2b): (i) a western sector formed by east-verging thrusts and limited amounts of backthrusts that exhume the Paleozoic basement. This sector has thick-skinned faults that to the east determine a basement wedge. The eastward boundary of this system is the Piedras Paradas fault, which uplifts the basement over the late Oligocene Auca Pan Formation. (ii) To the east, a system with a shallower decollement is associated with folds with characteristic short wavelength amplitude that to the east become more open. The geometry determined of the main depocenters is concordant with the described surficial faults interpreted as inverted normal faults that bound the main sedimentary thicknesses. This intermediate sector shows a series of halfgraben features limited to the east by a deeper east-verging N-thrust near the Junín de los Andes valley. (iii) The eastern system is dominated by west-verging thick-skinned faults that characterize the North Patagonian Precordillera. The westernmost fault through this system is the Media Luna fault that determines a triangular zone together with the previous east-verging fault array

orlando_a_p@yahoo.com.ar

with a decollement inferred at 15 km depth. The easternmost structures exhume the Sañicó depocenter exposing Late Triassic syn-rift sections.

This section was constrained by gravity data that allowed computing sedimentary infills at the intermediate region from the gravity density model identifying sections up to 3000 m in thickness. Calculated sedimentary depocenter geometries were introduced in the structural section, where 700 m corresponds to the maximum thickness of the Auca Pan Formation and 500 m for the Chimehuín Formation (Cucchi and Leanza 2005). An additional, not outcropping, sedimentary section needs to be added in depth that is considered corresponding to Mesozoic deposits buried beneath Cenozoic piles based on their direct exposure on the eastern analyzed zone (Fig. 2b).

4 Lower Crustal Structure

Dzierma et al. (2012) calculated Vp and Vs anomalies as deviations from a 1D background velocity model, shown in a series of horizontal sections at 10, 30, and 50 km deep, respectively. Along these, a low velocity anomaly at lower crustal and upper mantle levels is particularly pronounced beneath the Villarrica, Quetrupillán and Lanín Volcanoes. These authors regarded this to either an expression of a melt reservoir from which these volcanoes are fed or to a reduced mantle wedge density due to volatile addition from a highly serpentinizated subducted slab. This area lies at the crossing point between the Liquiñe-Ofqui Fault system and the extrapolation of the Valdivia fracture zone in the Nazca plate that are considered natural paths for fluids coming from the subducted slab.

Elastic thicknesses (Te) computed from gravity data show low values in an elongated area parallel to the Andean front, east of the Lanín volcano (Ramos et al. 2014). Te values at the arc front are relatively higher than in the described anomalous area, which is not consistent with Vp and Vs anomalies determined by Dzierma et al. (2012). However, seismic data are mostly missing at the southeast studied area, enabling direct comparison between both datasets. Finally, around the Lanín volcano area, there seems to be a consistency between low Vp and Vs values and low elastic thicknesses (Fig. 3).

5 Discussion

The fold and thrust belt between 39º and 40ºS is dominated by the inversion of previous normal faults that produced in the western analyzed area east-verging structures and in the east west-vergent faults that exposed the Neopaleozoic basement. These two systems interfere at the central part where younger successions of late Oligocene to Miocene age are differentially preserved. In the eastern section, Triassic–Jurassic extension affected the present foreland area concentrated in the

orlando_a_p@yahoo.com.ar

Sañicó and the Piedra del Aguila depocenters and the series of eastern depocenters that constitute the Huincul system. In the western section, the Auca Pan depocenter concentrates the Oligocene to early Miocene sedimentary record that could have a Triassic section beneath, as it is inferred from gravity data.

Contractional deformation is thought to have acted in two different stages, beginning in the Late Cretaceous (Fig. 4), as it is indicated by available cooling K/Ar ages in Neopaleozoic rocks (García Morabito and Ramos 2011). This deformational stage affected the whole Andes at these latitudes, from the Coastal Cordillera, through the Patagonian Andes and the North Patagonian Precordillera (Burns et al. 2006; García Morabito and Ramos 2012; Thomson 2002). Coetaneous to this process, the arc expanded from the western Chilean Andean slope to the retroarc zone (Ramos and Folguera 2005). This eastern volcanic front rested over the Argentinean side of the Andes until the early Eocene (Llambías and Rapela 1984, 1989; Franchini et al. 2003), when it retracted to the west (Fig. 4). After this, late Oligocene to early Miocene extensional Auca Pan (≤29 Ma)–Rancahue (≤26 Ma)–Cura Mallín (≤17 Ma) series of depocenters were developed at the western retroarc area with a volcanic front located over the Chilean Andean side (Suárez and Emparan 1995; Jordan et al. 2001; Radic et al. 2002; Franzese et al. 2011; García Morabito and Ramos 2012). These sections have been emplaced under low-pressure conditions associated with a normal crust as it is indicated by geochemical data (Ramos et al. 2014, and see references therein).

A second contractional event affected the area in late Miocene times, reactivating the Patagonian Andean and the North Patagonian Precordilleran systems. This is evidenced by deformation affecting late Miocene sedimentary sections. During this time, the arc retracted at the intra-arc Liquiñe-Ofqui fault system (Fig. 4).

Pliocene to Quaternary times is characterized by important volumes of basaltic plateaus that were emplaced at the retroarc area (Fig. 4). Low Vp and Vs anomalies would indicate a heated middle crust partly coincident with computed low elastic thicknesses.

As indicated, seismic tomographies allow inferring the presence of a subducted steeper older slab beneath the present subduction zone (Figs. 2, 4) (Pesicek et al. 2012). This has been considered an evidence of a slab tearing associated with the steepening of the subduction zone at these latitudes some 5–3 Ma ago (Fig. 4). This is potentially related to the upwelling of hot asthenospheric mantle, and thermal anomalies in the middle crust described by Dzierma et al. (2012), related low Te values, and retroarc volcanic eruptions.

Expansions and narrowings of the volcanic arc at the studied latitudes showed to be contemporaneous to the described contractional and extensional stages; while the subduction of the Valdivia transform fault and the strong tearing that the Nazca plate exhibits would explain the present seismic velocity structure of the crust.

orlando_a_p@yahoo.com.ar

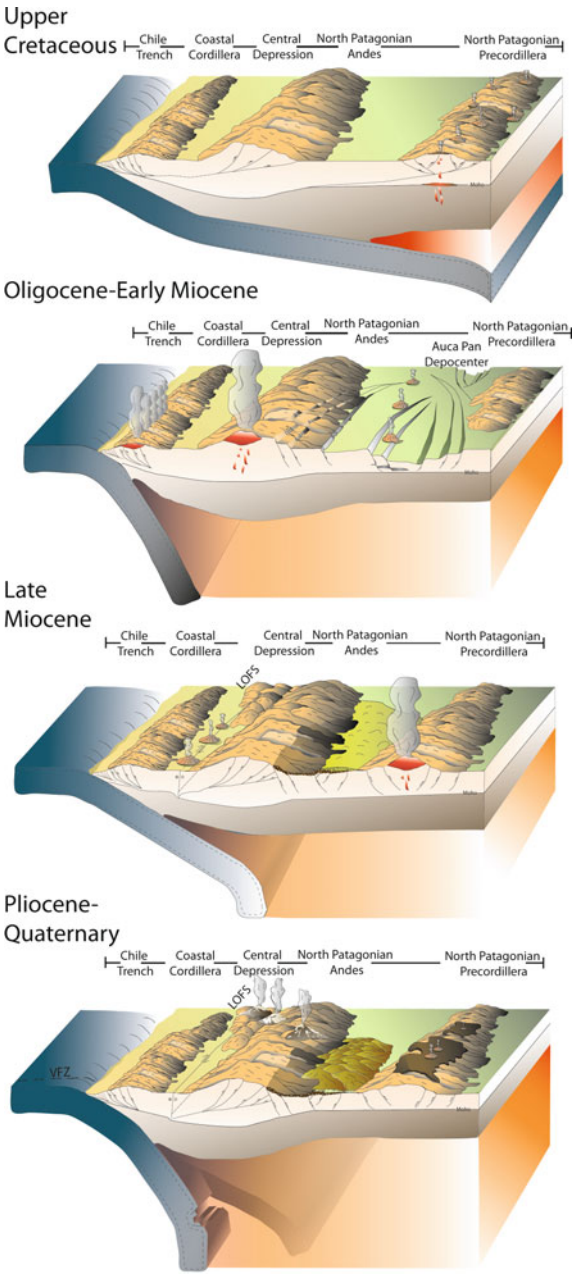


Fig. 4 Schematic block diagrams summarizing the evolution of the North Patagonian Andes since the latest Cretaceous to Pliocene–Quaternary times nearby the 40ºS (see text for further details)

orlando_a_p@yahoo.com.ar

6 Conclusions

The present chapter exemplifies how the North Patagonian Andes are characterized by a long and complex deformational history. Three different sectors have been described with characteristic behaviors. These sectors have been uplifted by the inversion of previous extensional structures from the Triassic–Jurassic and the Oligocene times. During this evolution, two main extensional periods occurred, first during the Triassic–Jurassic associated with Pangea breakup and then during Oligocene times. Contractional stages have taken place during the Late Cretaceous and the upper Miocene, respectively, affecting vast proportions of the fold and thrust belt. The first stage is determined at these latitudes mainly from K/Ar ages, interpreted as cooling ages, while the youngest by the age of sedimentary and volcanic sections deformed at the Andean front.

Recently, released seismic tomographies show the present geometry of the subduction system at these latitudes where slab detachment processes are described. This slab detachment would have given place to the injection of an asthenospheric inflow under this segment of the North Patagonian Andes. Thermal conditions revealed by low Vp and Vs velocities and Te values, together with the occurrence of less than 5 My mafic rocks at the retroarc zone, could be linked to this particular environment.

Oscillations of the subducted slab through time inferred by the arc behavior coincide with the deformational regimes that affected the North Patagonian Andes.

References

Bohm M, Lüth S, Echtler HP, Asch G, Bataille K, Bruhn C, Rietbrock A, Wigger P (2002) The Southern Andes between 36° and 40°S latitude: seismicity and average seismic velocities. Tectonophysics 356:275–289

Burns WM, Jordan TE, Copeland P, Kelley SA (2006) The case for extensional tectonics in the Oligocene- Miocene Southern Andes as recorded in the Cura Mallín basin (36°–38°S). In: Kay SM, Ramos VA (eds) Evolution of an Andean margin: a tectonic and magmatic view from the Andes to the Neuquén Basin (35°–39°S lat.). Geological Society of America, Special Papers, vol 407, pp 163–184

Cande SC, Leslie RB (1986) Late Cenozoic tectonics of the southern Chile trench. J Geophys Res 91:471–496

Cembrano J, Lara L (2009) The link between volcanism and tectonics in the southern volcanic zone of the Chilean Andes: a review. Tectonophysics 471:96–113

Cucchi R, Leanza H (2005) Hoja Geológica 3972-IV Junín de los Andes, provincia del Neuquén. Servicio Geol Min Nac Bol 357:1–102

D'Elia L, Muravchik M, Franzese JR, Lopez L (2012) Tectonostratigraphic analysis of the Late Triassic-Early Jurassic syn-rift sequence of the Neuquén Basin in the Sañicó depocentre, Neuquén Province, Argentina. Andean Geol 39:133–157

Diraison M, Cobbold PR, Rossello EA, Amos AJ (1998) Neogene dextral transpression due to oblique convergence across the Andes of northwestern Patagonia, Argentina. J S Am Earth Sci 11:519–532

orlando_a_p@yahoo.com.ar

Dzierma Y, Thorwart M, Rabbel W (2012) Moho topography and subducting oceanic slab of the Chilean continental margin in the maximum slip segment of the 1960 Mw 9.5 Valdivia (Chile) earthquake from P-receiver functions. Tectonophysics 530–531:180–192

Forsythe R, Nelson E (1985) Geological manifestations of ridge collision: evidence from del Golfo de Penas-Taitao Basin, Southern Chile. Tectonics 4:477–495

Franchini M, López-Escobar L, Schalamuk IB, Meinert L (2003) Magmatic characteristics of the Paleocene Cerro Nevazón region and other Late Cretaceous to Early Tertiary calc-alkaline subvolcanic to plutonic units in the Neuquén Andes, Argentina. J S Am Earth Sci 16:399–421

Franzese JR, Spalletti LA (2001) Late triassic–early jurassic continental extension in southwestern Gondwana: tectonic segmentation and pre-break-up rifting. J S Am Earth Sci 14:257–270

Franzese JR, D'Elia L, Bilmes A, Muravchik M, Hernández M (2011) Superposición de cuencas extensionales y contraccionales oligo-miocenas en el retroarco andino norpatagónico: la Cuenca de Aluminé, Neuquén. Andean Geol 38:319–334

García Morabito E, Ramos VA (2011) La Precordillera neuquina sur en el contexto de los Andes Norpatagónicos. In: Leanza HA, Arregui C, Carbone O, Danielli J, Vallés J (eds) Geología y Recursos Naturales de la Provincia de Neuquén. Relatorio del XVIII Congreso Geológico Argentino, Buenos Aires, pp 355–365

García Morabito E, Ramos VA (2012) Andean evolution of the Aluminé fold and thrust belt, Northern Patagonian Andes (38°30′–40°30′S). J S Am Earth Sci 38:13–30

García Morabito E, Götze HJ, Ramos VA (2011) Tertiary tectonics of the Patagonian Andes retro-arc area between 38°15′ and 40°S latitude. Tectonophysics 499:1–21

Giacosa RE, Afonso JC, Heredia CN, Paredes J (2005) Tertiary tectonics of the sub-Andean region of the North Patagonian Andes, southern central Andes of Argentina (41–42°30′S). J S Am Earth Sci 20:157–0170

González E (1989) Hydrocarbon resources in the coastal zone of Chile. In: Reinemund JA (ed) Ericksen GE, Cañas Pinochet MT. Geology of the Andes and its relation to hydrocarbon and mineral resources. Circum-Pacific council for energy and mineral resources earth science series, Houston, Texas, pp 383–404

Gulisano CA (1993) Precuyano. In: Riccardi A, Damborenea S (eds) Léxico Estratigráfico De La Argentina, Jurásico. Asoc Geol Argentina Serie "B" (Didáctica y Complementaria) No. 21. Buenos. Aires 9:334–335

Gulisano CA, Gutiérrez Pleimling AR, Digregorio RE (1984) Esquema estratigráfico de la secuencia jurásica del oeste de la provincia del Neuquén, IX Congreso Geológico Argentino (San Carlos de Bariloche). Actas 1:236–259

Hervé M (1976) Estudio geológico de la Falla Liquiñe-Reloncaví en el área de Liquiñe: antecedentes de un movimiento transcurrente. I Congreso Geológico Chileno (Valdivia). Actas 1:B39–B56

Hervé F (1984) Rejuvenecimiento de edades radiométricas y el sistema de fallas Liquiñe-Ofqui. Comunicaciones 35:107–116

Hervé F, Araya E, Fuenzalida JL, Solano A (1979) Edades radiométricas y tectónica neógena en el sector costero de Chiloé continental, X Región. II Congreso Geológico Chileno (Arica). Actas 1:F1–F8

Jordan TE, Burns WM, Veiga R, Pángaro F, Copeland P, Kelley SA, Mpodozis C (2001) Extension and basin formation in the southern Andes caused by increased convergence rate: a mid Cenozoic trigger for the Andes. Tectonics 20:308–324

Lara LE (2004) Geología del Volcán Lanín, Región de La Araucanía. Servicio Nacional de Geología y Minería, Carta Geológica de Chile. Serie Geología Básica 87: p 18

Lavenu A, Cembrano J (1999) Compressional- and transpressional-stress pattern for pliocene and quaternary brittle deformation in fore arc and intra-arc zones (Andes of Central and Southern Chile). J Struct Geol 21:1669–1691

Llambías EJ, Rapela CW (1984) Geología de los complejos eruptivos de La Esperanza, provincia de Río Negro. Rev Asoc Geol Argentina 39:220–243

Llambías EJ, Rapela CW (1989) Las volcanitas de Collipilli, Neuquén (37°S) y su relación con otras unidades paleógenas de la cordillera. Rev Asoc Geol Argentina 44:224–246

orlando_a_p@yahoo.com.ar

Lüth S, Wigger P, Mechie J, Stiller M, Krawczyk C, Bataille K, Reichert C, Flueh ER (2004) The crustal structure of the Chilean forearc between 36° and 40°S from combined offshore and onshore seismic wide-angle measurements. Bolletino di Geofisica Teorica ed Applicata. Electronic Files

Mazzoni M, Benvenuto A (1990) Radiometric ages of tertiary ignimbrites and the Collón Cura Formation, northwestern Patagonia, XI Congreso Geológico Argentino (Buenos Aires). Actas 1:87–90

Melnick D, Rosenau M, Folguera A, Echtler HP (2006) Neogene tectonic evolution of the Neuquen Andes western flank (37–39ºS). Geol Soc Am Spec Pap 407:73–95

Munizaga F, Hervé F, Drake R, Pankhurst RJ, Brook M, Snelling N (1988) Geochronology of the Lake Region of south-central Chile (39º–42ºS): preliminary results. J S Am Earth Sci 1:309–316

Muñoz J, Troncoso R, Duhart P, Crignola P, Farmer L, Stern CR (2000) The relation of the mid-Tertiary coastal magmatic belt in south-central Chile to the late Oligocene increase in plate convergence rate. Rev Geol Chile 27:177–503

Pankhurst RJ, Hervé F, Rojas L, Cembrano J (1992) Magmatism and tectonics in continental Chiloé, Chile (42°–42°30′S). Tectonophysics 205:283–294

Pankhurst RJ, Weaver SD, Hervé F, Larrondo P (1999) Mesozoic-Cenozoic evolution of the North Patagonian Batholith in Aysen, southern Chile. J Geol Soc 156:673–694

Pardo-Casas F, Molnar P (1987) Relative motion of the Nazca (Farallon) and s since late cretaceous time. Tectonics 6:233–248

Pesicek JD, Engdahl ER, Thurber CH, DeShon HR, Lange D (2012) Mantle subducting slab structure in the region of the 2010 M8.8 Maule earthquake (30–40°S). Chile Geophys J Int 191:317–324

Radic JP (2010) Las cuencas cenozoicas y su control en el volcanismo de los Complejos Nevados de Chillán y Copahue-Callaqui (Andes del Sur, 36º–39°S). Andean Geol 37:220–246

Radic JP, Rojas L, Carpinelli A, Zurita E (2002) Evolución tectónica de la cuenca terciaria de Cura Mallín, región cordillerana chileno argentina (36°30′–39°00′S). XV Congreso Geológco Argentino (Calafate). Actas 3:233–237

Ramos VA, Cortés JM (1984) Estructura e interpretación tectónica. In: Ramos VA (ed) Geología y Recursos Naturales De La Provincia De Río Negro. Asoc Geol Argentina, Buenos Aires, pp 317–346

Ramos VA, Folguera A (2005) Tectonic evolution of the Andes of Neuquén: Constraints derived from the magmatic arc and foreland deformation. In: Spalletti L, Veiga G, Schwarz E, Howell J (eds) The Neuquén Basin: a case study in sequence stratigraphy and basin dynamics, Geological Society of London, Special Publications, vol 252, pp 15–35

Ramos ME, Orts DL, Calatayud F, Pazos PJ, Folguera A, Ramos VA (2011) Estructura, Estratigrafía y evolución tectónica de la cuenca de Ñirihuau en las nacientes del río Cushamen, Chubut. Rev Asoc Geol Argentina 68:210–224

Ramos ME, Folguera A, Fennel L, Giménez M, Litvak VD, Dzierma Y, Ramos VA (2014) Tectonic evolution of the North Patagonian Andes from field and gravity data (39º–40°S). J S Am Earth Sci 51:59–75

Somoza R (1998) Updated Nazca (Farallon)-South America relative motions during the last 40 My: implications for mountain building in the central Andean region. J S Am Earth Sci 11:211–215

Spalletti LA, Dalla Salda LH (1996) A pull apart volcanic related Tertiary basin, an example from the Patagonian Andes. J S Am Earth Sci 9:197–206

Suárez M, Emparan C (1995) The stratigraphy, geochronology and paleophysiography of a Miocene fresh-water interarc basin, southern Chile. J S Am Earth Sci 8:17–31

Suárez M, Emparan C (1997) Hoja Curacautm. Regiones de la Araucania y del Bio Bio. Carta Geológica de Chile, 1:250 000. Servicio Nacional de Geologia y Mineria de Chile, Santiago, pp 71–105

Tašárová ZA (2007) Towards understanding the lithospheric structure of the southern Chilean subduction zone (36°S–42°S) and its role in the gravity field. Geophys J Int 170:995–1014

orlando_a_p@yahoo.com.ar

Thomson SN (2002) Late Cenozoic geomorphic and tectonic evolution of the Patagonian Andes between latitudes 42ºS and 46ºS: an appraisal based on fission track results from the transpressional intra-arc Liquiñe-Ofqui fault zone. Geol Soc Am Bull 114:1159–1173

Thomson SN, Hervé F (2002) New time constraints for the age of metamorphism at the ancestral Pacific Gondwana margin of southern Chile (42–52°S). Rev Geol Chile 29:1–16

Turner JCM (1965) Estratigrafía de Aluminé y adyacencias. Rev Asoc Geol Argentina 20:153–164

Turner JCM (1973) Descripción geológica de la Hoja 37a-b, Junín de los Andes, provincia del Neuquén. Servicio Nac Min Geol Bol 138:1–86

Vergara M, Munizaga F (1974) Age and evolution of the upper Cenozoic andesitic volcanism in central south Chile. Geol Soc Am Bull 85:603–606

orlando_a_p@yahoo.com.ar

Cenozoic Deformational Processes in the North Patagonian Andes Between 40° and 43°S

Darío L. Orts, Andrés Folguera, Mario Gimenez, Francisco Ruiz, Alfonso Encinas, Emilio Agustín Rojas Vera and Federico Lince Klinger

Abstract The Cenozoic tectonic evolution of the North Patagonian Andes is analyzed linking geological and geophysical data in order to decipher the deformational processes that acted through time and relate them to basin formation. Field observations and seismic reflection profiles reveal the shallow structure of the retroarc area where contractional structures, associated with Oligocene to early Miocene inverted extensional sections, are partially onlapped by early to late Miocene synorogenic deposits. From the construction of five structural cross sections along the retroarc area between 40° and 43° 30′S, constrained by surface, gravity, and seismic data, a shortening gradient is observed along Andean strike. The highest shortening of 18.7 km (15.34 %) is determined near to 41° 30′S where basement blocks were uplifted in the orogenic front area, and the deepest and broadest synorogenic depocenters were formed toward the foreland. Additionally, eastward shifting of Miocene calc-alkaline arc rocks occurred at these latitudes, which is interpreted as indicative of a significant change in the subduction parameters at this time. Deep crustal retroarc structure is evaluated through

D.L. Orts (✉)
Instituto de Investigación en Paleobiología y Geología, Universidad Nacional de Río Negro—CONICET, General Roca (Río Negro), Argentina
e-mail: dlorts@yahoo.com

A. Folguera · E.A. Rojas Vera
Departamento de Ciencias Geológicas, Facultad de Ciencias Exactas y Naturales, Instituto de Estudios Andinos "Don Pablo Groeber" UBA-CONICET, Buenos Aires, Argentina

M. Gimenez · F. Ruiz · F. Lince Klinger
Instituto Geofísico y Sismológico Ing. Volponi, Universidad Nacional de San Juan, Ruta 12-km17, San Juan, Argentina

M. Gimenez · F. Lince Klinger
Consejo Nacional de Investigaciones Científicas y Técnicas (CONICET), Buenos Aires, Argentina

A. Encinas
Departamento de Ciencias de la Tierra, Universidad de Concepción, Casilla 160-c, Concepción, Chile

© Springer International Publishing Switzerland 2016

A. Folguera et al. (eds.), *Growth of the Southern Andes*,
Springer Earth System Sciences, DOI 10.1007/978-3-319-23060-3_8

orlando_a_p@yahoo.com.ar

inversion of gravity models that made also possible to infer Moho attenuated zones. These coincide with the occurrence of younger than 5 Ma within-plate volcanics as well as with crustal thermal anomalies suggested by shallowing of the Curie isotherm calculated from magnetic data.

Keywords Miocene synorogenic sequences · North Patagonian Andes

1 Introduction

The Cenozoic evolution of the North Patagonian Andes shares common characteristics with other Andean segments as these are part of an active and long-lived subduction orogen, with different pulses of foreland sedimentation and magmatism (Fig. 1). The North Patagonian Andes between 40° and 43°S are ascribed in the literature as having undergone several different deformational stages during at least the last 100 Ma (Feruglio 1947, 1949; Ramos and Cortés 1984; Diraison et al. 1998; Giacosa and Heredia 1999). This work focuses on this area, where the fold and thrust belt has a differential eastward development in the Cenozoic, creating a

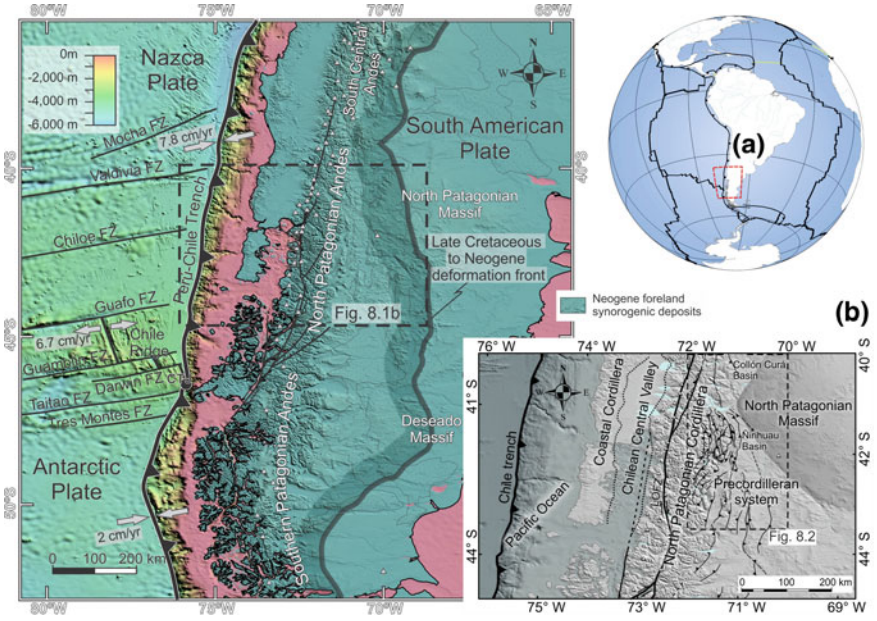


Fig. 1 **a** Present tectonic setting of the Patagonian Andes, plate configurations and location of the study zone. *LOFZ* Liquiñe-Ofqui fault zone; *CTJ* Chile triple junction; *Grey triangles* Active volcanoes; *Grey arrows* Present-day plate convergence and mid-ocean spreading rates (after Thomson et al. 2001). **b** Schematic regional map showing main morphotectonic units and structures of the Andes between 40° and 45°S

orlando_a_p@yahoo.com.ar

foreland curved feature, in comparison with northern and southern sections of the Andes (Figs. 1 and 2) (Feruglio 1947; Coira et al. 1975; Peroni et al. 1995; Figari 2005; Giacosa et al. 2010).

One of the most striking characteristics of the study area is the thick successions of late Oligocene to Miocene strata on the eastern fold and thrust belt, at the wedge-top zone, reaching 2500 m, that are condensed up to 300–500 m north of 39°S and south of 43° 30′S (Figs. 1a and 2) (Marshall and Salinas 1990; Radic et al. 2009; García Morabito et al. 2011; Flynn et al. 2008; Rojas Vera et al. 2010). These deposits are known in this region as the Ñirihuau and Collón Curá Formations, among other local denominations, extensively studied in early regional works (Feruglio 1949; González Bonorino and González Bonorino 1978; Cazau et al. 1989; Mazzoni and Benvenuto 1990). These together with the structural and stratigraphic relations with older units along strike are key elements to identify the deformational pulses that affected the fold and thrust belt in the Cenozoic.

In this work, we attempt to integrate geological mapping, based partially on previous studies, with geophysical and geochronological data from the cordilleran axis to the sub-Andean region. Field work has focused on the Main North Patagonian Andes and the frontal zone where synorogenic deposits accumulated. This allows us the identification of the main Cenozoic deformational stages that affected the fold and thrust belt and to relate them to the different geometries that adopted the magmatic arc through time.

2 Geological Framework

The Andean orogen between 40° and 43° 30′S is characterized by a series of morphotectonic elements that from west to east comprises (Fig. 1b): the Coastal Cordillera, the Chilean Central Valley, the North Patagonian Cordillera, and the Precordilleran System and its foreland where this study is focused (Figs. 1b and 2).

In the Coastal Cordillera (south of ∼38°S), a Late Paleozoic to Triassic accretionary prism outcrops, partly covered by Meso-Cenozoic strata (see Hervé et al. 2013 for a synthesis; Thomson and Hervé 2002; Willner et al. 2004). These metamorphic rocks were part of the proto-Pacific margin during the Gondwanian orogenic cycle, developed previously to the Andean cycle.

To the east, a low-lying area between the Coastal and the North Patagonian Cordilleras named as the Chilean Central Valley is composed of a series Eocene to Quaternary basins filled by volcaniclastic, marine, and glacial sediments (Elgueta and Mpodozis 2012; González 1989; Radic et al. 2009). This region, located in the Andean forearc, would have suffered subsidence due to subduction erosion in early Miocene times (∼17 Ma) allowing a Pacific-derived transgression and deposition of deep-marine sediments (Encinas et al. 2012). The North Patagonian Cordillera is characterized by the presence of the Quaternary volcanic arc of the Southern Andes Volcanic Zone including large stratovolcanoes that correspond to the highest elevations at these latitudes (see Stern 2004). A conspicuous feature of this region is

orlando_a_p@yahoo.com.ar

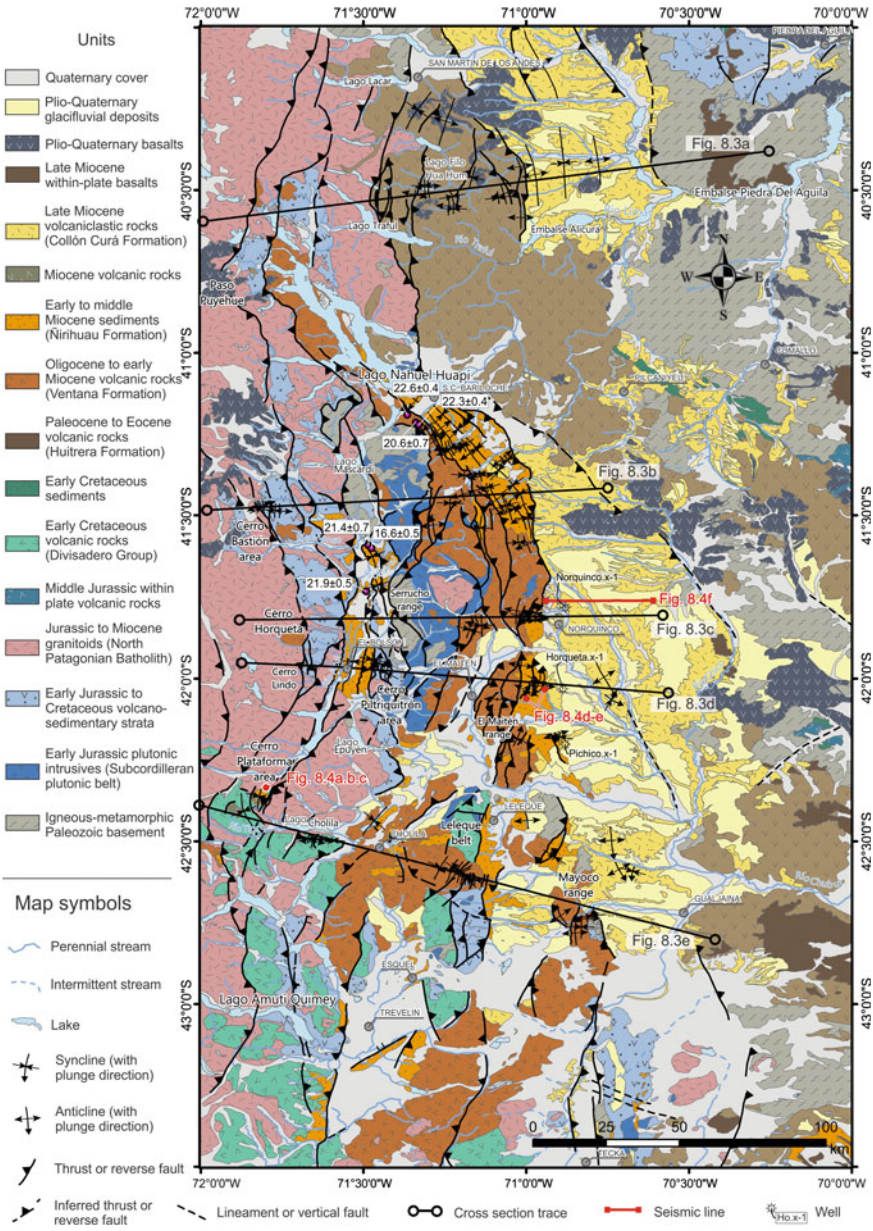


Fig. 2 Regional geological map of the retroarc area between 40° and 43° 30′S (based on Giacosa et al. 2001, 2005; Bechis and Cristallini 2006; Bechis et al. 2014; Orts et al. 2012, 2015). Location of the performed structural cross sections and seismic lines interpreted in this study are shown. See text for further details. New available geocronological data (Bechis et al. 2014) of the basal and intermediate volcaniclastic sections of El Bolsón and Ñirihuau basins are shown

orlando_a_p@yahoo.com.ar

the Liquiñe-Ofqui fault zone (LOFZ) (Figs. 1 and 3), a 1000 km long dextral strike-slip fault system that is developed along a thermally weakened crust within the active arc roots (Cembrano et al. 1996; Lavenu and Cembrano 1999; Thomson et al. 2010).

The basement of the Quaternary stratovolcanoes is constituted by the Patagonian Batholith, a ~2000 km long and average 120 km wide body parallel to the Pacific coastline, associated with smaller satellite plutons spread toward both Andean slopes (Hervé et al. 2000). In particular, the segment north of the Chilean Triple Junction (CTJ) (47°S; Fig. 1) corresponding to the North Patagonian Batholith (NPB) is constituted by Middle Jurassic to Miocene calc-alkaline intrusive rocks (Castro et al. 2011; Pankhurst et al. 1999) which are locally intruding the Paleozoic basement.

The North Patagonian Cordillera, east of the LOFZ, is structured by thick-skinned Andean thrust sheets that exhumed the eastern side of the NPB and widespread outcrops of basement rocks (Fig. 4) (Giacosa and Heredia 2004a; Thomson 2002; Giacosa et al. 2005; Orts et al. 2012; García-Sansegundo et al. 2009). These basement rocks are composed mostly of Paleozoic metamorphic and igneous rocks, deformed by the Gondwanic orogeny in Late Carboniferous-Triassic times (García-Sansegundo et al. 2009; von Gosen 2009; von Gosen and Loske 2004). This igneous–metamorphic basement is grouped in the Colohuincul Complex in the high Andes, whereas to the foreland , it is referred to as the Rio Chico Complex (Dalla Salda et al. 1991, 1994; Lucassen et al. 2004; Hervé et al. 2013; Pankhurst et al. 2006).

In the eastern parts of the North Patagonian Cordillera, volcanic rocks of the Divisadero Group (Skármeta and Charrier 1976) unconformably overlay Jurassic successions and older intrusive rocks. These volcanic successions with calc-alkaline affinities have Early Cretaceous ages, ranging between 100 and 120 Ma (Rapela et al. 1988; Suárez et al. 1996). Their outcrops are found between 41° and 48°S and are emplaced over an angular unconformity that would imply a late Early Cretaceous orogenic event that would have shaped the Andes at these latitudes (Ramos 1981; Suárez and De La Cruz 2001).

In the Precordilleran system (41° 30′–43°S), east of the North Patagonian Cordillera (Fig. 3), the Paleozoic basement is intruded by the Early Jurassic Subcordilleran Plutonic Belt (Gordon and Ort 1993) (Fig. 4). These rocks are covered by relatively concomitant volcano-sedimentary successions that were developed in a NNE-oriented intra-arc extensional system (Giacosa and Heredia 2004b; Orts et al. 2012). Further to the east, in the foreland region, Early to Middle Jurassic non-marine extensional depocenters of the Cañadon Asfalto Basin (Fig. 3) were developed (Figari 2005).

In this region, two Cenozoic magmatic belts were formed, related to extensional intra-orogenic events (Giacosa and Heredia 2004a), differing in age and composition: (i) the eastern Pilcaniyeu belt (60–42 Ma, Huitrera Formation) and (ii) the western El Maitén belt (33–23 Ma, Ventana Formation) (Rapela et al. 1988) (Fig. 4). The Paleocene to Eocene Pilcaniyeu magmatic belt is characterized by bimodal volcanic rocks from predominant rhyolitic ignimbrite facies to subordinate andesites and basalts (Mazzoni et al. 1991; Rapela et al. 1988). To the east, the

orlando_a_p@yahoo.com.ar

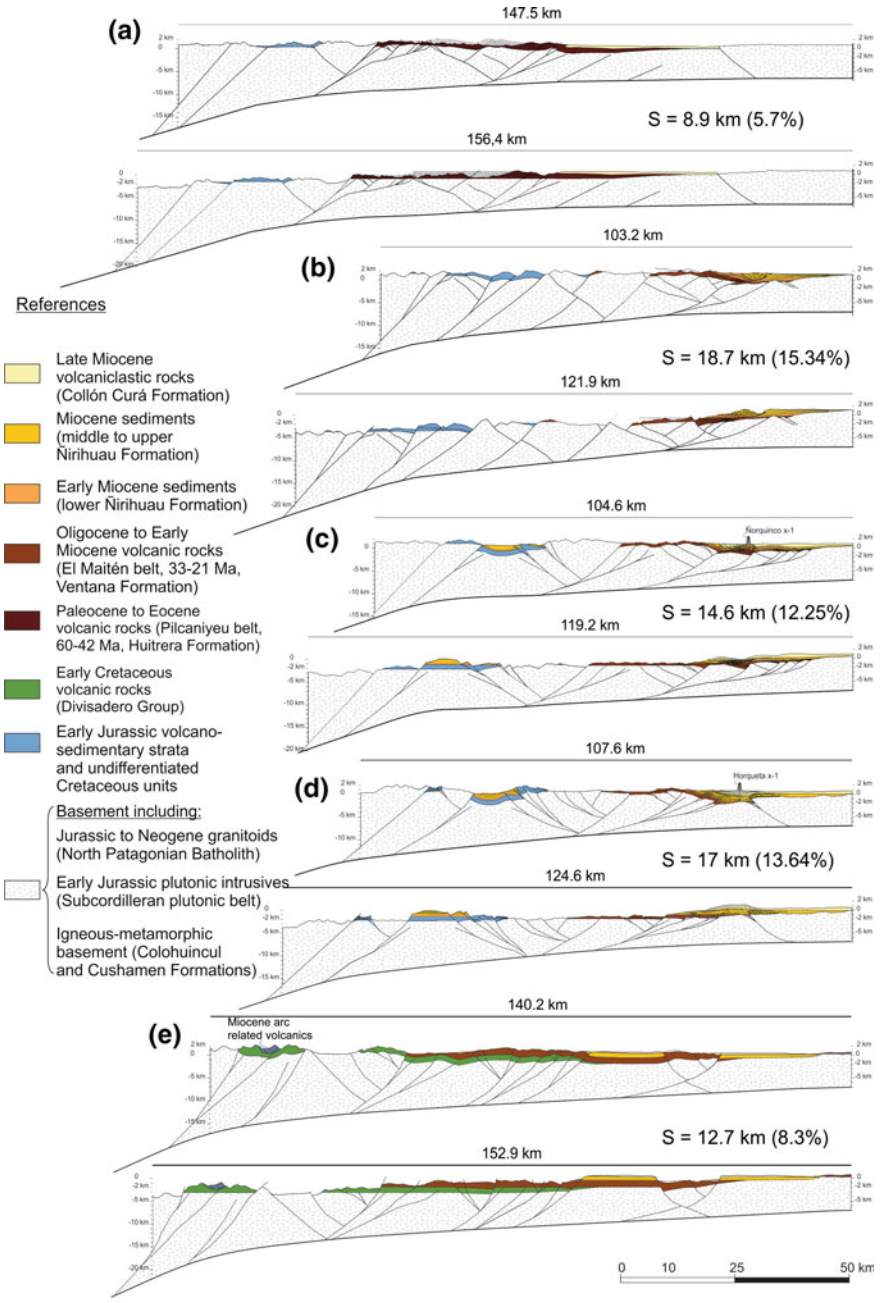


Fig. 3 Balanced cross sections from the retroarc area between 40° 30′ and 42° 45′S (see Fig. 2 for location). **a** Northernmost cross section from the Puyehue area to the foreland area across Traful and Filo-Hua-Hum lakes. **b** Cross section from Cerro Bastión and across the David syncline, which coincides with the maximum shortening in this Andean segment. **c** Cross section from Cerro Horqueta to the Ñorquinco foreland area. **d** Cross section from Cerro Lindo to the foreland region east of the El Maitén range. **e** Cross section from the divide area near Cholila lake to Mayoco ranges

orlando_a_p@yahoo.com.ar

Oligocene El Maitén magmatic belt is characterized by widespread outcrops of andesites and dacitic ignimbrites with subordinated basaltic lava flows and rhyolitic ignimbrites in a N–S trend along the Precordilleran system (Fig. 4). Associated

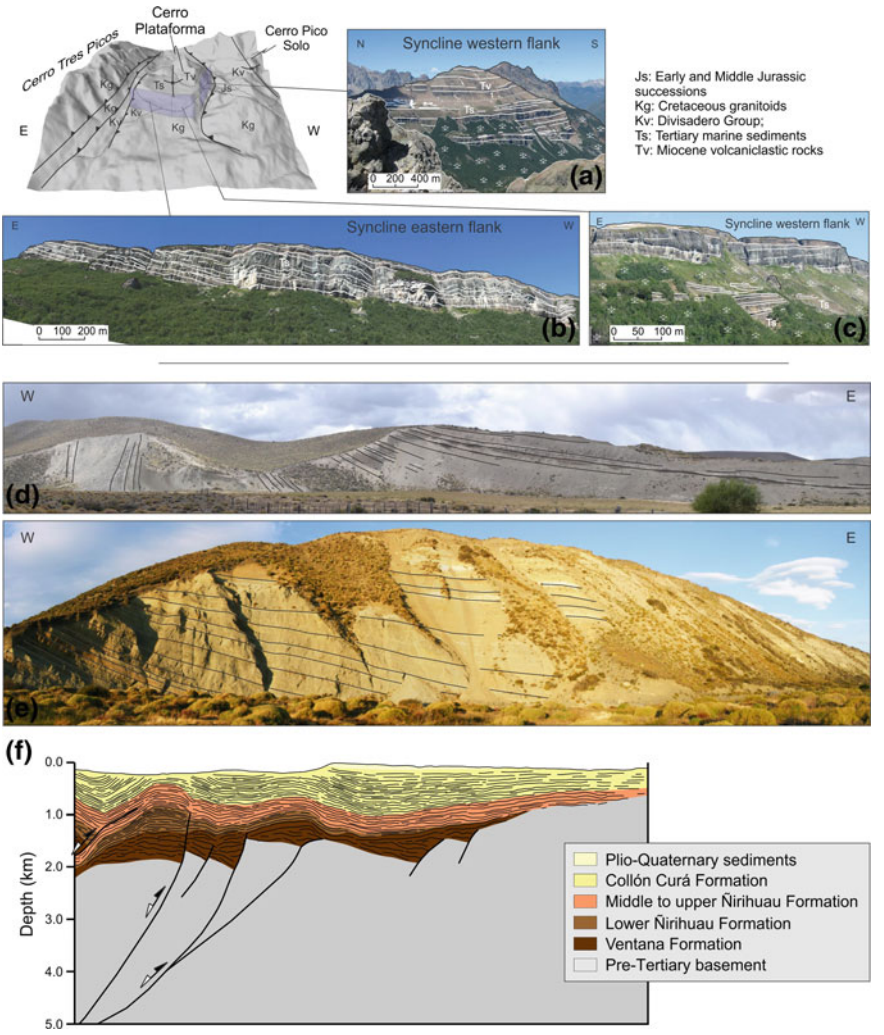


Fig. 4 **a**–**c** Progressive unconformities at the hinterland zone in marine successions in both limbs of the Cerro Plataforma syncline (see Fig. 2 for location). **d** and **e** progressive unconformities corresponding to growth strata at the backlimbs of main structures in the eastern slope of the El Maitén Belt (see Fig. 2 for location) corresponding to Collón Curá and upper Ñirihuau Formations, respectively. **f** Depth-converted 2D seismic line AR4A-103 (see Fig. 2 for location). East-vergent structures associated with inverted extensional depocenters of the Ventana Formation and lower Ñirihuau Formation. Growth strata related to these structures occurred at the time of deposition of the Collón Curá and upper Ñirihuau Formations which shows onlap relations in wedge-like geometries

orlando_a_p@yahoo.com.ar

products have accumulated in volcanic depocenters with wedge-like geometries recognized from field observations (Orts et al. 2012). These two magmatic belts have geochemical characteristics that indicate tholeiitic signatures (Rapela and Kay 1988; Rapela et al. 1988).

The late Cenozoic sedimentary infill in the study zone is accommodated in isolated depocenters on the eastern slope of the Andes. These sedimentary successions correspond to two partially superimposed sections, the Ñirihuau and the Collón Curá Formations (Fig. 2). These Miocene successions are characterized by volcaniclastic sections that onlap the flanks of the Cenozoic folds (Ramos et al. 2011; Orts et al. 2012; Bilmes et al. 2013).

Flat-lying Pliocene-Pleistocene basalts unconformably cover the Miocene successions (Fig. 4). These have been dated between 5 and 0.6 Ma by K/Ar methods (Haller et al. 2009; Mena et al. 2006; Pécskay et al. 2007). Their chemistry indicates a within-plate environment that differs from previous Andean arc-magmatic rocks (Massaferro et al. 2006).

3 General Methodology

In this study, we present an integration of the structure and the geology of the retroarc zone between 40° and 43° 30′S from the hinterland to the foreland area (Fig. 2). This was made through the compilation of previously published and our own data (e.g., Giacosa et al. 2001; Bechis and Cristallini 2006; Ramos et al. 2011; Tobal et al. 2012; Orts et al. 2012, 2015). The regional data integration has allowed the construction of five cross sections (Fig. 3) perpendicular to the strike of the main structures.

These were done combining surface and subsurface geophysical and geological information (Figs. 2, 4, and 5). The subsurface information consists of a series of reprocessed seismic profiles and five wells provided by the oil industry (YPF S.A) which are available in the Ñirihuau Basin after the 80s exploratory surveys. The construction of the cross sections was performed using the Move® software. Different modeling algorithms were used in their palinspastic restoration. Most of the structures were modeled using the fault parallel flow and flexural slip algorithms, computing minimum displacements to the eroded cut-off and leveling the same units in the hanging and foot walls.

In particular, structural data were collected from the highest sector along the North Patagonian Andes between the Traful lake (∼40° 30′S) and the Amuti Quimey lake (∼43°S), to the Precordilleran sector along the El Maitén, Leleque, Mayoco, and Esquel ranges (Fig. 4). Then, data were gathered in a GIS database for comparison with seismic and gravity and magnetometric data.

Gravity data consist of measurements along the main roads, seismic lines, and off-road through the area (see dataset in Fig. 5a). The onshore gravity dataset used in this work consists of a compilation of more than 7500 gravity stations from several different sources. The observations were carried out over the past 20 years

orlando_a_p@yahoo.com.ar

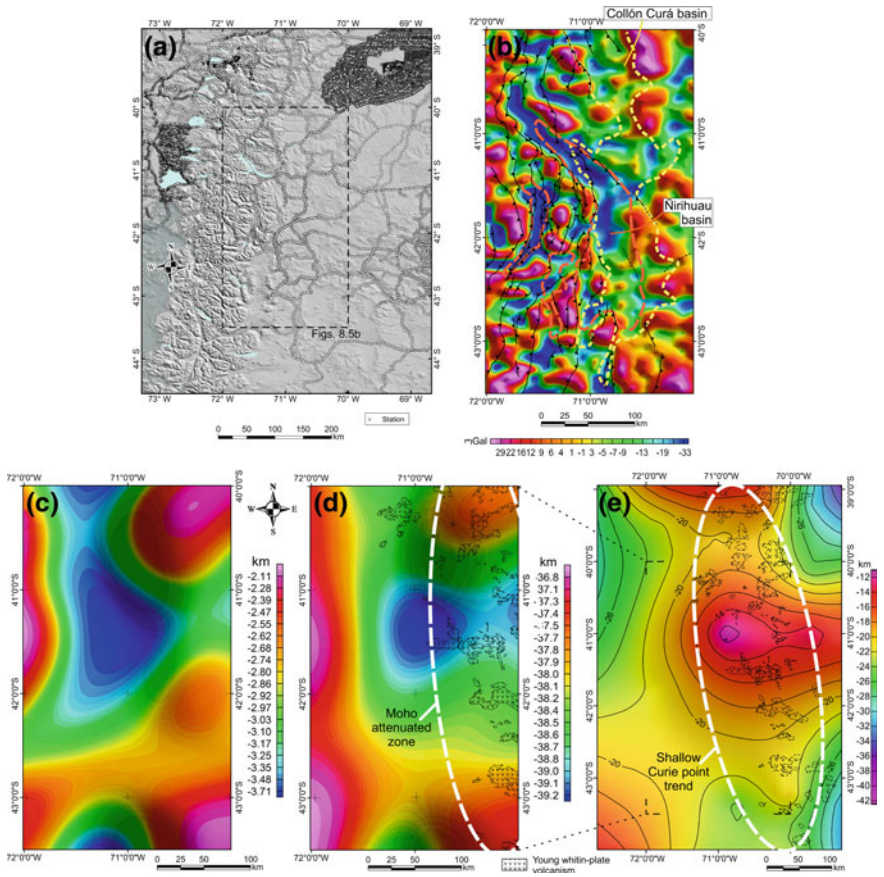


Fig. 5 **a** Gravity dataset used in this study. **b** Resulting gravimetric residuals after discounting an upward continued field up to 40 km from the Bouguer anomalies. Note a strong correlation between the residual anomalies, mapped retroarc structures, and main Cenozoic depocenters. **c** Basement topography obtained from the inversion of gravimetric residuals computed from an idealized crustal density model. **d** Moho geometry obtained from the inversion of the gravimetric residuals using a single 2-layered lithospheric density model. **e** Curie isoterm map obtained from the power-density spectra of magnetic anomalies. Within-plate volcanic units aligned in a NNW trend are superimposed to (**d**) and (**e**), showing a correlation with an attenuated and thermally weakened crustal zone

by the "Instituto Geofísico y Sismológico Volponi (IGSV)". Industry data were provided through agreements with YPF (Argentina). Additional data were taken from Araneda et al. (1999) and Götze et al. (2006). This data compilation resulted in a rather inhomogeneous dataset with large gaps in some parts of the modeled region (Fig. 5a). These gaps are mostly due to difficult access in some areas under study, for this reason, satellite data (GOCE missions) have been used to fill in these gaps across the highest Andes (Álvarez et al. 2012). This database was used to

orlando_a_p@yahoo.com.ar

compute gravimetric residuals and basement topography and Moho geometry inversions (Fig. 5b–d).

Additionally, the Curie isotherm (~580 °C) was computed from satellite and airborne magnetic data in order to infer the crustal thermal state at the retroarc zone (Fig. 5e). Mean depths of the base of the magnetized crust were calculated from the power-density spectra of magnetic data from the World Digital Magnetic Anomaly Map (Maus et al. 2007), by applying the Tanaka et al. (1999) method implemented by Ruiz and Introcaso (2004). The lower boundary is assumed to correspond to the Curie depth point (~580 °C). The total magnetic field long wavelengths were analyzed through 52 square windows, each side covering 1.75°. These are displaced around 0.25° along N–S and E–W directions, covering the retroarc region between 39°–44°S and 73°–69°W.

4 Balanced Cross Sections: Shortening Magnitudes

In this study, we present five published cross sections that have been constructed from the drainage divide to the foreland areas between 40° 15′ and 43°S (Fig. 3; see Fig. 2 for location). These were constructed in order to evaluate and validate the different deformation mechanisms as seen in the field and indirect observations, from seismic lines and borehole data.

The northernmost cross section goes from Paso Puyehue, north of Nahuel Huapi lake, to the upper Río Limay (Fig. 3a). Here, the hinterland in the western sector is characterized by the exposure of Jurassic-Cretaceous strata and Cretaceous to Tertiary granitoids of the Patagonian batholith. These granitoids are locally intruding the Paleozoic basement. The structures through this sector are high-angle reverse faults that produce long-wavelength anticlines cored by basement rocks. This sector ends with an eastern thrust that juxtaposes the Paleozoic-Mesozoic series over Cenozoic sections of the Huitrera Formation north of the El Traful lake (Fig. 2). The eastern sector is characterized by continuous outcrops of Cenozoic series exposed by short-wavelength structures that are related locally to a shallower decollement, of an average depth of 5 km. Thus, two decollements are used to model the measured structures, the mentioned before as an interrupted one between prominent basement blocks, and a continuous one at ~15 km depth for the larger structures. The eastern part of this segment is again formed by long-wavelength structures that are eastwardly bounded by an emergent deformational front associated with a narrow synorogenic accumulation corresponding to the Collón Curá Basin. No Ñirihuau depocenters are developed at these latitudes, or at least no direct evidences are available. The palinspastic restoration of this cross section (Fig. 3a) has yielded a total shortening of 8.9 km that corresponds to 5.7 % of the initial length (156.4 km).

The next balanced cross section is located to the south and goes from the Cerro Bastión to the foreland area across the David syncline (Fig. 3b). In the hinterland zone, a similar style of deformation with high-angle east-verging faulting is

orlando_a_p@yahoo.com.ar

observed as in the previous cross section. This thick-skinned deformation is also associated with tectonic inversion and folding of the Jurassic-Cretaceous successions with occasional backthrusting. To the east, near Mascardi lake pre-Mesozoic basement rocks, partially covered by the Oligocene volcanic rocks of the Ventana Formation, are uplifted as a long-wave pop-up structure. Further to the east, this volcanic cover is widely exposed through a frontal belt forming a long-wavelength antiform controlled internally by the inversion of previous Oligocene normal faults. This antiform is generated by a basement wedge that is inserted into the foredeep of the Ñirihuau Basin decoupling the sedimentary sections and generating the David syncline in the frontal area where the main thrust emerges. The David syncline is cored by the Ñirihuau and Collón Curá formations. Its west flank is associated with tight folds that are developed in the lower section of the Ñirihuau Formation near the contact with the Oligocene volcanic rocks. This tight deformation is interpreted by Giacosa et al. (2005) as a response of a rheological contrast between these lacustrine-pyroclastic sections and the lower volcanic sections of the Ventana Formation. The middle to upper sections of the Ñirihuau Formation are symmetrically folded by the fault bend geometry. The footwall of this emergent front is composed of synorogenic successions that are thinning eastwardly over partially to not be inverted extensional depocenters. The obtained shortening was 18.7 km (15.34 %) with an initial length of 121.9 km. This magnitude corresponds to the highest shortening values achieved along this Andean segment.

The cross section C, located to the south (Fig. 3c), goes from Cerro Horqueta to Ñorquinco area in the foreland. The hinterland zone is characterized by an east-vergent out-of-sequence thrust that uplifted the NPB rocks above Cenozoic sediments in the Bolson valley. The eastern margin of this valley at the El Serrucho range is formed by a series of backthrusts that uplift the Paleozoic igneous-metamorphic basement, cannibalizing the El Bolsón Subbasin successions. To the east, this basement block is uplifted by an east-vergent thrust system. Further east, this basement wedge propagates and deforms the Oligocene volcanic cover as long-wavelength structures. Even further east, these successions are deformed by the insertion of a nonemergent basement wedge. This wedge generates a broad frontal antiform with a backlimb deformed by a series of backthrusts, continuing to the east as an intercutaneous wedge in the basin. The wedge-top area is characterized by folded synorogenic sediments covering the nonemergent wedge and the inverted Oligocene–early Miocene extensional depocenters in the Ñorquinco area (Fig. 4f). Further east, these depocenters are mildly inverted to not inverted, generating mild long-wavelength folding toward the foreland area. From the restoration, a magnitude of 14.6 km (12.25 %) was obtained over an initial length of 119.2 km.

Immediately to the south, the cross section D (Fig. 3d) is located between Cerro Lindo, in the hinterland zone, and the Rio Chico area in the foreland zone. The NPB rocks are uplifted over the Cenozoic succession of the El Bolsón valley by the previous trend of high-angle reverse faults. Previously deformed Jurassic successions lie above these batholitic rocks, as roof-pendant structures (Giacosa et al. 2004a) and are partially affected by a backthrust. Toward the east of El Bolsón

orlando_a_p@yahoo.com.ar

valley and in the Cerro Piltriquitrón, Early Jurassic wedge-like depocenters are inverted and uplifted through backthrusts over the Cenozoic successions of the Ñirihuau Formation as previously stated by Giacosa and Heredia (2004b). Thus, the Cerro Piltriquitrón is characterized by a doubly vergent system that propagates to the east affecting the Oligocene volcanic successions. These volcanic rocks are exhumed again in the El Maitén belt by a series of backthrusts generated in an east-vergent system. This system is exposed as a dismembered belt that continues to the east under the wedge-top area where blind structures are onlaped by synorogenic sediments of the Ñirihuau and Collón Curá formations, inferred from seismic information (Orts et al. 2012). This synorogenic depocenter is bounded to the east by a blind west-verging basement structure which is also onlaped by condensed synorogenic strata. This cross section yielded a shortening of 17 km (13.64 %) over an initial length of 124.6 km.

The southernmost cross section (Fig. 3e) is characterized by long-wavelength basement structures in the hinterland zone deforming Jurassic strata and overlaying Cretaceous and Miocene andesitic rocks and exhuming the NPB. These structures leave a triangular zone that is covered by Miocene synorogenic sediments with growth strata in the Cerro Plataforma area to the north as part of the El Bolsón Subbasin (Orts et al. 2012). The east-vergent structures in the hinterland uplift the Cretaceous volcanics and the North Patagonian batholith units over the Oligocene volcanics of the Ventana Formation in the Precordilleran system. This system is characterized by long-wavelength structures of inverted Oligocene extensional depocenters. To the east, in the Mayoco range, the sedimentary infill of the Ñirihuau-Collón Curá basin is cannibalized in association with an inverted extensional depocenter cored by Paleozoic rocks, defining a broken foreland setting. This southernmost section yielded a total shortening of 12.7 km (8.3 %) over an initial length of 152.9 km.

From the analysis of the aforementioned sections, significant along-strike variations and common patterns along the North Patagonian deformational belt can be inferred. A prevailing deformational mechanism for the retroarc area is the thick-skinned deformation. This can be either related to basement anisotropies associated with tectonic inversion of (i) Early to Middle Jurassic successions and (ii) Oligocene to early Miocene volcano-sedimentary deposits or to (iii) primary faults without previous control. These faults are usually backthrusts and primary east-vergent out-of-sequence thrusts. On the other hand, the tectonic inversion of Mesozoic extensional depocenters determined NNW-contractional trends from Esquel to Paso Puyehue areas, north of Nahuel Huapi lake, through the hinterland zone. These extensional preorogenic depocenters are characterized by half-grabens, with changing polarities, that define alternate vergences after their inversion (Giacosa and Heredia 2004b; Orts et al. 2012).

The Oligocene to early Miocene inverted normal faults are widely spread east of the older ones, along the Precordilleran System and as nonemergent structures in the wedge-top foreland basin. These depocenters are also characterized by half-graben geometries with changing polarities, although they are predominately controlled by west dipping faults determining typical east-vergent deformational

orlando_a_p@yahoo.com.ar

belts. Frontal inverted systems associated with Cenozoic normal faults accommodate systematically higher amounts of shortening in comparison to the older ones in the hinterland zone. Finally, higher shortenings are achieved between the Nahuel Huapi lake area and the El Maitén range at the site of maximum eastward expansion of the emergent orogenic front (Figs. 2 and 3).

5 Synorogenic Character and Associated Tectonic Inversion

The Cenozoic structures in the North Patagonian Cordillera are spatially associated with the thick accumulations and exposures of Neogene sedimentary and volcaniclastic units (Giacosa and Heredia 1999; Paredes et al. 2009; Asensio et al. 2010; Bechis et al. 2014). These deposits are distributed in the narrow subbasin NNE-oriented in the El Bolsón Valley and an open external basin of Ñirihuau-Collón Curá formations, with a synorogenic character.

The western part of the study area (Fig. 2), where the main Andes are developed, exhibits an abrupt relief influenced largely by Plio-Pleistocene glacial erosion (Thomson 2002; Adriasola et al. 2005). Through these deep valleys, the Cerro Plataforma remains as an isolated remnant of early–middle Miocene marine clastic and volcanic rocks, which are equivalents to those deposited in the El Bolsón Subbasin. Particularly, the Cerro Plataforma area (Fig. 2) is formed by a basal section of Late Cretaceous granitoids (Gordon and Ort 1993) that locally intrude volcanic strata of the Divisadero Group. These rocks are unconformably covered by 450 m of early–middle Miocene marine clastic and volcanic rocks (Fig. 4a–c) whose age was initially inferred based on their paleontological content (Lizuaín 1979; Griffin et al. 2002). The uppermost volcanic succession (Fig. 4a) was subsequently dated by Lizuaín (1983) in 15 Ma (K/Ar), indicating a minimum age for the lower sedimentary deposits. The volcanic succession also crops out west of the Plataforma area in the Cerro Premolar, where they are strongly deformed (see Orts et al. 2012). The Miocene marine succession at the Cerro Plataforma consists of 300 m of fossiliferous sandstones, siltstones, and minor conglomerates that form two parasequences in an overall coarsening-upward arrangement. These Neogene strata are preserved in syncline cores. The thickest column preserved in the Cerro Plataforma is at the syncline axis and western flank (Fig. 4a), narrowing toward its eastern flank. Onlap relationships can be observed at both flanks, implying ongoing contraction at the time of sedimentation (Fig. 4b, c). Therefore, this narrowing is interpreted as related to syncline development at the time of sedimentation. Maximum sedimentary thicknesses have been found next to the Cerro Pico Solo fault which is related to an inverted normal fault that uplifts Mesozoic successions to the west (Fig. 4). This is here interpreted as a Neogene thrust front associated with a frontal foredeep that was later cannibalized.

orlando_a_p@yahoo.com.ar

In the Precordilleran region, east of the main Andean domain, an emergent deformational front is developed, together with series of discontinuous uplifted mountain ranges south of 42°S. The wedge-top area is located between this Precordilleran System and the foreland area. Two different areas can be differentiated north and south of the Chubut river, where the synorogenic wedge-top has been differentially cannibalized by the advancing deformation front (Fig. 4): Whereas the wedge-top area is characterized by up to 2500 m of Miocene strata of the Ñirihuau and Collón Curá formations in the northern section (Giacosa et al. 2005), to the south a series of basement uplifts have led to erosion and condensation of the Neogene cover and exposure of the Late Paleozoic rocks.

The Miocene Ñirihuau Formation is exposed east of the El Maitén range and comprises a basal interval of shales, sandstones, and coal deposited in a lacustrine environment. Toward the top of this unit, fluvio-lacustrine and volcaniclastic levels of reworked fluvial deposits and ash fall layers crop out. On top, Gilbert delta lobes have prograded in a lacustrine environment that passes upwardly into a high-energy fluvial setting (Ramos et al. 2011). The upper successions are denominated as the Collón Curá Formation and have been dated by Marshall et al. (1977), Cazau et al. (1989), and Mazzoni and Benvenuto (1990) at 16–10 Ma. These are tuffs, fluvial, and lacustrine deposits locally interfingered with ignimbrites. These two sections show particular internal geometries next to the Precordilleran emergent front (Fig. 4d, e) that are interpreted as progressive angular unconformities. These are found from the middle segments of the Ñirihuau Formation to the lower segments of the Collón Curá Formation (Fig. 4) (Ramos et al. 2011).

These progressive unconformities have also been identified in seismic sections that were recorded across the wedge-top area at the eastern slope of the El Maitén range (Orts et al. 2012) and at Ñorquinco locality (Fig. 4f). In the seismic line AR4A-103 (Fig. 4f), the two mentioned sedimentary packages are identified at depth, constrained by borehole data of the Ñorquinco $x - 1$ well. This seismic line shows the presence of progressive unconformities associated with the limbs of two anticlines. The development of the anticlines is shown in Fig. 4f and in other seismic lines along the basin is linked to tectonic inversion of previous normal faults. These extensional structures are associated with the Ventana Formation and the lower section of Ñirihuau Formation (Fig. 4f). However, in sectors, as in the David syncline, where the contractional structures are concentrated, some primary faults tend to bypass the previous extensional architecture.

6 Regional Structure and Crustal Thermal State Derived from Gravity and Magnetic Data

An analysis of the gravity field in the retroarc area was performed in order to determine crustal geometry at depth. Here, the computed gravity residuals depict a general correspondence with the mapped structures and the Cenozoic basin infills

orlando_a_p@yahoo.com.ar

(Fig. 5b). Positive anomalies up to 33 mGals either correspond to direct exposures of basement rocks or differentially elevated structures that are interpreted as thick-skinned blocks with a thin sedimentary cover. Negative anomalies correspond to sedimentary depocenters, as intermontane basins such as the one between the North Patagonian Cordillera and the Precordillera (El Bolsón Subbasin) and to synorogenic deposits in the frontal foreland area (Ñirihuau and Collón Curá basins) (Fig. 5c).

The basement inversion model shown in Fig. 5c reveals the average basement depth, where long-wavelength features represent the main sedimentary depocenters. The density contrasts used in this inversion model allow the differentiation of the Cenozoic volcanic and sedimentary depocenters from the basement crystalline rocks. In the model, the deepest depocenter reaches ∼3700 m and corresponds to the Ñirihuau Basin where the thickest synorogenic sections have accumulated. This open foreland depocenter narrows and thins northwards (∼41° 30′S) and then deepens again toward the Collón Curá area, never exceeding 2500 m. Even though these values have to be taken as an approximation since they depend on an assumed model, they imply the existence of late Oligocene volcanic sections at depth in order to reach the computed values.

The Moho inversion model, using an idealized lithospheric density model, reveals a complex picture of the crust-mantle boundary, where an attenuated zone is suggested in the retroarc zone (Fig. 5d). This N-oriented zone coincides at surface with the position of Pliocene to Quaternary within-plate volcanic rocks described by Massaferro et al. (2006) (Fig. 5d, e).

As stated, the crust thermal structure can be inferred from magnetic anomalies through the Curie point depth analysis (Tanaka et al. 1999). The resulting Curie isotherm depth map (Fig. 5e) shows an anomalous shallow position elongated in a N- direction, through the retroarc area (Fig. 5e). This anomaly is fairly coincident with the inferred Moho attenuation zone calculated from gravity data depicted in Fig. 6b. Therefore, a thermal anomaly can be inferred for the orogenic front-western foreland areas in coincidence with an attenuated Moho and the area of emplacement of younger than 5 Ma within-plate volcanics (Massaferro et al. 2006; Pécskay et al. 2007).

7 Tectonomagmatic Evolution

The structural crustal-scale characterization of the North Patagonian fold and thrust belt derived from the regional geological mapping constrained by geophysical data allows to address some key elements. This belt presents a series of structures, mostly high-angle reverse faults and related folds, describing a convex geometry with a symmetry axis around 41° 30′S. These curved features representing the fold and thrust belt reach their maximum eastward progression near 41° 30′S (Figs. 2, 5b and 6). This area from the hinterland to the Precordillera shows the deepest structural levels corresponding to wide outcrops of Neopaleozoic metamorphic

orlando_a_p@yahoo.com.ar

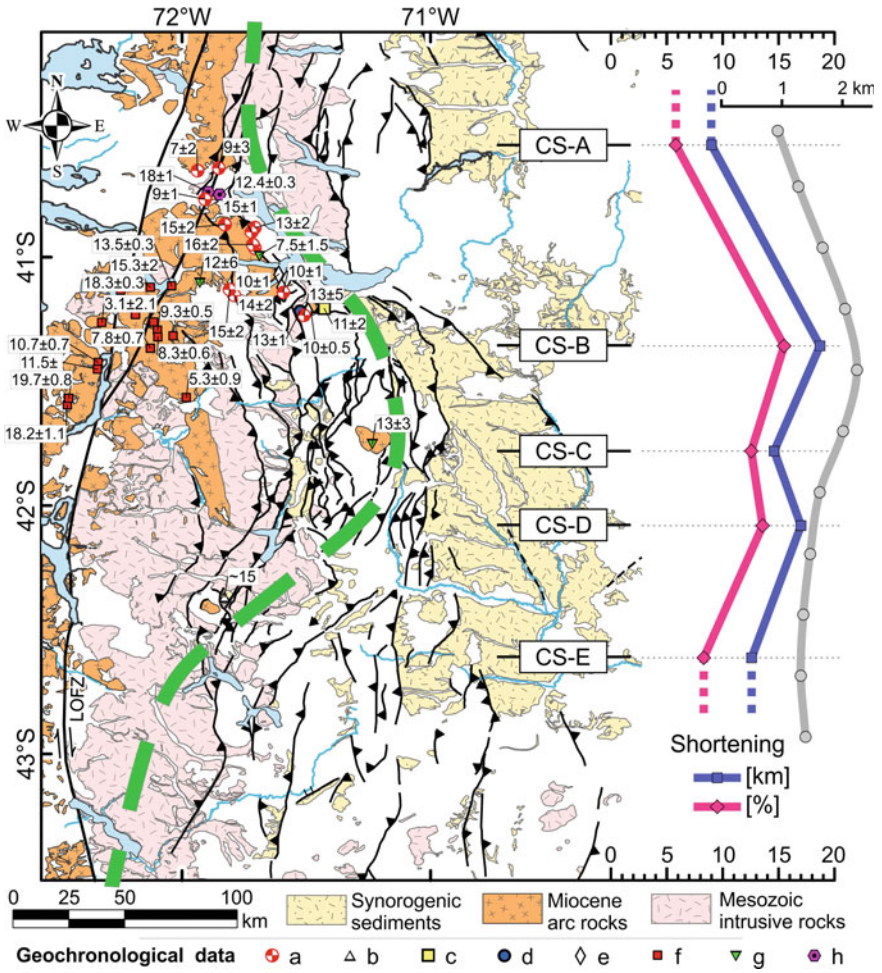


Fig. 6 Sketch map showing available ages of Miocene arc rocks and distribution of coeval synorogenic depocenters over the foreland area. Shortening magnitudes computed from the cross sections displayed in Fig. 3 are depicted on the *right side*, as well as computed Miocene sedimentary thicknesses obtained from the basement inversion gravity model along a 71°W longitude transect (*dotted grey line*). The *thick dashed green line* depicts the maximum foreland expansion of the Miocene arc rocks. Geochronological data are taken from: *a* González Diaz (1982); *b* Lizuaín (1983); *c* Rapela et al. (1983); *d* González Diaz and Lizuain (1984); *e* Rapela et al. (1987); *f* Adriasola et al. (2005); *g* Linares (2007); *h* Aragón et al. (2011)

rocks and plutons of the Subcordilleran batholith denoting a higher exhumation gradient than in areas located immediately north or south.

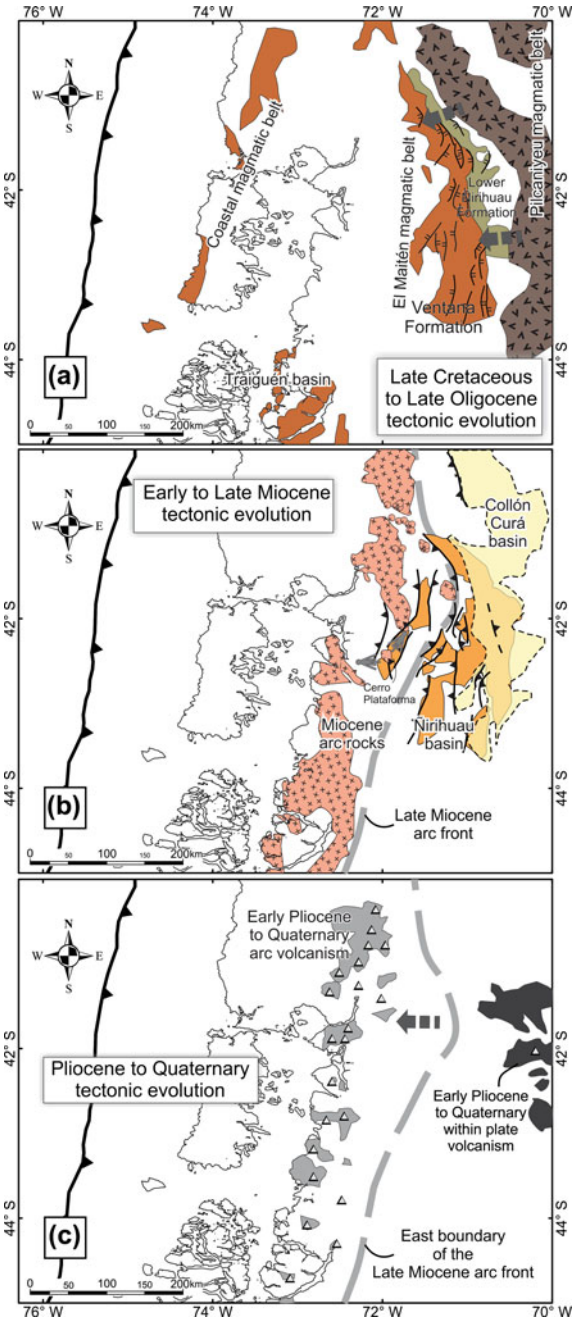
The structures along this internal belt are characterized by high-angle faults that can be related to tectonic inversion of previous extensional structures that had accommodated important volcano-sedimentary packages. Here, the tectonic

orlando_a_p@yahoo.com.ar

inversion is one of the principal mechanisms acting in the North Patagonian Andes. The first domain of extensional structures comprises the series of Early to Middle Jurassic peri-Gondwanic extensional basins. These are mostly constituted by half-grabens of changing polarities that were interpreted by Giacosa and Heredia (2004b) as developed in an intra-arc environment. These successions are thrust over Tertiary sediments, especially along the El Bolsón Valley (Giacosa and Heredia 2004b; Tobal et al. 2012; Bechis et al. 2014) and its south-west continuation in the Cerro Plataforma region (Orts et al. 2012). The structural and stratigraphic relationships in these units not only show a late Cenozoic contractional stage, but also a late Early Cretaceous one. A folded unconformity between the upper Lower Cretaceous volcanic rocks of Divisadero Group and the underlying Piltriquitrón Formation in the Cerro Plataforma area reveal an early contractional episode at these latitudes (Orts et al. 2012). This relation coincides with other observations of this contractional phase in neighboring areas to the south where it becomes more prominent (Echaurren et al. 2014; Gianni et al. 2015, see Chap. 8 for further details). After this contractional stage, a long-lived synextensional volcanic period affected the North Patagonian region and in particular the retroarc zone developing two clear magmatic belts differing in age, location, and composition (Rapela et al. 1988) (Fig. 7a). The Paleocene to Eocene Pilcaniyeu volcanic belt located to the east was followed by the Oligocene El Maitén volcanic belt in a more westward position (Fig. 7a). The latter belt presents broad wedge-like geometries visible in seismic data (Fig. 4f), as initially proposed by Mancini and Serna (1989), and surface observations (Orts et al. 2012). In this context, this spaciotemporal magmatic pattern could be interpreted as a magmatic westward migration as a result of a reconfiguration of the subduction system (Aragón et al. 2013). The structures found in this magmatic unit constitute the second domain of extensional structures that were affected by tectonic inversion in the development of the fold and thrust belt.

The shape of this fold and thrust belt and its differential exhumation gradient, revealed by the exposures of older units, correlate with the Neogene accumulation of synorogenic sedimentation in a open external foreland basin (Fig. 2, 6 and 7b). This foreland basin is the result of the advance of the orogenic front in last mountain building stage. This eastward progression began around 18 Ma at the hinterland zone, based on U/Pb zircon dating in the synorogenic strata at the Cerro Plataforma area, which is younger than in previous proposals (Giacosa and Heredia 2004b; Asensio et al. 2010, among others). This coincides with other recent proposals as Bilmes et al. (2013) or Bechis et al. (2014) that propose an even younger contractional deformation for equivalent units in the El Bolsón Subbasin. Provenance studies in Cerro Plataforma locality by Orts et al. (2012) demonstrate that the main Andes began their construction at the time of deposition of those successions. As a whole, the main pulse of deformation took place around 15 Ma and progressed from the hinterland zone to the Precordilleran system and the broken foreland area (Bilmes et al. 2013; Bechis et al. 2014). This process is clearly shown in the progressive unconformities and related growth strata described by Ramos et al. (2011) (Fig. 4d, e), in the eastern flank of the El Maitén belt, and further east by in equivalent rocks of the Gastre locality described by Bilmes et al. (2013). Also, this

orlando_a_p@yahoo.com.ar



orlando_a_p@yahoo.com.ar

◄ **Fig. 7** Tectonic sketches of the North Patagonian Andes for the last 60 Ma. **a** Westward retraction of the Paleogene magmatic belts after Rapela et al. (1988). By Oligocene times, arc rocks were re-established from the orogenic front area to the Coastal zone (El Maitén magmatic belt; Rapela et al. 1988; and the Coastal magmatic belt; Muñoz et al. 2000). These last volcanic rocks are associated with synextensional features. The synextensional character of the basal segments of the upperlying clastic Ñirihuau Formation has been described from seismic information by Mancini and Serna (1989), indicating that this period of arc retraction coincides with crustal stretching. **b** Early to late Miocene magmatic-tectonic evolution. Note an arc expansion which reaches its maximum expression at 41° 30′S respect to late Oligocene eastern rocks (González Díaz 1982; Heredia et al. 2005; among others) which coexists with contractional deformation dated between 18.3 and 10 Ma. Note also widespread development of synorogenic depocenters that are redefined in the foreland area. **c** Early Pliocene to Quaternary magmatic and tectonic setting. Within-plate volcanism (Massaferro et al. 2006; Pécskay et al. 2007) is developed at the foreland area coincident latitudinally with the site of former late Miocene arc expansion. Present arc is re-established in the hinterland zone, west of the late Miocene arc

progression can be clearly visualized in the relative eastward displacement between the Ñirihuau and Collón Curá basins (Fig. 7b) Additionally, evidence of a contractional context for this sedimentary infill is found in seismic data (Fig. 4f) as interpreted by Mancini and Serna (1989), Giacosa et al. (2005), and Orts et al. (2012).

In this context, middle to late Miocene granitoids form a plutonic belt (Fig. 6), located to the east of the present volcanic arc and the Coastal magmatic belt, considered the late Oligocene arc front, described by Muñoz et al. (2000) (Figs. 7b, c). In this belt, isolated plutons, with ages ranging from 19.7 to 7 Ma, are locally exposed in the eastern slope of the Andes, showing a maximum eastward expansion at 41° 30′S (Fig. 6, and references there in). These calc-alkaline rocks were interpreted as arc-related products similar to Quaternary arc rocks, based in geochemical characteristics (Pankhurst et al. 1999; Hervé et al. 2000). The nature of these eastern bodies implies an anomalous eastern expansion of the arc when compared to the present one (Fig. 7b, c). The scheme of Fig. 6 shows that satellite magmatic bodies were spread throughout the eastern Andean side, mainly south of the Nahuel Huapi lake, reaching the Precordillera. Ages for these eastern magmatic bodies go predominantly from 15 to 11 Ma. The particular geometry of this Miocene calc-alkaline eastern magmatic belt is interpreted as caused by the migration of the volcanic arc in Miocene times between 41° and 42° 30′S (Fig. 6). This migration of the arc front coincides temporally and spatially with the deepest and broadest synorogenic foreland depocenters and higher computed shortenings (Fig. 6).

In the last 5 Ma, the arc retracted to its present position along the axial zone of the Andes (Lara et al. 2001), leaving the former late Miocene arc to the east (Fig. 7c). Here, the LOFZ played an important role focusing magmatism and deformation in the Andean axis, with coeval retreat of the deformation front (Lavenu and Cembrano 1999). Additionally, the climatic cooling and consequent onset of glaciation played a fundamental role in sites of active deformation (Thomson et al. 2010). In the foreland area, less than 5 Ma within-plate volcanic rocks developed between 41 and 43°S (Massaferro et al. 2006; Pécskay et al. 2007),

orlando_a_p@yahoo.com.ar

defining a NNW-trending magmatic belt (Figs. 5d, e, 7c). These isolated basaltic effusive centers coincide with a Moho attenuated zone and a thermal anomaly computed from gravimetric and magnetometric data, respectively (Fig. 5d, e).

This framework, in which arc expansion coincides with a stage of mountain building and synorogenic basin formation, was described as related to shallow subduction in neighboring regions to the north and south along the Andes (James and Sacks 1999; Kay et al. 2006; Kay and Coira 2009; Espinoza et al. 2010; Spagnuolo et al. 2012; Ramírez de Arellano et al. 2012).

In these models, arc migration modifies the thermal state of the retroarc crust enabling the shallowing of brittle-ductile transitions developing broad deformation zones. Steepening of these shallow subduction configurations is associated with extension and within-plate magmatism as asthenospheric wedge broadens (James and Sacks 1999; Kay and Coira 2009). Thus, this situation could be applied to the North Patagonian Andes where the Neogene synorogenic successions seem to be the direct product of these processes as the arc and fold and thrust belt expanded. Finally, in the last 5 Ma, the foreland region registered the injection of within-plate basalts after the retraction of the magmatic arc to its present position.

8 Conclusions

The analysis of the retroarc geology at surface and the interpretation of seismic reflection profiles available in the foreland region show the synorogenic character of the retroarc basin infill dated at 18–10 Ma. It also showed the existence of previous synextensional depocenters (33–21 Ma) later affected by tectonic inversion. In particular, the construction of structural cross sections in the retroarc area shows a shortening gradient that has the highest values of 18.7 km (15.34 %) at 41° 30′S, corresponding to the point of maximum lateral development of the fold and thrust belt. This value is higher than in neighboring areas to the north and south, where the orogenic front retracts relatively to the Andean axis.

Available geochronological data in calc-alkaline granitoids emplaced over the Argentinean Andean slope show ages between 20 and 11 Ma that could indicate an arc migration toward the foreland area. This arc migration correlates in time and space with higher shortenings achieved in the retroarc zone, as well as with maximum foreland basin depth and amplitude. Thus, the Miocene contractional stage has led to a broken foreland with foreland basin formation contemporaneous to eastward arc expansion.

The subducted oceanic slab (Nazca plate) after 26 Ma, when heading toward the North Patagonian Massif at these latitudes, could have achieved a mild shallow configuration. The posterior steepening of the subducted slab could be associated with younger than 5 Ma within-plate volcanics in the retroarc zone at the time of arc-trenchward retraction and thinning of the Moho. These could be the result of the extensional relaxation of the Neogene fold and thrust belt after an orogenic cycle that could be enhanced by a shallow subduction in the area.

orlando_a_p@yahoo.com.ar

References

Adriasola AC, Thomson SN, Brix MR, Hervé F, Stöckhert B (2005) Postmagmatic cooling and late Cenozoic denudation of the North Patagonian Batholith in the Los Lagos region of Chile, 41°–42°15′S. Int J Earth Sci 95:504–528. doi:10.1007/s00531-005-0027-9

Álvarez O, Gimenez M, Braitenberg C, Folguera A (2012) GOCE satellite derived gravity and gravity gradient corrected for topographic effect in the South Central Andes region. Geophys J Int 190:941–959. doi:10.1111/j.1365-246X.2012.05556.x

Aragón E, Castro A, Díaz-Alvarado J, Liu D-Y (2011) The North Patagonian batholith at Paso Puyehue (Argentina-Chile). SHRIMP ages and compositional features. J South Am Earth Sci 32:547–554. doi:10.1016/j.jsames.2011.02.005

Aragón E, Pinotti L, D'eramo F, Castro A, Rabbia O, Coniglio J, Demartis M, Hernando I, Cavarozzi CE, Aguilera YE (2013) The Farallon-Aluk ridge collision with South America: Implications for the geochemical changes of slab window magmas from fore- to back-arc. Geosci Front 4:377–388. doi:10.1016/j.gsf.2012.12.004

Araneda M, Avendaño M, Götze H-J, Schmidt S, Muñoz J, Schmitz M (1999) South central Andes gravity, new data base. In: 6th international Congress of the Brazilian Geophysical Society. Braz Geophys Soc (Rio de Janeiro), p 3

Asensio M, Cornou M, Malumián N, Martínez MA, Quattrocchio ME (2010) Formación Río Foyel, Oligoceno de la cuenca de Ñirihuau: la transgresión pacífica en la Cordillera Norpatagónica. Rev Asoc Geol Argentina 66:399–405

Bechis F, Cristallini E (2006) Inflexiones en estructuras del sector norte de la faja plegada y corrida de Ñirihuau, provincia de Río Negro. Rev Asoc Geol Argentina, Publicación Especial 6:18–25

Bechis F, Encinas A, Concheyro A, Litvak VD, Aguirre-Urreta B, Ramos VA (2014) New age constraints for the Cenozoic marine transgressions of northwestern Patagonia, Argentina (41°–43°S): paleogeographic and tectonic implications. J South Am Earth Sci 52:72–93

Bilmes A, D'Elia L, Franzese JR, Veiga GD, Hernández M (2013) Miocene block uplift and basin formation in the Patagonian foreland: The Gastre Basin, Argentina. Tectonophysics 601:98–111

Castro A, Moreno-Ventas I, Fernández C, Vujovich G, Gallastegui G, Heredia N, Martino RD, Becchio R, Corretgé LG, Díaz-Alvarado J, Such P, García-Arias M, Liu D-Y (2011) Petrology and SHRIMP U-Pb zircon geochronology of Cordilleran granitoids of the Bariloche area, Argentina. J South Am Earth Sci 32:508–530

Cazau L, Mancini D, Cangini J, Spalletti L (1989) Cuenca de Ñirihuau. In: Chebli G, Sapalletti L (eds) Cuencas Sedimentarias Argentinas. Serie Correlación Geológica 6. Tucumán, Argentina, pp 299–318

Cembrano J, Hervé F, Lavenu A (1996) The Liquiñe Ofqui fault zone: a long-lived intra-arc fault system in southern Chile. Tectonophysics 259:55–66

Coira BL, Nullo FE, Proserpio C, Ramos VA (1975) Tectónica de basamento de la región occidental del Macizo Nordpatagónico (Prov. de Río Negro y Chubut) Republica Argentina. Rev Asoc Geol Argentina 30:361–383

Dalla Salda L, Cingolani C, Varela R (1991) El basamento pre-andino ígneo metamórfico de San Martín de los Andes, Neuquén. Rev Asoc Geol Argentina 46:223–234

Dalla Salda LH, Varela R, Cingolani C, Aragón E (1994) The Rio Chico Paleozoic crystalline complex and the evolution of Northern Patagonia. J South Am Earth Sci 7:377–386

Diraison M, Cobbold P, Rossello EA, Amos AJ (1998) Neogene dextral transpression due to oblique convergence across the Andes of northwestern Patagonia, Argentina. J South Am Earth Sci 11:519–532

Echaurren A, Henkel M, Rusconi F, Tobal J, Sagripanti L, Ramos M, Orts D, Folguera A. (2014) Geología y fases de deformación en la Cordillera Patagónica, norte de Chubut (Parque Nacional Los Alerces). XIX Congreso Geológico Argentino (Córdoba) Actas S22:19

Elgueta S, Mpodozis C (2012) Evolución tectono-sedimentaria de la cuenca del río Cruces (Valdivia) durante el Neógeno. XIII Congreso Geológico Chile (Antofagasta), Actas 649–651

orlando_a_p@yahoo.com.ar

Encinas A, Finger KL, Buatois LA, Peterson DE (2012) Major forearc subsidence and deep-marine Miocene sedimentation in the present Coastal Cordillera and Longitudinal Depression of south-central Chile (38° 30′S–41° 45′S). Geol Soc Am Bull 124:1262–1277

Espinoza F, Morata D, Polve M, Lagabrielle Y, Maury R, De la Rupelle A, Guivel C, Cotten J, Bellon H, Suarez M (2010) Volcanismo calcoalcalino durante el Mioceno Medio en Patogonia Central (47°S): petrogenesis e implicaciones en la dinamica de placas. Andean Geol 37:300–328

Feruglio E (1947) Descripción Geológica de la Hoja 40b, San Carlos de Bariloche, Río Negro, Carta Geológico-Económica de la República Argentina, scale 1:200,000. Dirección Nacional de Geología y Minería, Buenos Aires, Argentina

Feruglio E (1949) Descripción Geológica de la Patagonia. Dirección General de Yacimientos Petrolíferos Fiscales, Buenos Aires, p 334

Figari EG (2005) Evolución tectónica de la cuenca de Cañadón Asfalto (zona del valle medio del río Chubut). Unpublished PhD thesis, Universidad de Buenos Aires, p 177

Flynn JJ, Charrier R, Croft DA, Gans PB, Herriott TM, Wertheim JA, Wyss AR (2008) Chronologic implications of new Miocene mammals from the Cura-Mallín and Trapa Trapa formations, Laguna del Laja area, south central Chile. J South Am Earth Sci 26:412–423

Giacosa R, Heredia N (1999) La cuenca de antepais terciaria asociada a la faja plegada y corrida de los Andes Patagónicos entre los 41° y 42° S, SO de Argentina. Acta Geol Hispánica 32:103–111

García Morabito E, Götze H-J, Ramos VA (2011) Tertiary tectonics of the Patagonian Andes retro-arc area between 38°15′ and 40°S latitude. Tectonophysics 499:1–21. doi: 10.1016/j.tecto.2010.10.020

García-Sansegundo J, Farias P, Gallastegui G, Giacosa RE, Heredia N (2009) Structure and metamorphism of the Gondwanan basement in the Bariloche region (North Patagonian Argentine Andes). Int J Earth Sci 98:1599–1608

Giacosa RE, Heredia N (2004a) Structure of the North Patagonian thick-skinned fold-and-thrust belt, southern central Andes, Argentina (41°–42°S). J South Am Earth Sci 18:61–72

Giacosa R, Heredia N (2004b) Estructura de los Andes Nordpatagónicos en los cordones Piltriquitrón y Serrucho y en el valle de El Bolsón (41°30′–42°S), Río Negro. Rev Asoc Geol Argentina 59:91–102

Giacosa RE, Heredia N, Césari O, Zubia M (2001) Hoja Geológica 4172-IV, San Carlos de Bariloche (provincias de Río Negro y Neuquén). Servicio Geológico Minero Argentino, Boletín 279:1–67

Giacosa RE, Afonso JC, Heredia CN, Paredes J (2005) Tertiary tectonics of the sub-Andean region of the North Patagonian Andes, southern central Andes of Argentina (41–42° 30′S). J South Am Earth Sci 20:157–170

Giacosa R, Zubia M, Sánchez M, Allard J (2010) Meso-Cenozoic tectonics of the southern Patagonian foreland: Structural evolution and implications for Au–Ag veins in the eastern Deseado Region (Santa Cruz, Argentina). J South Am Earth Sci 30:134–150

Gianni G, Navarrete C, Orts D, Tobal J, Folguera A, Giménez M (2015) Patagonian broken foreland and related synorogenic rifting: the origin of the Chubut Group Basin. Tectonophysics 649:81–99

González E (1989) Hydrocarbon resources in the coastal zone of Chile. In: Ericksen GE, Canas Pinochet MT, Reinemund JA (eds) Geology of the Andes and its relation to hydrocarbon and mineral Resources, vol 11. Circum-Pacific Council for Energy and Mineral Resources Earth Science Series, Houston, Texas, pp 383–404

González Bonorino F, González Bonorino G (1978) Geología de la región de San Carlos de Bariloche. Rev Asoc Geol Argentina 33:175–210

González Díaz EF (1982) Chronological zonation of granitic plutonism in the northern Patagonian Andes of Argentina: the migration of intrusive cycles. Earth Sci Rev 18:365–393

González Diaz E, Lizuain A (1984) El Complejo volcano-clástico y plutónico del sector cordillerano. Geología y Recursos Naturales de la Provincia de Río Negro. Buenos Aires, pp 119–129

orlando_a_p@yahoo.com.ar

Gordon A, Ort MH (1993) Edad y correlación del plutonismo subcordillerano en la provincias de Río Negro y Chubut (41°–42°30′ L.S.). In: Ramos VA (ed). Geología y Recursos Naturales de la Provincia de Mendoza. Relatorio del XII Congreso Geológico Argentino, pp 120–127

Götze H, Alten M, Burger H, Goni P, Melnick D (2006) Data management of the SFB 267 for the Andes—from ink and paper to digital databases. In: Oncken O, Chong G, Franz G, Giese P, Götze H-J, Ramos VA, Strecker MR, Wigger P (eds) The Andes. Springer, Berlin, pp 539–556

Griffin M, Pérez LM, Muravchik M (2002) Moluscos terciarios del Cerro Plataforma, en el noroeste de Chubut. IX Congreso Argentino de Paleontología y Bioestratigrafía (Córdoba), p 101

Haller M, Pécskay Z, Németh K, Gméling K, Massaferro GI, Meister CM, Nullo FE (2009) Preliminary K-Ar geochronology of Neogene back arc volcanism in Northern Patagonia, Argentina. In: III International Maar Conference. IAVCEI (Malargüe), pp 40–41

Heredia N, Giacosa RE, Gallastegui G, Farias P, García-Sansegundo J (2005) Structural evolution of the North Patagonian Andes (41°–42°S), Argentina. In: VI international symposium on Andean geodynamics (Barcelona), Spain. Extended Abstracts, pp 364–367

Hervé F, Demant A, Ramos VA, Pankhurst RJ, Suárez M (2000) The Southern Andes. In: Cordani UG, Milani, EJ, Thomas Filho A, Campos AD (eds) Tectonic evolution of South America. XXXI International Geological Congress (Rio de Janeiro), pp 605–634

Hervé F, Calderón M, Fanning CM, Pankhurst RJ, Godoy E (2013) Provenance variations in the Late Paleozoic accretionary complex of central Chile as indicated by detrital zircons. Gondwana Res 23:1122–1135

James D, Sacks IE (1999) Cenozoic formation of the Central Andes: a geophysical perspective. In: Skinner BJ (ed) Geology and ore deposits of the Central Andes. Soc Econ Geol, pp 1–26

Kay S, Burns W, Copeland P, Mancilla O (2006) Upper cretaceous to Holocene magmatism and evidence for transient Miocene shallowing of the Andean subduction zone under the northern Neuquén Basin. In: Kay SM, Ramos VA (eds) Evolution of an Andean Margin: A Tectonic and Magmatic View from the Andes to the Neuquén Basin (35°–39°S Lat). Geol Soc Am, Special Paper 407: 19–60

Kay SM, Coira BL (2009) Shallowing and steepening subduction zones, continental lithospheric loss, magmatism, and crustal flow under the Central Andean Altiplano-Puna Plateau. In: Kay SM, Ramos VA, Dickinson WR (eds) Backbone of the Americas: Shallow Subduction, Plateau Uplift, and Ridge and Terrane Collision. Geol Soc Am Memoirs, vol 204, pp 229–259

Lara L, Rodriguez C, Moreno H, Pérez de Arce C (2001) Geocronología K-Ar y geoquímica del volcanismo plioceno superior-pleistoceno de los Andes del sur (39–42°S). Rev Geol Chile 28:67–90

Lavenu A, Cembrano J (1999) Compressional- and transpressional-stress pattern for Pliocene and Quaternary brittle deformation in fore arc and intra-arc zones (Andes of Central and Southern Chile). J Struct Geol 21:1669–1691

Linares E (2007) Catálogo de edades radimétricas de la Republica Argentina, Años 1957-2005. Asoc Geol Argentina, Buenos Aires

Lizuaín A (1979) La edad de las sedimentitas del cerro Plataforma, provincia del Chubut. Rev Asoc Geol Argentina 34(1):69–72

Lizuaín A (1983) Geología de la Cordillera Patagónica entre las localidades de Lago Puelo y Leleque. Unpublished PhD thesis, Universidad de Buenos Aires, p 128

Lucassen F, Trumbull R, Franz G, Creixell C, Vásquez P, Romer RL, Figueroa O (2004) Distinguishing crustal recycling and juvenile additions at active continental margins: the Paleozoic to recent compositional evolution of the Chilean Pacific margin (36–41°S). J South Am Earth Sci 17:103–119

Mancini D, Serna M (1989) Evaluación petrolera de la Cuenca de Ñirihuau, Sudoeste de Argentina. In: I Congreso Nacional de Exploración de Hidrocarburos (Argentina), vol 2, pp 739–762

Marshall L, Salinas P (1990) Stratigraphy of the Río Frías Formation (Miocene), along the Alto Río Cisnes, Aisén, Chile. Rev Geol Chile 17:57–87

orlando_a_p@yahoo.com.ar

Marshall LG, Pascual R, Curtis GH, Drake RE (1977) South American geochronology: radiometric time scale for middle to late tertiary mammal-bearing horizons in patagonia. Science 195:1325–1328. doi:10.1126/science.195.4284.1325

Massaferro GI, Haller MJ, D'Orazio M, Alric VI (2006) Sub-recent volcanism in Northern Patagonia: A tectonomagmatic approach. J Volcanol Geotherm Res 155:227–243

Maus S, Sazonova T, Hemant K, Fairhead JD, Ravat D (2007) National Geophysical Data Center candidate for the World Digital Magnetic Anomaly Map. Geochem Geophys Geosyst 8: Q06017. doi:10.1029/2007GC001643

Mazzoni MM, Benvenuto A (1990) Radiometric ages of Tertiary ignimbrites and the Collón Curá Formation northwestern Patagonia. XI Congreso Geológico Argentino (San Juan), pp 87–90

Mazzoni M, Kawashita K, Harrison S, Aragón E (1991) Edades radimétricas eocenas. Borde occidental del Macizo Norpatagónico. Rev Asoc Geol Argentina 46:150–158

Mena M, Ré GH, Haller MJ, Singer SE, Vilas JF (2006) Paleomagnetism of the late Cenozoic basalts from northern Patagonia. Earth Planets Sp 58:1273–1281

Muñoz J, Troncoso R, Duhart P, Crignola P, Farmer L, Stern CR (2000) The relation of the mid-Tertiary coastal magmatic belt in south-central Chile to the late Oligocene increase in plate convergence rate. Rev Geol Chile 27:177–203

Orts DL, Folguera A, Encinas A, Ramos M, Tobal J, Ramos VA (2012) Tectonic development of the North Patagonian Andes and their related Miocene foreland basin (41°30′–43°S). Tectonics 31: TC3012. doi:10.1029/2011TC003084

Orts DL, Folguera A, Gimenez M, Ruiz F, Rojas Vera E, Lince Klinger F (2015) Cenozoic building and deformational processes in the North Patagonian Andes. J Geodyn 86:26–41

Pankhurst RJ, Weaver SD, Hervé F, Larrondo P (1999) Mesozoic-Cenozoic evolution of the North Patagonian Batholith in Aysen, southern Chile. J Geol Soc London 156:673–694

Pankhurst RJ, Rapela CW, Fanning CM, Márquez M (2006) Gondwanide continental collision and the origin of Patagonia. Earth Sci Rev 76:235–257

Paredes JM, Giacosa RE, Heredia N (2009) Sedimentary evolution of Neogene continental deposits (Ñirihuau Formation) along the Ñirihuau River, North Patagonian Andes of Argentina. J South Am Earth Sci 28:74–88

Pécskay Z, Haller MJ, Németh K (2007) Preliminary K/Ar geochronology of the Crater Basalt volcanic field (CBVF), northern Patagonia. Rev Asoc Geol Argentina 62:25–29

Peroni GO, Hegedus AG, Cerdan J, Legarreta L, Uliana MA, Laffite G (1995) Hydrocarbon accumulation in an inverted segment of the Andean Foreland: San Bernardo Belt, Central Patagonia. In: Tankard AJ, Suárez R, Welsink HJ (eds) Petroleum basins of South America, Am Assoc Petrol Geol Memoir, vol 62. pp 403–419

Radic JP, Alvarez P, Rojas L, Czollak C, Parada R, Ortiz V (2009) La cuenca de Valdivia como parte del sistema de antearco de la plataforma continental de Chile Central entre los 36° y los 40°S. XII Congreso Geológico Chileno (Santiago), S10-032

Ramírez de Arellano C, Putlitz B, Müntener O, Ovtcharova M (2012) High precision U/Pb zircon dating of the Chaltén Plutonic Complex (Cerro Fitz Roy, Patagonia) and its relationship to arc migration in the southernmost Andes. Tectonics 31: TC4009. doi:10.1029/2011TC003048

Ramos VA (1981). Descripción geológica de la hoja 47ab, Lago Fontana: provincia del Chubut. Buenos Aires

Ramos VA, Cortés JM (1984) Estructura e interpretación tectónica. In: Ramos VA (ed) Geología y Recursos Naturales De La Provincia De Río Negro. Asociación Geológica Argentina, Buenos Aires, pp 317–346

Ramos M, Orts D, Calatayud F, Pazos PJ, Folguera A, Ramos VA (2011) Estructura, Estratigrafía y evolución tectónica de la cuenca de Ñirihuau en las nacientes del río Cushamen, Chubut. Rev Asoc Geol Argentina 68:210–224

Rapela CW, Spalletti LA, Merodio JC (1983) Evolución magmática y geotectónica de la Serie Andesítica Andina (Paleoceno-Eoceno) en la Cordillera Norpatagónica. Rev Asoc Geol Argentina 38:469–484

Rapela C, Kay S (1988) Late Paleozoic to Recent magmatic evolution of northern Patagonia. Episodes 11:175–182

orlando_a_p@yahoo.com.ar

Rapela CW, Munizaga F, Dalla Salda LH, Hervé F, Parada M, Cingolani CA (1987) Nuevas edades potasio-argón de los granitoides del sector nororiental de los Andes Patagónicos. X Congreso Geológico Argentino (Tucumán), pp 18–20

Rapela C, Spalletti L, Merodio JC, Aragón E (1988) Temporal evolution and spatial variation of early tertiary volcanism in the Patagonian Andes (40°S–42°30′S). J South Am Earth Sci 1:75–88

Rojas Vera EA, Folguera A, Valcarce GZ, Giménez M, Ruiz F, Martínez P, Bottesi G, Ramos VA (2010) Neogene to quaternary extensional reactivation of a fold and thrust belt: the Agrio belt in the Southern Central Andes and its relation to the Loncopué trough (38°–39°S). Tectonophysics 492:279–294

Ruiz F, Introcaso A (2004) Curie point depths beneath Precordillera Cuyana and Sierras Pampeanas obtained from spectral analysis of magnetic anomalies. Gondwana Res 7:1133–1142

Skármeta J, Charrier R (1976) Geología del sector fronterizo de Aysén entre los 45° y 46° de latitud sur, Chile. IV Congreso Geológico Argentino (Bahía Blanca), pp 267–286

Spagnuolo MG, Litvak VD, Folguera A, Bottesi G, Ramos VA (2012) Neogene magmatic expansion and mountain building processes in the southern Central Andes, 36–37°S, Argentina. J Geodyn 53:81–94

Stern C (2004) Active Andean volcanism: its geologic and tectonic setting. Rev Geol Chile 31:161–206

Suárez M, De La Cruz R (2001) Jurassic to Miocene K-Ar dates from eastern central Patagonian Cordillera plutons, Chile (45°–48°S). Geol Mag 138:53–66

Suárez M, De La Cruz R, Bell CM (1996). Estratigrafía de la región de Coyhaique (Latitud 45o-46oS), Cordillera Patagónica, Chile. XIII Congreso Geológico Argentino and III Congreso de Exploración de Hidrocarburos, pp 575–590

Tanaka A, Okubo Y, Matsubayashi O (1999) Curie point depth based on spectrum analysis of the magnetic anomaly data in East and Southeast Asia. Tectonophysics 306:461–470. doi:10.1016/S0040-1951(99)00072-4

Thomson S (2002) Late Cenozoic geomorphic and tectonic evolution of the Patagonian Andes between latitudes 42°S and 46°S: an appraisal based on fission-track results from the transpressional intra-arc Liquiñe-Ofqui fault zone. Geol Soc Am Bull 114:1159–1173

Thomson SN, Hervé F (2002) New time constraints for the age of metamorphism at the ancestral Pacific Gondwana margin of southern Chile (42–52°S). Rev Geol Chile 29:1–16

Thomson S, Hervé F, Stöckhert B (2001) Mesozoic-Cenozoic denudation history of the Patagonian Andes (southern Chile) and its correlation to different subduction processes. Tectonics 20:693–711

Thomson SN, Brandon MT, Tomkin JH, Reiners PW, Vásquez C, Wilson NJ (2010) Glaciation as a destructive and constructive control on mountain building. Nature 467:313–317

Tobal JE, Rojas Vera E, Folguera A, Ramos VA (2012) Deformación andina en el cordón del Hielo Azul al oeste de El Bolsón. Implicancias en la evolución tectónica de la Cordillera Norpatagónica en Río Negro, Argentina. Andean Geol 39:442–463

von Gosen W (2009) Stages of Late Palaeozoic deformation and intrusive activity in the western part of the North Patagonian Massif (southern Argentina) and their geotectonic implications. Geol Mag 146:48–71. doi:10.1017/S0016756808005311

von Gosen W, Loske W (2004) Tectonic history of the Calcatapul Formation, Chubut province, Argentina, and the "Gastre fault system". J South Am Earth Sci 18:73–88

Willner A, Glodny J, Gerya T, Godoy E, Massonne H-J (2004) A counterclockwise PTt path of high-pressure/low-temperature rocks from the Coastal Cordillera accretionary complex of south-central Chile: constraints for the earliest stage of subduction mass flow. Lithos 75:283–310

orlando_a_p@yahoo.com.ar

The North Patagonian Orogen: Meso-Cenozoic Evolution from the Andes to the Foreland Area

Guido Gianni, Andrés Folguera, César Navarrete, Alfonso Encinas and Andrés Echaurren

Abstract In the last decades, an important amount of studies have dealt with the Patagonian orogen evolution. However, a holistic approach on the evolution of this sector has not been addressed yet. A review of recent advances in different aspects of the Patagonian orogen and its related broken foreland system reveals a close relation between the evolution of both sectors. This enabled us to integrate them in an evolutionary model connecting tectonic events from the North Patagonian Andes to the broken foreland area throughout the Mesozoic and Cenozoic. During the breakup of Western Gondwana, beginning in Jurassic times, several extensional basins developed in the Patagonian region. In late Early Cretaceous to Paleocene, a switch in the tectonic regime caused the initial uplift of the North Patagonian Andes and the fragmentation of the foreland area. Synchronously, an eastward magmatic arc expansion is documented at the retroarc zone. At this moment, a series of mid-ocean ridges collided one after another against the Patagonian margin. A causative relation between young lithosphere subduction, slab shallowing, orogenesis and eruption of mafic magmatism at the arc and retroarc region has been proposed. In concert to regional compression, synorogenic foreland rifting occurred transversally to the main Andean trend in the San Jorge Gulf Basin, describing an exceptional setting for this type of rifting mechanism. From the Eocene to early Miocene, a westward retraction of the magmatic arc, possibly related to roll-back, was synchronous to the Traiguen Basin, formed over highly attenuated crust that

G. Gianni (✉) · A. Folguera · A. Echaurren
Departamento de Ciencias Geológicas, Facultad de Ciencias Exactas y Naturales,
Instituto de Estudios Andinos "Don Pablo Groeber" UBA-CONICET,
Buenos Aires, Argentina
e-mail: guidogianni22@gmail.com

C. Navarrete
Dpto. de Geología, F.C.N., Universidad Nacional de la Patagonia "San Juan Bosco". YPF,
Santo Domingo, Argentina

A. Encinas
Departamento de Ciencias de la Tierra, Universidad de Concepción, Casilla 160-C,
Concepción, Chile

© Springer International Publishing Switzerland 2016

A. Folguera et al. (eds.), *Growth of the Southern Andes*,
Springer Earth System Sciences, DOI 10.1007/978-3-319-23060-3_9

orlando_a_p@yahoo.com.ar

splitted the arc and forearc areas. To the east, extensive intraplate magmatism began in the Patagonian foreland covering partially the broken foreland orogen. During the Neogene, an acceleration of the convergence rate between Nazca and South American plates caused the renewal of Patagonian Andes uplift and reactivation of the broken foreland system. Patagonian orogenesis along with the Late Cenozoic global cooling event triggered aridization of the foreland zone, having dramatic consequences for the Patagonian fauna and flora.

Keywords Northern patagonia · Broken foreland · Ridge subduction

1 Introduction

The Patagonian Andes started their uplift immediately after the breakup of Western Gondwana as the result of the initial interaction between South America against Panthalassic oceanic plates. Thus, the Patagonian Andes preserve a key record of the earliest evolutionary stages of the Andean orogen (Ramos 1981; Folguera and Iannizzotto 2004; Suárez et al. 2009a; Ghiglione et al. 2013). Only recently, the effects of this early orogenic stage have been identified in the foreland region (Giacosa et al. 2010; Homovc and Constantini 2001; Marques and Navarrette 2011; Gianni et al. 2015 among others). In this area, a conspicuous NNW-trending intraplate belt has been defined as the Patagonian broken foreland (Homovc et al. 1995; Peroni et al. 1995; Bilmes et al. 2013). Even though, the main deformational stages leading to the orogenic building of this sector have been recently recognized, correlation to the building of the Patagonian Andes to the west has not been addressed yet. An intriguing aspect of this area is that the initial fragmentation of the foreland region would have occurred synchronously to transverse foreland rifting at the San Jorge Gulf Basin (Gianni et al. 2015).

The Early Cenozoic evolution of the Patagonian Andes is characterized by sudden interruption of the orogenic building by inception of generalized extension in Central Patagonia (Encinas et al. 2014; de Ignacio et al. 2001; Kay et al. 2007; Bruni et al. 2008 among others). During the Late Cenozoic, in a context of global cooling, the last orogenic phase raised an orographic barrier that left profound imprints in Patagonian fauna and flora (e.g. Marshall and Salinas 1990; Blisniuk et al. 2005).

Even though, an important amount of works have dealt with the geology of Central Patagonia, a holistic approach on the evolution of this sector has not been addressed yet. In order to tackle this issue, we review recent advances in different geological aspects of the Patagonian orogen and its related broken foreland system. Finally, we integrate these data from the Mesozoic to the Cenozoic in an evolutionary tectonic model.

orlando_a_p@yahoo.com.ar

2 Tectonic Setting

The present configuration of the Patagonian Andes is related to the subduction of the Nazca and Antarctic plates beneath the South American plate. The three plates presently interact along the South American margin at 46° 30′S in the Aysen triple junction (Fig. 1).

The Nazca plate subducts with aprox. 30°E, while the Antarctic plate subducts with a shallow dip angle locally south of the Chile triple junction, acquiring a "normal" (∼30°E) subduction angle further to the south (Heintz et al. 2005). The triple junction point separates two morphostructural domains along the Patagonian Andes: The Austral Patagonian Andes and the North Patagonian Andes (Fig. 1). This point has migrated from south to north along the trench in the last 14 Ma (Cande and Leslie 1986) producing an arc gap associated with the development of a slab window that separates the Austral volcanic zone from the South volcanic zone (Ramos and Kay 1992). This slab window generated a thermal anomaly that is currently affecting the Andean domain, producing its local structural collapse (Scalabrino et al. 2010) and regional dynamic uplift (Guillaume et al. 2010).

The Andes at 45°S are formed by three orogenic sectors (Fig. 2) from west to east: (i) the Coastal Cordillera, characterized by polyphasic deformation since the Mesozoic (see Hervé et al. 2008) and the development of extension during the Paleogene associated with the intra-arc Traiguén Basin (Hervé et al. 1995). (ii) The North Patagonian Andes are associated with the dextral strike-slip Liquiñe-Ofqui fault zone (LOFZ) of Neogene to Quaternary age (Cembrano and Hervé 1993, among others) that constitutes the latest reactivation of a Mesozoic ductile fault system (Cembrano et al. 2000) and controls the emplacement of the Quaternary volcanic arc. The core of the North Patagonian Andes is constituted by a Mesozoic to Cenozoic Patagonian batholith (Hervé et al. 1996). (iii) To the east, the Patagonian broken foreland system, also known at these latitudes as the Bernárdides system, was produced by the tectonic inversion of a Jurassic rift system (Feruglio 1949; Peroni et al. 1995).

3 Late Western Gondwana Stage and Breakup of Central Patagonia

The pre-Mesozoic tectonic evolution of the Patagonian basement is currently debated (e.g. Ramos and Naipauer 2014; Pankhurst et al. 2014). In Late Paleozoic times, the western paleo-margin of Gondwana was characterized by deposition of turbidites of the Eastern Andes Metamorphic Complex in a passive margin setting (Hervé 1988; Augustsson and Bahlburg 2008) (Fig. 1).

During the Late Triassic, this sector of the paleo-margin of Gondwana was associated with metaturbidites of the Chonos complex, as initially evidenced by fossil fauna and later confirmed by detrital zircon SHRIMP U-Pb age determinations

orlando_a_p@yahoo.com.ar

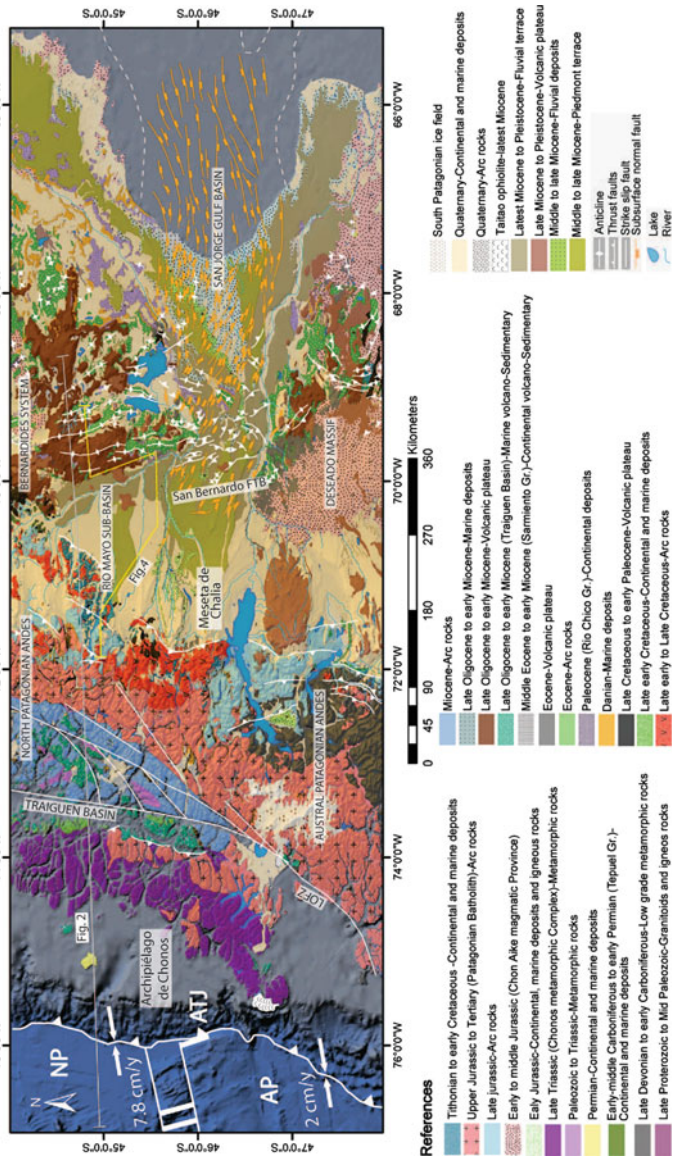


Fig. 1 Geological sketch map of the transitional segment between the North Patagonian Andes and the Austral Patagonian Andes. To the east, the Patagonian broken foreland and the San Jorge Gulf Basin are depicted. *AP* Antarctic plate, *NP* Nazca plate, *ATJ* Aysen triple junction

orlando_a_p@yahoo.com.ar

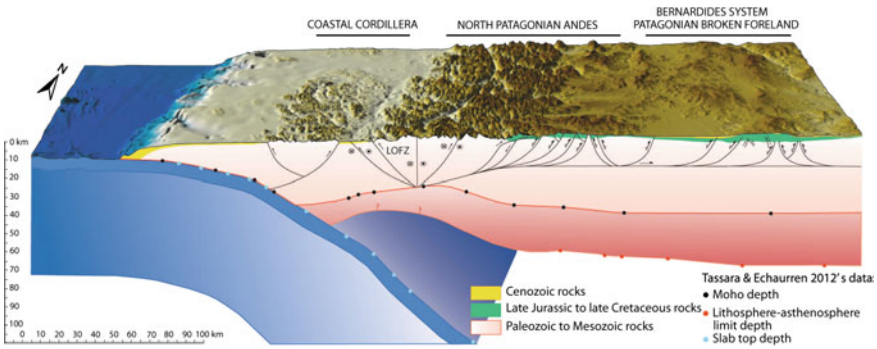


Fig. 2 Regional cross section depicting the general structure of the Andes at 45°S and the lithospheric geometry constructed with data taken from Tassara and Echaurren (2012). *LOFZ* Liquiñe-Ofqui fault zone

(Herve and Fanning 2001) (Fig. 1). This complex contains high-pressure low-temperature metamorphic rocks that reveal an early subduction event near the Triassic-Jurassic boundary (see Hervé et al. 2008). In Permian to Triassic times, the Patagonian extraandean zone (La Golondrina and El Tranquilo Basin) and part of the offshore area (San Julian Basin) suffered continued extension in NNW rift basins filled by fluvial and lacustrine deposits (Homovc and Constantini 2001). Later, in the Early Jurassic, coevally to the emplacement of I-Type granitoids of the Subcordilleran batholith, a NNW trending retroarc marine/continental basin developed in the extraandean zone filled by black shales and limestones intercalated with pyroclastic and andesitic volcanic rocks (Vicente 2005). Middle Jurassic times ushered in a period of rapid rift propagation into continental areas developing numerous fault-driven depocenters with NW and WNW orientations, accompanied by activity of one of the largest volcanic silicic provinces on the planet (Uliana et al. 1989; Pankhurst et al. 1998; Giacosa et al. 2010) (Fig. 1).

Hence, vast portions of the Patagonia extraandean zone were covered by acid volcanic rocks as a testimony of the imminent Pangea breakup (Fig. 3). Pankhurst et al. (2000) identified in this complex, three volcanic events in Patagonia younging from east to west, V1: 178–188 (Marifil Formation), 162–172 Ma (Chonaike Formation), and V3: 153–157 Ma (Ibañez and El Quemado Formations). These authors interpreted this volcanic pattern as the spreading of the Karoo plume-head towards the Pacific margin. The V3 volcanic event almost overlaps with the earliest known intrusions of the Patagonian batholith, a subduction related I-Type calc-alkaline body of Late Jurassic to Pliocene age that constitutes the core of the Patagonian Andes (Fig. 1). The youngest plutons lie near the main trace of the Liquiñe- Ofqui fault zone, which appears to have controlled their syntectonic emplacement (Thomson et al. 2001). From Late Jurassic to Early Cretaceous times, further fault-controlled subsidence was related to several extensional basins that crossed and broke apart western Gonwana (Uliana et al. 1989). These developed in the extraandean zone as well as in the Patagonian offshore area (Zambrano and

orlando_a_p@yahoo.com.ar

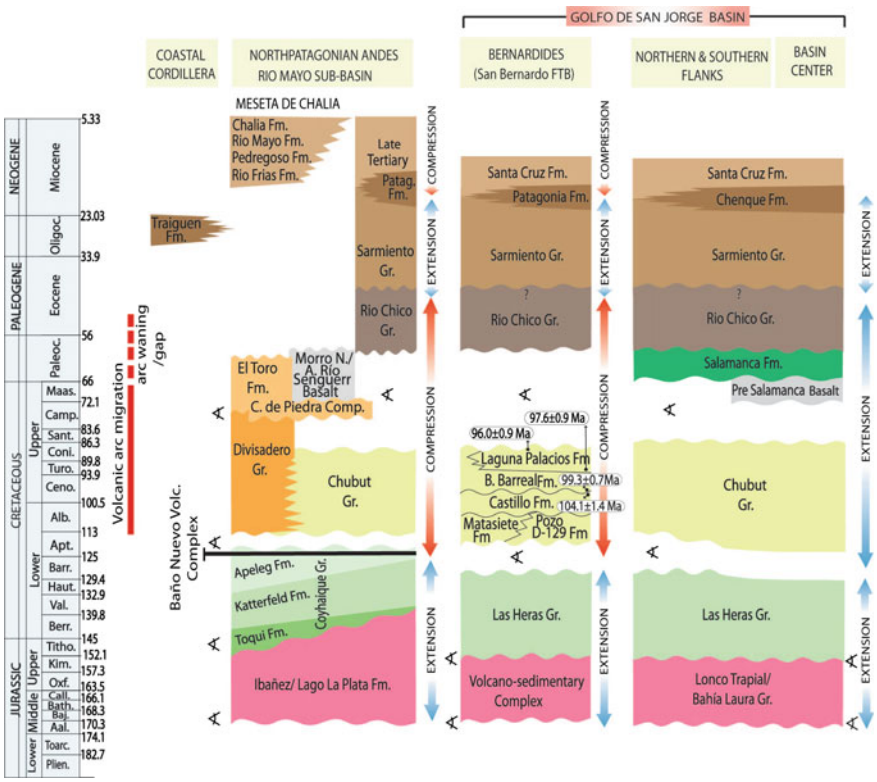


Fig. 3 Stratigraphic correlation among different units of the Patagonian Andes, San Bernardo FTB (broken foreland) and the eastern San Jorge Gulf Basin. (Based on Clavijo 1986; Barcat et al. 1989; Bruni et al. 2008; Suárez et al. 2009b; 2014; Sylwan 2001)

Urien 1970). After this, a Neocomian marine back-arc basin associated with the development of several NW- trending intra-arc and retroarc depocenters (Rolando et al. 2002, 2004), known as the Río Mayo Embayment/Sub-basin (Aguirre-Urreta and Ramos 1981) or Aysén Basin (Suárez et al. 2009a), formed during the last jump of the volcanic arc to the west between 150 and 140 Ma. The sedimentary and volcanic deposits accumulated in this basin were gathered in the Coyhaique Group. In Chile this unit is constituted, from base to top, by the Toqui, Katterfeld, and Apeleg Formations (Suárez et al. 1996) and in Argentina includes equivalents such as the Tres Lagunas Formation at the base (e.g. Ramos 1981; Iannizzotto et al. 2004). The Coyhaique Group is characterized by an easterly provenance coming from the San Jorge Gulf Basin and adjacent foreland areas (Bell et al. 1996). This unit begins with different shallow marine sedimentary facies with interbedded pyroclastic beds that are gathered in the Toqui Formation of Tithonian to early Hauterivian age, which represents a diachronous marine transgression that coexisted with a western volcanic arc chain (Suárez et al. 1996, 2009a and references therein). In Argentina, fossils in equivalent units (Tres Lagunas Formation) indicate

orlando_a_p@yahoo.com.ar

a Tithonian to early-late Valanginian age (Olivero and Aguirre-Urreta 2002). During Valanginian to Hauterivian times, the basin deepened and black shales of the Katterfeld Formation deposited in a shelf environment in Chile, while to the east it interfingered with prodelta turbidites (Olivero and Aguirre-Urreta 2002; Iannizzotto et al. 2004). In Hauterivian to early Aptian, black shales of the Katterfeld Formation deposited in a restricted environment that was later replaced by open marine sediments of de Apeleg Formation, related to a tide-dominated environment (Hervé et al. 2000 and references therein).

To the east, in the extraandean area Late Jurassic-Early Cretaceous extension gave place to the inicial opening of the San Jorge Gulf Basin (Neocomian stage). The western Neocomian half-grabens, are characterized by a WNW strike that interferes with another set of structures trending NNW (the latter, preferentially reactivated during Andean orogenesis). Contrastingly, the easternmost set of structures is dominated by E–W-trending faults (Zambrano and Urien 1970). The synextensional Neocomian deposits have been gathered in the Las Heras Group, which is formed, from base to top, by the Anticlinal Aguada Bandera (Tithonian-Valanginian) and Cerro Guadal Formations (Valanginian-Hauterivian) (Sylwan 2001 and references therein) (Fig. 3). Both units are separated by an erosional unconformity attributed to the intra-Valanginian phase (Barcat et al. 1989). According to Figari et al. (1999), these deposits represent mature half-grabens where the mainly pelitic lacustrine Anticlinal Aguada Bandera Formation constitutes the infill of a starved basin and the essentially sandy Cerro Guadal Formation corresponds to a maximun flooding stage with Pacific marine influence. Fitzgerald et al. (1990) interpreted the Las Heras Group as a late synrift phase of the rifting associated to the Liassic basin and the late to middle Jurassic volcano-sedimentary units (Fig. 3). The Neocomian deposits thicken towards the San Bernardo fold belt, where maximum stretching took place, thinning to the east against the Atlantic passive margin (Figari et al. 1999).

Finally, as the South Atlantic started to open by ~130 Ma, regional extension on the Patagonian region ceased (Fitzgerald et al. 1990).

4 Uplift of the North Patagonian Andes

During Aptian times, the Río Mayo Sub-basin underwent a major reorganization. As the Apeleg shallow sea progressively retreated, subduction-related surtseyan cones of the Baño Nuevo Complex were emplaced in the upper section of the Apeleg Formation (Suárez et al. 1996) (Fig. 3). Three amphibole Ar/Ar ages and one U–Pb SHRIMP zircon age, from samples of this complex, yielded concordant ages of 122 and 121 Ma (Suárez et al. 2007). Following the filling of the Río Mayo Sub-basin, subarerial subduction-related calcalkaline volcanics of the Divisadero Group, mainly silicic in character, were emplaced above Early Cretaceous volcanic and sedimentary rocks through an angular unconformity (Fig. 3). These volcanic arc rocks and equivalent units have been identified from 42° to 49°S (Suárez et al. 2009a,

orlando_a_p@yahoo.com.ar

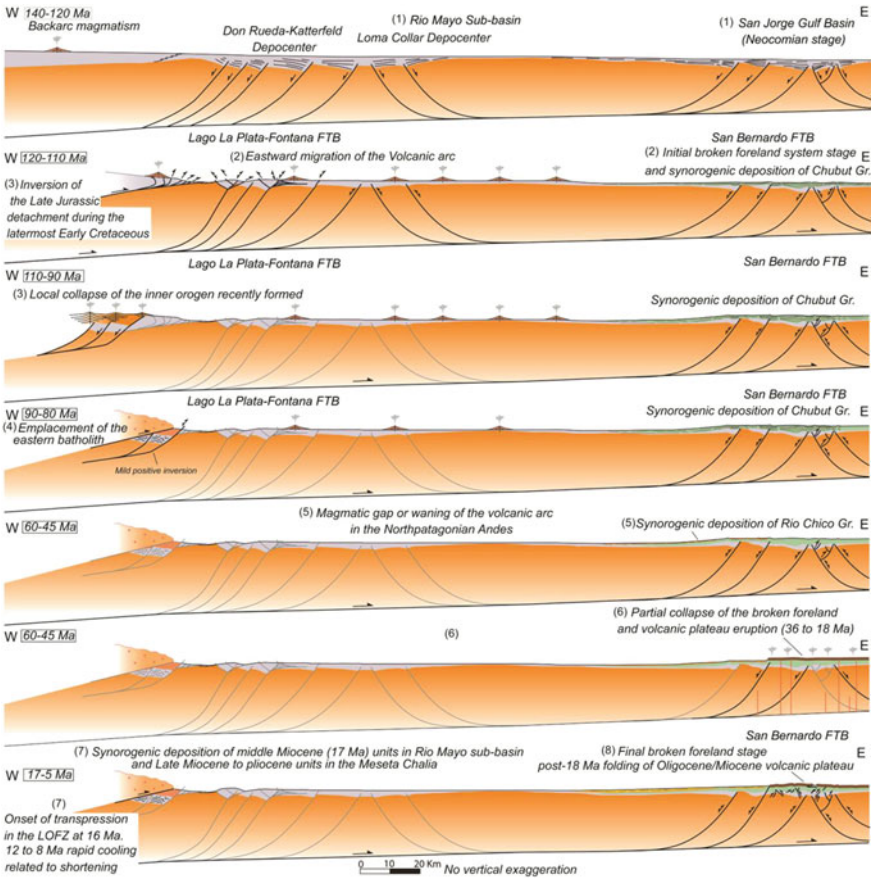


Fig. 4 Structural evolution of the North Patagonian Andes (Lago La Plata-Fontana FTB) and broken foreland system (San Bernardo FTB) during the Early Cretaceous to Pliocene, based on structural cross sections taken from Folguera and Iannizzotto (2004) and Gianni et al. (2015). See Fig. 1 for location

and references therein). Most radiometric ages from samples assigned to this unit in Chile are K–Ar and Ar–Ar ages, with a range from ~118 to 74 Ma (Suárez et al. 1996; Parada et al. 2001). However, U–Pb SHRIMP zircon ages range between ~118 to 102 Ma (Pankhurst et al. 2003; Suárez et al. 2009b). The local angular unconformity at the base of this unit has been interpreted as the earliest episode of Andean uplift at these latitudes. Based on geochronological data, this orogenic event has been constrained to the 121–118 Ma time interval (Aptian) (Ramos 1981; Iannizzotto et al. 2004; Folguera and Iannizzotto 2004; Suárez et al. 2009a) (Fig. 3, 4). Coincidently, in the northern part of the Austral Patagonian Andesat the Lago Pueyrredon area, Ghiglione et al. (2013) dated by U/Pb detrital zircons synorogenic strata of Río Belgrano Formation obtaining a maximum depositational age of ~122 Ma (Aptian).

orlando_a_p@yahoo.com.ar

This early orogenic event is well illustrated at the Lagos La Plata and Fontana area where it led to the construction of an east verging fold and thrust belt (Iannizzotto et al. 2004; Folguera and Iannizzotto 2004). This fold and thrust belt has an eastern inner sector characterized by a narrow belt of thin-skinned thrusts, detached at the turbidites of Ingenieros Formation (Berriasian-Hauterivian) and an external thick-skinned sector characterized by doubly vergent uplifted blocks (Fig. 4).

The presence of remnants of acid domes, basaltic lavas, and basaltic to dacitic lavas and plugs, with calc-alkaline affinities, indicate that subduction was an ongoing process during the Late Cretaceous (Fig. 3). These are represented by three subaerial calc-alkaline volcanic sequences identified in the area of Coihaique Alto (Demant and Suárez 2007). A compilation of ages and new geochronological data of these volcanic rocks has been provided by Demant and Suárez (2007). The oldest sequence represents rhyolitic to dacitic domes grouped in the Casa de Piedra volcanic Complex with ages ranging from ~84 to 77 Ma (Fig. 3). The second sequence known as the El Toro Formation consists of an association of andesitic to dacitic lava flows and breccias with ages ranging from ~77 to 63 Ma (Fig. 3). The third volcanic sequence corresponds to a basaltic succession defined as the Morro Negro basalts with K/Ar ages ranging from ~75 to 64 Ma (Butler et al. 1991), which correlate in the foreland area with the Alto Río Senguer basalts dated between ~79 and 60 Ma (Butler et al. 1991; Demant and Suárez 2007) and the Tres Picos Prieto basalts erupted between ~80 and 62 Ma (Franchi and Page 1980).

The El Toro Formation lies above the Divisadero Group in a gentle angular uncomformity (Fig. 3). This, together with different structural observations such as out-of-sequence thrusting in the Patagonian batholith in the Lago La Plata-Fontana region and more locally a K–Ar date of 105 Ma from cataclastic plutonic rocks, has been interpreted as a Late Cretaceous orogenic event (Iannizzotto et al. 2004; Folguera and Iannizzotto 2004; Suárez and De la Cruz 2001; Suárez et al. 2009a) (Fig. 4). Moreover, this tectonic pulse is coincident with the climax of tectonic emplacement of the Patagonian batholith (98 ± 4 Ma proposed by Ramos 1982). Suarez et al. (2009a) argued that the closure of the Río Mayo Sub-basin and the eastward advance of the arc volcanism were approximately synchronous and probably causally related (Figs. 3, 4). A broad dataset of radiometric ages of different arc-related units shows that eastward arc migration took place from ~120 to 75 Ma, falling into a period of magmatic arc waning and finally a volcanic gap from ~74 to 50 (Gianni et al. 2015) (Figs. 3, 4). This anomalous arc behavior is registered in a discrete latitudinal fringe between 42°30′S and 48°S. After this arc waning/gap period, the volcanic arc significantly retracted to the west and reappeared in Eocene times occupying the eastern flank of the Coastal Cordillera and the western flank of the North Patagonian Andes (Pankhurst et al. 1999; Hervé et al. 2000, see Fig. 6) (Fig. 1).

The Traiguen basin filling is exposed through a N–S trend, between the Coastal Cordillera and the western flank of the North Patagonian Andes (southern Chile, 43°45′−47°) (Fig. 1). Here, a marine volcano-sedimentary sequence, denominated Traiguen Formation, deposited unconformably over the Patagonian batholithic

orlando_a_p@yahoo.com.ar

rocks (Fig. 1) (Hervé et al. 1995). This unit consists of pillow basalts and basaltic andesites, geochemically representing mostly alkali-subduction related basalts, interbedded with sandstones, shales, and breccia deposited in a deep-marine environment, crosscut by basic dikes and gabbroic to granodioritic rocks (Hervé et al. 1995). In this area, extensional tectonics have created halfgrabens, 10–15 m in width, with basaltic dikes that intrude fault zones that feed pillow lavas and clastic dikes (Encinas et al. 2014; Folguera et al. 2014). The volcanic rocks have been metamorphosed from zeolite to greenshist facies, in a setting similar to ocean floor-type metamorphism (Hervé et al. 2000; Encinas et al. 2014). Recently, detrital zircons from this unit dated by U-Pb yielded maximum depositional ages between 26 and 23 Ma (late Oligocene-early Miocene) (Encinas et al. 2014). Deposition of this unit was relatively coetaneous to accelerated cooling and denudation in the late Oligocene (ca. 30–23 Ma) as revealed by apatite fission track data interpreted as related to shortening of the western part of the Patagonian Andean crust (Thomson et al. 2001). However, taking into account the development of a highly attenuated extensional basin in this sector and the regional extensional regime in the Andes at this time (see Jordan et al. 2001), another possibility would be that fission track data were indeed reflecting extension-related exhumation and cooling.

The Traiguen Basin has been related to an extensional genesis from 43°S to 47°S, in harmony with the regional stress field that affected a vast portion of the Andean crust between 33°S and 43°S in late Oligocene to early Miocene (see Encinas et al. 2014 for a recent discussion). Silva et al. (2003), speculated that this tectonic activity may have begun even earlier during the late Eocene.

The closure of the Traiguen Basin took place before the intrusion of 20 Ma granitoids producing north–south ample folds and metamorphic basement overthrusting (Hervé et al. 2000). Subsequently, continental sedimentation, mainly exposed east of the Andean front, took place as response to renewed Andean orogeny in Neogene times (Charrier and Malumian 1975; Ramos 1981). Consequently, a significant rain shadow was progressively established increasing the aridity on the foreland area, as revealed by oxygen isotopes on carbonates and changing 'Friasian' faunas from savanna-woodlands to pampas (Marshall and Salinas 1990 and references therein; Blisniuk et al. 2005). Synorogenic deposits are present at the subsurface sector of the Rio Mayo Subbasin and at surface exposed at the Meseta de Chalia (Ramos 1999; Dal Molin and Franchi 1996) (Figs. 1, 3). However, in this region, the volume of synorogenic sediments is small compared with in the Tertiary infill developed south of 47°S. Synorogenic deposits of the Santa Cruz Formation were deposited in the Austral Basin and the Río Frías Formation in the Río Mayo Subbasin (Ramos 1999, Fig. 1). Both the Santa Cruz and Río Frías Formations were deposited by high-energy fluvial systems dated between ~18 and 15 Ma (Marshall et al. 1986; Marshall and Salinas 1990) (Fig. 3). More recently, Blisniuk et al. (2005) proposed a longer interval of deposition between ~22 and 14 Ma based on Ar/Ar dating of intercalated tuffs in Santa Cruz Formation. The above-mentioned timing of deposition suggests that progressive compression in the Patagonian Andes started between ~22 and 18 Ma, although

orlando_a_p@yahoo.com.ar

the Andes did not attain sufficient height to produce a rain shadow effect by blocking moisture-laden Pacific winds until somewhat later ~16 Ma (Marshall and Salinas 1990; Blisniuk et al. 2005). At the Meseta de Chalía, Dal Molin and Franchi (1996) described fluvial deposits of synorogenic character overlying the Rio Frias Formation. These are the Pedregoso Formations, dated in 12, 18 ± 0.15 Ma, the Río Mayo Formation pelites, related to short periods of tectonic quiescence or retraction of the deformational front and the latest Miocene to Pliocene conglomerates of the Chalia Formation that registered a final reactivation of the Andean front (Dal Molin and Franchi 1996) (Fig. 3). Based on fission track data, Thomson (2002) identified a late Miocene period of enhanced cooling and denudation related to dextral transpressional tectonism at the Liquiñe-Ofqui fault system between ~16 and 10 Ma. These authors favored the models related to the collision of different segments of the Chile mid-ocean ridge, as the driving force behind this transpressional activity. Finally, deposition of the last synorogenic sequences at the Meseta de Chalia were relatively coetaneous with a phase of late Miocene rapid cooling and denudation between 12 and 8 Ma related to eastward propagation of the Andean front and 7–2 Ma associated with the activity at the Liquiñe-Ofqui fault system as revealed by fission track data (Thomson et al. 2001; Thomson 2002).

In latest Miocene to Pliocene times, approximation of the Chile mid-ocean ridge caused an increase in tectonic coupling between the continent and the subducted oceanic plates. A testimony of this is the emplacement of the Taitao ophiolites most probably around 6 Ma, when subduction of segment SCR-1 started (Kaeding et al. 1990; Mpodozis et al. 1985; Nelson et al. 1993; among others) (Fig. 1).

5 Uplift of the Patagonian Broken Foreland

East of the Patagonian Andes in the extraandean zone, an intraplate deformational belt developed as a product of tectonic inversion of Mesozoic rifts (Homovc et al. 1995; Peroni et al. 1995). It has been referred to as the Bernárdides system and more recently as Patagonian broken foreland system (Peroni et al. 1995; Bilmes et al. 2013). This belt is characterized by NNW–SSE trending structures that extend for more than 600 km to the south of the North Patagonian Massif, crossing the western border of the San Jorge Gulf Basin and reaching as far as the core of the Deseado Massif (Fig. 1).

Almost synchronously to the initial growth of the North Patagonian Andes during the late Early to Late Cretaceous, a new sedimentary cycle, represented by continental deposits of the Chubut Group (Lesta 1968), occupied an extensive area of the Patagonian and offshore sectors (Fig. 3). These rocks are characterized by a high proportion of distal, ash-fall deposits reworked in lacustrine and fluvial settings (Sciutto 1981). An increase in volcanic activity and a coeval eastward migration of the magmatic arc at this time, have been associated with the high pyroclastic component of this unit (Barcat et al. 1989; Paredes et al. 2007; Tunik et al. 2004; Umazano et al. 2009, 2012) (Fig. 3). These Cretaceous sections were

orlando_a_p@yahoo.com.ar

initially studied by Ameghino (1906) at the San Bernardo fold and thrust belt (FTB), where the most complete sections crop out (Figs. 1, 3). Here, this succession is stratigraphically arranged as follows: The Pozo D-129/Matasiete, Castillo, Bajo Barreal and Laguna Palacios Formations. The Matasiete Formation, and locally the equivalent Pozo D-129 Formation, are exposed dominantly in the western part of the San Jorge Gulf Basin over the San Bernardo FTB. There, this unit is composed of different fluvial and pyroclastic facies that laterally interfinger with the lacustrine Pozo D-129 Formation to the east of the basin (Fig. 3). The latter constitutes an organic-rich unit deposited between 121.5–112 Ma (Fitzgerald et al. 1990; Paredes et al. 2007) (Fig. 2). In the Deseado Massif, Césari et al. (2011) and Pérez Loinaze et al. (2013) constrained the age of a partially equivalent unit known as the Baqueró Group through U/Pb detrital zircons to the ~118–114 Ma time interval. Overlying the latter is the Castillo Formation, characterized by volcanoclastic fluvial to shallow lacustrine deposits (Sciutto 1981; Bridge et al. 2000). Its age has been assigned on the basis of pollen, charophytes, and ostracodes to the Aptian-Albian (Musacchio and Chebli 1975; Fitzgerald et al. 1990). Recently, a U/Pb zircon age of ~104 Ma provided an Albian age for this unit (Suárez et al. 2009b). Above, the Bajo Barreal Formation, was deposited in a fluvial to lacustrine environment (Umazano et al. 2009) (Fig. 3). Its upper section is a lateral equivalent of the Laguna Palacios Formation, a tuffaceous-loess-paleosol succession (Sciutto 1981) (Fig. 2). The age of these units has been variably assigned to the Senonian (Bonaparte and Gasparini 1978), Campanian-Maastrichtian (Lesta and Ferello 1972) and Santonian-Maastrichtian (Bellosi et al. 2002). However, Suárez et al. (2014), provided a new set of U/Pb zircon ages of ~99 Ma for the Bajo Barreal Formation and a 96–98 Ma age for the Laguna Palacios Formation, determining a Cenomanian to late Cenomanian-early Turonian (?) age (Fig. 3).

The plot of the detrital modes carried out by Tunik et al. (2004) showed that the Matasiete Formation presents a source corresponding to a non-dissected magmatic arc, while samples corresponding to the Castillo and Bajo Barreal Formations are most probably related to a provenance of a transitional magmatic arc or a dissected arc. According to the authors, the latter together with the presence of ash-fall deposits could be explained by migration of the arc and exposure of the roots of the volcanic arc due to deformation in the Patagonian Andes concomitant with active volcanism located in the North Patagonian Andes.

Through the Patagonian region the Chubut Group is separated from the underlying Neocomian units through a regional angular uncomformity, interpreted in terms of regional compression and traspression that affected the foreland area and the offshore San Julian Basin (Clavijo 1986; Barcat et al. 1989; Homovc and Constantini 2001; Giacosa et al. 2010; Ranalli et al. 2011; Marques and Navarrette 2011, among others) (Figs. 3, 4). This unconformity has been correlated with the initial growth of the Patagonian Andes and the tilting of the southern part of South American continent that closed the Pacific connection of previous basins (Barcat et al. 1989; Ramos 1981; Iannizzotto et al. 2004; Folguera and Iannizzotto 2004; Suárez et al. 2009a).

orlando_a_p@yahoo.com.ar

More recently, in the northern part of the Austral Patagonian Andes, Ghiglione et al. (2013) have dated through U/Pb detrital zircons in synorogenic deposits of Rio Belgrano and Rio Tarde Formations obtaining a maximum depositional age of ~122 Ma and ~118–111 Ma respectively. These detrital zircon populations yielded interesting results, instead of having a clear Andean provenance, these rather come from the Patagonian foreland. Hence, the authors pointed out that data could indicate a late Early Cretaceous post ~122 Ma uplift of different sectors of the foreland zone (the Deseado Massif and the western rim of the North Patagonian Massif). Uplift of this area is further supported by the synorogenic character of the Chubut Group based on seismic surveys (Homovc et al. 2011; Gianni et al. 2015). More recently, Gianni et al. (2015) provided surface data of growth strata and progressive unconformities related to contractional structures at the San Bernardo FTB in all units belonging to the Chubut Group. These authors suggested that deposition of the Chubut Group in the foreland area is related to the early development of the Patagonian broken foreland system, where fragmentation of the upper plate reached the offshore area 1200 km from the trench (distal broken foreland), inverting the San Julián, Rawson and Valdés basins.

Across the foreland and offshore areas the Chubut Group is capped by a regional angular unconformity, either by the Upper Cretaceous/Lower Paleogene retroarc basalts or marine transgressive deposits (Fig. 3). This unconformity has been interpreted as a Late Cretaceous major compressional event and seems to have affected the upper plate from the Andes to the offshore area (Feruglio 1949; Lesta et al. 1980; Ramos 1981, 2002; Proserpio 1978; Barcat et al. 1989; Anselmi et al. 2000; Panza et al. 2001; Thomson et al. 2001; Silva Nieto 2005; Continanzia et al. 2011; Micucci et al. 2011) (Fig. 3).

During Danian times, vast portions of the foreland area were flooded by a regional Atlantic marine trasgression of the Salamanca Formation and equivalent units that encountered several topographic highs uplifted during previous orogenic events (Feruglio 1949; Lesta et al. 1980). However, Ruiz et al. (2005) proposed that some sectors of the foreland area may have been uplifted in Danian times as suggested by synorogenic deposits of the marine Lefipan Formation in the northern sector of the Patagonian broken foreland.

The late Paleocene sedimentation was essentially continental with fluctuations between fluvial and lacustrine conditions (Raigemborn 2006). Seismic surveys carried out in the eastern Río Mayo Subbasin in the subsurface foreland area and at the San Bernardo FTB pointed out to a synorogenic character of this group evidencing ongoing foreland compression during late Paleocene times (Gianni et al. 2015) (Figs. 3, 4).

From Eocene to early Miocene times, the foreland region faced a series of intraplate magmatic events, where most of the Patagonian broken foreland was buried under extensive volcanic plateaus of alkaline to subalkaline composition (Baker et al. 1981; Kay et al. 2007; Bruni et al. 2008, among others) (Figs. 3, 1). During this period, extensive tuff deposits belonging to the Sarmiento Group (late Eocene to early Miocene) were deposited in a low-gradient, continental setting (Paredes et al. 2008). Around the San Bernardo FTB and the San Jorge Gulf Basin,

orlando_a_p@yahoo.com.ar

magmatic activity took place mainly during Oligocene to early Miocene times under an extensional regime that caused an important thermal event and reactivated basin subsidence (Baker et al. 1981; Rodriguez and Littke 2001; among others) (Fig. 4). During this time interval, half graben and graben structures have been identified in the San Jorge Gulf Basin (Giacosa et al. 2004). Coevally to extension and regional intraplate magmatism, a second Atlantic-derived transgression known as the Patagoniano flooded the foreland region (Ameghino 1906; Bellosi 1987) (Figs. 3, 4). During middle Miocene times, these marine sediments graded to high-sinuosity fluvial and aeolian deposits of the synorogenic Santa Cruz Formation that accompanied their regression (Feruglio 1949; Lesta et al. 1980). In late early–middle Miocene times, the Patagonian broken foreland suffered renewed contraction between 40 and 48°S (Homovc et al. 1995; Peroni et al. 1995; Giacosa et al. 2010; see Bilmes et al. 2013) (Fig. 4). At the San Bernardo FTB, folded plateau basalts have been dated by Bruni et al. (2008) in ~18 Ma above which Pliocene basaltic rocks of ~3 Ma rest unconformably not deformed, constraining this event to sometime between the ~18 and ~4 Ma interval (Gianni et al. 2015).

6 Synorogenic Foreland Rifting: Chubutian Stage of the San Jorge Gulf Basin

The Patagonian broken foreland is traversed by a roughly E–W rift basin known as the San Jorge Gulf Basin (Fig. 1). This basin is characterized by the spatial coexistence of at least two superposed subbasins differentiated in terms of their evolution (Figari et al. 1999). These are the Neocomian depocenters, related to generalized extension during Western Gondwana breakup and the Chubutian Basin, related to a renewed extensional/trasntensional reactivation (Uliana et al. 1989; Chelotti 1997; Figari et al. 1999) (Fig. 5). The beginning of the Chubutian stage in late Early Cretaceous was marked by dramatic basin reorganization (Hechem and Strelkov 2002). To the west, the arc turned vigorously active and migrated/expanded to the east and the Patagonian Andes and the San Bernardo FTB (broken foreland) were progressively constructed, causing the tilting of the regional slope to the east and widespread deposition of the Chubut Group throughout Central Patagonia (Clavijo 1986; Barcat et al. 1989; Hechem et al. 1990) (Fig. 4). Concomitantly in the San Jorge Gulf Basin, the general W–NW and NNW trend of the Neocomian depocenters, suddenly turned into an extensive E–W-trending tectonic depression with a main depocenter displaced to the east, in which the Chubut Group filled synextensionally (Uliana et al. 1989; Chelotti 1997; Figari et al. 1999) (Fig. 5).

Paradoxically, while syncontractional deposition of the Chubut Group has been described in the Patagonian broken foreland system (San Bernardo fold and thrust belt), an extensional character of this unit has been recognized at the San Jorge Gulf Basin. Here, 2D and 3D seismic data, suggest that rifting occurred at different times during the deposition of the Chubut Group, and even during the Early Paleogene

orlando_a_p@yahoo.com.ar

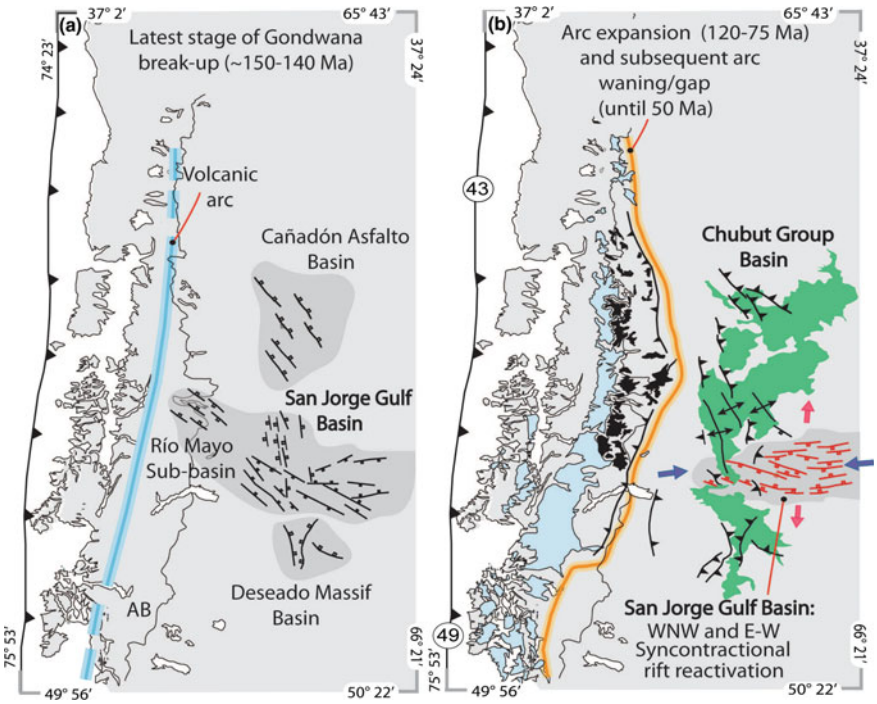


Fig. 5 Mesozoic evolution of Central Patagonia. **a** Late Jurassic to Early Cretaceous: this time was associated with a volcanic arc located next to the trench, a westward development of the Neocomian basins and regional extension related to the breakup of Western Gondwana. Several W–NW, NNW and E–W depocenters were outlined in Patagonia in this period. **b** Late Early Cretaceous to Late Cretaceous: the volcanic arc migrated eastwards associated with a slab shallowing according to previous hypotheses (see text for details). As a consequence, initial Andean uplift, broken foreland development and E–W syncontractional foreland rifting in the San Jorge Gulf Basin (Chubutian stage) took place. Note that E–W and WNW Neocomian structures of the San Jorge Gulf Basin were reactivated in the late Early Cretaceous. *Green color:* Deposits of the Chubut Group, *RMSB:* Rio Mayo Subbasin, *SGB:* San Jorge Gulf Basin

related to the deposition of Salamanca Formation and Río Chico Group (Hechem 1998; Figari et al. 1999; Georgieff et al. 2009; Foix et al. 2012, 2013; Paredes et al. 2013) (Fig. 3).

Hence, the Chubutian stage of the San Jorge Gulf Basin was coetaneous to strong compression that raised the Andes and broke the foreland area and extension that modified previous basin configuration turning into a general E–W rift transversal to the main Andean trend (Figs. 1, 5). Gianni et al. (2015) proposed a causative relation between these processes, where the Chubutian stage represents a synorogenic foreland rifting stage (Fig. 5).

These authors argued that the oblique disposition of the Chubutian stage rifting respect to the Andean trend and its temporal relation with Patagonian orogenesis somehow resembles impactogene rift basins (see Sengor et al. 1978) that form as a

orlando_a_p@yahoo.com.ar

consequence of continent-continent collision (e.g. Rhine and Baikal rift) (Figs. 1, 5). During collisional events, when properly oriented, compression may reactivate lithospheric weaknesses (terrane sutures or previous rift basins) in the upper plate, creating orogen-perpendicular extensional/transtensional systems.

Arc migration in central Patagonia since late Early Cretaceous times has been related to a slab shallowing triggered by subduction of buoyant lithosphere (Barcat et al. 1989; Folguera and Ramos 2011; Gianni et al. 2015) (Figs. 4, 5). Thus, regional compression related to slab shallowing could have reactivated extensionally/transtensionally the most favorable E–W and secondarily WNW-trending Neocomian structures. Consequently, a change in the general direction of the extensional axis between Neocomian and Chubutian rift depocenters could be explained by inception and propagation of the fold and thrust belt during shallow subduction conditions (Gianni et al. 2015) (Fig. 5).

According to Seton et al. (2012)'s global plate reconstruction, two mid-ocean ridges interacted with the Patagonian margin in the Cretaceous (Fig. 6). The Chasca/Catequil mid-ocean ridge collided between ~120 and ~93 Ma; then as the

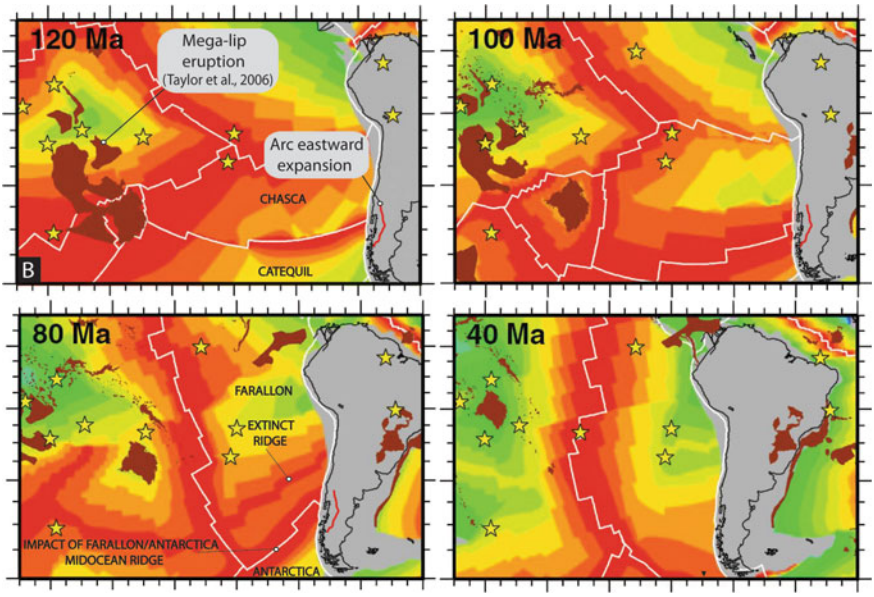


Fig. 6 Plate reconstruction modified from Seton et al. (2012). Eruption of a mega-lip and fragmentation of Panthalassic plates at 120 Ma (Taylor 2006), led to the breakup of an oceanic plate into a set of new ones (Chasca and Catequil plates). The Chasca-Catequil mid-ocean ridge and related young lithosphere propagated eastwards impacting with the Patagonian margin (from ~120 to 93 Ma), influencing the geometry of the subducted slab as reflected by magmatic arc migration. At ~86 Ma a new mid ocean (Antarctica-Farallon) replaced the previous one impacting at the same latitudes until 56 Ma. The collision of both mid-ocean ridges took place under a context of high-trench normal convergence and upper plate velocity (Maloney et al. 2013)

orlando_a_p@yahoo.com.ar

latter got extinct and migrated northwards, it was replaced by the Farallones/Antarctica mid-ocean ridge that interacted with the margin from ~86 to ~55 Ma (Fig. 6). Based on this reconstruction, less than ~10 Ma ocean lithosphere, generated in the two subsequent mid-ocean ridges, was subducted at the time of arc-magmatic expansion between ~120 and 75 Ma that led to an arc waning/gap until ~50 Ma (Gianni et al. 2015) (Fig. 6). Hence, the authors proposed that young lithosphere related to mid-ocean ridges, colliding against the previously weakened South American plate in a context of high convergence, would have been a key condition to maintain the shallow slab configuration for a prolonged time causing regional compression and consequent synorogenic foreland rifting (Gianni et al. 2015) (Figs. 5, 6).

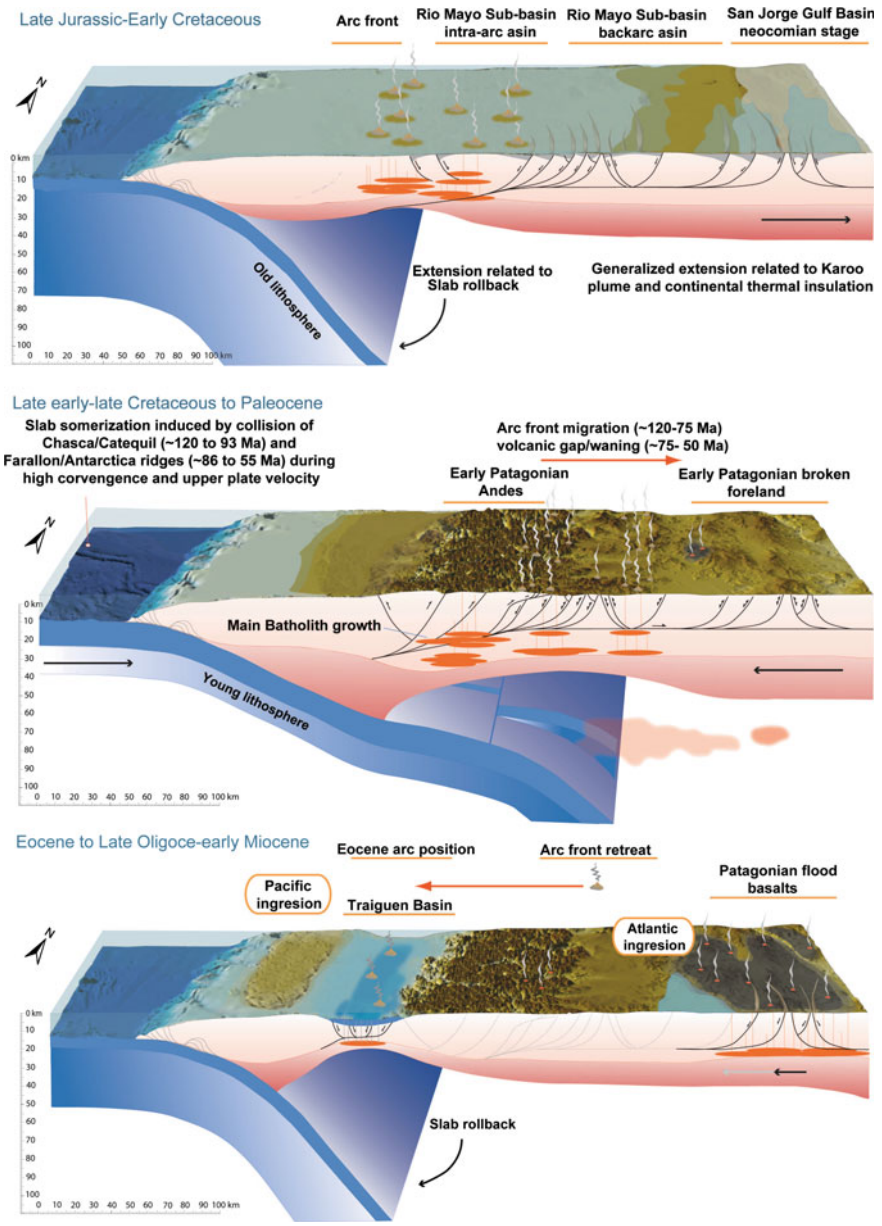
7 Meso-Cenozoic Evolution of the Patagonian Orogen

The different tectonic events reviewed above reveal a clear correlation between the geological evolution of the Patagonian Andes and the foreland region from Mesozoic to Cenozoic times. This enables us to put forward an evolutionary model that integrates the existing data from these Andean sectors (Fig. 7).

In Late Jurassic to Early Cretaceous times, in a context of generalized extension during westward migration of the volcanic arc, the NW- trending intra-arc and inner retroarc Río Mayo Subbasin developed at the western margin of South America (Rolando et al. 2002) (Fig. 5). To the east, in an intraplate position, the initial Neocomian stage of the San Jorge Gulf Basin was associated with several W–NW to NNW and E–W depocenters (Fig. 5). In this area, extension was mainly related to the opening of the Southern Atlantic ocean as a consequence of the Karoo plume activity (Pankhurst et al. 2000) or as recently demonstrated, to continental thermal insulation raising the ambient mantle temperature to 150 °C above current values (Brandl et al. 2013). However, in the western sector, upper plate extension may have triggered by slab rollback (Rolando et al. 2002; Folguera and Iannizzotto 2004). Roll-back related to extension may have been enhanced by subduction of an old slab (Maloney et al. 2013) (Fig. 8). During the late Early Cretaceous, the geodynamic context changed drastically as a consequence of global and local factors. Ultra-fast spreading of oceanic floor, product of superplume activity caused batholith emplacement and orogeny around the Pacific subduction ring between 120 and 80 Ma (Vaughan 1995; Charrier et al. 2007).

However, in this context of high-trench normal convergence and upper plate motion, orogeny may have been intensified at Patagonian latitudes by local collision of mid-ocean ridges (Fig. 6). As a consequence, the volcanic arc migrated eastward from ~120 to 75 Ma and eventually turned off until ~50 Ma, possibly related to a slab shallowing period that unleashed an orogenic wave that uplifted the North Patagonian Andes and almost coetaneously fragmented the foreland area to the east (Fig. 7). At this time, synorogenic sequences of the Chubut Group (late Early to Late Cretaceous) and the Río Chico Group (late Paleocene) deposited in a

orlando_a_p@yahoo.com.ar



orlando_a_p@yahoo.com.ar

◄ **Fig. 7** Evolution of the southern segment of the North Patagonian Andes and the Patagonian broken foreland. Late Jurassic- Early Cretaceous: Gondwana breakup related extension. In the eastern intraplate area, extension was mainly related to opening of the Southern Atlantic ocean. Extension in the arc and backarc region (Rio Mayo/Aysen Basin) was mainly related to rollback while the upper plate moved away from the trench. Late early-Late Cretaceous-Paleocene: the volcanic arc migrated eastwards from aprox. 120–75 Ma and entered in a volcanic gap stage from 75 to 50 Ma, associated with a slab shallowing, caused by subduction of mid-ocean ridges and related young lithosphere during high convergence and upper plate velocity. This produced a regional contractional stress field that uplifted the North Patagonian Andes and broken the foreland area. During the late Early Cretaceous, Panthalassic asthenosphere may have leaked through the Chasca/Catequil mid-ocean ridge influencing locally the volcanic arc. In Late Cretaceous-Paleocene times, the Antarctic/Farallon mid-ocean ridge may have evolved into a slab window responsible for the eruption of volcanic plateaux. Eocene-late Oligocene to early Miocene: During the Eocene the arc retracted to the west, where it was lately associated with further extension during the late Oligocene in the Traiguen Basin. To the east the broken foreland was partially collapsed and a vast volume of volcanic rocks poured over it

broken foreland system. Regional compression led to synorogenic reactivation of the San Jorge Gulf Basin in an impactogenic-like manner (Fig. 5). Parada et al. (2001) argued that around the Aysen area the arc was locally influenced by an upwelling asthenospheric source that justified the anomalous arc signature and an elevated gradient as evidenced by a thermal metamorphic event. We speculate that asthenosphere leaking through the Chasca/Catequil mid-ocean ridge may have been responsible for influencing the sources of the volcanic arc at that area (Fig. 7). A fully open slab window event may have been inhibited by the highly oblique collision of this mid-ocean ridge (60°<) as recently modeled by Quevedo et al. (2013) (Fig. 7a). In Late Cretaceous to Paleocene, due to a more favorable oblique angle of collision (60°>), the Antarctic/Farallon mid-ocean ridge may have evolved into a slab window responsible for the eruption of volcanic plateaus in the foreland (Alto Río Senguer, ~79 to 60 Ma and Tres Picos Prieto basalts, ~80 to 62 Ma). At around 75–72 Ma, scarce arc-related products at the western slope of the Andes are partially synchronous to Morro Negro basalts, interpreted as derived from a slab window (Demant and Suárez 2007) (Fig. 3). These authors also described some volcanic rocks with adakitic signature erupted at ~75 Ma (Fig. 7).

In Eocene times, the magmatic arc retracted to the west occupying the eastern flank of the Coastal Cordillera and the western flank of the North Patagonian Andes, possibly reflecting a slab roll back (Fig. 7). Here, the Traiguen Basin developed in a context of highly attenuated crust, possibly beginning in late Eocene and fully developing during the late Oligocene-early Miocene (Silva et al. 2003; Encinas et al. 2014) (Fig. 7). Recent analog modeling on intra-arc extension showed that the arc sector, because of its thermal state, tends to weaken the upper plate, focalizing extension during slab roll back (Boutelier and Cruden 2013). Similarly, we speculate that the position of the Eocene arc and the later arc front development of the extensional Traiguen Basin could be related to thermal weakening of the crust that further localized extension (Fig. 7). During the Eocene to late Oligocene-early Miocene intraplate magmatism spread over the Patagonian Broken foreland (Fig. 7). The eruption of these volcanic plateaux has been difficult to

orlando_a_p@yahoo.com.ar

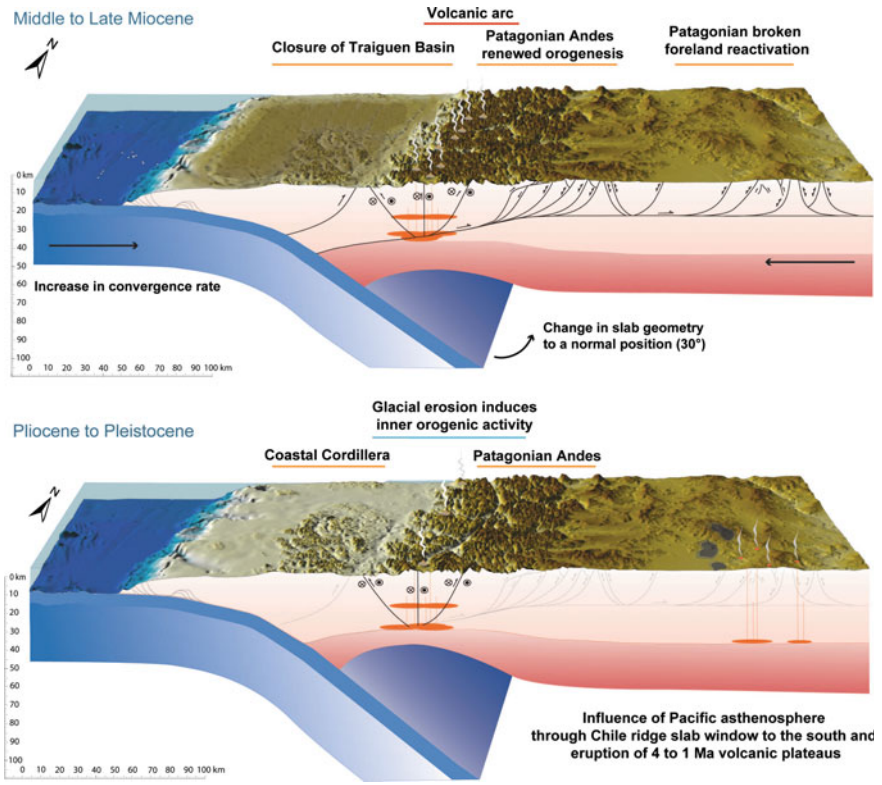


Fig. 8 Middle-late Miocene: closure of the Traiguen Basin between 23 and 20 Ma, renewed uplift in the North Patagonian Andes, transpression in the LOFZ, and broken foreland reactivation in a context of high-trench normal convergence. Pliocene to Pleistocene: continued activity in the Liquiñe-Ofqui fault system (LOFZ) and eruption of volcanic plateaux related to incoming asthenosphere from Chile mid-ocean ridge slab window to the south (Guillaume et al. 2010). Final retraction of the thrust front at 7–5 Ma to the inner sector of the North Patagonian Andes due to intense glacial erosion (Thomson et al. 2010)

explain, giving place to an ongoing discussion, with a high diversity of proposed models (mantle plumes, asthenospheric upwellings, slab windows, changes in slab geometry and lithospheric delamination) (de Ignacio et al. 2001; Kay et al. 2007; Bruni et al. 2008; Zaffarana et al. 2012; Remesal et al. 2012; among others).

In Miocene times, in a context of high-trench normal convergence (above 4 cm/yr), closure of the Traiguen Basin produced basement exhumation and basin inversion (Maloney et al. 2013) (Fig. 8). This event took place after deposition of the Traiguen Formation at ~23 Ma and before intrusion of ~20 Ma granitoids (Hervé et al. 2000; Encinas et al. 2014).

The timing of synorogenic deposition at the Andean front suggests that progressive compression in the Patagonian Andes began between ~22 and 18 Ma, and that at ~16 Ma it attained sufficient height to produce a rain shadow effect that

orlando_a_p@yahoo.com.ar

triggered aridization in the foreland region causing changes in Patagonian fauna and flora (Marshall and Salinas 1990, and references therein; Palazzesi et al. 2003; Blisniuk et al. 2005).

Between 16 and 10 Ma, the core of the Cordillera was affected by dextral transpressional tectonism related to the Liquiñe-Ofqui fault system that continued until Pleistocene times (Thomson et al. 2001; Thomson 2002) (Fig. 8). In late early–middle Miocene times, renewed uplift of the Patagonian broken foreland took place between 40°S and 48°S (Bilmes et al. 2013; Gianni et al. 2015) (Fig. 8). The Neogene broken foreland reactivation admits no simple explanation. Noteworthy, is that no general arc expansion has been reported in middle Miocene times along the arc front from 42°30′S to 46°30′S as documented in late Early Cretaceous times (Hervé et al. 2000, see Fig. 6). This precludes the possibility of a long-standing flat-slab segment, a conclusion to which Bilmes et al. (2013) had already arrived. Gianni et al. (2015) proposed that restructuration of the broken foreland in the middle Miocene would have been mainly by the presence of western Gondwana breakup-related heterogeneities in the Patagonian foreland, such as Mesozoic basins, enhaced by magmatic crustal weakening imposed by retroarc eruptions. These anisotropies may have reactivated due to a high-trench normal convergence (above 4 cm/yr) in Neogene times. During the late Miocene to Pliocene, the deformational front retreated from the broken foreland area to the North Patagonian foothills, where synorogenic deposits are well preserved at the Meseta de Chalía (Dal Molin and Franchi 1996). Recent thermochronological data from 38° to 49°S record a marked acceleration in erosion at 7–5 Myr ago coeval with the onset of major Patagonian glaciation and the retreat of deformation from the easternmost thrust front (Thomson et al. 2010). These authors proposed that intense glaciation at the core of the Patagonian Andes deactivated the easternmost deformational front leading to out of sequence thrusting and orogenic shrinkage (Fig. 8).

In latest Miocene to Pliocene, approximation of the Chile mid-ocean ridge caused the emplacement of the Taitao ophiolites, most probably around 6 Ma, and eruption of volcanic plateaux in the foreland region related to incoming asthenosphere from Chile mid-ocean ridge slab window to the south (Nelson et al. 1993; Guillaume et al. 2010) (Fig. 8).

References

Aguirre Urreta B, Ramos VA (1981) Estratigrafía y paleontología de la alta cuenca de río Roble, Cordillera Patagónica. VIII Congreso Geológico Argentino (San Luis). Actas 3:101–138

Ameghino F (1906) Les formations sedimentaires du Cretáce superieur et du Tertiare de Patagonie. Anales del Museo Nac de Historia, Buenos Aires 8:568

Anselmi GJL, Cortés JM, Genini A (2000) Hoja Geológica 4569 - II El Sombrero. Servisio Geol Min Nac Bol 271:92

Augustsson C, Bahlburg H (2008) Provenance of late Palaeozoic metasediments of the Patagonian proto-Pacific margin (southernmost Chile and Argentina). Int J Earth Sci 97:71–88

orlando_a_p@yahoo.com.ar

Baker PE, Rea WJ, Skarmeta J, Caminos R, Rex DC (1981) Igneous history of the Andean cordillera and Patagonian plateau around latitude 46°S. Philos Trans Roy Soc Lond Ser A Math Phys Sci 105–149

Barcat C, Cortiñaz JS, Nevistic VA, Zucchi HE (1989) Cuenca Golfo San Jorge. In: Chebli LS (ed) Cuencas Sedimentarias Argentinas, Serie Correlación Geológica 6, Tucumán: 319–345

Bell CM, De la Cruz R, Suarez M, Townsend, MJ (1996) The evolution of the Aysen Basin, an early Cretaceous epicontinental interior seaway in the southernmost South America. In: 3rd International Symposium of Andean Geodynamics (Saint Malo), pp 289–292

Bellosi ES (1987) Litoestratigrafía y sedimentación del "Patagoniano" en la Cuenca de San Jorge, Terciario de Chubut y Santa Cruz. Unpublished Ph.D. Thesis. Universidad de Buenos Aires, p 252

Bellosi E, González M, Genise J (2002) Paleosuelos y sedimentación cretácica de la Cuenca San Jorge (Grupo Chubut) en la Sierra San Bernardo, Patagonia Central. XV Congreso Geológico Argentino (Calafate). Actas 1:747–753

Bilmes A, D'Elia L, Franzese JR, Veiga GD, Hernández M (2013) Miocene block uplift and basin formation in the Patagonian foreland: the Gastre Basin, Argentina. Tectonophysics 601:98–111

Blisniuk PM, Stern LA, Chamberlain CP, Idleman B, Zeitler PK (2005) Climatic and ecologic changes during Miocene surface uplift in the Southern Patagonian Andes. Earth Planet Sci Lett 230:125–142

Bonaparte JF, Gasparini Z (1978) Los saurópodos de los Grupos Neuquén y Chubut y sus relaciones cronológicas. VII Congreso Geológico Argentino (Neuquén). Actas 2:393–406

Boutelier D, Cruden A (2013) Slab rollback rate and trench curvature controlled by arc deformation. Geology 41:911–914

Brandl PA, Regelous M, Beier C, Haase KM (2013) High mantle temperatures following rifting caused by continental insulation. Nat Geosci 6(5):391–394

Bridge JS, Jalfin GA, Georgieff SM (2000) Geometry, Lithofacies, and spatial distribution of cretaceous fluvial sandstone bodies, San Jorge Basin, Argentina: outcrop analog for the hydrocarbon-bearing Chubut group. J Sediment Res 70:341–359

Bruni S, D'Orazio M, Haller MJ, Innocenti F, Manetti P, Pécskay Z, Tonarini S (2008) Time-evolution of magma sources in a continental back-arc setting: the Cenozoic basalts from Sierra de San Bernardo (Patagonia, Chubut, Argentina). Geol Mag 145:714–732

Butler RF, Hervé F, Munizaga F, Beck M, Oviedo E (1991) Paleomagnetism of the Patagonian Plateau Basalts, southern Chile and Argentina. J Geophys Res 96:6023–6034

Cande S, Leslie R (1986) Late Cenozoic tectonics of the Southern Chile trench. J Geophys Res 91:47–496

Charrier R, Malumian N (1975) Orogénesis y epirogénesis en la región austral de América del Sur durante el Mesozoico y el Cenozoico. Rev Asoc Geol Argentina 30(2):193–207

Charrier R, Pinto L, Rodríguez MP (2007) Tectonostratigraphic evolution of the Andean orogen in Chile. In: Gibbons W (ed) Moreno T. The Geology of Chile, Geol Soc London, pp 21–114

Chelotti L (1997) Evolución tectónica de la Cuenca del Golfo San Jorge en el Cretácico y Terciario; algunas observaciones desde la interpretación sísmica. Bol Inf Pet 49:62–82

Cembrano J, Hervé F (1993) The Liquiñe Ofqui fault zone: a major Cenozoic strike-slip duplex in the southern Andes. In: 2nd international symposium of Andean geodynamics (Oxford), extended abstracts, pp 175–178

Cembrano J, Schermer E, Lavenu A, Sanhueza A (2000) Contrasting nature of deformation along an intra-arc shear zone, the LOFZ fault zone, southern Chilean Andes. Tectonophysics 319:129–149

Césari SN, Limarino CO, Llorens M, Passalia MG, Loinaze VP, Vera EI (2011) High-precision late Aptian Pb/U age for the Punta del Barco Formation (Baqueró Group), Santa Cruz Province, Argentina. J S Am Earth Sci 31:426–431

Clavijo R (1986) Estratigrafía del Cretácico Inferior en el sector occidental de la Cuenca del Golfo San Jorge. Bol Inf Pet 9:15–32

orlando_a_p@yahoo.com.ar

Continanzia J, Manceda R, Covellone GM, Gavarrino AS (2011) Cuencas de Rawson y Valdés: Síntesis del Conocimiento Exploratorio—Visión actual. In: Legarreta L, Boll A, Marshall PA (eds) Kozlowski E. VIII Congreso de Exploración y Desarrollo de Hidrocarburos, Simposio Cuencas Argentinas Visión Actual, pp 47–64

Dal Molin C, Franchi M (1996) Reinterpretación estratigráfica de las sedimentitas terciarias del sudoeste de Chubut. XIII Congreso Geológico Argentino, (Buenos Aires). Actas 1:473–478

de Ignacio C, López I, Oyarzu R, Márquez A (2001) The northern Patagonian Somuncura plateau basalts: a product of slab induced, asthenospheric shallow upwelling. Terra Nova 13:117–121

Demant A, Suárez M (2007) Geochronology and petrochemistry of Late Cretaceous- (?) Paleogene volcanic sequences from the eastern central Patagonian Cordillera (45°−45°40′S) Rev Geol Chile 34:3–21

Encinas A, Riffo R, Tapia F, Folguera A, Azúa P, Hervé F, Finger KL, Valencia V, Oliveros V (2014) Evidence of submarine volcanism and deep-marine sedimentation in the forearc of southern Chile (45°25`−45°50`) during the Late Oligocene-Early Miocene. XIX Congreso Geológico Argentino (Córdoba), Electronic files

Feruglio E (1949) Descripción Geológica de la Patagonia. Editorial Coni, Dirección General de Yacimientos Petrolíferos Fiscales, p 334

Figari EG, Strelkov E, Laffitte G, Cid De La Paz MS, Courtade SF, Celaya J, Vottero A, Lafourcade P, Martinez R, Villar H (1999) Los Sistemas Petroleros de la Cuenca del Golfo San Jorge: Sintesis Estructural, Estratigrafía y Geoquímica. IV Congreso de Exploración y Desarrollo de Hidrocarburos (Mar del Plata), Actas, pp 197–237

Fitzgerald MG, Mitchum RM Jr, Uliana MA, Biddle KT (1990) Evolution ofthe San Jorge Basin, Argentina. Am Assoc Petrol Geol 74:879–920

Foix N, Paredes JM, Giacosa RE (2012) Upper Cretaceous-Paleocene extensional phase in the Golfo San Jorge basin (Argentina): Growth-fault model, paleoseismicity and paleostress analysis. J S Am Earth Sci 33:110–118

Foix N, Paredes JM, Giacosa RE (2013) Fluvial architecture variations linked to changes in accommodation space: Río Chico formation (Late Paleocene), Golfo San Jorge basin, Argentina. Sediment Geol 294:342–355

Folguera A, Iannizzotto NF (2004) The lagos La Plata and Fontana fold-and-thrust belt: long-lived orogenesis at the edge of western Patagonia. J S Am Earth Sci 16:541–566

Folguera A, Ramos VA (2011) Repeated eastward shifts of arc magmatism in the Southern Andes: a revision to the long-term pattern of Andean uplift and magmatism. J S Am Earth Sci 32 (4):531–546

Folguera A, Orts D, Rojas Vera E, Encinas A, Sagripanti L, Tobal J, Ramos ME, Gianni G, Echaurren A, Fennell L, Colavitto B, Ramos VA (2014) Análisis general de los mecanismos que han construido Los Andes entre los 36° y 46°S. XIX Congreso Geológico Argentino (Córdoba), Electronic files

Franchi M, Page RFN (1980) Los basaltos Cretácicos y la evolución magmática del Chubut occidental. Rev Asoc Geol Argentina 35:208–230

Georgieff SM, Sosa Gómez JA, Ferreira L, Vides ME, Ibañez LM, Ovejero R, Bossi GE, Richter GAV, Anis KB, Pieroni EM, Moyano S (2009) Characterization of fluvial sandstones in the Cerro Guadal Norte oil field, Golfo San Jorge Basin, Santa Cruz, Argentina. In: 9th International conference on fluvial sedimentology (San Miguel de Tucumán), pp 35–36

Ghiglione MC, Naipauer M, Sue C, Barberón V, Blampied JN, Ronda G, Ramos VA, Aguirre Urreta BA, Valencia V (2013) Early Cretaceous (Aptian) uplift of Patagonia recorded on zircons detrital content from the northern Austral-Magallanes basin. Bolletino di Geofisica Teorica ed Applicata. Electronic Files, pp 64–66

Giacosa RE, Paredes JM, Nillni A, Ledesma M, Colombo F (2004) Fallas normales de alto ángulo en el Neógeno del margen Atlántico de la Cuenca del Golfo San Jorge (46°S–67° 30 O, Patagonia Argentina). Bol Geol y Min 115(3):537–550

Giacosa R, Zubia M, Sánchez M, Allard J (2010) Meso-Cenozoic tectonics of the southern Patagonian foreland: Structural evolution and implications for Au–Ag veins in the eastern Deseado Region (Santa Cruz, Argentina). J S Am Earth Sci 30:134–150

orlando_a_p@yahoo.com.ar

Gianni G, Navarrete C, Orts D, Tobal J, Folguera A, Giménez M (2015) Patagonian broken foreland and related synorogenic rifting: the origin of the Chubut Group Basin. Tectonophysics. doi:10.1016/j.tecto.2015.03.006

Guillaume B, Moroni M, Funiciello F, Martinod J, Faccenna C (2010) Mantle flow and dynamic topography associated with slab window opening: insights from laboratory models. Tectonophysics 496:83–98

Hechem JJ (1998) Arquitectura y paleodrenaje del Sistema Fluvial efímero de la Formación Bajo Barreal, Cuenca del Golfo San Jorge, Argentina. Bol Inf Pet 53:21–27

Hechem JJ, Strelkov E (2002) Secuencia sedimentaria mesozoica del Golfo San Jorge. In: Haller MJ (ed) Geología y Recursos Naturales de Santa Cruz. Relatorio del XV Congreso Geológico Argentino: 1–9

Hechem JJ, Homovc JF, Figari EG (1990) Estratigrafía del Chubutiano en las Sierras de San Bernardo, Cuenca del Golfo San Jorge, Chubut, Argentina. XI Congreso Geológico Argentino (San Miguel de Tucuman). Actas 2:173–176

Heintz M, Debayle E, Vauchez A (2005) Upper mantle structure of the South American continent and neighboring oceans from surface wave tomography. Tectonophysics 406:115–139

Hervé F (1988) Late Paleozoic subduction and accretion in southern Chile. Episodes 11 (3):183–188

Herve F, Fanning CM (2001) Late Triassic detrital zircons in meta-turbidites of the Chonos metamorphic complex, southern Chile. Rev Geol Chile 28:91–104

Hervé F, Pankhurst RJ, Drake R, Beck ME (1995) Pillow basalts in a mid-tertiary extensional basin adjacent to the Liquiñe Ofqui fault zone: the Isla Magdalena area, Aysén, Chile. J S Am Earth Sci 8:33–46

Hervé F, Pankhurst R, Demant A, Ramirez E (1996) Age and Al-in-Hornblende geobarometry in the North Patagonian batholith. In: 3rd international symposium of Andean geodynamics (St Malo), pp 579–581

Hervé F, Demant A, Ramos VA, Pankhurst RJ, Suárez M (2000) The Southern Andes. In: Cordani UG, Milani EJ, Thomaz Filho, A (eds) Tectonic evolution of South America, pp 605–634

Hervé F, Calderón M, Faúndez V (2008) The metamorphic complexes of the Patagonian and Fuegian Andes. Geol Acta 6:43–53

Homovc JF, Constantini L (2001) Hydrocarbon exploration potential within intraplate shear-related depocenters: Deseado and San Julián basins, southern Argentina. Am Assoc Petrol Geol Bull 85:1795–1816

Homovc J, Conforto G, Lafourcade P, Chelotti L (1995) Fold belt in the San Jorge Basin, Argentina: an example of Tectonic inversion. In: Buchanan P, Buchanan J (eds) Basin inversion, Geol Soc London, Special Publication, pp 235–248

Homovc J, Navarrete C, Marshall P, Masquere S, Cerdan J (2011) Inversión tectónica intra-cretácica de la Subcuenca de Río Mayo, Chubut, Argentina. XVIII Congreso Geológico Argentino (Neuquén), Actas, pp 1418–1419

Iannizzotto NF, Folguera A, Leal PR (2004) Control tectónico de las secuencias volcaniclásticas neocomianas y paleogeografía en la zona del Lago La Plata (45°S). Sector interno de la faja plegada y corrida de los lagos La Plata y Fontana. Rev Asoc Geol Argentina 59:655–670

Jordan T, Burns W, Veiga R, Pángaro F, Copeland P, Kelley S, Mpodozis C (2001) Extension and basin formation in the Southern Andes caused by increased convergence rate: a Mid-Cenozoic trigger for the Andes. Tectonics 20:308–324

Kaeding M, Forsythe RD, Nelson EP (1990) Geochemistry of the Taitao ophiolite and near-trench intrusions from the Chile Margin Triple Junction. J S Am Earth Sci 3:161–177

Kay SM, Ardolino AA, Gorring ML, Ramos VA (2007) The Somuncura large igneous Province in Patagonia: interaction of a transient mantle thermal anomaly with a subducting slab. J Petrol 48:43–77

Lesta PJ (1968) Estratigrafía de la Cuenca del Golfo San Jorge. III Jornadas Geológicas Argentinas (Buenos Aires), Actas: 251–289

orlando_a_p@yahoo.com.ar

Lesta P, Ferello R (1972) Chubut extraandino. In: Leanza A (ed) Academia Nacional de Ciencias. Córdoba, Geología Regional Argentina, pp 601–653

Lesta P, Ferello R, Chebli G (1980) Chubut extraandino. In: Turner JC (ed) II Simposio de Geología Regional Argentina. Córdoba, Academia Nacional de Ciencias, pp 1307–1387

Maloney KT, Clarke GL, Klepeis KA, Quevedo L (2013) The Late Jurassic to present evolution of the Andean margin: drivers and the geological record. Tectonics 32:1049–1065

Marques M, Navarrette C (2011) La tectónica compresiva pre-Aptiana-Albiana en la sierra de Pichiñañez, Chubut, Argentina. XVIII Congreso Geológico Argentino (Neuquén), Actas: 105–106

Marshall LG, Salinas P (1990) Stratigraphy of the Río Frías Formation (Miocene), along the Alto Río Cisnes, Aisén, Chile. Rev Geol Chile 17:57–87

Marshall LG, Drake RE, Curtis GH, Butler RF, Flanagan KM, Naeser CW (1986) Geochronology of type Santacrucian (middle Tertiary) land mammal age, Patagonia, Argentina. J Geol 449–457

Micucci EM, Continanzia J, Manceda R, Gavarrino AS (2011) Cuenca de San Julián: Síntesis del conocimiento exploratorio—visión actual. In: Legarreta L, Boll A, Marshall PA (eds) Kozlowski E. VIII Congreso de Exploración y Desarrollo de Hidrocarburos, Simposio Cuencas Argentinas Visión Actual, pp 17–46

Mpodozis C, Hervé M, Nasi C, Soffia J, Forsythe R, Nelson E (1985) El Magmatismo Plioceno de Península Tres Montes y su relación con la Evolución del Punto Triple de Chile Austral. Rev Geol Chile 25–26

Musacchio EA, Chebli GA (1975) Ostrácodos no marinos y carófitas del Cretácico inferior en las provincias del Chubut y Neuquén, Argentina. Ameghiniana 12:70–96

Nelson E, Forsythe R, Diemer J, Allen M, Urbina O (1993) Taitao ophiolite: a ridge collision ophiolite in the forearc of the southern Chile (46°S). Rev Geol Chile 20:137–165

Olivero EB, Aguirre-Urreta MB (2002) Sucesión de amonoideos de la Formación Katterfeld (Valanginiano–Hauteriviano) en su área tipo, Lago Fontana, Chubut. XV Congreso Geológico Argentino (Calafate). Actas 1:485–490

Palazzesi L, Barreda V, Prieto AR (2003) Análisis evolutivo de la vegetación cenozoica en las provincias de Chubut y Santa Cruz (Argentina) con especial atención en las comunidades herbáceo-arbustivas. Rev Museo Argentino Cs Naturales 5:151–161

Pankhurst RJ, Leat PT, Sruoga P, Rapela CW, Márquez M, Storey BC, Riley TR (1998) The Chon Aike province of Patagonia and related rocks in West Antarctica: a silicic large igneous province. J Volcanol Geotherm Res 81:113–136

Pankhurst RJ, Weaver SD, Hervé F, Larrondo P (1999) Mesozoic-Cenozoic evolution of the North Patagonian Batholith in Aysén, southern Chile. J Geol Soc Am 156(4):673–694

Pankhurst RJ, Riley TR, Fanning CM, Kelley SP (2000) Episodic silicic volcanism in Patagonia and the Antarctic Peninsula: chronology of magmatism associated with the break-up of Gondwana. J Petrol 41:605–625

Pankhurst RJ, Hervé F, Fanning M, Suárez M (2003) Coeval plutonic and volcanic activity in the Patagonian Andes: the Patagonian Batholith and the Ibáñez and Divisadero Formations, Aisén, southern Chile. X Congreso Geológico Chileno (Concepción), Electronic files

Pankhurst RJ, Rapela CW, De Luchi ML, Rapalini AE, Fanning CM, Galindo C (2014) The Gondwana connections of northern Patagonia. Geol Soc Lond 171:313–328

Panza JL, Cobos JC, Zubia M, Franchi MR (2001) Hoja geológica 4769-III: Destacamento La María. Servicio Geológico Minero Nacional Boletín 296

Parada MA, Lahsen A, Palacios C (2001) Ages and geochemistry of Mesozoic-Eocene back-arc volcanic rocks in the Aysén region of the Patagonian Andes. Rev Geol Chile 28:25–46

Paredes JM, Foix N, Colombo Piñol F, Nillni A, Allard JO, Marquillas RA (2007) Volcanic and climatic controls on fluvial style in a high-energy system: the lower Cretaceous Matasiete formation, Golfo San Jorge basin, Argentina. Sediment Geol 202:96–123

Paredes JM, Colombo F, Foix N, Allard JO, Nillni A, Allo M (2008) Basaltic Explosive Volcanism in a tuff-dominated intraplate setting, sarmiento formation (Middle Eocene-lower Miocene), Patagonia Argentina. Lat Am J Sediment Basin Anal 15(2):77–92

orlando_a_p@yahoo.com.ar

Paredes JM, Plazibat S, Crovetto C, Stein J, Cayo E, Schiuma A (2013) Fault kinematics and depocenter evolution of oil-bearing, continental successions of the Mina del Carmen Formation (Albian) in the Golfo San Jorge basin, Argentina. J S Am Earth Sci 46:63–79

Perez Loinaze VS, Vera EI, Passalia MG, Llorens M, Friedman R, Limarino CO, Césari SN (2013) High-precision U-Pb zircon age from the Anfiteatro de Ticó Formation: implications for the timing of the early angiosperm diversification in Patagonia. J S Am Earth Sci 48:97–105

Peroni GO, Hegedus AG, Cerdan J, Legarreta L, Uliana MA (1995) Hydrocarbon accumulation in an inverted segment of the Andean Foreland : San Bernardo Belt, Central Patagonia. In: Tankard AJ, Suárez R, Welsink HJ (eds) Petroleum Basins of South America, pp 403–419

Proserpio CA (1978) Descripción Geológica de la Hoja 42d, Gastre, Provincia del Chubut (1:200000). Servicio Geológico Minero Nacional, Boletín 159:76

Quevedo L, Hansra B, Morra G, Butterworth N, Müller RD (2013) Oblique mid ocean ridge subduction modelling with the parallel fast multipole boundary element method. Comput Mech 51:455–463

Raigemborn MS (2006) Análisis composicional y procedencia de la Formación Peñas Coloradas, Grupo Río Chico (Paleoceno superior-Eoceno?), en la región oriental de la Cuenca del Golfo San Jorge, Chubut, Argentina. Lat Am J Sediment Basin Anal 13(2):119–133

Ramos VA (1981) Descripción geológica de la hoja 47 a b Lago Fontana, Provincia de Chubut. Servicio Geológico Minero Nacional, Boletín 183:130

Ramos VA (1982) Geología de la región del lago Cardiel, provincia de Santa Cruz. Rev Asoc Geol Argentina 37:23–49

Ramos VA (1999) Los depósitos sinorogénicos terciarios de la Región Andina. In: Caminos R (ed). Geología Argentina. Instituto de Geología y Recursos Minerales, Anales 29: 651–682

Ramos VA (2002) Evolución tectónica. In: Haller MJ (ed), Geología y Recursos Naturales de La Provincia de Santa Cruz, Relatorio XV Congreso Geológico Argentino (Calafate): 365–390

Ramos VA, Kay SM (1992) Southern Patagonian plateau basalts and deformation: back-arc testimony of ridge collision. Tectonophysics 205:261–282

Ramos VA, Naipauer M (2014) Patagonia: where does it come from? J Iber Geol 40:367–379

Ranalli JN, Peroni GO, Boggetti DA, Manoni R (2011) Cuenca Cañadón Asfalto. Modelo tectosedimentario. In: Kozlowski E, Legarreta L, Boll A, Marshall PA (eds) VIII Congreso de Exploración y Desarrollo de Hidrocarburos, Simposio Cuencas Argentinas Visión Actual, pp 185–216

Remesal MB, Salani FM, Cerredo ME (2012) Petrología del complejo volcánico Barril Niyeu (Mioceno inferior). Patagonia Argentina. Rev Mex Ciencias Geológicas 29(2):463–477

Rodriguez JF, Littke R (2001) Petroleum generation and accumulation in the Golfo San Jorge Basin, Argentina: a basin modeling study. Mar Petrol Geol 18(9):995–1028

Rolando A, Hartmann L, Santos J, Fernández R, Etcheverry R, Schalamuk I, McNaughton N (2002) SHRIMP zircon U-Pb evidence for extended Mesozoic magmatism in the central Patagonian batholith and assimilation of Archean crustal components. J S Am Earth Sci 15 (2):267–283

Rolando A, Hartmann L, Orestes J, Fernandez R, Etcheverry R, Schalamuk I, McNaughton N (2004) SHRIMP U-Pb zircon dates from igneous rocks from the Fontana Lake region, Patagonia: implications for the age of magmatism, Mesozoic geological evolution and age of basement. Rev Asoc Geol Argentina 59(4):671–684

Ruiz L, Scasso RA, Aberhan M, Kiessling W, Bande A, Medina F, Weidemeyer S (2005) La Formación Lefipán en el Valle Medio del Río Chubut: ambientes sedimentarios y su relación con la tectónica del Cretácico Tardío-Paleoceno. XVI Congreso Geológico Argentino (La Plata). Actas 3:231–238

Scalabrino B, Lagabrielle Y, Malavieille J, Dominguez S, Melnick D, Espinoza F, Suarez M, Rossello E (2010) A morphotectonic analysis of central Patagonian Cordillera: negative inversion of the Andean belt over a buried spreading center? Tectonics 29. doi:10.1029/2009TC002453

Sciutto JC (1981) Geología del Codo del Río Senguerr, Chubut, Argentina. VIII Congreso Geológico Argentino (San Luis). Actas 3:544–568

orlando_a_p@yahoo.com.ar

Sengor AMC, Burke K, Dewey JF (1978) Rifts at high angles to orogenic belts; tests for their origin and the Upper Rhine Graben as an example. Am J Sci 278(1):24–40

Seton M, Müller RD, Zahirovic S, Gaina C, Torsvik T, Shephard G, Talsma A, Gurnis M, Turner M, Maus S, Chandler M (2012) Global continental and ocean basin reconstructions since 200 Ma. Earth Sci Rev 113:212–270

Silva C, Herrera C, Hervé F (2003) Petrogénesis de lavas y diques básicos de la Formación Traiguén, Región de Aysén (43°30′-46°S), Chile. X Congreso Geológico Chileno (Concepción), Actas, Electronic files: p 11

Silva Nieto D (2005) Hoja Geológica 4369-III, Paso de Indios, provincia del Chubut. Servicio Geológico Minero Nacional, Boletín 265:72

Suárez M, De la Cruz R (2001) Jurassic to Miocene K-Ar dates from eastern central Patagonian Cordillera plutons, Chile (45°–48°S). Geol Mag 138:53–66

Suárez M, De La Cruz R, Bell M (1996) Estratigrafía de la región de Coyhaique (45°–46° latitud S); Cordillera Patagónica, Chile. XIII Congreso Geológico Argentino and III Congreso de Exploración de Hidrocarburos (Buenos Aires): 575–90

Suárez M, De La Cruz R, Bell MC (2007) Geología del Area Ñireguao-Baño Nuevo, Región Aisén del General Carlos Ibáñez del Campo. Servicio Nacional de Geología y Minería, Carta Geológica de Chile, Serie Geología Básica 108:56

Suárez M, De La Cruz R, Bell M, Demant A (2009a) Cretaceous slab segmentation in southwestern Gondwana. Geol Mag 147:193–205

Suárez M, Márquez M, De La Cruz R, Fanning M (2009b) Aptian-Albian subaerial volcanic rocks in central Patagonia: Divisadero and Chubut Groups. XII Congreso Geológico Chileno (Santiago de Chile): 1–4

Suárez M, Márquez M, De La Cruz R, Navarrete C, Fanning M (2014) Cenomanian-? Early Turonian minimum age of the chubut group, Argentina: SHRIMP U-Pb geochronology. J S Am Earth Sci 50:64–74

Sylwan CA (2001) Geology of the Golfo San Jorge Basin, Argentina. J Iber Geol 27:123–157

Tassara A, Echaurren A (2012) Anatomy of the Andean subduction zone: three-dimensional density model upgraded and compared against global-scale models. Geophys J Int 189:161–168

Taylor B (2006) The single largest oceanic plateau: Ontong Java–Manihiki–Hikurangi. Earth Planet Sci Lett 241:372–380

Thomson SN (2002) Late Cenozoic geomorphic and tectonic evolution of the Patagonian Andes between latitudes 42°S and 46°S: an appraisal based on fission-track results from the transpressional intra-arc Liquiñe-Ofqui fault zone. Geo Soc Am Bull 114:1159–1173

Thomson SN, Hervé F, Stöckhert B (2001) Mesozoic Cenozoic denudation history of the Patagonian Andes (southern Chile) and its correlation to different subduction processes. Tectonics 20:693–711

Thomson SN, Brandon MT, Tomkin JH, Reiners PW, Vásquez C, Wilson NJ (2010) Glaciation as a destructive and constructive control on mountain building. Nature 467:313–317

Tunik MA, Vietto ME, Sciutto JC (2004) Procedencia de areniscas del Grupo Chubut en el área central de la Sierra de San Bernardo. Análisis preliminar. Rev Asoc Geol Argentina 59:601–606

Umazano AM, Bellosi ES, Visconti G, Jalfin GA, Melchor RN (2009) Sedimentary record of a Late Cretaceous volcanic arc in central Patagonia: petrography, geochemistry and provenance of fluvial volcaniclastic deposits of the Bajo Barreal Formation, San Jorge Basin, Argentina. Cretac Res 30:749–766

Umazano AM, Bellosi ES, Visconti G, Melchor RN (2012) Detecting allocyclic signals in volcaniclastic fluvial successions: Facies, architecture and stacking pattern from the Cretaceous of central Patagonia, Argentina. J S Am Earth Sci 40:94–115

Uliana MA, Biddle KT, Cerdan J (1989) Mesozoic extension and the formation of Argentine sedimentary basins. In: Tankard AJ, Balkwill HR (eds) Extensional tectonics and stratigraphy of the North Atlantic Margin: p 599–613

orlando_a_p@yahoo.com.ar

Vaughan AP (1995) Circum-Pacific mid-Cretaceous deformation and uplift: a superplume-related event? Geology 23:491–494

Vicente JC (2005) Dynamic paleogeography of the Jurassic Andean Basin: pattern of transgression and localization of main straits through the magmatic arc. Rev Asoc Geol Argentina 60:221–250

Zaffarana CB, Lagorio SL, Somoza R (2012) Paleomagnetism and geochemistry from the upper cretaceous Tres Picos Prieto locality (43°S), Patagonian Plateau basalts. Andean Geol 39 (1):53–66

Zambrano JJ, Urien CM (1970) Geological outline of the basins in Southern Argentina and their continuation off the Atlantic shore. J Geophys Res 75:1363–1396

orlando_a_p@yahoo.com.ar

Growth of the Southern Patagonian Andes (46–53°S) and Their Relation to Subduction Processes

Matías C. Ghiglione, Victor A. Ramos, José Cuitiño and Vanesa Barberón

Abstract The Cretaceous-Cenozoic evolution of the Southern Patagonian Andes is one of the most prominent examples of coupling between subduction processes and climatic, magmatic, deformational, and sedimentary events. Three orogenic and magmatic cycles can be particularly related to processes in the subduction zone (1) Late Cretaceous closure of the Rocas Verdes marginal basin, (2) Paleogene collision of the Farallón-Aluk seismic ocean ridge, and (3) Miocene subduction of the Chile seismic ridge beneath South America. Andean orogenic growth started during Late Cretaceous times, in a tectonic scenario that included the Rocas Verdes back-arc oceanic basin, widening from 49°S toward the south. The Andean segment south of 49°S experienced a strong Cenomanian–Santonian deformational event during the closure of the back-arc basin and progressive subduction of its ocean floor. The final closure produced the Coniacian–Santonian exhumation of the Sarmiento Ophiolitic Complex and propagation of the orogenic front toward the foreland. The second cycle, during Paleogene deformation, coincided with an Eocene volcanic arc gap, and seems to be related to the Fallarón-Phoenix seismic ridge collision. The resulting slab window produced OIB volcanic plateaux represented by the Chile Chico and Posadas Basalts, erupted in the foothills and retroarc. The third cycle of accelerated Andean uplift started during the Oligocene, as a consequence of orthogonal and fast subduction of young lithosphere, while the Chile seismic ridge between Antarctica and Nazca was approaching the trench. Kinematic plate reconstructions show that at approximately 14–18 Ma the Chile oceanic ridge entered the South America trench and migrated northward from 53°S to its present-day position at 46°S. The early Miocene ridge collision and resulting

M.C. Ghiglione (✉) · V.A. Ramos · V. Barberón
Departamento de Ciencias Geológicas, Facultad de Ciencias Exactas y Naturales, Instituto de Estudios Andinos "Don Pablo Groeber" UBA-CONICET, Buenos Aires, Argentina
e-mail: mcghiglione@gmail.com

J. Cuitiño
Departamento de Ciencias Geológicas, Facultad de Ciencias Exactas y Naturales, Instituto de Geociencias Básicas, Aplicadas y Ambientales (IGEBA) UBA-CONICET, Buenos Aires, Argentina

© Springer International Publishing Switzerland 2016

A. Folguera et al. (eds.), *Growth of the Southern Andes*,
Springer Earth System Sciences, DOI 10.1007/978-3-319-23060-3_10

orlando_a_p@yahoo.com.ar

slab window produced an extensive OIB magmatism between 10 and 3 Ma in extra-Andean Patagonia. The space-time unraveling of tectonic uplift is well known from geochronometers, and shows a migration from the basement domain to the external fold and thrust belt accompanied by lower Miocene synorogenic sedimentation. Orogenic growth led to middle Miocene rain shadow in the foothills, followed by the late Miocene—Pliocene desertification of Patagonia.

Keywords Patagonian andes · Patagonia · Austral basin · Magallanes basin · Rocas verdes basin · Fold and thrust belt · Subduction zone · Ridge subduction · Phoenix plate · Farallon plate

1 Introduction

The evolution of the Southern Patagonian Andes involved three main orogenic cycles with foreland sedimentation in the Austral or Magallanes basin (Fig. 1). Each orogenic cycle was related to a particular subduction scenario, including the closure of the Rocas Verdes marginal basin during the Late Cretaceous (Dalziel 1986; Ramos 1989), and Paleocene and Miocene ridge collisions (Cande and Leslie 1986; Ramos and Kay 1992). While the Late Cenozoic cycle affected the entire orogen, the initial Late Cretaceous orogeny took place only along the section influenced by the Rocas Verdes Basin south of 49° (Ghiglione et al. 2014a), controlling the age distribution of foreland sequences (Figs. 2 and 3). The Paleogene orogenic cycle occurred during the Farallón ridge subduction (Cande and Leslie 1986; Somoza and Ghidella 2012), which generated Eocene volcanic Mesetas (basaltic plateux) in Patagonia (Ramos 1989, 2005; Espinoza et al. 2005), and the eastward advance of the orogenic front and the foreland basin system.

At the end of the Early Cretaceous, the Pacific margin of Patagonia was concluding an extensional phase, characterized by the Jurassic development of the Rocas Verdes back-arc basin, that produced oceanic floor from 49°S and widened toward the south, in continuity with the Weddell Sea (Fig. 4a) (Katz 1973; Dalziel et al. 1974; Dalziel 1981; Stern et al. 1991). Orogenic growth and related foreland sedimentation began during basement uplift and erosion due to the closure of the Rocas Verdes basin, as shown by first detrital input into the Austral basin at around ~101–88 Ma (Wilson 1991; Fildani et al. 2003; Varela et al. 2012; McAtamney et al. 2011). The Late Cretaceous collision of the drifted rim of the marginal basin against the Patagonian craton (Fig. 4b) (Stern and de Witt 2003) produced a Coniacian–Santonian 80 km advance of the orogenic front (Ghiglione et al. 2014a) together with obduction and a 8 km exhumation of the Sarmiento Ophiolitic Complex in the inner cordillera (Calderón et al. 2012). As a result, the Andean orogen south of 49° was around 180 km wide at the end of the Campanian (Fosdick et al. 2011; Ghiglione et al. 2014a) and a more than 5000-m-thick foreland sedimentary sequence was already deposited in the Austral-Magallanes basin (Katz 1973; Wilson 1991).

orlando_a_p@yahoo.com.ar

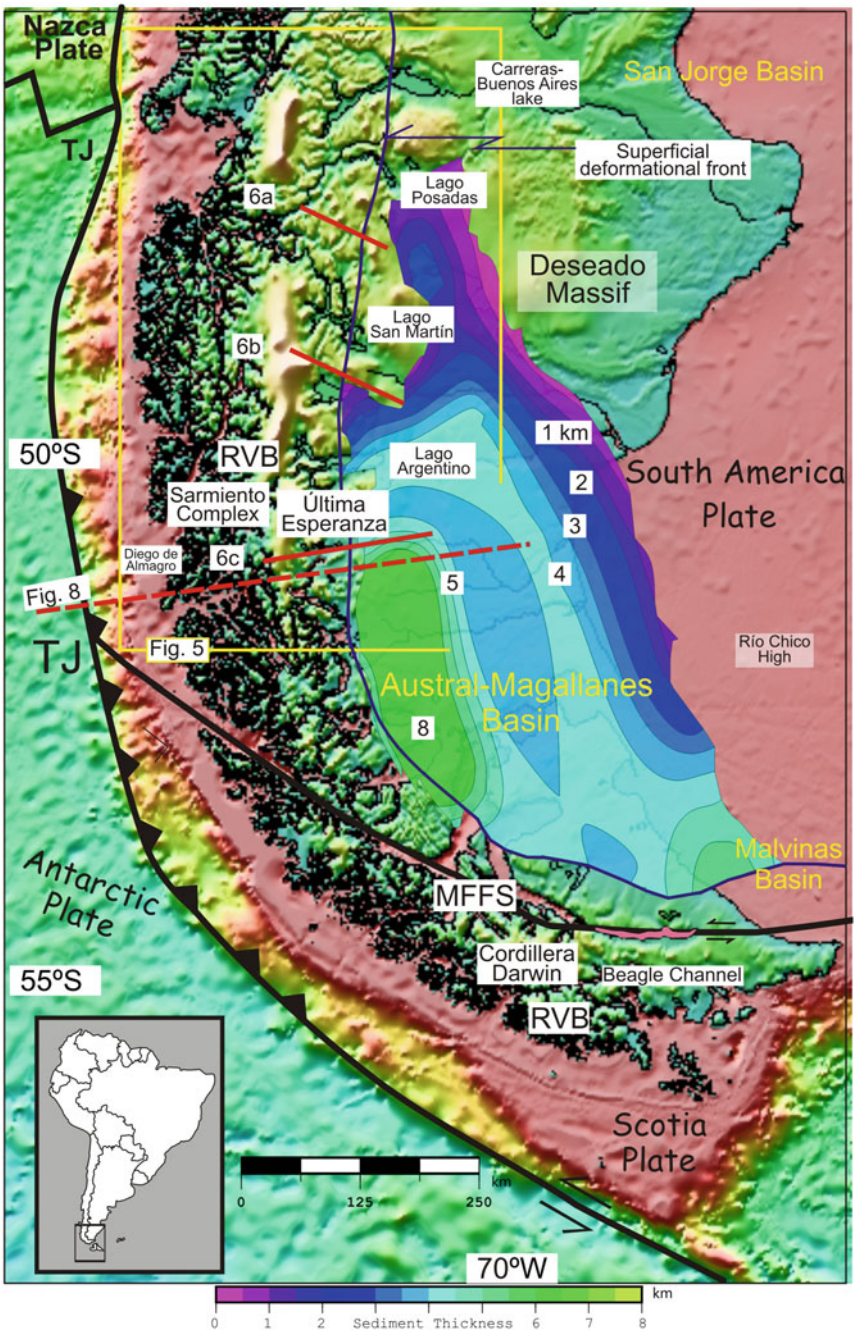


Fig. 1 Location map. *FTB* fold and thrust belt; *RVB* Rocas Verdes Marginal Basin; *TJ* Triple Junction; *MFFS* Magallanes-Fagnano fault zone. Modified from Ghiglione et al. (2010, 2014a)

orlando_a_p@yahoo.com.ar

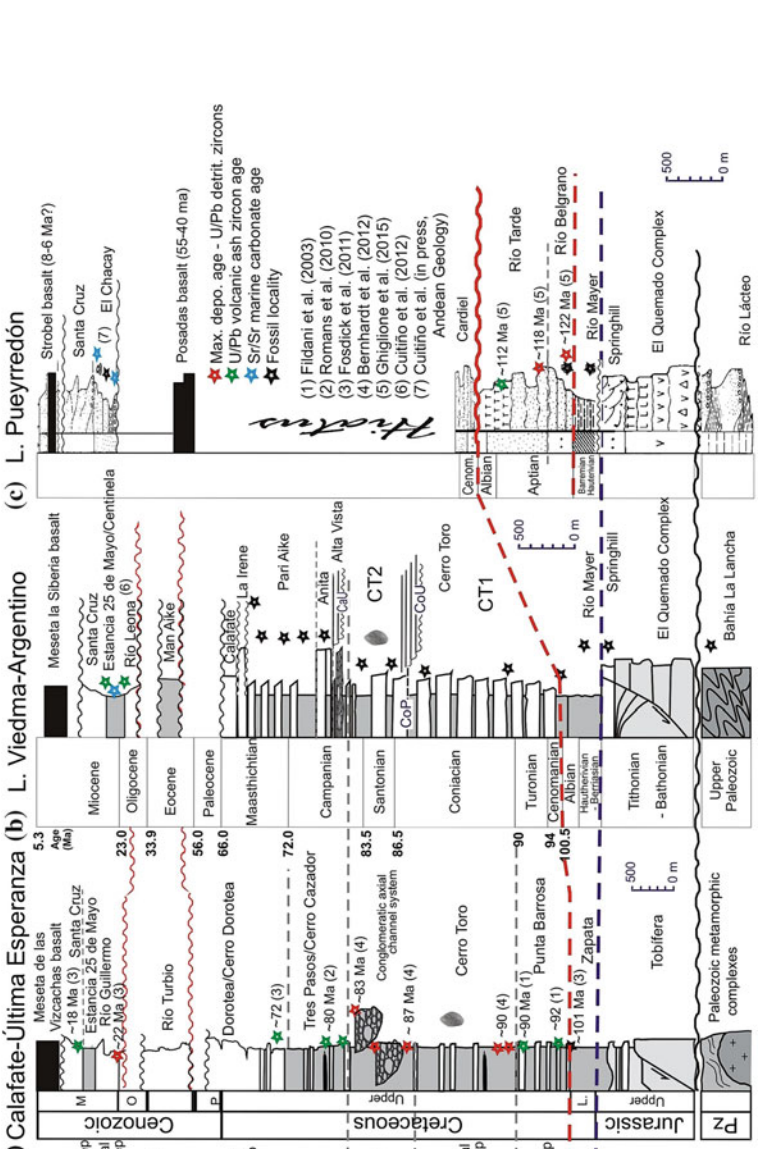


Fig. 2 Simplified stratigraphic columns across the Southern Patagonian Andes with location (**a**–**c**) shown in Fig. 3, and their correlation: **a** representative of Última Esperanza and Río Turbio sectors from Malumián et al. (2000) and Fosdick et al. (2011). **b** Sector between Argentino and Viedma lakes modified from Ghiglione et al. (2014a) after Kraemer and Riccardi (1997). **c** Column from Posadas lake modified from Ramos (1989). *CaU* Campanian syntectonic angular unconformity; *CoU* Coniacian syntectonic angular unconformity; *CoP* Coniacian Paraconformity

orlando_a_p@yahoo.com.ar

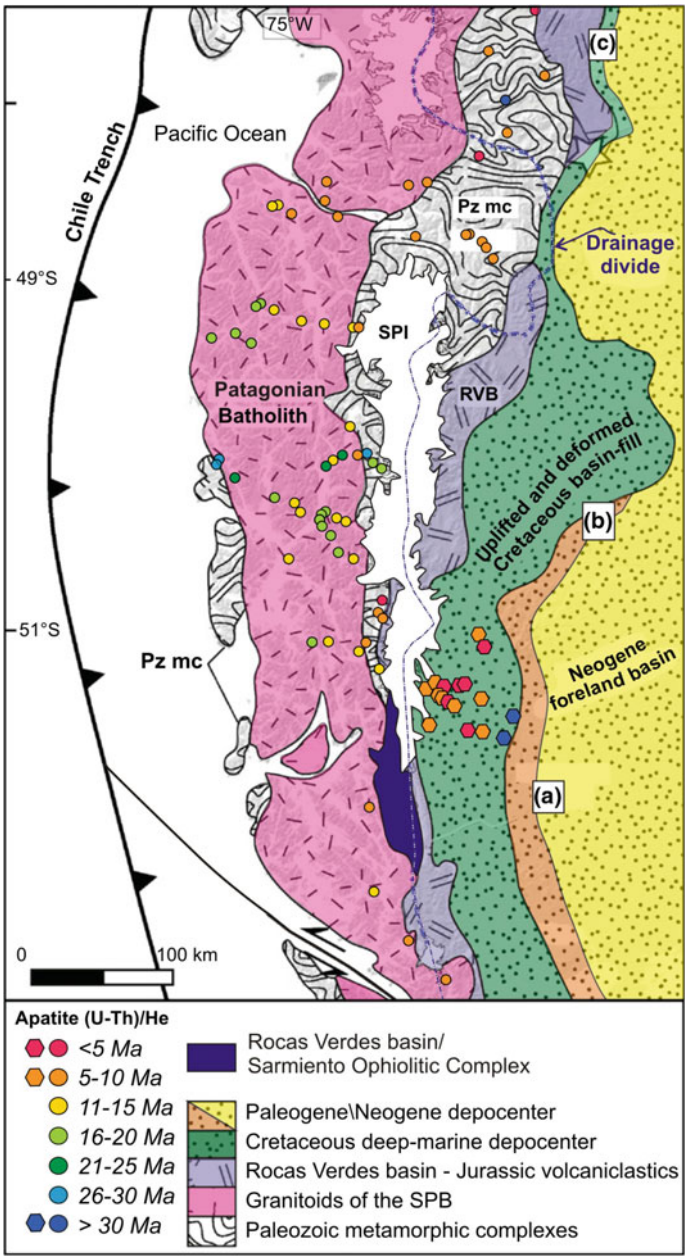


Fig. 3 Simplified lithotectonic units. (U–Th)/He ages from Fosdick et al. (2013) (*hexagons*) and Thomson et al. (2010) (*circles*). *SPI* Southern Patagonian Ice Field. Letters *a–c* indicate columns from Fig. 2. Modified from Fosdick et al. (2013)

orlando_a_p@yahoo.com.ar

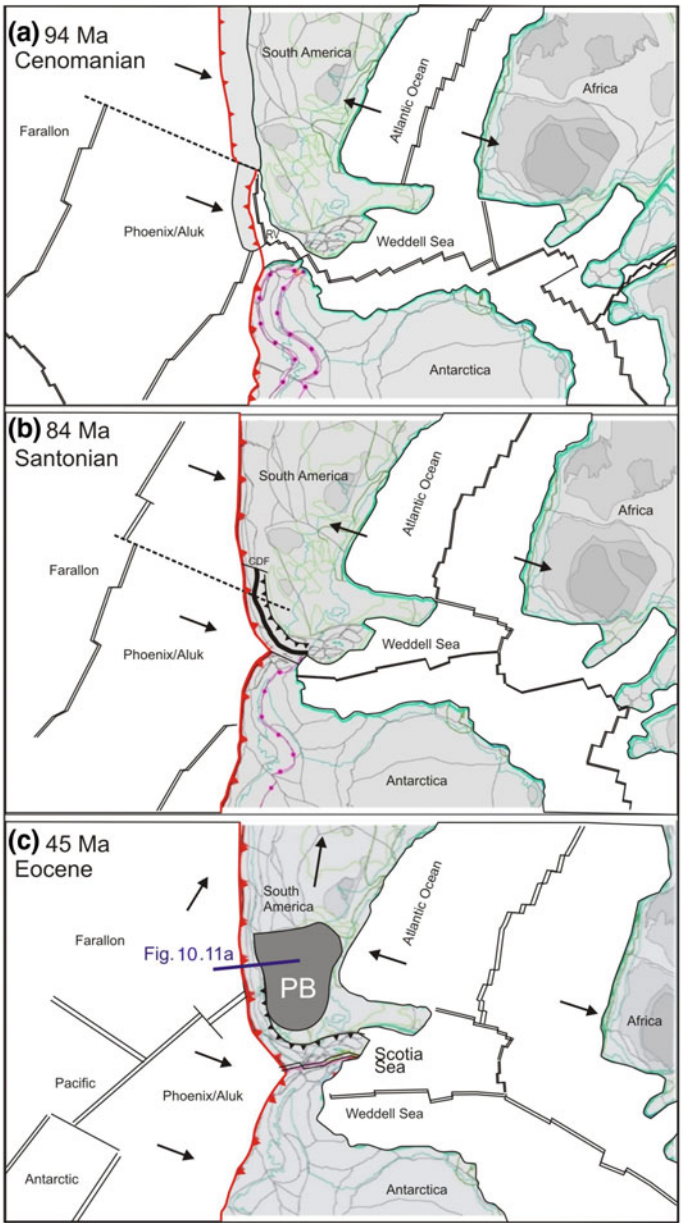


Fig. 4 Paleotectonic reconstructions for **a** *94 Ma* Final stages of Rocas Verdes basin closure, **b** *84 Ma* Basin closure trough collision of its western margin. *RV* Rocas Verdes Basin. **c** *45 Ma* Collision of Farallón-Phoenix seismic ridge. Distribution and convergence of Pacific oceanic plates is from Somoza and Ghidella (2012), and South America vectors from Somoza and Zaffarana (2008)

orlando_a_p@yahoo.com.ar

The ensuing Cenozoic evolution of the Southern Patagonian Andes is also intimately related to variable subduction processes and resulting magmatic, sedimentary and deformational events. One of the key points is that sustained subduction-related magmatism produced a characteristic continuous batholithic belt now outcropping in the windward side of the Andes (Figs. 5 and 6) (Ramos et al. 1982; Pankhurst et al. 1999; Hervé et al. 2007; Ramos and Ghiglione 2008).

Paleogene deformation retreated to the basement domain (Kraemer 1998), until the collision of the Farallon-Phoenix ridge during the middle Eocene (Fig. 4c) (Cande and Leslie 1986; Somoza and Ghidella 2005, 2012) that produced the reactivation of the orogenic front as shown by syntectonic angular unconformities and growth-strata at Río Turbio (Malumián et al. 2000). While there is scarce dated plutonic activity with Paleocene or Eocene ages (Suárez and de la Cruz 2001; Hervé et al. 2007), extensive volcanic plateaux represented by the Posadas Basalt were erupted between 44° and 52°S in the foothills and in extra-Andean Patagonia (Ramos and Kay 1992; Kay et al. 2002; Espinoza et al. 2005), coinciding in time and space with the region affected by the ridge subduction (Fig. 4c). The orogenic wedge widened (Kraemer 1998; Fosdick et al. 2011) while the active thrust front propagated to the east (Malumián et al. 2000). The sedimentary response was limited to a 600-m-thick molasse sequence of the Río Turbio and Man Aike Formations (Fig. 2b) (Kramer 1998; Malumián et al. 2000).

The Late Cenozoic evolution of the Southern Patagonian Andes and adjacent Patagonia is one of the most prominent examples of coupling between tectonic processes and climate, which can be unfolded as a series of events taking place since the Oligocene. During the period of normal subduction preceding ridge subduction (Gorring et al. 1997), the volcanic arc was active on the retroarc, now represented by some of the most world famous granite peaks like the Fitz Roy (3405 m, 17 Ma, Ramirez de Arellano et al. 2012) and Torres del Paine (2885 m; 12 Ma, Michel et al. 2008). The Chile ridge-collision was responsible for most of the magmatic and morphotectonic features recognized in the Patagonian Cordillera and extra-Andean Patagonia. The opening of an asthenospheric slab window resulting from slab breakoff produced the extensive Mio-Pliocene Patagonian basaltic Mesetas (Ramos and Kay 1992; Gorring et al. 1997; Espinoza et al. 2005; Lagabrielle et al. 2004; Guivel et al. 2006). Regional Oligocene exhumation across the orogen, was followed by late Miocene propagation of the eastern fold and thrust belt (Thomson et al. 2010; Fosdick et al. 2013). Initial subsidence produced a major Miocene transgression affecting Patagonia, known as Patagoniano, while fast infilling of the accommodation space resulted in progradation of synorogenic fluvial deposits of the Santa Cruz Formation from ~19 to 14 Ma (Blisniuk et al. 2005, Fosdick et al. 2011; Cuitiño et al. 2012).

We will first present a brief summary of the geological framework that preceded orogenesis. The account is arranged chronologically, and some debatable subjects are developed along the sections, while they are also reviewed on the discussion section.

orlando_a_p@yahoo.com.ar

2 Structure of the Southern Patagonian Andes

The structure of the Southern Patagonian Andes can be divided into three tectonomorphic zones, including from west to east (after Kraemer 1998; Coutand et al. 1999; Kraemer et al. 2002; Ghiglione et al. 2009, 2010; Giacosa et al. 2012) (Fig. 6): the Basement thick-skinned brittle domain, the Internal ductile fold and thrust belt and the External fold and thrust belt.

The Basement domain includes Paleozoic metamorphic rocks of the Bahía La Lancha and Río Lácteo Formations (Fig. 2) (Poiré et al. 1999; Giacosa et al. 2012). The Late Jurassic synrift deposits uncomformably overlie the Paleozoic basement near its eastern boundary, while all the sequence is intruded by Jurassic to Neogene calc-alkaline magmatic arc rocks from the Patagonian Batholith (Fig. 5) (Hervé et al. 2007; Calderón et al. 2007). The Upper Jurassic rocks form elongated outcrops with a N to NNE trend that represent an inverted main extensional depocenter, thrust toward the east over the fold and thrust belt (Kraemer 1998; Ghiglione et al. 2009, 2014a). In this sector there are westward verging back-thrusts uplifting eastward-thinning Jurassic synrift deposits, indicating the total inversion of an extensional depocenter along the western boundary (Kraemer 1998).

The internal fold and thrust belt is composed of ductile structures, characterized by N-S trending thrusts, back-thrusts and folds. The structural packages involved are mainly Upper Cretaceous foreland sequences (Fig. 6b, c). There are strong along-strike variations in width of the Internal domain that take place in discrete ~E–W transition zones (Ghiglione et al. 2009), especially noticeable on the southern shore of Lago Argentino (Fig. 5). In the northern sector of the basin, the Internal domain as defined here losses expression, and is replaced by a triangle zone where the Paleozoic basement interacts directly with the external fold and thrust belt (Fig. 6c).

The external thin-skinned domain, involving Late Cretaceous to Miocene sequences (Arbe 1989, 2002; Kraemer and Riccardi 1997), is thrust with westward vergence forming a frontal monocline, while thin-skinned folds and thrust with eastward vergence are developed to the east (Fig. 6). The structural style of the external domain is that of a monocline developing a triangle zone, where Maastrichtian to Cenozoic sequences are thrust to the west, over an Upper Cretaceous epidermic wedge (Ghiglione et al. 2009).

3 Late Paleozoic—Early Mesozoic Geological Framework

The metamorphic basement of the region (Fig. 5) was generated from Late Paleozoic to Early Mesozoic times as an accretionary prism developed along the Pacific margin of Gondwana (Dalziel 1981; Hervé et al. 1981). The western Basement domain is composed of the Paleozoic Eastern Andes Metamorphic

orlando_a_p@yahoo.com.ar

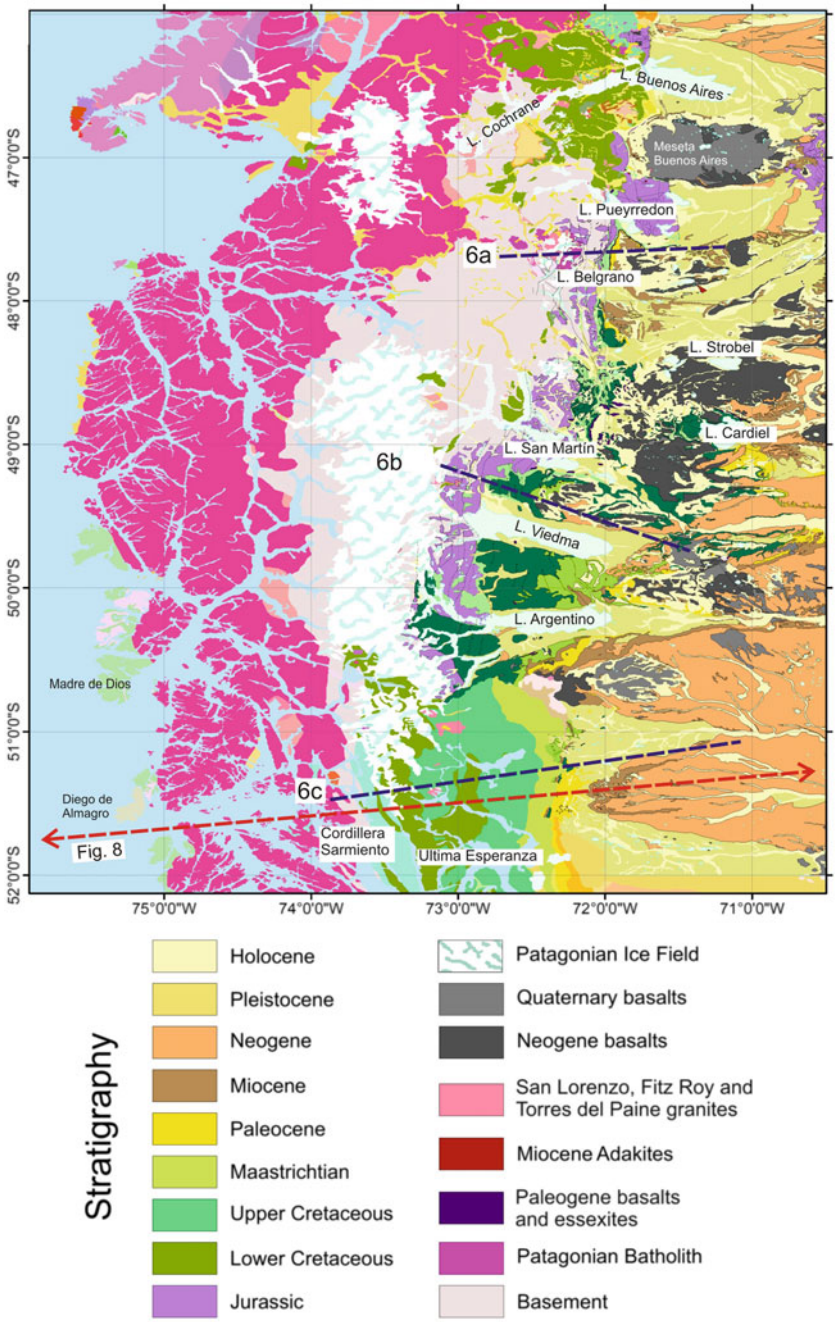


Fig. 5 Geologic map of the Southern Patagonian Andes at 1:1,000,000 scale, compiled from SERNAGEOMIN (2003) and SEGEMAR (2003)

orlando_a_p@yahoo.com.ar

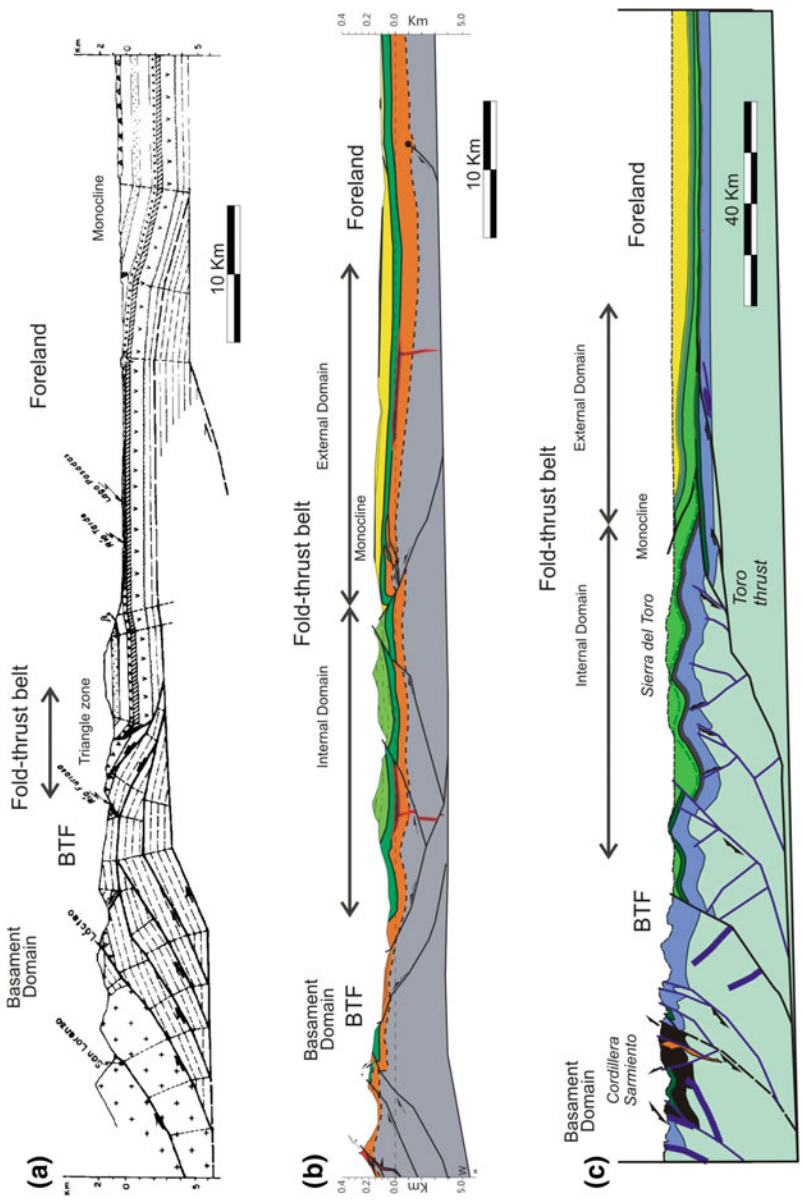


Fig. 6 Cross sections with location shown in Figs. 1 and 5: **a** Lagos Belgrano-Posadas, from Ramos (1989), **b** Lago Viedma, from Giacosa et al. (2012) and **c** Última Esperanza, from Ghiglione et al. (2014a). *BTF* Basement thrust front

orlando_a_p@yahoo.com.ar

Complex, including polideformed metaturbidites of Late Devonian to Late Permian age (Calderón et al. 2007).

Initial subsidence began in almost all of the Patagonian hydrocarbon-producing basins during the Triassic-Jurassic continental rifting of southern South America (Uliana et al. 1989). As a consequence, one of the largest known silicic igneous provinces (LIP) was formed in Patagonia, dominated by rhyolitic ignimbrites, which form a bimodal association with minor mafic and intermediated lavas (Pankhurst et al. 1998, 2000). A clear diachronism is recognized between the early Middle Jurassic volcanism of extra-Andean Patagonia (Marifil and Chon Aike formations) and the Middle-Late Jurassic volcanism of the Andean Cordillera (El Quemado and Tobífera Formations), showing a regular decrease of ages from the ENE (187 Ma) to the WSW (144 Ma) along 650 km (Pankhurst et al. 1998, 2000; Féraud et al. 1999). This progressive stretching culminated toward the SSW with the generation of oceanic crust in the Rocas Verdesmarginal basin along the Pacific margin of the continent during Late Jurassic times (Dalziel 1981; Mukasa and Dalziel 1996). The northern remnants of the sea floor and bimodal magmatism of the marginal basin are grouped into the Sarmiento Ophiolite Complex (Figs. 1 and 5) active between 152 and 142 Ma (Calderón et al. 2007).

The Late Jurassic extensional event produced NW to NNW trending depocenters controlled by normal faulting (Uliana et al. 1989; Baristeas et al. 2013; Ghiglione et al. 2013), filled up by an heterogeneous suite of siliceous volcanic and volcaniclastic rocks called El Quemado Complex in Argentina and Tobífera Formation in Chile (Fig. 2) (Thomas 1949). Toward the west, the Late Jurassic rocks form elongated outcrops with an N to NNE trend (Fig. 5) that represents an inverted main extensional depocenter (Fig. 6b, c).

The synrift sequences are uncomfortably overlain by extended lower Cretaceous sag deposits of the arenaceous Springhill and pelitic Zapata or Río Mayer formations (Fig. 2) recognized, respectively, as the main petroleum reservoir and source rocks of the Austral Basin.

4 Late Cretaceous Orogenic Cycle: Closure of Rocas Verdes Basin and Initiation of Foreland Basin Sedimentation South of 49°S

4.1 Tectonic Setting and Basement Uplift

The Aptian-Albian speeding up opening of the Atlantic Ocean (Rabinowitz and La Brecque 1979; Verard et al. 2012; Heine et al. 2013) produced intracontinental compressional stresses due to ridge-push forces and the uplift and denudation of extra-Andean Patagonia (Ghiglione et al. 2014b, 2015) during tectonic inversion of the Deseado and San Julián basins (Figueiredo et al. 1996; Soares et al. 2000; Homovc and Constantini 2001). The beginning of Late Cretaceous times ($\sim$100 Ma)

orlando_a_p@yahoo.com.ar

was a period of global reorganization of tectonic plates, involving an increase in spreading rate (Matthews et al. 2012), that initiated the orogenic growth of the Southern Patagonian Andes by accelerating the Pacific Ocean convergence rate against its western margin (Dalziel 1981, 1986; Ramos 1989; Verard et al. 2012). Accelerated convergence on the Pacific margin, plus a twofold increase in the South Atlantic spreading rate (Fig. 2 of Colli et al. 2014) produced the compressional state responsible for the progressive closure of the Rocas Verdes Basin during the middle of the Cretaceous (Fig. 4) (Halpern and Rex 1972; Halpern 1973; Dalziel et al. 1974; Bruhn and Dalziel 1977; Dalziel 1981, 1986; Hervé et al. 1981, 2007; Cunningham 1995).

Even though the Late Cretaceous deformational stage was also related to a ridge subduction by some authors (Ramos 2005), there are neither plate kinematic data for this period (Somoza and Ghidella 2012), nor evidence of retroarc magmatism, such as in the Paleogene and Neogene collisions (e.g., Figs. 4c and 7). A different hypothesis proposed a volcanic gap, deformation and closure of the Rocas Verdes Basin as result of flat-slab subduction (Stern et al. 1991; Suárez et al. 2000a; Suárez and de la Cruz 2001; Stern and de Witt 2003). However, even though there is a volcanic gap from 126 to 75 Ma, it only develops between ~48 and 51°, as shown by regional U–Pb SHRIMP zircon ages from the Patagonian Batholith (Hervé et al. 2007).

The onset of subduction conditions that ultimately led to the initiation of the marginal basin final closure, is indicated by the Barros Arana basalts (Albian, hornblende K/Ar age of 104 Ma) interpreted as mafic members of the mildly alkaline shoshonitic rock suite of subduction-related arcs, occurring within the sedimentary infill of the Rocas Verdes Basin (Stern et al. 1991).

The final history of the marginal basin has been recently well constrained by structural considerations and geochronological data of basement uplift and metamorphism. Age of metamorphism indicates that total closure took place approximately simultaneously on both its southern Fueguian Andes sector along the Beagle channel (prior to ~86 Ma; Klepeis et al. 2010) and on its northern, Patagonian rim, in Cordillera Sarmiento (at ~85 Ma; Calderón et al. 2012). The continued rise of the Southern Andes during the Coniacian also coincides with the westward acceleration of South America between 90 and 80 Ma (Somoza and Zafarana 2008).

An important mechanical aspect to be taken into account is that subduction of Rocas Verdes ocean floor during closure was directed toward the Pacific, beneath the western drifted magmatic arc (Fig. 4b) (Cunningham 1995; Hervé et al. 2007; Klepeis et al. 2010; Kraemer 2003; Calderón et al. 2012). This particular geometrical configuration produced the thrusting of the western margin and ophiolitic remains ramping on top of the continental craton during final closure (Fig. 8). In this manner, a small (~60-km wide) basement thrust wedge with cratonward vergence was created (Kraemer 2003; Klepeis et al. 2010; Calderón et al. 2012) that straightforwardly transferred shortening from the basement toward the foreland (Ghiglione and Cristallini 2007) along the Sarmiento Ophiolitic Complex (Figs. 6c and 8) and Beagle channel fault zone (Fig. 1). This pervasive structural configuration remained during the following pulses of Late Cretaceous and Cenozoic compressive deformation (Kraemer 2003), where tectonic basement uplift preceded

orlando_a_p@yahoo.com.ar

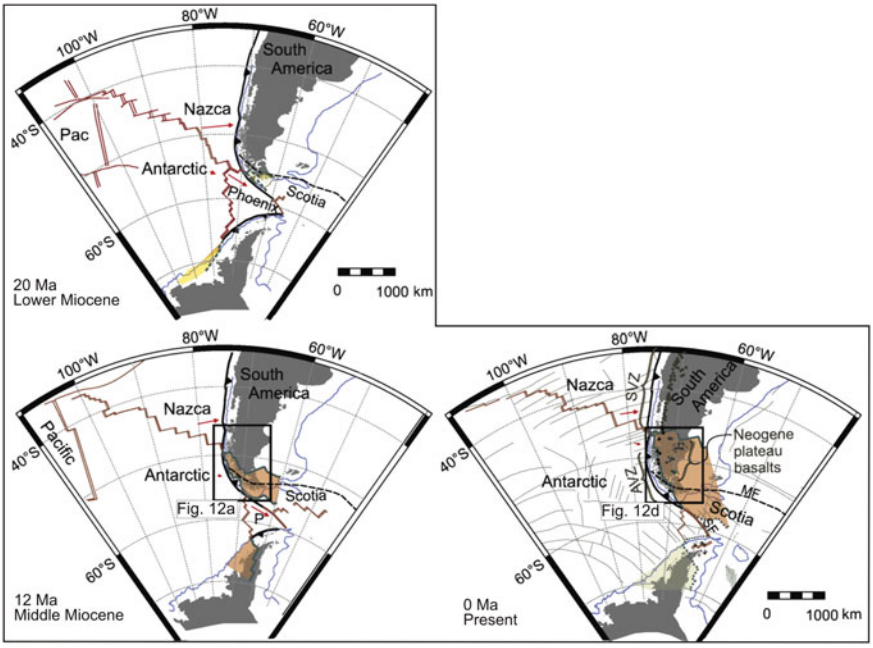


Fig. 7 Paleotectonic diagrams with Neogene to present kinematic reconstructions of ridge collisions and resulting slab windows. *AVZ* Austral volcanic zone; *MF* Magallanes–Fagnano fault; *P* Phoenix; *SF* Shackleton fault; *SVZ* Southern volcanic zone. From Breitsprecher and Thorkelson (2008)

deformation transferred to the sedimentary cover (Ghiglione and Ramos 2005; Klepeis et al. 2010).

The exposed metamorphic detachment of the basement wedge runs along a belt of highly strained rocks in the Canal de las Montañas shear zone, in the eastern flank of the Sarmiento Ophiolitic Complex (Fig. 8) (Stern and de Witt 2003; Calderón et al. 2012). Geobarometric considerations and $^{40}Ar/^{39}Ar$ age data suggest that this sector experienced fast uplift rates (1–2 mm/year) and a total exhumation of 8 km between ~85 and 80 Ma during progressive thrust sheet imbrications (D1) and subsequent doming and back folding (D2) of the basement thrust wedge (Calderón et al. 2012). The main compressive deformational event was dated at ~85 Ma by in situ $^{40}Ar/^{39}Ar$ in syntectonic phengite. The 78–81 Ma U–Pb zircon crystallization ages of crosscutting plutonic and hypabyssal rocks and $^{40}Ar/^{39}Ar$ amphibole age of ~79 Ma from lamprophyric dikes within the fold and thrust belt constrain an upper-age limit of the ophiolite tectonic emplacement deformation (Calderón et al. 2012). In general agreement with geobarometric data, a widespread remagnetizing event affecting pillow lavas and dikes from the Sarmiento Ophiolitic Complex was associated to a pervasive regional post-emplacement metamorphic overprint (Rapallini et al. 2008). Whole-rock K–Ar dating of this rocks gives rejuvenated ages clustered around 75 Ma, consistent with a greenschist facies

orlando_a_p@yahoo.com.ar

metamorphism associated with the final closure and inversion of the Rocas Verdes Basin between ~79 and 70 Ma (Rapalini et al. 2008).

Regionally, data from Canal de las Montañas shear zone (Fig. 8) are in agreement with a first episode of folding, thrusting, and rapid exhumation in Cordillera Darwin between 90 and 70 Ma with cratonward vergent thrusting concentrated at lower structural levels (Nelson et al. 1980; Nelson 1982; Kohn et al. 1995). Also, the presence of discontinuous outcrops of mylonitized rocks near the western boundary of the Sarmiento Ophiolitic Complex (Calderón et al. 2012) could be interpreted as evidence for a double vergent wedge, similar to the present along the Beagle channel (see Chap. 11, this book). The simultaneous closure of the northern and southern limbs of Rocas Verdes Basin (Kraemer 2003) is in coincidence with geodynamic reconstructions predicting the collision of its western and southern margin together with the Antarctic Peninsula against the Patagonian-Fuegian Andes (Suárez et al. 2010) between 95 and 84 Ma (Fig. 4b) (Vérard et al. 2012). It also clearly coincides with the westward acceleration of South America during the Late Cretaceous between 90 and 80 Ma, suggesting that the continent episodically overrode the Andean trench by those times (Somoza and Zaffarana 2008).

4.2 Late Cretaceous Foreland Sequences

Late Cretaceous basement uplift and erosion caused the deposition of coarse-grained detrital sediments on top of the sag units (Fig. 2), indicating the onset of a foreland phase in the Austral-Magallanes basin (Fig. 9a) (Wilson 1991). Along the axis of the Cordillera, the exposed Late Cretaceous foreland depocenter is involved in the internal domain of the fold and thrust belt, extending approximately between 72° and 73°W (Figs. 3 and 5 (Kraemer 1998; Kraemer et al. 2002; Ghiglione et al. 2009, 2014a; Giacosa et al. 2012; Fosdick et al. 2011).

There are two key constrains provided by the distribution of the Late Jurassic rifting on the evolution of the following foreland sedimentation. First, the compressional and subsidence effects of Rocas Verdes basement uplift took place south of 49°S (Fig. 4b), therefore delimiting the sector where the Late Cretaceous foreland basin system was developed (Figs. 3 and 5). On the other hand, the segment north of 49°S presents an important hiatus for the Turonian-Paleocene stage (Fig. 2c).

Second, a peculiar feature of the southern foreland depocenter is a strong north to south axial sediment dispersal pattern with a deepening of the accommodation space, water depth, and thickening of the foreland sequences from around 1450 m in Lago Viedma (49°30′S) to more than 5000 m in Última Esperanza (51°S) (Katz 1963; Scott 1966; Arbe 1986, 2002; Macellari et al. 1989; Fildani and Hessler 2005; Hubbard et al. 2008, 2010; Romans et al. 2010; Bernhardt et al. 2011). This situation produced a remarkable Coniacian–Campanian scenario, where a shallow to platform depositional system north of Lago Argentino prograded southward, to a deeper water marine trough in Ultima Esperanza region (Fig. 9b, c), filled by

orlando_a_p@yahoo.com.ar

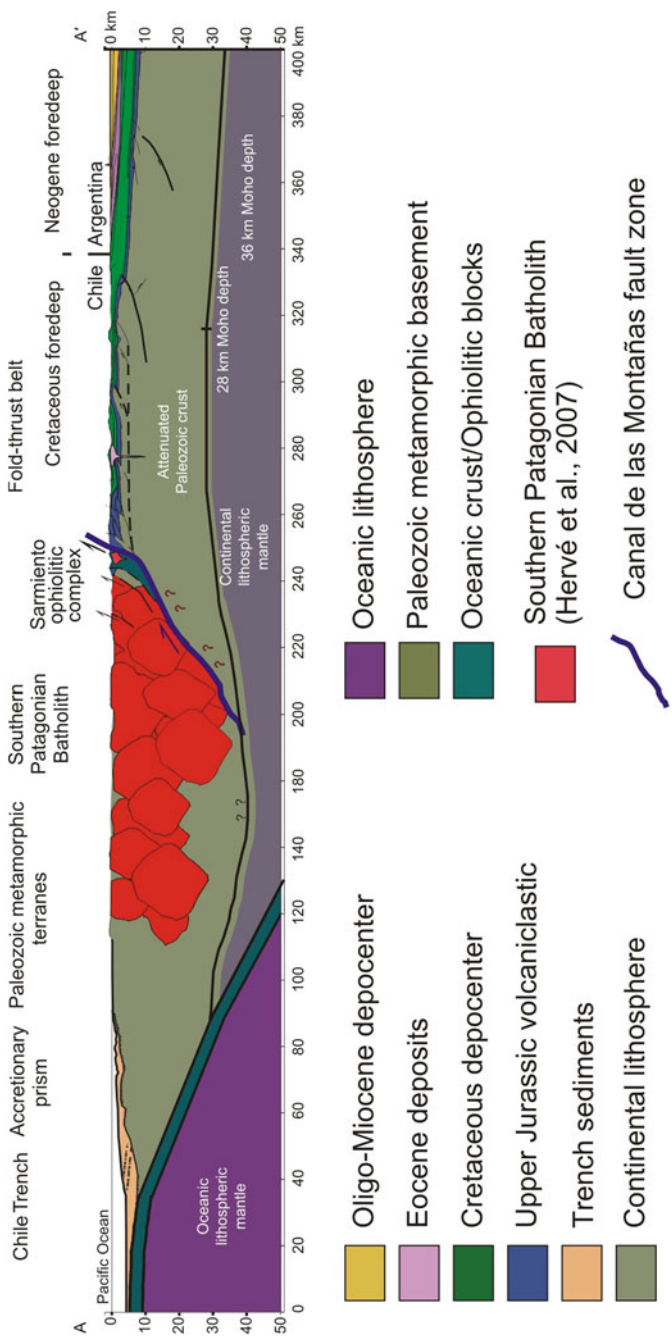


Fig. 8 Lithospheric section across the Southern Patagonian Andes, with location shown in Figs. 1 and 5. Modified from Fosdick et al. (2011)

orlando_a_p@yahoo.com.ar

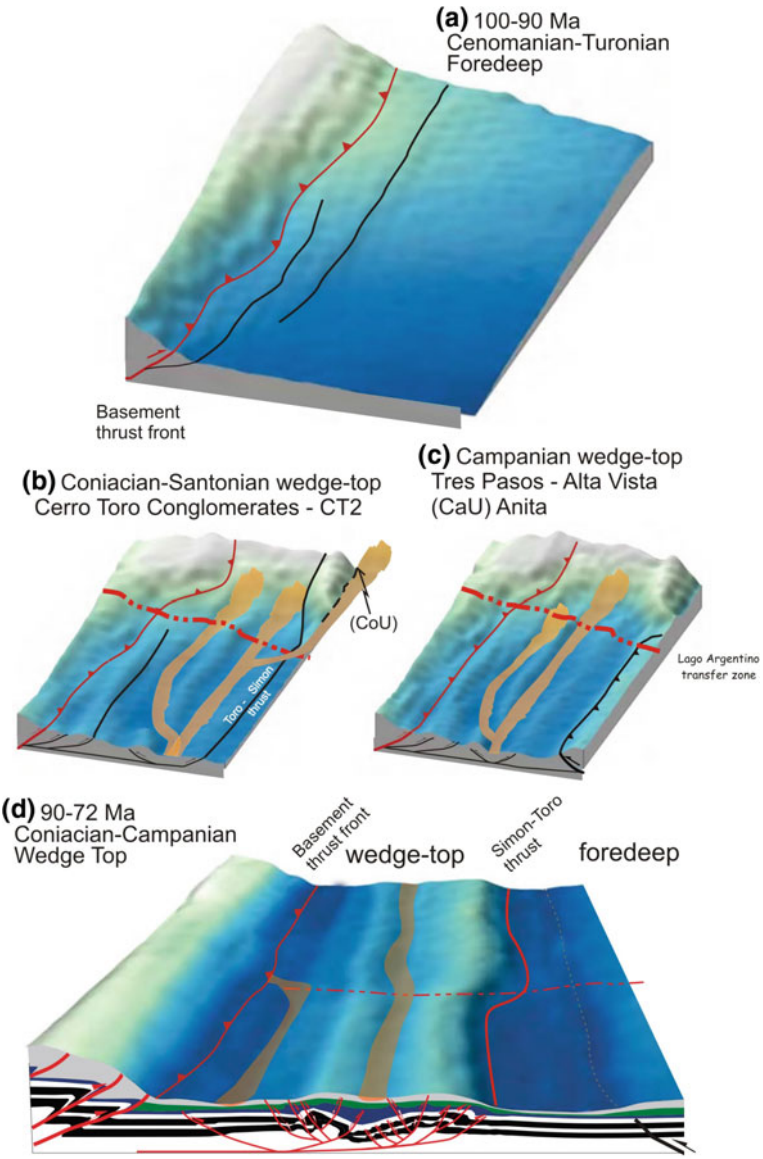


Fig. 9 **a–d** Cenomanian to Campanian paleogeographic reconstructions for the deposition of Late Cretaceous Austral Basin foreland sequences in a foredeep and wedge-top depozones. Modified from Ghiglione et al. (2014a)

abyssal turbidites (Arbe 2002). The southward increase in sedimentary thickness within the foredeep depocenter is associated with a similar lateral increase in pre-existing Jurassic lithospheric stretching beneath the foreland basin, and a corresponding weaker response to tectonic loading (Dott et al. 1982; Wilson 1991;

orlando_a_p@yahoo.com.ar

Kraemer 1998; Ghiglione et al. 2009; Romans et al. 2010; Likerman et al. 2013). This variable stretching and loading response are expressed regionally in an increase in total sedimentary thickness and depth to basement toward the south, from a few hundred meters at Lago Posadas (47°) up to 8 km between 51° and 54°S (Figs. 1 and 2).

Before the discussion and integration of uplift data and sedimentary response, we will present the Late Cretaceous stratigraphic data from north to south divided into three sectors, each encompassing a similar composited sedimentary column: (1) Lago San Martín–Lago Viedma (49°00′–49°30′S); (2) Lago Viedma–Lago Argentino (49°30′–50°15′S); and (3) Calafate—Última Esperanza—(50°15′–53°00′S). Although depositional ages from U/Pb in detrital zircons and volcanic ashes are available mainly south of 51°S, they are similar to stratigraphic ages based on abundant ammonoid associations. Therefore, a regional stratigraphic correlation using a combination of fossils and isotope ages seem to be adequate (Ghiglione et al. 2014a), and indicates that basal foreland deposits are of Latest Albian–Cenomanian age (Fig. 2).

4.3 Lago San Martín–Lago Viedma Sector (49°00′–49°30′S)

The northernmost outcrops of the Upper Cretaceous depocenter are located between the Lagos Viedma and San Martín, and include 1100–m–thick marine to deltaic sediments from the Lago Viedma and Puesto El Alamo Formations (Arbe 2002) of Late Albian to Turonian age based on ammonite fossil content (Leanza 1970; Aguirre-Urreta 1989). North of 49°, the Río Mayer Formation is overlaid by the Kachaike Formation (Fig. 5) (Riccardi and Rolleri 1980) deposited in deltaic environments (Arbe 2002) that became progressively fluvial-continental to the top of the unit (Nullo et al. 1999). The Kachaike sequence has a well-constrained Late Aptian–Early Cenomanian age, based on ammonite fauna and abundant palynological assemblages (Nullo et al. 1999; Guler and Archangelsky 2006; Archangelsky and Llorens 2005). To the east of Viedma and San Martín lakes, the Upper Cretaceous units located on top of the marine sag represent shallow environments, composed of the deltaic to fluvial Piedra Clavada, Mata Amarilla and Anita Formations that complete a ~400-m-thick sequence (Varela et al. 2012). A tuff layer of the Mata Amarilla Formation intercalated at 140 m above the base of Piedra Clavada Formation, yielded a U–Pb concordia age of ~96 ± 1 Ma, which corresponds to the middle Cenomanian (Varela et al. 2012). Even though these authors interpreted that the Mata Amarilla Formation represents the onset of the foreland stage, the sudden apparition of the 60-m-thick deltaic sandstones of the Piedra Clavada on top of the marine sag may represent a forced regression and the onset of uplift. Further north along the external foothills, the Piedra Clavada Formation is covered by continental deposits of the Cardiel Formation (Ramos 1989; Arbe 2002;

orlando_a_p@yahoo.com.ar

Andreis et al. 2007). The Cardiel Formation is about 270-m thick and is considered Cenomanian in age due to the presence of rare Classopolis torosus (Andreis et al. 2007) in concordance with the tuff U–Pb age of Mata Amarilla Formation. The Cardiel Formation includes different types of volcaniclastic deposits, mainly represented by fine tuffs and massive bentonites (Andreis et al. 2007), that extended further north up to Belgrano and Puerredón lakes, where it is found covering the Río Tarde Formation (Ramos 1989; Arbe 2002).

4.4 Lago Viedma– Lago Argentino Sector (49°30'–50°15'S)

Between the Viedma and Argentino lakes (Fig. 2b), the basal foreland units overlaying the sag deposits of the Rio Mayer Formation are represented by the Cerro Toro Formation, including abundant age-diagnostic ammonites and inoceramids of late Albian to early Campanian age (Arbe and Hechem 1984; Kraemer and Riccardi 1997). This contact represents the transition from deep-water turbiditic mudstones to a shale-dominated platform. The Cerro Toro Formation is composed of 1000-m-thick turbiditic mudstones and sandstones, and can be divided in two members CT1 and CT2 separated by an unconformity CoU and laterally corresponding paraconformity CoP to the west (Fig. 2b) (Kraemer and Riccardi 1997). The fossil content of member CT1 indicates a late Albian to early Coniacian age (Arbe and Hechem 1984; Kraemer and Riccardi 1997; Riccardi 2002) and its basal section can be correlated with the Punta Barrosa Formation from the Ultima Esperanza region (Ghiglione et al. 2014a). The upper section of CT1 plus the CT2 member of early middle Coniacian to early Campanian age are time-equivalent to the Cerro Toro Formation of Última Esperanza in Chile (Ghiglione et al. 2014a). The westward onlap of member CT2 over CoU during early middle Coniacian to early Campanian times (Fig. 2b) (Kraemer and Riccardi 1997) is contemporaneous with the onset and deposition of deep-water Cerro Toro-Lago Sofía conglomeratic channels to the south of Lago Argentino (Ghiglione et al. 2014a). The member CT2 presents a syntectonic angular unconformity evidenced by the westward onlap and thinning of horizons in seismic lines from the northern shore of Lago Argentino (CoU in Fig. 2b) (Kraemer and Riccardi 1997; Kraemer 1998). In a recent work, it has been argued that the CT2 Coniacian–Santonian syntectonic unconformity is the product of the tectonic uplift of the whole internal domain of the fold and thrust belt, from Viedma lake up to río Turbio (Ghiglione et al. 2014a). The foreland sequence between the Viedma and Argentino lakes continues with 1000 m of the Alta Vista (late Santonian-early Campanian) and Anita Formations (lower Campanian) (Arbe and Hechem 1984; Kraemer and Riccardi 1997). These last two formations are separated by a syntectonic angular unconformity of ∼ lower Campanian age (CaU, Fig. 2b), outcropping in the southern coast of Lago Viedma and visualized in seismic lines north of Lago Argentino (Ghiglione et al. 2014a). The rest of the Cretaceous foreland sequence is completed by a coarsening upward

orlando_a_p@yahoo.com.ar

sequence of the shallow marine Pari Aike and fluvial La Irene Formations, outcropping further east, along the Leona river and in Cerro Fortaleza (Kraemer and Riccardi 1997; Arbe 1986, 2002).

4.5 Calafate-Última Esperanza Sector (50°15′–52°00′S)

At these latitudes, the first coarse-grained clastic infill overlaying the sag deposits of the Zapata Formation is represented by Late Albian to Cenomanian turbiditic sandstones of the Punta Barrosa Formation (Fig. 2a) (Katz 1963; Scott 1966; Natland et al. 1974; Winn and Dott 1979; Dott et al. 1982; Wilson 1991). The age span of this unit has been the subject of intense geochronological U/Pb dating of zircons from volcanic ashes and sandstones over the last decade, yielding an age between Turonian (~92 ± 1 Ma) for its base and ~91 ± 3 Ma for the top (Fildani et al. 2003). Fosdick et al. (2011) dated a volcanic ash at the Zapata/Punta Barrosa formations transition zone yielding a Late Albian U/Pb zircon age of 101 ± 1.1 Ma (Fig. 2a), indicating that provenance from uplifted western basement blocks could have occurred as early as the latest Albian. Sandstone petrography, detrital zircon geochrononology, and mudstone geochemistry indicate that Punta Barrosa sediments were derived from the uplifted Paleozoic metamorphic and Jurassic ophiolitic basement complexes, and a juvenile volcanic arc (Fildani and Hessler 2005; Fildani et al. 2008). Sandstone modal analyses and U–Pb detrital zircon spectra from equivalent units 700 km to the south at Bahía Brookes on Tierra del Fuego, indicates that foreland basin sedimentation began around ~85–89 Ma (Fig. 1) (McAtamney et al. 2011). This event coincided with increased arc volcanism and the partial obduction of the basaltic Rocas Verdes basin floor (McAtamney et al. 2011).

The Cerro Toro Formation represents the climax of deep-water sedimentation with up to 2000-m-thick shale-rich sequences (Fig. 2a) (Katz 1963; Winn and Dott 1979; Hubbard et al. 2008; Crane and Lowe 2008; Bernhardt et al. 2011; Jobe et al. 2010), and a strong age-peak of zircons between 160 and 145 Ma indicating that the Tobífera Formation started to provide detritus to the basin during the Santonian (Fildani et al. 2008), as a consequence of the uplift of the basement thrust front (Fig. 9b) (Ghiglione et al. 2014a). The Cerro ToroFormation in Ultima Esperanza spans a Turonian to Campanian interval from U/Pb detrital and volcanic ash zircon ages (ca. 90–76 Ma; see review from Bernhardt et al. 2012). In early Coniacian times (ca. 87 Ma, Bernhardt et al. 2012), the pelitic abyssal platform was incised by the abrupt inception of coarse-grained deep-water channels up to 400-m thick of the upper Cerro Toro Formation, known as the Lago Sofía conglomerates in Argentina (Winn and Dott 1979; Dott et al. 1982; Arbe and Hechem 1984; Jobe et al. 2010). The conglomerates were deposited by low-sinuosity, N-S oriented axial channel belts that served as a conduit for turbidity currents transporting coarse clastic detritus from a feeding sector along the northern shore of Lago Argentino toward the southern deepening marine trough in Ultima Esperanza (Fig. 9b, c) (Winn and Dott 1979; Scott 1966; Arbe 1989, 2002; Hubbard et al. 2008). A 4 to 8 km wide

orlando_a_p@yahoo.com.ar

and >100 km-long deep-water Sierra del Toro axial channel system and secondary channels located to the west were active until the Santonian–Campanian with southward transport along the axis of the trough (Fig. 9d) extending at least from SW of Lago Argentino to Seno Última Esperanza (Fig. 5) (Arbe and Hechem 1984; Crane and Lowe 2008; Hubbard et al. 2008; Bernhardt et al. 2012; Ghiglione et al. 2014a). Recent works presented structural and sedimentary indications of confinement and synsedimentary tectonic uplift for the western secondary axial channel system along the Silla Syncline (Crane and Lowe 2008; Gonzales and Aydin 2008; Bernhardt et al. 2011). Specifically, the locations of coarse-grained channel deposits within the syncline were controlled by first-order thrust and strike–slip faults, and their related folds that initiated prior to the coarse sediment deposition (Gonzales and Aydin 2008). Synsedimentary deformation included positive inversion of N-S oriented Jurassic extensional structures creating the elongated geometry of the depocenter (Likerman et al. 2013). Further evidence of thrust-related growth strata served as the basis for a new geodynamic model (Fig. 9d), concluding that the deposition of the Cerro Toro conglomerates was tectonically triggered in a wedge-top depozone (Ghiglione et al. 2014b).

The conglomerates are overlaid by Campanian–Maastrichtian slope and deltaic systems of the Tres Pasos and Dorotea formations in Chile that prograded southwards, cropping out along the base of the Monocline (Fig. 6c) (Katz 1963; Natland et al. 1974; Wilson 1991; Macellari et al. 1989; Covault et al. 2009). These units represent the final amalgamation of the basin, putting end to the ~65 m-year-old deep-marine trough (Fig. 2a). The basal prograding slope sandstones of the Tres Pasos Formation reached a lower Campanian detrital zircon age of 78–82 Ma, while the basal sandstones of the Dorotea Formation reached ~72 Ma, corresponding to the base of the Maastrichtian (Romans et al. 2010; Fosdick et al. 2014). On the Argentinean side these units are called differently, and have ages established by foraminifera assemblages (Malumián and Caramés 1997). The Cerro Cazador Formation (Campanian–Maastrichtian) is equivalent to Tres Pasos Formation, while the Cerro Dorotea Formation equal the Dorotea Formation (Fig. 2a, Upper Maastrichtian-Danian) (Leanza 1972; Malumián and Caramés 1997; Malumián et al. 2000).

The petrographic composition of the Campanian–Danian sequences is similar, and indicates provenance from a dissected arc (Smith 1977; Macellari et al. 1989; Manassero 1988), while analysis of their detrital zircons show abundant Tobífera volcanic zircons (157–145 Ma), Cretaceous arc material (110–70 Ma), and minor components of Paleozoic basement (Romans et al. 2011).

4.6 Late Cretaceous Foreland Basin System of the Magallanes-Austral Basin

We here present a summarized account of uplift and deformational data and their corresponding sedimentary response, to broadly classify the different sequences of the foreland basin system between Lago San Martín and Última Esperanza (Fig. 1)

orlando_a_p@yahoo.com.ar

in their corresponding wedge-top, foreland and forebulge depocenters (F1-F6 stages from Fig. 2a; sensu DeCelles and Giles 1996).

The geochemical signature of the Late Albian upper Zapata Formation shows a close affinity to ophiolitic source rocks, in agreement with the initial marginal basin inversion (Fildani and Hessler 2005), starting after ~104 Ma (Stern et al. 1991). The paucity of coarse-grained material in the upper Zapata Formation can be explained by an initial basin partition due to a partially inverted horst within the Rocas Verdes basin that isolated the eastern depocenters of Ultima Esperanza from the uplifted basement blocks (Fildani and Hessler 2005; Fildani et al. 2008). This scenario suggests a distal foredeep depocenter for the deposition of upper Zapata Formation (F1 in Fig. 2). The presence of a nearby bulge would be in agreement with an alternative eastern source for the Zapata Formation, as indicated by the presence of slumped intervals (Wilson 1991).

The Cenomanian basal coarse-grained turbidite sedimentation between 101 and 90 Ma coincides with the partial obduction of the Rocas Verdes basaltic floor, and Paleozoic basement denudation as shown by the clastic composition of the Punta Barrosa Formation and equivalent units to the south (Fildani et al. 2003; Romans et al. 2011; Fosdick et al. 2011; McAtamney et al. 2011). It seems that while progressive closure was underway, the outcropping deformational front was concentrated on Sarmiento Cordillera (Fildani and Hessler 2005), more probably on its eastern side, along the Canal de las Montañas shear zone (Calderón et al. 2012), or even further east, along the present basement thrust front (Ghiglione et al. 2014a). Despite these different interpretations, the calculated distance from the studied section of Punta Barrosa Formation at Río Chico anticline, and these possible Cenomanian–Turonian thrust fronts are similar, around ~45–60 km before shortening, placing Punta Barrosa Formation and its northern equivalents CT1 member from Cerro Toro Formation and Piedra Clavada Formation in a proximal foredeed depocenter (F2 in Fig. 2).

During the late Turonian–Coniacian, a well-developed proximal foredeep foreland sequence existed dominated by the southward progradation of littoral sequences (Subciclo Mata Amarilla from Arbe 2002). This scenario included the deltaic Mata Amarilla Formation to the shallow marine Puesto El Alamo Formation depositional system north of Lago Viedma, prograding toward a southern deep water marine N-S trough filled by abyssal turbidites of the Cerro ToroFormation (Arbe 1986, 2002; Kraemer 1998).

Late Coniacian–Santonian syntectonic angular unconformities within the CT2 member of Cerro Toro Formation along the northern shore of Lago Argentino, indicates that the abrupt inception and development of submarine conglomerate channels was probably tectonically triggered (Ghiglione et al. 2014a). In this remarkable scenario, the Santonian (~85 Ma) first input of abundant Tobífera detritus into the basin represents the uplift of the basement domain (Romans et al. 2011).

Denudation was probably concentrated along the basement thrust front, since it is the only structure exposing significant outcrops of the Tobífera Formation across the Southern Patagonian Andes (Figs. 3 and 5) (Ghiglione et al. 2014a). There are synsedimentary indications that changes in sediment supply and general confinement

orlando_a_p@yahoo.com.ar

in the western conglomerate channels were the product of laterally confinement by active faults (Gonzales and Aydin 2008; Bernhardt et al. 2011), in agreement with a wedge-top setting (F3 in Fig. 2; Ghiglione et al. 2014a). The eastward migration of foreland depocenters and development of a wedge-top depozone was produced by the Coniacian–Santonian 80 km advance of the thrust front due to the final closure of the Rocas verdes Basin (Fig. 9d).

The significant input of Tobífera detritus into the Tres Pasos/Cerro Cazador and Dorotea/Cero Dorotea formations (Romans et al. 2011) is an indication of continuous shortening and denudation concentrated along the basement thrust front, i.e., a proximal foredeep (F4 in Fig. 2), since there is no evidence of syntectonic deposition. Southward and westward progradation of sequences was still very dominant during this period (Fig. 10) (Subciclo Anita from Arbe 2002; Macellari et al. 1989; Manassero 1988).

5 Paleogene Orogenic Cycle: Uplift, Sedimentation, Eocene Ridge Subduction and Related Magmatism

5.1 Tectonic Setting, Time of Deformation, and Sedimentary Response

The Eocene was a period of rapid convergence (Pardo Casas and Molnar 1987), associated with the Incaic orogeny of the Central Andes, when the Farallón-Phoenix ridge collided against the Southern Patagonian Andes (Cande and Leslie 1986). Modern reconstructions based on plate kinematics calculate that during the ~50 to 45 Ma collision of the active ridge, the Phoenix oceanic plate was converging at > 10 cm/year rate with a SE direction, while the Farallon plate was NE directed with a 6 cm/yr convergence rate (Somoza and Ghidella 2005, 2012). Therefore, besides the more immediate and direct effects produced by the collision of the seismic ridge, the collision point also suffered a long-lasting change from ESE (Phoenix plate) to NE (Farallon plate) directed subduction (Fig. 4c) (Ghiglione and Ramos 2005; Somoza and Ghidella 2005; Ghiglione and Cristallini 2007). Paleogene deformational data along the basement domain of the Southern Patagonian Andes from apatite fission track thermochronology are scarce, with a few points on the western side, and a predominance of Miocene exhumation (Fig. 3) (Thomson et al. 2001, 2010).

Forward modeling of He dates suggests post-depositional 54–45 Ma (Early Eocene) heating of the Maastrichtian-Danian Dorotea/Cerro Dorotea Formation up to 180°C due to sedimentary burial along the Monocline (Fig. 10b). The early Eocene burial was followed by a middle Eocene episode of rapid exhumation along the eastern boundary of the Internal Domain, which can be interpreted from zircon (U–Th)/He cooling (200–160°C) ages between 44 and 42 Ma of samples located on the hanging wall of the Toro thrust (Fosdick et al. 2013). The older ZHe ages from

orlando_a_p@yahoo.com.ar

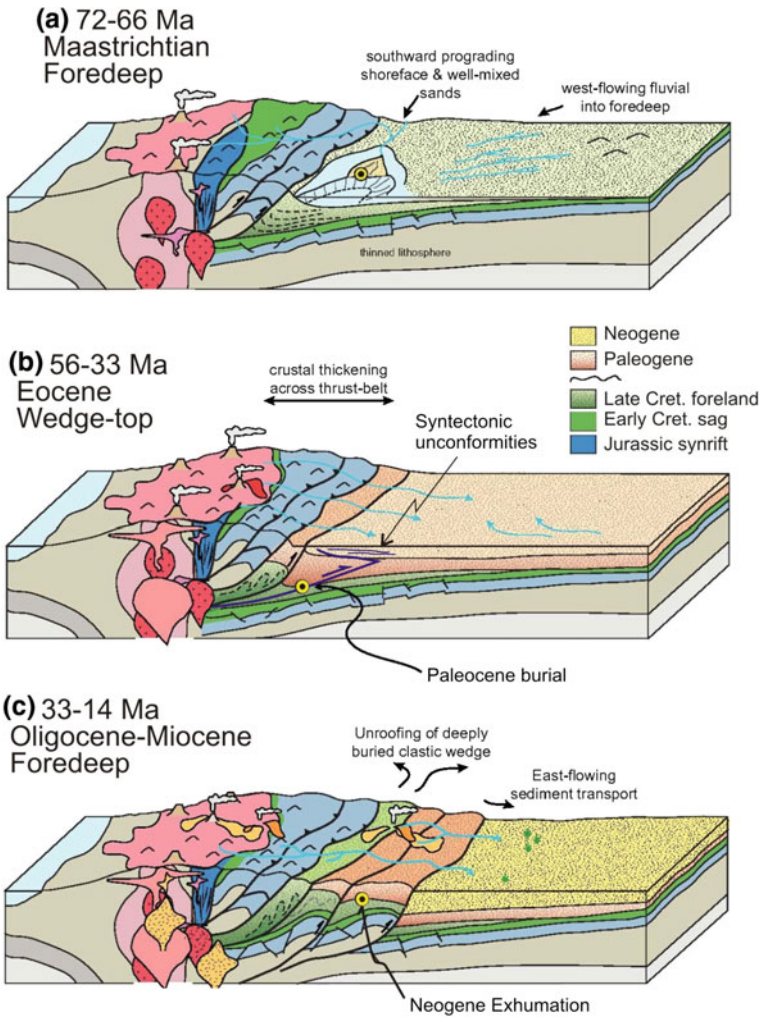


Fig. 10 Paleogeographic reconstructions during: **a** Maastrichtian foredeep southward progradation of Dorotea/Cerro Dorotea Formations, **b** Eocene wedge-top deposition of Río Turbio and Manaike Formations, and **c** Oligocene-Miocene foredeep with eastward sediment transport. Modified from Fosdick et al. (2014)

the Toro thrust hanging wall present larger spread of partially-reset single-grain ages yielding evidence for Paleocene burial, followed by middle Eocene exhumation (Fosdick et al. 2013, 2014).

Deformation of the frontal Monocline located immediately to the east of the Toro thrust, and synsedimentary eastward tilting of its flank during the middle and late Eocene (~46–34 Ma) is recorded on progressive unconformities from the Río Turbio and Río Guillermo formations (Fig. 2a) (Malumián et al. 2000). These

orlando_a_p@yahoo.com.ar

syntectonic sequences onlap on top of the Dorotea/Cerro Dorotea Formation (Mpodozis in Alvarez et al. 2006), bracketing an upper Paleocene-lower Eocene hiatus spanning from ~60 to 46 Ma (Fig. 2) (Malumián et al. 2000). From structural modeling, the Frontal Monocline has been interpreted as a passive wedge of the Cerro Toro thrust sheet (Fig. 6c), and therefore their respective deformational ages and kinematics can be associated (Ghiglione et al. 2014a).

Propagation of the fold and thrust belt from the Basement domain up to the eastern boundary of the Internal domain, related to the Eocene ridge collision, has also been proposed for the sector between Lagos Argentino and Viedma (Kraemer 1998; Kraemer et al. 2002). There, the stratigraphic and environmental response to deformation is very similar to the Río Turbio sector (Camacho et al. 2000; Marenssi et al. 2002). The shallow marine and lagoon deposits of the middle to upper Eocene Man Aike Formation (Russo et al. 1980; Malumián and Nañez 1988; Malumián 1990) rest uncomformably on top of the marine Maastrichtian Calafate Formation, bracketing a Paleocene-lower Eocene hiatus (Camacho et al. 2000), related to the Eocene deformational event (Marenssi et al. 2002). Near Calafate locality, a passage from a paraconformity to a discordant onlap and overlap relations has been observed for the contact between Man Aike and Calafate formations (Marenssi et al. 2002), which is typical of syntectonic unconformities and growth onlaps, and very alike the stratigraphic situation described for the Río Turbio locality by Mpodozis (Alvarez et al. 2006). The Oligocene-early Miocene fluvial systems of the Río Leona Formation uncomformably rest on top of the Man Aike Formation (Marenssi et al. 2005), and is transitionally covered by the shallow marine early Miocene Estancia 25 de Mayo (Centinela) Formation (Cuitiño and Scasso 2010; Cuitiño et al. 2012).

Further north, there are isolated continental deposits of Paleogene age preserved on the external foothills between Lagos Belgrano and Cardiel (Fig. 5). These deposits bearing coal seams in littoral shallow facies have been interpreted as molasse related to deformation in the Basement domain (Kraemer et al. 2002). These deposits are better developed in the Chilean Cosmelli basin (approx. 47°S, south of Lago Cochrane, Fig. 5) where Suárez et al. (2000b) and Troncoso et al. (2002) described a continental sequence bearing coal seams of late Paleocene–early Eocene age. This conglomeratic unit defined as Ligorio Márquez Formation has an oligomitic clastic composition of quartz, indicating a provenance from metamorphic basement sources.

5.2 *Paleogene Foreland Basin System of the Magallanes-Austral Basin*

There are multiple aspects to account for the depositional setting of the Paleogene foreland sequences. Paleogene deposits are missing in the Internal Domain of the fold and thrust belt, while only very restricted Paleocene units (Dorotea/Cerro Dorotea Formation) are present along the External domain (Fig. 5), characterized by a Paleocene-lower Eocene hiatus (Malumián et al. 2000). The middle upper Eocene

orlando_a_p@yahoo.com.ar

shallow marine to costal Río Turbio and Man Aike formations, and following continental fluvial systems of the Río Guillermo and Río Leona formations are present along the external domain of the fold and thrust belt from Lago Cardiel to Río Turbio and continue to the east, bellow the Patagonian steppe (Russo et al. 1980; Malumián et al. 2000; Camacho et al. 2000; Marenssi et al. 2002). A west-east transect of the Paleogene basin along 52°S shows an asymmetric section, typical of a foreland basin with a rapid thickening toward the west, from 1150 m along the foothills to 400 m 120 km further east, and 80 m along the Atlantic coast (see Fig. 1 of Malumián 2002). Accordingly, the subsidence curve of the basin indicates a rapid Paleocene increase of the subsidence rate (Biddle et al. 1986).

Previous studies interpreted that the present distribution of Paleogene units indicates uplift and erosive denudation of the internal fold and thrust belt, producing a cratonward migration of the foreland depocenter (Biddle et al. 1986; Fosdick et al. 2011). For the Internal domain it is very uncertain whether the Paleocene deposits were present at one point and eroded afterwards, being the only evidence partially-reset zircon ages yielding evidence for Paleogene burial (Fosdick et al. 2013, 2014). It seems quite clear, however, that the middle upper Eocene shallow marine to costal Río Turbio and Man Aike formations were deposited in a wedge-top depozone (F5 in Fig. 2) with high sedimentation rates, along the eastern boundary of the active internal domain (Fig. 10).

5.3 *Paleogene Arc Volcanic Gap and Retroarc Volcanism*

The Patagonian Batholith and the satellite bodies located further east along the foothills (Fig. 5) recorded a persistent magmatic activity related to subduction since Jurassic times (Hervé et al. 2007). However, there is no dated plutonic activity with Paleocene to Eocene ages (65–34 Ma) between 45° and 48°S (Ramos et al. 1982; Suárez and de la Cruz 2001). In a database of 70 U–Pb zircon ages, a 55 to 26 Ma plutonic gap can be noticed between 48° and 52°S (Hervé et al. 2007).

Contemporaneously with the Paleogene volcanic arc gap, widespread alkaline basalts were spread on the retroarc and foreland (Figs. 5 and 11a). These basalts have typical OIB signature reflecting deep mantle origin, and have been interpreted as evidence of an asthenospheric window formed during the Farallon-Phoenix ridge collision (Ramos and Kay 1992; Kay et al. 2002; Espinoza et al. 2005). The majority of these retroarc volcanic plateaus, known as the Posadas Basalt, were erupted between 44° and 52°S (Figs. 4, 11) (Kay et al. 2002; Ramos 2005). The Eocene basalts are spread on top of Cretaceous-Paleogene sequences (Fig. 2), and crop-out along the foothills between Buenos Aires and Belgranolakes, particularly on the *Mesetas* Chile Chico, Buenos Aires and Posadas (Figs. 5 and 11). Others outcrops are concentrated on the shores of Cardiel lake, while the complete extent of the Eocene plateau covered most of the extra-Andean Patagonia as shown by well data (Ramos 2005). These Eocene plateau basalts are associated with the Eocene Río Carbón essexite suite, composed of dike swells, necks and sills

orlando_a_p@yahoo.com.ar

emplaced at lower stratigraphic levels along the fold and thrust belt between Belgrano and Argentino lakes (Riccardi 1971; Nullo 1983; Ramos 2005).

The Meseta Chile Chico (46°S) constitute the westernmost exposure of the Posadas basalts, including intercalation of the Eocene (55–40 Ma, K–Ar ages) and Mio–Pliocene (16–4 Ma, K–Ar ages) flood basalts (Fig. 11) (Espinoza et al. 2005). Data from this area distinguish two main pulses of Eocene activity, one between ~44 and 41 Ma, and a younger around ~39–40 Ma (K/Ar in whole rock, Flynn et al. 2002). The oldest basalt corresponds to a ~59 ± 2 Ma reported by Morata et al. (2000) in the same area. These ages are also similar to $^{40}Ar/^{39}Ar$ ~ 43 Ma ages (Kay et al. 2002), and 43 ± 7 Ma K/Ar ages from Meseta Posadas (Ramos and Drake 1987). The main outcrops of the Río Carbón essexites are located between Lago San Martín and Tutu-Tucu (Fig. 5), including the remarkable Cerro Kachaike volcanic neck and sills several kilometers long and up to 30–40 m thick, with whole-rock dating of 48 ± 4 and 32 ± 3 Ma (Riccardi 1971). The overall ~55–40 Ma K/Ar dating indicate a lower to middle Eocene age for the Posadas Basalt and the Río Carbón essexite, overlapping with the moment when the orogenic front along the fold and thrust belt was reactivated.

5.4 *Unfolding of Paleogene Events*

It seems clear that during the middle Eocene the Internal Domain was reactivated (Kraemer 1998), as shown by 44 and 42 Ma samples located along the thrust front (Fosdick et al. 2013) and ~46–34 Ma growth strata (Malumián et al. 2000). The Eocene orogenic wedge widened by around 40 km (Kraemer 1998; Malumián et al. 2000). Stratigraphic geometry and sedimentary response is in agreement with renovated Paleogene uplift and an Eocene wedge top to proximal–distal foredeep depocenter. The overall ~55–40 Ma K/Ar dating for the Posadas Basalt and the Río Carbón essexite overlaps with reactivation of the orogenic front and a wedge-top to proximal foredeep (Fig. 2). The calculated time of the Farallon-Phoenix ridge collision against South America by means of kinematic reconstructions is mostly speculative, since the most nearby constraint is the position of the Antarctic-Phoenix-Farallon triple junction (Fig. 4c) (Somoza and Ghidella 2005; Eagles and Jokat 2014). Therefore, the age of the collision is better constrained by geological data from the continental margin as expressed by Somoza and Ghidella (2012). The Miocene case-study shows a 4 to 6 myr delay between the ridge-subduction and the main spread of retroarc plateaus (Fig. 12) for convergence rates of around 6 cm/yr (Breitsprecher and Thorkelson 2008). It seems reasonable to think that during the Eocene, with a 10 cm/yr convergence rate (Somoza and Ghidella 2005), the retroarc volcanism concentrated on a major ~50–45 Ma peak (Fig. 11c) (Espinoza et al. 2005), indicating a 52–50 Ma onset for the collision, in agreement with most recent plate reconstructions (Somoza and Ghidella 2012; Eagles and Jokat 2014). The volcanic gap broadly coincides with and postdates the Farallon-Aluk ridge passage along the margin (Herve et al. 2007), while the retroarc

orlando_a_p@yahoo.com.ar

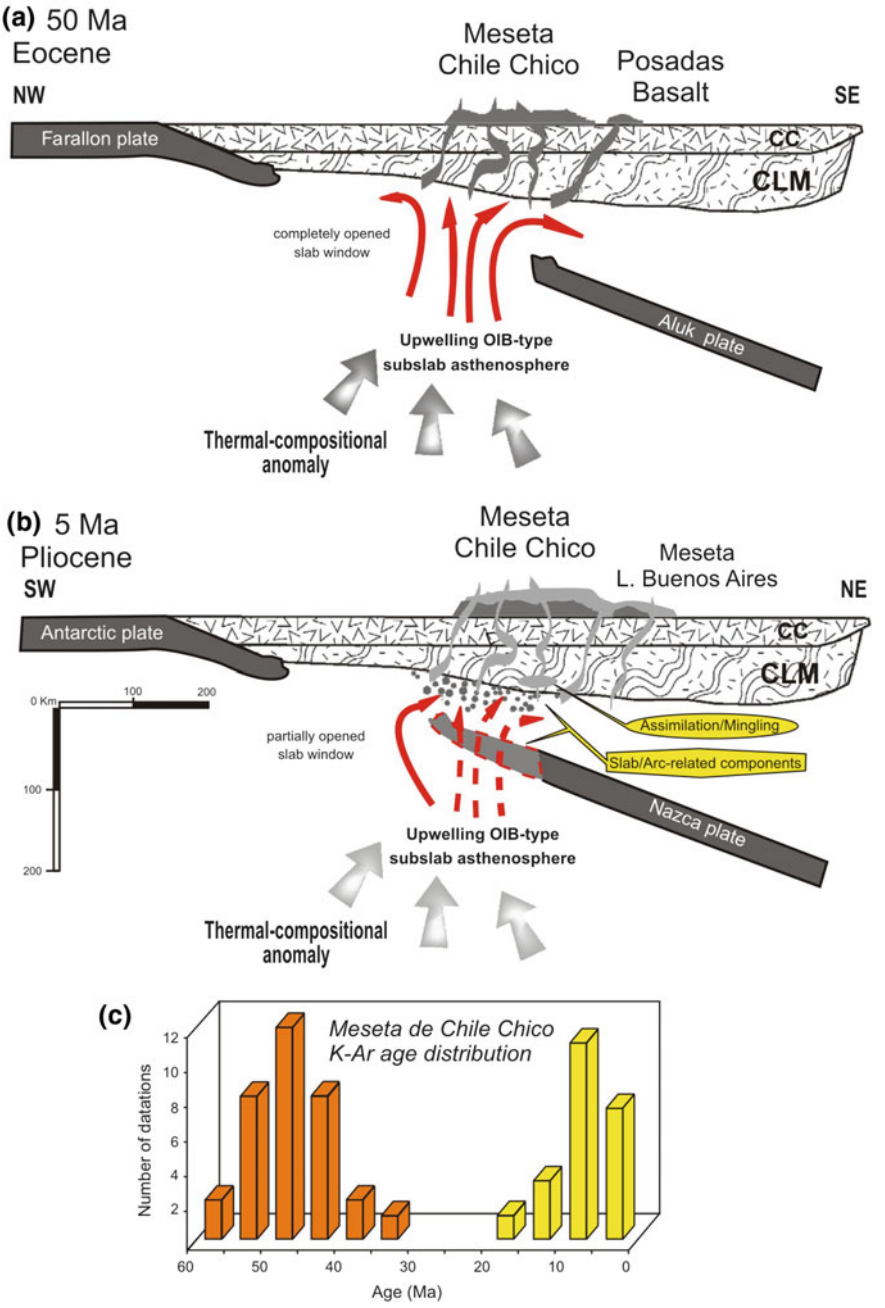


Fig. 11 Tectonic-sections of Patagonian Lithosphere during the **a** Eocene, with location marked as *solid blue line* in Fig. 4c. **b** Pliocene, marked as *solid red line* in Fig. 12c; **c** Histogram showing Meseta Chile Chico K–Ar age distribution. From Espinoza et al. (2005)

orlando_a_p@yahoo.com.ar

volcanism seems to be a more accurate indicator bracketing the time of ridge-subduction. It can be seen that there is a close correlation in time and space between the approach and collision of an oceanic spreading center, deformation in the fold and thrust belt, sedimentation in the foreland, cessation of arc volcanism, and development of alkaline retroarc basalts.

6 Neogene Orogenic Cycle: Uplift, Sedimentation, Ridge Subduction and Related Magmatism

6.1 Tectonic Setting

The Neogene tectonic evolution of the Southern Patagonian Andes is probably one of the better studied cases of coupling between subduction processes and magmatic, deformational, and sedimentary events. During the Miocene, the Chile oceanic ridge dividing the Nazca and Antarctic plates entered the South America trench at ~54°S and migrated northward to its present-day position at 46°S west of Taitao Península (Fig. 12) (Forsythe and Nelson 1985; Cande and Leslie 1986; Forsythe et al. 1986). The Chile ridge collided almost parallel to the South America trench, and from the moment of ridge collision at 14–12 Ma an astenospheric slab window increasingly opened beneath Patagonia (Figs. 9 and 12) (Forsythe et al. 1986; Ramos and Kay 1992; Gorring et al. 1997; Bourgois and Michaud 2002; Lagabrielle et al. 2004). Once the ridge reached the trench, its eastern side, belonging to the Nazca plate, kept *a* ~10 cm/year subduction rate (Somoza and Ghidella 2012), while the Antarctic border started a lower ~2–2.5 cm/year rate (De Mets et al. 1994; Sdrolias and Müller 2006); the speed difference produced the still opening slab window (Fig. 12).

Kinematic reconstruction of the geometry of the Patagonia and Antarctic slab windows through Neogene time indicate that approximately at 17–18 Ma during an unstable quadruple-junction event, the Phoenix–Nazca–Antarctic ridge collided at 53°–54°S against South America (Fig. 9) (Breitsprecher and Thorkelson 2008). From ~14 to 3 Ma, a series of at least four ridge-segments separated by transform faults collided against the South America trench from 53°S to its present-day position at 46°S (Fig. 12), as indicated by the time-space distribution of alkali Patagonian plateau lavas (Ramos and Kay 1992; Kay et al. 1993; Gorring et al. 1997, 2003). The current position of the Antarctic plate edge at ~250 km from the trench is indicated by distribution of adakitic Holocene volcanoes (Fig. 12).

The middle Miocene ridge collision at 13–14 Ma and resulting slab window produced an extensive OIB magmatism between 10 and 3 Ma in extra-Andean Patagonia. The ridge collision produced a change from precollisional normal subduction (14 Ma) to syncollisional shallow subduction (12 Ma) and slab window (10), to the modern slow-rate subduction of Antarctic plate beneath South America (Fig. 11b) (Gorring et al. 1997). During the period of "normal subduction" preceding ridge subduction, the volcanism was active on the retroarc, such as the Fitz

orlando_a_p@yahoo.com.ar

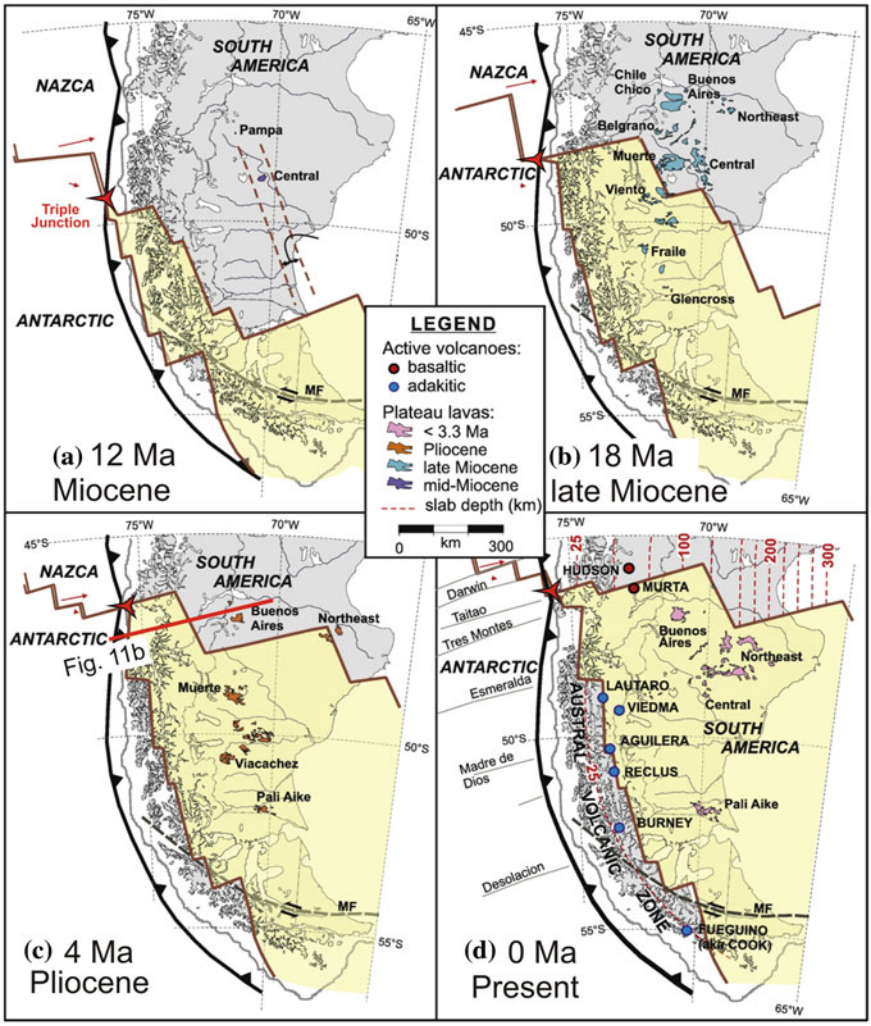


Fig. 12 Maximum extent of the Patagonia slab window through the Neogene. Heavy lines are the kinematically defined slab edges. *Red arrows* indicate the relative displacement of each subducting plate relative to South America. *Red dashed lines* represent present-day depth contours to tops of slabs. From Breitsprecher and Thorkelson (2008)

Roy-Torre (∼17–16 Ma, Ramirez de Arellano et al. 2012) and Torres del Paine plutons (12 Ma, Michel et al. 2008). The Patagonian retroarc region record erosion-driven cooling through the apatite partial retention zone (80–50°C) between 7 and 4 Ma producing the exposition of those plutons (Fosdick et al. 2013).

It has also been proposed a cause to effect relationship between ridge collision and the beginning of Neogene orogeny (Ramos 1989, 2005), although there is a time lag between rapid uplift and collision. Apatite fission track data show

orlando_a_p@yahoo.com.ar

increased denudation starting at 30–23 Ma in the basement domain and migrating eastward until 12 Ma (Thomson 2002). ZHe geochronometers reflect synchronous regional exhumation across the orogen between 22 and 18 Ma, while lower temperature chronometers such as AHe give exhumation ages between 10 to 4 Ma concentrated on the eastern fold and thrust belt (Thomson et al. 2010; Fosdick et al. 2013). The compressional period between 22 and 18 Ma was interpreted as the result of increased coupling due to orthogonal subduction of young and buoyant oceanic lithosphere while the active Chile ridge was approaching the trench (Folguera and Ramos 2002). Miocene–Pliocene exhumation concentrated on the eastern retroarc is also shown by the exposition of the Miocene plutons emplaced at 5–6 km depth and now forming some of the most world famous granite peaks like the Fitz Roy (3405 m.a.s.l.) and Torres del Paine (2885 m.a.s.l.).

6.2 *Neogene Foreland Basin System of the Magallanes-Austral Basin*

The Neogene cycle of sedimentation is represented by a foredeep clastic wedge that thickens to the west and to the south of the basin. This cycle represents one of the most widespread stratigraphic portions of the basin, extending to areas beyond than that occupied by Paleogene and Cretaceous units, especially to the eastern portion where these beds onlap over basement rocks of the Deseado and Río Chico highs.

The cycle starts with fluvial conglomerates and sandstones of the Río Guillermo and Río Leona formations (Malumián et al. 2000), which rest on a discontinuity formed during the late Eocene and early Oligocene times (F6 in Fig. 2). This depositional phase of fluvial sedimentation is restricted to the southwest area of the proximal foreland. The Rio Guillermo Formation is restricted to the Río Turbio-Ultima Esperanza region while the Rio Leona covers the former and extends north up to the Lago Cardiel Area (Fig. 5). Both units are dated as late Oligocene to early Miocene (Barreda et al. 2009; Fosdick et al. 2014). Marenssi et al. (2005) described a southward thickening and a fining upward trend for Rio Leona Formation which indicates an upward increase in accommodation space. This trend ends with the flooding of the shallow marine "Patagoniense" transgression.

During the early Miocene, the widespread marine depositional event known as the Patagoniense transgression took place in the entire basin. This depositional event is recorded in a narrow band that borders the Patagonian fold and thrust belt and extend to the east at the southern part of the basin. This N-S narrow shape is the result of flexural subsidence caused by tectonic loading in the adjacent Andean belt. From North to South, lithostratigraphic units related to the Patagoniense transgression are the El Chacay Formation at Lago Posadas/Pueyrredón (Chiesa and Camacho 1995) and the Estancia 25 de Mayo Formation (previously known as Centinela) at Lago Argentino (Cuitiño and Scasso 2010). To the east, the Monte León Formation represents a distal equivalent for this transgression. The age for the Patagoniense transgression at the western trough is constrained between 20 and

orlando_a_p@yahoo.com.ar

18 Ma (early Miocene; Cuitiño et al. 2012). These deposits represent a T-R cycle which coincides in age with a low eustatic sea level interval (Miller et al. 2005), suggesting an origin caused by a strong basin floor subsidence event related to tectonic loading at the Andean belt. A low-hierarchy erosional event (sequence boundary) is recognized in within the marine units in some sections possibly caused by tectonic uplift (Cuitiño and Scasso 2010).

The Miocene cycle ends with the fluvial Santa Cruz Formation. This units display a transitional contact with the various underlying marine units. This gradual contact is evidenced by estuarine deposits everywhere it crops out in the entire basin (Feruglio 1938; Cuitiño and Scasso 2010; Cuitiño et al. 2013). The Santa Cruz Formation is about 500 m thick in the western portion of the basin and thins to the east to about 200 m in the coastal zone of Santa Cruz. It is composed of a coarsening upward succession of fluvial deposits that show a high aggradation rate. The pattern of sediment dispersal during the deposition of this unit suggests a drainage system flowing to the east and partially to the north. This northward direction suggests an axial component in the sediment dispersal pattern, controlled by relatively high flexural subsidence rates in the foredeep. The Santa Cruz Formation is truncated at its top by a regional unconformity produced by the erosion of fluvial and glaciofluvial processes which resulted in widespread deposition of late Miocene-Pliocene conglomeratic beds (Panza 2002).

Both the marine Patagoniense units and the Santa Cruz Formation show distal foredeep sedimentation features at the western border of the basin (F7 in Fig. 2). Coarse alluvial deposits or wedge-top sedimentary units are not preserved due to eastward migration of the fold and thrust belt after the early Miocene deposition of these beds.

A large amount of pyroclastic material is present within the Neogene succession of the Magallanes Basin. This is registered in the Lago Argentino-Ultima Esperanza region where the marine Estancia 25 de Mayo and the fluvial Santa Cruz Formation bear a large amount of pyroclastic beds (Cuitiño and Scasso 2013). To the north, the Lago Posadas region shows less amounts of pyroclastic material, suggesting that the explosive volcanism was restricted to the southern portion.

The rapid uplift of the Patagonian Andes caused an extraordinary rain shadow on the Andean foothills since $\sim$16.5 Ma according to tectonic and isotopic evidence (Blisniuk et al. 2005). Patagonian desertification most likely occurred during the last 6 m year due to a combination of global climate change during the onset of glaciations in the Patagonian Andes (Palazzesi et al. 2014). The Patagonian Batolith was denudated by rain shadow and glaciation during the Miocene (Thomson et al. 2010).

7 Concluding Remarks

The Cretaceous–Cenozoic evolution of the Southern Patagonian Andes is one of the most prominent examples of coupling between deep processes at lithospheric scale (subduction) and climatic, magmatic, deformational, and sedimentary events.

orlando_a_p@yahoo.com.ar

The main driving force for the Late Cretaceous orogeny was the progressive closure of the Rocas Verdes Basin. These compressional and subsidence effects, south of 49°S, provide a key constraint for the areal distribution of the Late Cretaceous foreland basin system (Figs. 3 and 5). As a result of this particular subduction scenario, the Andean orogen south of 49° was around 180 km wide at the end of the Campanian and a more than 5000-m thick foreland sedimentary sequence was already deposited in the Austral-Magallanes Basin (Fig. 2 a) (Katz 1973; Wilson 1991).

The next important deformational event and migration of the locus of sedimentation toward the east was produced by the Farallón-Phoenix ridge collision against the Southern Patagonian Andes (Cande and Leslie 1986). There is a close correlation in time and space between the approach and collision of the oceanic spreading center, deformation in the fold and thrust belt, sedimentation in the foreland, cessation of arc volcanism, and development of alkaline retroarc basalts. The retroarc volcanism indicates a 52–50 Ma onset for the collision, in agreement with the most recent plate reconstructions (Somoza and Ghidella 2012; Eagles and Jokat 2014).

During the Miocene, the Chile oceanic ridge entered the South America trench at ~54°S and an astenospheric slab window increasingly opened beneath Patagonia (Figs. 9 and 12) (Ramos and Kay 1992; Gorring et al. 1997; Lagabrielle et al. 2004). The space-time unraveling of tectonic uplift is well known from geochronometers, and shows a migration from the basement domain to the external fold and thrust belt accompanied by lower Miocene synorogenic sedimentation. The rapid uplift of the Patagonian Andes caused an extraordinary rain shadow on the Andean foothills (Blisniuk et al. 2005), followed by the late Miocene–Pliocene desertification of Patagonia (Palazzesi et al. 2014).

Acknowledgments M.C.G. wants to acknowledge Fabián Suarez for the possibility to start working in the Southern Patagonian Andes during a 2008 project leaded by him. The present work is part of research projects conducted in the Southern Andes financially supported by grants Agencia PICT-2013-1291, and CONICET PIP 0048 and PIP 2014–2016 GI. The authors are grateful to Parques Nacionales de Argentina for allowing access to National Parks.

References

Aguirre-Urreta MB (1989) The Cretaceous decapod crustacea of Argentina and the Antarctic Peninsula. Palaeontology 32:499–552

Alvarez P, Elgueta S, Mpodozis C, Briceño M, Vieytes H, Radic JP, Mella P (2006) Proyecto Tranquilo-Otway: Unpubl. report. Empresa Nacional del Petróleo (ENAP) Chile 1: p 290

Andreis RR, Zalba PE, Morosi ME (2007) Composición y procesos diagenéticos de los depósitos de arenisca y toba de la Formación Cardiel (Cenomaniano), área Lago Cardiel, provincia de Santa Cruz. Rev Asoc Geol Argentina 62:257–266

Arbe HA (1986) El Cretácico de la Cuenca Austral: sus ciclos de Sedimentación. Unpubl. PhD thesis, Facultad de Ciencias Exactas y Naturales, Universidad de Buenos Aires, p 300

orlando_a_p@yahoo.com.ar

Arbe HA (1989) Estratigrafía y evolución sedimentaria del Cretácico en la Cuenca Austral, provincia de Santa Cruz. In: Chebli G, Spalleti L (eds), Cuencas Sedimentarias Argentinas, pp 442–449

Arbe HA (2002) Análisis estratigráfico del Cretácico de la Cuenca Austral. In Haller MJ (ed) Geología y Recursos Naturales de Santa Cruz. Relatorio del XV Congreso Geológico Argentino, pp 103–128

Arbe HA, Hechem JJ (1984) Estratigrafía y facies de depósitos marinos profundos del Cretácico Superior, Lago argentino, Provincia de Santa Cruz. IX Congreso Geológico Argentino (Bariloche). Actas 5:7–41

Archangelsky A, Llorens M (2005) Palinología de la Formación Kachaike, Cretácico Inferior de la Cuenca Austral, Provincia de Santa Cruz 2: Esporas. Ameghiniana 42:311–328

Baristeas N, Anka Z, di Primio R, Rodriguez JF, Marchal D, Dominguez F (2013) New insights into the tectono-stratigraphic evolution of the Malvinas Basin, offshore of the southernmost Argentinean continental margin. Tectonophysics 604:280–295

Barreda VD, Palazzesi L, Marenssi S (2009) Palynological record of the Paleogene Río Leona Formation (southernmost South America): Stratigraphical and paleoenvironmental implications. Rev Palaeobot Palynol 151:22–33

Bernhardt A, Jobe ZR, Lowe DR (2011) Stratigraphic evolution of a submarine channel-lobe complex system in a narrow fairway within the Magallanes foreland basin, Cerro Toro Formation, southern Chile. Mar Petrol Geol 28:785–806

Bernhardt A, Jobe ZR, Grove M, Lowe DR (2012) Palaeogeography and diachronous infill of an ancient deep-marine foreland basin, Upper Cretaceous Cerro Toro Formation, Magallanes Basin. Basin Res 24:269–294

Biddle KT, Uliana MA, Mitchum RM, Fitzgerald MG, Wright RC (1986) The stratigraphy and structural evolution of the central and eastern Magallanes Basin, southern South America. In: Allen A, Homewood P (eds) Foreland Basins, Blackwell Scientific Publications, London. Int Assoc Sediment Special Publication 8, 41–61

Blisniuk PM, Stern LA, Page Chamberlain C, Idleman B, Zeitler PK (2005) Climatic and ecologic changes during Miocene surface uplift in the Southern Patagonian Andes. Earth Planet Sc Lett 230:169–186

Bourgois J, Michaud F (2002) Comparison between the Chile and Mexico triple junction areas substantiates slab window development beneath northwestern Mexico during the past 12–10 Myr. Earth Planet Sc Lett 201:35–44

Breitsprecher K, Thorkelson DJ (2008) Neogene kinematic history of Nazca-Antarctic-Phoenix slab windows beneath Patagonia and the Antarctic Peninsula. Tectonophysics 464:10–20

Bruhn RL, Dalziel IWD (1977) Destruction of the Early Cretaceous marginal basin in the Andes of Tierra del Fuego. Island arcs, deep sea trenches and back-arc basins, 395–405

Calderón M, Fildani A, Hervé F, Fanning CM, Weislogel A, Cordani U (2007) Late Jurassic bimodal magmatism in the northern sea-floor remnant of the Rocas Verdes basin, southern Patagonian Andes. J Geol Soc 164:1011–1022

Calderón M, Fosdick JC, Warren C, Massonne HJ, Fanning CM, Fadel Cury L, Schwanethal J, Fonseca PE, Galaz G, Gaytán D, Hervé F (2012) The low-grade Canal de las Montañas Shear Zone and its role in the tectonic emplacement of the Sarmiento Ophiolitic Complex and Late Cretaceous Patagonian Andes orogeny, Chile. Tectonophysics 525:165–185

Camacho HH, Chiesa JO, Parma SG, Reichler V (2000) Invertebrados marinos de la Formación Man Aike (Eoceno medio), Provincia de Santa Cruz, Argentina. Academia Nacional de Ciencias, Córdoba, Boletín 64:187–208

Cande S, Leslie RB (1986) Late Cenozoic tectonics of the southern Chile trench. J Geophys Res 91:471–496

Chiesa JO, Camacho HH (1995) Litoestratigrafía del Paleógeno marino en el noroeste de la provincia de Santa Cruz, Argentina. Monografías de la Academia Nacional de Ciencias Exactas, Físicas y Naturales de Buenos Aires 11:9–15

Colli L, Stotz I, Bunge HP, Smethurst M, Clark S, Iaffaldano G, Tassara A, Guillocheau F, Bianchi MC (2014) Rapid South Atlantic spreading changes and coeval vertical motion in

orlando_a_p@yahoo.com.ar

surrounding continents: Evidence for temporal changes of pressure-driven upper mantle flow. Tectonics 33(7):1304–1321

Coutand I, Diraison M, Cobbold PR, Gapais D, Rossello EA, Millar M (1999) Structure and kinematics of a foothills transect, Lago Viedma, southern Andes (49° 30`S). J S Am Earth Sci 12:1–15

Covault JA, Romans BW, Graham SA (2009) Outcrop expression of a continental margin-scale shelf-edge delta from the Cretaceous Magallanes Basin, Chile. J Sediment Res 79:523–539

Crane WH, Lowe DR (2008) Architecture and evolution of the Paine channel complex, Cerro Toro Formation (Upper Cretaceous), Silla Syncline, Magallanes Basin, Chile. Sedimentology 55:979–1009

Cuitiño JI, Scasso RA (2010) Sedimentología y paleoambientes del Patagoniano y su transición a la Formación Santa Cruz al sur del Lago Argentino Patagonia Austral. Rev Asoc Geol Argentina 66(3):406–417

Cuitiño JI, Scasso RA (2013) Reworked pyroclastic beds in the early Miocene of Patagonia: Reaction in response to high sediment supply during explosive volcanic events. Sediment Geol 289:194–209

Cuitiño JI, Pimentel MM, Ventura Santos R, Scasso RA (2012) High resolution isotopic ages for the early Miocene "Patagoniense" transgression in Southwest Patagonia: Stratigraphic implications. J S Am Earth Sci 38:110–122

Cuitiño JI, Ventura Santos R, Scasso RA (2013) Insights into the distribution of shallow marine/estuarine early Miocene oysters from Southwestern Patagonia: sedimentologic and stable isotope constraints. Palaios 28:583–598

Cunningham WD (1995) Orogenesis at the southern tip of the Americas: the structural evolution of the Cordillera Darwin metamorphic complex, southernmost Chile. Tectonophysics 244 (4):197–229

Dalziel IWD (1981) Backarc extension in the southern Andes: a review and critical reappraisal. Philos Trans R Soc London 300:319–335

Dalziel IWD (1986) Collision and Cordilleran orogenesis: an Andean perspective. In: Coward MP, Riers AC (eds) Collision Tectonics, Geol Soc London, Special Publication 19, 389–404

Dalziel IWD, De Wit MF, Palmer KF (1974) Fossil marginal basin in the southern Andes. Nature 250:291–294

DeCelles PG, Giles KA (1996) Foreland basin system. Basin Res 8:105–123

De Mets C, Gordon RC, Argus DF, Stein S (1994) Effect of recent revisions to the geomagnetic reversal time scale on estimates of current plate motions. Geophys Res Lett 21:2191–2194

Dott RH, Winn RD, Smith C (1982) Relationship of late Mesozoic and early Cenozoic sedimentation to the tectonic evolution of the southernmost Andes and the Scotia Arc. In: Craddock, C (ed) Antarctic Geoscience, University of Wisconsin Press, Madison, Wisconsin, pp 193–202

Eagles G, Jokat W (2014) Tectonic reconstructions for paleobathymetry in Drake Passage. Tectonophysics 611:28–50

Espinoza F, Morata D, Pelleter E, Maury RC, Suárez M, Lagabrielle Y, Polvé M, Bellon H, Cotten J, de la Cruz R, Guivel C (2005) Petrogenesis of the Eocene and Mio-Pliocene alkaline basaltic magmatism in Meseta Chile Chico, southern Patagonia, Chile: evidence for the participation of two slab windows. Lithos 82:315–343

Féraud G, Alric V, Fornari M, Bertrand H, Haler M (1999) $^{40}Ar/^{39}Ar$ dating of the Jurassic volcanic province of Patagonia: migrating magmatism related to Gondwana break-up and subduction. Earth Planet Sc Lett 172:83–96

Feruglio E (1938) Relaciones estratigráficas entre el Patagoniano y el Santacruciano en la Patagonia Austral. Rev Museo de La Plata, Geología 4:129–159

Figueiredo AMF, Pellon de Miranda A, Ferreira RF, Zalan PV (1996) Cuenca de San Julián. Relatorio del XIII Congreso Geológico Argentino y III Congreso Exploración de Hidrocarburos: 193–212

Fildani A, Hessler AM (2005) Stratigraphic record across a retroarc basin inversion: Rocas Verdes Magallanes Basin, Patagonian Andes. Geol Soc Am Bull 117:1596–1614

orlando_a_p@yahoo.com.ar

Fildani A, Cope TD, Graham SA, Wooden JL (2003) Initiation of the Magallanes foreland basin: Timing of the southernmost Patagonian Andes orogeny revised by detrital zircon provenance analysis. Geology 31:1081–1084

Fildani A, Romans BW, Fosdick JF, Crane WH, Hubbard SM (2008) Orogenesis of the Patagonian Andes as reflected by basin evolution in southernmost South America. In: Spencer JE, Titley S.R. (eds) Circum-Pacific Tectonics, Geologic Evolution, and Ore Deposits, Arizona Geol Soc Digest 22: 259–268

Flynn JJ, Novacek MJ, Dodson HE, Frassinetti D, McKenna M, Norell M, Sears K, Swisher C, Wyss A (2002) A new fossil mammal assemblage from the southern Chilean Andes: Implications for geology, geochronology, and tectonics. J S Am Earth Sci 15:285–302

Folguera A, Ramos VA (2002) Partición de la deformación durante el Neógeno en los Andes Patagonicos Septentrionales (37°–46° S). Rev Soc Geol España 15:81–93

Forsythe R, Nelson E (1985) Geological manifestations of ridge collision: evidence from the Golfo de Penas-Taitao basin, southern Chile. Tectonics 4:477–495

Forsythe R, Nelson E, Carr MJ, Keading ME, Hervé M, Mpodozis C, Soffia JM, Harambour S (1986) Pliocene near trench magmatism in Southern Chile: a possible manifestation of ridge collision. Geology 14:23–27

Fosdick JC, Romans BW, Fildani A, Bernhardt A, Calderón M, Graham SA (2011) Kinematic evolution of the Patagonian retroarc fold-and-thrust belt and Magallanes foreland basin, Chile and Argentina, 51°30'S. Geol Soc Am Bull 123:1679–1698

Fosdick JC, Grove M, Hourigan JK, Calderón M (2013) Retroarc deformation and exhumation near the end of the Andes, southern Patagonia. Earth Planet Sc Lett 361:504–517

Fosdick JC, Grove M, Graham SA, Hourigan JK, Lovera O, Romans BW (2014) Detrital thermochronologic record of burial heating and sediment recycling in the Magallanes foreland basin, Patagonian Andes. Basin Res 1–27:doi: 10.1111/bre.12088

Ghiglione MC, Ramos VA (2005) Chronology of deformation in the Southernmost Andes of Tierra del Fuego. Tectonophysics 405:25–46

Ghiglione MC, Cristallini EO (2007) Have the southernmost Andes been curved since Late Cretaceous times? An analog test for the Patagonian Orocline. Geology 35:13–16

Ghiglione MC, Suarez F, Ambrosio A, Da Poian G, Cristallini EO, Pizzio MF, Reinoso RM (2009) Structure and evolution of the Austral basin fold–thrust belt, southern Patagonian Andes. Rev Asoc Geol Argentina 65:215–226

Ghiglione MC, Quinteros J, Yagupsky D, Bonillo-Martínez P, Hlebszevtich J, Ramos VA, Vergani G, Figueroa D, Quesada S, Zapata T (2010) Structure and tectonic history of the foreland basins of southernmost South America. J S Am Earth Sci 29:262–277

Ghiglione MC, Likerman J, Barberón V, Giambiagi L, Aguirre-Urreta MB, Suarez F (2014a) Geodynamic context for the deposition of coarse-grained deep-water axial channel systems in the Patagonian Andes. Basin Res 26(6):726–745

Ghiglione MC, Naipauer M, Barberón V, Ronda G, Pereyra-Fernández E, Ramos VA, Aguirre-Urreta MB, Valencia V (2014 b) Early Cretaceous (Aptian) uplift of Patagonia recorded on detrital zircons population from the Patagonian Andes. XIII Congreso Geológico Argentino (Córdoba), Actas, Electronics files

Ghiglione MC, Navarrete-Rodríguez AT, González-Guillot M, Bujaleski G (2013) The opening of the Magellan Strait and its geodynamic implications. Terra Nova 25:13–20

Ghiglione MC, Naipauer M, Sue C, Barberón V, Valencia V, Aguirre-Urreta MB, Ramos VA (2015) U–Pb zircon ages from the northern Austral basin and their correlation with the Early Cretaceous exhumation and volcanism of Patagonia. Cretac Res 55:116–128

Giacosa R, Fracchia D, Heredia N (2012) Structure of the Southern Patagonian Andes at 49°S. Geológica Acta 10:265–282

Gonzales J, Aydin A (2008) Structural characterization of deep-water deposits in a foreland basin, Silla Syncline (Chilean Patagonia), with applications to depositional processes. J Struct Geol 30:1095–1108

orlando_a_p@yahoo.com.ar

Gorring ML, Kay SM, Zeitler PK, Ramos VA, Rubiolo D, Fernandez MI, Panza JL (1997) Neogene Patagonian plateau lavas: Continental magmas associated with ridge collision at the Chile Triple Junction. Tectonics 16:1–17

Gorring ML, Singer B, Gowers J, Kay SM (2003) Plio-Pleistocene basalts from the Meseta del Lago Buenos Aires, Argentina: Evidence for asthenosphere-lithosphere interactions during slab window magmatism. Chem Geol 193:215–235

Guivel C, Morata D, Pelleter E, Espinoza F, Maury RC, Lagabrielle Y, Polvé M, Hervé B, Cotten J, Benoit M, Suárez M, de la Cruz R (2006) Miocene to Late Quaternary Patagonian basalts (46–47S): Geochronometric and geochemical evidence for slab tearing due to active spreading ridge subduction. J Volcanol Geotherm Res 149:346–370

Guler MV, Archangelsky S (2006) Albian dinoflagellate cysts from the Kachaike Formation, Austral Basin, southwest Argentina. Rev Museo Argentino Cs Naturales, Nueva Serie 8:179–184

Halpern M (1973) Regional geochronology of Chile South of 50°. Latitude. Geol Soc Am Bull 84 (7):2407–2422

Halpern M, Rex DC (1972) Time of folding of the Yahgan Formation and age of the Tekenika beds, southern Chile, South America. Geol Soc Am Bull 83:1881–1886

Heine C, Zoethout J, Müller RD (2013) Kinematics of the South Atlantic rift. Solid Earth 4:215–253

Hervé F, Nelson E, Kawashita K, Suárez M (1981) New isotopic ages and the timing of orogenic events in the Cordillera Darwin, southernmost Chilean Andes. Earth Planet Sc Lett 55 (2):257–265

Hervé F, Pankhurst RJ, Fanning CM, Calderón M, Yaxley GM (2007) The South Patagonian batholith: 150 My of granite magmatism on a plate margin. Lithos 97:373–394

Homovc JF, Constantini LA (2001) Hydrocarbon exploration potential within intraplate shear-related depocenters, Deseado and San Julián basins, southern Argentina. Am Assoc Petrol Geol Bull 85(10):1795–1816

Hubbard SM, Romans BW, Graham SA (2008) Deep-Water foreland basin deposits of the Cerro Toro Formation, Magallanes basin, Chile: architectural elements of a sinuous basin axial channel belt. Sedimentology 55:1333–1359

Hubbard SM, Fildani A, Romans BW, Covault JA, McHargue TR (2010) High-relief slope clinoform development; insights from outcrop, Magallanes Basin, Chile. J Sediment Res 80:357–375

Jobe ZR, Bernhardt A, Lowe DR (2010) Facies and architectural asymmetry in a conglomerate rich submarine channel fill, Cerro Toro formation, Sierra del Toro, Magallanes Basin, Chile. J Sediment Res 80:1085–1108

Kay SM, Ramos VA, Marquez M (1993) Evidence in Cerro Pampa volcanic rocks for slab melting prior to ridge-trench collision in southern South America. J Geol 101:703–714

Kay SM, Ramos VA, Gorring ML (2002) Geochemistry of Eocene Plateau Basalts related to ridge collision in Southern Patagonia. XV Congreso Geologico Argentino (Calafate), Actas, Electronic files

Katz HR (1963) Revision of Cretaceous stratigraphy in Patagonian Cordillera of Ultima Esperanza, Magallanes Province, Chile. Am Assoc Pet Geol Bull 47:506–524

Katz HR (1973) Contrasts in tectonic evolution of orogenic belts in the southwest Pacific. J Royal Soc New Zealand 3:333–362

Klepeis K, Betka P, Clarke G, Fanning M, Hervé F, Rojas L, Mpodozis C, Thomson S (2010) Continental underthrusting and obduction during the Cretaceous closure of the Rocas Verdes rift basin, Cordillera Darwin, Patagonian Andes. Tectonics 29(3) doi:10.1029/2009TC002610

Kohn MJ, Spear FS, Harrison TM, Dalziel IWD (1995) Ar-40/Ar-39 Geochronology and P-T-T Paths from the Cordillera Darwin Metamorphic Complex, Tierra del Fuego, Chile. J Metamorphic Geol 13:251–270

Kraemer PE (1998) Structure of the Patagonian Andes. Regional balanced cross section at 50° S.L. Argentina. Int Geol Rev 40:896–915

orlando_a_p@yahoo.com.ar

Kraemer PE (2003) Orogenic shortening and the origin of the Patagonian orocline (56°S.Lat). J S Am Earth Sci 15:731–748

Kraemer PE, Riccardi AC (1997) Estratigrafía de la región comprendida entre los lagos Argentino y Viedma (49°40–50°10 lat. S), Provincia de Santa Cruz. Rev Asoc Geol Argentina 52:333–360

Kraemer PE, Ploszkiewicz JV, Ramos VA (2002) Estructura de la Cordillera Patagónica Austral entre los 46° y 52°S, provincia de Santa Cruz, Argentina. In: Haller MJ (ed) Geología y Recursos Naturales de Santa Cruz. Relatorio del XV Congreso Geológico Argentino, Buenos Aires, pp 353–364

Lagabrielle Y, Suarez M, Rossello EA, Hérail G, Martinod J, Régnier M, De la Cruz R (2004) Neogene to Quaternary tectonic evolution of the Patagonian Andes at the latitude of the Chile Triple Junction. Tectonophysics 385:211–241

Leanza AF (1970) Ammonites nuevos o poco conocidos del Aptiano, Albiano y Cenomaniano de los Andes Australes, con notas acerca de su posición estratigráfica. Rev Asoc Geol Argentina 25(2):197–261

Leanza AF (1972) Andes Patagónicos Australes. Geología Regional Argentina, Academia Nacional de Ciencias, Córdoba, pp 689–706

Likerman L, Burlando JF, Cristallini EO, Ghiglione MC (2013) Along-strike structural variations in the Southern Patagonian Andes: insights from physical modeling. Tectonophysics 590:106–120

Macellari CE, Barrio CA, Manassero MJ (1989) Upper Cretaceous to Paleocene depositional sequences and sandstone petrography of Southwestern Patagonia (Argentina and Chile). J S Am Earth Sci 23:223–239

Malumián N (1990) Foraminíferos de la Formación Man Aike (Eoceno, Sureste Lago Cardiel) Provincia de Santa Cruz. Rev Asoc Geol Argentina 45:365–385

Malumián N (2002) El Terciario marino. Sus relaciones con el eustatismo. In: Haller MJ (ed) Geología y Recursos naturales de Santa Cruz. Asociación Geológica Argentina, Relatorio XV Congreso Geológico Argentino, pp 237–244

Malumián N, Caramés A (1997) Upper Campanian-Paleogene from the Río Turbio coal measures in southern Argentina: Micropaleontology and the Paleocene/Eocene boundary. J S Am Earth Sci 10:189–201

Malumián N, Náñez C (1988) Asociaciones de foraminíferos del Terciano medio de Cuenca Austral: sus relaciones con eventos eustaticos globales. Rev Asoc Geol Argentina 43 (2):257–264

Malumián N, Panza JL, Parisi C, Nañez C, Caramés A, Torre E (2000) Hoja Geológica 5172-III-Yacimiento Río Turbio, provincia Santa Cruz, 1:250.000. Servicio Geológico Minero Argentino, Boletín 247: p. 108

Manassero MJ (1988) Petrografía y procedencia de las areniscas cretacicas superiores de la Cuenca Austral Argentina. Rev Asoc Geol Argentina 43:175–187

Marenssi SA, Casadío S, Santillana S (2002) La Formación Man Aike al sur de El Calafate (Provincia de Santa Cruz) y su relación con la discordancia del Eoceno medio en la cuenca Austral. Rev Asoc Geol Argentina 57:341–344

Marenssi SA, Limarino CA, Tripaldi A, Net L (2005) Fluvial systems variations in the Rio Leona Formation: tectonic and eustatic controls on the Oligocene evolution of the Austral (Magallanes) Basin, southernmost Argentina. J. S Am. Earth Sci 19:359–372

Matthews KJ, Seton M, Muller RD (2012) A global-scale plate reorganization event at 105-100 Ma. Earth Planet Sc Lett 355:283–298

McAtamney J, Klepeis K, Mehrtens C, Thomson S, Betka P, Rojas L, Snyder S (2011) Along-strike variability of back-arc basin collapse and the initiation of sedimentation in the Magallanes foreland basin, southernmost Andes (53–54.5°S). Tectonics 30(5). doi:10.1029/2010TC002826

Michel J, Baumgartner L, Putlitz B, Schaltegger U, Ovtcharova M (2008) Incremental growth of the Patagonian Torres del Paine laccolith over 90 k.y. Geology 36(6):459–462

orlando_a_p@yahoo.com.ar

Miller KG, Kominz MA, Browning JV, Wright JD, Mountain GS, Katz ME, Sugarman PJ, Cramer BS, Christie-Blick N, Pekar SF (2005) The Phanerozoic Record of Global Sea-Level Change. Science 310:1293–1298

Morata D, de la Cruz R, Suárez M, Demant A (2000) Mantle xenoliths and xenocrysts in the late Paleocene Patagonian continental flood basalts from Aysen, southern Chile. IX Congreso Geologico Chileno (Puerto Varas). Actas 2:226–229

Mukasa SB, Dalziel IWD (1996) Southernmost Andes and South Georgia island, north Scotia Ridge: zircon U-Pb and muscovite Ar/Ar age constraints on tectonic evolution of southwestern Gondwanaland. J S Am Earth Sci 9:349–365

Natland M, González E, Cañón A, Ernst M (1974) A system of stages for correlation of Magallanes basin sediments. Geol Soc Am Memoirs 139:1–117

Nelson EP (1982) Postectonic uplift of the Cordillera Darwin orogenic core complex: evidence for fission track geochronology and closing temperature time relationships. J Geol Soc 139:755–761

Nelson EP, Dalziel IWD, Milnes AG (1980) Structural geology of the Cordillera Darwin-collision style orogenesis in the southernmost Andes. Eclogae Geol Helv 73:727–751

Nullo FE (1983) Descripción Geológico-Económica de la Hoja 59 a-b, Cordón de los Cristales, provincia de Santa Cruz. Unpubl, Servicio Geológico Nacional Buenos Aires

Nullo FE, Panza JL, Blasco G (1999) Jurásico y Cretácico de la Cuenca Austral. In Caminos R (ed) Geología Argentina, Instituto de Geología y Recursos Minerales, Anales 29(17–7): 528-535

Palazzesi L, Barreda VD, Cuitiño JI, Guler MV, Tellería MC, Santos RV (2014) Fossil pollen records indicate that Patagonian desertification was not solely a consequence of Andean uplift. Nature communications 5:35–58

Pankhurst R, Leat PT, Sruoga P, Rapela CW, Márquez M, Storey BC, Ryley TR (1998) The Chon Aike province of Patagonia and related rocks in west Antarctica: A silicic large igneous province. J Volcanol Geotherm Res 81:113–136

Pankhurst RJ, Weaver SD, Hervé F, Larrondo P (1999) Mesozoic-Cenozoic evolution of the North Patagonian Batholith in Aysen, southern Chile. J Geol Soc London 156:673–694

Pankhurst RJ, Riley TR, Fanning CM, Kelley SP (2000) Episodic silicic volcanism in Patagonia and the Antarctic Peninsula: chronology of magmatism associated with the break-up of Gondwana. J Petrology 41:605–625

Panza JL (2002) La cubierta detrítica del Cenozoico superior. In Haller MJ (ed) Geología y Recursos Naturales de Santa Cruz, Relatorio XV Congreso Geológico Argentino: 259–284

Pardo-Casas F, Molnar P (1987) Relative motion of the Nazca (Farallon) and South American plates since Late Cretaceous time. Tectonics 6:233–248

Poiré D, Morel E, Maggi J (1999) Facies diamictíticas en la Formación Bahía de la Lancha (Paleozoico), Estancia La Lila, Lago San Martín, Santa Cruz. XIV Congreso Geológico Argentino (Salta). Actas 1:425–428

Rabinowitz PD, La Brecque J (1979) The Mesozoic South Atlantic Ocean and evolution of its continental margins. J Geophys Res B: Solid Earth 84:5973–6002

Ramírez de Arellano C, Putlitz B, Müntener O, Ovtcharova M (2012) High precision U/Pb zircon dating of the Chaltén Plutonic Complex (Cerro Fitz Roy, Patagonia) and its relationship to arc migration in the southernmost Andes. Tectonics 31(4). doi:10.1029/2011TC003048

Ramos VA (1989) Andean foothills structures in Northern Magallanes Basin, Argentina. Am Assoc Pet Geol Bull 73:887–903

Ramos VA (2005) Seismic ridge subduction and topography: Foreland deformation in the Patagonian Andes. Tectonophysics 399:73–86

Ramos VA, Ghiglione MC (2008) Tectonic evolution of the Patagonian Andes. Late Cenozoic of Patagonia and Tierra del Fuego. In Rabassa J (ed) Developments in Quaternary Science, Elsevier 11: 57–71

Ramos VA, Drake R (1987) Edad y significado de la Formación Río Tarde (Cretácico), Lago Posadas, Provincia de Santa Cruz. X Congreso Geológico Argentino (Tucumán). Actas 1:143–147

orlando_a_p@yahoo.com.ar

Ramos VA, Kay SM (1992) The Southern Patagonian plateau basalts: retroarc testimony of a ridge collision. Tectonophysics 205:261–282
Ramos VA, Niemeyer H, Skarmeta J, Muñóz J (1982) Magmatic evolution of the Austral Patagonian Andes. Earth-Science Rev 18:411–443
Rapallini AE, Calderón M, Singer S, Hervé F, Cordani U (2008) Tectonic implications of a paleomagnetic study of the Sarmiento Ophiolitic Complex, Southern Chile. Tectonophysics 452:29–41
Riccardi AC (1971) Estratigrafía en el oriente de la bahía La Lancha, Lago San Martín Santa Cruz. Rev Museo de La Plata, Notas, Geología 7:245–318
Riccardi AC (2002) Invertebrados del Cretácico Superior. In: Haller MJ (ed) Geología y Recursos Naturales de Santa Cruz. Relatorio del XV Congreso Geológico Argentino, Buenos Aires, pp 461–479
Riccardi AC, Rolleri E (1980) Cordillera Patagónica Austral. II Simposio de Geología Regional Argentina, Academia Nacional de Ciencias, Córdoba, pp 1173–1306
Romans BW, Fildani A, Graham SA, Hubbard SM (2010) Importance of Predecessor basin history on the sedimentary fill of a retroarc foreland basin: provenance analysis of the Cretaceous Magallanes basin, Chile (50–52°S). Basin Res 22:640–658
Romans BW, Fildani A, Hubbard SM, Covault JA, Fosdick JC, Graham SA (2011) Evolution of deepwater stratigraphic architecture, Magallanes Basin, Chile. Mar Petrol Geol 28:612–628
Russo A, Flores MA, Di Benedetto H (1980) Patagonia Austral Extraandina. II Simposio de Geología Regional Argentina, Actas 2:1431–1462
Scott KM (1966) Sedimentology and dispersal pattern of a Cretaceous Flysch sequence, Patagonian Andes, southern Chile. Am Assoc Pet Geol Bull 50:72–107
Sdrolias M, Müller RD (2006) Controls on back-arc basin formation. Geochem Geophys Geosyst 7(4). doi:10.1029/2005GC001090
SEGEMAR (2003) Mapa Geológico de Santa Cruz 1:750,000. Servicio Geológico Minero de la Rep, Argentina, Buenos Aires, Argentina
SERNAGEOMIN (2003) Mapa Geológico de Chile: versión digital, escala 1:1,000,000. Servicio Nacional de Geología y Minería, Santiago, Chile
Soares F, Miranda AP, Figueiredo AMFD (2000) Geological and geophysical interpretation of the San Julian Basin—offshore Argentina. Atlantic Rifts and Continental Margins: 193–209
Smith CHL (1977) Sedimentology of the Late Cretaceous (Santonian–Maastrichtian) Tres Pasos Formation, Ultima Esperanza District, Southern Chile. Unpubl. M.S. thesis: Madison, Wisconsin, University of Wisconsin, p 129
Somoza R, Ghidella ME (2005) Convergencia en el margen occidental de América del sur durante el Cenozoico: Subducción de Nazca, Farallon y Aluk. Rev Asoc Geol Argentina 60:797–809
Somoza R, Ghidella ME (2012) Late Cretaceous to recent plate motions in westrn South America revisited. Earth Planet Sc Lett 331:152–163
Somoza R, Zaffarana CB (2008) Mid-Cretaceous polar standstill of South America, motion of the Atlantic hotspots and the birth of the Andean Cordillera. Earth Planet Sc Lett 271:267–277
Stern CR, De Witt MJ (2003) Rocas Verdes ophiolites, southernmost South America: remnants of progressive stages of development on oceanic-type crust in a continental margin back-arc basin. In Dilek Y, Robinson PT (eds) Ophiolites in Earth History. Geol Soc London, Special Publication 218: 1–19
Stern CR, Mohseni PP, Fuenzalida R (1991) Petrochemistry and tectonic significance of Lower Cretaceous Barros Arana Formation basalts, southernmost Chilean Andes. J S Am Earth Sci 4:331–342
Suárez M, De la Cruz R (2001) Jurassic to Miocene K-Ar dates from eastern central Patagonian Cordillera plutons, Chile (45° - 48°S). Geol Mag 138(1):53–66
Suárez M, de la Cruz R, Bell CM (2000a) Timing and origin of deformation along the Patagonian fold and thrust belt. Geol Mag 137:345–353
Suárez M, de la Cruz R, Troncoso A (2000b) Tropical/subtropical Upper Paleocene-Lower Eocene fluvial deposits in eastern central Patagonia, Chile. J S Am Earth Sci 13:527–536

orlando_a_p@yahoo.com.ar

Suárez M, de la Cruz R, Bell M, Demant A (2010) Cretaceous slab segmentation in southwestern Gondwana. Geol Mag 147:193–205

Thomas CR (1949) Geology and Petroleum Exploration in Magallanes Province, Chile. Am Assoc Petrol Geol Bull 33:1553–1578

Thomson SN (2002) Late Cenozoic geomorphic and tectonic evolution of the Patagonian Andes between latitudes 42°S and 46°S: an appraisal based on fission-track results from the transpressional intra-arc Liquine-Ofqui fault zone. Geol Soc Am Bull 114:1159–1173

Thomson SN, Herve F, Stockhert B (2001) The Mesozoic-Cenozoic denudation history of the Patagonian Andes (southern Chile) and its correlation to diferent subduction processes. Tectonics 20:693–711

Thomson SN, Brandon MT, Reiners PW, Tomkin JH, Vásquez C, Wilson NJ (2010) Glaciation as a destructive and constructive control on mountain building. Nature 467:313–317

Troncoso A, Suárez M, de la Cruz R, Palma Heldt S (2002) Paleoflora de la Formación Ligorio Márquez en su localidad tipo: sistemática, edad e implicancias paleoclimáticas. Rev Geol Chile 29:113–135

Uliana VMA, Biddle KT, Cerdan J (1989) Mesozoic extension and the formation of Argentine sedimentary basins. In: Tankard AJ, Balkwill HR (eds) Extensional Tectonics and Stratigraphy of the North Atlantic Margins. Am Assoc Pet Geol Bull, Memoirs 46: 599–613

Varela AN, Poiré DG, Martin T, Gerdes A, Goin FJ, Gelfo JN, Hoffmann S (2012) U-Pb zircon constraints on the age of the Cretaceous Mata Amarilla Formation, southern Patagonia, Argentina: its relationship with the evolution of the Austral Basin. Andean Geol 39:359–379

Vérard C, Flores K, Stampfli G (2012) Geodynamic reconstructions of the South America-Antarctica plate system. J Geodyn 53:43–60

Wilson TJ (1991) Transition from Back-Arc to Foreland Basin Development in the Southernmost Andes—Stratigraphic Record from the Ultima-Esperanza-District, Chile. Geol Soc Am Bull 103:98–111

Winn RD, Dott RH (1979) Deep-water fan-channel conglomerates of late Cretaceous age, southern Chile. Sedimentology 26:203–228

orlando_a_p@yahoo.com.ar

Orogenic Growth of the Fuegian Andes (52–56°) and Their Relation to Tectonics of the Scotia Arc

Matías C. Ghiglione

Abstract The tectonic evolution of the Fuegian Andes is strongly related to their southern neighbors, the Scotia Sea and Antarctica. During Mesozoic times, extensional and magmatic processes in the southernmost Andes developed in continuity with the Antarctic Peninsula. The Rocas Verdes back-arc oceanic basin opened during the Jurassic along the Patagonian–Fuegian margin, widening toward the south were it connected with the Weddell Sea. Jurassic volcaniclastic deposits from the large igneous province Chon Aike of Patagonia and the Antarctic Peninsula Volcanic Group were part of the same volcanic event related to Gondwana breakup. It was followed by Late Cretaceous compression, closure and inversion of the Rocas Verdes Basin that culminated with the onset of orogenesis and foreland sedimentation in the Austral or Magallanes Basin. The beginning of compression coincided with geodynamic reconstructions predicting the collision of the Antarctic Peninsula against the Fuegian Andes due to accelerated convergence rates. Afterward, three phases of Cenozoic deformation in the southernmost Andes that can also be tied to tectonics of the Scotia Arc occurred: (1) a Paleocene–early Eocene continental stretching on the Austral, Malvinas, and South Malvinas basins, produced by the slow, N–S separation of South America and Antarctica. After 50 Ma, crustal extension was concentrated in the Drake Passage due to an acceleration in South America—Antarctica separation rate, while regional continental stretching ceased. (2) The Fuegian Andes were affected by middle Eocene–Oligocene compressional deformation producing the forward advance of the orogenic front. Shortening was due to the synergetic combination of rapid convergence and northward-directed subduction of the Farallon plate against South America, and the fast opening of the Scotia Sea producing ridge-push forces. (3) The development of the present seismically active Magallanes–Fagnano continental strike-slip plate boundary between South America and Scotia Plates produces widespread deformation in the Fuegian Andes since the latest Oligocene.

M.C. Ghiglione (✉)
Departamento de Ciencias Geológicas, Facultad de Ciencias Exactas y Naturales,
Instituto de Estudios Andinos "Don Pablo Groeber" UBA-CONICET,
Buenos Aires, Argentina
e-mail: mcghiglione@gmail.com

© Springer International Publishing Switzerland 2016

A. Folguera et al. (eds.), *Growth of the Southern Andes*,
Springer Earth System Sciences, DOI 10.1007/978-3-319-23060-3_11

orlando_a_p@yahoo.com.ar

Keywords Fuegian Andes · Southernmost Andes · Scotia Plate · Antarctica · Drake Passage · Eocene–Oligocene global cooling · Austral basin · Magallanes basin · Malvinas basin · Magallanes–Fagnano fault · Scotia ridge

1 Introduction

The tectonic evolution of the Fuegian Andes is strongly related to its southern neighbors: the Scotia Sea and Antarctica (Fig. 1a, b). Mesozoic extensional and magmatic processes in the southernmost Andes and Patagonia developed in continuity with the Antarctic Peninsula and the Weddell Sea. One of the most outstanding characteristics was the Jurassic development of the Rocas Verdes marginal Basin (Fig. 2a), producing oceanic crust in connection with the Weddell Sea (Katz 1973; Dalziel et al. 1974; Dalziel 1981; Stern and de Wit 2003; Calderón et al. 2007, 2012). Thereafter, during the onset of subduction, accelerated convergence on the Pacific margin, plus South Atlantic ridge-push forces, produced a compressional state of stress responsible for the progressive closure of the oceanic basin during the mid-Cretaceous (Halpern and Rex 1972; Bruhn and Dalziel 1977; Dalziel 1986; Cunningham 1995). Final closure of the Rocas Verdes Basin and collision of its drifted margin together with the Antarctic Peninsula against the Patagonian–Fuegian Andes (Fig. 2a) occurred between 95 and 84 Ma (Vérard et al. 2012). The Late Cretaceous was therefore a period of consolidation of the Basement Domain (Ghiglione and Cristallini 2007), and the onset of foreland depocenters from the Austral–Magallanes and Malvinas basins (Fig. 1b).

Throughout the Cenozoic, the Fuegian Andes were affected by competing tectonic processes, giving as a result the superposition of different kinematic events. For one side, Andean uplift and compression were sustained due to subduction (Cande and Leslie 1986; Folguera and Ramos 2002; Somoza and Ghidella 2005, 2012; Ghiglione and Cristallini 2007), while strike-slip and extensional tectonics were mainly related to the opening of the Scotia Sea (Livermore et al. 2005; Eagles et al. 2005; Ghiglione et al. 2008, 2010; Baristeas et al. 2013) and the northward drift of South America during its separation with the Antarctic Peninsula (Livermore et al. 2005; Somoza 2007; Ghiglione et al. 2013). Subduction of Pacific oceanic plates and seismic ridges against the western margin sustained continuous Andean orogenic growth from Cretaceous to Neogene times (see Chap. 10, this book).

An important debate involves the Paleogene evolution of the orogen, with seemingly contrasting evidence of extensional (Dalziel and Brown 1989; Kohn et al. 1995; Ghiglione et al. 2008, 2010; Bry et al. 2004; Baristeas et al. 2013) and

orlando_a_p@yahoo.com.ar

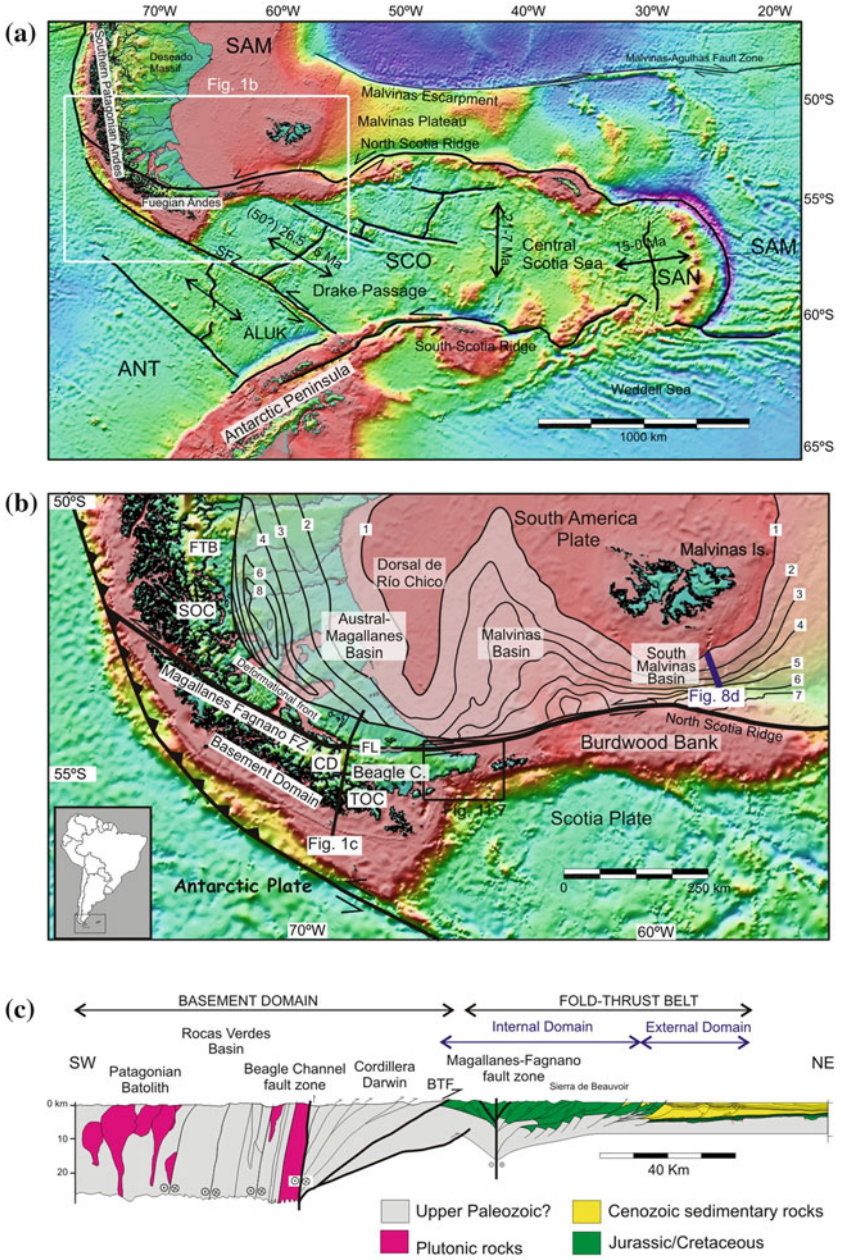


Fig. 1 **a** Major tectonic plates enclosing the Southernmost Andes (Antarctica ANT, Sandwich SAN, Scotia SCO, and South America SAM), *SFZ* Shackleton Fault Zone; *SSR* South Scotia Ridge. **b** Location of main morphostructural units. Contours indicate foreland sediment thickness within the undeformed depocenters in kilometers, *CD* Cordillera Darwin; *FL* Fagnano Lake; *FTB* fold–thrust belt; *SOC* Sarmiento Ophiolitic Complex; *TOC* Tortuga Ophiolitic Complex. **c** Regional structural cross-section. BTF Basement thrust front. From Ghiglione et al. (2010), after Cunningham (1995) and Kraemer (2003)

orlando_a_p@yahoo.com.ar

compressional tectonics (Cunningham 1995; Ghiglione and Ramos 2005; Gombosi et al. 2009; Klepeis et al. 2010; Torres Carbonell et al. 2011). However, an extensional event followed by compression can be accounted (Ghiglione et al. 2008, 2010). Nevertheless, there is an agreement in that a rapid propagation of the fold and thrust belt occurred from Middle to Late Eocene times (Ghiglione et al. 2002; Ghiglione and Ramos 2005; Barbeau et al. 2009).

Some events in the evolution of the Fuegian Andes are related to the process of global significance, such as the opening of the Drake Passage, somehow linked to Late Cenozoic cooling (Fig. 2b, c). Before 50 Ma, a wide and relatively shallow epicontinental sea developed between the Antarctic Peninsula and South America drowning the Weddellian Isthmus (Lawver et al. 2014) and preventing the faunal interchange for cursorial terrestrial forms (Reguero et al. 2014). During the phase of late Paleocene to early Eocene, slow separation between South America and Antarctica (Fig. 2b, c) (Livermore et al. 2005), a continental stretching regime existed in Tierra del Fuego (Ghiglione et al. 2008, 2010) and offshore Malvinas Basin (Baristeas et al. 2013). Analysis of geophysical data in the Scotia Sea indicates that an eightfold increase in the separation rate started at about 50 Ma (phase II of Livermore et al. 2005; Eagles et al. 2006). It seems that it was South America who broke away by drifting northwards about 5° latitude, as shown by the relative Eocene paleomagnetic position of Patagonia (Somoza 2007). The onset of phase II (Fig. 2b) produced the Late Eocene opening of small extensional basins in the embryonic Drake Passage (Lawver and Gahagan 2003; Eagles et al. 2006).

Relative movement between South America and Antarctica was accommodated by spreading in the West Scotia Sea from about 28 Ma (Lodolo et al. 2006) until ~16 Ma when the future Scotia Plate started to move independently of the South American plate (Eagles et al. 2005; Lagabrielle et al. 2009) by means of a sinistral strike-slip fault zone on the North Scotia Ridge—Magallanes–Fagnano fault zone (Klepeis and Austin 1997; Thomas et al. 2003). A still active rifting system perpendicular to the orogen produced the opening of the eastern Magallanes strait (Diraison et al. 1997, 2000) and the transverse segmentation of the external fold and thrust belt (Ghiglione et al. 2013). This fault system is responsible for the position of mayor Quaternary features such as the position of glacial valleys (Diraison et al. 1997, 2000) and the distribution of seismic events (Ghiglione et al. 2013).

In the following sections, a chronological account of major Cenozoic tectonic events and features that affected the southernmost Andes is given, considering mainly the Fuegian Andes, and complementary data from the Southern Patagonian Andes, offshore Austral and Malvinas basins, and the Scotia Sea. This work does not aim to present an extensive account of the geology of the region, but it emphasizes on geodynamic processes and the most controversial issues.

orlando_a_p@yahoo.com.ar

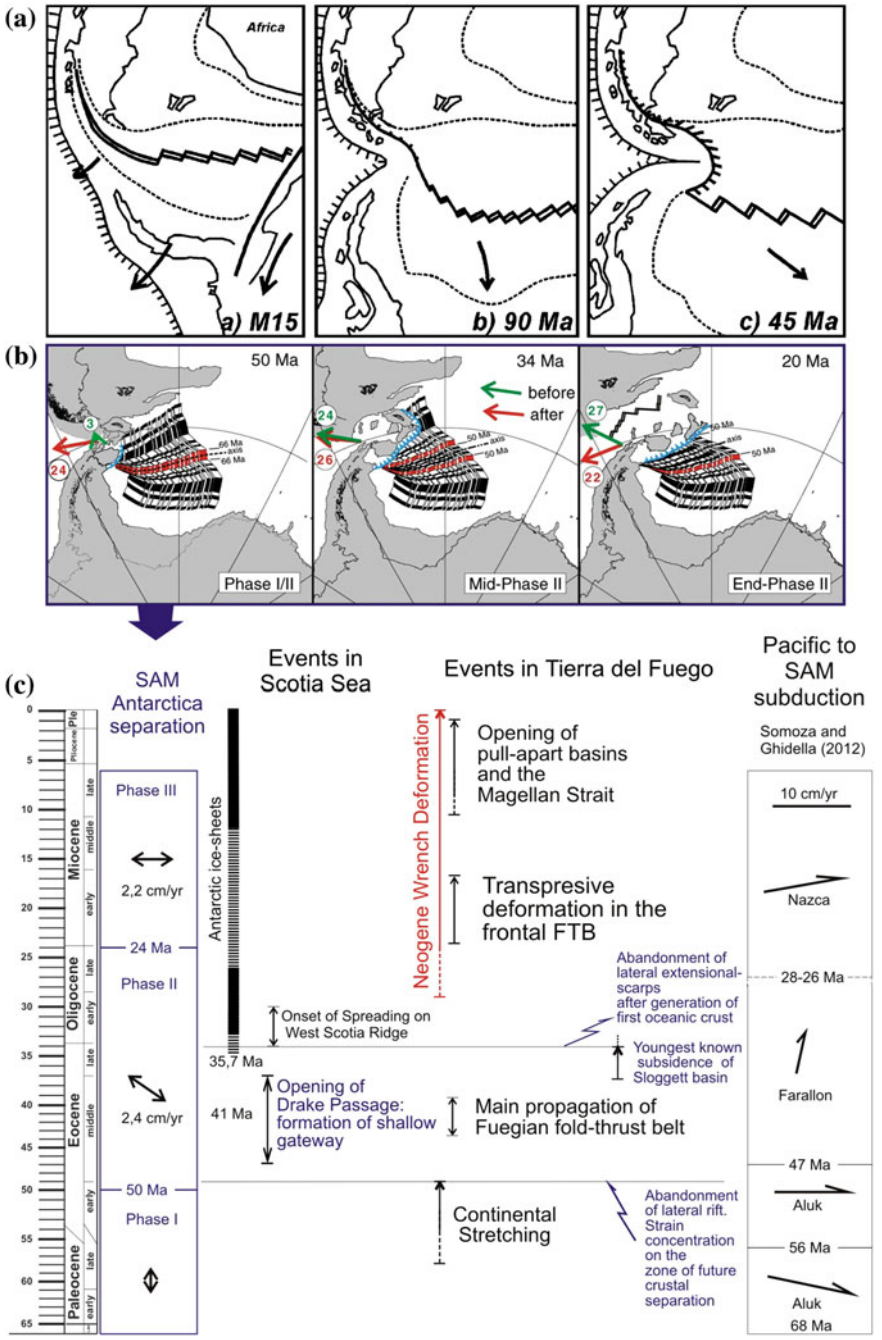


Fig. 2 **a** and **b** Mesozoic–Cenozoic reconstructions of South America and Antarctica. Modified from Barker (2001) and Livermore et al. (2005) respectively. **c** Correlation between events in Tierra del Fuego with main tectonic events from West Scotia Sea, modified after Ghiglione et al. (2008)

orlando_a_p@yahoo.com.ar

2 Structure of the Southern Andes

The southernmost Andes progressively change their strike from the N–S-oriented Southern Patagonian Andes to the ESE–WNW-trending Fuegian Andes (Fig. 1a, b) forming the Patagonian Orocline (Carey 1958; Dalziel et al. 1973; Cunningham 1993; Ghiglione and Cristallini 2007; Maffione et al. 2010). See Poblete et al. (2014) for a review of the kinematic development of the curvature and implications for the structural evolution of the mountain belt. Kinematic analysis of fault-slip data indicates that regional shortening directions vary in trend from ENE in the Patagonian Andes to NNE–SSW in the Fuegian Andes (Diraison et al. 2000).

The orogen can be divided into three main structural domains: (after Diraison et al. 2000; Kraemer 2003) (Fig. 1c) (i) a Basement thick-skinned Domain to the west and south (Fig. 1b), composed of Paleozoic metamorphic rocks, sedimentary and magmatic remnants of the Rocas Verdes Basin, and intrusive rocks of the Patagonian Batholith; and (ii) a fold and thrust belt (Figs. 3, 4), subdivided into a thick-skinned Internal domain exposing Jurassic to Cretaceous sequences and a thin-skinned External domain affecting the Tertiary foreland sequence. The boundary between the Basement domain and the thin-skinned fold and thrust belt is the basement thrust front (Figs. 1c, 3) (Kraemer 2003; Ghiglione et al. 2010). Calculated total shortening through the Fuegian fold and thrust belt with some constrains on the length of folded sequences ranges between ~75 km (~50 %) (Kley et al. 1999; Ghiglione, 2003) and 52 km (32 %) (Fig. 3).

3 Late Paleozoic–Early Cretaceous Geological Background

Subduction along the Pacific margin of Gondwana formed an accretionary prism from the Late Paleozoic to the Early Mesozoic that comprises the metasedimentary and metavolcanic basement of the Southern Andes (Nelson et al. 1980; Dalziel 1981; Hervé et al. 1981; Mukasa and Dalziel 1996). In Tierra del Fuego, basement rocks are concentrated in Cordillera Darwin (Figs. 1b, c), a high-grade metamorphic complex exposing kyanite–staurolite schist (Dalziel et al. 1974; Herve et al. 1981; Nelson 1982; Kohn et al. 1995; Maloney et al. 2011).

Patagonia was affected by widespread Jurassic extension and related silicic volcanic activity during Gondwana breakup (Dalziel 1981; Uliana et al. 1989; Pankhurst et al. 2000). The extension-related silicic volcanism formed part of Chon Aike large igneous province, distributed from the North Patagonian Massif throughout Andean and extra-Andean Patagonia toward the Antarctic Peninsula Volcanic Group (Fig. 5) (Storey et al. 1996; Féraud et al. 1999; Pankhurst et al. 2000; Calderón et al. 2007). The heterogeneous suite of siliceous volcanic and volcaniclastic rocks is known as Lemaire Formation in Argentinean Tierra del Fuego (Caminos et al. 1981; Yrigoyen 1989), and Tobífera Formation in Chile (Thomas 1949).

orlando_a_p@yahoo.com.ar

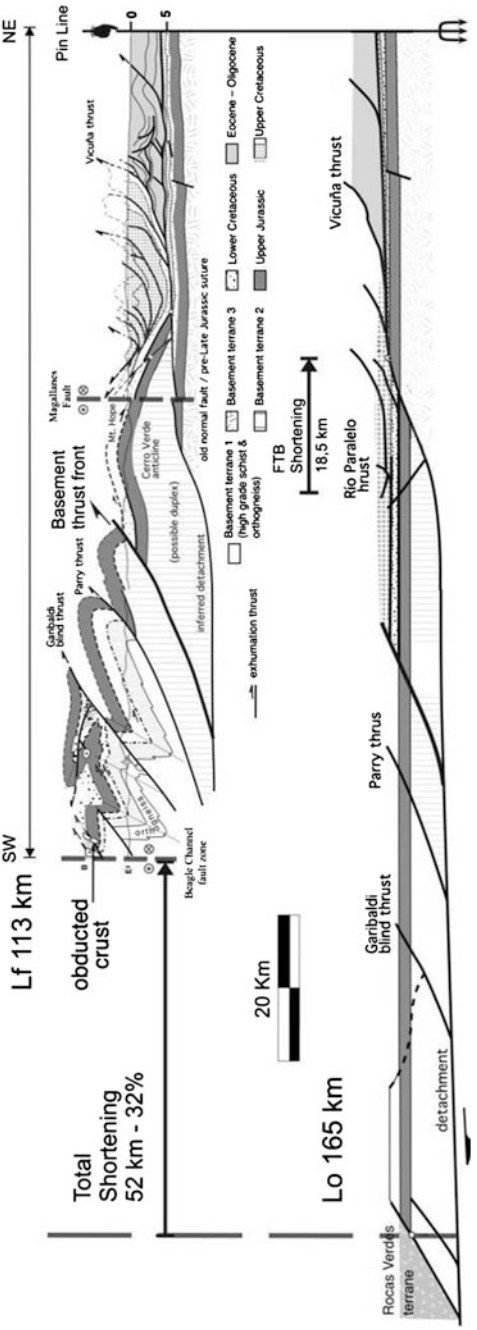


Fig. 3 Composite profile of Cordillera Darwin and south-central Tierra del Fuego, and restored section. Modified from Klepeis et al. (2010)

orlando_a_p@yahoo.com.ar

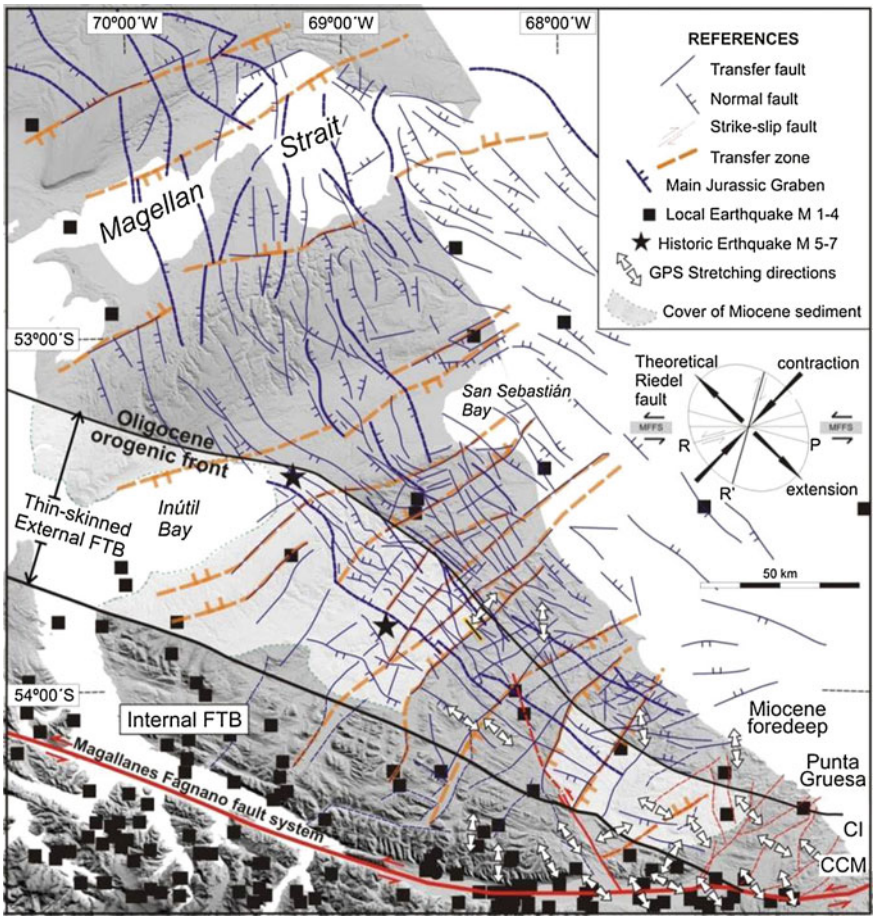


Fig. 4 Jurassic faults array from Tierra del Fuego. Main extensional grabens from the Chilean side are from Moraga et al. (2004) and Navarrete-Rodríguez (2006). *FTB* fold–thrust belt; seismicity of Tierra del Fuego from: Pelayo and Wiens (1989); Sabbione et al. (2007); Buffoni et al. (2009). GPS stretching directions are from Mendoza et al. (2011). *CI* Irigoyen cape; *CCM* Campo del Medio Cape. From Ghiglione et al. (2013)

Maximum extension produced the opening of the Late Jurassic to Early Cretaceous Rocas Verdes Basin, floored by basaltic crust with mid-ocean ridge affinities extending along the Pacific rim of the Southern Andes in the NW to the Weddell Sea in the SE (Fig. 2a) (Katz 1973; Dalziel et al. 1974; Dalziel 1981; Grunow et al. 1992; Mukasa and Dalziel 1996). Deformed remnants of this basin and its clastic infill are now exposed as the upper part of ophiolite complexes in the hinterland (Fig. 1b, 5) (Katz 1973; Wilson 1991; Mukasa and Dalziel 1996). The northern remnants of the pillow lavas ocean floor and interfingered bimodal 152–142 Ma old magmatism (Calderón et al. 2007; Hervé et al. 2007) are grouped

orlando_a_p@yahoo.com.ar

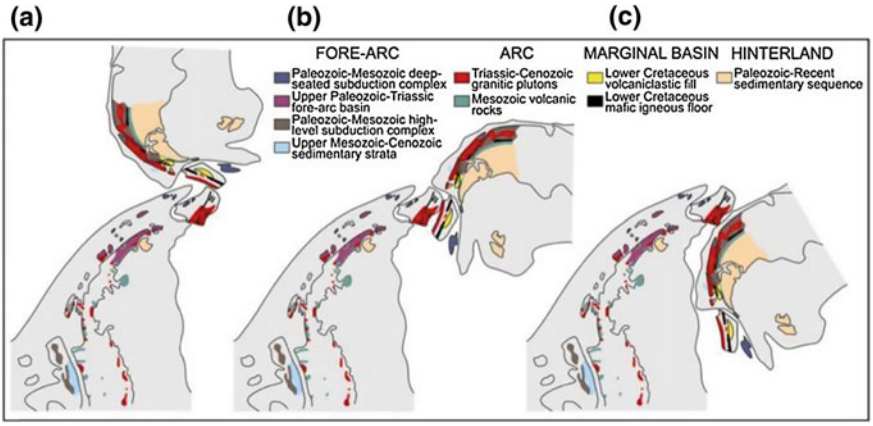


Fig. 5 **a**–**c**. Possible tectonostratigraphic reconstructions showing a time before the Eocene. From Eagles and Jokat (2014)

into the Sarmiento Ophiolite Complex in the Southern Patagonian Andes (Fig. 1b) (Stern and De Witt 2003). Detrital-zircon ages from sediments that covered the Tortugas ophiolitic complex on the southern part of the basin (Fig. 1b, c) provide a maximum depositional age of ~148 Ma, suggesting that the basin opened approximately simultaneously along its length during the Late Jurassic (Klepeis et al. 2010). Extension was followed by a Lower Cretaceous sag phase of the Yahgan and Beauvoir formations (Halpern and Rex 1972; Dalziel et al. 1974; Hervé et al. 1981; Suárez et al. 1985; Wilson 1991).

4 Late Cretaceous: Basement Consolidation and Onset of Foreland Basin

A first event of folding, thrusting, and rapid exhumation and cooling of Cordillera Darwin occurred between 90 and 70 Ma (Halpern and Rex 1972; Nelson et al. 1980; Kohn et al. 1995). This deformational event coincides in time with the final closure of the Rocas Verdes ocean basin, and collision of its para-autochthon western margin and the Antarctic Peninsula against the Patagonian–Fuegian Andes, between 95 and 84 Ma (Fig. 2a) (Vérard et al. 2012; Ghiglione et al. 2014). A mid-Cretaceous wrench component of bulk transpressional deformation that accommodated the movement between Antarctica and the southernmost Andes along the Beagle Channel fault zone (Cunningham 1993, 1995), is also recognized in Cooper Bay shear zone in South Georgia (Curtis et al. 2010), and in the Elephant Island along the South Scotia Ridge (Grunow et al. 1992). Subduction inception in the northern rim of the Rocas Verdes basin and the ensuing ophiolitic obduction in

orlando_a_p@yahoo.com.ar

the Sarmiento Cordillera occurred at ~85 Ma, as shown by means of combined zircon U–Pb and phengite ^{40}Ar-^{39}Ar age data representing cooling synchronous with mica crystallization (Calderón et al. 2012). Structural data and U–Pb isotopic ages on zircon from granite plutons near the Beagle Channel (Fig. 1c) show that basin inversion involved initially a small (~60 km-wide) thrust wedge that placed the basaltic floor of the Rocas Verdes Basin on top of adjacent continental crust prior to ~86 Ma (Klepeis et al. 2010). U–Th–Pb in situ dating of S2 monazite indicates that staurolite and kyanite growth and thus exhumation was underway before ~71 Ma (Maloney et al. 2011). Rocks of the Beagle granite suite, with zircon U–Pb and ^{40}Ar-^{39}Ar ages of ~68–70 Ma were emplaced post-tectonically within the uplifted marginal basin floor (Mukasa and Dalziel 1996).

The magmatic arc of the Fuegian Andes presents a mid-Cretaceous monzonitic suit plutons intruded by small calc–alkaline dykes and sills known as the Ushuaia Peninsula Andesites (Guillot et al. 2011). Radiometric dating indicates that the andesites are related to a transition from normal to flat subduction which additionally caused the widening and landward migration of the magmatic arc, as well as crustal deformation (Guillot et al. 2011). Rear-arc magmatism due to flat subduction endured ca. 22 m.y. and retracted southward afterward (Guillot et al. 2011).

Exhumation of the Basement Domain caused the deposition of coarse clastic sediments on top of the sag units, indicating the onset of a foreland phase in the evolution of the Austral and Malvinas basins (Natland et al. 1974; Biddle et al. 1986; Ghiglione et al. 2010). First foreland deposits are Coniacian—Campanian in the western part of Tierra del Fuego (Winslow 1982; Alvarez-Marrón et al. 1993) and Campanian–Maastrichtian (Fig. 6; Bahía Thetis Formation) in the eastern part (Malumián and Jannou 2010). Load subsidence and sedimentary supply to the offshore Malvinas and South Malvinas basins seem to be roughly synchronous with the first stages of Austral foreland basin (Ghiglione et al. 2010).

A phase of thrusting culminating in the Paleogene, shortened the basement and the Upper Jurassic igneous cover in the internal part of the belt by at least ~50 km (Kraemer 2003), forming a bivergent thrust wedge (Maloney et al. 2011). The exact age of this out-of-sequence thrust event that involved the Internal domain is uncertain (Klepeis et al. 2010). However, stratigraphic relationships suggest that they all post-date emplacement of the post-tectonic Beagle suite granite (~68–70 Ma, Mukasa and Dalziel 1996), as for example along the northern boundary of Cordillera Darwin in Bahía Parry where Late Cretaceous Beagle granites intruding the basement have been displaced by the basement thrust front (Klepeis et al. 2010). The presence of faulted pebble conglomerates and coarse-grained turbidites of Paleocene or younger age unconformably overlying the Upper Cretaceous sections at the northern end of Bahía Brookes suggest that back thrusting has occurred after the Paleocene (Klepeis et al. 2010).

orlando_a_p@yahoo.com.ar

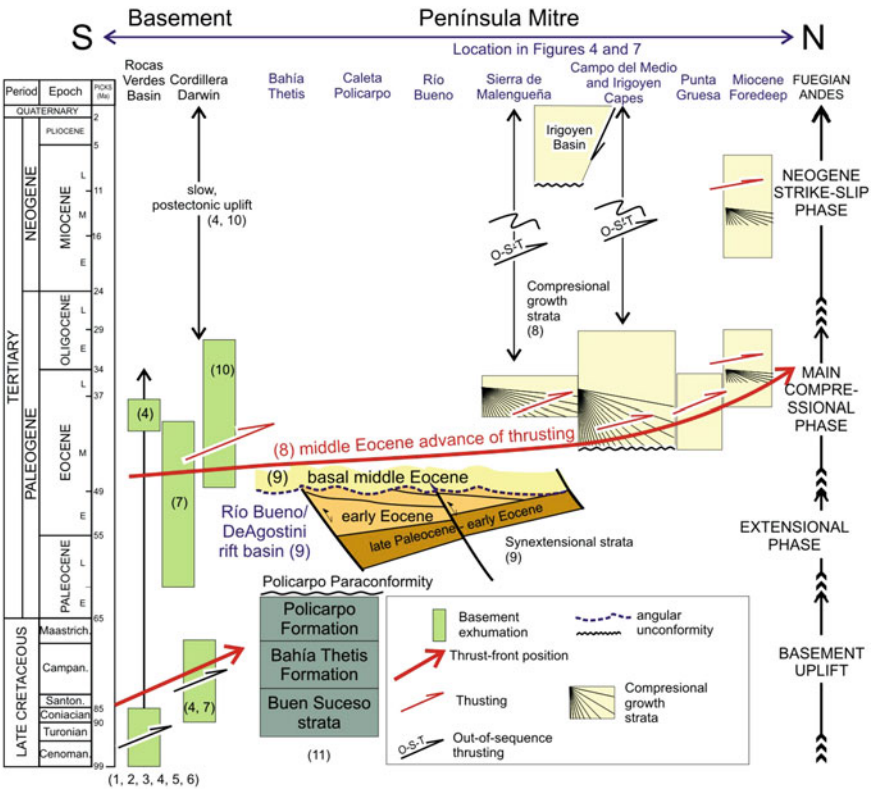


Fig. 6 Schematic time–space section through the Fuegian orogenic wedge in Peninsula Mitre illustrating patterns of faulting, uplift, sedimentation, and erosion. References are indicated with numbers: *1*, Halpern and Rex (1972); *2* Natland et al. (1974); *3* Hervé et al. (1981); *4* Nelson (1982); *5* Ramos et al. (1986); *6* Cunningham (1993, 1995); *7* Kohn et al. (1995); *8* Ghiglione and Ramos (2005); *9* Ghiglione et al. (2008); *10* Gombosi et al. (2009); and *11* Malumián and Jannou (2010)

5 Paleogene

The Late Cretaceous closure and compressional uplift of the Rocas Verdes Basin involved indentation of the magmatic arc and ocean floor against the foreland basement during the Late Cretaceous (Fig. 2c). These processes resulted in the consolidation of the basement domain and the formation of the thin-skinned fold and thrust belt probably by latest Cretaceous–Early Paleocene time (Kraemer 2003; Ghiglione and Cristallini 2007). A complex Paleogene stage of deformation involved Late Paleocene–Early Eocene continental stretching (Galeazzi 1998; Bry et al. 2004; Baristeas et al. 2013) associated with the slow separation of South America and Antarctica plates (Ghiglione et al. 2008, 2010) and followed by Middle to Late Eocene basement uplift and propagation of the fold and thrust belt (Figs. 2a, 6) (Ghiglione and Ramos 2005).

orlando_a_p@yahoo.com.ar

Although balanced cross-section of the fold and thrust belt were constructed (i.e., Fig. 3) (Alvarez-Marrón et al. 1993; Kley et al. 1999; Kraemer 2003; Klepeis et al. 2010), only few studies include a direct constrain on the age of Cenozoic deformation. Timing of exhumation and uplift was studied by multiple methods such as analysis of growth strata (Ghiglione et al. 2002; Bry et al. 2004; Ghiglione and Ramos 2005; Navarrete-Rodríguez 2006), fission tracks (Nelson 1982; Kohn et al. 1995; Gombosi et al. 2009), and exhumation of provenance sectors using U/Pb detrital-zircon geochronology (Barbeau et al. 2009).

A Cenozoic pulse of exhumation in Cordillera Darwin at 65–40 Ma (Fig. 6; Early Palaeocene–Middle Eocene) (Nelson 1982; Kohn et al. 1995) was originally related to exhumation due to normal faulting (Dalziel and Brown 1989; Kohn et al. 1995). Following interpretations, however, proposed that Paleocene–Eocene exhumation of Cordillera Darwin was contemporaneous, and therefore related to, shortening in the fold and thrust belt (Klepeis and Austin 1997; Kraemer 2003; Ghiglione and Ramos 2005; Torres Carbonell et al. 2011; Gombosi et al. 2009) and/or transpression along the Beagle Channel fault zone (Cunningham 1993, 1995). Recent structural and geophysical data from the Fuegian fold and thrust belt indicate however, Paleocene–Early Eocene continental stretching (Ghiglione et al. 2008) that can be connected to the conspicuous development of Paleocene extensional depocenters in the Austral and offshore basin of the South American oceanic platform (Platt and Philip 1995; Galeazzi 1998; Thomson et al. 2002; Bry et al. 2004; Baristeas et al. 2013), reviving the extensional versus compressional tectonics debate (Ghiglione et al. 2010) that would be discussed later in this chapter.

5.1 Paleogene Basement Exhumation and Deformation

The first episode of rapid exhumation and cooling of the Darwin Metamorphic Complex, from 500–600 °C to 350 °C, took place between 90 and 70 Ma (Fig. 6) (Kohn et al. 1993, 1995). Dalziel and Brown (1989) proposed that the northwest arm of the Beagle Channel marks the locus of a regional-scale detachment structure that accommodated extensional unroofing of the Cordillera Darwin following mid-Cretaceous shortening, i.e., the "core complex" interpretation. A second pulse of exhumation in the Darwin Metamorphic Complex, occurred during the Paleocene–Early Eocene (Fig. 6) (Nelson 1982; Kohn et al. 1993, 1995). Models of K–Ar release spectra show a complex P–T-t history between 60 and 40 Ma (temperatures of 325 and 200 °C, respectively), including rapid cooling at ~50 Ma between two slow-cooling episodes (Kohn et al. 1995). During its Paleogene exhumation, the Cordillera Darwin underwent extension distributed at relatively high structural levels that Kohn et al. (1995) ascribed to extension related to faulting along the Beagle Channel.

Thermal modeling of fission-track and (U–Th–Sm)/He data from the Basement Domain in the Fuegian Andes reveals rapid cooling (~12–48 °C Ma^{-1}) during the middle and late Eocene (~48–30 Ma) followed by slow cooling (~1.5 °C Ma^{-1})

orlando_a_p@yahoo.com.ar

from that time to the Recent (Gombosi et al. 2009). These data are in accordance with previous fission-track geochronology data, showing accelerated (0.5–1.5 mm/yr) middle Eocene basement uplift, followed by slower rates (0.05–0.20 mm/yr) of Neogene post-tectonic uplift of Cordillera Darwin (Nelson 1982). The Eocene rapid cooling (Fig. 6) is interpreted by Gombosi et al. (2009) as a result of exhumation from contractional uplift within the crystalline interior of the orogen.

Rock- and surface-uplift of the Cordillera Darwin complex and adjacent hinterland thrust sheets are also interpreted on the basis of provenance analysis using U/Pb detrital-zircon geochronology on foreland basin sequences exposed on the external fold and thrust belt (Barbeau et al. 2009): from the Late Cretaceous through most of the middle Eocene, detrital zircons reaching the foreland basin were dominantly contributed from ≤140 Ma sources, most likely derived from the Patagonian–Fuegian magmatic arc (Patagonian Batholith; Fig. 1c). In contrast, detrital-zircon populations of upper Eocene and Oligocene sequences are dominated by 150–190 Ma from synrift volcanism exposed on the Basement Domain (Fig. 1c) and pre-Mesozoic grains from metasedimentary rocks of Cordillera Darwin (Barbeau et al. 2009). This dramatic sediment provenance shift at c. 39 Ma in the Magallanes foreland basin is interpreted as evidence of basement uplift in the southernmost Andes related to important geodynamic changes in the Scotia Sea (Gombosi et al. 2009; Barbeau et al. 2009).

5.2 *Paleocene–Early Eocene Extension*

Despite the seemingly continuous orogeny affecting the southernmost Andes since Late Cretaceous times, there are conspicuous indications for Paleocene–early Eocene continental stretching. First studies related Late Cretaceous and Paleocene exhumation data of Cordillera Darwin to normal faulting (Dalziel and Brown 1989; Kohn et al. 1995). Other studies, focused on the sedimentary depocenters of the offshore basins on the Argentinean platform (Fig. 1b), also defined a Paleocene–middle Eocene extensional phase (Galeazzi 1998; Bry et al. 2004; Ghiglione et al. 2010; Baristeas et al. 2013).

The presence of extensional and strike-slip faulting in the early Paleocene–early Eocene sequences located near the deformational front lead Galeazzi (1998) to interpret this interval as a foredeep transition phase dominated by extensional and strike-slip deformation. Similar normal faulting is observed in the Austral basin in onshore and offshore seismic sections (Robbiano et al. 1996). The latter are thought to be transtensive because of their *en échelon* distribution in map view (Bonillo-Martinez et al. 2006). Extensional faults affecting post-sag sequences from the South Malvinas Basin were previously interpreted by Platt and Philip (1995) as evidence of extensional deformation that dominated the early evolutionary stages of the foredeep. A cluster of these normal faults is concentrated ahead of the deformational front and was synchronous with the first foreland sequences, as shown by the presence of growth faulting and fault-cutting relationships (Fig. 8d) (Thomson

orlando_a_p@yahoo.com.ar

et al. 2002; Bry et al. 2004). Normal faulting extends through the flexed plate decreasing its displacement and age toward Malvinas Islands. This observation leads Bry et al. (2004) to suggest that normal faulting was contemporaneous with the compressional phase. The authors interpret these normal faults as flexural-related, i.e., intrinsically related to a compression-driven tectonic load and not to an overall extensional phase. However, the *en échelon* distribution in map view (Bonillo-Martinez et al. 2006) and the important displacement shown by a few of the normal faults generating small extensional depocenters located closer to the deformational front in the Malvinas Basin (Fig. 8d) (Ghiglione et al. 2010) are more in agreement with the interpretation of a Paleocene–middle Eocene extensional and strike-slip deformation phase by Galeazzi (1998).

A recent study proposes a latest Paleocene–early Eocene extensional phase in southeast Tierra del Fuego that can be connected with the early stretching between South America and Antarctica (Ghiglione et al. 2008). Field-data showing synextensional growth strata and an S–SE thickening wedge-shape (Fig. 8a–c) allowed to interpret the upper Paleocene–Lower Eocene sequences from the southern tip of Peninsula Mitre as synrift deposits (Figs. 2a, 6) (Ghiglione et al. 2008). The upper Campanian–Lower Eocene marine sequences is characterized by agglutinated foraminiferous deposited in low-oxygen shallow environments that are in accordance with the existence of isolated extensional basins (Malumián and Jannou 2010). Extensional depocenters located offshore north of Isla de los Estados (Tassone et al. 2008) had a similar tectonostratigraphic architecture and can be broadly age-correlated with the onshore dopocenters (Fig. 7) (Ghiglione et al. 2008, 2010). A post-rift unconformity (Figs. 6, 8a–b) indicates that extensional faulting ended in that area at $\sim$49 Ma (Ghiglione et al. 2008). As shown in the correlation from Fig. 2c, extension ended in concurrence with an eightfold increase in South America–Antarctica separation rate (Livermore et al. 2005), and the proposed onset of oceanic basins in the incipient Drake Passage (Eagles et al. 2006). Early stages of extension during the Late Paleocene produced a relative shallow epicontinental sea between the Antarctic Peninsula and South America, preventing the faunal interchange of terrestrial forms (Reguero et al. 2014).

These events conducted to the Oligocene–Miocene full development of the Antarctic Circumpolar Current (Lawver and Gahagan 2003; Barker et al. 2007), which could have contributed to Oligocene global cooling and Antarctic glaciation by changes in ocean circulation that reduced heat transport to low latitudes (Kennett 1977). Others argue that a shallow early opening of the Drake Passage during the middle Eocene influenced a circulation-induced biogenic productivity increase that may have sequestered CO_2 (Scher and Martin 2006; Eagles et al. 2006) producing a fall in atmospheric CO_2 that could have caused Oligocene cooling without a global change in ocean circulation (De Conto and Pollard 2003). Conspicuous evidence of Paleocene–Eocene isolated rift depocenters in the Austral and Malvinas basins bolster interpretations of an early marine gateway (Bry et al. 2004; Ghiglione et al. 2008, 2010; Baristeas et al. 2013) by confirming the prediction of a continental extensional regime in the region prior to the opening of the Drake Passage (Eagles et al. 2006).

orlando_a_p@yahoo.com.ar

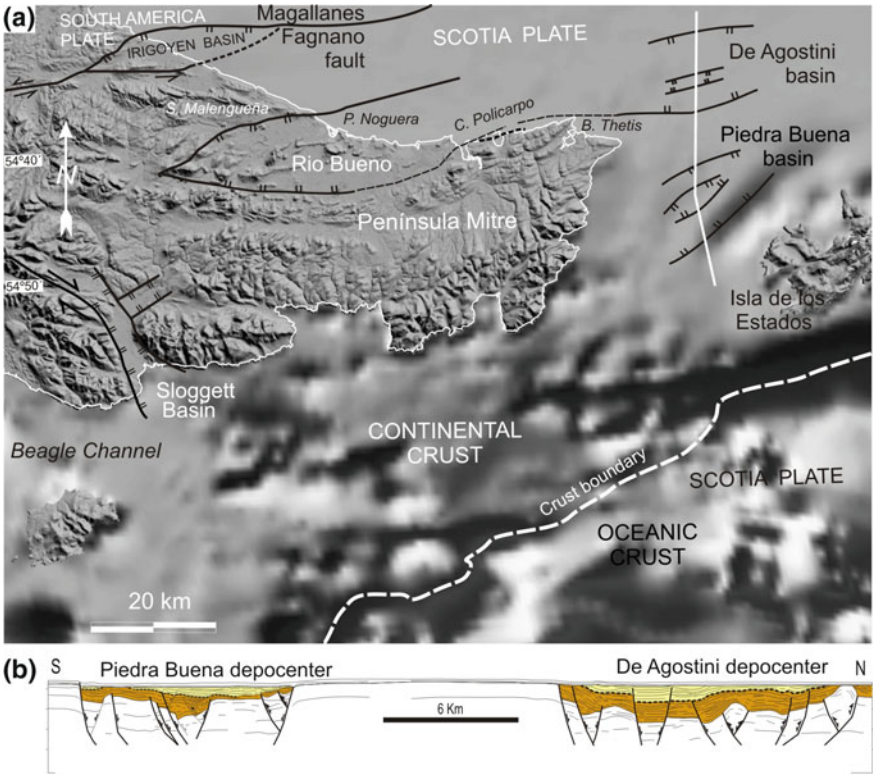


Fig. 7 **a** Mayor extensional features from the southern tip of the Andes at Peninsula Mitre (Ghiglione et al. 2008) with location of **b** line drawings of multichannel seismic reflection profile NW of Isla de los Estados (stratigraphic colors are from Fig. 6). From Ghiglione et al. (2008) after Tassone et al. (2008)

5.3 *Middle to Late Eocene Propagation of the Fold and Thrust Belt*

From middle Eocene to Oligocene, a combination of active deformation, tectonic loading and rapid subsidence produced conspicuous syntectonic sequences recognized between outcropping foreland basin sequences of Austral Basin in onshore Tierra del Fuego (Fig. 6) (Ghiglione et al. 2002; Ghiglione and Ramos 2005; Navarrete-Rodríguez 2006), and seismic data from offshore Malvinas and South Malvinas basins (Ghiglione et al. 2010). These sequences were deposited in a depositional wedge-top depozone where the frontal structures of the fold and thrust belt stayed below the depositional base level of the Austral and Malvinas flexural foreland depocenter (Ghiglione et al. 2010). Among the synorogenic features, the most conspicuous are syntectonic and intraformational angular unconformities and progressive unconformities constituting growth strata (Ghiglione et al. 2002;

orlando_a_p@yahoo.com.ar

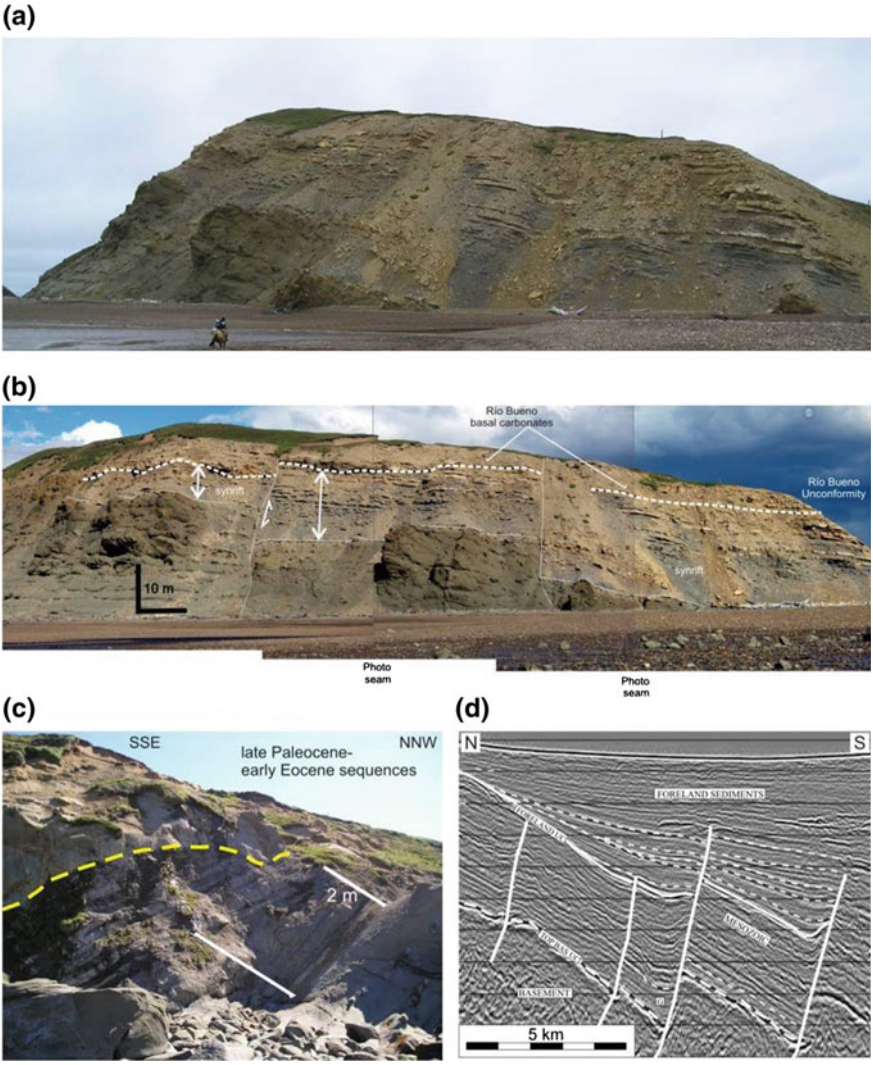


Fig. 8 **a–c** Composite field-photographs of the Río Bueno depocenter, showing synsedimentary extensional growth strata at Punta Noguera (see location in Fig. 7); **d** Seismic reflection profile from South Malvinas Basin located in Fig. 1b, showing normal faults cutting sequences of a foredeep wedge. These faults show clear evidence of intermittent synextensional stratigraphic growth within foreland package. From Bry et al. (2004)

Ghiglione and Ramos 2005). Eocene compressional growth strata have a ~49 to 34 Ma age, and therefore they were deposited a posteriori of synextensional growth strata of 60 to ~49 Ma age. Stratigraphic correlations along the Atlantic coast of Tierra del Fuego (Fig. 6) (Malumián and Olivero 2006; Malumián and Jannou 2010), also place the herein interpreted as compressional growth strata

orlando_a_p@yahoo.com.ar

(La Despedida Group) on top of the extensional Río Bueno—D´Agostini extensional depocenter (Río Claro Group). The Middle–Late Miocene subsidence due to tectonic load produced a pronounced transgression, represented by the Despedida Group, covering the previous isolated depocenters (Malumián and Olivero 2006; Malumián and Jannou 2010). The Middle Eocene orogenic front migration is disclosed by the distribution in space and time of syntectonic and progressive unconformities between dated growth strata shown in Fig. 6. This Middle Eocene compressional phase produced an orogenic front migration of at least 40 km (Ghiglione and Ramos 2005).

Middle to Late Eocene compressional deformation in the fold and thrust belt (Ghiglione and Ramos 2005) is in agreement with rapid cooling of the Basement Domain from ~48 to 30 Ma (Fig. 6) (Nelson 1982; Gombosi et al. 2009). Compressional basement exhumation and denudation produced a dramatic sediment provenance shift at ~39 Ma interpreted as evidence of geodynamic changes in the Scotia Sea (Gombosi et al. 2009; Barbeau et al. 2009).

Through the fold and thrust belt, flanking the Malvinas Basin, there is a series of piggy-back basins developing angular and progressive unconformities that can be clearly seen in seismic reflection profiles (Fish 2005; Ghiglione et al. 2010). These synkinematic sequences are of Eocene to Early Oligocene ages, based on correlation of seismic reflectors and well data (Yagupsky 2003; Tassone et al. 2008). Growth strata of similar Middle to Late Eocene age (Fig. 6), based on foraminifera assemblages (Malumián and Jannou 2010), crop-out along the Atlantic coast of Tierra del Fuego (Ghiglione et al. 2002; Ghiglione and Ramos 2005).

6 Neogene–Quaternary: Strike-Slip Tectonics

During the Neogene, deformation in southern South America slowed dramatically and changed in character from compressional to transpressional (Winslow 1982). Relative movement between South America and Antarctica was accommodated by spreading in the independent Central Scotia Plate from about 28 Ma (Lodolo et al. 2006) until ~16 Ma, when spreading ceased at the West Scotia Ridge and part of South America and the Central Scotia Plate amalgamate (Eagles et al. 2005; Lagabrielle et al. 2009). This event formed the modern Scotia Plate independent of South America (Eagles et al. 2005), which moved between two sinistral, dominantly strike-slip fault zones on the South Scotia Ridge–Shackleton fault zone and North Scotia Ridge–Magallanes Fagnano fault zone ever since (Fig. 1b) (Winslow 1982; Thomas et al. 2003; Lodolo et al. 2003). South America's northward drift of about 5° latitude since Eocene times (Somoza 2007) should be summed to the westward vector produced by the opening of the Atlantic ocean to produce an overall northwestward movement during the Oligocene–Neogene (Fig. 2b).

This passage from compressional tectonics to wrench kinematics has been registered at similar times in different parts of the Fuegian fold and thrust belt. In the Andes of western Tierra del Fuego, Cenozoic shortening has been overlaid by

orlando_a_p@yahoo.com.ar

left-lateral transtensional deformation since the Oligocene to early Neogene (Winslow 1982; Diraison et al. 2000; Lodolo et al. 2003; Ghiglione 2002, 2003; Ghiglione and Ramos 2005). Some authors suggested that a left-lateral offset of 20–30 km, mapped in the sequences cut by the Magallanes–Fagnano fault system in Tierra del Fuego, took place since at least the latest Eocene (Olivero and Martinioni 2001), while others calculated a 48 km offset by means of low displacement since 7 Ma (Torres Carbonell et al. 2008).

The development of the present seismically active Magallanes–Fagnano continental strike-slip plate boundary between South America and Scotia Plates produced the generalized strike-slip deformation observed everywhere in the southernmost Andes since the Oligocene (Wilson 1991; Cunningham 1993; Ghiglione 2002, 2003; Lodolo et al. 2003). Orientation of satellite image lineaments coincide with a theoretical Riedel shear system (Ghiglione 2002; Lodolo et al. 2003), while recent GPS studies (Mendoza et al. 2011) show stretching of the crust oriented in a NW–SE direction, and subordinate contraction with a SW–NE trend (Fig. 4). Some of the younger tectonic-driven morphostructural features related to Late Cenozoic strike-slip tectonics are pull-apart basins such as the Irigoyen (Fig. 8a) (Ghiglione 2003) and Fagnano lake basins along the strike-slip plate boundary (Figs. 1b, 3) (Lodolo et al. 2003). The Irigoyen Basin is filled by a transgresive upper Miocene–Pliocene marine sequence, containing foraminifera with Pacific affinities suggesting that the basin was part of an ocean connection (Malumián and Jannou 2010). A still active rifting system perpendicular to the orogen produced the opening of the eastern Magallanes strait (Diraison et al. 1997, 2000) and the transverse segmentation of the external fold and thrust belt (Ghiglione et al. 2013) (Fig. 4).

6.1 Neogene–Quaternary Rift System and the Magellan Strait

The Magellan strait that connects the Atlantic and Pacific oceans (Fig. 4) consists of a NW–SE western section controlled by the transtensional Magallanes–Fagnano fault zone within the Cordillera (Lodolo et al. 2003) and an east section-oriented E to NE along the Magellan rift. Diraison et al. (1997) interpreted the Magellan strait and the depressions of glacial valleys as extensional grabens, as for example the Inútil and San Sebastián bays (see also Lodolo et al. 2003; Menichetti et al. 2008). The intense volcano-tectonic activity in the Pali Aike area (Corbella 2002) marks a major Pliocene–Quaternary phase in the development of the Magellan rift system (Mazzarini and D'Orazio 2003). This volcanic field shows alignment of volcanoes indicating ascent of magma throughout reactivated NW trending Jurassic extensional faults (Corbella et al. 1996; Corbella 2002). The widespread spatial distribution of mainly shallow (depth <10 km) low-magnitude (Ms <4) earthquakes recorded on the recently installed local seismic network (Sabbione et al. 2007; Buffoni et al. 2009) also seems to be associated with modern tectonic activity in the Magellan rift (Fig. 4).

orlando_a_p@yahoo.com.ar

Recent structural mapping using seismic sections shows a good match between the orientation of the NE trending Jurassic transfer zones that coincide with Neogene grabens proposed by Diraison et al. (1997), developed at right angles of SW–NE strike-slip extensional directions (Ghiglione et al. 2013) (Fig. 4). Thus, it seems that Jurassic transfer zones were extensionally reactivated during Neogene strike-slip deformation generating the Magellan rift system (Ghiglione et al. 2013).

The Neogene rift system produced a transverse segmentation of the external fold and thrust belt, where some segments are outcropping while others are covered by Miocene sediments (Fig. 4). The transition from compression to strike-slip deformation occurred without a significant change in shortening direction, thus a synergetic transition took place from Eocene–Oligocene compression to Neogene transpression (Figs. 2a, 6). Transpression and inversion was also facilitated by the SW–NE orientation of the strike-slip maximum compressive stresses (Fig. 4), orthogonal to both previous compressional structures and to Jurassic extensional faults, facilitating reactivation by inversion. This fault system is responsible for the position of some Quaternary features such as the disposition of glacial valleys (Diraison et al. 1997, 2000) and the distribution of seismic events (Ghiglione et al. 2013).

7 Discussion and Concluding Remarks

There is a plethora of evidence op. cit. for the onset of a Late Cretaceous compressional tectonic setting related to subduction that produced the closure of the Rocas Verdes oceanic basin, ophiolitic obduction, high-grade metamorphism, and arc magmatism. From that grounding point, together with the existence of an important orogenic wedge, including a well-developed fold and thrust belt involving thick Paleogene–Neogene sequences, existed a conceptual understanding that orogeny continued uninterruptedly throughout the Paleogene.

Recent structural and geophysical data from the Fuegian fold and thrust belt indicate however a late Paleocene–early Eocene event of continental stretching (Ghiglione et al. 2008), that can be connected to the conspicuous development of Paleocene extensional depocenters in the Austral and offshore basin of the South America platform (Fig. 1) as described by many authors (Platt and Philip 1995; Galeazzi 1998; Thomson et al. 2002; Bry et al. 2004; Baristeas et al. 2013; among others). The latest Paleocene–early Eocene extensional phase coincided with a slow, N–S separation of South America and Antarctica (phase I of Livermore et al. 2005) and represented a crustal stretching event before the onset of seafloor spreading between the tips of South America and Antarctica (Livermore et al. 2005, 2007; Eagles et al. 2006). The depicted tectonic scenario included the opening of small and shallow, isolated extensional depocenters, in agreement with the paleoecological background of their foraminiferous content (Malumián and Jannou 2010). The Late Paleocene continental stretching documented in Tierra del Fuego (Ghiglione et al. 2008) produced a wide and relatively shallow epicontinental sea

orlando_a_p@yahoo.com.ar

(see Map 3 of Lawver et al. 2014) producing faunistic isolation between Antarctica and South America (Reguero et al. 2014). An accurately dated post-rift unconformity indicates that extensional faulting ended in the Río Bueno—De Agostini basins located in Peninsula Mitre and the surrounding offshore area at ~49 Ma (Fig. 8).

Extension ended in coincidence with a threefold increase in the separation rate between South America and Antarctica at ~50 Ma that was followed by the opening of a gap between South America and Antarctica from 50 to 34 Ma (Livermore et al. 2005). In major rift systems, the time at which crustal separation is achieved is largely a function of plate interaction and is usually preceded by a gradual reduction of tectonic activity in lateral graben systems, while tensional strain concentrates on the zone of future crustal separation. In terms of rifting dynamics, the deactivation of Río Bueno—De Agostini Basin can thus be explained as the abandonment of the lateral rift after strain concentration on the zone of future crustal separation due to a drastic acceleration in tectonic separation. After 50 Ma, crustal extension concentrated in Drake Passage allowing the formation of a shallow seaway across Protector and Dove basins (Livermore et al. 2005; Eagles et al. 2006) that ultimately lead to a 41 Ma blend of Pacific waters into the South Atlantic (Scher and Martin 2006). Even though an ancestral South Sandwich Arc would have been a barrier to the Antarctic Circumpolar Current (Dalziel 2014) until a deep water Drake Passage opened in the Miocene (Lawver et al. 2014), there is a general agreement for a shallow Late Eocene passage. The age of latest sedimentation from Sloggett—Piedra Buena basins can only be constrained in Sloggett Bay outcrops as Late Eocene (~33–37 Ma; Olivero and Martinioni 2001), coinciding with the suggested ~34–30 Ma onset of spreading in the west Scotia Sea (Livermore et al. 2005). Thus, abortion of Sloggett—Piedra Buena basins seem to be reflecting the final abandonment of marginal graben-scarps after generation of the first oceanic crust (Fig. 2) just 25–50 km to the southeast (Fig. 8). The extensional phases show a gradual concentration of extensional strain from southernmost South America toward the Drake Passage, where the spread of oceanic crust finally took place.

7.1 Middle Eocene–Oligocene Compression

It has been proposed a stage of the fold and thrust belt propagation during the Paleogene sensu lato, that shortened the basement domain and inner fold andthrust belt by at least ~50 km (Kraemer 2003), forming a bivergent thrust wedge uplifting Cordillera Darwin (Maloney et al. 2011). However, the exact age of this post Cretaceous out-of-sequence thrusting event that involved the Inner domain of the fold and thrust belt is uncertain (Klepeis et al. 2010), and present data do not account for fold and thrust belt propagation during the Paleocene–Early Eocene. Despite the fact that the Cenozoic pulse of exhumation in Cordillera Darwin at 65–40 Ma was originally ascribed to exhumation due to normal faulting (Dalziel and Brown 1989; Kohn et al. 1995), following interpretations proposed that

orlando_a_p@yahoo.com.ar

Paleocene–Eocene exhumation of Cordillera Darwin was contemporaneous with shortening in the fold and thrust belt, and therefore related to compression (Klepeis and Austin 1997; Kraemer 2003; Ghiglione and Ramos 2005; Torres Carbonell et al. 2011). A problem with later interpretations is that saving some exceptions (Ghiglione et al. 2002, 2010; Gombosi et al. 2009) in general they do not provide an independent timing for fault propagation in the fault thrust belt. Furthermore, it is interesting to notice that except from the Paleocene–Early Eocene exhumation data from Kohn et al. (1995), all the other data point out for a Middle to Late Eocene basement uplift concomitant with orogenic front propagation in the fold and thrust belt.

Recent thermochronometry data indicating rapid Middle to Late Eocene (~48–30 Ma) uplift in the Fuegian Andes (Gombosi et al. 2009) were connected with a dramatic sediment provenance shift at ~39 Ma in the Austral foreland basin to suggest a dramatic reorganization of the Fuegian Andes orogeny, consistent with Middle Eocene shortening and exhumation of the orogenic hinterland (Barbeau et al. 2009; Gombosi et al. 2009). These studies are in agreement with previous works describing Eocene growth strata (~49 to 34 Ma) deposited in a wide wedge top depocenter, recording a major propagation of the blind thrust front of ~40 km (Ghiglione et al. 2002; Ghiglione and Ramos 2005). For Barbeau et al. (2009) this interpreted kinematic reorganization demonstrates a temporal relationship between Fuegian Andes deformation and the opening of the adjacent Drake Passage. Ghiglione et al. (2008) proposed that the region was affected by Middle Eocene–Oligocene coeval strike-slip and compressional deformation. This was due to the fast (2.4 cm/year) left-lateral motion between South America and Antarctica (Livermore et al. 2005), and the synergetic combination of fast spreading rates in the Drake Passage with rapid convergence and northward-directed subduction of the Farallon plate against South America (Ghiglione and Cristallini 2007). This constitutes an important discussion, because both tectonic stages relate deformation in South America with the Scotia sea development. There is a striking coincidence between the end of extension in the Early Eocene and the start of the Middle to Late Eocene compression (Figs. 2c, 6).

7.2 *Magallanes Strait and the Role of Ancient Transfer Zones*

The Patagonian Jurassic fault array was prone to reactivation under small amounts of stretching in an orthogonal direction (Glasser and Ghiglione 2009; Likerman et al. 2013; Ghiglione et al. 2014), developing the Magallanes strait with maximum depths of over 500 m joining the Atlantic and Pacific Oceans (Ghiglione et al. 2013). Tertiary riftings and shear zones around the Scotia Arc region and southernmost South America, including those associated with the opening of the Drake Passage, show a similar latitudinal orientation when are mapped on a Late Eocene paleogeographic reconstruction (Fig. 9). Even if the Dove and Protector basins

orlando_a_p@yahoo.com.ar

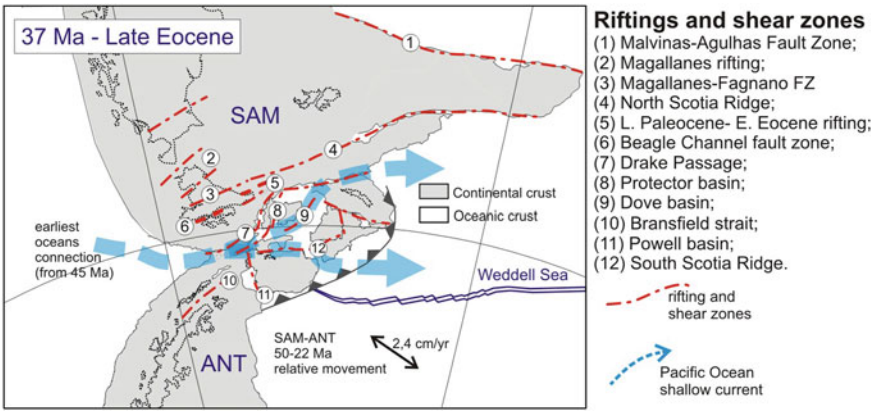


Fig. 9 Paleogeographic reconstruction for the Late Eocene (37 Ma) modified from Livermore et al. (2007). Riftings and shear zones around the Scotia Arc region and southernmost South America were added in dashed lines with dots and are signaled with numbers

show certain rotation at 37 Ma due to previous oceanic spreading (Fig. 9), they were parallel to the Neogene rifting before their opening (Fig. 2 from Livermore et al. 2007).

Here, it is proposed that transfer zones reactivated during Magallanes rift could have also controlled Cenozoic riftings around the Scotia sea (Fig. 9). In particular, relative left-lateral plate motion along the Magallanes–Fagnano fault system is ~0.6 cm/year, while the north–south separation rate is around ~0.6 cm/year (Smalley et al. 2003; Mendoza et al. 2011). Then, transfer zones located in the West Scotia Sea were easily reactivated during the phase of 2.4 cm/yr NW–SE separation between South America and Antarctica that started at 50 Ma (Eagles et al. 2006; Livermore et al. 2007).

Acknowledgments The present work is a part of the research projects conducted in the South Andes financially supported by grants Agencia PICT 2010-36, PICT-2013-1291 and CONICET PIP48.

References

Alvarez-Marrón J, McClay KR, Harambour S, Rojas L, Skarmeta J (1993) Geometry and evolution of the frontal part of the Magallanes foreland thrust and fold belt (Vicuna-Area), Tierra del Fuego, Southern Chile. Am Assoc Petrol Geol Bull 77:1904–1921

Baristeas N, Anka Z, di Primio R, Rodriguez JF, Marchal D, Dominguez F (2013) New insights into the tectono-stratigraphic evolution of the Malvinas Basin, offshore of the southernmost Argentinean continental margin. Tectonophysics 604:280–295

Barbeau DL, Olivero E, Swanson-Hysell N, Zahid K, Murray K, Gehrels G (2009) Detrital-zircon geochronology of the eastern Magallanes foreland basin: Implications for Eocene kinematics of the northern Scotia Arc and Drake Passage. Earth Planet Sci Lett 20:23–45

orlando_a_p@yahoo.com.ar

Barker PF (2001) Scotia Sea regional tectonic evolution: implications for mantle flow and palaeocirculation. Earth Sci Rev 55:1–39

Barker PF, Filippelli GM, Florindo F, Martin EE, Scher HD (2007) Onset and role of the Antarctic circumpolar current. Deep-Sea Res II 54:2388–2398

Biddle KT, Uliana MA, Mitchum RM, Fitzgerald MG, Wright RC (1986) The stratigraphy and structural evolution of the central and eastern Magallanes Basin, southern South America. In: Allen A, Homewood P (eds) Foreland basins, Blackwell Scientific Publications, London. Int Assoc Sediment Special Publication, vol 8, pp 41–61

Bonillo-Martinez P, Ghiglione MC, Figueroa D (2006) Structural styles and tectonic framework of the fold and thrust belt in Tierra del Fuego and offshore Austral-Malvinas basins, Argentina. Simposio Bolivariano (Cartagena de Indias), pp 1–8

Bruhn RL, Dalziel IWD (1977) Destruction of the early cretaceous marginal basin in the Andes of Tierra del Fuego. Island arcs, deep sea trenches and back-arc basins, pp 395–405

Bry M, White N, Singh S, England R, Trowell C (2004) Anatomy and formation of oblique continental collision: South Falkland basin. Tectonics 23(4):TC401

Buffoni C, Sabbione NC, Connon G, Ormaechea JL (2009) Localización de hipocentros y determinación de su magnitud en Tierra del Fuego y zonas aledañas. Geoacta 34:75–86

Calderón M, Fildani A, Hervé F, Fanning CM, Weislogel A, Cordani U (2007) Late Jurassic bimodal magmatism in the northern sea-floor remnant of the Rocas Verdes basin, southern Patagonian Andes. J Geol Soc 164:1011–1022

Calderón M, Fosdick JC, Warren C, Massonne HJ, Fanning CM, Fadel Cury L, Schwanethal J, Fonseca PE, Galaz G, Gaytán D, Hervé F (2012) The low-grade Canal de las Montañas Shear Zone and its role in the tectonic emplacement of the Sarmiento Ophiolitic complex and Late Cretaceous Patagonian Andes orogeny, Chile. Tectonophysics 525:165–185

Caminos R, Haller M, Lapido J, Lizuain O, Page A, Ramos VA (1981) Reconocimiento geológico de los Andes Fueguinos, Territorio Nacional de Tierra del Fuego. VIII Congreso Geológico Argentino (San Luis) Actas 1:759–786

Cande S, Leslie RB (1986) Late Cenozoic tectonics of the southern Chile trench. J Geophys Res 91:471–496

Carey SW (1958) The tectonic approach to continental drift. Continental drift: a symposium: Hobart. Geology Department, University of Tasmania, Tasmania, pp 177–355

Corbella H (2002) El campo volcano-tectónico de Pali Aike. In: Haller MJ (ed) Geología y Recursos Naturales de la Provincia de Santa Cruz. Relatorio del XV Congreso Geológico Argentino, pp 285–302

Corbella H, Chelotti L, Pomposiello C (1996) Neotectónica del rift Jurásico austral en Pali Aike, Patagonia extrandina, Santa Cruz, Argentina. XIII Congreso Geológico Argentino y III Congreso Exploración de Hidrocarburos (Buenos Aires). Actas 2:383–393

Cunningham WD (1993) Strike-slip faults in the southernmost Andes and the development of the Patagonian Orocline. Tectonics 169–186

Cunningham WD (1995) Orogenesis at the southern tip of the Americas: the structural evolution of the Cordillera Darwin metamorphic complex, southernmost Chile. Tectonophysics 244 (4):197–229

Curtis ML, Flowerdew MJ, Riley TR, Whitehouse MJ, Daly JS (2010) Andean sinistral transpression and kinematic partitioning in South Georgia. J Struct Geol 32(4):464–477

Dalziel IWD (1981) Backarc extension in the southern Andes: a review and critical reappraisal. Philos Trans R Soc Lond 300:319–335

Dalziel IWD (1986) Collision and Cordilleran orogenesis: an Andean perspective. In Coward MP, Riers AC (eds) Collision Tectonics, Geol Soc London, Special Publication, vol 19, pp 389–404

Dalziel IWD (2014) Drake passage and the scotia arc: a tortuous space-time gateway for the Antarctic circumpolar current. Geology 42:367–368

Dalziel IWD, Klingfield R, Lowrie W, Opdyke ND (1973) Paleomagnetic data from the southernmost Andes and the Antarctandes. In: Tarling DH, Runcom SK (eds) Implications of continental drift to the earth sciences 1: San Diego, Academic Press, pp 87–101

orlando_a_p@yahoo.com.ar

Dalziel IWD, De Wit MF, Palmer KF (1974) Fossil marginal basin in the southern Andes. Nature 250:291–294
Dalziel IWD, Brown RL (1989) Tectonic denudation of the Cordillera Darwin metamorphic core complex, Tierra del Fuego: implications for cordilleran orogenesis. Geology 17:699–703
De Conto R, Pollard D (2003) Rapid Cenozoic glaciation of Antarctica induced by declining atmospheric CO2. Nature 421:245–249
Diraison M, Cobbold PR, Gapais D, Rossello EA (1997) Magellan Strait: part of a Neogene rift system. Geology 25:703–706
Diraison M, Cobbold PR, Gapais D, Rossello EA, Le Corre C (2000) Cenozoic crustal thickening, wrenching and rifting in the foothills of the southernmost Andes. Tectonophysics 316:91–119
Eagles G, Jokat W (2014) Tectonic reconstructions for paleobathymetry in Drake Passage. Tectonophysics 611:28–50
Eagles G, Livermore RA, Fairhead JD, Morris P (2005) Tectonic evolution of the west Scotia Sea. J Geophys Res 110 doi:10.1029/2004JB003154
Eagles G, Livermore RA, Morris P (2006) Small basins in the Scotia Sea: the Eocene drake passage gateway. Earth Planet Sci Lett 242:343–353
Féraud G, Alric V, Fornari M, Bertrand H, Haler M (1999) ^{40}Ar-^{39}Ar dating of the Jurassic volcanic province of Patagonia: migrating magmatism related to Gondwana break-up and subduction. Earth Planet Sci Lett 172:83–96
Fish (2005) Frontier South, East Falkland basins reveal important exploration potential. Oil Gas J 103:34–40
Folguera A, Ramos VA (2002) Partición de la deformación durante el Neógeno en los Andes Patagonicos Septentrionales (37º–46º S). Rev Soc Geol España 15:81–93
Galeazzi JS (1998) Structural and stratigraphic evolution of the Western Malvinas Basin, Argentina. Am Assoc Petrol Geol Bull 82:596–636
Ghiglione MC (2002) Diques clásticos asociados a deformación transcurrente en depósitos sinorogénicos del Mioceno inferior de la Cuenca Austral. Rev Asoc Geol Argentina 57:103–118
Ghiglione MC (2003) Estructura y evolución tectónica del Cretácico-Terciario de la costa Atlántica de Tierra del Fuego. Unpubl. PhD thesis, Facultad de Ciencias Exactas y Naturales, Universidad de Buenos Aires, p 150
Ghiglione MC, Cristallini EO (2007) Have the southernmost Andes been curved since Late Cretaceous times? An analog test for the Patagonian Orocline. Geology 35:13–16
Ghiglione MC, Ramos VA (2005) Chronology of deformation in the Southernmost Andes of Tierra del Fuego. Tectonophysics 405:25–46
Ghiglione MC, Ramos VA, Cristallini EO (2002) Fuegian Andes foreland fold and thrust belt: structure and growth strata. Rev Geol Chile 29:17–41
Ghiglione MC, Yagupsky D, Ghidella M, Ramos VA (2008) Continental stretching preceding the opening of the drake passage: evidence from Tierra del Fuego. Geology 36:643–646
Ghiglione MC, Quinteros J, Yagupsky D, Bonillo-Martínez P, Hlebszevtich J, Ramos VA, Vergani G, Figueroa D, Quesada S, Zapata T (2010) Structure and tectonic history of the foreland basins of southernmost South America. J S Am Earth Sci 29:262–277
Ghiglione MC, Navarrete-Rodríguez AT, González-Guillot M, Bujaleski G (2013) The opening of the Magellan Strait and its geodynamic implications. Terra Nova 25(1):13–20
Ghiglione MC, Likerman J, Barberón V, Giambiagi L, Aguirre-Urreta MB, Suarez F (2014) Geodynamic context for the deposition of coarse-grained deep-water axial channel systems in the Patagonian Andes. Basin Res 26(6):726–745
Glasser N, Ghiglione MC (2009) Structural, tectonic and glaciological controls on the evolution of fjord landscapes. Geomorphology 105:291–302
Gombosi DJ, Barbeau DL, Garver J (2009) New thermochronometric constraints on the rapid Paleogene exhumation of the Cordillera Darwin complex and related thrust sheets in the Fuegian Andes. Terra Nova 21:507–515
Grunow AM, Dalziel IWD, Harrison TM, Heizler MT (1992) Structural geology and geochronology of subduction complexes along the margin of Gondwanaland: new data from the Antarctic Peninsula and southernmost Andes. Geol Soc Am Bull 104:1497–1514

orlando_a_p@yahoo.com.ar

Guillot MG, Escayola M, Acevedo R (2011) Calc-alkaline rear-arc magmatism in the Fuegian Andes: Implications for the mid-cretaceous tectonomagmatic evolution of southernmost South America. J S Am Earth Sci 31(1):1–16

Halpern M, Rex DC (1972) Time of folding of the Yahgan Formation and age of the Tekenika beds, southern Chile, South America. Geol Soc Am Bull 83:1881–1886

Hervé F, Nelson E, Kawashita K, Suárez M (1981) New isotopic ages and the timing of orogenic events in the Cordillera Darwin, southernmost Chilean Andes. Earth Planet Sci Lett 55 (2):257–265

Hervé F, Pankhurst RJ, Fanning CM, Calderón M, Yaxley GM (2007) The South Patagonian batholith: 150 My of granite magmatism on a plate margin. Lithos 97:373–394

Katz HR (1973) Contrasts in tectonic evolution of orogenic belts in the southwest Pacific. J Roy Soc N Z 3:333–362

Kennett JP (1977) Cenozoic evolution of Antarctic glaciation, the Circum-Antarctic ocean, and their impact on global paleoceanography. J Geophys Res 82:3843–3860

Klepeis KA, Austin JA (1997) Contrasting styles of superposed deformation in the southernmost Andes. Tectonics 16:755–776

Klepeis K, Betka P, Clarke G, Fanning M, Hervé F, Rojas L, Mpodozis C, Thomson S (2010) Continental underthrusting and obduction during the Cretaceous closure of the Rocas Verdes rift basin, Cordillera darwin, Patagonian andes. Tectonics 29(3) http://dx.doi.org/10.1029/2009TC002610

Kley J, Monaldi CR, Salfity JA (1999) Along-strike segmentation of the Andean foreland: causes and consequences. Tectonophysics 301:75–94

Kohn MJ, Spear FS, Dalziel IWD (1993) Metamorphic P-T paths from Cordillera Darwin, a core complex in Tierra del Fuego. Chile J Petrol 34:519–542

Kohn MJ, Spear FS, Harrison TM, Dalziel IWD (1995) Ar-40/Ar-39 geochronology and P-T-T paths from the Cordillera Darwin metamorphic complex, Tierra del Fuego, Chile. J Metamorph Geol 13:251–270

Kraemer PE (2003) Orogenic shortening and the origin of the Patagonian orocline (56 S Lat). J S Am Earth Sci 15:731–748

Lagabrielle Y, Goddéris Y, Donnadieu Y, Malavieille J, Suarez M (2009) The tectonic history of drake passage and its possible impacts on global climate. Earth Planet Sci Lett 279(3):197–211

Lawver LA, Gahagan LM (2003) Evolution of Cenozoic seaways in the circum-Antarctic region. Palaeogeo Palaeoclim Palaeoecol 198:11–37

Lawver LA, Gahagan LM, Dalziel IWD (2014) Reconstructions of the southern ocean and Antarctic regions. In: De Broyer C, Koubbi P, Griffiths HJ, Raymond B, Udekem d'Acoz C d' (eds) Biogeographic Atlas of the Southern Ocean, Cambridge, pp 36–42

Likerman L, Burlando JF, Cristallini EO, Ghiglione MC (2013) Along-strike structural variations in the Southern Patagonian Andes: insights from physical modeling. Tectonophysics 590:106–120

Livermore RA, Nankivell AP, Eagles G, Morris P (2005) Paleogene opening of drake passage. Earth Planet Sci Lett 236:459–470

Livermore R, Hillenbrand CD, Meredith M, Eagles G (2007) Drake passage and cenozoic climate: an open and shut case? Geochem Geophys Geosyst 8:Q01005

Lodolo E, Menichetti M, Bartole R, Ben-Avraham Z, Tassone A, Lippai H (2003) Magallanes-Fagnano continental transform fault (Tierra del Fuego, southernmost South America). Tectonics 22:1076

Lodolo E, Donda F, Tassone A (2006) Western Scotia Sea margins: improved constraints on the opening of the drake passage. J Geophys Res 111(6):B06101

Maffione M, Speranza F, Faccenna C, Rossello E (2010) Paleomagnetic evidence for a pre-early Eocene (~50 Ma) bending of the Patagonian orocline (Tierra del Fuego, Argentina): paleogeographic and tectonic implications. Earth Planet Sci Lett 289(1):273–286

Maloney KT, Clarke GL, Klepeis KA, Fanning CM, Wang W (2011) Crustal growth during back-arc closure: Cretaceous exhumation history of Cordillera Darwin, southern Patagonia. J Metamorph Geol 29(6):649–672

orlando_a_p@yahoo.com.ar

Malumián N, Jannou G (2010) Los Andes Fueguinos: el registro micropaleontológico de los mayores acontecimientos paleooceanográficos australes del Campaniano al Mioceno. Andean Geol 37(2):345–374

Malumián N, Olivero EB (2006) El Grupo Cabo Domingo, Tierra del Fuego: bioestratigrafía, paleoambientes y acontecimientos del Eoceno-Mioceno marino. Rev Asoc Geol Argentina 61 (2):139–160

Mazzarini F, D'Orazio M (2003) Spatial distribution of cones and satellite-detected lineaments in the Pali Aike Volcanic Field (southernmost Patagonia): insights into the tectonic setting of a Neogene rift system. J Volcanol Geotherm Res 125:291–305

Mendoza L, Perdomo R, Hormaechea JL, Del Cogliano D, Fritsche M, Richter A, Dietrich R (2011) Present-day crustal deformation along the Magallanes-Fagnano Fault System in Tierra del Fuego from repeated GPS observations. Geophys J Int 184:1009–1022

Menichetti M, Lodolo E, Tassone A (2008) Structural geology of the Fuegian Andes and Magallanes fold thrust belt—Tierra del Fuego Island. Geologica Acta 6:19–42

Moraga J, Briceño M, Mella P, Alvarez P, Vieytes H, Laval E, Méndez D (2004) Potencial de hidrocarburos en la cuenca de antepais Magallanes. Empresa Nacional del Petróleo (ENAP), Chile, Unpubl. report 1, p 85

Mukasa SB, Dalziel IWD (1996) Southernmost Andes and South Georgia island, north Scotia Ridge: zircon U-Pb and muscovite Ar/Ar age constraints on tectonic evolution of southwestern Gondwanaland. J S Am Earth Sci 9:349–365

Navarrete-Rodríguez AT (2006) Análisis estructural del área de lago Mercedes, cuenca de Magallanes, Chile. Unpubl. MSc Thesis, Universidad Nacional de Colombia, Bogotá: p 103

Natland M, González E, Cañón A, Ernst M (1974) A system of stages for correlation of Magallanes basin sediments. Geol Soc Am Mem 139:1–117

Nelson EP (1982) Post-tectonic uplift of the Cordillera Darwin orogenic core complex: evidence for fission track geochronology and closing temperature time relationships. J Geol Soc 139:755–761

Nelson EP, Dalziel IWD, Milnes AG (1980) Structural geology of the Cordillera Darwin-collision style orogenesis in the southernmost Andes. Eclogae Geol Helv 73:727–751

Olivero EB, Martinioni DR (2001) A review of the geology of the Argentinian Fuegian Andes. J S Am Earth Sci 14(2):175–188

Pankhurst RJ, Riley TR, Fanning CM, Kelley SP (2000) Episodic silicic volcanism in Patagonia and the Antarctic Peninsula: chronology of magmatism associated with the break-up of Gondwana. J Petrol 41:605–625

Pelayo A, Wiens D (1989) Seismotectonics and relative plate motions in the Scotia Sea region. J Geophys Res 94:7293–7320

Platt NH, Philip R (1995) Structure of the southern Falkland Islands continental shelf: initial results from new seismic data. Mar Petrol Geol 12:759–771

Poblete F, Roperch P, Hervé F, Diraison M, Espinoza M, Arriagada C (2014) The curved Magallanes fold and thrust belt: Tectonic insights from a paleomagnetic and anisotropy of magnetic susceptibility study. Tectonics 33:2526–2551

Ramos VA, Haller MJ, Butrón F (1986) Geología y Evolución tectónica de las Islas Barnevelt. Rev Asoc Geol Argentina 15:137–154

Reguero MA, Gelfo JN, López GM, Bond M, Abello A, Santillana SN, Marenssi SA (2014) Final Gondwana breakup: The Paleogene South American native ungulates and the demise of the South America-Antarctica land connection. Glob Planet Change 123:400–413

Robbiano JA, Arbe H, Gangui A (1996) Cuenca Austral Marina. In: Turic MA (ed) Ramos VA. Geología y Recursos Naturales de la Plataforma Continental Argentina, Buenos Aires, pp 323–342

Sabbione N, Connon G, Hormaechea JL, Rosa ML (2007) Estudio de sismicidad en la provincia de Tierra del Fuego. Geoacta 32:41–50

Scher H, Martin E (2006) Timing and climatic consequences of the opening of drake passage. Science 312:428–430

orlando_a_p@yahoo.com.ar

Smalley R, Kendrick E, Bevis MG, Dalziel IWD, Taylor F, Lauría E, Piana E (2003) Geodetic determination of relative plate motion and crustal deformation across the Scotia-South America plate boundary in eastern Tierra del Fuego. Geochem Geophys Geosyst 4(9) doi:10.1029/2002GC000446

Somoza R (2007) Eocene paleomagnetic pole for South America: Northward continental motion in the Cenozoic, opening of drake passage and Caribbean convergence. J Geophys Res 112:B03104

Somoza R, Ghidella ME (2005) Convergencia en el margen occidental de América del sur durante el Cenozoico: Subducción de Nazca, Farallon y Aluk. Rev Asoc Geol Argentina 60:797–809

Somoza R, Ghidella ME (2012) Late Cretaceous to recent plate motions in westrn South America revisited. Earth Planet Sci Lett 331:152–163

Stern CR, De Witt MJ (2003) Rocas Verdes ophiolites, southernmost South America: remnants of progressive stages of development on oceanic-type crust in a continental margin back-arc basin. In Dilek Y, Robinson PT (eds) Ophiolites in Earth History. Geol Soc London, Special Publication, vol 218, pp 1–19

Storey BC, Vaughan APM, Millar IL (1996) Geodynamic evolution of the Antarctic Peninsula during Mesozoic times and its bearing on Weddell Sea history. Geol Soc London, Special Publication 108:87–103

Suárez M, Hervé M, Puig A (1985) Hoja Isla Hoste e islas adyacentes. Carta Geológica de Chile Servicio Nacional de Geología y Minería, Santiago p 65

Tassone A, Lodolo E, Menichetti M, Yagupsky D, Caffau M, Vilas JF (2008) Seismostratigraphic and structural setting of the Malvinas Basin and its southern margin (Tierra del Fuego Atlantic offshore). Geol Acta 6:55–67

Thomas CR (1949) Geology and Petroleum Exploration in Magallanes Province, Chile. Am Assoc Petrol Geol Bull 33:1553–1578

Thomson K, Hegarty KA, Marshallsea SJ, Green F (2002) Thermal and tectonic evolution of the Falkland Islands: implications for hydrocarbon exploration on the adjacent offshore region. Mar Petrol Geol 19:95–116

Thomas T, Livermore RA, Pollitz F (2003) Motion of the Scotia Sea plates. Geophys J Int 155:789–804

Torres Carbonell PJ, Olivero EB, Dimieri LV (2008) Control en la magnitud de desplazamiento de rumbo del Sistema Transformante Fagnano, Tierra del Fuego. Argentina Rev Geol Chile 35 (1):63–77

Torres Carbonell PJ, Dimieri LV, Olivero EB (2011) Progressive deformation of a Coulomb thrust-wedge: the eastern Fuegian Andes Thrust-Fold Belt. In: Poblet J, Lisle R (eds) Kinematic evolution and structural styles of fold-and-thrust belts. Geol Soc London, Special Publication, vol 349, pp 123–147

Uliana VMA, Biddle KT, Cerdan J (1989) Mesozoic extension and the formation of Argentine sedimentary basins. In: Tankard AJ, Balkwill HR (eds) Extensional tectonics and stratigraphy of the North Atlantic Margins. Am Assoc Pet Geol Bull Mem 46:599–613

Vérard C, Flores K, Stampfli G (2012) Geodynamic reconstructions of the South America-Antarctica plate system. J Geodyn 53:43–60

Wilson TJ (1991) Transition from Back-Arc to Foreland Basin development in the Southernmost Andes—stratigraphic record from the Ultima-Esperanza-District, Chile. Geol Soc Am Bull 103:98–111

Winslow MA (1982) The structural evolution of the Magallanes basin and neotectonics in the southernmost Andes. In: Craddrock C (ed) Antarctic geosciences, symposium on antarctic geology and geophysics. University of Wisconsin Press, Madison, pp 143–154

Yagupsky DL (2003) Estudio sismoestratigráfico y estructural del sector meridional de las cuencas de Magallanes y Malvinas. Unpubl. Master Thesis, Facultad de Ciencias Exactas y Naturales, Universidad de Buenos Aires, p 111

Yrigoyen MR (1989) Cuenca de Malvinas. In: Chebli GA, Spalletti LA (eds) Cuencas Sedimentarias Argentinas, Serie Correlación Geológica 6, Universidad Nacional del Tucumán, pp 481–491

orlando_a_p@yahoo.com.ar

Index

A
Abanico basin, 67, 77, 81
Accretionary prism, 149, 208
Aconcagua, 69, 79
Aconcagua fold and thrust belt, 70, 75, 79, 81, 84, 87
Aconcagua volcanic complex, 74
Active convergent margin, 64
Adakitic, 228
Agrio fold and thrust belt, 101, 104–106, 108, 110, 111, 116
Agrio formation, 43, 47–50, 52, 128
Airy model, 17
Alta Vista, 218
Alto Tunuyán basin, 74, 79
Aluk, 201, 226
Aluk ridge, 226
Aluminé depocenter, 136
Amuti Quimey lake, 154
Anacleto Formation, 51
Andacollo Group, 101
Andean Cordillera, 36
Andean cycle, 125, 149
Andean deformation, 36
Andean fold and thrust belt, 139
Andean forearc, 149
Andean front, 139, 142
Andean magmatic arc, 36, 41, 47, 50, 51
Andean margin, 115
Andean orogen, 149
Andean orogeny, 76, 182
Andean retroarc, 120
Andean structure, 11
Andean system, 125
Andean uplift, 36, 48
Andean volcanic arc, 41, 46, 47
Andes, 173–178, 180–183, 185–187, 189, 192, 193
Angular unconformity, 122, 125
Anita Formation, 217, 218
Antarctica, 242, 244, 249, 251, 254, 257, 259, 260, 262
Antarctic and Nazca Plates, 135
Antarctic Circumpolar Current, 254, 260
Antarctic Peninsula, 214, 242, 244, 246, 249, 254
Antarctic Peninsula Volcanic Group, 246
Antarctic plate, 175, 176
Antiformal stack, 107
Antiñir- Copahue fault system, 120
Arc expansion, 104, 117, 165, 166
Arc front, 120, 121
Arc gap, 201, 225
Arc migration, 125–127
Arc retraction, 165
Arc roots, 151
Argentino lake, 218, 226
Arroyo Tocuyo, 118
Asthenospheric anomaly, 120, 128
Asthenospheric mantle, 140
Asthenospheric wedge, 166
Atlantic marine ingression, 76, 125
Atlantic Ocean, 211
Atuel basin, 75
Atuel depocenter, 44
Auca Pan depocenter, 138, 140
Auquilco Formation, 41, 101, 106
Austral Basin, 202, 211, 216, 220, 224, 230, 253, 255
Austral Patagonian Andes, 175, 176, 180

B
Backbulge, 76
Backthrust, 135, 138, 157, 158
Bahía Brookes, 219, 250
Bahía La Lancha, 208
Bahía Parry, 250
Bajada del Agrio group, 41, 43

© Springer International Publishing Switzerland 2016

A. Folguera et al. (eds.), *Growth of the Southern Andes*,
Springer Earth System Sciences, DOI 10.1007/978-3-319-23060-3

orlando_a_p@yahoo.com.ar

Bajo de Carpa formations, 53
Barreal-Las Peñas deformation zone, 71
Barros Arana basalts, 212
Basaltic plateux, 202
Basement, 202, 207, 208, 210–212, 214, 217, 219, 221, 224, 230, 232, 246, 249–253, 261
Basement blocks, 11
Basement domain, 208, 222, 224, 242, 246, 250, 251, 257, 260
Basement overthrusting, 182
Basement thrust front, 219, 221, 222
Basement topography, 155, 156
Basement wedge, 138
Beagle Channel, 212, 214, 249, 252
Beagle Channel fault zone, 249
Beagle granite suite, 250
Beauvoir formation, 249
Belgrano, 180, 185, 210, 224
Belgrano lake, 218, 225
Benioff zone, 5
Black shales, 47
Bouguer anomaly, 18–21
Brittle-ductile transition, 70, 117, 125, 166
Broken foreland, 24, 124, 158, 163, 166
Broken foreland system, 174, 175, 180, 183, 185, 186, 191
Buoyan foreland sedimentation lithosphere, 188
Butalón valley, 118

C

Cacheuta basin, 72, 75, 82
Calafate, 217, 219, 224
Calafate Formation, 224
Calc-alkaline affinities, 151
Cañadon Asfalto Basin, 25, 151
Canal de las Montañas shear zone, 213, 214, 221
Candeleros Formation, 44, 50, 53, 54
Cardiel Formation, 217
Cardiel lake, 225
Cenozoic, 12
Central Depression, 34, 68, 69, 73, 77, 82, 83, 135
Central Depression basin, 73
Central valley, 25
Cerrilladas Pedemontanas, 68, 72, 82
Cerro Cazador, 220, 222
Cerro Dorotea Formation, 220, 222, 224
Cerro Fortaleza, 219
Cerro Pico Solo, 159
Cerro Piltriquitrón, 158
Cerro Plataforma, 153, 158, 159, 163
Cerro Toro, 218, 219, 221, 224
Cerro Toro Formation, 219, 221
Cerro Villegas syncline, 107
Chacaico depocenter, 45
Chacay Melehue Formation, 46
Chachahuén volcanic complex, 116, 118, 124, 125, 127
Chachil Limestone, 46
Challacó Formation, 46
Charilehue Formation, 127
Chasca-Catequil mid-ocean ridge, 188
Chihuidos High, 105, 106
Chilean Central Valley, 149
Chilean Trench, 16
Chilean Triple Junction, 151
Chile mid-ocean ridge, 183, 193
Chilenia terrane, 38
Chile ridge, 207, 228, 230
Choiyoi Group, 47, 101
Choiyoi magmatic province, 40, 45, 47, 48, 53
Cholar Anticline, 106
Chon Aike, 211, 246
Chonaike Formation, 177
Chos Malal fold and thrust belt, 101, 102, 106–108, 110, 116, 118, 120, 126–128
City of Santiago, 69
Clastic wedges, 122
Coastal Batholith, 25, 40
Coastal Cordillera, 35, 39, 40, 135, 149, 175, 181, 191
Coastal Ranges, 69, 74, 77
Cola de Zorro formation, 104
Collision, 202, 207, 212, 214, 222, 224–226, 228, 232
Collón Curá Basin, 137, 156, 158, 161, 165
Collón Curá Formation, 149, 154, 157–160
Colohuincul Complex, 151
Continental deposits, 34, 44
Contractional pulse, 118, 126
Contractional structures, 120, 138
Convergent margin, 51
Convolution approach method, 20
Cordillera Darwin, 214, 243, 246, 249, 250, 252, 253, 260
Cordillera de las Yaretas, 71
Cordillera del Tigre, 71, 81
Cordillera del Viento, 40, 46, 48, 101, 106, 108, 110, 115, 116, 118, 125, 127
Cordillera del Viento Formation, 119
Cordillera Sarmiento, 212
Cordón de la Ramada, 71, 79
Cordón del Burrero Volcanic Complex, 78
Cordón del Plata, 71
Cordón del Portillo, 71
Cosmelli basin, 224

orlando_a_p@yahoo.com.ar

Costal Cordillera, 5
Cretaceous zircons, 48, 50
Cross section, 115, 150, 152, 154, 156–158, 162, 166
Crust, 68, 79, 81
Crustal extension, 67
Crustal inhomogeneities, 10
Crustal root, 17–19, 23, 25, 79, 81, 82
Crustal shortening, 64, 66, 85, 87
Crustal stretching, 165
Crustal thermal state, 156, 160
Crustal thickening, 66
Crustal thickness, 18, 20, 64, 68, 80, 85
Crustal thinning, 77
Crust-mantle boundary, 161
Crust-mantle discontinuity, 9
Crust thermal structure, 161
Cura Mallín Basin, 105, 126, 136
Cura Mallín Formation, 104, 107
Curie depth point, 156
Curie isotherm, 156, 161
Cuyania, 11, 23
Cuyania terrane, 38, 122
Cuyo Basin, 23, 67, 72, 84
Cuyo Group, 41, 45, 46, 53, 101, 105

D
Darwin Metamorphic Complex, 252
David syncline, 152, 156, 157
Decóllement, 70, 78, 156
Deep-marine environment, 182
Deep-marine sediments, 149
Deformational stage, 140
Degree and order of the harmonic expansion, 10, 15
Density, 10, 13, 15, 20, 24
Density contrast, 20
Depocenters, 118
Deseado basin, 211, 230
Deseado Massif, 12, 25, 183, 185
Detrital zircon, 34, 38, 40, 50–53
Direct approach method, 10
Disturbing potential, 13
Divisadero Group, 151, 159, 163
Domuyo, 101
Domuyo anticline, 101, 108
Dorotea Formation, 220, 222, 224
Downward continuation, 13
Drake Passage, 244, 254, 260, 261

E
Early orogenic stage, 174
Earth gravity field model, 9, 13
Effective elastic thickness, 19, 22
EGM2008, 9, 10, 13, 15, 17, 23
Elastic thicknesses, 133, 137, 139
El Bolsón Subbasin, 157, 158, 161, 163
El Bolsón valley, 157, 159, 163
El Chacay Formation, 230
Elephant Island, 249
El Freno formation, 44
El Maitén magmatic belt, 153, 165
El Quemado, 211
El Tranquilo Basin, 177
Emergent deformational front, 156, 160
Endogenic processes, 64
Esquel, 154, 158
Estratos de Molina depocenter, 122
Exhumation, 118, 122, 125
Exogenic processes, 64
Extension, 174, 175, 177, 179, 186, 187, 189, 191
Extensional reactivation, 110
Extensional stage, 126, 136
Extensional structures, 70, 77, 104, 106, 142, 160, 162, 163, 220
Extensional/trasntensional reactivation, 186
External domain, 208, 224
External fold and thrust belt, 208, 232
Extra-Andean, 207, 211, 225, 228
Extra-Andean Basin, 76

F
Famatinian magmatic arc, 38, 48, 122
Famatinian zircon ages, 51
Farallon Plate, 222, 261
Farallón ridge, 202
Farallones /Antarctica mid ocean ridge, 189
Farellones Formation, 69, 79, 81
Fission track, 116–118, 125
Fitz Roy, 207, 229
Flat slab subduction, 64
Flexural rigidity, 20
Flexural slip algorithm, 154
Fluvial drainage pattern, 120
Fluvial network, 120
Fold and thrust belt, 11, 36, 101, 105, 110, 148, 149, 161, 163, 166, 244, 246, 251–253, 255, 257, 258, 260
Forearc, 16, 24, 25, 126
Forearc Basin, 74
Forearc structure, 136
Foredeep, 116, 121, 125, 157, 159, 216, 221, 222, 226, 231
Foreland, 10, 12, 22, 24, 116, 117, 122–127, 148, 149, 151, 152, 154, 156–158, 160–163, 165, 166, 173–175, 178, 180–187, 189, 191

orlando_a_p@yahoo.com.ar

Foreland Basin, 34, 43, 50, 53, 75, 79, 82, 138, 166, 202, 211, 214, 219, 220, 224, 230, 232
Foreland crustal deformation, 117
Foreland magmatism, 118
Foreland sedimentation, 148, 202, 214, 241
Foreland systems, 34, 173, 174, 180, 191
Free-air gravity, 24
Frontal Cordillera, 11, 14, 34, 63, 66, 68, 71, 74, 75, 79, 81, 83, 84, 87
Frontal monocline, 208, 223
Fuegian Andes, 214, 242, 244, 246, 249, 250, 252, 261

G
Geochemical analysis, 44
Geochemical data, 140
Geochronological analyses, 115
Geochronological data, 149, 162, 166
Geophysical data, 161
Gilbert delta, 160
Glacial sediments, 149
GOCE satellite, 9
Gondwana, 11, 25, 66, 67, 208
Gondwana breakup, 186, 193
Gondwana margin, 38
Gondwanian orogenic cycle, 149
Gondwanian orogeny, 101
Gravimetric residuals, 155, 156
Gravity, 10, 13, 20, 23, 25
Gravity anomaly, 13–15, 23
Gravity data, 104, 133, 137, 139, 154, 155, 161
Gravity model, 136
Gravity residuals, 160
Grenville basement, 38
Grenvillian zircon ages, 124
Growth-strata, 207
Guañacos fold and thrust belt, 107, 109, 110, 116, 117

H
Half-grabens, 115, 119, 138, 179
Hauterivian, 47
Heat flow, 20, 24
Heavy minerals, 43
High-stand sea level, 125
Hinterland, 153, 154, 156–159, 161, 163, 165
Homogeneous precision, 10, 16
Huincul deformation zone, 39
Huincul Formation, 44, 52
Huincul High, 25, 35, 39, 45, 46, 48, 53
Huincul system, 140
Huitrera Formation, 43, 151, 156
Hydrostatic Moho, 18

I
Igneous–metamorphic basement, 151, 157
Impactogene rift basins, 187
Intermontain basin, 73
Internal Domain, 208, 214, 218, 222, 224–226
Internal fold and thrust belt, 208, 225
Interplate dynamics, 64, 85, 87
Interplate seismicity, 136
Intra-arc basin, 67, 136
Intra-orogenic events, 151
Intraplate belt, 174
Intraplate magmatism, 174, 186, 191
Inversion, 134, 139, 142
Inversion gravity models, 162
Irigoyen Basin, 258
Isla de los Estados, 254, 255
Isolated rift depocenters, 36
Isostatic, 17, 20
Isostatic compensation, 77, 82
Isostatic lithospheric flexure model, 9, 20
Isostatic modeling, 17
Isostatic rebound, 77, 82

J
Juan Fernández Ridge, 23, 24
Junín de los Andes, 136, 138
Jurassic, 36, 41, 45, 48, 50, 53
Jurassic Andean magmatic arc, 47
Jurassic synrift, 208

K
Kachaike Formation, 217

L
La Carrera fault system, 71
Lacustrine environment, 160
La Despedida Group, 257
Lago Argentino, 208, 214, 217–221, 230
Lago Belgrano, 224
Lago Cardiel, 225, 230
Lago Cochrane, 224
La Golondrina Basin, 177
Lago Posadas, 217, 230, 231
Lago San Martín, 217, 220, 226
Lago Sofía, 218, 219
Lago Viedma, 210, 214, 217, 218, 221
Lago Viedma Formation, 217, 221
La Irene Formation, 219
La Manga Formation, 41
La Ramada fold and thrust belt, 69, 79, 84, 87
Lajas Formation, 41
Lanín volcano, 139
Lanalhue Lineament, 35, 40

orlando_a_p@yahoo.com.ar

Landscape, 64
Lapa Formation, 45
Las Matras-Chadileuvú block, 34
Las Peñas Basin, 75
Late Cenozoic cooling, 244
Laurentia, 11
Lemaire Formation, 246
Leona river, 219
Ligorio Márquez Formation, 224
Liquiñe-Ofqui fault system, 120
Liquiñe–Ofqui fault zone, 12, 148, 151, 165, 175
Lithosphere, 17, 20, 24
Lithospheric strength, 66, 85
Loma Rayoso Anticline, 106
Loncopué Trough, 104, 105
Long wavelength, 10
Los Molles Formation, 46
Lotena Group, 41, 47, 101

M
Mafic magmatism, 173
Magallanes, 230
Magallanes Basin, 202, 214, 231, 232, 242, 253
Magallanes–Fagnano, 244, 257, 258, 262
Magallanes-Fagnano fault, 244, 257, 258, 262
Magallanes-Fagnano fault system, 11, 14, 16, 25
Magallanes-Fagnano fault zone, 203
Magallanes strait, 244, 258, 261
Magmatic arc, 208, 212
Magmatic arc migration, 188
Magnetometric data, 154, 166
Main Andes, 36, 44, 104, 105, 107, 124
Main Cordillera, 11, 14, 23, 126
Malargüe Basin, 73, 75, 82
Malargüe fold and thrust belt, 69, 70, 79, 82, 83, 100, 101, 108–110
Malargüe Group, 42, 43, 101, 122, 125
Malvinas, 242, 244, 250, 253, 254
Malvinas Basin, 242, 244, 250, 253–255, 257
Malvinas fault, 72
Malvinas Islands, 254
Man Aike, 207, 224, 225
Manantiales basin, 74
Mantle wedge, 139
Marginal Basin, 202, 211, 212, 221
Marifil, 211
Marine terraces, 69
Marine transgression, 33, 36, 41, 46, 47, 53, 178
Marussi tensor, 13
Mascardi lake, 157
Mata Amarilla Formation, 217, 218, 221
Maximum depositional age, 39, 40
Media Luna fault, 138
Melipilla fault, 69
Mendoza Group, 41, 44, 45, 47, 50, 101
Meseta Buenos Aires, 225
Meseta Posadas, 226
Mesetas Chile Chico, 225
Meso-Cenozoic Evolution, 189
Mesoproterozoic basement, 38
Mesozoic, 12
Metamorphic Complex, 211
Mid-ocean ridges, 173, 188, 189, 191
Mid-ocean spreading rates, 148
Modeling algorithms, 154
Moho attenuation, 161
Moho geometry, 155, 156
Monocline, 220, 222, 224
Monte León Formation, 230
Morphology, 66
Morphometric analyses, 115, 120
Morphotectonic units, 148
Mountain building, 85
Mountain ranges, 11, 24
Mulichinco Formation, 43, 101

N
Nacientes del Bío Bío Formation, 105
Nahuel Huapi lake, 156, 158, 159, 165
Navidad basin, 74
Nazca Plate, 12, 23, 24, 134, 135, 139, 140, 176
Neo-Proterozoic, 11
Neotectonic, 115, 116, 120, 121, 128
Neotectonic activity, 72
Neuquén, 42
Neuquén Basin, 34, 36, 38, 40–44, 46, 48, 50, 51, 53, 67, 70, 77, 100, 101, 116, 124, 127
Neuquén Embayment, 11, 12, 34, 36, 40, 41
Neuquén Group, 43, 44, 49–53, 101, 125
Ñirihuau Basin, 150, 154, 157, 161
Ñirihuau Formation, 153, 157, 158, 160, 165
Normal crust, 140
Normal faults, 116, 118, 119
Normal subduction, 64, 75, 82, 84, 88
Ñorquinco area, 157
Northern Patagonia, 25
North Patagonian Andes, 100, 133–136, 138, 142, 148, 149, 154, 163, 165, 166
North Patagonian Batholith, 151, 157, 158
North Patagonian Cordillera, 34, 149, 151, 159, 161
North Patagonian Massif, 25, 34, 36, 38, 40, 44, 51, 183, 185

orlando_a_p@yahoo.com.ar

North Patagonian orogen, 40, 147–149, 173
North Patagonian Precordillera, 137, 138, 140
North Scotia Ridge, 244, 257

O
Obduction, 202, 219, 221, 249, 259
Oblique convergence, 120
Ocean floor, 212
Oceanic floor, 202
Ophiolites, 202, 211–213, 219, 221
Orogenesis, 173, 179, 187
Orogenic front, 36, 43, 50, 51, 53, 79, 80, 82, 83, 115, 116, 121, 122, 124, 125, 127, 133, 138, 202, 207, 226
Orogenic wedge, 7, 64, 100, 116, 134, 226, 251, 259
Orogenic width, 64
Osorno and Llanquihue basins, 135
Out-of-sequence, 116, 120, 128
Out-of-sequence deformation, 70
Out-of-sequence thrusts, 70

P
Pacific margin, 202, 208, 212
Pacific Ocean, 212
Palauco Basin, 76, 126
Palauco Formation, 122, 125
Paleoelevation, 75
Paleo-margin, 175
Paleo-Pacific Ocean, 36, 41, 43, 46, 48
Paleozoic, 11, 12, 23
Paleozoic basement, 208, 220
Palinspastic restoration, 106, 154, 156
Pampa de Carrizalito depocenter, 122, 123
Pampa Tril anticline, 125
Pampean flat slab, 24, 104
Pampean zircon ages, 179, 184, 219, 220
Pampia terrane, 38, 122
Pangea breakup, 138
Panthalassic oceanic plates, 174
Panthalassic plates, 188
Paranaense marine regression, 76
Paraná-Etendeka LIP, 49
Pari Aike, 219
Patagonia, 25, 202, 207, 208, 211, 212, 221, 222, 225, 228, 230–232, 242, 244, 246
Patagonian Andes, 207, 208, 212, 222, 231, 232, 244, 249
Patagonian Batholith, 151, 156, 158, 175, 177, 181, 208, 246
Patagonian broken foreland system, 175, 183, 185, 186
Patagonian Cordillera, 12, 23
Patagoniano, 207
Patagonian Orocline, 246
Patagonia terrane, 38, 40
Patagoniense, 230, 231
Pattern of detrital zircon, 34, 40, 51
Payenia, 24, 68, 72
Payenia volcanic field, 104
Payenia volcanic plateau, 120
Peneplains, 69, 83
Peninsula Mitre, 254, 260
Peripheral bulge, 51, 53, 54
Phoenix plate, 222
Phoenix ridge, 207, 222, 225, 226, 232
Piedra Buena basin, 260
Piedra Clavada Formation, 217
Piedra del Águila Formation, 45
Piedra del Águila-Sañicó depocenter, 45
Piedra Santa Formation, 39
Piedras Paradas fault, 138
Pilcaniyeu belt, 151
Pilcaniyeu magmatic belt, 151
Pincheiras basin, 76
Pircala Formation, 125
Plate configuration, 148
Plate convergence, 148
Plate reconstruction, 188
Poisson ratio, 20, 22
Portezuelos Colorados syncline, 109
Posadas Basalt, 207, 225, 226
Positive dilatancy, 124
Potential methods, 115
Power-density spectra, 155, 156
Pre-Andean basement, 34, 39
Pre-Andean structures, 71
Precambrian, 38, 47, 48
Precordillera, 11, 14, 23, 63, 66, 68, 71, 74, 75, 78, 79, 81, 83, 84, 87
Precordilleran System, 149, 151, 153, 158, 160, 163
Pre-Cuyano, 101
Precuyano cycle, 41, 44–48
Principal Cordillera, 34, 63, 68–70, 74–77, 79–81, 83, 84, 86, 87
Progressive unconformities, 138
Proto-Andes, 101
Proto-Pacific margin, 66
Provenance analysis, 51

orlando_a_p@yahoo.com.ar

Puesto El Alamo Formation, 217, 221
Pull-apart, 137
Pull-apart basin, 258
Punta Barrosa Formation, 218, 219, 221
Puntilla de Huicán, 108

Q
Quetrupillán, 135, 137, 139

R
Radiometric ages, 117
Rayoso formation, 43, 48, 49, 51, 52
Reference depth, 20
Reference ellipsoid, 13
Regional angular unconformity, 185
Regional compression, 173, 184, 188, 189, 191
Retroarc, 133, 134, 136, 137, 140, 142, 150, 152, 154–156, 158, 160, 161, 163, 166
Retro-arc basin, 73
Retroarc foreland basins, 36
Retro-arc magmatism, 68
Retro-arc volcanism, 72, 225, 226, 228, 232
Retroarc zone, 100, 102, 104, 110, 120, 121, 166
Rheological and compositional properties, 20
Ridge collision, 228
Ridge subduction, 207, 212, 222, 228
Rift basin, 67
Rift phase, 46, 258, 262
Rift systems, 50, 54
Right-lateral displacements, 120
Rio Belgrano Formation, 225
Río Carbón essexite, 225, 226
Rio Chico Complex, 151
Río Chico high, 230
Río Claro Group, 257
Rio Damas Formation, 47
Rio de la Plata cratón, 24, 122
Río Grande basin, 76
Rio Guillermo Formation, 230
Río Lácteo Formation, 208
Rio Leona Formation, 230
Río Mayer Formation, 211, 217
Río Mayo Subbasin, 179, 181, 182, 185, 189
Río Turbio, 207, 218, 224, 225, 230
Río Turbio Formation, 207, 223
Roca Formation, 43
Rocas Verdes, 202, 212, 214, 242, 246, 248–251, 259
Rocas Verdes Basin, 202, 211, 212, 214, 219, 221, 222, 232
Rocas Verdes marginal basin, 202, 203, 211
Roll-back, 173, 189
Roof-pendant, 157

S
San Bernardo fold and thrust belt, 184, 186
Sañicó depocenter, 138, 139
San Jorge Gulf Basin, 173, 174, 176, 178, 179, 183–187, 189, 191
San Julian Basin, 177, 184
San Rafael basement block, 124
San Rafael Block, 11, 14, 24, 34, 38–40, 44, 68, 72, 73, 86
San Rafael orogenic phase, 40
San Rafael orogeny, 66
Santa Cruz Formation, 207, 231
Santa Isabel thrust, 72
Santiago valley, 69
Sarmiento Cordillera, 250
Sarmiento Ophiolite Complex, 249
Sarmiento Ophiolitic Complex, 212–214
Satellite, 10, 23
Satellite only models, 10
Satellite plutons, 151
Scotia Arc, 261, 262
Scotia plate, 25, 244, 257, 258
Scotia Ridge, 244, 249, 257
Scotia Sea, 242, 244, 253, 257, 260–262
Sedimentary depocenters, 136
Sedimentary prisms, 134
Sedimentary provenance analysis, 34, 43, 44
Sedimentation rates, 24
Seismic data, 139
Seismic information, 106
Seismic profiles, 154
Seismic reflection profile, 166
Shallow subduction, 116, 117, 124, 166
Shortening, 152, 156–159, 162, 165, 166, 182
Shortening gradient, 147, 166
Sierra Azul, 101
Sierra de Cara Cura, 101, 109
Sierra del Toro, 220
Sierra de Reyes, 101, 115, 116, 121, 122, 125–127
Sierras Pampeanas, 11, 24, 38, 49, 63, 68, 72, 73, 79, 81–84, 87, 125
Silla Syncline, 220
Slab breakoff, 207
Slab detachment, 142
Slab shallowing, 173, 187–189, 191
Slab tearing, 140
Slab window, 175, 191–193, 207, 228
Sloggett Bay, 260
Somuncura massif, 12, 25
Source areas, 44, 47, 51, 53, 54
South America, 206, 211, 212, 214, 226, 228, 232
South American Plate, 25, 120, 174, 175, 189

orlando_a_p@yahoo.com.ar

South Atlantic, 212, 242, 260
South Atlantic Ocean, 49
Southern Andes, 9, 11, 22, 212, 232
Southern Andes Volcanic Zone, 149
Southern Atlantic ocean, 189, 191
Southern Central Andes, 34–36, 38, 39, 43, 53, 54, 100, 110, 115, 116
Southernmost Andes, 242–244, 249, 253, 258
Southern Volcanic Zone, 120
South Georgia, 249
South Malvinas, 250, 253, 255
South Scotia Ridge, 243, 249, 257
Spatial resolution, 10
Springhill, 211
Stratovolcanoes, 149, 151
Strength, 20, 23
Strike-slip, 135
Structural cross-section, 124
Structural evolution, 180
Sub-Andean region, 149
Subcordilleran batholith, 162, 177
Subcordilleran Plutonic Belt, 151
Subducted geometry, 134, 188
Subducted slab, 125, 134, 136, 139, 142
Subduction, 173, 175, 177, 179, 181–183, 188, 191
Subduction erosion, 149
Subduction orogen, 148
Subduction zone, 134, 140
Subsidence, 135
Synextensional, 118
Synextensional deposits, 133
Synextensional geometries, 101, 104
Synorogenic depocenter, 99, 110, 124, 147, 158, 162, 165
Synorogenic deposits, 74–76, 116, 138, 158, 162, 165, 162, 165, 182, 185, 193
Synorogenic foreland rifting, 173, 186, 187
Synorogenic strata, 109, 110
Synrift, 208, 211, 253, 254
Syn-rift sections, 139
Synrift stage, 101
Synsedimentary, 220, 221, 223
Syntectonic, 207, 213, 218, 221, 222, 224

T

Tábanos formation, 41
Tearing, 134, 140
Tectonic, 9, 24
Tectonic events, 173, 189
Tectonic evolution, 34, 36
Tectonic inversion, 70, 105, 106, 116, 118, 157–160, 162, 163, 166
Temuco Basin, 126
Teniente volcanic complex, 77
Tesseroids, 13
Thermal anomalies, 140
Thermally weakened crust, 151, 155
Thermal sag stage, 34
Thermal state, 20
Thermal structure, 10, 20
Thermal weakening, 120
Thick-skinned, 11, 208
Thick-skinned deformation, 70, 157
Thick-skinned faults, 138
Thick-skinned system, 107
Thick-skinned thrusts, 71
Thin-skinned, 11, 208
Thin-skinned deformation, 70, 116
Thin-skinned structures, 105, 108, 110
Thin-skinned thrusts, 181
Tholeiitic magmatism, 77
Tholeiitic signatures, 154
Thrust front, 207, 221, 222, 226
Thrusts, 135, 138
Thrust sheets, 70
Tierra del Fuego, 219, 244–247, 250, 254, 255, 257, 259
Tithonian, 47
Tobífera Formation, 211, 219, 221, 246
Tomography contours, 136
Topographic effect, 13–17
Topographic elevation, 64, 82, 85, 87
Topographic load, 17, 19, 20
Topography, 13, 15, 17, 20, 24, 63, 64, 84, 85, 87
Topography reduced, 13
Tordillo Formation, 41, 44, 45, 47–49, 51, 52, 101
Toro thrust, 222
Torres del Paine, 207, 229
Tortuga Ophiolitic Complex, 243, 249
Traful lake, 154, 156
Traiguén marine basin, 173, 175, 181, 182, 191, 192
Transfer zones, 259, 261, 262
Transgression, 149
Transition zone, 100
Transtensional event, 67
Trench, 23, 24
Tres Pasos, 220, 222
Triangular zone, 119, 138, 158

orlando_a_p@yahoo.com.ar

Triassic, 11, 36, 41, 45
Triple junction, 226
Tromen volcanic plateau, 104, 115, 116, 120, 121, 127, 128
Tutu-Tucu, 226

U
Ultima Esperanza, 214, 218, 219, 221, 230, 231
Uncomformity, 181, 184
Unroofing sequence, 122, 127
U/Pb detrital zircon, 122, 124
U-Pb zircon age, 34, 38–40, 45, 49
Uplift, 173–175, 179–181, 183, 185, 187, 192, 193
Upwelling, 140
Ushuaia Peninsula Andesites, 250
Uspallata Basin, 75

V
Vaca Muerta Formation, 43, 44, 47, 101
Vacas Basin, 74
Valdivia Basin, 135
Valdivia fracture zone, 139
Velocity anomaly, 137, 139
Ventana Formation, 151, 153, 157, 158
Vertical gravity gradient, 14–17
Viedma, 204, 217, 218, 224
Villarrica-Lanín volcanoes, 134
Volcanic arc, 68, 79, 116, 137, 140, 149, 165
Volcanic eruptions, 140
Volcanic gap, 212, 225, 226
Volcanic Mesetas, 202
Volcanic Plateaus, 185, 191, 207
Volcano-sedimentary sequence, 181
Vp anomalies, 137
Vs anomalies, 137, 139, 140

W
Weddell Sea, 202, 242, 248
Wedge-like geometries, 153, 154, 163
Wedge-top, 216, 220, 221, 225, 226, 231
Wedge-top area, 157, 158, 160
Western Andean domain, 122
Western Gondwana, 40, 50
Western Sierras Pampeanas, 24
West Scotia, 244, 245, 257, 260, 262
West Scotia Ridge, 257
Within-plate environment, 154
Within-plate volcanics, 161
Within-plate volcanism, 117

Y
Yahgan, 249
Young lithosphere, 173, 188, 189, 191
Young modulus, 20, 22

Z
Zapata Formation, 219, 221
Zircon pattern, 51

orlando_a_p@yahoo.com.ar